nrsc

Remote Sensing Applications

P. S. Roy
R. S. Dwivedi
D. Vijayan

National Remote Sensing Centre

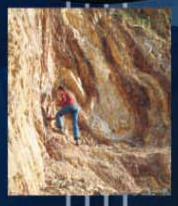

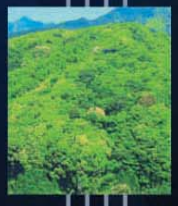

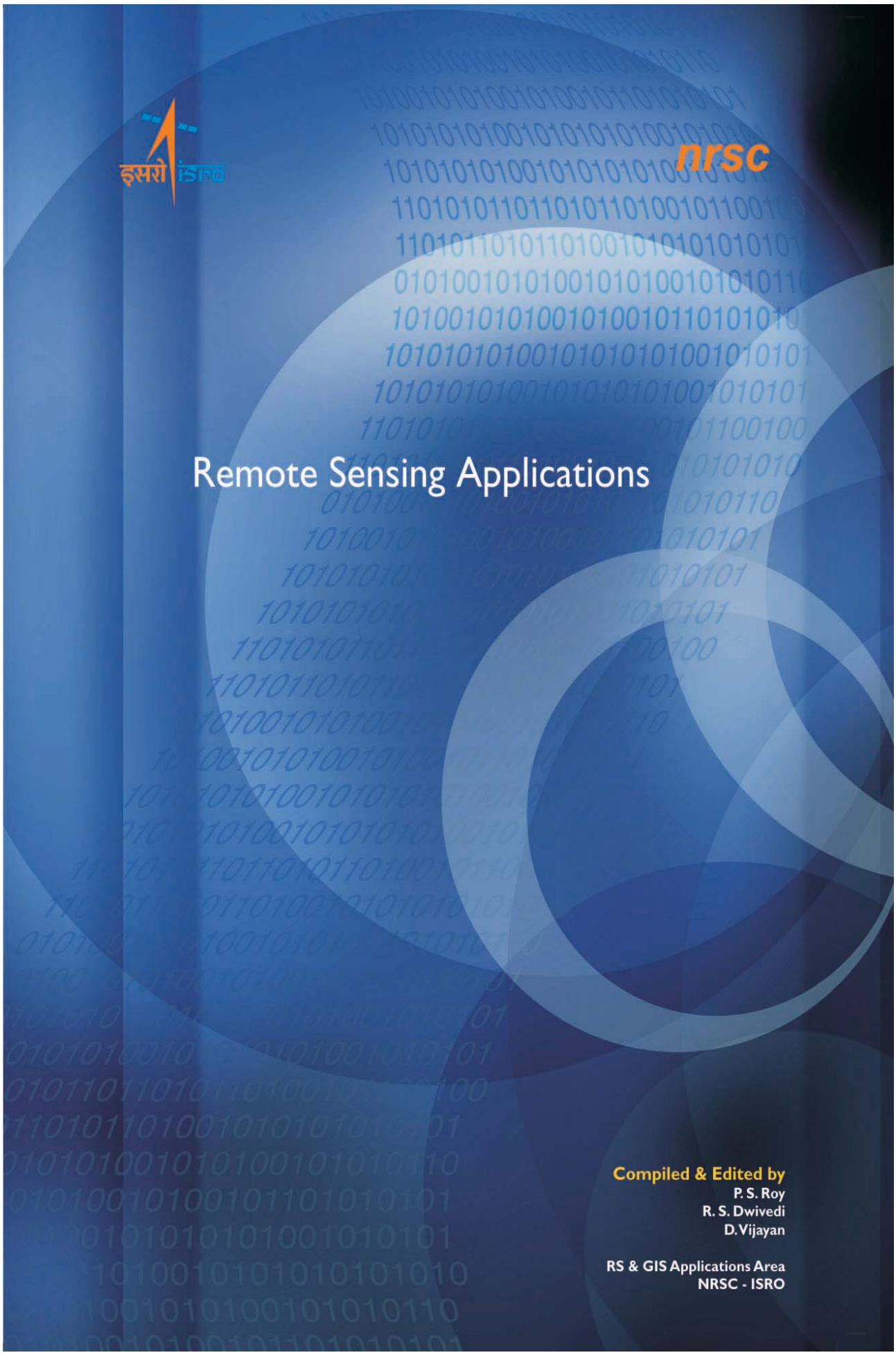
इसरो ISRO
nrsc
Remote Sensing Applications
Compiled & Edited by
P. S. Roy
R. S. Dwivedi
D. Vijayan
RS & GIS Applications Area
NRSC - ISRO

Earth Observation (EO) Programme focus in India has been to support operational remote sensing for sustainable natural resources management, address national needs and provide space based information support for disaster management and grassroot planning. NRSC (ISRO) has carried out many application projects for various government agencies under the aegis of National Natural Resources Management System (NNRMS) to utilize the satellite data for various natural resources applications and disaster related information support. NRSC is mandated to build the capacity in country for usage of Remote Sensing and Geo-information for its utilization and institutionalization is arranged to support capacity building initiative by Remote Sensing and GIS Applications Area.

First edition January, 2010
Second edition April, 2010

Remote Sensing Applications

Compiled and Edited by
Dr. P. S. Roy, Deputy Director,
Remote Sensing & GIS Applications Area, NRSC

Dr. R.S. Dwivedi and D.Vijayan
RS & GIS Applications Area, NRSC

Published by
National Remote Sensing Centre
Indian Space Research Organisation
Dept. of Space, Govt. of India,
Balanagar, Hyderabad – 500 625

Designed by
Imagiccreatives, Bangalore

ISBN 978-81-909460-0-1

Printed at
M/s Vamsi Art Printers Pvt. Ltd., Hyderabad - 500 004.
Ph : 040 23311858, 9866022137, 9866022138. Email : info@vamsi.com

Acknowledgements

The Editors would like to acknowledge all the authors who contributed various chapters in this book. Special thanks are to Director, NRSC for giving the message which encouraged us to bringout this volume. Thanks also to Dr. V. Hari Prasad, NRSC for extending his support in bringing out this book.

Remote Sensing Applications

Contents

भारत सरकार
अन्तरिक्ष विभाग
राष्ट्रीय सुदूर संवेदन केन्द्र
बालानगर, हैदराबाद-500 625, आं प्र, भारत
टेलिफोन : +040-23878360
+040-23884000-04
फैक्स : +040-23877210

सत्यमेव जयते

Government of India
Department of Space
National Remote Sensing Centre
Balanagar, Hyderabad-500 625, A P, India
Telephone : +040-23878360
+040-23884000-04
Fax : +040-23877210

V. Jayaraman
Director

MESSAGE

The recent times have seen galloping advances in space science, technology and applications, primarily due to ever improving advances in devices, computing, data handling and networking capabilities. Particularly the Earth Observation (EO) community has seen the advent of improved capabilities in imaging and non-imaging sensors as well as various advances in enabling techniques such as Geographical information system, Image Processing as well as the Global Positioning System, aided well by the information communication technology advances, resulting in vast outreach of EO potentials, touching almost every facet of human life.

India has conscientiously pursued with the EO applications for societal developments through multifarious activities in agriculture, land and water resources, environment and energy domains. With the continuous explosion of developments with the availability of newer sensors with enhanced capabilities and emerging demands with increasing expectations, the avenues for exploiting newer applications have broadened further. Obviously, these advances need corresponding concurrent efforts in the capacity building activities. It is well appreciated that capacity building itself is more than just training & education, and that it is also encompasses human resources development, organisational strengthening and institutional building to ensure a sustainable follow-up. At the same time, it is realised that in the chain of capacity building, bringing up talent and skill at every level is very important. For that to happen, it is of paramount importance that organised courses with appropriate contents are periodically organised, imparting both the theoretical basics for understanding the technology and techniques; and practical hands-on exposure to EO applications to ensure adoption and assimilation by the user community.

Towards the above, National Remote Sensing Centre has been conducting short duration and appraisal courses on Remote Sensing and allied technologies, meeting the needs of around 500 trainees at various levels every year. This comprehensive publication, principally addressing the Remote Sensing Applications segment has been expanded with the above intention, both in terms of depth of treatment as well as coverage of topics, supported by appropriate case studies. This effort, I am sure, will promote not only for a better understanding of the operational Remote Sensing applications, but also will trigger sufficient interests and imagination for taking up research in this domain.

I wish that this publication will reach all those in need, thus serving the larger purpose for which it is intended for.

(V. Jayaraman)

भारतीय अन्तरिक्ष अनुसंधान संगठन इसरो isro **Indian Space Research Organisation**

भारत सरकार
अन्तरिक्ष विभाग
राष्ट्रीय सुदूर संवेदन केन्द्र
बालानगर, हैदराबाद-500 625, आं प्र,. भारत
टेलिफोन : +040-23879677, 23884210
फैक्स : +23875932
ई-मेल : psr@nrsc.gov.in
ddapp@nrsc.gov.in

सत्यमेव जयते

Government of India
Department of Space
National Remote Sensing Centre
Balanagar, Hyderabad-500 625, A P, India
Telephone : +040-23879677, 23884210
Fax : +040-23875932
E-mail : psr@nrsc.gov.in
ddapp@nrsc.gov.in

डॉ. पी.एस. रॉय
उप-निदेशक
सु.सं. एवं भौ.सू.प्र. -अ. क्षेत्र

Dr. P. S. Roy
Deputy Director
RS & GIS Applications Area

PREFACE

Space technology has immense influence in the decision making process in almost all social spheres. It encompasses information generation on natural resource viz., land use, agriculture, climate, urban systems for better management of resources and in protecting ourselves from the impact of natural calamities like flood, cyclone, drought, forest fire and landslide etc. by being informed about the probability of occurrence and preparing contingency to face it. Natural resource management is dependent on the availability and quality of the geo-information on every sphere of human activity and its interaction with the environment. The recent advances in information technology and earth observation have facilitated unprecedented growth and need of spatial information in various facets of our life.

The information and its dissemination have created awareness among people and an informed society can be considered a precursor to development. In this direction, National Remote Sensing Centre (NRSC) is carrying out various nationwide application projects so that the end use of remote sensing and Geo-information technology reaches common man at the grass root level. Capacity building through training creates skilled professionals in specific area of applications to bridge the demand and requirement of trained manpower in India.

To share the expertise gained in Remote Sensing and GIS applications of natural resources and their management through capacity building, a comprehensive study material in the form of this publication has been prepared. This publication consist of 16 chapters convey remote sensing & GIS applications in land, water and atmosphere besides natural disasters.

This publication has been made possible due to the efforts of so many scientists of NRSC who are experts in their own field. This publication is lucid with appropriate well supported illustrations, diagrams, tables, figures, references and case studies for ease of understanding even for a non-expert. I take this opportunity to thanks all the authors for their contributions. I feel that providing access and sharing of resources will fasten the growth and use of geo-informatics technology for societal benefits. I hope that the readers will derive maximum benefit from this publication and use it for further development of Remote Sensing Applications in the country.

(P.S. ROY)

भारतीय अन्तरिक्ष अनुसंधान संगठन इसरो isro **Indian Space Research Organisation**

NATIONAL REMOTE SENSING CENTRE

Realizing the importance of space technology in national developmental programmes, the Department of Space was established in 1972. The utility of aerospace data for management of natural resources was then demonstrated through R&D efforts and pilot studies with the users. The need for upscaling such studies at operational level was subsequently visualized which had led to the establishment of National Remote Sensing Agency (NRSA) in 1974 at Hyderabad under Department of Science and Technology. In 1980, NRSA was brought into the folds of Department of Space, Govt. of India as an autonomous body. In September, 2009, NRSA had attained the status as government organization, rechristened as National Remote Sensing Centre (NRSC), and had become part of Indian Space Research Organization (ISRO), Department of Space.

Commensurating with its mandate, NRSC (erstwhile NRSA) has been striving for operationalization of space technology in India for management of natural resources, environment and natural disasters by way of acquisition, processing, dissemination and value addition of aerospace data. In order to realize its goal, NRSC operates through its five wings, namely Satellite Data Acquisition, Data Processing, Remote Sensing and GIS Applications, Aerial Survey and Digital Mapping, and capacity building facilities at the Indian Institute of Remote Sensing, Dehradun and Training and Education facility under RS & GIS Applications Area at Hyderabad. The satellite data acquisition facility (ground station) is located at Shadnagar about 60 km south of Hyderabad. The NRSC Data Centre (NDC) is responsible for dissemination of satellite data to the users. The Aerial Survey and Digital Mapping wing is equipped with state-of-the art facilities i.e., medium format digital camera, Differential GPS, Airborne Laser Terrain Mapper (ALTM) and digital photogrammetry systems and two aircrafts (Beach craft 200) for infrastructure and utilities surveys, and for generation of DEM.

The Remote Sensing and GIS Applications Area (RS&GIS AA) plays a vital role towards achieving the national goal of food, water, energy and environmental securities. NRSC undertakes the operational projects on applications of space technology for natural resources and disaster management at national level apart from carrying out research in frontier areas of space applications. Additionally, the RS&GIS AA strives for capacity building and promotion of space technology applications through State Remote Sensing Centres across the country. This book provides an overview of the applications of geospatial data for the benefit of resource scientists and technologists.

nrsc

Remote Sensing Applications

P. S. Roy
R. S. Dwivedi
D. Vijayan

National Remote Sensing Centre

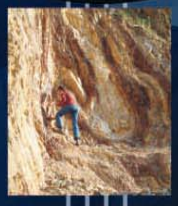

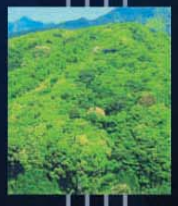

Remote Sensing Applications

Agriculture

1.1. Introduction

Agricultural is the backbone of Indian economy, providing livelihood to about 67.0 per cent of the population and contributing approximately 35.0 per cent to the Gross National Product. Food grain production has increased from 51 millions tons in 1951 to 230.67 million tons in 2007-08. On the other end, the Indian population crossed the billion mark and needs around 250 million tons of food grains and calling for efficient agricultural management involving appropriate application of production and conservation practices for development of land and water resources on a sustainable basis. Substantial increase in crop production is possible by bringing additional land under cultivation (horizontal approach) and improved crop management (vertical approach) technologies such as use of high yielding input responsive, energy intensive and stress tolerant varieties, increased irrigation and integrated crop nutrition and protection. In addition, reliable and timely estimates and seasonal crop acreage and production estimates are important for formulation of marketing strategies such as export/import, price fixation, public distribution. Conventional techniques to provide this information are highly tedious, time consuming, more often subjective, whereas satellite remote sensing has the requisite potential to provide this information on a regular, synoptic, temporal, timely and in a more objective manner.

The remarkable developments in space borne remote sensing (RS) technology and its applications during the last three decades have firmly established its immense potential for mapping and monitoring of various natural resources. Remote Sensing can be defined as the science and art of acquiring information about objects from measurements made from a distance, without coming into physical contact of the object. Human eye, cameras and scanners are some of the examples. Satellite remote sensing and Geographic Information System (GIS) offer great promise for natural resources management with the ability to depict the spatial distribution of the extent and monitoring capability. These techniques have potential to predict and zonate different levels of crop response to the inputs and can also provide solutions to various management problems in increasing the performance of the cropping system in a spatial and temporal dimension, when coupled with the relevant ancillary information. A suitable blend of these technologies aid in efficient management of our resources to enhance the crop productivity on a sustainable basis.

The spatial resolution of the sensors of the Indian Remote Sensing satellites range from very fine resolution multi-spectral data of 5.8 meters to moderate resolution Wide Field Sensor (WiFS) data of 180 m through 56 m data of Advanced Wide Field Sensor and 24 meter multi-spectral linear imaging self scanner data (LISS-III) with the revisit period ranging from 5 days to 24 days and swath ranging from 70 km to about 800 km. LISS-III data provides district level information of the natural resources whereas regional level information is derivable from both AWiFS and WiFS data.

The satellite data at regular temporal interval enables monitoring of the natural resources for their effective management. The science of remote sensing of agricultural crops along with the capabilities of the remote sensing technology in providing information about the spatial distribution and extent and inter seasonal variations in cropping patterns, cropping systems analyses and interface with the agricultural drought assessment are discussed in this chapter.

1.2. Remote Sensing in Optical and Reflective Infra Red (IR) region

Remote sensing is largely concerned with the measurement of surface reflectance from the object and drawing of inference from such reflectance for identification of objects of interest. An understanding of the physical and physiological properties of plants and their interaction with the incident radiation is the key element in crop identification through remote sensing.

1.2.1. Reflectance Characteristics of Green Plants

Plant parameters such as pigmentation, nutritional status, leaf architecture, internal structure of the leaves and water content affect spectral response of the leaves. The plant leaves have both diffused and specular characteristics. The diffused leaf reflectance emanates primarily from the interior of the leaf through multiple scattering. The specular character of the leaf reflectance at the surface of the leaf is primarily affected by the topography of the cuticular waxes and leaf hairs.

The green plant has spectral reflectance characteristics as shown in Figure 1.1 as green curve, which is quite

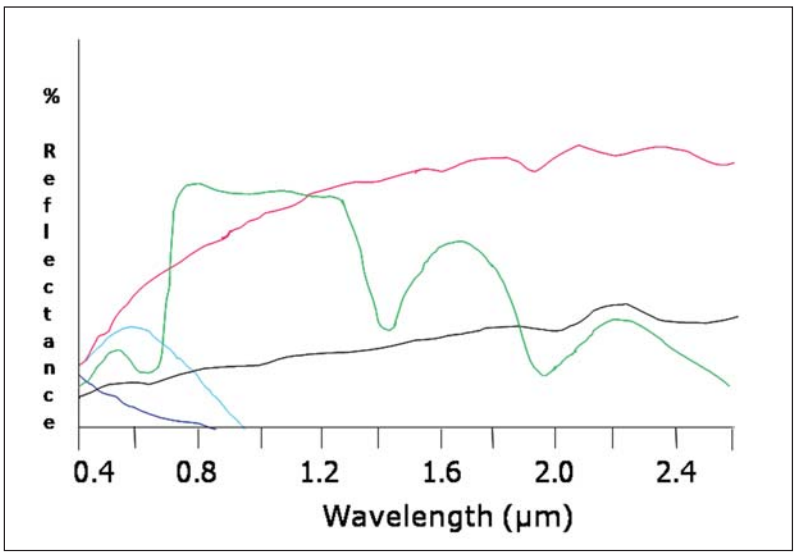

Figure 1.1: Typical spectral reflectance curves (source: Swain and Davis, 1978)

distinct from other objects such as dry/ wet soil in pink/black colour and turbid/ clear water in cyan/blue curves. The reflection of sun's radiation by green leaves is relatively low in the visible portion of the electro-magnetic spectrum of 400-700 nm wavelength region. Leaf pigments (chlorophyll) absorb a high portion of incident sunlight energy in the blue region (400-500 nm) and red region (600-700 nm) of the spectrum. Light energy in the green (500-600 nm) region of the spectrum is reflected to a slightly higher degree. Due to relatively high green sensitivity of human eye, the green colour of plant is sensed as the dominant colour.

Radiant energy in infrared part (700-900 nm) of the spectrum is reflected by the healthy plant, is much higher than most other objects. The high reflectance from 900 nm to about 1300 nm in IR is caused by internal structure of the leaf. The water content of the leaves profoundly influences the spectral region from 1300-2300 nm (near / mid infrared) and the main water absorption zones are at 1450 nm, 1950 nm and 2600 nm.

The healthier plant will be greener due to higher content of chlorophyll in leaves resulting in high absorption particularly, in blue and red regions of the electromagnetic spectrum. Decrease in infrared reflectance is one of the earliest symptoms of the reduction in vigor in many plants. During the drought, the spongy and palisade mesophyll cells become flaccid resulting in reduced infrared reflectance. Cell structure of the leaves affected by adverse conditions such as disease or pest also leads to reduction in infra-red reflection. The process of maturity / senescence will also cause changes.

1.3. Crop Inventory

The intrinsic ability of spectral reflectance data to identify and distinguish crops is very helpful in deriving crop acreages, production estimates, to monitor and assess the crop condition. Remote sensing based crop identification and discrimination is centered around the concept that each crop has a unique spectral signature due to its own architecture, growing period etc., when two crops with similar spectral signatures occur in a given date, multi date data is required to identify them.

1.3.1. Acreage Estimation

The acreage estimation procedure broadly involves 1) selection of single date data corresponding to the maximum vegetative growth stage of crop 2) identification of representative sites of various crops and their heterogeneity on image based on ground truth 3) generation of representative signatures for the training sites 4) classification of image using training statistics and 5) estimation of area of the crop using administrative boundary like district mask.

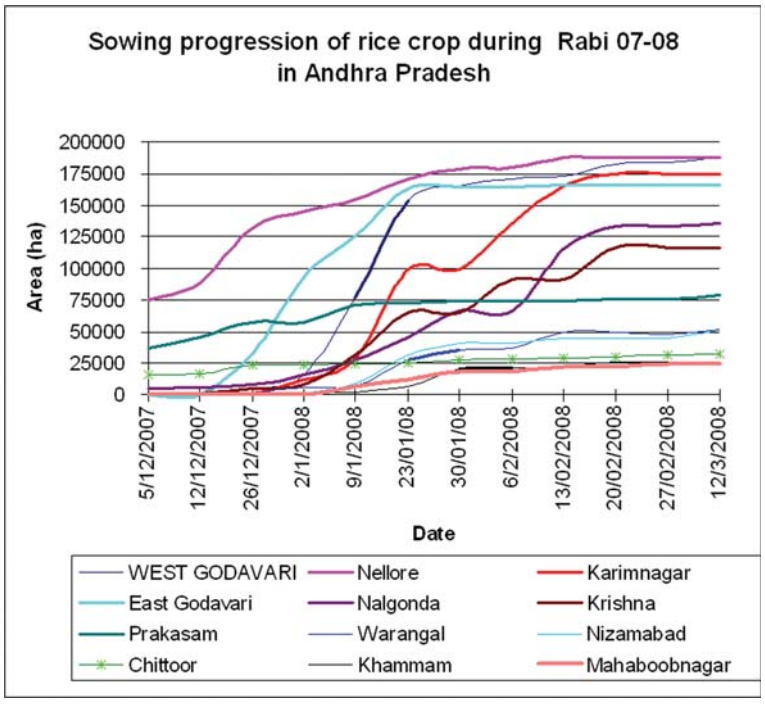

Figure 1.2: Sowing progression for the rabi rice areas in Andhra Pradesh

In the cases of estimation of crop acreages for large areas like states wherein analysis of large amount data and ground data collection are involved, stratified sampling procedure is being used operationally. The study area is divided into homogenous strata based on crop proportion and vigor as manifested on the satellite data and each strata is subdivided into segments of required size usually 5 X 5 km. About 10-15 percent of the sample segments are randomly selected for digital analysis and standard statistical methods are employed to aggregate crop estimates at district / state levels.

The analysis can also be carried out for the entire area of interest like district or taluk. The administrative boundary of the study area is overlaid on the image to extract all the pixels and the classification is carried out for the entire area to obtain the area under cultivation for the desired crops. In this procedure district crop map showing spatial distribution of different crops can also be generated.

In order to choose most optimum bio-window, it is necessary to obtain the crop calendar and sowing progression of different crops cultivated in the study area for better crop discrimination. The crop sowing progression shown in Figure 1.2 is an example depicting the variations in crop progression among the districts of A.P. The districts of Nellore, West and East Godavari districts need an early data sets compared to the other districts.

1.3.1.1. Major Crops

Using single date cloud free optical data during the maximum vegetative stage of the crop growth, district level pre-harvest acreage and production of large area covering crops viz., paddy, wheat, sorghum, ground nut, rapeseed-mustard and cotton is being estimated on operational basis under the crop acreage and production estimation (CAPE) project (Navalgund *et al.*, 1991, Navalgund and Ray, 2000, Dadhwal, 1999, Dadhwal and Ray, 2000 and Dadhwal *et al.*, 2002). The remote sensing based acreage estimations are aimed to be made available at least one month before the harvest of the crop, to enable the administrators and planners to take strategic decisions on import-export policy matters and trade negotiations. An extended project viz., forecasting agricultural output using Satellite, Agro-meteorological and Land Observations (FASAL) is in progress to provide multiple forecasts at district, state and national level (Parihar and Oza, 2006).

Moderate resolution data from WiFS sensors can provide regional level information of crops at state level. This sensor can also be used for deriving information at district level if the crops are concentrated. Inter seasonal and intra seasonal variations in the crop condition and cropping pattern can also be derived from WiFS data due to its regular revisit periodicity of five days. Figure 1.3 shows the spatial distribution of kharif rice in Andhra Pradesh during 2001.

1.3.1.2. Multiple Crop and Small Land Holding Situations

IRS LISS-III data acquired during optimal bio-window period of crops enabled better discrimination of rice and cotton crops for generating cropping pattern information at district level. The major kharif cropping pattern of Guntur district during 2004 using IRS-LISS III data is depicted in Figure 1.3. Thus, using LISS-III and AWiFS data crop inventory information at different spatial hierarchical levels can be generated. In addition, the high revisit period of AWiFS data at 5 days enables crop monitoring, besides increasing the probability of getting cloud free data during kharif season.

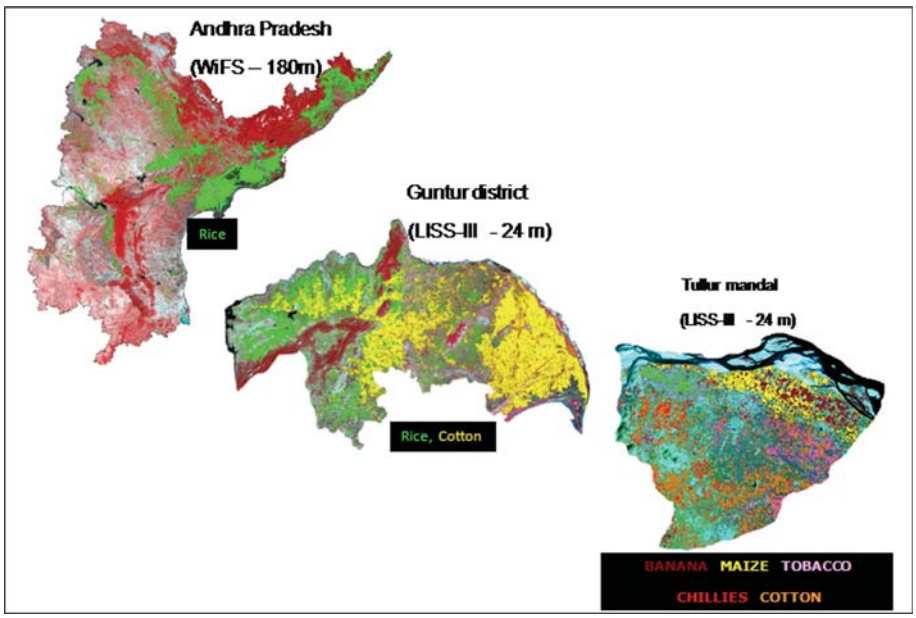

Figure 1.3: Crop inventory using satellite data

Availability of better spatial resolution from IRS LISS-III

enabled identification of crops, which are grown under multiple crop situations. Commercially important crops like chillies, tobacco etc., which are cultivated in small landholdings under intense input management practices can also be identified and their acreages can be estimated. These pre-harvest estimates have special importance from commercial point of view. Figure 1.3 shows utilization of IRS LISS-III data for discrimination of multiple crops in Tulluru mandal of Guntur district, AP (Krishna Rao *et al.*, 1997).

1.3.1.3. Commercially important crops

Inventory of commercially important crops and high value crops has the unique applications in making strategic decisions for enhancing the use efficiency of the economic resources. For example, area of the crops of soybean and sunflower enable location and planning for the optimal designs for oil extraction plants. (NRSA, 1992, Venkataratnam *et al.*, 1996, Krishna Rao *et al.*, 1997); Jute (NRSA, 1991); Cotton (Venkataratnam *et al.*, 1993) and Tobacco (Ranganath *et al.*, 1991) were studied. The remote sensing information also provides valuable information to enhance the area under hinterland for providing raw material to the agro-based industries. As an illustration, utilization of two-date data for sugarcane inventorying is presented below.

Sugarcane: Integration of the information of distribution of sugarcane crop along with the corresponding spatial data of soil attributes enables to derive the information for assessing the scope of expansion of sugarcane cropped area by matching the climate, soil and water requirements of the standing crops vis-à-vis other crops. In one specific study carried out for M/s EID Parry Ltd., the cropping pattern information was derived using two-date IRS-LISS III data (Figure 1.4). This information along with the corresponding soils information revealed that sugarcane crop could be expanded by 556 and 1108 ha, replacing the standing banana crop in the Alangudi and Arantangi divisions of Tamil Nadu. However, the ultimate choice of the crops depends upon the socio-economic returns and the efforts towards maintenance of soil fertility (Krishna Rao *et al.*, 2000; Hebbar *et al.*, 2003).

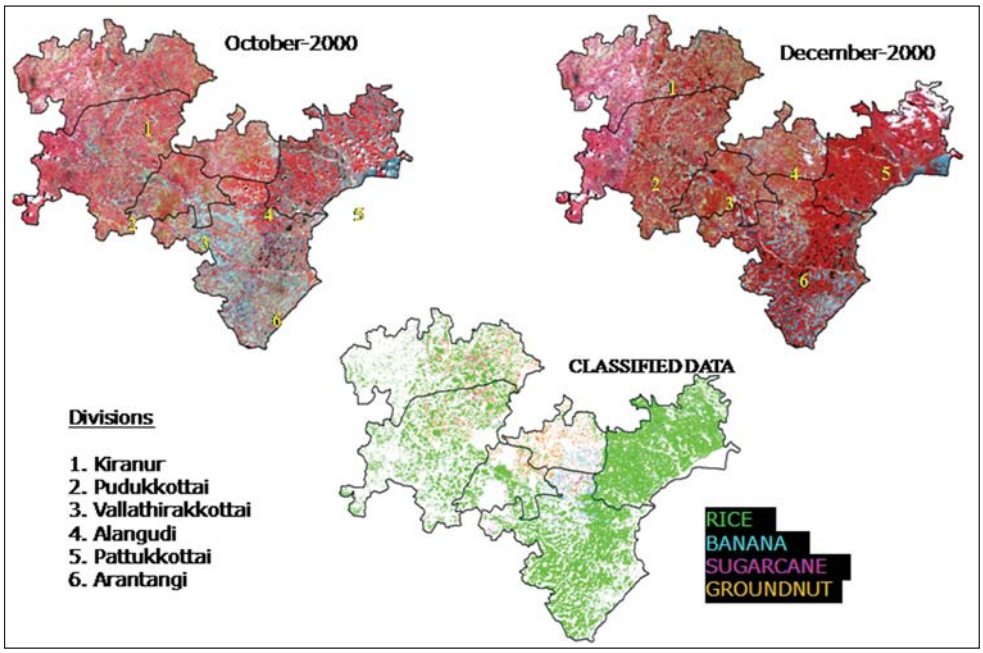

Figure 1.4: Cropping pattern of EID factory command derived from LISS-III data

1.3.2. Horticultural Crops

The high spatial resolutions LISS-III data also enabled identification of many horticultural crops viz., mango, coconut, oranges

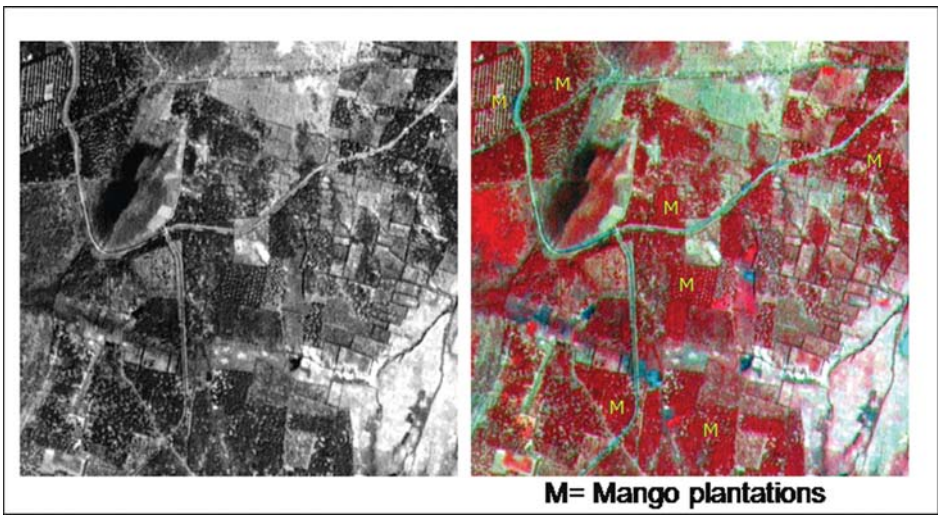

Figure 1.5: IRS LISS-III and PAN merged data showing mango plantations

and banana. Mandal level acreages of mango crop of Krishna district and banana crop of Guntur district, Andhra Pradesh were estimated. Using satellite data, the area under arecanut (RRSSC, 1991) and grape (Krishna Rao *et al.*, 1996) were reported. Dakshinamurthy *et al.*, (1971) demonstrated the utility of aerial photographs in identification of coconut trees with wilt disease in parts of East Godavari district, Andhra Pradesh. The very high spatial resolution PAN data adds a new dimension of geometric fidelity to the satellite data for better identification of plantation crops. The young and the fully-grown mango plantations were clearly discernible in the fused data products of LISS-III and PAN (Figure 1.5).

1.4. Cropping System Analysis

Remote sensing provides valuable information on the distribution and condition of crops at different spatial hierarchies and has the highest compatibility for analysis in GIS environment. Information on other natural resources that are of significant importance towards agricultural production can be integrated to generate information for sustainable agriculture. Integration of soil suitability for the cultivation of cotton crop along with the spatial distribution of cotton crop, as derived from remote sensing data through a conformity analysis enabled to delineate cotton crop grown under different suitability regimes. This information is useful towards planning for efficient production of cotton crop by apportioning those land parcels that are highly suitable for cultivation of cotton (Sesha Sai *et al.*, 2003). The rainy season (kharif) fallows in Madhya Pradesh which could have been used for a short duration crop like soybean were identified. Madhya Pradesh is endowed with well distributed rains ranging from 700 to 1200 mm. Vertisols with good moisture holding capacity can be used to grow short-duration soybean by adopting sound land management practices. This will help increase income to the farmers besides preventing land degradation due to runoff erosion (Wani *et al.*, 2002). Remote Sensing derived information of the rice-wheat and rice–fallow cropping systems of India, Pakistan, Nepal and Bangladesh are presented hereunder, as a case study (Subba Rao *et al.*, 2001; Krishna Rao *et al.*, 2002).

Rice Cropping System: Rice is the major food grain cereal crop grown in South Asia and is cultivated mostly during the monsoon (rainy) season. Since the scope is limited for horizontal expansion, increased cropping intensity on the existing agricultural lands is one of the best crop management options. In this context, post kharif rice fallows offer a considerable scope for achieving sustainable production by introduction of short duration leguminous crops.

IRS-WiFS data of 1999 kharif season and rabi 2000 season were analysed following total enumeration approach for deriving spatial distribution of kharif rice and rice fallows in different States of India and in the neighboring Pakistan, Nepal and Bangladesh Nations. Information on the spatial distribution of kharif rice and rabi fallow lands were logically combined to derive the distribution and area of post kharif rice-fallow lands (Figure 1.6). The analysis indicated that good potential for the utilization of post kharif rice fallow lands existed in India, Bangladesh and Nepal with marginal potential in Pakistan.

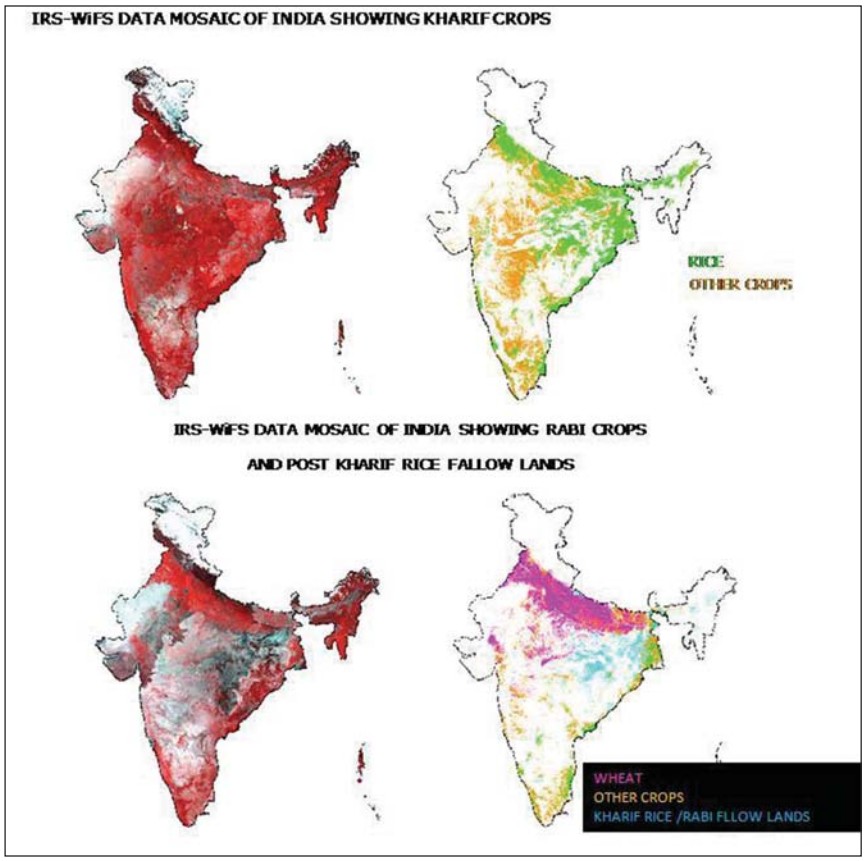

Figure 1.6: IRS WiFS data mosaic of India during kharif and rabi seasons during 1999-2000

Spatial information layer of rice derived from remote sensing data in India, Bangladesh, Nepal and Pakistan nations, in conjunction with soil and climate layers enabled ICRISAT for preparing GIS maps of potential areas for

rice- fallow cultivation with a suitable short duration leguminous crop. This information along with pedo-climate regimes and the socio-economic conditions in GIS environment enables for better utilization of the post kharif rice fallow lands towards enhancing the crop productivity in a sustainable manner in South Asia.

1.5. Production Estimation

Crop yield is influenced by many factors such as genotype, soil characteristics, cultural practices adopted, meteorological conditions and influence of pests and diseases. Spectral data of a crop is the integrated manifestation of the effect of all theses factors. Development of reliable crop yield models with minimal data is a major thrust area.

A major challenge often confronted in agricultural crop production, despite the development of advanced agricultural technology, is the damage caused to agricultural crops by pest and diseases. Crop losses can be due to biotic factors like pests, diseases, weeds and abiotic factors like flood, drought, cyclones hailstorms etc. Damage is known only after considerable damage has been occurred.

Statistical, meteorological and / or spectral models are used for crop yield estimation. Remote sensing based models adopt two approaches viz., single date spectral index and multi-date spectral index-growth profile are in vogue. The single date data spectral index approach relies solely upon the data acquisition within a narrow critical period of maximum vegetation growth phase while multi-date approach depends spectral data at different stages of crop growth within the season.

The multi-date approach has the constraint of obtaining the cloud-free multi-temporal satellite data within the crop growth cycle. To overcome this problem, studies are in progress to explore the potential of the microwave data, which has the all weather and cloud penetrating capability. Remotely sensed data directly or its derived parameters are related to the yield or to the biometric parameters.

In addition, attempts are also underway to incorporate the spectral information in the process-based models and crop simulation models to improve the predictive capabilities of the remote sensing based crop production estimation.

1.6. Crop Monitoring and Condition Assessment

Condition of the crop is affected by factors such as availability of water and nutrients, pest attack, disease outbreak and weather conditions. These stresses cause physiological changes which alter the optical and thermal properties of the leaves and bring about the changes in canopy geometry and reflectance / emission. Monitoring and assessment of crop condition at regular intervals during the crop growth cycle is essential to take appropriate curative measures and to assess the probable loss in production.

Regular monitoring of satellite data on crops at different phases of the crop growth would reveal any departure from normal growth, for inferring occurrence of any anomalies to incidence of pest and disease damage with the support of ground observations. In view of large area coverage in a short time and of repetitive nature, remote sensing techniques if used in complementary to ground surveys, it can provide real time data for early detection and warning of out break of the disease or insect damage before they reach higher severity levels.

1.7. Significance of NDVI in Agricultural Drought Assessment

The variations in the progression of NDVI, in terms of the magnitude and rate of progression, in relation to its respective normal NDVI provide information of the prevailing status of the vegetation. Exclusion of the permanent non-agricultural features like forests, wastelands, water bodies and settlements, reveal the status of the agricultural situation. In order to circumvent the problem of non-availability of cloud free optical data, time composited NDVI over an aggregated period of a fortnight or a month is generated, covering the entire crop growth season (NRSA, 1991; Sesha Sai *et al.*, 2004).

1.8. Thermal Remote Sensing

Thermal infrared radiation refers to electromagnetic waves with a wavelength of between 3.5 and 20 micrometers. The windows normally used from aircraft platforms are in the 3-5 µm and 8-14 µm wavelength regions. Some space borne sensors commonly use transmission windows between 3 and 4 µm and between 10.5-12.5 µm. None of the windows transmits 100 percent because water vapor and carbon dioxide absorb some of the energy across the spectrum and ozone absorbs energy in the 10.5-12.5 µm interval. In addition, solar reflectance contaminates the 3-4 µm windows to some degree during daylight hours, so we use it for earth studies only

when measurements are made at night. Unlike remote sensing of reflected light from surfaces in which only the topmost layers (a few molecular layers thick) are involved, thermal remote sensing includes energy variations extending to varying shallow depths below the ground surface. Thermal remote sensing is an observation of the status of the surface energy balance (SEB) at a specific time of day.

1.8.1. Parameter retrieval

The developments in satellite meteorology enabled the retrieval of basic agro-meteorology parameters viz., cloud cover, albedo, solar radiation, surface temperature/air temperature, rainfall, absorbed photo-synthetically active radiation, soil moisture and evapo-transpiration etc., which contribute significantly to the understanding of agricultural production forecasting. The following were some of the parameters that can be mapped and monitored through the use of satellite remote sensing data.

1.8.1.1. Surface Temperature

The parameter-surface temperature figures in nearly all equations for energy fluxes through a surface element. It is routinely derived from satellite radiances over the ocean. However, over land the changing surface emissivity, strong daytime heating as well as night time cooling and the difficulty of defining surface temperature for a canopy, have prevented a routine application. Water vapour continuum is the dominant absorber within the thermal infrared window from 10 to 13 mm. Also the aerosols and the optically thin clouds also attenuate the signal. The inversion of temperature in the lower atmosphere also alters the derived surface temperature.

Air temperature is significantly related to crop development and conditions. Operational crop and soil moisture models require daily minimum and maximum shelter temperature and dew point temperature. Canopy (or skin) temperature may be more directly related to growth and evapo-transpiration than the shelter temperature. The difference between the two is a measure of crop stress. The ability to observe canopy temperature directly is an advantage of satellite observations. However, it is to be noted that the satellite derived “skin temperature” and “crop canopy temperature” are equivalent only when a satellite field of view (FOV) is filled with vegetation. If FOV constitutes a mixture of bare soil, water bodies, etc., the relation between the two becomes complex. Satellite observations in the thermal IR window (10-12 mm) are used to obtain estimates of canopy or skin temperature.

1.8.1.2. Methods for LST Retrieval

Land surface temperature can be retrieved from remote sensing data applying different techniques, as for example single-channel, split-window and dual-angle algorithms. In order to retrieve land surface temperature (LST) from thermal infrared remote sensing data, different methods and algorithms have been published. A full revision of methods is given by Sobrino *et al.*, [2002] and Dash *et al.*, [2002], among others. The three well-known methods that use one or two thermal channels: single-channel [e.g., Qin *et al.*, 2001; Jime´nez-Mun˜oz and Sobrino, 2003], split-window [e.g., Price, 1984; Becker and Li, 1990a; Sobrino *et al.*, 1991; Prata, 1993; Sobrino *et al.*, 1994] and dual-angle [e.g.,Prata, 1994; Sobrino *et al.*, 1996, 2004]. In the literature other methods can be also found using three or more thermal channels or algorithms based on different techniques (Becker and Li, 1990b; Wan and Li, 1997).

Most of them are based on the radiative transfer equation, from which the at-sensor radiance is given by:

$$L_i^{at-sensor} \equiv B_i(T_i) = \left[\varepsilon_i B_i(T_S) + (1-\varepsilon_i)L_i^{atm\downarrow}\right]\tau_i + L_i^{atm\uparrow} \qquad (1)$$

ε_i is the channel surface emissivity,
B is the radiance emitted by a blackbody,
T_s^i is the surface temperature or LST,
T_i is the at sensor brightness temperature,

$L_i^{atm\uparrow}$ is the down-welling irradiance,
τ_i is the total transmission of the atmosphere (transmissivity) and
$L_i^{atm\downarrow}$ is the up-welling atmospheric radiance.

When equation (1) is applied only to one thermal channel, single-channel algorithms are obtained, and when equation (1) is applied to two thermal channels located in the spectral range from 10 to 12 mm, split-window

algorithms are obtained. It is also possible to apply equation (1) to one thermal channel with two different view angles, obtaining in this way the dual-angle algorithms. Land surface temperature can be retrieved from remote sensing data applying different techniques, as for example single-channel, split-window and dual-angle algorithms.

For single-channel algorithms, the best wavelength in order to retrieve the LST depends on the atmospheric water vapor and varies from 11 mm to 10.5 mm when the water vapor varies from 1 g/cm^2 to 4 g/cm^2. With regard to the split-window technique, the best simulated results have been obtained for wavelength combinations near to 11 mm and 12 mm. Single-channel methods provide similar or better results than split-window methods for low atmospheric water vapor content, whereas split-window methods always provide better results for high atmospheric water vapor content. Both the methods assume that land surface emissivity is known and need the atmospheric water vapor content in order to retrieve the LST. Total errors for split-window algorithms of around 1.5 K, and less than 1 K for dual-angle algorithms have been reported. The errors can largely be attributed to imperfect knowledge about atmospheric water vapor content and wavelength dependent surface emissivity.

1.8.1.3. Precipitation

The objective of precipitation measurement is to determine the spatial and temporal distribution of precipitation, primarily rain and snow. Historically, precipitation has been measured with gauges, which capture samples of the precipitation for direct measurement. Gauge measurements of precipitation have limitations, especially for operational meteorological and hydrological purposes such as short period weather and flash flood forecasting. These limitations include:

The density of measurements in most gauge networks is not sufficient for assessment of precipitation from thunderstorms in small watersheds. More-or-less typical precipitation networks for climatological purposes have a gage density of about one gage every 30 km (900 km^2 area). The highest precipitation intensities in a thunderstorm cell occupy a much smaller area, so could easily be missed in a fixed gage network.

Many areas of interest are not suitable for direct measurement of precipitation with gauges. These areas include mountains (for water supply assessment) and oceans (for earth heat and moisture budgets). The cost of direct measurements (including equipment, maintenance, personnel, data acquisition and processing) precludes expansion of gauge networks for operational uses.

Remote sensing of precipitation is widely used to obtain increased spatial and temporal accuracy. With remote sensors, the precipitation is not captured or directly measured. The precipitation is inferred from physical, statistical, and/or empirical relationships between precipitation characteristics and the emitted or reflected radiation from the earth and atmosphere. Remote sensing provides additional information to the existing network of ground based precipitation gauges, for mapping the extent and amount of precipitation. It is unlikely that remotely sensed data will replace the existing network of precipitation gauges.

There are several remote sensing techniques which have potential to assist in mapping the extent of precipitation patterns. Several reviews provide background on the use of satellite remote sensing to estimate precipitation (Arkin and Ardanuy, 1989; Barrett and Beaumont, 1994; Petty, 1995; Rasmussen and Arkin, 1992). Estimation of precipitation using remote-sensing techniques may be divided into three categories - Visible/Infra red, Passive microwave and Radar. The oldest and still most used precipitation-estimation technique is cloud indexing, assigning a rain rate to each cloud type.

In infrared-based methods, the most common approach is to find cold clouds (say, colder than 250^o K) within an overcast area. The raining potential of the clouds is proportional to the fractional area covered by cold clouds, and thus the rainfall derived. More complex techniques use both visible and infrared observations to create a bi-spectral histogram of the cloud images. Bi-spectral histogram method is a simple technique in which the clouds can be classified based on the combination of cloud signatures in visible and infrared frequencies. Then the rainfall is derived by estimating the extent of each type of cloud and multiplying it by the a-priori rain potential of respective classes. However, all the rain-retrieval techniques based on visible/IR observations are basically “inferential” in nature, because these sensors can sense the clouds (that too, the top surfaces of the clouds) but not the actual rain, that occurs at several layers below the clouds. Visible/IR techniques make a “guess” about the rainfall based on the cloud features. Due to this shortcoming, the estimates of rainfall based on visible/IR technique are not very accurate on instantaneous time scale. However, long time averages (e.g., daily, weekly, and monthly) of rainfall are better and usable for practical purposes.

The use of microwave techniques is that microwave radiation penetrates clouds and the precipitaion drops interact with the microwave radiation. The main disadvantage is the poor spatial and temporal resolution of passive microwave sounders. Passive microwave remote sensing of rainfall over land was more achievable since the 1987 launch of the Special Sensor Microwave Imager (SSM/I) on board the (USA) Defense Meteorological Satellite Program (DMSP). International research indicates that integrating geostationary thermal measurements with other data to make rainfall rate estimates provides more promise than using remotely sensed data alone.

There are several integration techniques, which may allow rainfall to be better predicted by combining the thermal GMS data with other data sets (Ebert and Le Marshall, 1995). These include:

- Use of pattern recognition or visible data to determine cloud type (Ebert, 1987); Integrating short wave infrared (SWIR) based inferences of cloud top droplet size may be linked to the presence of rainfall (Rosenfield and Gutman, 1994); and
- Combining the outputs from numerical weather prediction (NWP) to include some information about current meteorological conditions (Grassotti and Garand, 1994). Herman *et al.*, (1997) have developed an operational system using this approach for Africa to provide 10-day estimates for the entire continent

Using the high spatial resolution offered by remote sensing should assist in rainfall mapping for drought events especially in areas with a sparse rainfall measurement network. However, remote sensing only provides a snapshot which may have a revisit time of, at best hourly (geostationary satellites) to every 12 hours (polar orbiting sun-synchronous satellites). During that time clouds will move and intense periods of rainfall may occur and be over before the next revisit time. Providing accurate, precise and thoroughly validated space-time images of precipitation derived from using remote sensing is, and should continue to be, a major research area for issues like drought, climate prediction and thorough understanding of the global hydrologic cycle.

The first satellite whose primary mission is to measure precipitation is the Tropical Rainfall Mapping Mission (TRMM), a joint research project between the US (NASA) and Japan (National Space Development Agency: NASDA). A basic objective of TRMM is to obtain estimates of the vertical profile of the latent heat (heat resulting from a change of state), released through condensation of water vapor in the atmosphere, especially in the Equatorial Intertropical Convergence Zone (ITCZ). Potential flood areas can be derived using the precipitation intensity as described from TRMM (figure 1.7) and other collateral data.

Figure 1.7: Potential flood areas as derived from TRMM (source: http://trmm.gsfc.nasa.gov/publications_dir/instant_2.html)

1.8.1.4. Solar Radiation

Incoming solar radiation is the primary source of energy for plant photosynthesis. Solar radiation also plays a key role in evapotranspiration. Visible observations from satellites provide an excellent source of information about the amount of solar radiation reaching the plant canopy. A measurement of solar energy reflected to space from earth-atmosphere system immediately specifies the maximum amount of solar energy that can be absorbed at the surface. Incoming solar radiation can be known by adjusting the amount absorbed. Hence, for the computation of down welling solar radiation, the albedo of the surface must be known. This is especially important over the regions of high reflectivity such as snow and desert. Tarpley (1979) used a statistical regression technique to obtain surface fluxes over the land from Visible channel observations from geostationary satellites. In this model, cloud amount is estimated for a given location from satellite visible data. Three separate regression equations are then used to estimate solar radiation for three categories of clouds. This method provides an accuracy of 10% for

clear sky, 30% for partly cloudy and 50% for overcast conditions Other algorithms like those by Moser and Raschke (1984), and Pinker and Ewing (1985) used physical approaches, and treated the interaction of incoming and reflected solar radiation with the atmosphere and land surfaces in physical manner. The transmittance of solar radiation in these approaches is solved by the use of radiative transfer equations that take into account the concentration profile of different atmospheric components. These physical schemes also take into account the cloudiness and atmospheric water vapor. These methods provide relatively higher accuracy. However, statistical techniques have remained the choice for operational use. These methods require coincident satellite and ground (pyranometer) observations to develop the coefficients in the regression equations. These methods produce daily total insolation, based on hourly estimates made from geostationary satellite data between 0800 and 1600 LST, with interpolation used toward both sunrise and sunset and for any other missing hourly values.

For clear sky and near clear-sky conditions the average daily deviation of GMS based estimates compared to ground-based pyranomter measurements was 4.3%. This is within the error limits of well-maintained and calibrated pyrometers. Under heavy cloud conditions the error between GMS based estimates compared to ground based pyranomter measurements increased to about 15%. The relative error may appear large; however, the absolute error is small since the amount of incoming solar radiation is low due to the heavy cloud cover conditions.

1.8.2. Agro Meteorological Applications

The derived parameters viz., solar radiation, precipitation and surface temperature can be used to study the net primary productivity levels, assess the risk of flood occurrence and quantify the stress and its impact on yield. Previous studies have shown that the surface temperature measured over crop canopy can be used as a suitable indicator of crop water stress as well as irrigation scheduling. The most established method for detecting crop water stress remotely is through the measurement of a crop surface temperature. The correlation between surface temperature and water stress is based on the assumption that as a crop transpires, the evaporated water cools the leaves below that of air temperature. As the crop becomes water stressed, transpiration will decrease, and thus the leaf temperature will increase. Other factors need to be accounted for in order to get a good measure of actual stress levels, but leaf temperature is one of the most important. Many canopy temperature based indices have been developed for detecting plant water stress and scheduling irrigation viz., canopy-air temperature difference (CATD) and stress degree days (SDD), canopy temperature variability (CTV), temperature stress day (TSD) and crop water stress index (CWSI) (Jackson 1982). Of all these, crop water stress index has received much of the researchers as well as farm managers attention for its use in the day to day operations.

Stress degree day is the cumulative difference between the canopy temperature (Ts) and air temperature (Ta) measured post-noon near the time of maximum heating (Idso *et al.*, 1977; Jackson *et al.*, 1977). It is assumed that the canopy temperatures would account for the effect of environmental factors such as vapour pressure, net radiation and wind. The SDD increases with increasing plant water stress. A crop is considered stressed if the value is high and positive and unstressed if it is negative. This change over is, however, arbitrary and may not be valid for all environments.

The canopy temperature validity (CTV) is the variability of temperatures encountered in a field during a particular measurement period. It is expressed as the standard deviation of mid-day canopy temperature within a field. The basis for CTV index is that soils are inherently non-homogeneous. Some areas within the field becomes stressed earlier than others. As water limiting in the former, the canopy temperature would show a greater variability. This variability can be used to signal the onset of deficit and schedule irrigation (Gardner *et al.*, 1981).

The temperature stress day (TSD) is the difference in temperature between a stressed plot and a well irrigated plot (Gardner *et al.*, 1981). Use of well watered plot as reference compensates for environmental effects. It needs to be in the vicinity of the field to be irrigated.

The Crop Water Stress Index (CWSI) (Idso *et al.*, 1981; Jackson *et al.*, 1981), based on the difference between canopy and air temperatures, was a significant advance in this respect. The CWSI has been commonly applied to the detection of water stress of plants, but difficulties in measuring canopy temperature of crops with less than 100% vegetation cover has limited its operational application.

Crop Water Stress Index (CWSI):

$$CWSI = \frac{(dT - dT_l)}{(dT_u - dT_l)}$$

where,

dT is the measure of difference between crop canopy and air temperature,

dT_u is the upper limit of canopy minus air temperature (non-transpiring crop), and

dT_l is the lower limit of canopy minus air temperature (well-watered crop).

A CWSI of 0 indicates no water stress, and a value of 1 represents maximum water stress. The crop water stress that signals the need for irrigation is crop specific and should consider factors such as yield response to water stress, probable crop price, and water cost.

The Water Deficit Index (WDI) (Moran *et al.*, 1994) offered a means to overcome this limitation by combining spectral vegetation indices with composite surface temperature, based on the same theory as CWSI, to estimate water deficit for partially vegetated fields

1.9. Hyperspectral Sensors & Applications in Agriculture

1.9.1. Introduction

Hyperspectral remote sensing, also known as imaging spectroscopy, is a relatively new technology that is currently being investigated by researchers and scientists with regard to the detection and identification of minerals, terrestrial vegetation, and man-made materials and backgrounds. Recent advances in sensor technology have led to the development of hyperspectral sensors capable of collecting imagery containing several hundred bands over the spectrum. In comparison to multi-spectral remote sensing, which records reflectance from a target in a few broad channels, a hyperspectral imaging system acquires information in more than 100 very narrow, defined continuous spectral bands (Lillesand and Kiefer, 2000). In this system, radiation from any specified target has been obtained continuously, making it possible to gain detailed information on the materials.

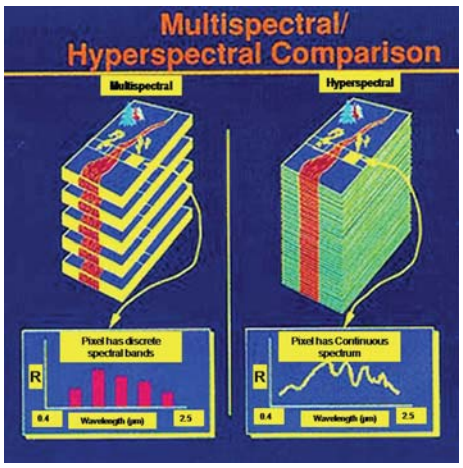

Figure 1.8: Depiction of discrete multispectral and continuous Hyperspectral band information

Using these narrow bands, the features that have diagnostic absorption and reflection properties in such narrow wavelength intervals can be differentiated, which was not possible with the wider wavebands used in multispectral sensors. These narrow wavebands make hyperspectral remote sensing systems powerful tools that have the potential to avoid time consuming and labor intensive ground data collection methods. Hyperspectral data sets are generally composed of about 100 to 200 spectral bands of relatively narrow bandwidths (5-10 nm), whereas, multispectral data sets are usually composed of about 5 to 10 bands of relatively large bandwidths (70-400 nm) as in figure 1.8. A hyperspectral sensor covers the visible and shortwave infrared regions of the spectrum. The Earth Observing-1 (EO-1) satellite, launched in November, 2000 (NASA), carries onboard hyperspectral sensors (Hyperion) is an example of such a system.

Hyperspectral imagery is typically collected (and represented) as a data cube with spatial information collected in the X-Y plane, and spectral information (l) represented in the Z-direction. Hyperspectral AVIRIS data cube is presented in figure 1.9.

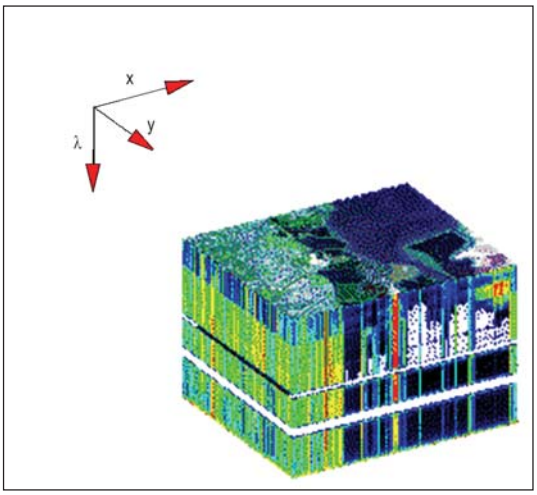

Figure 1.9: AVIRIS hyper spectral data cube over Moffett Field, CA (source: http://www.csr.utexas.edu/projects/rs/hrs/hyper.html)

Hyperspectral imaging sensors collect radiance data from either airborne or space-borne platforms which must be converted to apparent surface reflectance before analysis techniques can take place. Atmospheric correction techniques have been developed that use the data themselves to remove spectral atmospheric transmission and scattered path radiance.

While hyperspectral imagery is capable of providing a continuous spectrum ranging from 0.4 to 2.5 microns (in the case of AVIRIS) for a given pixel, it also generates a vast amount of data required for processing and analysis. Due to the nature of hyperspectral imagery (i.e., narrow wavebands), much of the data in the 0.4-2.5 micron spectrum is redundant. A minimum noise fraction (MNF) transformation is used to reduce the dimensionality of the hyperspectral data by segregating the noise in the data. The MNF transform is a linear transformation which is essentially two cascaded Principal Components Analysis (PCA) transformations. The first transformation decorrelates and rescales the noise in the data. This results in transformed data in which the noise has unit variance and no band to band correlations. The second transformation is a standard PCA of the noise-whitened data.

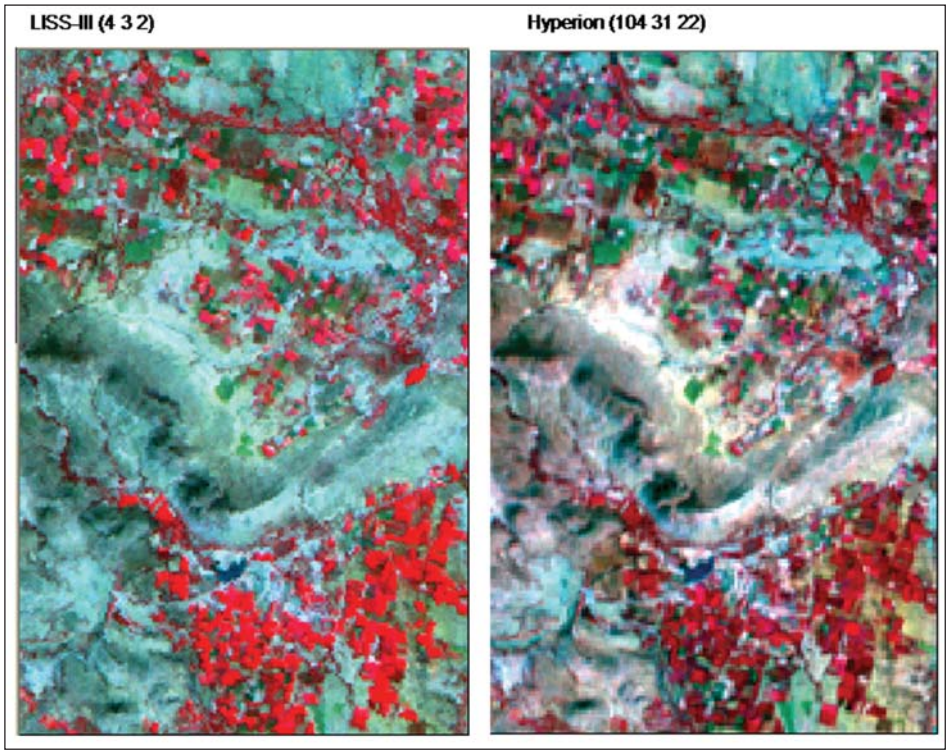

Figure 1.10: Comparision of LISS-III and Hyperion FCC image

The Pixel Purity Index (PPI) is a processing technique designed to determine which pixels are the most spectrally unique or pure. Due to the large amount of data, PPI is usually performed on MNF data which has been reduced to coherent images. The most spectrally pure pixels occur when there is mixing of endmembers. The PPI is computed by continually projecting n-dimensional scatterplots onto a random vector. The extreme pixels for each projection are recorded and the total number of hits are stored into an image. These pixels are excellent candidates for selecting endmembers which can be used in subsequent processing. Several classification techniques were being tried for deriving the required information from the huge data sets were Spectral Angle Mapper Classification, Spectral Unmixing/Matched Filtering and N-Dimensional visualization etc.

The figure 1.10 shows part of Prakasam district, Andhra Pradesh wherein the LISS-III multispectral and the Hyperion Hyperspectral FCC images from comparable bands. The sharpness in the Hyperion image may be attributed to the improved spectral resolution.

1.9.2. Parameter retrieval

Hyperspectral remote sensing has been proven to be a very effective tool for the estimation of crop variables such as LAI, pigment and water content and crop biomass accumulation, either directly or indirectly through other variables. Thenkabail *et al.*, (2002) showed that the narrowband vegetation indices provided a more accurate estimation of crop parameters than did equivalent broadband-based indices. Similarly, Blackburn (1999) reported that for estimation of chlorophyll a, chlorophyll b and carotenoids, wavebands of 680 nm, 635 nm and 470 nm, respectively, were optimal. The literature supports the fact that hyperspectral data could provide considerable additional information in the estimation of various crop characteristics compared to similar

information obtained from broadband sensors (Blackburn, 1998; Carter, 1998; Elvidge and Chen, 1995; Thenkabail *et al.*, 2002 and 2000; Asner *et al.*, 2000). Gong *et al.*, (2003) found that the wavelengths of 820, 1040, 1200, 1250, 1650, 2100, and 2260 nm were the most valuable bands for estimation of LAI. In Potato crop, the indices (NDVI, SAVI, RVI) based on reflectance of 780 and 680 nm showed maximum correlation to LAI. Among the other narrow-band indices, maximum of second derivative reflectance in the red edge region (680) and normalized difference of maximum of first derivative reflectance of the green and minimum of first derivative reflectance in the green showed high correlation were highly related to LAI in potato crop. (Ray et.al., 2006).

1.9.3. Stress Detection

With hyperspectral data, it is possible to identify not only the stress-free areas of the field but also those that are under water, nitrogen and weed stresses (Borregaard *et al.*, 2000, Cho *et al.*, 2002; Goel *et al.*, 2002, Karimi *et al.*, 2004). The derivative chlorophyll index (DCI) calculated as D_{705}/ D_{722} based on the double peak of derivative reflectance is proposed for mapping vegetation stress. (Zarco-Tejada *et. al.*, 2003). Ray *et.al.*, (2006) reported that the five best bands to discriminate between irrigation treatments were 540, 610, 630, 700, and 1000 nm. The optimum set of narrow bands found to be suitable for discriminating between different irrigation treatments were 540, 610, 630, 700, and 1000 nm, which were in green, red, red-edge and moisture-sensitive NIR region. These narrow bands centered at 540 nm is near green peak which is sensitive to total chlorophyll, 610 and 630 nm are absorption pre-maxima in red regions and sensitive to biomass and soil background, 700 nm is in red edge, which is sensitive to crop stress and 1000 nm is in moisture sensitive NIR region. Analysis of several narrow-band indices calculated from the reflectance values showed the indices that were able to differentiate best between the different rates of N application were reflectance ratio at the red edge (RE740/720) and the structure insensitive pigment index (SIPI).

1.9.4. Varietal discrimination

Thenkabail (2002) had found that to discriminate between agricultural crops (wheat, barley, chickpea, cumin, lentil and vetch) four most optimum hyperspectral bands are 547, 675, 718 and 904 nm. Apan *et al.*, (2004) found 550, 680 and 800 nm useful in discriminating between sugarcane varieties. The figure 1.11 shows the profile of the red edge shifts in different varieties in paddy crop grown under similar management practices, which can used as an indicator of stress/ characterization of variety.

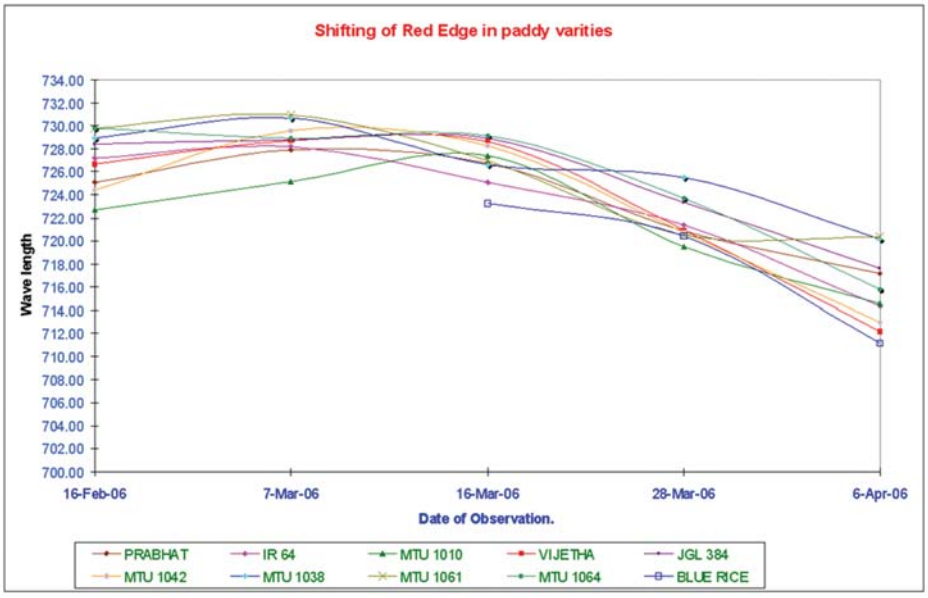

Figure 1.11: Red edge dynamics of few commonly grown rice varieties

1.9.5. Disease identification

Hyperspectral imaging can also aid in distinguishing the signatures of healthy and infested plants to allow intervention before there is significant damage. The reflection curves between healthy and diseased sugar beets showed a significant difference in the diseased crop. The reflection of healthy plants in comparison to diseased ones is clearly higher at most portions of the spectrum, especially at the near infrared sector. Additionally, the “green peak” at circa 550 nm is visible, in contrast to the reflectance curves of unhealthy sugar beets. These facts were also visible using two vegetation indices. The indices of diseased sugar beets presented lower values. (Laudien *et al.*, 2003).

The analysis of spectral reflectance pattern of cowpea infested with disease (Cowpea rust) was carried out and the reflectance at centered at 740, 660, 680 and 1448 nm was found to give significant difference compared to normal crop as shown in figure 1.12. The ratio of reflectance at 550/680, 800/1660, 1660/680, 1660/550 and (800-550/1660+680) wavelengths also were found to give significant differences.

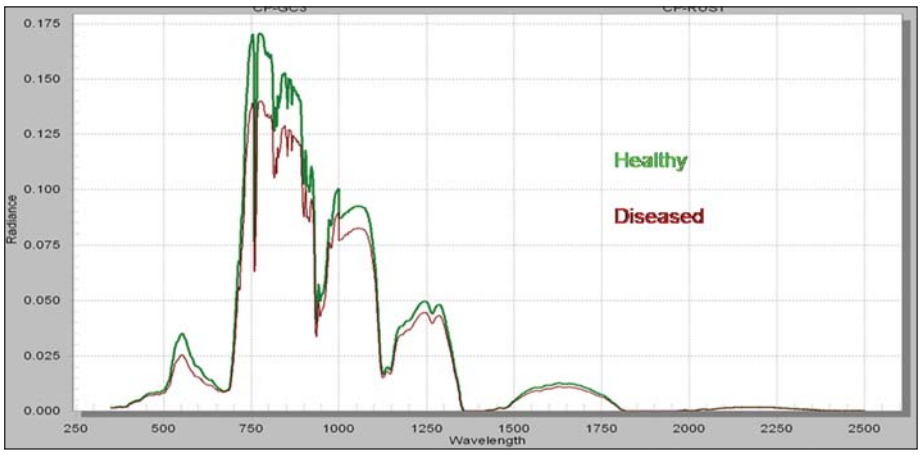

Figure 1.12: Hyperspectral signature for a diseased (cowpea rust) and a healthy cowpea crop

1.10. Microwave Remote Sensing

Non availability of adequate number of cloud free optical satellite datasets is a major constraint for using optical remote sensing data for agricultural applications during monsoon season. In light of this, all weather capability of RADAR, an active sensor, is an attractive option to rely upon. Microwave remote sensing techniques have all weather capability as atmosphere is transparent to microwaves at lower frequencies, penetrate clouds and are suitable for day/night operations owing to the independence of microwave sensors on Sun's illumination.

Radar response measured in terms of backscatter coefficient is dependent upon sensor (frequency, polarization and look angle) and target parameters (dielectric constant, surface roughness, and vegetation cover). In addition, SAR being an active sensor, frequency of data acquisition is two fold increased with the possibility of data availability during ascending and descending passes.

Sensitivity of microwave radiation to surface roughness (due to soil or crop), and water content (in soil or crop) as a function of look angle and polarization at a given frequency makes SAR an attractive remote sensor for obtaining information on several crop and soil parameters. Microwave response from an agricultural field depends on both standing crop and the underlying soil conditions. Contribution to the microwave backscatter from an agricultural field is maximum from the soil during the initial stages when crop cover is negligible, mixed from soil and crop during the growth period and mostly from the crop canopy when crop cover is at its peak. Hence, to put SAR data to full use in agricultural environment, complete information of soil as well as crop conditions is an essential requirement.

Geometrical and dielectric characteristics of crops influence the interaction of microwaves and thus determine the microwave backscatter measured by the sensor (Ulaby, 1975). Crop phenology governs the plant water content and thus crops dielectric properties. As crops mature the water content decreases, which in turn reduces contribution to radar backscatter from the plants. Besides crop geometry, several crop parameters such as leaf area index, plant biomass, plant water content and plant height show significant correlations with radar backscatter coefficient (Ulaby, 1975; Le Toan *et al.*, 1984, Bouman *et al.*, 1991). It is through these correlations monitoring of crop condition is possible.

Earlier studies reported in the literature includes the use of X band VV polarization data acquired by Canadian Intera Airborne SAR system during October 1988 that was capable of discriminating the plantations from crops. Later with the increased availability of SAR data from space borne platforms, the potential of multi-temporal SAR data for rice crop monitoring have been demonstrated by a number of investigators (e.g., Hoogeboom, 1983; Kurosu *et al.*, 1995; Premlatha and Rao, 1994; Patel, 1994; Chakraborty and Panigrahy, 1999). Apart from area monitoring and condition assessment, retrieval of different biophysical parameters viz., leaf area index, plant height, biomass, etc., have been attempted relating these with SAR backscatter.

1.10.1. National Kharif Rice Acreage Estimation

RADARSAT ScanSAR Narrow B – (SNB) data having an incidence angle of 31-46 degrees was found to give distinct signature to wetland rice crop. The pattern of change in backscatter from ploughed/puddled fields to the water-filled fields at transplanting stage is similar to that observed in case of ERS SAR data. However, unlike ERS SAR, wind-induced roughness has less effect on the backscatter from water bodies. This was attributed partly to

the HH polarization of RADARSAT and partly to the shallow angle of SNB. This resulted in better separation of rice fields from water, which generally overlap in ERS SAR data. Overall, 94 per cent classification accuracy was obtained for rice. It was also feasible to separate rice sub-classes based on its growth stages and crop rotation practice with 90 per cent accuracy (Chakraborty and Panigrahy 2000). The 300 km swath with 50 m resolution of SCNB data was found more cost effective for large area crop monitoring. In

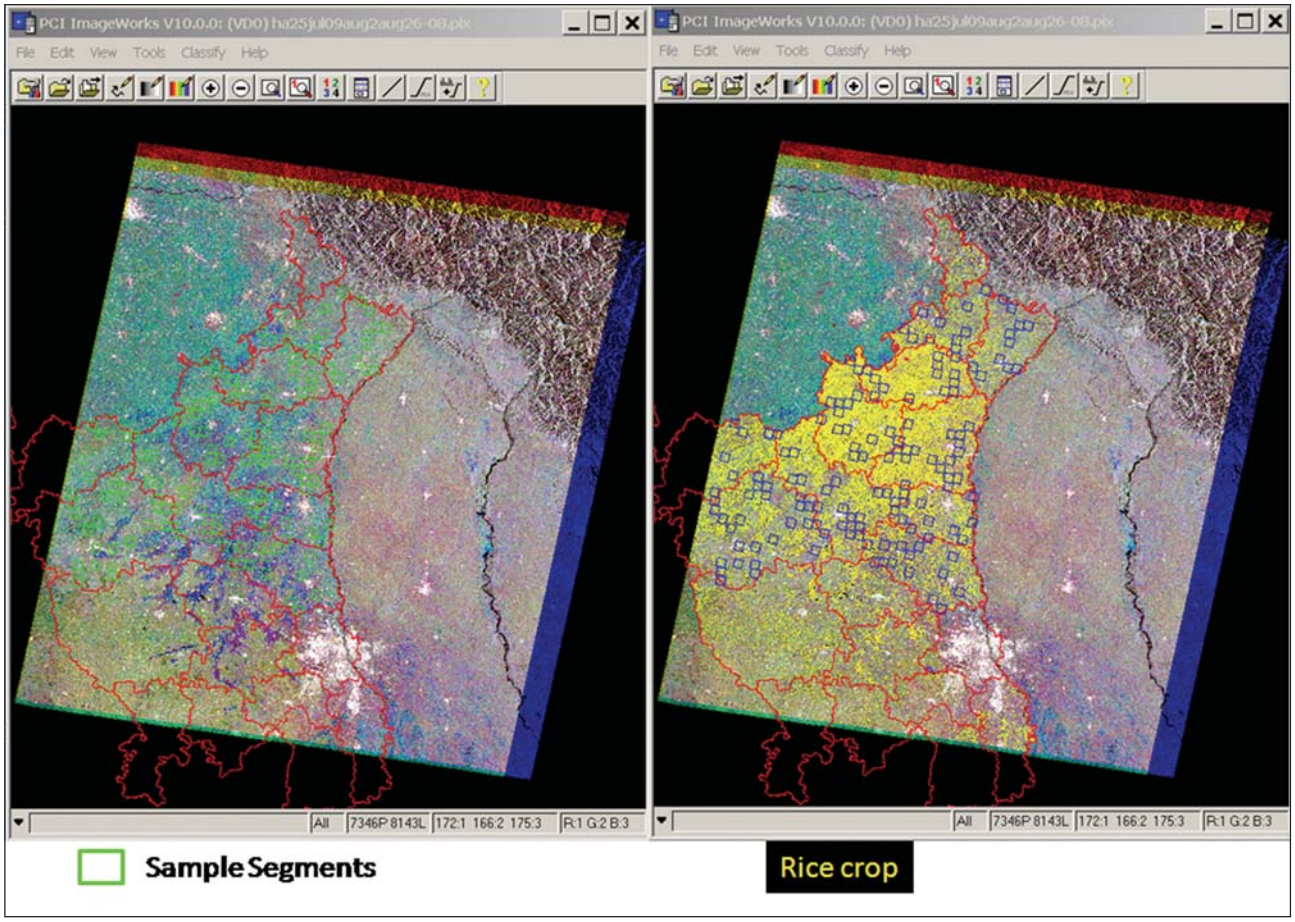

Figure 1.13: Temporal FCC of RADARSAT SN-2 data showing rice crop

order to obtain crop acreage estimates of large area within a reasonable time and cost, sampling approach rather than complete enumeration, was adopted in the ongoing National Kharif Rice Acreage estimation project at NRSC, Hyderabad. Figure 1.13 is the temporal FCC of RADARSAT ScanSAR Narrow B data covering the state of Haryana with the district boundaries and the sampling grids overlaid on to it.

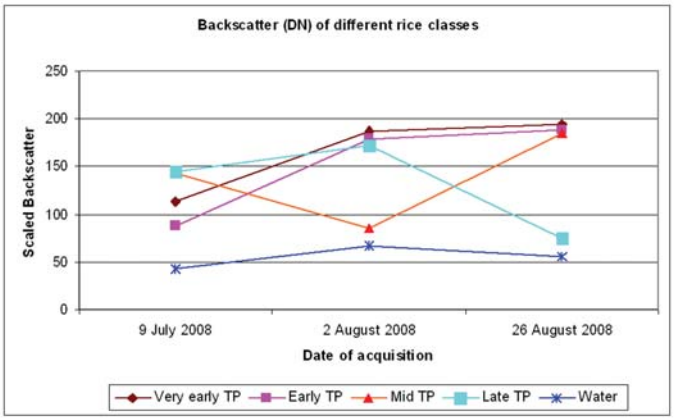

Figure 1.14: Temporal backscatter profile of different rice classes in Kaithal district, Haryana

The categories of very early, early, mid and late transplanted rice can be discriminated from the temporal data sets and the figure 1.14 depicts the temporal behavior of the various rice classes in Kaithal district, Haryana. It can be observed that the very early rice crop is transplanted some time prior to July 9 and developed sufficient biomass by the time of first date of pass, early, mid and late transplanted rice crop more or less coincided with the satellite pass on July 9, August 2 and 26.

1.11. Customized softwares for crop acreage estimations

The crop acreage estimation by sampling or total enumeration method can be accomplished by the commercially available image analysis and GIS software's. To facilitate speedy and accurate implementation of procedure on an

operational basis, a menu driven semi-automated software, 'CAPEMAN' followed by a advanced version 'CAPEWORKS', has been developed for data analysis interfacing with commercially available software Geomatica and ERDAS Imagine (RRSSC, 1996). In order to process the SAR data for National Kharif Rice. specific software called 'SARCROPS' was developed for semiautomatic proces g of of SAR data using Geomatica Software.

1.12. Conclusions

Satellite remote sensing techniques are being operationally used to provide intra seasonal and inter-seasonal information on the spatial distribution of crops at different levels. Analysis of satellite data for crops along with the information on other natural resources in GIS environment provides valuable information towards sustainable agriculture. Time compositing techniques, applied for normalized difference vegetation index parameter circumvent the problem of non-availability of cloud free optical data and enable generation of the in situ crop condition information. The continuous improvements in the satellite technology in terms of providing improved spatial and spectral resolutions and revisit periods will greatly enhance the capabilities of mapping and monitoring of crops, aiming towards sustainable agriculture.

References

Apan A, Held A, Phinn S and Markley J, 2004, Detecting sugarcane 'orange rust' disease using EO-1 hyperion hyperspectral imagery, *International Journal of Remote Sensing*, **25**:489–498.

Arkin PA and Ardanuy PE, 1989, Estimating Climatic-Scale Precipitation from Space: A Review *Journal of Climate*, **2**: 1229-1238.

Asner GP, Wessman CA, Bateson CA and Privette JL, 2000, Impact of tissue, canopy and landscape factors on the hyperspectral reflectance variability of arid ecosystems, *Remote Sensing of Environment*, **74(1)**: 69-84.

Barrett EC and Beaumont MJ, 1994, Satellite Rainfall Monitoring: an overview, *Remote Sensing Reviews*,**11**: 23-48.

Becker F and Li ZL, 1990a, Towards a local split window method over land surfaces, *International Journal of Remote Sensing*, **11**: 369– 394.

Becker F and Li ZL, 1990b, Temperature-independent spectral indices in thermal infrared bands, *Remote Sensing Enviroment*, **32**: 17–33.

Blackburn GA, 1998, Spectral indices for estimating photosynthetic pigment concentrations: a test using senescent tree -leaves, *International Journal of Remote Sensing,* **19(4)**: 657 - 675.

Blackburn GA, 1999, Relationships between spectral reflectance and pigment concentrations in stacks of deciduous broadleaves, *Remote Sensing of Environment*, **70(2)**: 224-237.

Borregaard T, Nielsen H, Norgaard L and Have H, 2000, Crop-weed Discrimination by Line Imaging Spectroscopy, *Journal of Agricultural Engineering Research*, **75**: 389-400.

Bouman BAM, 1991, Crop parameter estimation from ground based x-band (3-cm Wave) radar backscattering data, *Remote Sensing of Environment*, **37**: 193-205.

Carter GA, 1998, Reflectance bands and indices for remote estimation of photosynthesis and stomatal conductance in pine canopies, *Remote Sensing of Environment*, **63**: 61-72.

Chakraborty M and Panigrahy S, 2000, A processing and software system for rice crop inventory using multi-date RADARSAT ScanSAR data, *ISPRS Journal of Photogrammetry and Remote Sensing*, **55(2)**: 119-128.

Chakraborty M and Panigrahy S, 1996, Evaluation of Four Per-pixel Classifiers Using ERS-1 SAR Data for Classification of Rice Crop, In Proceedings of Indo-US Symposium, IIT, Bombay, October, 1996.

Cho SI, Lee DS and Jeong JY, 2002, Weed–plant discrimination by machine vision and Artificial Neural Network, *Biosystems Engineering*, **83(3)**:275–280.

Dadhwal VK, Singh RP, Dutta S and Parihar JS, 2002, Remote sensing based crop discrimination and area estimation: A review of Indian experience, *Tropical Ecology,* **43**: 107–122.

Dadhwal VK, 1999, Remote sensing and GIS for agricultural crop acreage and yield estimation, pp. 58-67, International Archives of Photogrammetry and Remote Sensing, XXXII, 7-W9, (ISPRS Commission VII/ WG 2 Symposium on Application of Remote Sensing and GIS for Sustainable Development), March 11, Dehradun, India.

Dadhwal VK and Ray SS, 2000, Crop Assessment using remote sensing – Part II: Crop condition and yield assessment, *Indian Journal of Agricultural Economics*, **55**(2, Suppliment): 55-67.

Dakshinamurthy C, Krishnamurthy B, Summanwar AS, Santhur P and Pisharoty PR, 1971, Remote sensing of coconut wilt, Proceedings of 6th International symposium on Remote sensing of Environment, Ann Arbor p. 25

Dash P, Go¨ttsche FM, Olesen FS and Fischer H, 2002, Land surface temperature and emissivity estimation from passive sensor data: Theory and practice-Current trends, *International Journal of Remote Sensing*, **23**: 2563–2594.

Ebert EE and Le Marshall JF, 1995, An evaluation of infrared satellite rainfall estimation techniques over Australia, *Australian Meteorological Magazine,* **44**: 177-190.

Ebert EE, 1987, A pattern recognition technique for distinguishing surface and cloud types in polar regions, *Journal of Climate and Applied Meteorology*, **26**: 1412-1427.

Elvidge CD and Chen Z, 1995, Comparison of broad-band and narrow-band red and near-infrared vegetation indices, *Remote Sensing of Environment*, **5:** 38–48.

Gardner BR, Blad BL and Watts DG, 1981, Plant and air temperature in differentially-irrigated corn, *Agricultural Meteorology*, **25**, 207–217

Goel PK, Prasher SO, Patel RM, Smith DL and DiTommaso A, 2002, Use of airborne multi-spectral imagery for weed detection in field crops, *Transactions of the ASAE*, **45 (2)**: 443–449.

Gong P, Pu R, Biging GS and Larrieu MR, 2003, Estimationof forest leaf area index using vegetation indices derived from Hyperion hyperspectral data, *IEEE Transaction on Geoscience and Remote Sensing*, **41 (6)**: 1355-1362.

Grassotti CG and Garand L, 1994, Classification-based rainfall estimation using satellite data and numerical forecast model fields, *Journal of Applied Meteorology*, **33**: 159-178.

HebbarR, Krishna Rao MV and Sesha Sai MVR, 2003, Inventory of major crops in EID-PARRY sugar factory command for possible expansion of sugarcane cropped area using RS & GIS, SISSTA *Sugar Journal - 2003* .

Herman A, Kumar VB, Arkin PA and Kousky JV, 1997, Objectively determined 10-day African rainfall estimates created for famine early warning systems, *International Journal of Remote Sensing*, **17**: 2147-2159.

Hoogeboom P, 1983, Classification of Agricultural Crops in Radar Images, *IEEE Transactions on Geoscience and Remote Sensing*, **23**: 329-336.

Idso SB, Jackson RD, Pinter PJ Jr., Reginato RJ and Hatfield JL,1981, Normalizing the stress-degree-day parameter for environmental variability, *Agricultural Meteorology*, **24**: 45–55.

Idso SB, Jakson RD and Reginato RJ,1977a, Remote-sensing for agicultural water management and crop yield production, *Agricultural Water Management*, **1(4)**: 299-310.

Jackson RD, Idso SB and Reginato RJ, 1977, Remote Sensing of Crop Canopy Temperatures for Scheduling Irrigation and Estimating Yield, Proceedings of the Symposium on Remote Sensing of Natural Resources, Utah State University, Logan, UT.

Jackson RD, Idso SB, Reginato RJ and Pinter PJ,1981, Canopy temperature as a crop water stress indicator, *Water Resources Research,* **17**: 1133–1138.

Jackson RD,1982, Canopy temperature and crop water stress, Hillel DI, Editor, Academic Press, *Advances in Irrigation*, **1**: 43-85.

Jime´nez-Mun˜oz JC and Sobrino J A, 2003, A generalized singlechannel method for retrieving land surface temperature from remote sensing data, *Journal of Geophysical Research*, **108(22)** :4688, doi:10.1029/2003JD003480.

Karimi Y, Prasher SO, McNa irn H, Bonnell RB, Dutilleul P and Goel PK, 2004, Discriminant analysis of hyperspectral data for assessing water and nitrogen stresses in corn, *Transaction of the ASAE*, **48(2)**: 805-813.

Krishna Rao MV, Hebbar R, Sesha Sai MVR and Venkataratnam L, 2002, Inventory of post kharif rice fallow lands of South Asia for introduction of legumes- an endeavour towards macro level sustainable agriculture IAPRS & SIS,**34**, Part 7, Resource and Environmental Monitoring, Hyderabad, India, 30-34.

Krishna Rao, MV, Hebbar R and Venkatratnam L, 1997, Evaluation of IRS-1C data for discrimination and acreage estimation of crops grown under multiple cropping situation, In Remote Sensing for Natural Resources, Joint publication of ISRS & NNRMS, 205-211.

Krishna Rao MV, Sesha Sai MVR and Hebbar R, 2004, Remote sensing and GIS applications for Crops studies, In: Soils & Crops, NRSA, Hyderabad, 161-173.

Krishna Rao PV, Sesha Sai MVR, Ramana KV, Venkataratnam L and Sudhakara Babu SN, 1996, Estimation of sunflower crop yield using Remote Sensing techniques, Proceedings of National Symposium on Remote Sensing for Natural Resources with special emphasis on Water Management, Pune, India.

Krishna Rao PV, Venkataratnam L, Venkateswara Rao V and Venkataramaiah,2000, Remote sensing studies on sugarcane fields in KCP Sugar and Industries corporation Sugar factory Zones, *SISSTA Sugar journal*, **25**: 129-138.

Krishna Rao V, Krishna Rao PV and Venkataratnam L, 1996, Grapevine acreage estimation using IRS LISS-II data, *Asian*

Pacific Remote Sensing and GIS Journal, **8(2)**: 61 – 64.

Krishna Rao MV, Sesha Sai MVR, Hebbar R, Krishna Rao PV and Venkataratnam L, 1997, Acreage and production estimation of soybean crop using remote sensing technique In: Remote Sensing for Natural resources - A Joint *Publication of Indian Society of Remote Sensing* and NNRMS: 239-246.

Kurosu T, Fujita M and Chiba K, 1995, Monitoring of rice crop growth from space using the ERS-1 C -band SAR, *IEEE Transactions on Geoscience and Remote Sensing,* **33(4)**: 1092-1096.

Laudien R, Bareth G and Doluschitz R, 2003, Analysis of Hyperspectral field data for deletion of sugarbeet diseases, EFITA 2003 conference, Debrecen, Hungary.

Le Toan T, Lopes A and Huet M, 1984, On the relationships between radar backscattering coefficient and vegetation canopy characteristics, International Geoscience and Remote Sensing Symposium Proceedings, Strasburg, France, 155-160.

Lillesand TM and Kiefer RW, 2000, Remote Sensing and Image Interpretation, John Wiley & Sons. Inc. (4th edition).

Moran MS, Clarke TR, Inoue Y and Vidal A, 1994, Estimating crop water deficit using the relation between surface-air temperature and spectral vegetation index, *Remote Sensensing of Environment*, **49**: 246–263.

Moser W and Raschke E, 1984, Incident solar radiation over Europe estimated from METEOSAT data, *Journal of Climate and Applied Meteorology*, **23**: 166-170.

Navalgund RR, Parihar JS, Ajai and Nageshwar Rao PP, 1991, Crop inventory using remotely sensed data, *Current Science*, **61**: 162–171.

Navalgund RR and Ray SS, 2000, Geomatics in natural resources management, In Proceedings of Geomatics-2000, Pune, India, NR1-NR14.

NRSA, 1991, Hectarage estimation of jute crop in Cooch Behar district of West Bengal, NRSA Technical report, p 23.

NRSA, 1990, National Agricultural Drought Assessment and Monitoring System, NRSA, Hyderabad, p. 124.

NRSA, 1992, Acereage estimation of soyabean and sunflower crops, Hyderabad, p. 42.

Parihar JS and Oza MP, FASAL: 2006, An integrated approach for crop assessment and production forecasting, Proc. of SPIE, Agricultural and hydrology applications (eds: Robert, J, Kuligowski, J S, Parihar, Genya Saito), **6411**: 641101–641113.

Patel NK, Medhavy TT, Patnaik C and Hussain A, 1995, Multi Temporal ERS-1 SAR Data for Identification of Rice Crop, *Journal of Indian Society of Remote Sensing*, **23**: 33-39.

Petty GW, 1995, The Status of Satellite-Based Rainfall Estimation Over Land, *Remote Sensing of Environmen*t, **51**: 125-137.

Pinker RT and Ewing JA, Modeling surface solar radiation : Model formulation and validation, *Journal of Climate and Applied Meteorology*, **24**: 389-401.

Prata AJ, 1993, Land surface temperatures derived from the AVHRR and ATSR: 1, Theory, *Journal of Geophysical Research*, **98**: 689–16,702.

Prata AJ, 1994, Land surface temperatures derived from the advanced very high resolution radiometer and the along-track scanning radiometer, *Journal of Geophysical Reserach*, **99**: 13,025–13,058.

Premlatha M and Rao PPN, 1994, Crop Acreage Estimation Using ERS-1 SAR Data, *Journal of Indian Society of Remote Sensing*, **22**: 139-147.

Price JC, 1984, Land surface temperature measurements from the split window channels of the NOAA 7 AVHRR, *Journal of Geophysical Reserach*, **89**: 7231– 7237.

Qin Z A, Karnieli and Berliner P, 2001, A mono-window algorithm for retrieving land surface temperature from Landsat TM data and its application to the Israel-Egypt border region, *International Journal of Remote Sensing*, **22**:3719–3746.

Rasmussen EM and Arkin PA, 1992, Observing Tropical Rainfall from Space: a review, In: JS Theon, TMatsumo, T Sakata and N Fugono (Editors), The Global Role of Tropical Rainfall, Deepak, Hampton, VA, 105-188.

Ray SS, Das G, Singh JP and Panigrahy S, 2007, Evaluation of hyperspectral indices for LAI estimation and discrimination of potato crop under different irrigation treatments, *International Journal of Remote Sensing*, **27(24)**:5373-5387.

Rosenfield D and Gutman G, (1994), Retrieving microphysical properties near the tops of potential rain clouds by multispectral analysis of AVHRR data, *Atmospheric Research,* **34**: 259-283.

RRSSC, 1991, Identification and acereage estimation of tobacco through satellite remote sensing, Project report.

RRSSC, 1996, CAPEWORKS Reference Manual, Vol 1.0.

Sesha Sai MVR, Hebbar R, and Krishna Rao MV, 2004, Remote Sensing Based Crop Inventorying for Agricultural Drought Assessment, Workshop on Regional Workshop on Agricultural Drought Assessment and Monitoring using Space Technology, 25-32.

Sesha Sai MVR and Hebbar KR, 2008, Alternating polarization Envisat-ASAR data for agricultural management, , Scientific Report, EOAM/NRSA/RiSAT-JEP/Agril/2008, NRSA.

Sesha Sai MVR, Ramana KV and Hebbar R, 2007, Satellite remote sensing for efficient coastal agriculture, Presented in the International Symposium on Management of Coastal Eco-systems, Kolkata.

Sesha Sai MVR, Hebbar R, Krishna Rao PV, Narasimha Rao PV, Vijayshankar Babu M, Dwivedi RS and Roy PS, 2007, Alternating polarization Envisat-ASAR data for agricultural management, published in Conference of Joint Experiment Project towards Microwave Remote Sensing Data Utilization (JEP-MW), SAC, Ahmedabad, 77-89.

Sesha Sai MVR, Hebbar R and Krishna Rao MV, 2003, Planning for sustainable cotton production through conformity analysis using RS and GIS techniques, Theme: Application of RS & GIS in Agriculture for the ISPRS TC VII/3 Workshop on Intergraded Monitoring Systems & ISRS Annual Convention 2003.

Sobrino JA, Coll C and Caselles V, 1991, Atmospheric correction for land surface temperature using NOAA-11 AVHRR Channels 4 and 5, *Remote Sensensing of Environment,* **38**: 19– 34.

Sobrino JA, So‘ ria G and Prata AJ, 2004, Surface temperature retrieval from Along Track Scanning Radiometer 2 data: Algorithms and validation, *Journal of Geophysical Reserach*, **109**, D11101, doi:10.1029/2003JD004212.

Sobrino JA, Jime´nez-Mun˜oz JC, Labed-Nachbrand J and Nerry F, 2002, Surface emissivity retrieval from Digital Airborne Imaging Spectrometer data, *Journal of Geophysical Reserach*, **107**(**23)**: 4729, doi:10.1029/2002JD002197.

Sobrino JA, Li ZL, Stoll MP and Becker F, 1994, Improvements in the split-window technique for land surface temperature determination, *IEEE Transaction on Geoscienses and Remote Sensensing*, **32**: 243– 253.

Sobrino JA, Li ZL, Stoll P and Becker F, 1996, Multi-channel and multi-angle algorithms for estimating sea and land surface temperature with ATSR data, *International Journal of Remote Sensensing,* **17**: 2089– 2114.

Subbarao GV, Kumar Rao JVDK, Kumar J, Johansen C, Deb UK, Ahmed I, Krishna Rao MV, Venkataratnam L, Hebbar KR, Sesha Sai MVR and Harris D, 2001, Spatial distribution and quantification of rice-fallows in South Asia – potential for legumes, Published by ICRISAT, Hyderabad.

Swain PH and Davis SM, 1978, Remote sensing: The Quantitative Approach, McGraw Hill, New York.

Tarpley JD, 1979, Estimating incident solar radiation at the surface from geostationary satellite data, *Journal of Applied Meteorology,* **18**: 1172-1181.

Thenkabail PS, 2002, Optimal hyperspectral narrow bands for discriminating agricultural crops, *Remote Sensing Reviews*, **20**: 257–291.

Thenkabail PS, Smith RB and De-Pauw E, 2002, Evaluation of narrowband and broadband vegetation indices for determining optimal hyperspectral wavebands for agricultural crop characterization, *Photogrammetric Engineering and Remote Sensing*, **68**: 607–627.

Ulaby FT, 1975, Radar response to vegetation, *Transactions on Antennas and Propagation*, **23**: 36-45.

Venkataratnam L, Krishna Rao MV, Ravishankar T, Thammappa SS and Gopi S, 1993, Cotton acreage estimation and condition assessment through remote sensing method, Proc. National Seminar on Oilseeds Research and Development in India: Status and Strategies, p 217.

Venkataratnam L, Krishna Rao PV, Ramana KV, Sudhakara Babu SN, Koteswara Rao K, and Babu VVR, 1994, Acreage estimation of sunflower crop using remote sensing techniques, In PrasadMVR et. al. Ed. Sustainability in oilseeds, Indian Society of Oilseeds Research, Hyderabad, 433 – 435.

Wan Z and ZL Li, 1997, A physics-based algorithm for retrieving land-surface emissivity and temperature from EOS/ MODIS Data, *IEEE Transaction on Geosciense and Remote Sensensing*, **35**: 980– 996.

Wani SP, Dwivedi RS, Ramana KV, Vadivelu A, Navalgund RR and Pande AB, 2002, Spatial distribution of rainy season fallows in Madhya Pradesh: Potential for increasing productivity and minimizing land degradation, Global Theme 3: Water, Soil and Agrobiodiversity Management for Ecosystem Health, Report no. 3. Patancheru 502 324, Andhra Pradesh, India: International Crops Research Institute for the Semi- Arid Tropics, p 40.

Zarco-Tejada PJ, Pushnik JC, Dobrowski S and LUS, 2003, Steady-state chlorophyll a fluorescence detection from canopy derivative reflectance and double-peak red-edge effects, *Remote Sensing of Environment*, **84**: 283-294.

http://trmm.gsfc.nasa.gov/publications_dir/instant_2.html

http://www.csr.utexas.edu/projects/rs/hrs/hyper.html

nrsc

Remote Sensing Applications

P. S. Roy
R. S. Dwivedi
D. Vijayan

National Remote Sensing Centre

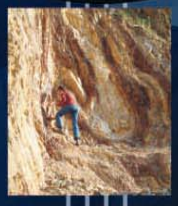

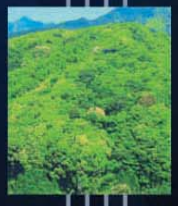

Remote Sensing Applications

Land Use and Land Cover Analysis

2.1. Introduction

Economic development and population growth have triggered rapid changes to Earth's land cover over the last two centuries, and there is every indication that the pace of these changes will accelerate in the future. These rapid changes are superposed on long-term dynamics associated with climate variability. Land cover change can affect the ability of the land to sustain human activities through the provision of multiple ecosystem services and because the resultant economic activities cause feedbacks affecting climate and other facets of global change. Accordingly, systematic assessments of Earth's land cover must be repeated, at a frequency that permits monitoring of both long-term trends as well as interannual variability, and at a level of spatial detail to allow the study of human-induced changes.

Land cover, defined as the assemblage of biotic and abiotic components on the Earth's surface, is one of the most crucial properties of the Earth system. There are three fundamental ways in which it is important (Turner *et al.*, 1994). The first lies in the interaction of land cover with the atmosphere, which leads to regulation of the hydrologic cycle and energy budget, and as such is needed both for weather and climate prediction (DeFries *et al.*, 2002). For example, most climate models are now coupled with Land Surface Parameterizations (LSPs) which use digital land cover data to produce databases of albedo, surface roughness, evapotranspiration and respiration. Second, land cover plays a major role in the carbon cycle acting as both sources and sinks of carbon. In particular, the rates of deforestation, afforestation and regrowth play a significant role in the release and sequestering of carbon and consequently affect atmospheric CO_2 concentration and the strength of the greenhouse effect (IPCC, 2000; Janetos and Justice, 2000; Houghton, 1999). Finally, land cover also reflects the availability of food, fuel, timber, fiber, and shelter resources for human populations, and serves as a critical indicator of other ecosystem services such as biodiversity. Information on land cover is fundamental to many national/global applications including watershed management and agricultural productivity. Thus, the need to monitor land cover is derived from multiple intersecting drivers, including the physical climate, ecosystem health, and societal needs.

Although the terms "land cover (LC)" and "land use (LU)" are sometimes used interchangeably, they are actually different. Simply put, land cover is what covers the surface of the earth and land use describes how the land is used. Examples of land cover classes include: water, snow, grassland, deciduous forest, and bare soil. Land use examples include: wildlife management area, agricultural land, urban, recreation area etc. Two land parcels may have similar land cover, but different land use. For instance, A golf course and an office building are both commercial land uses. The former would have a land cover of grass, while the latter would be considered built up.

2.2. LULC Mapping

2.2.1. Conventional Approach

Compilation from revenue records by the Directorate/Bureau of Economic and Statistics (DES/BES) of respective states has been the conventional approach of collecting LULC information in the country. The land use information "derived" from the agricultural inventory carried out at individual plot level is available in a nine-fold classification system. These data are available in the form of statistical records without any reference to the spatial locations. Topographical maps from Survey of India that represent very broad land use categories mapped using mainly ground information on 1:50,000 to 1:25,000 scale is another source of LULC information. However, this land use information does not represent current situation of land use and also does not reflect changes. Land use maps generated by Soil Survey organizations that are based on soil mapping units forms another source, from which land use information can be deciphered. However, such maps are generated and available for only specific project areas. For most part, they have worked independently and without coordination with other agencies. Too often this has meant duplication of effort, or it has been found that data collected for a specific purpose were of little or no value for a similar purpose only a short time later.

There are many different sources of information on existing land use and land cover and on changes that are occurring at different levels. Local planning agencies make use of detailed information generated during ground surveys involving enumeration and observation. Major problems that surface during the application and interpretation of these data sets include changes in definitions of categories and data collection methods by source agencies, incomplete data coverage, varying data age, and employment of incompatible classification systems. In addition,

it is nearly impossible to aggregate the available data because of the differing classification systems used. These limitations of traditional approaches had been partly overcome by adopting modern approaches like remote sensing.

2.2.2. Remote Sensing based Approach

Land cover mapping is a product of the development of remote sensing, initially through aerial photography. Remote sensing technology, because of the benefits it offers (wide area coverage, frequent revisits, multispectral**,** multisource**,** and storage in digital format to facilitate subsequent updating and compatibility with GIS technology) proved very practical and economical means for an accurate classification of land cover.

There are several important considerations that determine the characteristics of land cover information generated using remote sensing data.

Purpose: Land cover information is obtained for numerous scientific, policy, planning or management purposes. Within each of these areas, a wide range of needs exists. For example, land use inventories, forest inventories, planning as well as other biophysical resource inventories require land cover information. Specific models of vegetation–atmosphere interactions require different types of land cover information (Dickinson *et al.*, 1986, Sellers *et al.*, 1994) including productivity models (Liu *et al.*, 1997) and hydrological models (Wigmosta *et al.*, 1994)

Thematic content: The information may be needed for few cover types (e.g., forest–non-forest); for all cover types and at the same (or varying) levels of detail; tailored to specific model requirements; or as continuous variables (e.g., percentage coniferous forest). The thematic content also has a strong effect on the frequency of land cover mapping

Scale: Over large areas, land cover information may be required locally (at specific sites), at regional scales, or continental to global scales

Data: The quality and availability of remote sensing data limit the type and accuracy of information that may be extracted

Processing and analysis techniques: The characteristics of processing and analysis techniques employed at various stages are of critical importance

2.2.3. LULC Classification System

There is no one ideal classification of land use and land cover, and it is unlikely that one could ever be developed. There are different perspectives in the classification process, and the process itself tends to be subjective, even when an objective numerical approach is used. There is, in fact, no logical reason to expect that one detailed inventory should be adequate for more than a short time, since land use and land cover patterns change in keeping with demands for natural resources. Each classification is made to suit the needs of the user.

In order to address the issues associated with classification like class definitions, multiple land uses on a single land parcel, minimum representable area and to standardize the LULC information that could be generated using remote sensing data. Anderson (1971) developed some criteria for classification systems.

- The minimum level of interpretation accuracy in the identification of land use and land cover categories from remote sensor data should be at least 85 percent
- The accuracy of interpretation for the several categories should be about equal
- Repeatable or repetitive results should be obtainable from one interpreter to another and from one time of sensing to another
- The classification system should be applicable over extensive areas
- The categorization should permit vegetation and other types of land cover to be used as surrogates for activity
- The classification system should be suitable for use with remote sensor data obtained at different times of the year
- Effective use of subcategories that can be obtained from ground surveys or from the use of larger scale or enhanced remote sensor data should be possible
- Aggregation of categories must be possible

- Comparison with future land use data should be possible
- Multiple uses of land should be recognized when possible

Accordingly, he proposed a multilevel land use and land cover classification system, wherein LULC information at Levels I and II would generally be of interest to users who desire data on a nationwide, interstate, or statewide basis. More detailed land use and land cover data such as those categorized at Levels III and IV usually will be used more frequently by those who need and generate local information at the intrastate, regional or municipal level. It was intended that these latter levels of categorization would be developed by the user groups themselves, so that their specific needs might be satisfied by the categories they introduced into the structure. The system satisfied the three major attributes of the classification process (1) it gave names to categories by simply using accepted terminology; (2) it was amenable to further refinement on the basis of more extended and varied use and (3) it allowed inductive generalizations to be made. At the more generalized levels it met the principal objective of providing a land use and land cover classification system for use in land use planning and management activities.

Later on, many refinements and customizations were effected in the LULC classification systems, commensurating with the needs of users and it is beyond the scope of this chapter to discuss the LULC classification systems developed all over the globe.

2.3. Historical perspective of LULC mapping projects using remote sensing in India

The Indian experience on use of satellite data for LULC analysis is mentioned in the Manual on National land Use Mapping at 1:250000 scale using IRS-P6 AWiFS data (NRSA, 2004), The work was carriedout by National Remote Sensing Centre (erstwhile NRSA). Department of Space, Government of India, in collaboration with various central and state government organisations. Realizing the need for an up-to-date nationwide LULC maps by several departments in the country, as a prelude, a LULC classification system with 24 categories up to Level-II, suitable for mapping on 1:250,000 scale, was developed by NRSC by taking into consideration the existing land use classification adopted by NATMO, CAZRI, Ministry of Agriculture, Revenue Department, AIS & LUS, etc., and the details obtainable from satellite imagery. After discussions with nearly 40 user departments / institutions in the country a 22 fold classification system was finalized and adopted for Nationwide LULC Analysis.

2.3.1. Nationwide LULC Analysis for Agro-Climatic Zone Planning

The district-wise LULC analysis of all the 15 agro-climatic zones, using the 22 fold LULC classification system was completed using satellite data for the period 1988 – 89. The IRS - LISS-I data of kharif (July-October) 1988 and Rabi (November– March) 1989 were used to generate details on crop land in Kharif (July-October) and Rabi seasons, the area under double crop, fallow lands, different types of forests, degradation status, wasteland, water bodies, etc., using hybrid methodology i.e., visual as well as digital analysis approach. NRSC along with Regional Remote Sensing Centres (RRSC's), State Remote Sensing Centres and other institutions completed this task. Out of 442 districts in the country, 274 districts were analyzed using visual techniques and remaining 168 districts by digital techniques. The Planning Commission of India was the main user for this project.

2.3.2. National Wastelands Inventory Project (NWIP)

Until recently, no attempt had been made to prepare map showing different types of wastelands in India. The area reported by various government agencies under wastelands varies from 38 M ha, to 175M. ha. In 1985, NRSC prepared wasteland maps of all states and union territories at a 1:1 million scale. The total area of wastelands in the country during 1980 – 1982 was estimated at 53.3 million ha or 16.2 per cent of the geographical area of the country.

The National Wastelands Development Board (NWDB) was setup in 1985 with an objective of rehabilitating 5 million ha of land each year for fuel wood and fodder production through a massive programme of seeding and afforestation. This programme required a very reliable database that provided details on the type, extent, location and ownership of wastelands. In view of varying estimates of the extent of wasteland, including the one provided by NRSC based on remote sensing, the need for precise definitions of various categories of wastelands realized. The Technical Task Force established by the NWDB proposed a classification system consisting of thirteen categories of wastelands.

Subsequently waste land mapping on 1 : 50,000 scale was taken up in five phases and about 5000 wasteland

maps covering entire country were prepared. The methodology developed based on pilot studies were used for identification and delineation of different types of wastelands using satellite data. Both Landsat Thematic Mapper (TM) and an Indian satellite (LISS-II and LISS-III) data were used for mapping purposes. Hybrid methodology i.e., both visual and digital techniques were used to derive information on the wastelands. About 63,87 million ha (20.17 per cent) have been estimated as wastelands through this study. Second cycle wasteland analysis has been completed using 2003 satellite data. An estimated 55.27 million ha. (17.45%) of land area has been mapped as wastelands. Currently, the 3rd cycle of mapping is in progress.

2.3.3. National Natural Resource Census

Land Use and Land Cover (IRS AWiFS data) : A composite Land Use/ Land Cover data set has been generated using multi temporal IRS-AWiFs data. Analysis is being carried out on 1: 250, 000 scale using level I and some Level II classes of land use classification. This project was aimed to analyse annual land use distribution for next three years i.e., 2004-05, 2005-06 and 2006-07.

Land Use / Land Cover inventory using IRS P6 LISS III data: Under the national level Project, LULC mapping on 1:50,000 scale for entire country has been taken up after conducting prototype studies for development of legend, standardization of methodology including digital data base creation and to generate spatial statistics. These studies are being carried out using 2005-06 databases to create the bench mark database which can later be used to understand the degree and magnitude of LULC changes at time intervals of 5 years.

2.4. Methodology of Land Use / Land Cover Analysis

In principle, land cover mapping from satellite data is straightforward and consists of four steps: data acquisition, pre-processing, analysis/classification, product generation and documentation.

2.4.1. Pre-processing

In principle, it entails geometric and radiometric corrections. Geometric corrections will not be discussed here as it is beyond the scope of present topic. Details on radiometric corrections is presented in the subsequent paragraphs.

Coarse resolution data:

In the past, some classification projects employing coarse resolution data were carried out with single-date, relatively cloud-free images. However, this approach is fundamentally limited because the probability of cloud-free scenes decreases as the area covered by one scene increases. It is thus very difficult to obtain useful images for land cover mapping, especially if the eligible time interval is short. Furthermore, such images contain systematic errors due to atmospheric effects (as a function of the path length) as well as monotonically changing spatial resolution for most coarse resolution sensors. Their classification is therefore difficult and requires interactive fine tuning for each input scene used, as well as post-classification operations to reconcile differences between adjacent scenes to ensure consistency across the mapped area. For these reasons, research in recent years has emphasised the use of image composites.

In a compositing process, the image product is prepared so as to contain, as far as possible, information about the land surface itself. Since a large fraction of the pixels typically contain clouds, the main objective of the procedure is to select the most cloud-free measurement from those available for a given pixel of the composite image. At present, the selection is most often based on the maximum value of the Normalized Difference Vegetation Index (NDVI) (Holben, 1986), Advantages of the NDVI criterion include high sensitivity to atmospheric contamination, ease of computation and wide acceptance in previous studies, thus creating a de facto standard. The pixel compositing approach yields nominally cloud-free composites every few days, thus providing a potentially large data set for land cover classification. However, in this form the data are far from adequate for such a purpose. This is because the composites have built-in noise from the varying satellite sensing geometry and from residual clouds or variable atmospheric properties (water vapour, aerosols, ozone). These effects are normally present between adjacent composite pixels and can lead to large radiometric differences for the same land cover type, thus causing classification errors. They also have a strong impact on the consistency of satellite data, both within and among years.

The degree of corrections following compositing varies among investigations. Atmospheric corrections are frequently carried out, although nominal / climatological values of some critical parameters are typically used or their effect is ignored (e.g., aerosol). While the nominal corrections account for systematic effects such as Rayleigh scattering,

they are incapable of discerning pixel-specific atmospheric contamination caused by translucent or small clouds, haze, or snow patches, Sellers *et al.,* (1994) used the NDVI temporal trajectory to flag contaminated pixels and Cihlar (1996) extended this approach in CECANT (Cloud Elimination from Composites using Albedo and NDVI Trend). Since the detection is NDVI-based, it can identify the above sources of noise because they tend to decrease the measured NDVI (compared to the 'expected value' for that pixel and compositing period). CECANT requires that data for the entire growing season be available so that the NDVI curve can be modeled. However, it is also applicable to new (current year) data provided that comparable full-season data are available for a previous year and some degradation of performance can be traded for timeliness (Cihlar *et al.,* 1999). Bidirectional corrections are possible but have not yet been frequently implemented because of the perceived complexity of the problem.

Fine resolution data:

In the past, most land cover studies employing high resolution data were carried out with single images (hereafter called 'scenes'), parts of scenes or an assembly of such scenes from different areas. In these cases, radiometric consistency was not an issue because the classification could be optimized individually for each scene. When classifying a scene composite (i.e., a mosaic of scenes), the situation is more complicated. In principle, two options are possible. First (case I), one can classify each scene separately and subsequently reconcile the classes across the mosaic. Another approach (case II) is to assemble a mosaic of scenes for the entire area, establish radiometric uniformity across the mosaic, and then classify it as one entity. In case I, each scene is treated as a separate data set to be classified, using ancillary data that are appropriate for the classification procedure employed. It is thus slow and labour-intensive. The reconciliation of classification across the boundaries between adjacent scenes can be difficult and may require changes in the classification(s) or labelling to be carried out within individual scenes. Even with these measures, discontinuities between scenes are not necessarily removed if significant radiometric differences were present at the outset. Thus, even with much intervention by the analyst, post-classification reconciliation does not guarantee success. On the other hand, case I is highly flexible and can cope with various limitations of the input data.

Because of the infrequent satellite revisits, the compositing of fine resolution data over large areas (case II) employs entire scenes, as opposed to individual pixels in the coarse resolution data. Thus, although radiometric noise is still present, it takes on different forms. First, atmospheric contamination is less limiting because only mostly cloud- and haze-free scenes (preferably <10%) are used for this purpose. Second, bidirectional problems are much less severe, particularly in the case of nadir-looking sensors with a narrow field of view such as the Landsat Thematic Mapper (TM) or Satellite Probatoire d'Observation de la Terre High Resolution Visible Imaging System (SPOT HRV) in nadir mode.

A substantial amount of research has been carried out in the area of radiometric equalization across scene composites. Typically, the algorithms utilize overlaps between adjacent scenes to establish the correction factors. These corrections have been carried out interactively or they can be automated (Chavez ,1988, Schott *et al.,* 1988, Elvidge *et al.,* 1995, Atzberger,1996, Yuan and Elvidge, 1996, Guindon, 1995). However, reconciling adjacent scenes may not be sufficient in larger scene composites. An overall adjustment within the scene composite is preferable, in which the inconsistencies and radiometric differences are balanced to an overall optimum. This is conceptually similar to block adjustment employed in photogrammetry, and can be implemented for scene compositing purposes. With such adjustments, the radiometric errors are minimized across the composite, based on the magnitude of the differences detected in the overlapping areas. These differences can conveniently be detected using overlaps with adjacent scenes or orbits. Because of the scale relationships between scene size and the size of atmospheric high-pressure areas, adjacent scenes along the orbit often have similar cloud contamination.

Even in radiometrically corrected scene composites, some noise will remain. The most important sources are local atmospheric effects such as haze, smoke or cumulus clouds in an otherwise clear-sky scene. Small but potentially significant bidirectional reflectance effects may also be present (Staenz *et al.*, 1984), These residual effects must be dealt with in the classification process.

In addition to purely radiometric noise, the uniformity is also affected by phenological differences among scenes that are more difficult to address. Potential solutions include enlarging the window during which acceptable data are acquired, usually by adding years from which data may be used; using data from other similar sensors; or attempting a 'phenological correction' based on seasonal trajectories established for similar targets. Such corrections

would be required prior to scene compositing. The use of scenes from various sensors in a composite has not yet been explored. In principle, it requires pre-processing the data from the added sensor to resemble the initial one. both spatially and spectrally. Spatial resolution presumes resampling to the same pixel size – a routine operation. Spectral adjustment is conceptually more difficult, and its feasibility will depend on the differences between the two sensors and the spectral characteristics of the targets in the imaged scene. The solution is easiest when the added sensor has more than one spectral band where the initial sensor has only one. The inverse situation has no satisfactory solution and may render the added data set unsuitable. It should be noted that the last two options (phenological correction and compositing scenes from various sensors) will also add radiometric noise of their own. Some form of between-scene reconciliation is therefore likely to be required in many cases. This and the inevitable residual noise in the scene composite suggest that while the case II application may be the preferred solution, in practice it may often have to be supplemented by case I to obtain quality land cover maps.

2.4.2. Classification

Land cover information that can be gleaned from satellite images is the spectral and spatial attributes of individual cover types, There are some differences between coarse and fine resolution data, mainly in the relative importance of these two kinds of attributes. Because of the reduced resolution, the spectral dimension is the most important source of cover type information in coarse resolution images. For fine resolution data, the relative importance of the spatial dimension is higher, although the spectral content still dominates in most cases. In the following discussion, no distinction is therefore made between the two data types.

2.4.2.1. Digital Classification

Numerical techniques for satellite image classification have a long tradition, dating back to at least the early 70s, two types of approaches have evolved and, in spite of recent developments, have remained as the basic options. They differ in the assumptions made about the knowledge of the scene to be classified. In supervised classification, a priori knowledge of all cover types to be mapped within the classified scene is assumed. This knowledge is used to define signatures of the classes of interest, to be applied to the entire scene. In unsupervised classification, no prior information about the land cover types or their distribution is required. Unsupervised classification methods divide the scene into more or less pure spectral clusters, typically constrained by pre-defined parameters characterizing the statistical properties of these clusters and the relationships among adjacent clusters. The assignment of land cover labels to individual spectral clusters is made subsequently on the basis of ground information, obtained in the locations indicated by the resulting clusters. In recent years, numerous variants of these two basic classification methods have been developed. These include decision trees (Hansen *et al.*, 1996); neural networks (Foody *et al.*, 1997), fuzzy classification (Foody, 1998, Mannan *et al.*, 1998) and mixture modeling (van der Meer, 1995) for supervised classification; and classification by progressive generalization(Cihlar *et al.*,1998e),classification through enhancement, and post- processing adjustments (Lark 1995 a, b) for unsupervised techniques.

It seems evident that when one knows what classes are desired and where they occur (at least as a sample), supervised classification strategies are preferable. However, over large areas the distribution of classes is not known a priori. This is compounded by the spatial trends in spectral signatures, resulting in the well known signature extension problem. These complexities render sample selection very difficult and often arbitrary. Thus, where spatial distribution information is not available, e.g., when mapping a large area previously not well known, unsupervised classification is arguably the better strategy, although a supervised method has also been used in such case (Hansen *et al.*, 2000). Unsupervised classification provides more comprehensive information on the spectral characteristics of the area, presents spectrally pure clusters for the labelling step, and gives the opportunity to the analyst to group similar clusters into a smaller number of land cover classes. Perhaps the major problem with unsupervised classification is the effect of controlled parameters (e.g., number of clusters, allowable dispersion around a cluster mean), for the same data set, changes in these can produce different final clusters. A recent way of circumventing this limitation has been to produce a large number of clusters, typically 100–400 (Homer *et al.*, 1997, Cihlar *et al.*, 1998e, Vogelmann *et al.*, 1998). The large number of clusters is then reduced by well defined merging steps. The merging procedure can be based on statistical measures (i.e., again unsupervised), or can be carried out interactively by the analyst. Given the large number of clusters in relation to the small number of resulting land cover types, the impact of control parameters on the final product is diminished in this case. Another

important limitation of unsupervised classification is the potential mismatch between spectral clusters and thematic classes. The hyperclustering approach also mitigates this problem, but additional steps may be necessary (Lark, 1995b). Independent ground information is required by both the supervised and unsupervised method. The important advantage of the latter is that concerns about the location and representativeness of the ground data are much reduced because the clusters are homogenous by definition.

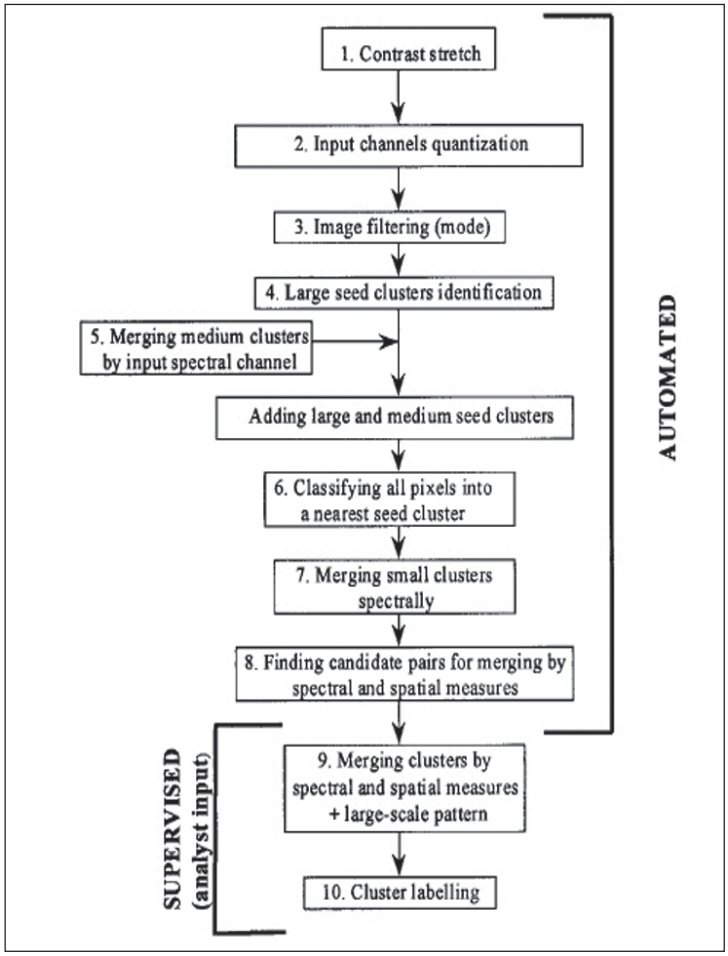

Figure 2.1: Flowchart for Classificationby Progressive Generalization (source: Cihlar et al., 1998)

While most classification strategies have focused on the use of the spectral dimension, the spatial domain also contains important information, especially in fine resolution data. Although numerous algorithms have been developed to quantify spatial relations within images such as texture (Gong *et al.*, 1992), segment homogeneity (Kartikeyan *et al.*,1998) and various others, the spatial dimension has not been used effectively in image classification so far. Spatial measures can be employed in supervised or unsupervised classification as additional channels, in unsupervised classification for cluster merging, as a pre-classifying step resulting in homogenous patches (perfield classifiers), and in other ways. Given the fact that spatial attributes can aid land cover classification, their increased use is most desirable. Recent interest in an effective use of spatial and spectral information (Shimabukuro *et al.,* 1997, Kartikeyan *et al.,* 1998) is therefore encouraging.

An important consideration in land cover classification is consistency and reproducibility. That is, the same result should be obtained by various analysts given the same input data or ideally, even different input data over the same area. In practice, this means that as much as possible of the analysis should be done with objective, analyst-independent procedures. On the other hand, the analyst cannot be entirely excluded from the process because any classification is a human construct, imposing an artificial scheme on the natural world. One way of dealing with this dichotomy is to separate the tasks into distinct phases. For example, Cihlar *et al.,* (1998) described 'classification by progressive generalization', a non-iterative unsupervised classification procedure in which the selection of training samples, classification and initial merging of clusters are automated and thus fully reproducible (figure 2.1), In the last stage preceding labelling, the analyst is presented with suggestions for merging the remaining clusters but the decision is his/hers. The suggested merging is based on both spectral and spatial relations between the remaining cluster pairs. In this way, the number of clusters can be reduced to a few dozen (typically 70–120) without the need for ground information.

Over large areas, applications of frequent mapping and at high spatial resolution are rare at the present time. High resolution satellite data are routinely employed over large areas, e.g., for annual crop assessment (de Boissezon *et al.,* 1993), but in a sampling mode. The minimum required temporal frequency for land cover mapping at present appears to be about 5 years (Ahern *et al.,* 1998, GCOS, 1997), nevertheless, it is desirable to know about the changes in land cover composition, though not the location of these changes for policy purposes, to satisfy reporting requirements, to assess the impact of management measures, or for other reasons. Figure 2.2 illustrates the Lan Use/Land Cover map generated through digitatal classification using multispectral satellite data.

Numerous studies have demonstrated the effectiveness of combining coarse and fine resolution images in estimating the area of one class, e.g., forests (Mayaux and Lambin, 1995, 1997, DeFries *et al.,* 1997, Mayaux *et al.,* 1998),

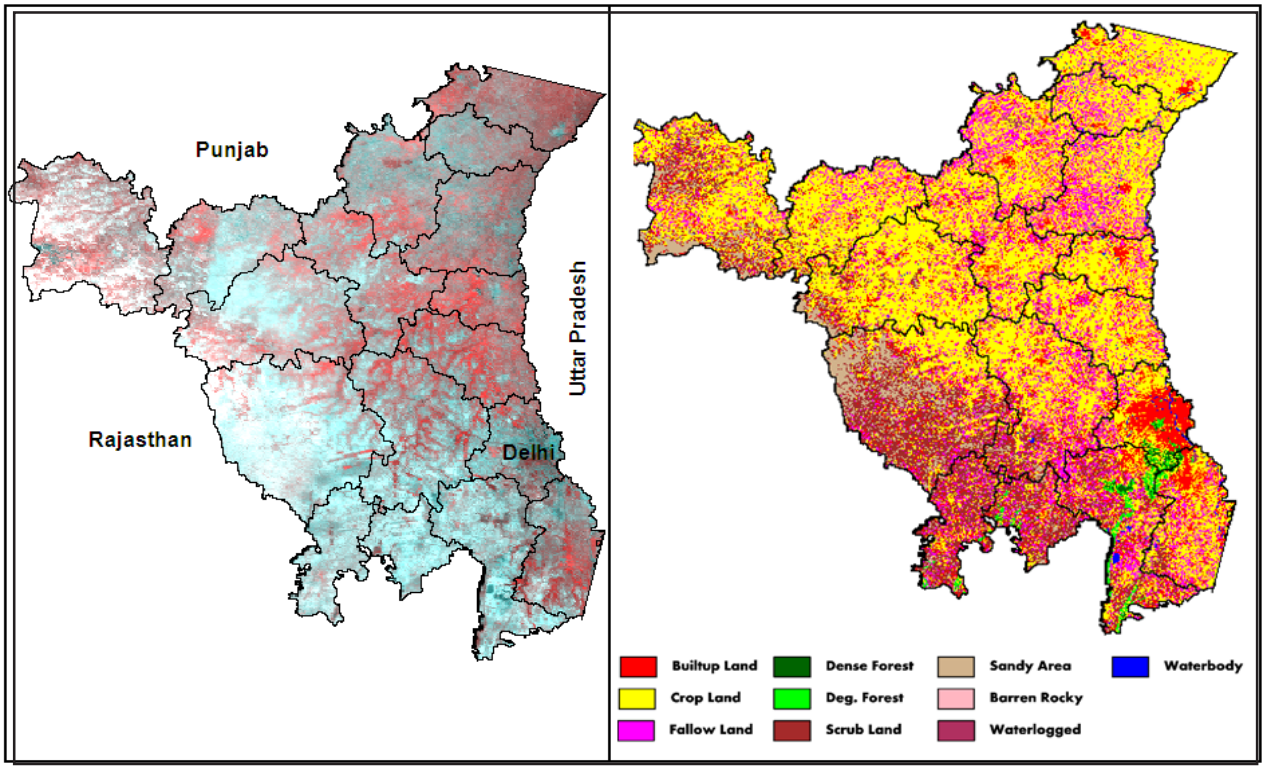

Figure 2.2: Land Use/ Land Cover Map of Haryana State generated through digital supervised classification technique from IRS-WiFS image of February 2002

When dealing with many classes, the methodological considerations are more complex (Walsh and Burk 1993, Moody and Woodcock, 1996). Given a coarse resolution land cover map for an area (domain), it may be used to stratify the domain into units with a similar composition, then sample these with high resolution data. The challenge is in finding appropriate stratification and sampling framework that uses the domain coverage effectively.

2.4.2.2. Manual Classification

Manual, or visual, classification of remotely sensed data is an effective method of classifying land cover especially when the analyst is familiar with the area being classified. This method uses skills that were originally developed for interpreting aerial photographs. It relies on the interpreter to employ visual cues such as tone, texture, shape, pattern, and relationship to other objects to identify the different land cover classes (figure 2.3), The primary advantage of manual interpretation is its utilization of the brain to identify features in the image and relate them to features on the ground. The brain can still beat the computer in accurately identifying image features. Another advantage is that manual classification can be done without a computer, instead using a hardcopy version of a satellite image.

The downside of manual interpretation is that it tends to be tedious and slow when compared with automated classification and because it relies solely on a human interpreter it is more subjective. Another drawback is that it is only able to incorporate 3 bands of data from a satellite image since the interpretation is usually done using a color image comprised of red, green, and blue primary colours.

The technique used in manual interpretation is fairly simple. The analyst views the image on either a computer screen or a hardcopy printout and then draws a polygon around areas that are identified as a particular land cover type. If the land cover delineations are done on a computer screen the land cover map is created during the delineation process. If the interpretation is done on a hardcopy image the resulting map will have to be digitized to convert it into a machine readable format.

2.4.2.3. Hybrid Approach

A hybrid approach combines the advantages of the automated and manual methods to produce a land cover map that is better than if just a single method was used. One hybrid approach is to use one of the automated classification methods to do an initial classification and then use manual methods to refine the classification and correct

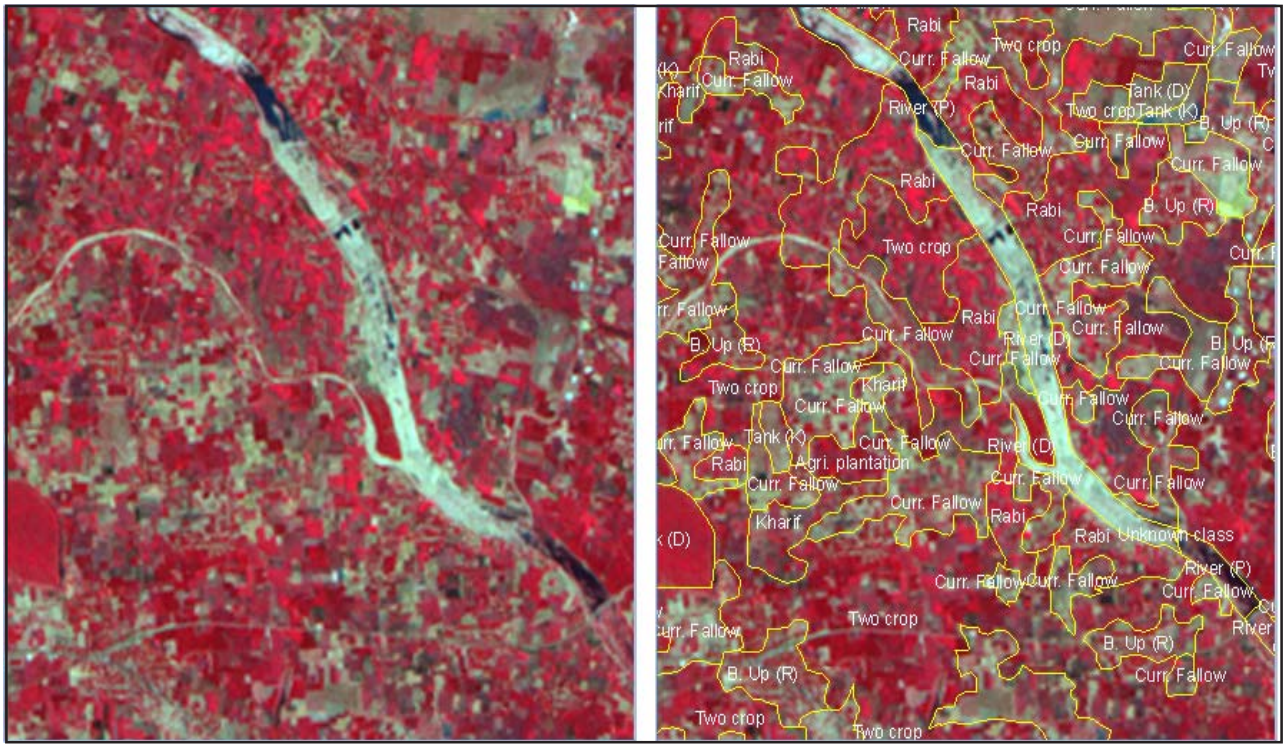

Figure 2.3: Land use /Land Cover map of part of Karaikal, Pondichery generated using manual classification Heads-Up digitisation approach. The FCC pertains to IRS-P6 LISS-III data of February, 2006

obvious errors. With this approach a reasonably good classification can be obtained quickly with the automated approach and then manual methods can be used to refine the classes that did not get labeled correctly.

The editing process requires that the analyst be able to compare the classified map with either the original satellite image or some other imagery that can be used to identify land cover features. To compare a classified map with imagery it is helpful to have access to software that allows the analyst to flicker between two images (the land cover image and the original satellite image) or slide one image over the other on the computer display using a technique often called “swiping”. By doing these comparisons the analyst gets a sense of the quality of the classification. When errors are spotted they can be edited using tools common in many image processing software packages. In most cases, visually editing a classified map will improve the accuracy of the final product.

2.4.3. Other methods of classification in vogue

A wide variety of methods exist to derive measures of vegetation cover from remotely sensed data. These methods range widely in complexity, sophistication, and accuracy. The discrepancies are important for researchers to consider when incorporating or generating vegetation data for larger studies. Since the accuracy disparity between techniques is well documented, it should concern researchers who rely on simple linear vegetation indexes for accurate vegetation cover estimates. It is important to determine precisely how different the vegetation measurements will be between a simple, easy method, as compared to a more sophisticated, yet perhaps less accessible one.

Arguably the most widely used of these techniques is the Normalized Difference Vegetation Index (NDVI), It is a simple operation, needing little time, expertise, or processing capacity, which uses two bands of data to generate an index of relative vegetation abundance. Spectral Mixture Analysis (SMA) is a more sophisticated approach, using all bands of data in an image to generate percent cover of various specified ground covers within each pixel. Unfortunately field data was not available to assess the absolute accuracy of either of these techniques. However, a good evaluation is possible based on data comparisons, detailed image interpretation, reviews of possible error sources, and reviews of the wealth of literature on both these techniques.

2.4.3.1. Normalized Difference Vegetation Index

The dominant method for identifying vegetation using remotely sensed data is through vegetation indexes. Vegetation indexes are algorithms aimed at simplifying data from multiple reflectance bands to a single value correlating to physical vegetation parameters (such as biomass, productivity, leaf area index, or percent vegetation ground

cover) (Tucker, 1979). These vegetation indexes are based on the well-documented unique spectral characteristics of healthy green vegetation over the visible to infrared wavelengths.

Healthy green vegetation generally reflects very little solar energy in the visible wavelengths (0.4-0.7 μm), with a sharp increase in reflectance in the near-infrared wavelength region (0.7-1.1 μm), This "red edge" is unique to vegetation as a surface material. Dead or senescent vegetation and soil generally reflect relatively greater amounts of energy in the visible wavelengths and less in the near-infrared. This unique spectral property of green vegetation is used in various indexes ranging in complexity from applying correlation coefficients to brightness values of a near-infrared band, to multi-band ratioing combined with complex algorithms. Arguably the most successful and commonly used of these techniques is the Normalized Difference Vegetation Index (NDVI).

NDVI is the traditional vegetation index used by researchers for extracting vegetation abundance from remotely sensed data (Tucker, 1979). It divides the difference between reflectance values in the visible red and near-infrared wavelengths by the overall reflectance in those wavelengths to give an estimate of green vegetation abundance (Tucker, 1979). In essence, the algorithm isolates the dramatic increase in reflectance over the visible red to near infrared wavelengths, and normalizes it by dividing by the overall brightness of each pixel in those wavelengths. Specifically NDVI is:

$$NDVI = IR-Red / IR+Red$$

where the values in either band have been converted from raw DN values to radiance of solar electromagnetic radiation, The result of this algorithm is a single band data set, ranging from -1 to 1, with values corresponding to photosynthetic vegetation abundance. NDVI has been used extensively to measure vegetation cover characteristics on a broad-scale worldwide, and has been incorporated into many large-scale forest and crop assessment studies (Peterson *et al.*, 1987; Asrar *et al.*, 1984), It is used to provide weekly vegetation maps, monitor crops over large regions, monitor vegetation change in much of the tropics, and estimate biomass.

Despite this wide use, some well-documented accuracy limitations exist. The limitations of vegetation indexes emanate from the fact that relationships between vegetation abundance and electromagnetic reflectance values in complex vegetation structures (and areas with high vegetation abundance) are many times nonlinear, whereas vegetation indexes are simple linear algorithms. Therefore, because of increased mutual shadowing in mature stands, aging forests may show a decrease in NDVI while actual biomass increases. Consequently, once vegetation indexes reach a threshold level they no longer accurately correlate to actual vegetation abundance (Wiegand *et al.*, 1991),

Studies have also shown that background soil color affects NDVI, especially in heterogeneous scenes (Huete, 1988). Because the difference between the bands is divided by the overall brightness of the two bands, extreme variations in background soil brightness can cause NDVI values to be artificially high or low. In theory, pixels with dark soil backgrounds, such as the basaltic soil patches, have a lower overall brightness. Therefore NDVI values would be artificially higher in these areas, as the difference between the visible and near infrared would be divided by less. Similarly, bright soil backgrounds would raise the overall brightness levels and therefore vegetation values derived through NDVI would be artificially lower than areas with similar abundance that have dark soil backgrounds. This background soil effect is additionally complicated by multiple scattering effects between vegetation and soil (Huete, 1988).

While NDVI has been shown to correlate reasonably well in medium to low vegetation abundance with various ecological parameters (such as leaf area index or green leaf biomass) (Anderson *et al.*, 1993), the literature suggests that in certain environments specific types of changes in vegetation may not be accurately depicted by NDVI (Asrar, 1984; Peterson *et al.*, 1987).

2.4.3.2. Spectral Mixture Analysis

Many other means of quantifying vegetation cover from remotely sensed data have been developed. One of the most promising is Spectral Mixture Analysis (SMA), a more sophisticated technique that utilizes all available bands of data to separate each pixel into fractions of specified land covers (Huete, 1986). The conceptual model used to develop SMA is that most pixels in scenes are mixtures of a few specific ground covers (or endmembers), especially in arid areas and mixed land use environments. If pure spectra of spectrally distinct primary land cover materials (i.e., vegetation, water and soil) in a scene can be found, a data set can be converted to fractions of each pre-defined land cover for each pixel (Adams *et al.*, 1995; Huete, 1986).

Linear mixture modeling assumes that endmembers (pre-defined primary land covers) are arranged in spatially distinct areas in each pixel and can therefore be extracted through the application of specific algorithms. Each pixel is modeled as a spatial mixture of endmember spectra to determine the physical abundance of land cover types in each pixel area.

The results of SMA are the percent coverage of each defined ground cover material, or endmember, in each pixel. This method had the advantage of deriving not only vegetation data, but land cover fractions for all the endmembers used, as well. Additionally, the data is generated into a physically-based measure, and therefore easily integrated into studies as measures of percent live cover rather than an indexed, relative measure. Elmore *et al.*, 2000 found percent live cover estimates using Spectral Mixture Modeling to be accurate within 4.0% and change in percent live cover to have a precision of 3.8%, Specific examples of research using SMA include monitoring rural land use changes and their effects on soil characteristics in Europe (Sommer *et al.*, 1998), estimating erosion (Metternicht & Fermont, 1998).

Despite the utility and accuracy of this method, limitations to SMA exist. In addition to being limited in the total number of possible endmembers. SMA is limited by the type of endmembers that can be used, especially when using multispectral data (Adams, *et al.*, 1995; Roberts *et al.*, 1993). Endmembers must be spectrally distinct from one another and generally account for the dominant land cover and spectral characteristics of the scene. Therefore, without hyperspectral data, it is virtually impossible to use this method to generate fractions of different types of photosynthetic vegetation. Generally researchers are limited to vegetation, soil, sand, and shade when using multispectral satellite imagery. Additionally, this process requires a good deal of processing capabilities and expertise in order to find pure spectra of appropriate endmembers in the scene. However, it is important to emphasize the advantage of additional datasets of endmember surface cover that are generated using SMA, as these can be used to extract more information from scenes than vegetation index information alone.

2.5. Ground Data Collection

Although land cover maps are often made without visiting the field, there are good reasons why field visits should be made. The two primary reasons for visiting the area that is being mapped are to collect data that can be used to train the algorithm or the interpreter and to collect data that can be used to evaluate the land cover map and estimate the accuracy of the individual classes (a process called validation). At a minimum, these data can be collected in one trip but often two or more trips are preferred so that validation information can be systematically collected using a sampling design based on the classification results.

Data collected in the field must be geo-referenced so that the point where the data were collected can be located on the imagery. GPS receivers are commonly used to record this location information. The type of information collected can range from detailed notes describing a site to a photograph of the site. Some of the detailed information that can be recorded includes: type of vegetation, crown closure, slope, aspect, soil type, and other bio-physical characteristics that are important to identify the land cover type. If photographs are taken it is a good idea to record the direction the camera was pointed and to make notes about the area to supplement the content in the photograph. For example, you could add information about species composition, tree height, and possibly land use.

When land cover maps are created without using field data from the region of interest it is difficult to predict the accuracy of the final land cover map. An analyst with significant experience may be able to produce a land cover map of high quality but without validation information the true accuracy of the image classification quality is not known.

2.6. Accuracy Assessment

No land cover classification project would be complete without an accuracy assessment. It may well be noted that concern about the accuracy of land cover maps did not exist before the advent of satellite-based methods and photo interpretation-based maps were assumed 100% accurate (this is still often the case, e.g., in forest inventories). The need for accuracy assessment initially arose as part of algorithm development, and it was extended into an important tool for users of land cover products. Many papers have been written on the methods of accuracy assessment, and various accuracy measures have been defined (e.g., Hord and Brooner, 1976, Thomas and Allcock ,1984, Rosenfield and Fitzpatrick-Lins,1986, Congalton, 1991, Hammond and Verbyla, 1996, Edwards *et al.,* 1998). At this point, the principles of accuracy assessment are well known. The ideal requirements are based

on sampling theory, but practical considerations regarding access, resources, etc., constrain the 'desirable'. There are also methodological difficulties with respect to spatial resolution, mixed pixels in coarse resolution satellite data being of special relevance. At the coarse resolution, many pixels contain a mixture of cover types even in a fairly general classification scheme such as land versus water, thus creating a difficulty in deciding on the correctness of the assigned label. An obvious approach is to assign the pixel to the single largest cover type within the pixel (e.g., Cihlar *et al.,* 1996, Hansen *et al.,* 2000). This can be accomplished with the aid of fine resolution maps where these are available. However, it is questionable when the dominant land cover type covers much less than 50% of the pixel. Furthermore, since the high resolution maps have errors (as do maps obtained through airborne techniques such as aerial photographs, airborne video, etc.), a definitive accuracy assessment needs to contain 'ground truth' as part of the sampling design. In addition to purely methodological considerations, accuracy assessment tends to be strongly constrained by the resources available. The acquisition of verification data can be expensive, especially if a statistical design is rigorously followed, access is difficult etc. Within these constraints, however, creative solutions are possible,

For example, Kalkhan *et al.,* (1998) described the combined use of air photo interpretation and a sample of ground data to assess the accuracy of Landsat-derive proportions of land cover types, with 200 samples at the first stage and only 25 among these described in the field. To complicate matters further, ground truth may not necessarily be correct either; its errors can be due to incorrectly specified location, very small land cover patches being used, the inability of the surveyor to see a larger area of the surface, inconsistencies in labelling, etc. Thus, in practice, accuracy assessment is likely to remain a matter of compromise between the ideal and the affordable, or 'A balance between what is statistically sound and what is practically attainable must be found (Congalton, 1996).

2.7. Land Use Land Cover Mapping - Issues

Since land cover changes over time, the temporal resolution is a critical consideration in choosing the appropriate data type. Figure 2.4 portrays the relationships between spatial resolution, temporal resolution and satellite data sources. The dotted line identifies the principal domain of interest to large-area land cover mapping employing satellite data. Such mapping is not required for very small areas or very frequently (i.e., the lower left part of the graph). Thus, the domain of interest spans the range between two extremes: 'coarse' resolution at frequent time intervals (lower right part of the plot), and 'fine' resolution at long intervals (upper left). It should be noted that the labels 'coarse' and 'fine' are relative and that each covers a range of resolutions; for example, 'coarse' is appropriate for AVHRR 8 km data but not for MODIS 250 m data. The terms are used for brevity to categorize a sensor but the qualification must be kept firmly in mind.

The range between the above extremes is a continuum accessible through satellite remote sensing techniques. Theoretically, the entire range could be covered using satellite data from the lower left corner of the range. i.e., data obtained very frequently and at a high spatial resolution. However, this is a practical impossibility at the present and a cost-ineffective solution at any time because land cover does not change rapidly enough in all places. Thus, a more realistic approach is to consider the range as consisting of discrete components.

Region A in the figure represents mapping with frequently obtained coarse resolution data. With such data it is possible to prepare higher level data sets through pixel compositing procedures (Holben, 1986), thus allowing global land cover maps to be produced at short intervals. In region B, fine resolution data are obtained relatively infrequently. Therefore, along with unavoidable cloud contamination and seasonal phenological effects, data sets suitable for land cover analysis can be compiled only over longer time periods. A coverage of large areas is thus produced through 'scene compositing', i.e., by mosaicking the individual images. Region C can utilize land cover products generated by methods in A or B. So far, the approach has been to employ A for mapping and B for training and/or validation (e.g., Cihlar and Beaubien, 1998, DeFries *et al.,* 1998, Hansen *et al.,* 2000). Region D presents the greatest challenge, requiring frequent coverage at fine resolution. While this is not now realistically possible over large areas, it should be feasible to synergistically combine data and products from parts A and B. So far, satellite-based large-area mapping has been mostly performed in region A because of the availability of data and the manageable computational demands. Land cover maps at 8 km resolution or coarser were prepared from AVHRR Global Area Coverage (GAC) data (DeFries and Townshend 1994, DeFries *et al.*, 1998). Maps for landscape regions (e.g., Cihlar *et al.*, 1997a,b, Steayert *et al.*, 1997, Laporte *et al.*, 1998) or larger areas (Loveland *et al.*, 1991, 1995, Cihlar and Beaubien, 1998) have been produced in recent years with 1 km AVHRR data. With the availability of the global AVHRR 1 km data set , intensive activities led to global products at the same resolution (Loveland and Belward, 1997, Hansen *et al.* 2000, Loveland *et al.*, 2000). So far, region A maps have been

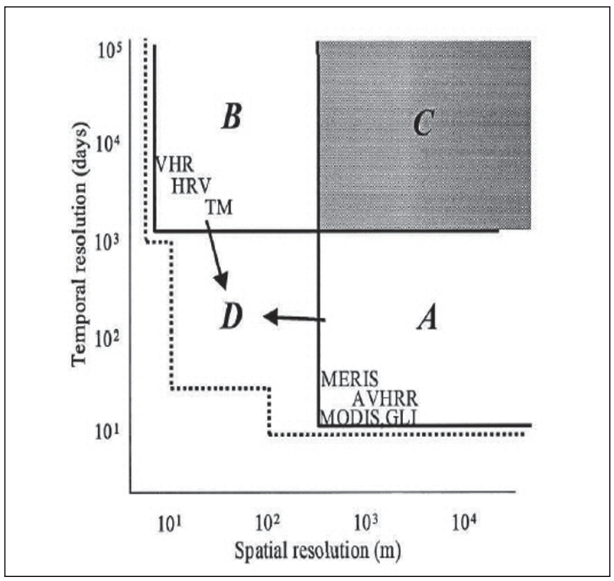

Figure 2.4: Land Cover Mapping requirements expressed in spatial and temporal resolutions. The acronomy represents satellite sensors at both fine and coarse resolutions; VHR – very high resolution sensors (Source: Cihlar,2000)

produced infrequently. However, the same techniques can be used to generate land cover maps at shorter time intervals, as short as the minimum compositing period resulting in a usable data set. For region B, the work so far has been limited mostly to studies over small areas, such as a Landsat scene or less. Among the exceptions is the US GAP program (Jennings, 1995), through which maps over entire states have been produced (Homer *et al.*, 1997), humid tropical deforestation studies, and other experimental products prepared through scene compositing (Guindon 1995, Homer *et al.*,1997, Beaubien *et al.*, 1999, Vogelmann *et al.*, 1998). Apart from some methodological studies (e.g., Moody and Woodcock, 1996, Cihlar *et al.*, 1998e), little work on region D has been carried out.

2.8. Research needs and Opportunities

In general, research needs and opportunities are related to present and upcoming information requirements over large areas, and the expected evolution in the relevant data and technological tools. In all these areas, land cover mapping applications will receive a strong boost due to: increased demand for information because of concerns about climate change and sustainable development; several new sensors designed with land cover mapping as an important application; and the continuing rapid growth in computing technology.

2.8.1. Pre-processing

Assuming that the range of land cover mapping requirements is represented by all four areas A–D, the focus needs to be maintained on improving the methods for optimally using data from new coarse and fine resolution sensors. For coarse resolution sensors, this means improved methods for image corrections, especially atmospheric, sensing geometry and pixel contamination. The objective should be to produce a cloud-free composite image which has radiometric properties of a single-date, fixed geometry image obtained during the same period. The availability of high quality, calibrated data from MODIS, MERIS, VGT and GLI will make major improvements possible. This goal cannot be fully achieved for most sensors because of the changing spatial resolution with the viewing angle, although in some cases (e.g., SPOT VGT, Saint 1992) the resolution is view angle-independent. Innovative ways must be found to define and implement robust, accurate and automated algorithms for the generation of superior composite products. Newly available tools are calibrated data, improved spectral coverage (new as well as sharpened bands), and the considerable progress made in recent years in defining algorithms for atmospheric parameters extraction, bidirectional corrections, etc. Although the ultimate solution is an accurate detection of contaminated pixels and retention of all remaining ones with the associated angular information, compositing will be a necessary pre-processing step for land cover classification in the foreseeable future. Further work on compositing algorithms thus appears warranted, with the currently ubiquitous maximum NDVI criterion used as the basis for comparison. In the case of fine resolution sensors, the main pre-processing need is for accurate and robust scene compositing. This implies accurate sensor calibration and atmospheric corrections, although these measures alone are not sufficient. Local atmospheric effects (thin clouds, haze, smoke), subtle bidirectional effects, or small phenological changes may yield to algorithmic solutions but they pose a significant challenge. Much more research is needed on the preparation of large-area scene composites, to work out the theoretical and practical problems of dealing with residual atmospheric, phenological and other types of noise. Research is also required on compositing images from different sensors, with the objective of producing mosaics of the same consistency as from one sensor. Once these techniques are developed sufficiently well to be automated, it should be possible to produce 'virtual scene composites', on the basis of which the user could routinely order data set(s) covering the geographic area of interest over the specified compositing period(s). Of course, if any of the above radiometric differences within the composite are not resolved at the pre-processing stage, they must be dealt with during classification.

2.8.2. Classification

Cihlar *et al.,*(1998e) proposed that classification algorithms should ideally satisfy the following requirements: accuracy; reproducibility by others given the same input data; robustness (not sensitive to small changes in the input data); ability to fully exploit the information content of the data; applicability uniformly over the whole domain of interest; and objectiveness (not dependent on the analyst's decisions). Many present digital image classification methods do not meet these criteria, and none meets them completely. Yet, such criteria are fundamental to a scientifically based methodology. Some of the implications are briefly discussed below. The interest and innovation in image classification methods has continued in recent years, as has the 'creative tension' between supervised and unsupervised approaches and their variants. This will undoubtedly continue, and it is a healthy and beneficial process which should lead to better algorithms. Work is needed especially in mitigating the limitations of the two basic approaches, supervised and unsupervised, stemming from the fundamental assumptions (Chuvieco and Congalton, 1988, Bauer *et al.,*1994, Lillesand ,1996).

Although initially digital spectral values were the main input for classification, various types of data have been considered more recently, either during classification (DeFries *et al.,*1995) or at the labelling stage (Brown *et al.,*1993). This will be a continuing requirement, especially as the number of spectral bands increases and new bands may prove to carry unique information content (e.g., Eva *et al.,*1998). There is a strong need to make better use of spatial information. After all, useful land cover maps were produced from this attribute alone before the advent of colour photography and digital classification. In addition to texture (which is easily computed but not necessarily an informative attribute), more attention needs to be given to other measures such as pattern, shape and context (Rabben 1960). Another problem is in optimally and synergistically combining spectral and spatial elements, using one to improve the quantity and quality of land cover information obtained from the other.

A special challenge in image classification is to isolate, and minimize if possible, the role of the analyst in the classification. This is important because reproducibility is a fundamental requirement for any method or product. When the analyst's input is distributed throughout the classification procedure, the result is not reproducible. On the other hand, as long as discrete (thus artificial to some degree) classification legends continue to be used, the analyst's role cannot be eliminated because the class distinctions do not necessarily correspond to equivalent distinctions in reality. However, it is possible to assign a more precise role to the analyst, and to limit his input to specific portions of the classification procedure. This will improve the reproducibility of the entire process, and will highlight the impact of the analyst's decisions. A range of options are possible here. For example, in fuzzy classification approaches, the analyst's role can be reduced to defining the acceptable fractional composition of each class in terms of individual components.

A further step in reducing the subjective component in classifications is to first prepare specific biophysical products with continuous variables. For example, Running *et al.,*(1995) proposed that three variables (permanence of above ground live biomass, leaf area index, leaf longevity) characterize vegetated land cover. If such separate products can be derived from satellite data, individual users can construct an optimized classification legend for all the land cover types or conditions present in the area to meet their specific objective. This does not eliminate need for classifications but renders the whole process more useful because of a better fit of the classification with specific user needs. The challenges here stem from the fact that 'land cover' can imply various characteristics, not all easily translated into biophysical variables that can be derived from satellite data (e.g., the hydrological regime). Nevertheless, this area needs to be pursued because of the potential gains in the utility of satellite-derived information products. The work done so far on two or a few classes (e.g., Iverson *et al.,*1994, Zhu and Evans 1994, DeFries *et al.,*1997) needs to be extended to multiple cover types.

Although for scene composites (Region B, figure 2.4) the desirable approach is classifying the entire mosaic as one entity, it is very likely that data limitations will make this impossible in many cases. Local adjustments will thus be needed to achieve optimum results. The locations of these should be evident based on input image quality, but algorithms will be required to make this process reproducible and consistent.

Further research is needed on the synergistic use of data from coarse and fine resolution sensors to span the entire range of requirements represented in figure 2.4. Region D is the most demanding, with high spatial and temporal resolutions. It is also an area where large progress can be expected.

2.9. Land Use Land Cover Change

Changes in land use and land cover impact both environmental quality and the quality of life, two aspects that impact human wellbeing. Changes in habitat, water and air quality and the quality of life are some of the environmental, social and economic concerns associated with land use and land cover changes.

Habitat: Land use by human leads to changes in land cover that can negatively impact biodiversity. Conversion of natural wood- and grass-lands to more developed uses decreases the amount of habitat available. The pattern of human land use also tends to result in a patchy landscape, fragmenting habitats. Some species of plants and animals do better in patchy, fragmented environments, while others need large, uninterrupted areas.

Water Quality: Changes in land use can affect the volume, timing and quality of runoff water. More-developed land uses have higher proportion of impervious surface (areas where water can not soak into the ground, such as roadways, parking lots, and building roofs). As the amount of impervious surface increases, rainstorm runoff increases in volume, increasing the risk of flooding and increasing the amount of pollutants carried into streams and lakes. Human use of land also disturbs natural land cover, increasing the potential for soil erosion into streams and lakes.

Quality of Life (aesthetics, recreation, congestion): Land use and land cover changes can affect quality of life when those changes impact landscapes that have aesthetic value (scenic views), or when the quality and quantity of the landscapes are reduced in areas that are attractive for recreational activities. Also, changes in Land Use and Land Cover can affect traffic patterns that can have positive or negative effects on congestion.

Air Quality: The pattern of land use in a region can affect its air quality. If residential areas are located far from shopping and work centers, automobile use and emissions will be higher. If forests or other natural areas that purify air are developed, local air quality can worsen. Changes in vegetative cover can also lead to local changes in climate.

Global Carbon Cycles: More-natural landscapes can capture and store carbon in the soil, decreasing the amount of carbon dioxide in the atmosphere. If vegetation is cut and/or the soil is disturbed, stored soil carbon can be released back into the atmosphere. Several studies have examined the social and economic factors that drive Land Use and Land Cover change. These include:

Population Growth or Decline: As a region's population grows, the new residents need housing, as well as places to work and shop. In a region with declining population, there will be less new construction of homes and businesses.

Economic Growth: A booming regional economy will result in construction of new commercial and industrial buildings to house that activity. As the economy grows, the new jobs created will attract workers, leading to population growth, leading to construction of new homes and places to shop. As incomes rise, household may choose to build new larger homes on larger lots, leaving smaller, older houses vacant.

Demographics: The average number of people living in a household has been decreasing over time. Therefore, more housing units are needed to house the same number of people. The number of retired households is increasing, and these households tend to have few members. Meanwhile, the proportion of non-white households is also increasing, These households tend to have more members on average than white households.

Agricultural and forest products: A change in the price of agricultural or forest products can affect landowners' decisions whether to keep the land in those uses. Policies aimed at supporting agricultural prices provide an incentive to keep land in farming.

Regional and local planning and policies: Regions can influence the rate at which land use and land cover change through a variety of means.

2.9.1. Land Use & Land Cover Change Detection with Remote Sensing data

An increasingly common application of remotely sensed data is for change detection. Change detection is the process of identifying differences in the state of an object or phenomenon by observing it at different times (Singh, 1989). Change detection is an important process in monitoring and managing natural resources and urban development because it provides quantitative analysis of the spatial distribution of the population of interest. Change detection is useful in such diverse applications as land use change analysis, monitoring shifting cultivation, assessment of deforestation, study of changes in vegetation phenology, seasonal changes in pasture production, damage assessment, crop stress detection, disaster monitoring, day/night analysis of thermal characteristics as well as other environmental changes (Singh, 1989).

Macleod and Congalton (1998) list four aspects of change detection which are important when monitoring natural resources:

- Detecting that changes have occurred
- Identifying the nature of the change
- Measuring the areal extent of the change
- Assessing the spatial pattern of the change

The basic premise in using remote sensing data for change detection is that changes in land cover result in changes in radiance values which can be remotely sensed. Techniques to perform change detection with satellite imagery have become numerous as a result of increasing versatility in manipulating digital data and increasing computing power.

A wide variety of digital change detection techniques have been developed over the last two decades. Singh (1989) and Coppin & Bauer (1996) both provide excellent and comprehensive summaries of methods and techniques of digital change detection. Coppin & Bauer (1996) summarize eleven different change detection algorithms that were found to be documented in the literature. These include:

- monotemporal change delineation
- delta or post-classification comparison
- multidimensional temporal feature space analysis
- composite analysis
- image differencing
- image ratioing
- multitemporal linear data transformation
- change vector analysis
- image regression
- multitemporal biomass index
- background subtraction

The scientific literature reveals that digital change detection is a difficult task to perform accurately and unfortunately, many of the studies concerned with comparative evaluation of these applications have not supported their conclusions by quantitative analysis (Singh, 1989). Digital change detection is affected by spatial, spectral, temporal, and thematic constraints. The type of method implemented can profoundly affect the qualitative and quantitative estimates of the change. Even in the same environment, different approaches may yield different change maps. The selection of the appropriate method therefore takes on considerable significance. Not all detectable changes, however, are equally important to the resource manager. On the other hand, it is also probable that some changes of interest will not be captured very well, or at all by any given system. Figure 2.5 illustrates LULC change detection capabilities of satellite data.

According to recent research by Coppin & Bauer (1996), image differencing appear to perform generally better than other method of change detection; and such monitoring techniques based on multispectral satellite data have demonstrated potential as a means to detect, identify, and map changes in forest cover. Image differencing is probably the most widely applied change detection algorithm for a variety of geographical environments (Singh, 1989). It involves subtracting one date of imagery from a second date that has been precisely registered to the first.

The vegetation index (VI) differencing is one of the most popular change detection algorithms. The fundamentals for this technique rely on the idea that if VIs are correlated to biomass, then the decrease of vegetation can be detected by a difference of VI images (one before and other after the land cover change). In this method, the first step is to calculate a differencing image by subtracting two coregistered images, followed by the application of a threshold to distinguish significant spectral differences as areas of land cover change. Four types of VI can be tested: (1) Normalised Difference Vegetation Index (NDVI) one of the most common indices used in remote sensing studies, (2) the Atmospherically Resistant Vegetation Index (ARVI), which accounts for the atmospheric influence in the sensor output, (3) the Soil Adjusted Vegetation Index (SAVI) (Huete, 1988) that accounts for the

background effect, and (4) the Modified Soil Adjusted Vegetation Index (MSAVI2), which is an improvement of SAVI. Change Vector Analysis (CVA) is another well-accepted change detection technique. The change vector of a pixel is defined as the vector difference between the multi-band digital vectors of the pixel on two different dates. When a forest suffers a change, its spectral characteristics also change. The vector describing this change is known as the pixel change vector and describes the intensity and the direction of the change that occurred between the first and the second date. The CVA is applied to two co-registered bands of an image, in two different dates. With this method, two images are computed: one image for the vector intensity and another for the vector direction. The first image contains the information of change, while the second contains information on the type of change. CVA can be applied to two different spectral data sets: original TM bands and the components of the Tasseled Cap transformation, brightness (B), greenness (G) and wetness (W).

Principal Components Analysis (PCA) is another technique available. PCA is one of the most popular multivariate analysis techniques for data reduction. The PCA transformation leads to the description of multidimensional data in which axis variables are uncorrelated. In the transformed data, the first variable or component (PC1) contains the higher variance present in the data while the subsequent variables contain decreasing proportions of data scatter. Experiments have shown that the first components contain the unchanged spectral information, while the changed information is contained in the latter components (Byrne et al., 1980). PCA can be performed on original or standardised data, The former uses the covariance matrix, and the latter uses the correlation matrix.

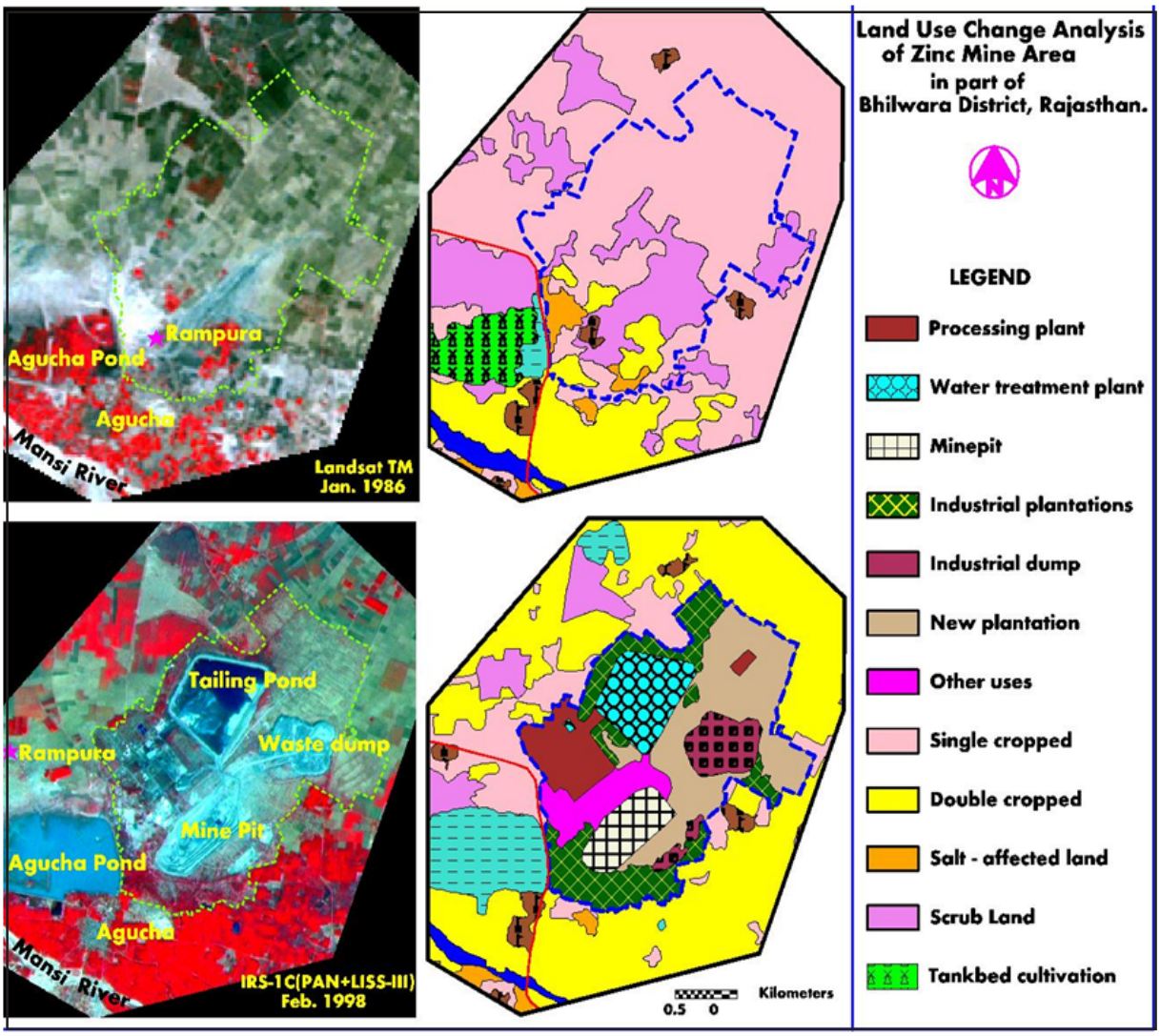

Figure 2.5: Land Use/Lland Cover Chage detection using post-classification comparision technique

2.10. Land Use Modeling

Land is a dynamic canvas through which human and natural systems interact. Understanding the many factors influencing Land Use Cover Change (LUCC) has been the focus of scientific study across multiple disciplines, locations, and scales. But direct measurements alone are not sufficient to provide an understanding of the forces driving change. Linking observations at a range of spatial and temporal scales to empirical models provides a comprehensive approach to understanding land-cover change (Turner *et al.*,1994).

The primary utility of models is to provide a systematic approach to understanding a research problem. An important aspect is the link between direct observations, case studies, and models in an effort to test or identify dominant features of land-cover change. Development of diagnostic models can lead to an improved understanding of the current and recent situation and at the same time provide credible, geographically-referenced predictions. The length of time over which a prediction is valid is a function of the persistence of the observed phenomena. There is evidence to suggest that much, if not most, land-cover change is spatially and temporally persistent over 10 to 15 year intervals. It should be noted, however, that certain events can alter trends significantly and rapidly. Changes in political, institutional, and economic conditions can cause rapid changes in the rate or direction of land-cover change. Therefore, an effort to understand the primary kinds of influences which cause land-cover change trends to diverge rapidly is also an important component of this programme.

Several different approaches are used to project future Land Use and/or Land Cover. These can be divided into two broad categories: a) models that predict total land use change for a region, and b) models that predict Land Use for specific parcels or grid cells. If the analyst wants to know the total amount of land use change that will occur in a large region like a state, then the first type of model is appropriate. On the other hand, if the analyst wants to know where in the region land use change will occur, or to project what will happen at a specific place, then the second type of model is appropriate.

The goal of this discussion is to provide a broad overview of these models, offer our perspective on their potential role in LUCC modeling, discuss some key issues related to their development and implementation, and briefly review ongoing research based on this modeling paradigm.

2.10.1. Approaches to Modeling Land-Use/Cover Change

The strengths and weaknesses of seven broad, partly overlapping, categories of models: mathematical equation-based, system dynamics, statistical, expert system, evolutionary, cellular, and hybrid are discussed for comparison. This review is not exhaustive and only serves to highlight ways in which present techniques are complemented by those models that combine cellular and agent-based models. More comprehencive overview of LUCC Modeling techniques is given by Agarwal, 2000.

Equation-Based Models

Most models are in some way mathematical, but some are especially so in that they rely on equations that seek a static or equilibrium solution. The most common mathematical models are sets of equations based on theories of population growth and diffusion that specify cumulative land-use/cover change over time (Sklar and Costanza, 1991). A variant of this model is based on linear programming (Howitt, 1995), potentially linked to GIS information on land parcels (Cromley and Hanink, 1999). A major drawback of such models is that a numerical or analytical solution to the system of equations must be obtained, limiting the level of complexity that may practically be built into such models.

System Models

System models represent stocks and flows of information, material, or energy as sets of differential equations linked through intermediary functions and data structures. Time is broken into discrete steps to allow feedback. Human and ecological interactions can be represented within these models, but they are dependent on explicit enumeration of causes and functional representation, and they accommodate spatial relationships with difficulty (Sklar and Costanza, 1991).

Statistical Techniques

Statistical techniques are a common approach to modeling land-use/cover change, given their power, wide acceptance, and relative ease of use. They include a variety of regression techniques applied to space and more

tailored spatial statistical methods . Unless they are tied to a theoretical framework, statistical techniques may downplay decision making and social phenomena such as institutions. Successful examples of combining theory and statistics are provided by spatial econometrics (Leggett and Bockstael, 2000).

Expert Models

Expert models combine expert judgment with nonfrequentist probability techniques such as Bayesian probability or Dempster-Schaefer theory or symbolic artificial intelligence approaches such as expert systems and rule-based knowledge systems (Lee *et al.*, 1992). These methods express qualitative knowledge in a quantitative fashion that enables the modeler to determine where given land uses are likely to occur. It can be difficult to include all aspects of the problem domain, however, which leaves room for gaps and inconsistencies.

Evolutionary Models

Within the field of artificial intelligence, symbolic approaches such as expert systems are complemented by a biologically inspired evolutionary paradigm. Exemplars of this field, such as artificial neural networks and evolutionary programming, are finding their way into LUCC models (e.g., Balling *et al.*,1999). In brief, neural networks are silicon analogs of neural structure that are trained to associate outcomes with stimuli. Evolutionary programming mimics the process of Darwinian evolution by breeding computational programs over many generations to create programs that become increasingly able to solve a particular problem.

Cellular Models

Cellular models (CM) include cellular automata (CA) and Markov models. Each of these models operates over a lattice of congruent cells. In CA, each cell exists in one of a finite set of states, and future states depend on transition rules based on a local spatiotemporal neighborhood. The system is homogeneous in the sense that the set of possible states is the same for each cell and the same transition rule applies to each cell. Time advances in discrete steps, and updates may be synchronous or asynchronous (Hegselmann 1998). In Markov models, cell states depend probabilistically on temporally lagged cell state values. Markov models may be combined with CA for LUCC modeling as evidenced by joint CA-Markov models (Balzter, Braun, and Kohler 1998). Global land-use/cover change in response to climate change (Alcamo, 1994).

Cellular models have proven utility for modeling ecological aspects of land-use/cover change, but they face challenges when incorporating human decision making. It is necessary to use complex hierarchical rule sets to differentiate between the kinds of decision making that apply to groups of cells, such as local land tenure structure (e.g., Li, 2000). While effective, these deviations from generic cellular automata come at the potential cost of moving away from the advantages of the generic approach. In particular, “in order to converse with other disciplines, from biology and physics to chemistry, it may be necessary that the form of CA preserve as many features of strict and formal CA models as possible” (Torrens and O’Sullivan, 2001).

2.10.2. Hybrid Models

Hybrid models combine any of the above-mentioned techniques, each of which is a fairly discrete approach unto itself. A prime example is estuarine land-use/cover transition modeling that has an explicit, cellular model tied to a system dynamics model (Costanza, Sklar, and Day, 1986). Other examples that combine statistical techniques with cellular models and system models include larger-scale models such as CLUE family (Veldkamp and Fresco, 1996).

A distinct variant of hybrid models is dynamic spatial simulation (DSS), which portrays the landscape as a two-dimensional grid where rules represent the actions of land managers based on factors such as agricultural suitability (Lambin, 1994). Dynamic spatial simulation typically does not represent heterogeneous actors, institutional effects on decision making, or multiple production activities. However, due to their ability to represent individual decision making and temporal and spatial dynamics, they represent an important advance over previous models (Lambin, 1994).

2.10.3. Agent-Based Models

While cellular models are focused on landscapes and transitions, agent-based models focus on human actions. Agents are the crucial component in these models. Several characteristics define agents: they are autonomous,

they share an environment through agent communication and interaction, and they make decisions that tie behavior to the environment. Agents have been used to represent a wide variety of entities, including atoms, biological cells, animals, people, and organizations (Conte *et al.*, 1997; Janssen & Jager, 2000).

One key difference exists between agent-based modeling and other techniques. Complex systems are often characterized by nonlinear relationships between constantly changing entities while systems theory typically studies static entities linked by linear relationships defined by flows and stocks of energy, information, or matter. Similarly, systems theory emphasizes quantities of flow and not necessarily their quality, while complexity research attempts to examine qualitative attributes such as learning and communication. Complex behavior is seen as emerging from interactions between system components while system models tend to favor parameterized flows and stocks that assume that the system exists in equilibrium due to fixed relationships between system elements. Agent-based modeling relies on the idea that emergent or synergistic characteristics are understood by examining subcomponent relationships.

2.10.3.1. Multi-Agent Systems (MAS) for Land-Use/Cover Change

The exploration of modeling thus far has raised three key points. First, of the host of methods used to model land-use/cover change, dynamic spatial simulation offers a promising degree of flexibility. Second, as noted above, cellular models successfully replicate aspects of ecological and biogeophysical phenomena, but they may not always be suited to modeling decision making. Third, agent-based modeling is a promising means of representing disaggregated decision making. When all three points are taken together, they suggest the use of a dynamic, spatial simulation-like MAS/LUCC model that consists of two components. The first is a cellular model that represents biogeophysical and ecological aspects of a modeled system. The second is an agent-based model to represent human decision making. The cellular model is part of the agents' environment, and the agents in turn act on the simulated environment. In this manner, the complex interactions among agents and between agents and their environment can be simulated in a manner that assumes equilibrium conditions. Rather, equilibria or transient but reoccurring patterns emerge through the simulated interactions between agents and their environment.

2.10.4. Current Applications of MAS/LUCC Modeling

Many well-developed techniques for modeling land-use/cover dynamics exist. However, each of these techniques has some limitations. Equation-based models may require simplifying assumptions to achieve analytical or computational tractability, and they are often based on empirically implausible assumptions regarding static market equilibria. System models directly address the shortcomings of equation-based models in terms of representing feedbacks and dynamic processes, but these models also operate at a very aggregated level, or, equivalently, at a very coarse temporal and spatial resolution. Therefore, where local heterogeneity and interactions are important, such models may have limited explanatory power.

Some insight into the impacts of spatial heterogeneity, neighborhood effects, and spatial spillovers can be gleaned through estimation of statistical models. However, these models distill information into parameter estimates that represent average effects over available data. Thus, such models may be useful for projecting spatial dynamics and interactions only for processes which are stationary and uniform over space and time. While the impacts of spatial influences occurring at hierarchical spatial scales can be represented to some extent through statistical techniques that account for regional heterogeneity (such as generalized least-squares, fixed-effect, and random-effect models), feedbacks across scales cannot be effectively modeled. While cellular modeling techniques offer greater flexibility for representing spatial and temporal dynamics, these dynamics also are based on stationary transition probabilities. Therefore, such models have limited ability to reflect feedbacks in the system under study, as global changes in the system do not influence transitions at the cellular level. Perhaps most significant, none of the above modeling techniques can represent the impacts of autonomous, heterogeneous, and decentralized human decision making on the landscape.

Many of these limitations are potentially overcome by MAS/LUCC models. In particular, MAS/LUCC models may be well suited for representing socioeconomic and biophysical complexity. They also might be well suited for the related goal of modeling interactions and feedbacks between socioeconomic and biophysical environments.

2.11. Land Use/Cover Change, Climate and Environment

2.11.1. Effect of land use/land cover on local climate

Land surface changes can affect local precipitation and temperatures. Vegetation patterns and soil composition

can influence cloud formation and precipitation through their impact on evaporation and convection i.e., the rise of air, The effect of land cover on climate depends on the type of land cover that is present in a specific region. For example, barren lands tend to heat more rapidly and can transmit this heat to the lower atmosphere.

A recent study of the United States on summer climate using computer models of NASA and the National Oceanic and Atmospheric Administration found that land cover changes from grassland to agriculture in part of the Great Plains and the Midwest brought as a result a significant cooling effect. A possible explanation is that farmlands tend to create lower temperatures due to increase in evaporation. In the same study, a warming effect associated to land use change from forest to croplands was found along the Atlantic cost of the United States. Within the climate system, forests are more efficient in transpiration processes where the evaporation of plants during photosynthesis and helps to cool the air.

Land surface changes can affect local temperatures not only in forests or agricultural land but also in urban areas. For example, average temperatures in downtown areas of a city can increase due to the high density of construction materials such as pavements and roofs. Higher temperatures in urban areas compared to lower temperatures in surrounding rural areas, has been called by scientists the urban heat island effect.

2.11.2. Effect of land use/land cover on global climate

Every new building constructed consumes energy both in its construction and use. Single family homes use more energy per person than multifamily homes. Larger homes use more energy than smaller homes. The farther new homes are from existing population centers, from work and shopping, the greater the additional energy use in transportation per home and per person. Because of the strong links between energy use, greenhouse gas emissions and climate change, rates of new construction are strongly related to rates of climate change, especially when this new construction is relatively distant from existing population centers.

Moreover, the consequences of new construction for climate change go beyond their effects on Green House Gases (GHG) emission rates. Areas under forest, wetland, even agricultural fields serve as Carbon 'sinks'. That is, they absorb and retain Carbon from the atmosphere. New construction then not only increases rates of GHG emission, it reduces the amount of Carbon that is stored in areas with vegetative cover. There are differences in carbon storage of 'undeveloped' areas: forests store more carbon than farmland; different forest-types store different amounts of carbon; farming practices with minimal tillage and/or which include trees or perennials store more carbon than those with complete tillage and only annual row crops.

2.11.3. Impact of climate change on land use/land cover

The effect of climate's impact on land cover refers to the direct and indirect influence that climate has on the vegetation, or other features that cover the land (Ecosystems). Climate change produces alterations in water, energy and carbon fluxes. It also could also produce environmental disturbances that directly or indirectly affect land cover. For example, species respond to disturbances produced by climate change through migration, extinction or adaptation to new disturbances.

Most of the work that has looked at the impacts of climate change on Land Use has focused on agricultural land and forests. Variability in climate can affect agricultural land patterns due to a) rainfall patterns. b) temperatures (particularly night temperatures) and c) CO_2 enrichment. Controlled experiments have found that greater variability in rainfall patterns result in lower overall plant growth due to decreased water availability in the upper 30 cm of soil. Higher temperatures are likely to make growing seasons longer, allowing the possibility of more than one cropping cycle during the same season as well as the expansion of agricultural and forest land towards the poles and to higher elevations. At the same time, increases in night time temperatures can affect biological processes such as respiration and could result in reduction of potential yields.

Scientists are trying to understand the responses of CO_2 enrichment (higher volumes of CO_2 in the atmosphere) on different species. Wheat, rice and soybeans are crops that seem to have a positive response (increased overall observed growth) to higher CO_2 levels in the atmosphere. Crops such as corn are likely to be less responsive to CO_2 enrichment. Other potential impacts of climate change on land cover include: Natural fire frequency, intensity and duration and potential rise of sea level and floods, especially in coastal areas.

Given all the factors mentioned above, the net impact on agriculture in a particular area could be positive or negative. If climate change makes agriculture less productive in an area, then more farm land will be converted to other uses. If climate change offers more agricultural produce in an area, land that is currently in forests may be converted to agricultural uses.

Humans can also respond to climate change through migration. If warmer places are considered amenities to humans, population density can increase in areas with higher temperatures. The new population settlements indirectly affect land cover as more development and land fragmentation occurs. Proactive land use planning can be used to anticipate and adapt to Climate Change. The following are examples of potential strategies to minimize the potential negative impacts from climate change:

- One possible impact from climate change is an increase in severity of storms, which would lead to an increase in flash flooding. Adaptation strategies include banning new construction in vulnerable areas with high risk of flooding, minimizing flashy runoff from impervious surfaces, changing the requirements for stormwater retention structures in new developments, and protection of wetlands that buffer runoff from heavy rainstorms
- Increased temperatures will make urban heat effects more severe. Land use planning should reduce urban heat effects, through maintenance of green areas, use of different building materials
- The global climate in future is expected to become more variable. This will increase stress on natural ecosystems. Species that rely on natural, undisturbed habitat will have difficulty surviving droughts and storms, particularly if that habitat exists only in small patches. These habitats will be more resilient to climate variation if they are connected, so that populations can move and repopulate areas that are impacted by drought or severe storms. Land use planning can include provisions for habitat corridors that connect isolated patches of suitable habitat
- As sea levels rise, the shoreline along coastal areas will erode. Where there are beachfront or bayfront houses, the owners will try to protect their property, through shoreline hardening for example. It is much easier to adapt to sea level rise if those properties are not built to begin with. Land use policies that discourage shoreline building will leave communities more flexibility to deal with sea level rise
- Climate change will make some agricultural areas more suitable for production and other areas less so. The impacts of climate change on agriculture will be less if production is allowed to move in response to changing climate. Some land that is not currently suitable for agriculture because of climate may become suitable in the future. If that land is not available because it has already been developed, then the farming sector will be less able to adapt. It may make sense to preserve land for future agricultural production, even if it is not currently being used for that purpose. Similarly, forest land that is currently dominated by lower-valued species may become more valuable in the future, and vice versa.

2.12. Conclusions

Earth observations have the potential to respond to the growing and urgent demand for timely and accurate land cover information over large areas. In the recent past, land cover mapping from satellites has come of age, Through research on various issues regarding data pre-processing, classification and accuracy assessment, new and unique data / land cover products are being generated which could not be produced by earlier techniques. Many of the technical limitations hampering further improvements in land cover mapping need to be removed in the next few years, especially in the quality of satellite data (improved calibration, spatial and spectral resolution, spectral coverage, geolocation accuracy) and the computing capability, founded on the accumulated knowledge and experience in the use of digital analysis methods. This will require strong, ongoing research activities as well as new initiatives in the production of land cover maps. The future research in LULC studies needs to address the best ways of taking advantage of satellite-derived land cover databases through LULC change modeling techniques which provide important inputs for studies in the emerging areas of environmental monitoring, global warming and climate change.

References

Adams JB, Sabol DE, Kapos V, Filho RA, Roberts DA , Smith MO and Gillespie AR, 1995, Classification of Multispectral Images based on Fractions of Endmembers: Application to land-cover change in the Brazilian Amazon, *Remote Sensing of the Environment,* **52** :137-154.

Agarwal C, Green GM, Grove JM , Evans T and Schweik C, 2000, A review and assessment of land-use change models: Dynamics of space, time, and human choice, Paper presented in the Fourth International Conference on Integrating GIS and Environmental Modeling (GIS/EM4), September 2–8, Banff, Canada.

Ahern FJ, Janetos AC and Langham E, 1998, Global Observation of Forest Cover: a CEOS' Integrated Observing Strategy, Proceedings of 27th International Symposium on Remote Sensing of Environment,Troms,Norway, p. 103–105.

Alcamo J, 1994, *IMAGE 2.0: Integrated Modeling of Global Climate Change*, Kluwer Academic Publishers, Dordrecht, Germany.

Anderson GL, Hanson JD and Haas RH,1993, Evaluating landsat thematic mapper derived vegetation indices for estimating above–ground biomass on semiarid rangelands*, Remote Sensing of Environmen*t, **45**: 165–175.

Anderson JR, Hardy EE , Roach JT and Witmer RE, 1976: A land use and land cover classification system for use with remote sensor data, US Geological Survey Professional Paper 964, 28 pp.

Asrar G, Fuchs M, Kanemasu ET and Hatfield JL, 1984, Estimating absorbed photosynthetic radiation and leaf area index from spectral reflectance in wheat, *Agronomy Journal,* **76**: 300-306.

Atzberger CG, 1996, The spectral correlation concept: an effective new image-based atmospheric correction methodology over land areas, In Progress in *Environmental Remote Sensing Research and Applications*, edited by Parlow A (Rotterdam: Balkema), 125–132.

Balling RJ, Taber JT, Brown M and Day K, 1999, Multi-objective urban planning using a genetic algorithm, *ASCE Journal of Urban Planning and Development,* **125 (2)** : 86-99.

Balzter, H, P W Braun and W Kohler, 1998, Cellular automata models for vegetation dynamics, *Ecological Modelling,* **107 (2/3)**: 113-125.

Barnes W L, Pagano TS and Salomonson VV, 1998, Prelaunch characteristics of the Moderate Resolution Imaging Spectrometer (MODIS) on EOS-AM/1, *IEEE Transactions on Geoscience and Remote Sensing*, **36**: 1088–1100.

Brown JF, Loveland TR, Merchant J W, Reed BC and Ohlen, DO, 1993, Using multisource data in global land cover characterization: concepts, requirements and methods, *Photogrammetric Engineering and Remote Sensing*, **59**: 977–987.

Burk TE, Ek AR, Coppin PR, Lime SD, Walsh TA, Walters DK, Befort W and Heinzen DH, 1994, Satellite inventory of Minnesota forest resources, *Photogrammetric Engineering and Remote Sensing*, **60**: 287–298.

Carpenter GA, Gjaja MN, Gopal S and Woodcock CE, 1997, ART neural networks for remote sensing: vegetation classification from Landsat TM and terrain data, *IEEE Transactions on Geoscience and Remote Sensing*, **35**: 308–325.

Chavez P, 1988, An improved dark-object subtraction technique for atmospheric scattering correction of multispectral data, *Remote Sensing of Environment*, **24**: 459–479.

Chavez P,1989, Radiometric calibration of Landsat Thematic Mapper multispectral images, *Photogrammetric Engineering and Remote Sensing*, **55**: 1285–1294.

Chuvieco E and Congalton RG,1988, Using cluster analysis to improve the selection of training statistics in classifying remotely sensed data, *Photogrammetric Engineering and Remote Sensing,* **54**: 1275–1281,

Cihlar J, 2000, Land cover mapping of large areas from satellites: status and research priorities, *International Journal of Remote Sensing,* **21(6-7)**: 1093-1114.

Cihlar J, 1996, Identification of contaminated pixels in AVHRR composite images for studies of land biosphere, *Remote Sensing of Environment*, **56**: 149–163.

Cihlar J and Beaubien J, 1998, Land Cover of Canada 1995, Version 1.1. Digital data set documentation, Natural Resources Canada, Ottawa, Ontario.

Cihlar J, Latifovic R, Chen J and Li Z, 1999, Near-real time detection of contaminated pixels in AVHRR composites, *Canadian Journal of Remote Sensing,* **25**: 160–170.

Cihlar J, Ly H and Xiao Q, 1996, Land cover classification with AVHRR multichannel composites in northern environments, *Remote Sensing of Environment*, **58**: 36–51.

Cihlar J, Xiao Q, Beaubien J, Fung K and Latifovic R, 1998, Classification by Progressive Generalization: a new automated methodology for remote sensing multichannel data, *International Journal of Remote Sensing*, **19**: 2685–2704.

Colwell RN, (editor) 1960, *Manual for Photographic Interpretation*, The American Society of Photogrammetry, Washington, D.C.

Congalton RG, 1991, A review of assessing the accuracy of classifications of remotely sensed data, *Remote Sensing of Environment,* **37**: 35–46.

Congalton RG, 1996, Accuracy assessment: a critical component of land cover mapping, In Gap Analysis: A Landscape Approach to Biodiversity Planning, edited by Scott JM, Tear THandDavis F (Bethesda, Maryland: *American Society for Photogrammetry and Remote Sensing*), 119–131.

Conte R, Hegselmann R and Terna P, eds., 1997, *Simulating Social Phenomena*, Springer, Berlin.

Coppin, Pol R and Marvin E Bauer, 1996, Digital Change Detection in Forest Ecosystems, *Remote Sensing Reviews*,13207-234.

Costanza R, Sklar FH and JDay W Jr., 1986, Modeling spatial and temporal succession in the Atchafalaya/Terrebonne Marsh/estuarine complex in South Louisiana, P, 387-404 in D, A, Wolfe, ed, *Estuarine Variability*, Academic Press.

Cracknell A P and Paithoonwattanakij K, 1989, Pixel and sub-pixel accuracy in geometrical image correction of AVHRR imagery, *International Journal of Remote Sensing*, **10**: 661–667.

Cromley RG and Hanink DM, 1999, Coupling land-use allocation models with raster GIS, *Journal of Geographic Systems,* **1**: 137-153.

De Boissezon H, Gonzales G, Pus B and Sharman M, 1993, Rapid estimation of crop acreage and production at a European scale using high resolution imagery—operational review, Proceedings of the International Symposium 'Operationalization of Remote Sensing', ITC Enschede, The Netherlands, 94–105.

DeFries RS, Hansen M and Townshend JRG, 1995, Global discrimination of land cover types from metrics derived from AVHRR Pathfinder data, *Remote Sensing of Environment*, **54**: 209–222.

DeFries R S, Hansen M, Townshend JRG and Sohlberg R, 1998, Global land cover classification at 8 km spatial resolution: the use of training data derived from Landsat imagery in decision tree classifiers, *International Journal of Remote Sensing,* **19**: 3141–3168.

DeFries R, Hansen M, Steininger M, Dubayah R, Sohlberg R and Townshend J, 1997, Subpixel forest cover in central Africa from multisensor, multitemporal data, *Remote Sensing of Environment*, **60**: 228–246.

DeFries RS and Townshend JRG, 1994, NDVI-derived land cover classification at global scales, *International Journal of Remote Sensing*, **15**: 3567–3586.

DeFries RS, Bounoua L and Collatz GJ, 2002, Human modification of the landscape and surface climate in the next fifty years, *Global Change Biology*, **8**: 438-458.

Dickinson RE, Henderson-Sellers A, Kennedy PJ and Wilson MF, 1986, Biosphere-atmosphere transfer scheme (BATS) for the NCAR community climate model, NCAR Technical Note NCAR/TN275+STR, Boulder, CO, USA.

Elmore, Andrew J, Mustard, John F, Manning, Sara J, Lobell and David B, 2000, Quantifying Vegetation Change in Semi-Arid Environments: Precision and Accuracy of Spectral Mixture Analysis and the Normalized Difference Vegetation Index, *Remote Sensing of the Environment*, **73(1)**: 87 - 102.

Elvidge CD, Yuan D, Weerackoon RD and Lunetta RS, 1995, Relative radiometric normalization of Landsat Multispectral Scanner (MSS) data using an automatic scattergram-controlled regression, *Photogrammetric Engineering and Remote Sensing,* **61**: 1255–1260.

Eva HD, Malingreau JP, Gregoire JM, Belward AS and Mutlow CT, 1998, The advance of burnt areas in Central Africa as detected by ATSR-1, *International Journal of Remote Sensing,* **19**: 1635–1637.

Foody GM, 1998, Sharpening fuzzy classification output to refine the representation of sub-pixel land cover distribution, *International Journal of Remote Sensing,* **19**: 2593–2599.

Foody GM, Lucas RM, Curran PJ and Honzak M, 1997, Non-linear mixture modeling without end-members using an artificial neural network, *International Journal of Remote Sensing,* **18**: 937–953.

Friedmann DE, 1981, Operational resampling for correcting images to a geocoded format, Proceedings of the Fifteenth International Symposium Remote Sensing of Environment, Ann Arbor, MI (Environmental Research Institute of Michigan), 195–199.

GCOS, 1997, GCOS/GTOS plan for terrestrial climate-related observations, Report GCOS-32, WMO/TD-No. 796, World Meteorological Organization.

Gong P, Marceau DJ and Howarth PJ, 1992, A comparison of spatial feature extraction algorithms for land-use classification with SPOT HRV data, *Remote Sensing of Environment,* **40**: 137–151.

Guindon B, 1995, Utilization of Landsat Pathfinder data for the creation of large area mosaics, Proceedings of the 1995 ACSM/ASPRS Conference, Charlotte, NC (*American Society of Photogrammetry and Remote Sensing*), **2**: 144–153.

Hammond TO and Verbyla DL, 1996, Optimistic bias in classification accuracy assessment, *International Journal of Remote Sensing*, **17:** 1261-1266.

Hansen MC, DeFries RS, Townshend, JRG and Sohlberg R, 2000, Global land cover classification at 1 km spatial resolution using a classification tree approach, *International Journal of Remote Sensing*, **21**: 1331–1364.

Hansen M, Dubayah R and DeFries R, 1996, Classification trees: an alternative to traditional land cover classifiers, *International Journal of Remote Sensing*, **17**: 1075–1081.

HolbenB, 1986, Characteristics of maximum-value composite images from temporal AVHRR data, *International Journal of Remote Sensing*, **7**: 1417–1434.

Homer CG, Ramsey RD, Edwards T C Jr. and Falconer A, 1997, Landscape cover type modeling using a multi-scene Thematic Mapper mosaic, *Photogrammetric Engineering and Remote Sensing*, **63**: 59–67.

Hord RM, and Brooner W, 1976, Land-use map accuracy criteria, *Photogrammetric Engineering and Remote Sensing*, **42**: 671–677.

Houghton RA , 1999, The annual net flux of carbon to the atmosphere from changes in land use 1850-1990, *Tellus Series B-Chemical And Physical Meteorology*, **51**: 298-313.

Howitt RE, 1995, Positive mathematical programming, *American Journal of Agricultural Economics,* **77 (2)**: 329-42.

Huete AR,1986, Separation of Soil-plant Spectral Mixtures by Factor Analysis, *Remote Sensing of the Environment*, **19**: 237 - 251.

Huete AR, 1988, A soil-adjusted vegetation index (SAVI), *Remote Sensensing of Environment,* **25**: 295-309.

IGBP,1990, The International Geosphere-Biosphere Programme: a study of global change, The initial core projects, IGBP Report #12, Stockholm, Sweden.

Intergovernmental Panel on Climate Change (IPCC), 2000, *Land use, Land-use Change, and Forestry: A Special Report*, R Watson *et al.* (Eds.), Cambridge University Press, Cambridge, U.K.

Iverson LR, Cook EA and Graham RL, 1994, Regional forest cover estimation via remote sensing: the calibration center concept, *Landscape Ecology,* **9**: 159–174.

Janetos AC and Justice CO, 2000, Land cover and global productivity: a measurement strategy for the NASA programme, *International Journal of Remote Sensing,* **21**: 1491-1512.

Janssen M A and Jager W, 2000, The human actor in ecological economic models, *Ecological Economics,* **35 (3)**: 307-310.

Kalkhan M A, Reich RM and Stohlgren TJ, 1998, Assessing the accuracy of Landsat Thematic Mapper classification using double sampling, *International Journal of Remote Sensing*, **19**: 2049–2060.

Kartikeyan B, Sarkar A and Majumder KL, 1998, A segmentation approach to classification of remote sensing imagery, *International Journal of Remote Sensing*, **19**: 1695–1709.

Lambin EF, 1994, *Modelling Deforestation Processes: A Review*, European Commission, Luxemburg.

Lark RM, 1995a, A reappraisal of unsupervised classification, I: correspondence between spectral and conceptual classes, *International Journal of Remote Sensing*, **16**: 1425–1423.

Lark RM, 1995b, A reappraisal of unsupervised classification, II: optimal adjustment of the map legend and a neighbourhood approach for mapping legend units, *International Journal of Remote Sensing,* **16** : 1445–1460.

Lee RG, Flamm R, Turner MG, Bledsoe C , Chandler P, DeFerrari C ,Gottfried R , Naiman RJ ,Schumaker N and Wear D, 1992, Integrating sustainable development and environmental vitality: A landscape ecology approach, pp 499-521 in R J Naiman, ed. *Watershed Management: Balancing sustainability and environmental change*, Springer-Verlag, New York.

Leggett CG and Bockstael NE, 2000, Evidence of the effects of water quality on residential land prices, *Journal of Environmental Economics and Management*, **39**: 121-144.

Li BL, 2000, Fractal geometry applications in description and analysis of patch patterns and patch dynamics, *Ecological Modelling,* **132 (1 / 2)**: 33-50.

Lillesand TM, 1996, A protocol for satellite-based land cover classification in the Upper Midwest, In Gap Analysis: A Landscape Approach to Biodiversity Planning, edited by Scott JM, Tear TH and Davis F(Bethesda, Maryland: *American Society for Photogrammetry and Remote Sensing*), 103–118.

Liu J, Chen JM, Cihlar J and Park W, 1997, A process-based boreal ecosystem productivity simulator using remote sensing inputs, *Remote Sensing of Environment,* **62**: 158–175.

Loveland TR and Belward AS, 1997, The IGBP-DIS global 1 km land cover dataset, DISCover: first results, *International Journal of Remote Sensing*, **18**: 3289–3295.

Loveland TR, Merchant JW, Brown JF, Ohlen DO, Reed BC, Olson P and Hutchinson J, 1995, Seasonal land-cover regions of the United States, *Annals of the Association of American Geographers*, **85**: 339–355.

Loveland TR, Merchant JW, Ohlen DO and Brown JF, 1991, Development of a land-cover characteristics database for the conterminous U.S., *Photogrammetric Engineering and Remote Sensing*, **57**: 1453–1463.

Loveland TR, Reed BC, Brown JF, Ohlen DO, Zhu Z, Yang L and Merchant JW, 2000, Development of a global land cover characteristics database and IGBP DISCover from 1-km AVHRR data, *International Journal of Remote Sensing*, **21** : 1303–1330.

Macleod RD and Congalton RG, 1998, *Photogrammatry Engineering and Remote Sensing*, **64**: 207–216.

Mannan B, Roy J and Ray AK, 1998, Fuzzy ARTMAP supervised classification of multi-spectral remotely-sensed images, International Journal of Remote Sensing, **19**: 767–774.

Mathews E, 1983, Global vegetation and land use: new high resolution data bases for climate studies, *Journal of Climate and Applied Meteorology*, **22**: 474–487.

Mayaux P, Achard F and Malingreau JP, 1998, Global tropical forest area measurements derived from coarse resolution satellite imagery: a comparison with other approaches, *Environmental Conservation*, **25** : 37–52.

Mayaux P and Lambin EF, 1995, Estimation of tropical forest area from coarse spatial resolution data: a two-step correction function for proportional errors due to spatial aggregation, *Remote Sensing of Environment*, **53**: 1–16.

Mayaux P and Lambin EF, 1997, Tropical forest area measured from global land-cover classifications: inverse calibration models based on spatial textures, *Remote Sensing of Environment,* **59**: 29–43.

Mertens B and Lambin EF, 1997, Spatial modelling of deforestation in southern Cameroon, *Applied Geography,* **17 (2)**: 143-162.

Metternich GI and Fermont A, 1998, Estimating erosion surface features by linear mixture modeling, *Remote Sensing of the Environment,* **64(3)**: 254-265.

Moody A and Woodcock CE, 1996, Calibration-based models for correction of area estimates derived from coarse resolution land-cover data, *Remote Sensing of Environment*, **58**: 225–241.

National Remote Sensing Agency, 2004, Manual on National Land use /land Cover mapping on 1:250,000 scale using multi-temporal IRS P6-AWiFS data, NRSA, Dept. of Space, Govt. of India, Balanagar, Hyderabad.

Peterson DL, Spanner MA, Running SW and Tenber KB,1987, Relationship of Thematic Mapper Simulator data to Leaf Area, *Ecology* , **67 (1)**: 1273-1276.

Rabben EL, 1960, Fundamentals of photo interpretation, In Manual of Photographic Interpretation, edited by R N Colwell (Washington, DC: *The American Society of Photogrammetry*), 99–168.

Roberts DA, Smith MO and Adams JB, 1993, Green Vegetation, Nonphotosynthetic Vegetation, and soils in AVIRIS Data, *Remote Sensing of Environment,* **44(2-3)**: 255-269.

Rosenfield GH and Fitzpatrick-Lins K, 1986, A coefficient of agreement as a measure of thematic classification accuracy, *Photogrammetric Engineering and Remote Sensing*, **52**: 223–227.

Rosenzweig C and Hillel D,1998, Climate Change and the Global Harvest: Potential Impacts of the Greenhouse Effect on Agriculture, *Journal of Agricultural and Environmental Ethics*, **11 (1)**: 71-74.

Running SW, Justice CO, Salomonson V, Hall D, Barker J, Kaufmann YJ, Strahler A H, Huette A R, Muller JP, Vanderbilt V, Wan ZM, Teillet P and Carneggie D, 1994, Terrestrial remote sensing science and algorithms planned for EOS/MODIS, *International Journal of Remote Sensing,* **15**: 3587–3620.

Running SW, Loveland TR, Pierce LL, Nemani RR and Hunt ER Jr., 1995, A remote sensing based vegetation classification logic for global land cover analysis, *Remote Sensing of Environment*, **51**: 39–48.

Schott JR, Salvaggio C and Volchok WJ, 1988, Radiometric scene normalization using pseudoinvariant features, *Remote Sensing of Environment*, **26**: 1–16.

Sellers PJ, Los SO, Tucker CJ, Justice CO, Dazlich DA, Collatz J A and Randall DA, 1994, A global 1º by 1º NDVI data set for climate studies, Part 2: The generation of global fields of terrestrial biophysical parameters from the NDVI, *International Journal of Remote Sensing*, **15**: 3519–3545.

Shimabukuro YE, Mello EM K, Moreira JC and Duarte V, 1997, Segmentacao e classi, cacao da imagemsombra do modelo demistura paramapear des• orestamento na Amazona, Report INPE-6147-PUD/029, InstitutoNacional de Pesquisas Espacias, Sao Jose dos Campos, Brazil.

Singh HC,1989, Rural Environment Development and Planning, Chugh Publications, Allahabad, India.

Sklar FH and Costanza R, 1991, The development of dynamic spatial models for landscape ecology: A review and prognosis: in M G Tuner and R H Gardner, eds, *Quantitative Methods in Landscape Ecology*, Springer-Verlag, New York, 239-288.

Sommer S, Hill J and Megier J,1998, The Potential of Remote Sensing for Monitoring Rural Land Use Changes and Their Effects on Soil Conditions, *Agriculture Ecosystems & Environment*, **67(2-3)**: 197-209.

Staenz K, Brown RJ and Teillet PM, 1984, Infl uence of the viewing geometry on vegetation measures, Proceedings of the 8th Canadian Symposium on Remote Sensing, Montreal, QUE, (Canadian Remote Sensing Society), 5–12.

Steyaert LT, Hall FG and Loveland TR, 1997, Land cover mapping, fire regeneration, and scaling studies in the Canadian boreal forest with 1 km AVHRR and Landsat TM data, *Journal of Geophysical Research*, **102**: 29581–29598.

Thomas IL and McKallcock G, 1984, Determining the confidence level for a classification, *Photogrammetric Engineering and Remote Sensing*, **50**: 1491–1496.

Torrens PM and O'Sullivan D, 2001, Cellular automata and urban simulation: Where do we go from here? *Environment and Planning,* **28 (2)**: 163-168.

Townshend JRG, Justice CO, Skole D, Malingreau JP, Cihlar J, Teillet P, Sadowski F and Ruttenberg S, 1994, The 1 km resolution global data set: needs of the International Geosphere – Biosphere Programme, *International Journal of Remote Sensing*, **15**: 3417–3441.

Tucker CJ, 1979, Red and photographic infrared linear combinations for monitoring vegetation, *Remote Sensing of Environment* , **8**: 127-150.

Turner BL II, Mayer WB and Skole DL,1994, Global Land Use and Land Cover Change: Towards an integrated programme of study, *Ambio,* **23(1)***: 91-95.*

Van der Meer F, 1995, Spectral unmixing of Landsat Thematic Mapper data, *International Journal of Remote Sensing*, **16**, 3189–3194.

Veldkamp A and Fresco LO, 1996, CLUE: A conceptual model to study the conversion of land use and its effects, *Ecological Modelling,* **85 (2/3)**: 253-270.

Viovy N, Arino O and Belward AS, 1992, The Best Index Slope Extraction (BISE): a method for reducing noise in NDVI time-series, *International Journal of Remote Sensing*, **13**: 1585–1590.

Vogelmann J E, Sohl T and Howard S M, 1998, Regional characterization of land cover using multiple sources of data, *Photogrammetric Engineering and Remote Sensing*, **64**: 45–57.

Walsh T A and Burk TE, 1993, Calibration of satellite classifications of land area, *Remote Sensing of Environment*, **46** : 281–290.

Wiegand CL, Richardson AJ, Escobar DE and Gerbermann AH, 1991, Vegetation indices in crop assessments, *Remote Sensensing of Environment,* **35**: 105-119.

Wigmosta MS, Vail LW and Lettenmaier DP, 1994, A distributed hydrology vegetation model for complex terrain, *Water Resources Research*, **30**: 1665–1679.

Yuan D and Elvidge CD, 1996, Comparison of relative radiometric normalization techniques, *ISPRS Journal of Photogrammetry and Remote Sensing*, **51**: 117–126.

Zhu Z and Evans DL, 1994, U,S, forest types and predicted percent forest cover from AVHRR data, *Photogrammetric Engineering and Remote Sensing,* **60**: 525–531.

nrsc

Remote Sensing Applications

P. S. Roy
R. S. Dwivedi
D. Vijayan

National Remote Sensing Centre

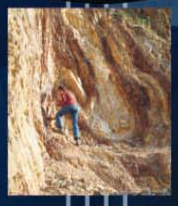

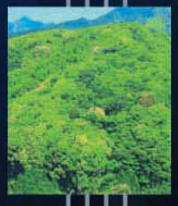

Remote Sensing Applications

Forest and Vegetation

3.1. Introduction

Forests are the natural resource, which provide mankind with numerous benefits both in goods and services. Managing this important resource base both spatially as well as temporally dynamic, can be a daunting task without the utilization of proper spatial tool. Space technology has immense influence in the decision-making processes especially in areas like forest resource management. Remote sensing as a tool has facilitated systematic and hierarchical approach of forest resources assessment and its monitoring using sensors of different spatial and spectral capabilities, the characterization, quantification and monitoring including specific efforts towards understanding the structure, composition and function of different natural habitats/ecosystems. These studies have provided key inputs for the regulation of the impact of developmental activities and to sustain the delivery of natural ecosystem goods and services. Forest resource assessment in India is being carried out in different levels e.g., bi-annual forest cover mapping using satellite remote sensed data.

With the availability of basic spatial coarse scale databases for important ecosystems, efforts have been made for understanding ecosystems structure and processes. The spatial information generated using remote sensing data is used in conjunction with ground based information in geospatial domain. Subsequently values have been added in terms of spatially explicit quantification for growing stock and biodiversity assessment. Process understanding related to landscape change and simulation, carbon sequestration, hydrology, generic ecosystem patterns, species niche models and regional climate models have also been addressed. The web-enabled information systems with significant impact factors are also useful to efficiently process, query and disseminate the data.

Optimal sampling designs for forest timber volume estimation; Automated forest cover retrieval and change assessment; Species exploration and niche modeling; Biodiversity monitoring and change modeling; Vegetation stress analysis; Forest ecosystem responses to climate change and anthropogenic impacts; Ecological Foot Printing analysis for sustainable development and Forest vulnerability and change assessment are the thrust areas identified for the retrieval of forest parameters using high resolution and hyperspectral data. But gaps in the information still exist in areas like forest fragmentation causes, invasion of exotics, rapid fire alarm system, shifting cultivation assessment and biodiversity assessment. This can be achieved through development of sensors with higher spatial and temporal resolution as well as enhanced spectral capabilities. Ground based information database is also lacking in Indian sub-continent region and this needs to be looked into urgently for spatial understanding of the ecosystem processes and their subsequent upscaling for regional level management.

3.2. Global and National Issues, Scenarios and Developments

3.2.1. Global Scenario

Retrieving information about forest resources is a process for obtaining information on the quality and quantity of forest resources and forms the foundation of forest planning and forest policy. While early concepts of sustainable forest management and forest inventory focused on timber production, modern forest inventory concepts support a holistic view of forest ecosystems addressing not only timber production but also the multiple functions of forest as well as the need to understand the functioning mechanisms of forest ecosystems.

Forest resources assessment facilitates a multifaceted analysis and study of forests is not only an important source of subsistence, employment, revenue, earnings, and raw materials to a number of industries but also critical for their vital role in ecological balance, environmental stability, biodiversity conservation, food security, and sustainable development of countries and the entire biosphere. Forests have to be managed judiciously not only for environmental protection and other services but also for various products and industrial raw material. In some parts of the world biological resources are being depleted faster than they can regenerate. Following the 1992 United Nations Conference on Environment and Development (UNCED) conference in Rio de Janeiro, considerable progress has been made in the area of sustainable forest management (Table 3.1). For example, the International Tropical Timber Organization (ITTO) and the Forest Stewardship Council (FSC) developed criteria and indicators for sustainable forest management and certification. The Kyoto Protocol of the United Nations Framework Convention of Climate Change (UNFCCC) describes measures to mitigate greenhouse gasses effects and addresses in Article 3.3 in particular the impact of deforestation and afforestation in global climate change. The Convention of Biological Diversity (CBD) that was ratified in 1994 deals with the protection and maintenance of biodiversity.

The information requirements from forest owners, policy planners, the scientific community, and society in general concerning forest resources have been growing steadily since the 1950s when the main focus was on information about timber supply. The multiple functions of forests biomass, global warming, biodiversity, and non-wood goods and services have since gained prominence.

The thematic scope of forest inventories can vary considerably. UNCED criteria and indicators for sustainable forest management have been formulated through several international, national, and nongovernmental processes. These include the Pan-European (or Helsinki) process (for European forests), the Montreal Process (for temperate and boreal forests), the Tarapoto Proposal of Criteria and Indicators for Sustainability of the Amazon Forest the United Nations Environment Program (UNEP) Food and Agriculture Organisation (FAO) Expert Meeting on Criteria and Indicators for Sustainable Forest Management in Dry-Zone Africa, or the Lepaterique Process of Central America. The ITTO, the Tarapoto Process (TARA), the Centre for International Forestry Research (CIFOR), the African Timber Organization (ATO) and the Central American Commission for Environment and Development (CCAD) developed systems of criteria and indicators for sustainable forest management which cover administrative, economic, legal, social, technical and scientific issues which affect natural forests and plantations. The criteria define the essential factors of forest management against which forest sustainability may be assessed. Each criterion relates to a key management factor which may be described by one or more qualitative, quantitative, or descriptive indicators. Through measurement and monitoring of selected indicators, the effects of forest management action, or inaction, can be assessed and evaluated and action adjusted to ensure that forest management objectives are more likely to be achieved. Table 3.2 summarizes the criteria and indicators identified by the processes and initiatives and should facilitate the definition of inventory objectives.

Table 3.1: Increase in information needs about forest lands in the USA (source: Franklin, 2001)

Timber	Multiple resources Timber	Biomass Multiple resources Timber	Global warming Biomass Multiple resources Timbers	Ecosystems biodiversity NWGS Global warming Biomass Multiple resources Timber	Non forest lands habitats, old growth and primary forests Ecosystems biodiversity NWGS Global warming Biomass Multiple resources Timber
1950s	1960s	1970s	1990s	1990s	2000+

3.2.2. National Scenario

The Indian sub-continent is known for its diverse bioclimatic regions supporting one of the richest floras and fauna in the world. The continent is a confluence point of three major terrestrial biogeographical realms (viz., the Indo-Malayan, the Eurasian and the Afro-tropical) and the Antarctic realm and is ranked as one of the mega-biodiversity countries in the world with 49,219 numbers of plant species and 89,451 animal species. According to an estimate about 30 percent plant species are endemic to India.

The natural terrestrial ecosystems like forests, grasslands, scrub lands, fresh water & ocean systems, microbial ecosystems, managed vegetation systems-agriculture and plantations provide immense potential in terms of Bioresources. India has a forest cover of 67.8 million ha (covering 20.64% of total geographic area). Forests are widely distributed across the country across different bioclimatic and topographic zones. Indian forests offer valuable ecosystem services as carbon sinks, soil erosion control, flood mitigation and various goods. Its rich floral diversity is represented by 47,000 plant species. Much of the demand for timber, fuel wood and fodder are met through these forests.

The need for understanding and assessment of this multiplicity of biodiversity in terms of ecosystem services and goods is important in order to design appropriate conservation strategies. Wood products removed from forests and other wooded land constitutes an important component of the productive function. The standing stock volumes

Table 3.2: Criteria and indicators for sustainable management
(source: Franklin, 2001)

Extent of forest resources and global carbon cycles:
Area of forest cover
Wood-growing stock
Successional stage
Age structure
Rate of conversion of forest to other use.
Forest ecosystem health and vitality external influences:
Deposition of air pollutants
Damage by wind erosion
Forest vitality indicators
Incidence of defoliators
Reproductive health
Forest influence indicators
Insect / disease damage
Fire and storm damage
Wild – animal damage
Anthropogenic influence indicators
Competition from introduction of nonnative plants
Nutrient balance and acidity
Trends in crop yields
Biological diversity in forest ecosystem :
Ecosystem indicators
Distribution of forest ecosystems
Extent of protected areas
Habitat suitability
Forest fragmentation
Area cleared annually of endemic species
Area and percentage of forest lands with fundamental ecological changes
Forest fire control and prevention measures
Species indicators
Number of forest- dependent species
Number of forest-dependent species at risk
Reliance on natural regeneration
Resources exploitation systems used
Measures for in situ conservation of species at risk
Genetic indicators
Number of forest-dependent species with reduced range
Productive functions of forests:
Percentage of forests/other wooded lands managed according to management plans
Growing stock
Wood production
Production of non-wood forest products
Annual balance between growth and removal of wood products
Level of diversification of sustainable forest production
Degree of utilization of environmentally friendly technologies

and the volume of wood removed indicate the condition of the forests and economic and social utility of forest resources to national economies and local communities. This information contributes to monitoring the use of forest resources by comparing actual removal with the sustainable potential.

Besides, there has been growing recognition of the role of Non Wood Forest Products as an integral part of sustainable forest management in developed and developing countries. A wide variety of products are collected from forests, woodlands and trees outside forests – a major portion of which are consumed by households or sold locally, while some find export markets. Understanding the potential contribution of NWFPs to sustainable rural development, especially in poverty alleviation and food security, requires good statistical data, which in most cases are gathered sporadically and are often unreliable.

Traditional rural population, particularly the tribes / aboriginal people depend heavily on very large spectrum of bio-resources associated with forest landscapes. Around 20,000 plant species are believed to be used for medicine in the developing world. In India the knowledge about medicinal value of plants has evolved in the form of traditional systems of medicinal sciences like, Unani, Ayurveda and Siddha. More than 8,000 species are used in some 10,000 drug formulations. It is estimated that about 0.5 million ton (dry weight) of plant material is collected each year from the forests. The global plant based drug trade is projected around US$ 62 billion with a 7% annual growth rate but India has only 2.5% share in it. The disproportionate demand and destructive methods of extraction have put unreasonable pressure on our wild phyto-resources. Due to this, pressing need is felt to have a reliable database on phyto resources such that a sustainable strategy can be formulated.

However, anthropogenic pressures are taking a heavy toll on the country's forests. About 2.5 Mha of the areas are under shifting cultivation. Forest fires cause a loss of nearly 10 million US$ every year. 95 % of these forest fires is man-made. Other types of biotic disturbances are grazing, mining activities, and construction of dams, agricultural conversions and urbanization. In view of the above, the precise estimates of Bioresources, their availability, location and extent, extraction and renewal systems are very important.

3.3. Conventional / Ground / Recent methods – Remote sensing

The forestry or vegetation science is one of the established and well flourished branches of science and we have at least one century old tradition of forestry management records. Similarly in the last decade several ecology and forest schools have contributed significantly in the development of basic concepts on structure and function of ecosystems. However, these so called conventional methods stand alone had several limitations. One of them was that they were not spatially explicit as well as there was lot of difficulty in revising those observations as well as there was no surrogate available to model them for different scenarios or for different niche conditions. Here came the advantages of remote sensing technology. With the mapping and stratification through remote sensing, the area coverage could be very large with even low intensity sampling by taking the advantage of stratification. The temporal revisit of the satellites have made it possible to assess and analyse changed scenario with better accuracy and precision. Additional applications include such as forest land appraisal, timber harvest planning, monitoring, logging and reforestation, planning and assessing plant vigor and health in forest nurseries, mapping "Forest fuels" to accesses fire potential, planning fire suppression activities, assessing potential slope features and soil erosion, planning forest roads, inventorying forest recreation resources, wildlife and assessing wildlife habitat, and monitoring vegetation regrowth in fire lanes and power line rights-of-way.

The terrestrial vegetation systems like forests, grasslands, scrub and agriculture provide unique reflectance properties of electromagnetic radiation received enabling to characterize using satellite remote sensing. In view of the very large extent and heterogeneity of the country, the modern tools like satellite remote sensing technology which can help in deriving synoptic and periodic information on Bioresources from forests, grasslands and scrub is considered as one of the potential complimentary tools for conventional ground assessment.

3.3.1. Satellite Remote Sensing Applications in Forestry

Remote sensing refers to the phenomenon of recording/observing/perceiving objects or events at remote places. In remote sensing, the sensors are not in direct physical contact with the objects or events being observed. The process of acquiring information about earth surface features, from orbiting satellites is known as Satellite remote sensing.

Technically, remote sensing usually refers to the technology of acquiring information about the earth surface and atmosphere using sensors onboard airborne (aircraft, balloons) or space borne (satellites, space shuttles) platforms. Most remote sensing is performed from orbital or sub orbital platforms using instruments, which measure electromagnetic radiation reflected or emitted from the terrain. Some sensors use other mediums such as magnetic fields, sound waves, *etc*. Remote sensing is a technique that can be used in a wide variety of disciplines, but is not a discipline or subject itself. Digital image processing helps scientist to manipulate and analyze the image data produced by these remote sensors in such a way as to reveal information that may not be immediately recognizable in the original form. The primary goal of remote sensing is not only the pursuit of knowledge, but also the application of any knowledge gained.

Optical sensors detect solar radiation in the visible and near infrared wavelength regions, reflected or scattered from the earth, forming images resembling photographs taken by a camera high up in space.

Different materials such as water, soil, trees, buildings and roads reflect visible and infrared light in different ways. Knowledge of spectral reflectance signatures of various materials on earth is thus required for interpretation of optical remote sensing images. Satellites acquire the digital data and transmit it to the ground stations, which can then be used to reconstitute an image of the earth's surface. Acquisition of images of earth from space has opened new frontiers in mapping. The multi-spectral satellite images provide definitions of vegetation patches, which are

related to phenological types, gregarious formations and communities occurring in unique environmental setup. The temporal images help in monitoring all back processes a landscape has experienced (Delcourt and Delcourt, 1988). Satellites provide nearly global coverage of the Earth with spatial resolutions and repetition rates that vary from one platform to another. Improvements in spatial resolution have enabled availability of data in varying scales (Figure 3.1).

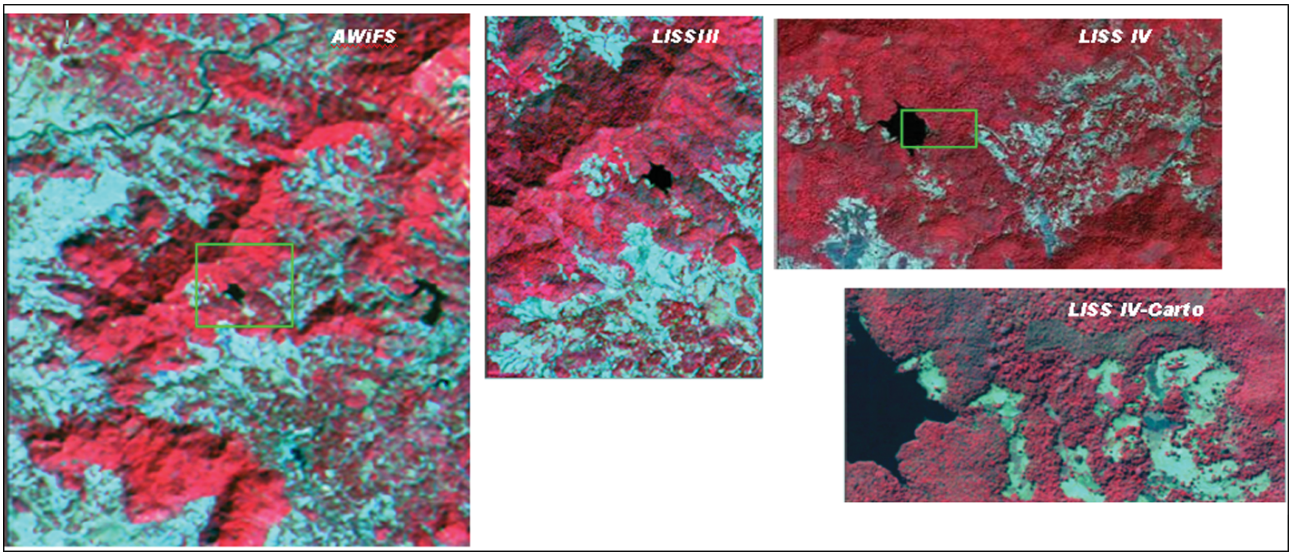

Figure 3.1: Scale diversity of remote sensing data

The images also provide digital mosaic of the spatial arrangement of landcover and vegetation types amenable to computer processing (Coulson *et al.*, 1990; Chuvieco, 1999). Biophysical spectral modeling techniques allow stratifying vegetation types based on the canopy closure (Roy *et al.*, 1996). Such an approach allows mapping and monitoring the forest condition and degradation processes.

Attempts have also been made to quantify forest biomass/volume and productivity using stratified sampling and spectral response modeling (Roy, 1994; Roy & Ravan, 1996). It is reported that the microwave remote sensing provides better estimation of biomass / volume due to better penetration. The surface and volume backscatter have strong relationship with the density and biomass (Hussin *et al.* 1991; Dobson *et al.* 1992; Luckeman, 1998). Recent studies indicate that the multi-wavelength, multi-polarization and varying look angle microwave sensors further improve mapping of structural parameters (Sardar, 1997; Pierce, 1998).

3.3.2. Multispectral basis of Remote Sensing and Vegetation

Spectral Signatures is the variability in the remote sensing data to identify the earth surface features spectrally. The proportions of energy reflected, absorbed, and transmitted will vary for different earth features, depending upon their material type and conditions. These differences permit us to distinguish different features on an image. The wavelength dependency means that, even within a given feature type, the proportion of reflected, absorbed, and transmitted energy will vary at different wavelengths. A graph of the spectral reflectance of an object as a function of wavelength is called a spectral reflectance curve. The configuration of spectral reflectance curves provides characteristics of an object and has a strong influence on wavelength regions in which remote sensing data are acquired for a particular application. Figure 3.2 shows the typical spectral reflectance curves for three basic types of earth features vegetation, soil, water and snow. The spectral reflectance of vegetation canopy varies with wavelength. Chlorophyll, contained in a leaf, has strong absorption at 0.45 µm and 0.67 µm, and the plant structure contributes to the high reflectance at near infrared (0.7-0.9 µm).

This results in a small peak at 0.5-0.6 (green color band), which makes vegetation green to the human observer. Near infrared is very useful for vegetation surveys and mapping because such a steep gradient at 0.7-0.9 µm is produced only by vegetation. Soil reflectance depends on the chemical and physical properties of the components such as moisture, organic matter, iron oxide, texture, surface roughness and sun angle. In visible spectrum, soils

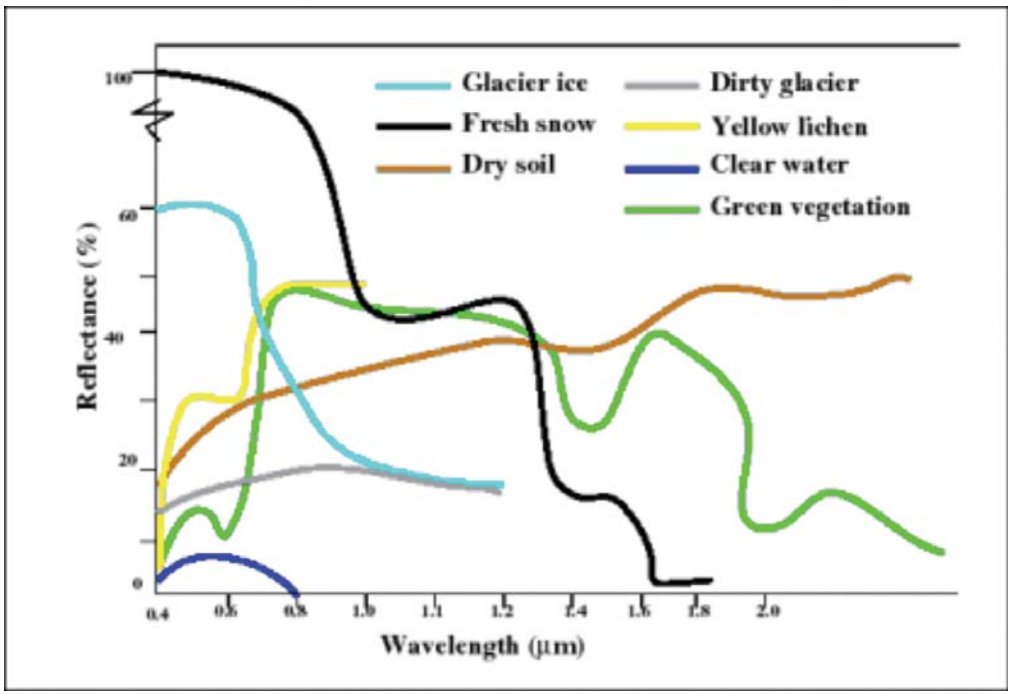

Figure 3.2: Spectral Reflectance curve

usually have higher reflectance than plants. However, it is opposite in case of near infrared band, where plants have higher reflectance than soil. The reflectance of EMR from water is affected by a number of variables such as suspended particles, floating materials and water depth. Water gives low reflectance in visible and almost nil reflectance in near infrared regions.

Microwave Remote Sensing: Optical remote sensing is not suitable for all atmospheric conditions. It cannot penetrate through clouds and haze. Microwave remote sensing is very useful as it provides continuous observation of the earth's surface regardless of the atmospheric conditions. The basic principle of Radar is to send out a signal and measure the time taken until it returns to the source, thus measuring the distance to that target. The microwaves are the electromagnetic waves with frequencies between 1300 MHz to 300 GHz. Advantage of Radar is its all weather, day and night capability to provide image data. Microwave portion ranges from the wavelength 1 mm to 1 m in the Electromagnetic spectrum.

By measuring the time delay between the transmission of a pulse and the reception of the backscattered "echo" from different targets, their distance from the radar and thus their location can be determined. As the sensor platform moves forward, recording and processing of the backscattered signals builds up a two-dimensional image of the surface. Depending on wavelength and polarization, radar can penetrate the canopy to different depths, and can sense plant parts of different sizes, shapes, and water content. This ability of radar to probe the canopy, and the expectation of retrieving biophysical forest descriptions, underlie much of the international impetus for forest radar research.

Backscatter is the outgoing radar signal that the target redirects back towards the antenna. Radar images are composed of many dots, or picture elements. In the image, darker areas represent low backscatter and brighter areas represent high backscatter. Backscattering from a diffused reflector is more than the backscattering from a specular reflector. Microwave interaction depends on the Angle of Incidence and Wavelength of the Radar. Radar remote sensing is also used to achieve Biomass Estimates and Carbon accounting. Radar data can also provide information about terrain surface and vegetation canopies. SAR provides important characteristics of soil and vegetation covers, for instance, inundation below closed canopies, fresh woody biomass of forested areas, freeze/thaw conditions of soil and vegetation, soil moisture and surface roughness in areas of low vegetation, and information on the orientation and structure of objects on the ground that reflect the incoming microwave radiation. Presently ERS-1, ERS-2 (European Space Agency), RADARSAT (Canadian Space Agency), and ENVISAT data are being used for analysis with specific reference to crop assessment, Soil moisture retrieval, Forest biomass etc. The role of multi-spectral, multi resolution sensors in quantifying the various forestry components as well as their sensitivity is described in Tables 3.3, 3.4 and 3.5.

Table 3.3: Role of Multi – Spectral RS derived parameters for various forestry components (H-high; M-medium; L-low)

S.No	Parameter	Pigmentation	Canopy structure and gaps	Composition	Temperature canopy water regimes
1	Phenology	H	M	H	M
2	Crown Closure	L	H	L	L
3	Vegetation Types	M	H	H	M
4	Species	M	H	H	H
5	LAI	H	H	M	
6	Biomass	H	H	H	M
7	Biochemistry	H	L	H	L
8	Transpiration	L	M	H	H

Table 3.4 : Sensitivity of RS wavelength bands in the quantification of forestry structural and functional parameters

Band	Wavelength	Description	Where it can be used	Index
Blue	**435-500**			
	415	Chlorophyll degradation, detects early stress	Drought, pathogen attack	NPQI
	420	Plant stress status	Drought, pathogen attack	PI1
	430	Carotinoid/chlorophyll-a content	Senescence, phenology	SRPI
	435	Chlorophyll degradation, detects early stress	Drought, pathogen attack	NPQI
	440	Vegetation health index, chlorophyll fluoresence ratios	Drought, pathogen attack	PI3, PI4
	500	Index of vegetation cover	Primary productivity	SGR
Green	**520-565**			
	531	Xanthophyll light response ~ photosynthetic efficiency, Sensitive to carotenoid/chlorophyll ratio	plant pathogen attack, senescence	PRI
Red	**565-740**			
	570	Xanthophyll light response ~ photosynthetic efficiency, Sensitive to carotenoid/chlorophyll ratio	plant pathogen attack, senescence	PRI
	599	Index of vegetation cover	Primary productivity	SGR
	600	Anthocyanins / Chlorophyll		RGR
	665	Index of green vegetation cover	Precision farming, soil organic content	SR, NDVI
	680	Carotinoid/chlorophyll-a content	plant pathogen attack, senesence	SRPI
	690	Vegetation health index, chlorophyll fluoresence ratios	Drought, pathogen attack	PI3

Band	Wavelength	Description	Where it can be used	Index
	695	Plant stress status		PI1, PI2
	699	Anthocyanins / Chlorophyll		RGR
	705	Leaf chlorophyll content	Detects trace quantities of vegetation cover in arid and semi-arid regions	mNDVI
	740	Vegetation health index, chlorophyll fluorescence ratios	Drought, pathogen attack	PI4
NIR	**750-1000**			
	750	Leaf chlorophyll content	Detects trace quantities of vegetation cover in arid and semi-arid regions	mNDVI
	760	Plant stress status	Drought, pathogen attack	PI2
	800	Carotinoid/chlorophyll-a concentration		SIPI
	840	Discriminates soil and dry matter	Precision farming, soil organic content	NDI, SACRI
	845	Index of green vegetation cover		SR, NDVI
	860	Leaf water content	Drought, precision farming	NDWI
	900	Leaf water content	Drought, precision farming	WBI
	970	Leaf water content	Drought, precision farming	WBI
SWIR	**1000-3000**			
	1240	Leaf water content	Drought, precision farming	NDWI
	1510	Foliar Nitrogen content	Impact of nitrogen loading	NDNI
	1650	Discriminates soil and dry matter	Precision farming, soil organic content	NDI, SACRI
	1680	Foliar Nitrogen content, Foliar lignin content	Impact of nitrogen loading	NDNI, NDLI
	1754	Foliar lignin content	Non-leaf based biomass	NDLI
	2020	Cellulose & lignin absorption features, discriminates plant litter from soils.	Precision farming, soil organic content	CAI
	2100	Cellulose & lignin absorption features, discriminates plant litter from soils.	Precision farming, soil organic content	CAI
	2220	Cellulose & lignin absorption features, discriminates plant litter from soils.	Precision farming, soil organic content	CAI

Table 3.5 : Role of sensors of different spatial resolutions in studying the major forestry components

S.No	Sensors	Greenness	Structure	Composition
1	Coarse (~1 km)	H	M	L
2	High (~20-250 m)	H	H	M
3	Very High (=10 m)	H	H	H

3.3.2.1. Red Edge

The region of the red-near infrared (NIR) transition has been shown to have high information content for vegetation spectra. This region is generally referred to as the “red edge”. It represents the region of abrupt change in leaf

reflectance between 680 and 780 nm caused by the combined effects of strong chlorophyll absorption in the red wavelengths and high reflectance in the NIR wavelengths due to leaf internal scattering. Increases in the amount of chlorophyll, for example, results in a broadening of the major chlorophyll absorption feature centered around 680 nm, causing a shift in the red edge slope and wavelength of maximum slope towards longer wavelengths. The latter is termed the red edge position (REP). Shifts in the REP to longer or shorter wavelengths has been used as a means to estimate changes in foliar chlorophyll content and also as an indicator of vegetation stress.

Since the REP is defined as the inflection point of the red-NIR slope, an accurate determination of the REP requires a number of spectral measurements in narrow bands in this region. Fortunately, recent developments in imaging spectrometry have provided additional bands (contiguous spectra of less than 10 nm bandwidths) within the red edge region compared to broadband imagery such as Landsat Thematic Mapper. Subsequently, the REP is defined by the maximum first derivative of the reflectance spectrum. However, the limitation of this approach is that the maximum first derivatives of contiguous spectra have been well documented to occur within two principal spectral regions (around 700 and 725 nm) causing a bimodal distribution of REP data around 700 and 725 nm and a discontinuity in the REP/chlorophyll relationship. Several other studies have revealed the existence of this double-peak feature in the first derivative of contiguous spectra, identified two peaks in winter wheat at 703 and 735 nm, also found peaks in canopy spectra of grass near 702 and 725 nm. Using analytical Spectral Devices (ASD) FieldSpec FR spectroradiometer with a 1 nm spectral resolution, observed two peaks in canopy spectra of grass near 700 and 720 nm and also observed the double-peak feature at 690–710 nm and found out that it is a function of natural fluorescence emission at 690 and 730 nm.

3.3.3. Retrieval of forest parameters and integrated analysis

The figure 3.3 shown below explains the conjunctive use of ground data, Remote Sensing, GIS and GPS in forestry applications. The integrated use of these technologies helps in describing the four major components – the greenness, crown closure, mixed vegetation types and the species assemblages, both qualitatively and quantitatively.

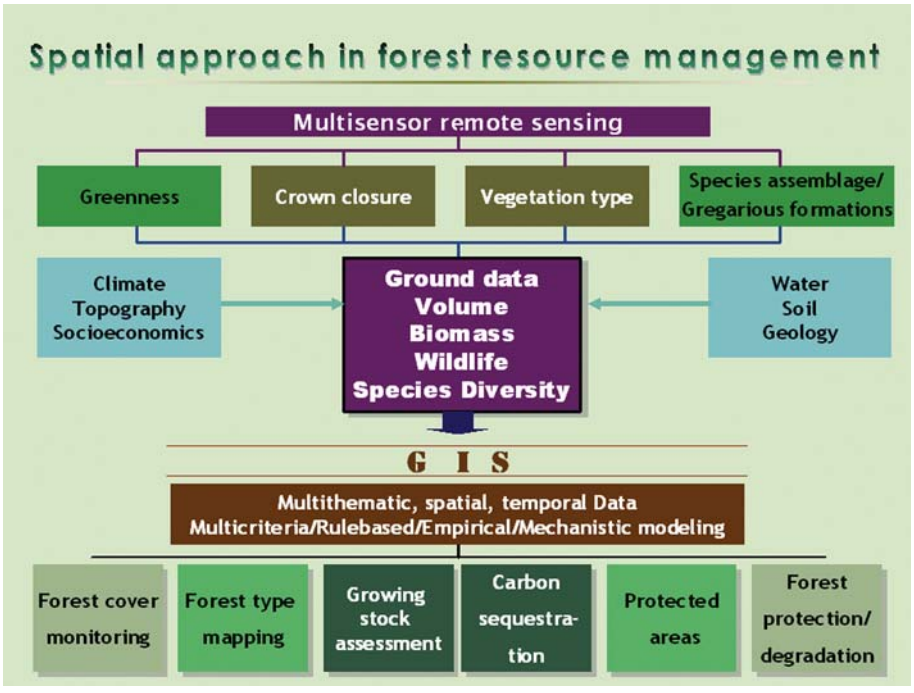

Figure 3.3: Spatial Resource in Forest resource Management

The availability of large possibility of spatial, temporal and radiometric resolutions have made it possible to address the described components almost directly. However, ground measured parameters such as climatic, topographic and socio-economic need to be collected from ground and to be integrated with remotely sensed data into the GIS domain. With the help of various GIS analysis (described later in this chapter), various forestry products required for the forest managers, researchers and academia can be obtained as shown in Figure 3.3.

3.3.3.1. Greenness

The seasonality of vegetation also called phenology is one of the key elements of vegetation study. The understanding of greenness amount and its cycle along different season and its spatial distribution is crucial to any climate change study as it is directly linked to the role of vegetation in carbon and water cycle. The leafy biomass controls these two cycles and can be monitored comprehensively through the daily, weekly or seasonally orbiting remotely sensed data. The time series data of spectral vegetation index provide a powerful tool to learn from past events,

monitor current conditions and prepare for future change. Comparison of current vegetation data records with historic long-term averages have been used to support ecosystem monitoring, and help evaluate the impact of rising global temperature and CO_2 levels and provide evidence of the impact of the 1989 and 1998 El Niño events around the world.

Global, regional and local natural resource survey and assessment strategies are increasingly incorporating remotely sensed imagery to monitor current and historical vegetation dynamics and often rely on the combined use of multi-sensor vegetation data. A rising number of national, regional and local users and applications are employing geospatial tools that incorporate time series of spectral vegetation index data and other reference data such as roads, rivers and soil information for spatially and temporally explicit natural resource and agricultural monitoring.

Although a variety of satellite sensor options are now available, practical considerations (i.e. data and processing costs, free distribution, the inherent trade-off between spatial and temporal resolution, and the influence of cloud cover) favor platforms that provide frequent images that are systematically processed into products useful for the assessment of vegetation. Two sensors among those that currently meet these criteria are the NOAA Advanced Very High Resolution Radiometer and NASA's Moderate Resolution Imaging Spectroradiometer. Since SPOT VEGETATION and Sea-viewing Wide Field-of-view Sensor (SeaWiFS) NDVI data are not freely distributed, these data are not included in the analysis. Among other products, both AVHRR and MODIS reflectance data are transformed into the Normalized Difference Vegetation Index, the most widely used vegetation index.

3.3.3.2. Forest type Mapping

Digital method:

The general methodology flow of forest type and forest density classification is shown in the following flow chart (Figure 3.4) .

Multi-spectral images are primarily subjected to digital image classification using both supervised and unsupervised approaches depending upon the land-cover class response in spectral sensing. Supervised classification presumes occurrence of Digital Number (DN) value to a particular category. Image processing module is provided with sample areas of distinctive spectral zones over which computation is extrapolated over whole image. Unsupervised approach generates spectrally explicit classes without consideration for thematic distinction which is subjected to a posteriori grouping. Statistical comparison of each given pixel(s) with overall image statistics in iterative mode helps to cluster spectral associations in unsupervised technique.

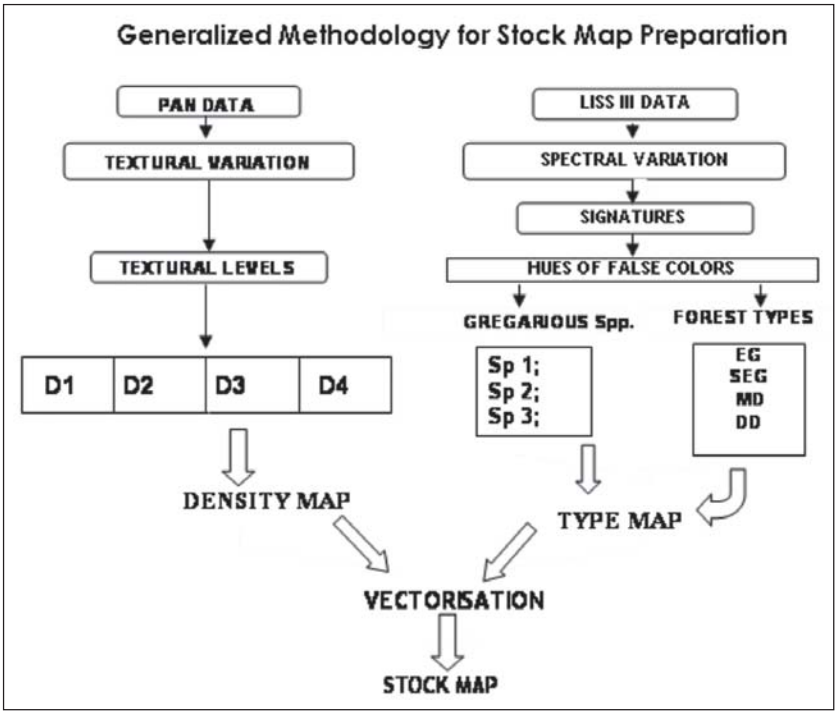

Figure 3.4: Generalised methodology for stock map preparation

Land-cover and vegetation classes of a typical area meant for forest management would usually be patterned with forested, agricultural and man-made features. Supervised classification is operated upon forested as well as agricultural tracts. Forests stand out uniquely due to the spectral distinction due to grades of foliage prevalence. Agricultural tracts consisting of cropped and fallow areas respond spectrally due to their separate class of near infrared / red reflectance relations. Bamboo dominated regions represents another spectral distinction. Other obviously distinguishable categories like water, barren areas, sand could also be recognized spectrally. Specimen spectral signatures are generated using Area Of Interest (AOI) facility in 'Signature editor' in Image processing S/W. The facility captures complete variation in a given irregular patch of pixels in terms of basic statistical parameters for each band viz., near infrared, red etc., which

form the centre for segregation of classes. Spectral homogeneity, corresponding generally to a homogenous theme strata on ground, can be attained either using qualitative visual interpretation or region growing algorithms available. Region growing algorithms search all around the designated pixel for specified DN value range and envelop selected ones for signature collection.

Signature sets thus generated are purified iteratively, based on the contingency matrix depicting commission and omission, as well as using feature space based spectral ellipses of respective spectral classes. Supervised classification algorithm based on maximum likelihood algorithm is operated upon the image using these purified signature sets. The output classes are compared for theme-wise and subjected to class merging, if there is high similarity between classes.

Classified image was standardised for required number of land-cover classes and subjected to image smoothing using majority 3X3 filter to dampen spurious noise. These filters consider the modal value of nine pixels and resample the area for proper re-alignment. The area statistics are generated.

Visual method:

The image characteristics of shape, size, pattern, shadow, tone and texture are used by interpreters in tree species identification. For example, individual tree species have their own characteristic crown shape and size. Some species have rounded crowns, some have cone-shaped, and some have star-shaped crowns. Variations of these basic crown shapes also occur. In dense stands, the arrangement of tree crowns produces a pattern that is distinct for many species. When trees are isolated, shadows often provide a profile image of trees that is useful in species identification. In pure stands (plantation), the canopy is regular in pattern and tree height is even or changes gradually with the quality of site.

Phenological correlations are useful in tree species identification. Changes in the appearance of trees in different seasons of the year some times enable discrimination of species that are indistinguishable on a single date. The most obvious example is the separation of deciduous and evergreen trees that is easily made on images acquired when the deciduous foliage has fallen.

Visual image interpretation is used extensively for growing stock estimation, biomass and carbon stock estimation. The Primary objective of such operations is to determine the volume of timber that might be harvested from an individual or more stand of trees. To be successful in image-based timber cruising, biomass and carbon stock studies, one requires the skill of an integrated interpretation of both aerial or satellite and ground data. Image measurements on individual trees or stands are statically related to ground measurements of tree volume, biomass and carbon mass in selected plots. The results are then extrapolated to large areas. The parameters of interest in forestry derived from image analysis most often are (1) tree height or stand height, (2) tree-crown diameter, (3) density of stocking, and (4) stand area etc.

3.3.3.3. Preparation of Forest Crown Density Maps.

Forest crown density is used as one of the critical parameter in forest cover assessment, growing stock estimations and monitoring in India. Satellite remote sensing based crown density mapping started during 1984 and technology is made as operational activity at national level. Since then Forest Survey of India has carried out nine national biennial surveys using remote sensing. Since 1995 IRS LISS II and LISS III sensors satellite data with 36.25 and 23.5 m resolution respectively are used for the purpose. With the increasing spatial resolution of the sensors and the advancement in satellite data processing, the crown density mapping has progressed from two crown density classes viz., 10-40% and >40% to three crown density classes 10-40%, 40-70%, >70%. Based on the latest report of 2005, national forest cover is estimated as 67.7 M ha covering 20.6% of the total geographical area of the country. This database also stands as one of the important input for national forest growing stock assessments.

Detailed forest crown density mapping with crown density interval of 20% is also prepared using IRS PAN, IRS LISS IV sensors data at 1:25,000 scale for forest division and micro level planning. These databases are used for monitoring and evaluation of afforestation, reforestation activities and as stratification input for developing optimal sampling designs for growing stock assessments. Based on the forest crown density levels, rehabilitation and selection working circle are demarcated to facilitate conservation and harvest plans respectively. With the availability of CARTOSAT, IKONOS and QUICKBIRD series of satellite data, detailed forest crown based information viz. crown diameter, number of crowns, degree of overlap etc., are amenable for mapping. These data bases are prepared for microlevel monitoring and forest condition assessment.

Based on the interpretation key developed as shown in (Figure 3.5) , the respective satellite data is interpreted for forest crown density delineation on screen based standardisation and correlation from field experience along with ancillary information available.

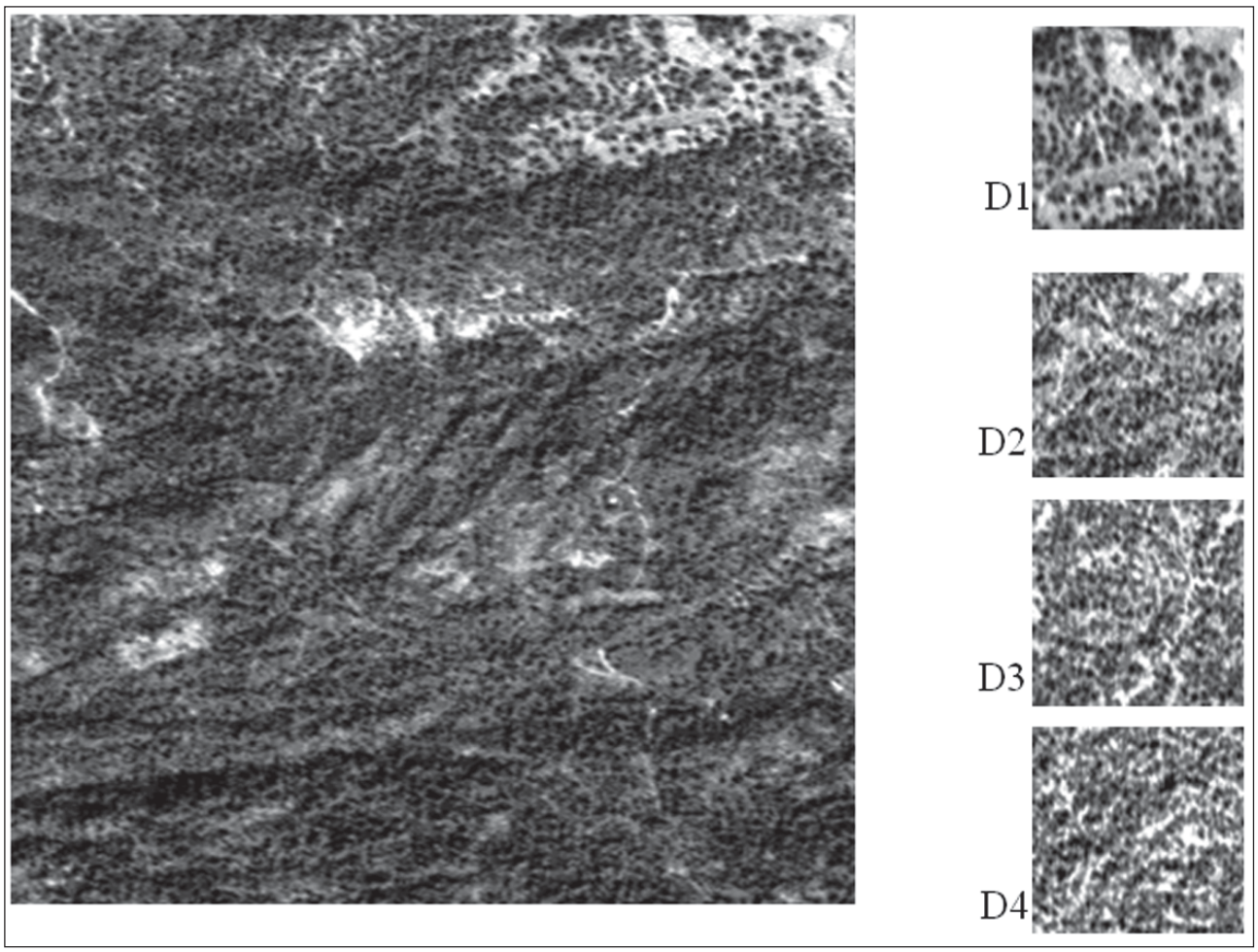

Figure 3.5: IRS Pan data for forest crown density mapping

Chandrashekhar *et al.*, 2005 demonstrated the test-assessment and practicability of forest canopy density mapping using satellite remote sensing data and biophysical spectral response modelling. Forest canopy density stratification through object oriented image analysis and conventional method of visual interpretation also have been compared with the Forest Canopy Density (FCD) Mapper semi expert system. In this study, forest canopy density was effectively stratified through linear multi-parametric approach by utilizing advanced vegetation index, bare soil index, shadow index and thermal index. Isodata cluster analysis of forest canopy density map derived from FCD Mapper and conventional methods were shown similar results with respect to percent area of forest and non-forest. The high percentage (10-30%) occurrence of bushy vegetation like *Lantana Camera* in ground canopy poses challenge in delineation of forest canopy density as its spectral reflectance is similar to that of the forest. Similarly, Roy *et al.*, 1996 conducted a study in which a three way crown density model was developed for the classification of forest crown density classes which utilizes the vegetation index, bare soil index and canopy shadow index.

3.3.3.4. Forest Quantification - Inventory Approaches

The precise estimation of forest ecosystem parameters depends on the efficiency of three stages of quantification process viz. design stage, estimation stage and inference stage. The design stage means selecting the design by which the data is gathered, the estimating stage selecting and using the estimators for the parameters of interest i.e., population means and totals, and the inference stage analyses the accuracy of these estimators i.e. calculation of standard errors and confidence levels. Geoinformatics based approaches involving remote sensing, GIS, GPS and information science enhances the development of reliable, time and cost effective approaches. In forested ecosystems selected features are typically identified by their location. Consequently, any quantitative assessment needs spatial perspective: sampling in space. There are two scientifically robust approaches for sampling and extrapolating from a sample to an entire population i.e. design and model based methods. The principle difference between the design and model-based approaches lies in the source of randomness they

utilize. Both these approaches are effectively used in the development of different quantitative database on growing stock, biomass and species diversity in the country.

3.3.3.5. Forest Quantification – Biomass, LAI from NDVI

One of the important ways of enhancing the efficiency of estimation is to bring out reliable stratification of the complex population and optimally sample subpopulations. The satellite remote sensing provides precise stratification in terms of forest crown density, vegetation types, communities and species formations which can form the basis for reducing the strata variance and make precise estimates. This assumes larger relevance in the context of high degree of variability of spatial distribution of vegetation types in India. The spatial explicitness in the estimates was brought out at desired scale and accuracy through geostatistical tools and GIS based spatial balancing methods. However, the resolution of spatial explicitness depends on the details of stratification and intensity of ground sampling required for scale and type of assessments.

Broad leaf tropical forests exhibit unique structural and environmental responses in the spectral domain. The increase in biomass levels results in the increase of reflectance values. NDVI, LAI and biomass are significantly correlated with ground estimated biophysical parameters. The regression models developed as part of several studies can also help in generating spatial biomass map. The attempt made in this direction showed strong possibility of using spectral response-based models for biomass estimation. However it is noteworthy that remote sensing-based Above Ground Biomass (AGB) estimation is a complex procedure in which many factors such as atmospheric conditions, mixed pixels, data saturation, complex biophysical environments, insufficient sample data, extracted remote sensing variables, and the selected algorithms, may interactively affect AGB estimation. The increase in reflectance of the NIR provides a remarkable capability for distinguishing vegetation from almost any other surface material, especially soil and water. Thus, this contrast is the basis for the application of vegetation indices in the estimation of vegetation parameters.

Studies have established relationships between the LAI of the canopy and vegetation indices from the signal reflected from the top of the canopy in the NIR and Red regions of the spectrum. The IRS LISS-IV data could be successfully used for forest patch level estimation with better accuracy.

3.4. Review of Literature

3.4.1. Coarse-resolution remote sensing

Over the past few years, global datasets from coarse spatial resolution sensors have become more and more readily available (e.g. Townsend *et al.* 1994, Arino & Melinotte 1995). Use of satellite image data for mapping and monitoring (Table 3.6) global land-cover, biomass burning, estimating geophysical and biophysical characteristics of terrain features, or monitoring continental-scale climate shift, is a primary input for biodiversity assessment. The rapid revisit time of AVHRR helps better understanding of land cover, burnt area, etc., at both global and regional levels (Stone *et al.*1994, Loveland & Belward 1997, Eva & Lambin 1998). The global vegetation type maps, analyses of land-cover changes and burnt areas in conjunction with trends in human disturbance, are effectively used to generate coarse-scale biodiversity maps and identification of biodiversity hotspots. In addition, the Moderate Resolution Imaging Spectroradiometer (MODIS) is designed to provide consistent spatial and temporal comparisons of global vegetation conditions that can be used to monitor photosynthetic activity, which facilitate understanding the biodiversity function.

During broad-scale mapping of Western Ghats (1:1,000,000 scale), 205 patches belonging to 11 different landscape types consisting of topography, climate, population, agriculture and vegetation cover, were delineated using IRS 1B data (Nagendra & Gadgil, 1998). In a detailed analysis in the tropical forests of the Western Ghats of India, Nagendra & Gadgil (1999) mapped a landscape into seven habitat types ranging from secondary evergreen forests to paddy fields, using supervised and unsupervised classification of IRS-1B LISS-II satellite imagery. The nature and the extent of forest degradation and its causes have been intensely debated, using mesoscale analyses of forest condition in the region of Western Ghats (Lele *et al.,* 1998).

Table 3.6: Satellite Remote Sensing sensors and potential in biodiversity assessment (Murthy *et al.*, 2003)

Scale	Data sources	Forest attributes	Spatial resolution	Temporal frequency	Mapping scale	Monitoring cost
Global	NOAA-AVHRR MODIS WIFS	Phenology types Forest / Non Forest Net Primary Productivity Deforestation Biomass burning	180 - 1 Km^2	Daily	>1:5000,000	Low
Regional	IRS LISS	Forest / Habitat types Secondary types	5 - 90 m	5 - 25 days	>1:50,000	Low to high
	IRS PAN	Disturbance - logging/roads/fire /encoarchments Plantations Ecotones				
	Landsat Spot	Wetlands Gregarious formations				
	JERS-1	Target species with gregarious distribution				
	ASTER					
Local	IKONOS	Target species with gregarious distribution	< 5 m	User defined	>1:10,000	High
	Aerial photography	Species assemblages / Communities				
	Aerial multispectral scanner	Regeneration				
	LIDAR	Forest disturbance				
	CASI	Agriculture Logging / roads Canopy gaps Plantations Harvest rates Level of degradation				

3.4.2. High-resolution remote sensing

Rapid change in land-use in tropical areas and the need to map changes in land use over large areas effectively, calls for application of high- or very-high-resolution satellite sensors. At the national or local level, IRS, Landsat or SPOT imagery can provide finer-scale information on forest type distribution and agricultural expansion. Radar systems, such as JERS and Radarsat, are not affected by clouds, and are useful for determining the extent of forest and non-forest landscapes where topographic relief is not substantial (<200m). Vegetation type and land-cover mapping of the entire North-East India, Western Himalayas and Western Ghats of India, were mapped on a 1:250,000 scale by using IRS LISS data (IIRS, 2002). Tropical evergreen forest along with other phenological types and major disturbed habitats (grassland, orchards, mangroves, Myristica swamps and Ochlandra) were mapped. The spatial data generated by remote sensing is useful in many ways in biodiversity monitoring and conservation efforts. Datasets from IRS 1C/1D LISS-III have been used effectively in mapping the pure plant colonies of *Hippophae rhamnoides* in the Spiti region of India with prior knowledge of their occurrence and vegetation types of the area by using remote sensing (Roy *et al.* 2001). IRS 1C/1D LISS-III FCC has been used for stratification of *Ephedra gerardiana* in complex terrain conditions of Lahul and Spiti district (Porwal *et al.,* 2003).

In areas where vegetation structure varies greatly, structural rather than species differences may predominate in imagery. These methods may then prove less suitable for determining species composition and facilitate delineation of specific vegetation types and habitats. In 1995, White *et al.* used LANDSAT TM imagery for an unsupervised classification of the forest of the Lassen Volcanic National Park. Genus-level mapping into Pinus and Abies forest classes was achieved with an accuracy of 63%. Treitz *et al.,* (1992) carried out a study in the Presquile Provincial Park, Canada. MEIS-II data, with five bands of 3 nm, was related to species-based community classification. Franklin (1994) carried out an analysis using satellite imagery to differentiate compositionally distinct vegetation communities. LANDSAT TM was used for estimation of species richness, indicating biodiversity hotspots in riparian and ecotonal areas (Gould 2000).

Remote sensing based on habitats, in conjunction with information on species habitat associations, can be generally used to derive information on the distribution of species, although a few exceptions may exist (e.g., Treitz *et al.* 1992). The degree of correspondence between habitat and species distributions depends on the degree of habitat map generalization, and this should also be optimized to get maximum information on species diversity (Stoms 1992, Coops & Catling, 1997). Habitat appears capable of providing information on the distribution

of large numbers of species in a wide variety of areas. However, this is restricted to the spatial scale of tens of square kilometers. In smaller, local areas with limited species diversity, direct mapping can provide detailed information on the distribution of certain canopy tree species or associations.

3.4.3. Very-high-resolution remote sensing

Applications of very-high-resolution remote sensing techniques to the conservation of biodiversity, assessment of protected areas, and species protection, show that fine-grain remote sensing is underused in conservation of forest ecosystems. Very high-resolution data (1m panchromatic and 4 m multispectral), which are now available from the commercial IKONOS II satellite, may be useful for determining the actual activities on the ground that have led to forest clearing. Although such data can detect very small clearings, the scientific community as yet has very little experience with these data. In addition, laser scanner data in combination with very-high-resolution satellite images, e.g. IKONOS, Terra Aster platform, or aerial multispectral scanner data, can be applied to the assessment of heights of single trees, tree-wise timber volume calculations, and the detection of even single trees of other species, especially for forest inventory tasks. The synergy of these different data sources can guarantee foresters a high level of information extraction for these applications.

Mapping of diversity estimates is often accomplished by analyzing the variation in spectral signal, and correlating this variation with measures of landscape or taxonomic diversity (Rey-Benayas & Pope 1995, Jorgensen & Nohr 1996). Mapping individual trees by using high-resolution data, poses problems not encountered when mapping associations or habitat patches. Pixels covering different component of a tree, such as bark and leaf, can be extremely variable in intensities. This makes the spectral signature of a tree species difficult to define. The factors like crown closure, crown geometry, stand density, topography, soil type, etc., regulate the reflectance properties of vegetated surfaces, so characterization of individual species, communities and vegetation types is a complex process. However, few studies have reported on the use of hyperspectral image data for differentiation of several tropical species (Franklin, 1994, Martin *et al.*, 1998) as well as discrimination of coniferous species (Cochrane, 2000, Gong *et al.*, 2001). Researchers in the Yellowstone National Park used Landsat and a Geographic Information System (GIS) to categorize habitats a priori and then determined the relationship between remotely sensed habitat categories and species distribution patterns (Debinski & Humphrey 1997, Debinski *et al.* 1999, Van Horssen *et al.*, 1999).

3.4.4. Temporal monitoring

The amount of change that is occurring in tropical parts of the World has been of considerable interest in the past ten years. Remote sensing offers perhaps the only practical method of analyzing large areas over time. Green & Sussmann (1990) used a combination of aerial photography, forest maps, and satellite images to estimate deforestation rates in Madagascar from 1950 to 1985, spanning a total of 35 years. With the advent of availability of satellite remote-sensing data, several countries have recently launched temporal monitoring of forest cover, which facilitates analyzing biodiversity losses. However, these studies do not provide information on vegetation type transition and losses, which is primarily necessary for understanding shifts and losses in biodiversity.

A few examples of the studies conducted in southern Western Ghats of India and Vindhyans of central India and North-East India have provided details about vegetation type transitions. These transitions, when coupled with ground-based species databases, help in analyzing and quantifying biodiversity losses. Prediction of the spatial distribution and relative abundance of wildlife on the basis of multitemporal satellite data and simulation models is also a recent development; Coops & Catling (2002) extensively reviewed such approaches.

3.4.5. Hyperspectral remote Sensing

Hyperspectral remote sensing is a relatively new technology. It is currently being investigated by researchers and scientists with regard to the detection and identification of minerals, terrestrial vegetation, and man-made materials and backgrounds. The ability of imaging sensor to acquire the reflectance spectrum of pixel in significant detail leads to substantial difference in the reflectance values of pixel belonging to disparate material of earth surface. Actual detection of materials is dependent on the spectral coverage, spectral resolution, and signal-to-noise ratio of the spectrometer, the abundance of the material and the strength of absorption features for that material in the wavelength region measured. There are many applications which can take advantage of hyperspectral remote sensing.

- Atmosphere: water vapor, cloud properties, aerosols
- Ecology: chlorophyll, leaf water, cellulose, pigments, lignin
- Earth Science: mineral and soil types
- Coastal Waters: chlorophyll, phytoplankton, dissolved organic materials, suspended sediments
- Snow/Ice: snow cover fraction, grainsize, melting
- Biomass Burning: subpixel temperatures, smoke
- Commercial: mineral exploration, agriculture and forest production

Current and recent important Hyperspectral Sensor and Data providers include spaceborne Hyperion onboard EO-1 providing data from 220 spectral bands and airborne sensors such as AVIRS with 224 bands, Hydice with 210 bands are operating in 0.4-2.5 µm. Hymap and DAIS 21115 are working in visible and thermal IR regions is providing data in 200 and 210 bands, respectively. Based on the international and domestic experience the following hyperspectral sensor configuration will be of immense use in the Indian space programme. Hyperspectral sensors are able to discriminate, identify and determine many characteristics about earth's features. Hyperspectral image analysis requires more attention to issues of atmospheric correction and relies more on physical and biophysical models than statistical techniques. Physical modeling and Empirical modeling are the approaches that can be employed to relate digital remote sensing data to biophysical variables.

3.4.6. Microwave and LIDAR sensing of forests

Recent advances in instrumentation and techniques are producing estimates of biomass with unprecedented accuracies in even the most densely forested ecosystems. Traditionally, these attributes have been measured in the field using handheld equipment. Field methods are accurate but are time-consuming and therefore limited to either mapping at fine scales or relatively sparse sampling at the landscape scale. Multi-spectral and hyper-spectral remote sensing have been used to map some aspects of structure at moderate resolution and broad scales. However, passive optical sensors have difficulty penetrating beyond upper forest layers and are better suited for mapping horizontal components, such as land cover type. Synthetic aperture radar (SAR) and interferometric synthetic aperture radars (InSARs) can provide measures of vertical structure at landscape scales at varying degrees of accuracy. Scientists used a ratio of P- and C-bands and the HV polarization (PHV/CHV) as well as L to C ratios (LHV/CHV) to predict biomass in boreal forests. Researchers found a direct correlation between biomass and X and L-band with HV polarization (LHV/CHV) backscatter, again in a boreal forest. Many other studies reported accurate results for biomass retrieval are in plantations or in very simple (in terms of either physiognomy or floristics or both) forest types. SAR and InSAR appear to be suited for structurally homogeneous, simple forest types at the present time, although advances in technology should improve estimates in other ecosystem types.

Light detecting and ranging (LiDAR) provides highly accurate measurements of forest structure. Due to the high cost of flight time, the need to limit scanning to near nadir in order to prevent ranging errors, and the presence of coverage gaps due to aircraft pitch and roll, many LiDAR studies provide samples at the stand level or image small areas, most missions do not provide the same wall-to-wall coverage at the same scale as a Landsat TM scene or SAR image. In India, this technique could be utilized to address various aspects of forest ecosystem management, not possible earlier with the data available from aerial photographs, optical and radar satellites or even by ground measurements (Behera and Roy, 2002).

The optimal strategy for mapping forest structure would include the finely-detailed measurements of the vertical dimension that currently only field sampling provides as well as the broad spatial coverage and lower cost per unit area provided by remote sensing. Although no single technology is capable of providing this level of forest structural information at the present time, improvements in Radio Detecting and Ranging (RaDAR) and Light Detecting and Ranging (LiDAR) will likely lead to broad-scale mapping of vertical structure in the near future.

Direct measurements of forest structure that are highly correlated with biomass include diameter at breast height (dbh), basal area, canopy height, and crown volume. RaDAR and LiDAR systems make measurements of some of these variables directly, e.g., canopy height, and/or make measurements which can be used to infer these variables. Numerous researchers, have shown that these different LiDAR or RaDAR measurements, considered separately, can be used to estimate forest biomass. It has been demonstrated through experiments that if these different LiDAR and RaDAR forest canopy measurements, considered jointly, produce more accurate, precise estimates of above ground forest biomass. It can also be determined which of the LiDAR height and RaDAR height

and cross-sectional returns most accurately predict total above ground forest biomass in arid, relatively heterogeneous ponderosa pine stands.

3.4.7. Geomatics and Forestry

Geoinformatics (geographic information science, geomatics) aims at the development and application of methods for solving specific problems - with special emphasis on the geographical position of objects.

The future research direction and opportunities will be significantly affected both by the availability and utilization of Information Technology. As the complexities of processes are only recently being recognized through the application of new technologies, it is evident that an enormous gain in understanding can be realized only if multidisciplinary data are evaluated numerically, and integrated geospatially through the utilization of Information Technology. Ever-growing understanding and acceptance that the Earth functions as a complex system composed of myriad interrelated mechanisms have made scientists realize that existing information systems and techniques used are inadequate. Currently, the uncoordinated distribution of available data sets, a lack of documentation about them, and the lack of easy-to-use access tools and computer codes are major obstacles for scientists and educators alike. These obstacles have hindered scientists and educators in the access and full use of available data and information, and hence have limited scientific productivity and the quality of education. Recent technological advances, however, provide practical means to overcome such problems. Advances in computer design, software, disk storage systems as well as the growth of the World Wide Web (www) now permit for the first time the management of gigabytes to terabytes of data for distribution to scientists, educators, students, and the general public.

Remote Sensing and GIS are disciplines that are strongly data driven, and researchers and government agencies often develop large data basis. The complexity of the fundamental scientific questions being addressed requires integrative and innovative approaches employing these data basis if we are to find solutions. Although a number of databases exist, the ultimate goal is to create a fully integrated data system populated with high quality, freely available data, as well as, a robust set of software to analyze and interpret the data. This system would feature rich and comprehensive databases and convenient access. These capabilities are needed to attack a variety of basic and applied Earth Science problems.

The present day problems are inherently four-dimensional (x,y,z,t) in nature involving variation with time. Thus, their solution requires data analysis that is far more complex than provided by traditional Geographic Information Systems (GIS). The extent, complexity, and sometimes primitive form of existing data sets and data bases, as well as the need for the optimization of the collection of new data, dictate that only a large, cooperative, well -coordinated, and sustained effort will allow the community to attain its scientific goals. With a strong emphasis on ease of access and use, the resulting data system would be a very powerful scientific tool to reveal new relationships in space and time, and would be an important resource for students, teachers, the public at large, governmental agencies and industry. Fundamental new discoveries will require the availability of databases that encompass a variety of temporal and spatial scales. Because of the need to integrate heterogeneous data sets and tools to analyze them, Geoinformatics provides the focus for community participation in a national experiment to enhance and retain the pre-eminent role in the world.

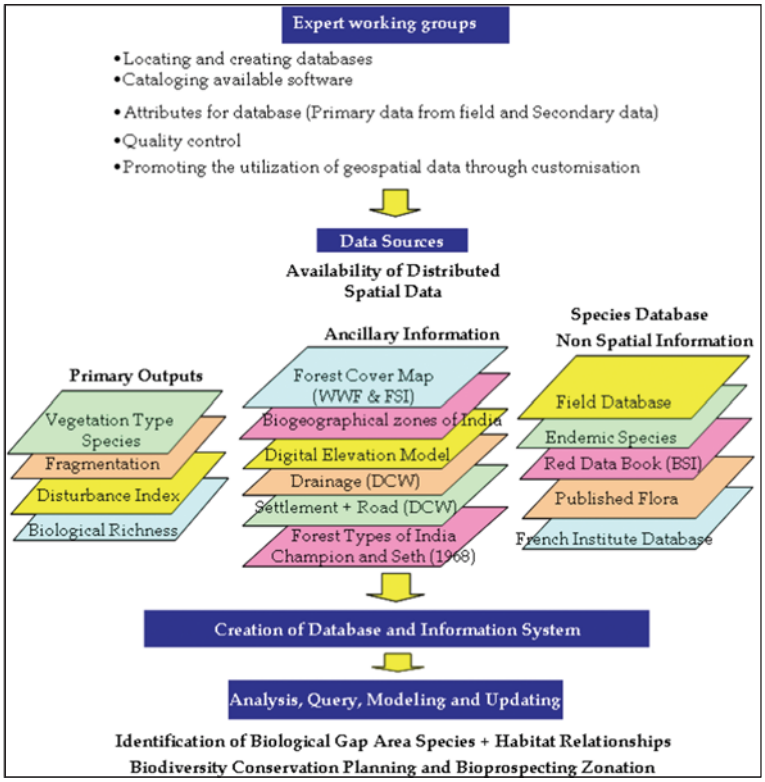

Figure 3.6: Steps in geoinformatics for creating biodiversity information system

The environmental control on the forest vegetation is well documented (Mueller-Dombois, Dieter and Ellenberg 1974). Physiography, topography, climate and

human interventions largely control the distribution of vegetation and biodiversity. The developments in computer based Geographic Information System (GIS) enables the integration of spatial and non-spatial information for defining the habitats and improving vegetation type descriptions in space and time. A review on GIS and database for vegetation mapping and monitoring is given by Skole *et al.*, 1993. It is also possible to evolve geospatial models using multi criterion to present disturbance regimes and landscape diversity. Landscape ecology has evolved as an operational tool with the availability of geospatial modeling techniques. Tomlin (1990), Mc Guire *et al.*, 1988, Antencci *et al.* (1991) and Miller (1994) provide number of examples of application relevant to biodiversity. The power of having all information and knowledge along with access, modeling, and visualization tools at the finger tips of a user has great potential in advancing science, accelerating the discovery process, and enhancing the quality of science and education. The steps in Geoinformatics for creating Biodiversity Information System are given Figure 3.6.

Table 3.7: Components of biodiversity assessment and measurement tools (Murthy *et al.*, 2003)

No	Parameters	Remote sensing	Ground Measurement / GPS	GIS Based (Derived/Integrated Spatial layer)
A	Human interventions	√	√	√
1	Logging	√	√	√
2	Grazing	√	√	√
3	Fire	√	√	√
4	NTFP resouces extraction	√	√	√
5	Trampling	√	√	√
6	Plantation	√	√	√
7	Agriculture	√	√	√
8	Encoarchment/ Clearances	√	√	√
9	Infrastructure	√	√	√
B	Natural Processes	√	√	
10	Climate	√	√	√
11	Erosion	√	√	√
12	Topography	√	√	√
13	Soil	√	√	√
C	Structure and Function		√	
14	Vertical structure	√	√	√
15	Size class distribution		√	
16	Relative abundance		√	
17	Gap frequency	√	√	√
18	Canopy openness	√	√	√
19	Standing and fallen dead wood		√	√
20	Trophic dynamics		√	√
21	Other structural elements		√	
D	Landscape level			
22	Vegetation type and extent	√		√
23	Landscape diversity	√		√
24	Species diversity	√	√	√
25	Number of patches per unit area	√		√
26	Neighbourhood	√		√
27	Patch shape	√		√
28	Core-edge ratio	√		√
E	Habitat level			
29	Species assemblages / Communities	√	√	√
30	Species diversity	√	√	√
31	Interior to exterior habitat	√	√	√
32	Regeneration	√	√	√
33	Habitat extinction	√	√	√
F	Species level			
34	Reproduction		√	
35	Dispersal		√	
36	Regeneration		√	
37	Migration		√	
38	Location extinction		√	

The holistic understanding of the complex mechanisms that control biodiversity, as well as their spatial and temporal dynamics, requires synergetic adoption of measurement approaches, sampling designs and technologies. The data requirements include data of both spatial and non-spatial nature and also of various time scales. In view of this, the combination of satellite remote sensing, Global Positioning System (GPS), and integrative tools (such as GIS and information systems) is an important complimentary system to ground-based studies. It has been well explained by Murthy *et al.* 2003 that these technologies together form the basis for geoinformatics. The various parameters required for biodiversity assessment and their amenability for measurements by different techniques is given in Table 3.7.

3.5. Major Application Projects

3.5.1. Different IRS satellite sensors and use for bioresources assessment

IRS P6 satellite provides unique opportunity of having different resolution sensors on the same platform. AWiFS (56 m), LiSS III (23.5 m), LiSS IV (5.6 m) provide the capability to study and assess different forest parameters at various spatial scales. Cartosat I data with 2.5 m resolution help in detailed assessment of forest structure and species composition. A large range and scale of information can be acquired by making use of all these sensors. Coarse resolution sensors with high repetivity as the AWiFS are being used effectively for monitoring forest fires, rapid forest cover monitoring, vegetation phenology, carbon sequestration and forest productivity studies at global and regional scale. LiSS III sensor having spatial resolution of 23.5 m has wide application for studying forest composition, gregarious formations, monitoring of forest stands and plantation activities. High resolution LiSS IV and Cartosat sensors have applicability in studies pertaining to canopy density, canopy height and mapping of individual

trees of economic importance as Teak and Sal and NTFP (Non Timber Forest product) such as canes, gums, resins, fibre yielding forest species. Satellite remote sensing capabilities have undergone significant advancement over the years. Starting from coarse resolution MSS sensors of 1970's a range of sensors as the Cartosat, LiSS IV, LiSS III, AWiFS are available now which can be applied for sensing and monitoring various forest parameters. Similarly from simple mappings carried out with the earlier sensors in 1980's forest remote sensing has come a long way passing through the whole gamut of applications as monitoring and change assessments, biodiversity studies, fire detection and species prediction. Now the focus lies on developing Information systems and model ecological processes.

3.5.2. Forest Cover Assessment

At the backdrop of increased developmental activities, demand for land and forest as bioresource, the Government of India has taken up the task of assessing forest cover in 1986, National forest cover mapping was initiated by NRSA for the periods 1972-75 & 1981-83 using Landsat MSS data at 1:1 million scale. Forest cover mapping provides total forest area information in terms of crown density classes, an index of condition of forests. Forest crown density refers to the per cent area covered by tree crown per unit ground area. NRSA initial study has revealed significant loss of forests during 1972-83 and given alert signal to the country for conservation of forests.

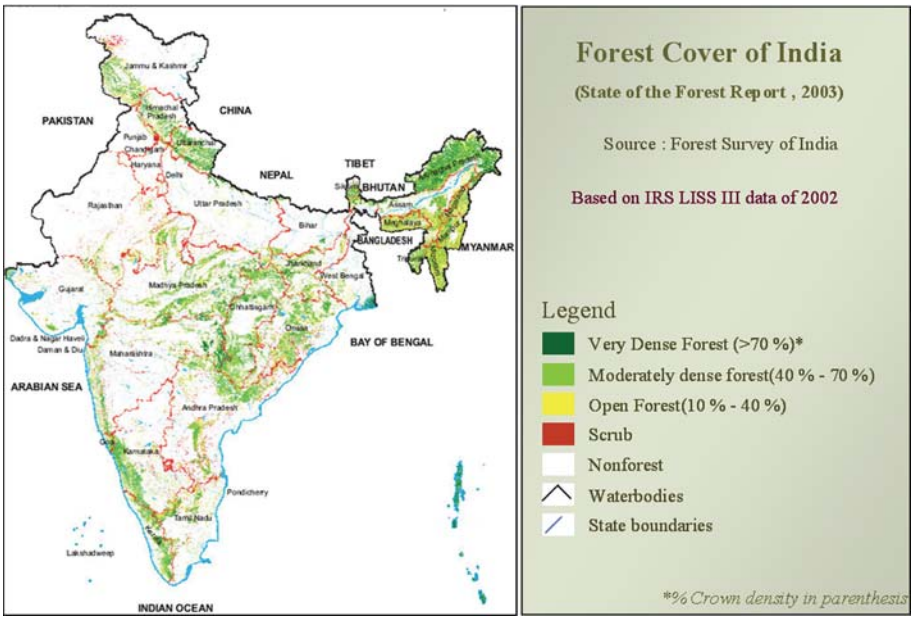

Figure 3.7: Forest cover assessment of India

In addition, the study has also established the operational methodology for national cover mapping and technology was transferred to Forest Survey of India (FSI). Since then, FSI has made ten biennial assessments. Forest cover was interpreted visually for first seven cycles at 1:250,000 scale, and then digital approaches are followed for the subsequent cycles (1:50,000) for two crown density classes 10-40% and >40%. As spatial resolution improved classes > 70 %, 40 – 70%, 10-40 % and scrub have been delineated in addition to the tree cover outside the Reserve forest areas (Figure 3.9). The present assessment (2005) represents >70 %, 40-70%, 10-40 % scrub and tree cover with multitemporal, sensor capability with total forest area reported as 67.7 Mha of the country (Figure 3.7).

3.5.3. Vegetation type mapping as potential base of bioresource

India has diverse climatic, geological, topographical and anthropogenic disturbance gradient. This has resulted in the formation of diverse vegetation communities e.g., major Eco-regions like Eastern and Western Himalayas, Shivaliks, Vindhyans, Eastern and Western Ghats and Coast constituting region specific vegetation type. Champion & Seth (1968) based on extensive ground surveys brought out forest type classification using forest structure, composition and environment (climate, topography). They identified 16 major type groups and 221 forest types. Champion & Seth (1968) classification scheme does not have spatial explicitness and with the increasing pressure on forests during the last three decades, changes at several places were noticed in forest composition. In view of this, satellite remote sensing is used as one of the effective tools to delineate forest types for better management. Forest types based on structure (canopy, height, branching, and tree density), composition (species mixture) and phenology (leaf onset/offset – leaf fall) provides unique spectral signatures. Based on the Phenological / structural properties, the 16 major type groups of the country were mapped using multi temporal SPOT and IRS WiFS data.

As part of joint initiative of Department of Space and Department of Biotechnology, 120 vegetation types covering mixed formations, gregarious formations, locale specific formations, grasslands, degradational stages, plantations, scrub and orchards were mapped for the entire country using IRS LISS-III data and available as digital database (figure 3.8). Vegetation type map for Orissa state has been shown separately in figure 3.9 depicting Sal mixed moist deciduous forest as the dominant vegetation type. This geo-database encompasses the whole

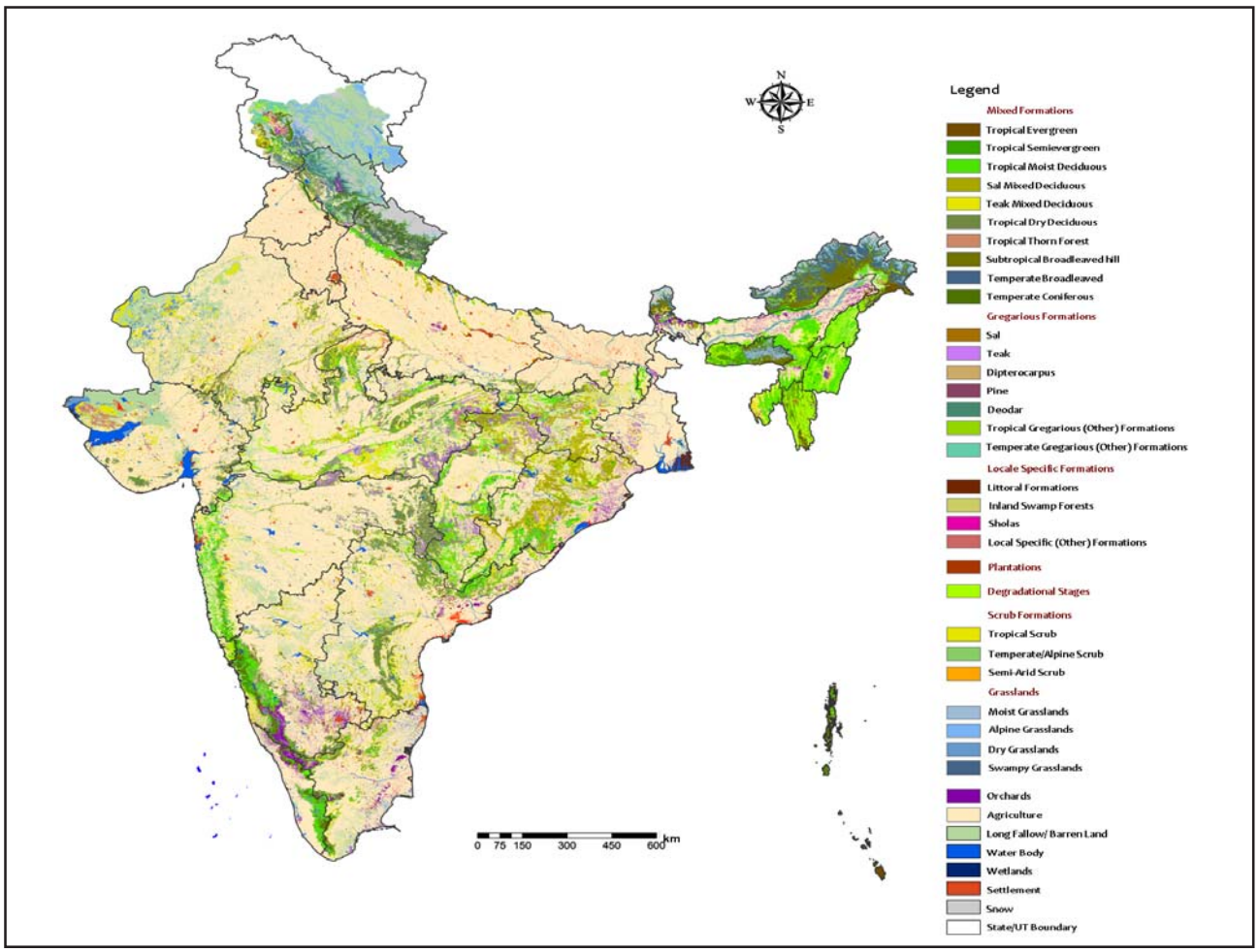

Figure 3.8: Vegetation type map of India(source: Roy et al., 2010 communicated)

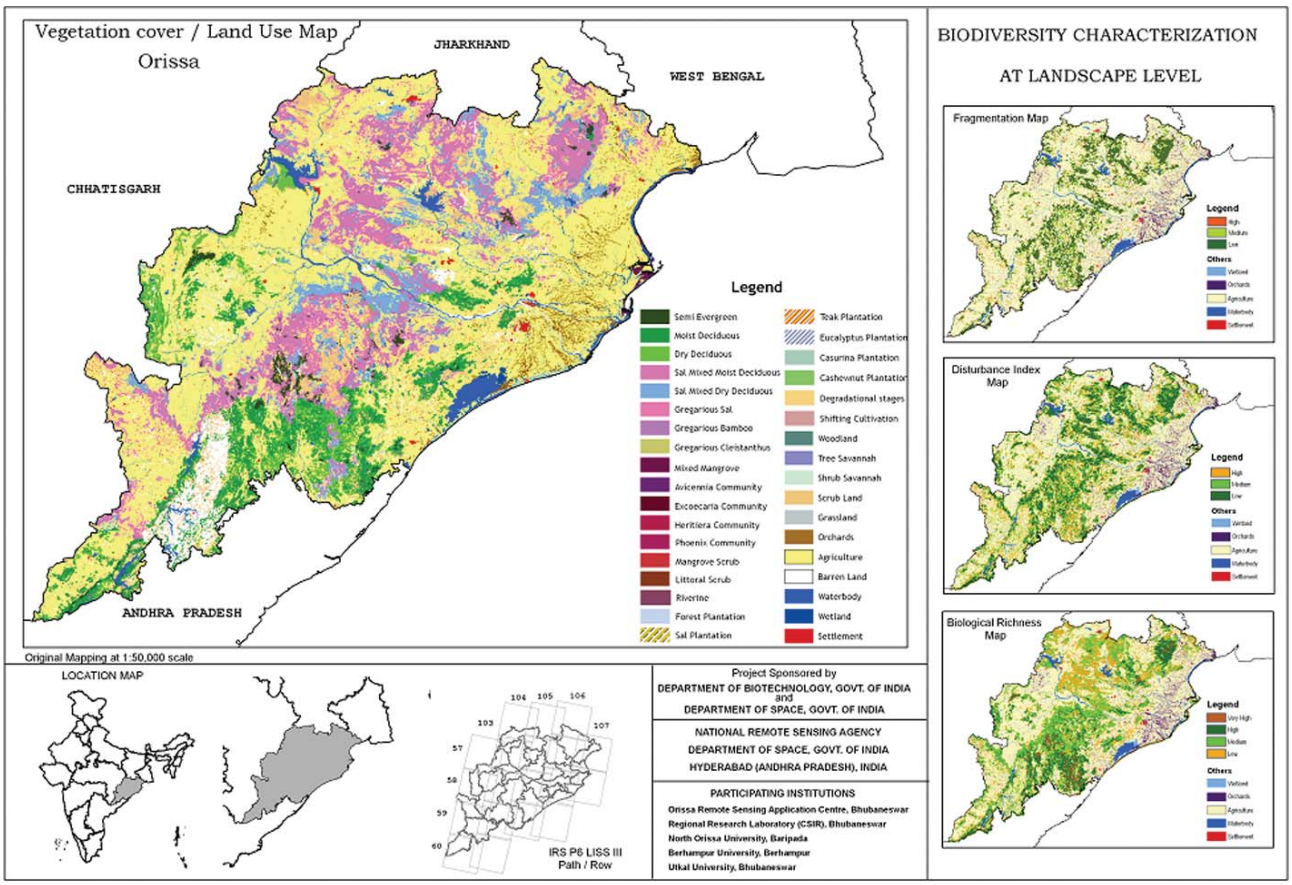

Figure 3.9: Vegetation type map of Orissa state

range of variability across climatic, edaphic and disturbance regimes across the country and also addresses the natural and man-made vegetation formations. Identification of gregarious formations (such as Red Sanders, Ephedra, Hippophae, Acacia, Sal, Teak,Dipterocarpus, Deodar etc.) along with grasslands and deciduous formations rich in medicinally important plants provide unique database for bio-prospecting prioritization. Spatial databases on locale specific formations like riverine, alpine and coastal vegetation and different degradational stages of vegetation stand as key database for conservation planning.

Currently FSI is preparing detailed forest type map for the entire country on 1:50,000 scale. These forest types have unique species composition having different economic and ecological value which can be effectively quantified using optimal ground surveys.

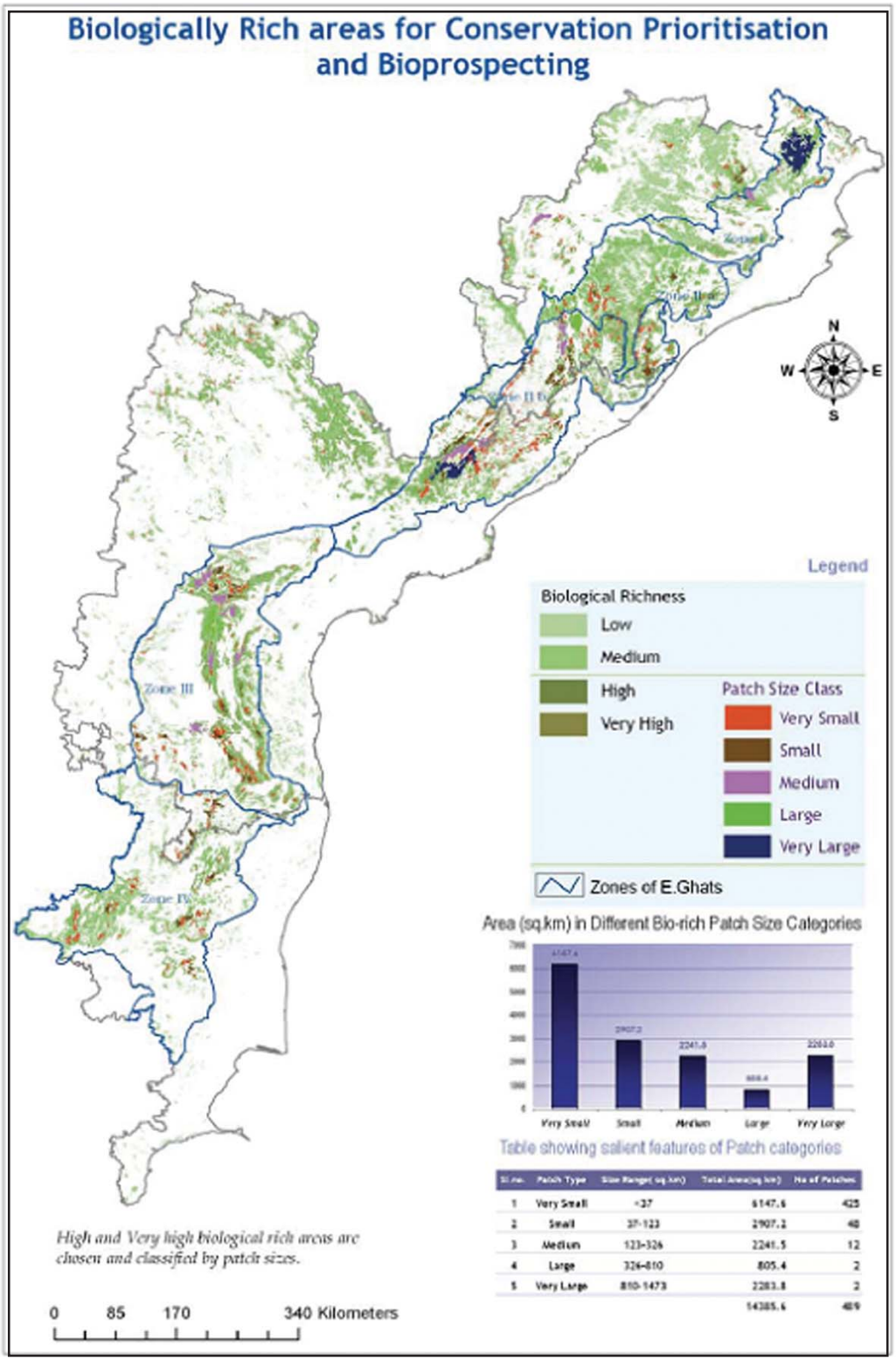

Figure 3.10: Biologically rich areas for conservation prioritization and bioprospecting in Eastern Ghats

3.5.4. Landscape level biodiversity assessment- Input for Bioresources assessment

On global to local scales, the only feasible way to monitor the Earth's surface to prioritize and assess the success of conservation efforts is through remote sensing. Currently a suite of remote sensing satellites, having various resolutions, are available to generate spatial information on vegetation and land-cover from global to local level. The remote-sensing-based information on vegetation and land cover provides a potential spatial framework and works as one of the vital input layers for the following:

- Vegetation, land cover losses and conversion
- Stratification base for optimal ground sampling and assessment of diversity
- Fragmentation and neighborhood analysis
- Delineation of broader vegetation types and analysis of species assemblages along with ancillary data
- Identification of gregarious and ecological by important species
- Inputs for species habitat models
- Spatial delineation of biologically rich zones
- Developing conservation strategies

In a major initiative, 50 Mha (80%) forests were characterized for intact and critical habitats of biodiversity under the project 'Biodiversity Characterization at Landscape Level'. The project was carried out in two phases the first phase the Western Himalayas, North East, the Andaman and Nicobar Islands and the Western Himalayas were covered. In the second phase central India, West Bengal and Eastern Ghats and East coast (Figure 3.10) was covered. The study is an outcome of the efforts of 27 Universities and 11 National institutions involving 63 scientists and 56 research scholars. Ten spatial layers comprising Vegetation types derived from remote sensing data, forest fragmentation, settlement and road buffers, ecosystem uniqueness, species diversity and economic value derived from 12,000 sample plots among others was integrated in geospatial domain to derive index of Biological Richness. The data is organized in web based 'Biodiversity Information System' facilitating query and analysis. The data provides spatial extent and relative abundance of vegetation patches of medicinal and economic value for prioritizing the plan for bioprospecting.

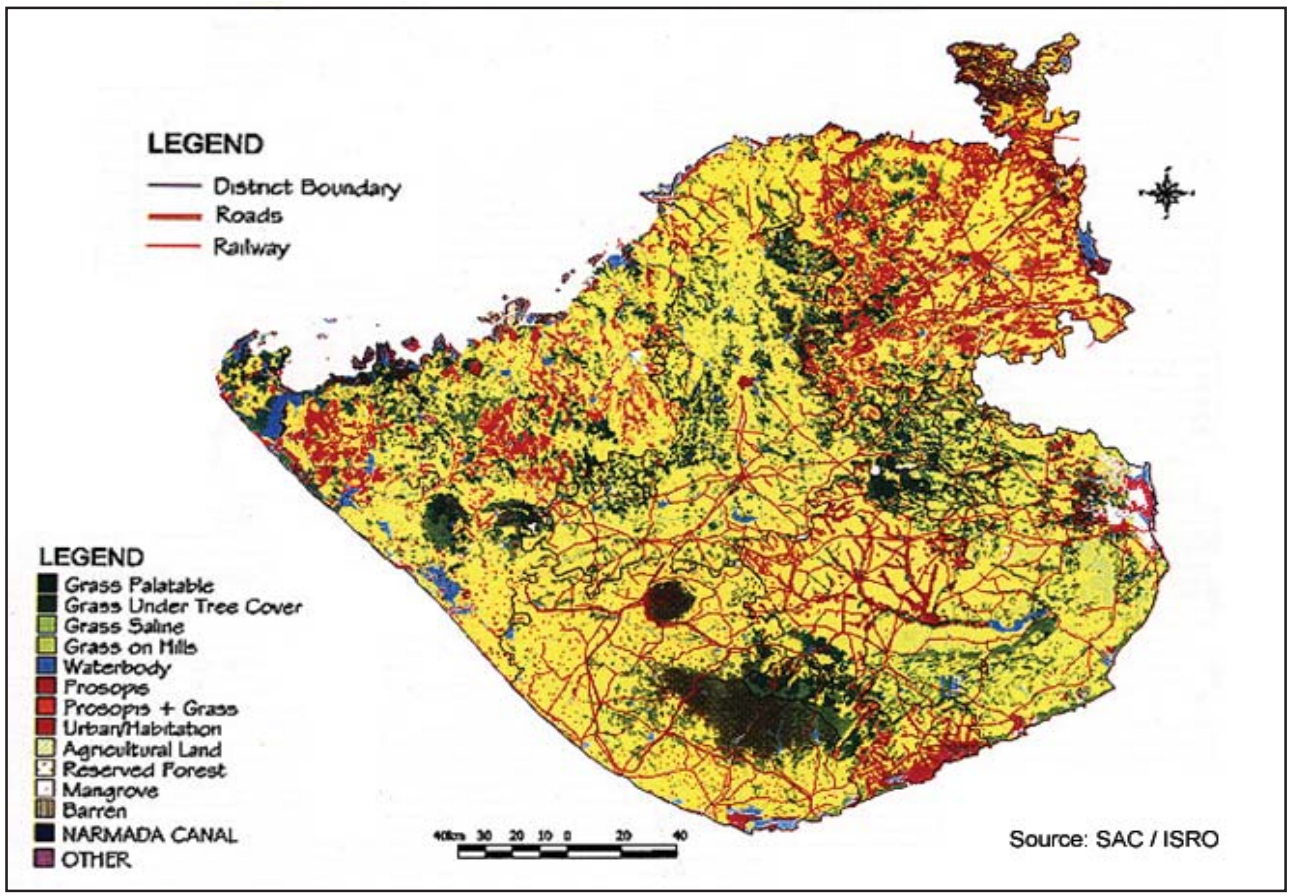

Figure 3.11: Grassland map of Saurashtra region of Gujarat

nrsc

Remote Sensing Applications

P. S. Roy
R. S. Dwivedi
D. Vijayan

National Remote Sensing Centre

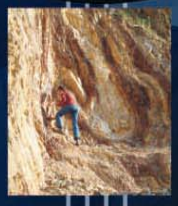

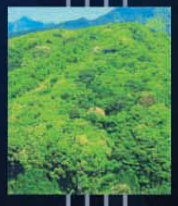

Remote Sensing Applications

Soils and Land Degradation

4.1. Introduction

The soil is a life supporting system upon which human beings have been dependent from the dawn of the civilization. Therefore, comprehensive information on soil resources, its potential / limitations / capabilities, is required for a variety of purposes such as command area development, soil conservation in catchment areas, sustainable agriculture, watershed management, reclamation of degraded lands etc. In this context, characterization and mapping of different types of soils, developing rational / scientific criteria for land evaluation and interpretation of soils for multifarious land uses attains greater importance.

Remote sensing technology has been successfully used in studying the various aspects of soils in spatial and temporal domain. The data obtainable from the sensors placed in a satellite or aircraft or ground level could be interpreted as a function of soil properties. Therefore, spectral reflectance of soils plays an important role in extracting information on different types of soils and land degradation. The techniques make use of data obtained from different regions of electromagnetic spectrum viz., visible, infrared, thermal and microwave regions.

A good number of studies carried over nearly three decades testifies the role of remote sensing in soil related studies. The interpretation techniques have also undergone change over a period of time on par with satellite spatial and spectral resolutions. In this chapter, application of geospatial technology (Remote Sensing, GIS, GPS) in the study of spectral reflectance of soils, land degradation mapping, monitoring of degraded lands, soil moisture along with important issues and prospects are discussed.

4.2. Spectral Reflectance of Soils

Understanding the spectral reflectance properties of soils is fundamental to many applications of remote sensing in soils. The soil reflectance data can be acquired in the laboratory or in the field and from air / space. In the laboratory the soil reflectance measurements are made under controlled conditions, which may enable to understand the relationship between the physical and chemical properties of soil and soil reflectance. In the field, reflectance measurements are made with the help of portable field spectrometers / radiometers. Field soil spectroscopy will help in rapid point to point measurement of soil properties. However, the measurements are affected by variations in viewing angle or illumination condition and roughness factors. In the case of soil reflectance from air / space, the soil reflectance values can be obtained over a large area and reflectance can be studied in spatial domain. But factors like low signal to noise ratio and atmospheric attenuations have critical effect on these measurements.

Nevertheless, information about soils from reflectance spectra in the visible (0.4 µm to 0.7 µm), near infrared (NIR – 0.7 to 1.1 µm) and short wave infrared (SWIR- 1.1 to 2.5 µm) regions of electromagnetic spectrum (EMS) represent most of the data the passive remote sensors can provide. Besides this thermal infrared regions (3 to 5 µm and 8 to 12 µm) do provide diagnostic information about soils. Spectrometers, radiometers and polarimeters provide quantitative measurement of reflected energy from soil and have found applications in studying the various aspects of soils as mentioned previously.

The shape and nature of a soil reflectance curve depends upon the physical and chemical properties of soils. The important physical properties are soil colour, soil texture, structure, soil moisture, surface conditions / roughness etc. The chemical properties of soils result in absorption of incident radiation and is seen on reflectance curve as troughs whose positions are attributed to specific chemical groups in various structural configurations. It includes soil mineralogy, organic matter, salinity, carbonates etc.

The most important soil properties that influence the reflectance are soil moisture content, texture, structure and iron oxide content (Hofer, 1978; Stoner and Baumgardner, 1981). These factors are interrelated and the spectral reflectance of soil is a cumulative property of combination of these factors (Baumgardner *et al.*, 1985 and Irons *et al.*, 1989).

Soil color, particularly the Munsell color value component, has been identified in many studies affecting the amount of energy reflected from soil surfaces (Post *et al.*, 1994). Post *et al.*, 1993 also evaluated using a Chroma Meter to measure soil colors and concluded that commercial colorimeters have great potential as tools to precisely measure soil colors. They also demonstrated how color changes from the dry to a wet condition. The greatest change for the Munsell color value component was also strongly correlated with soil albedo. The observed darkening

of wet soil is due to the optical effects of a thin liquid layer on the soil surface. Soil color is mostly influenced by mineralogy, chemical composition, soil moisture, and organic matter content. It is an important parameter that allows the diagnosis of soil types and their properties, as well as the detection of changes affecting ecosystems like erosion, salinization and / alkalization. A detailed investigation by Escadafal (1993) revealed that for measuring soil colour, remote sensing sensors capable of sensing in blue (450-500 nm), green (500-550 nm) and red (650-700 nm) are very important.

Organic matter in soils has profound influence on soil spectral characteristics. The increase in organic matter has been found to result in a decrease in reflectance. The organic matter has effect on spectral reflectance of soils throughout the visible, NIR and SWIR region of EMS and many workers have studied organic matter extensively from a remote sensing point of view. The absorption features of reflectance spectra are related to functional groups in the organic matter (Elvidge, 1990; Chen and Inbar, 1994) and models were developed to predict the humus / organic carbon content in soils (Buamgardner *et al.*, 1985; Shepherd and Walsh, 2002). The absorption features representing organic matter were found at 1720 nm, 2180 nm and 2309 nm.

Particle size or soil texture (refers to relative proportions of sand, silt and clay in soil) is another soil property that influences the spectral reflectance of soils significantly (Buamgardner *et al.*, 1985). Finer the particle size, the soil becomes smooth and more incoming energy is reflected. An increase in particle size causes a decrease in reflectance. However, silt content of soil is considered as major controlling factor for spectral reflectance. The spectral reflectance decreases with decrease in silt content. However, it is commonly observed that sandy soil exhibits higher reflectance than that of clayey soil, which is due to abundance of macro pores and air-soil interface. Under field conditions the soil structure play a dominant role in altering the reflectance from soil (Buamgardner *et al.*, 1985).

It was reported that an increase in iron oxide content in soils can cause decrease in reflectance, in visible wavelengths (Obukov and Orlov, 1964; Vincent, 1973). Many of the absorption features in soil reflectance spectra are due to the presence of iron in one or other form (as Hematite) and provide significant evidence on soil weathering process. Soils dominant in ferrous and ferric ions exhibit high response in the red region of spectrum. The ferric ion response bands are approximately at 0.40, 0.70 and 0.87 µm and a sharp and narrow absorption band is evident at 0.9 µm. The ferrous ion on the other hand, has been found to respond at 0.43, 0.45, 0.51, 0.55 and 1.0 µm.

Clay minerals are layered crystalline aluminosilicate minerals and are characterized by hydroxyl bands at 1.4 µm and 2.2 µm. Most of the work done on soil spectral reflectance on clay mineralogy is mostly on pure minerals under laboratory conditions (Mulders, 1987; Kruse *et al.*, 1991). These studies shows that absence of appreciable amount of bound water in Kaolinite shows a weak band at 1.9 µm due to absence of appreciable amounts of bound water while montmorillonite shows very strong bands at 1.9 µm as well as at 1.4 µm. Quartz and feldspar show very high reflectance and the spectrum in the visible and near infrared is almost devoid of spectral features (such as absorption maxima denoted as bands) unless impurities occur. Carbonate response bands were noticed at 1.90, 2.00, 2.16, 2.35 and 2.55 µm. Soils with Gypsic minerals reflect highly because of the inherent reflectance properties of gypsum.

Soil crusting too has influence on soil reflectance. The work carried out by De Jong (1992) and Savin, (1996) shows an evidence that it is feasible to provide information with respect to the crusting status with reflectance spectroscopy. Significant spectral changes resulting from the structural crust formation were detected on the soil surface and these changes were attributed to both particle-size distribution and mineralogical composition (Ben-Dor *et al.*, 2003).

In the Indian context very limited studies has been carried out on spectral behavior of soils (Venkataratnam,1980; Dwivedi et al 1981; Sinha 1986; Kalra and Joshi , 1994; Rao et al 1995). Ravisankar and Rao (2004) studied the spectral response pattern of major soil types in Guntur district of AP. In this study, the MODIS reflectance data was correlated with soil properties using stepwise multiple linear regression (SMLR). Good correlations were obtained for pH (r^2 = 0.87), Organic Carbon (r^2 = 0.71), Cation Exchange Capacity (r^2 = 0.77) and Clay content (r^2 = 0.61).

The study of spectral reflectance of soils has ability to provide non-destructive rapid prediction of soil physical, chemical and biological properties under laboratory conditions, for sensing soil organic matter content in the field and for the discrimination of major soil types from satellite data and hyperspectral data. There has been little focus on development of soil spectral libraries for using in prediction and interpretation of soil properties. In

India, spectral libraries were developed using ASD FieldSpec@Pro radiometer (with spectral range of 350 nm - 2500 nm) for about 600 pedons and 2500 surface and subsurface soils covering all major soil orders in major physiographic units in the country (NBSS&LUP Report no.835) under 'Development of spectral libraries for major soils of India' project. Such hyperspectral libraries will be of immense use for characterization of soils.

4.3. Recent Developments in Soil Spectroscopy

In the recent developments, importance is being given to utilization of hyper-spectral domain for soil physical and chemical characterization. Development of soil reflectance libraries is being given utmost importance with parallel developments in hyperspectral profile matching algorithms. In this direction, an attempt has been made to calibrate soil properties to soil reflectance using Multivariate Adaptive Regression Splines (MARS). Spectral analysis techniques and screening tests were also being developed to address the soil / plant nutrient status and fertility constraints (Shepherd and Walsh, 2002). Since the mid-1980s, developments in instrument technology and chemometrics (the application of mathematical and statistical techniques to chemical data) have led to the increased use of spectroscopy in the laboratory and field and from space platforms (Clark, 1999).

Recent research studies demonstrated the ability of reflectance spectroscopy to provide nondestructive rapid prediction of soil physical, chemical, and biological properties in the laboratory (Ben-Dor et al, 1997 and Reeves *et al.*, 1999). Sudduth and Hummel (1993) could successfully apply reflectance spectroscopy for sensing of soil organic matter in the field. Despite of good potential, there are few examples of the application of reflectance spectroscopy for non-destructive assessment of soils (Janik *et al.*, 1998; Myer, 1998). Although geological spectral libraries exist that include soil mineral spectra (Clark, 1999), there are few examples of soil spectral libraries that include a wide diversity of soils with information on physical, chemical, and biological properties. Development of soil spectral libraries for application to risk-based approaches to soil evaluation explicitly accounting uncertainty in predictions and interpretation of soil properties is need of the hour.

Fundamental features in reflectance spectra occur at energy levels that allow molecules to rise to higher vibrational states. For example, the fundamental features related to various components of soil organic matter generally occur in the mid- to thermal-infrared range (2.5–25 μm), but their overtones (at one half, one third, one fourth etc. of the wavelength of the fundamental feature) occur in the near-infrared (0.7–1.0 μm) and short-wave infrared (1.0–2.5 μm) regions. Soil clay minerals have very distinct spectral signatures in the shortwave infrared region because of strong absorption of the overtones of sulphate, carbonate and hydroxyl combinations of fundamental features of H_2O and CO_2 (Hunt, 1982; Clark, 1999). The visible (0.4–0.7 μm) region has been widely used for color determinations in soil applications as well as in the identification of Fe oxides and hydroxides (Ben-Dor *et al.*, 1999).

4.4. Soil Mapping

Soil mapping comprises of identification, description and delineation of different kinds of soils based on physiography, climate and vegetation of the area, confirmation through field work and laboratory data and depicting on a standard base map. The different soils observed within an area are put into a limited number of groups. Each group of soils is typified by a pedon or their association. A pedon is morphologically described in the field and sampled for laboratory investigations for their characterization and classification. Such groups of soils may occur on the landscape in a repeated manner and are delineated on a map as "map unit". The delineated units on a map will be given a specific symbol, colour and name. Soil maps contain several mapping units along with a legend that give description of each soil unit. The soil maps are prepared on different scales varying from 1:1 million to 1:4,000 to meet the requirements of planning at various levels.

The scale of a soil map is of importance as it has direct correlation with the information content and field investigations that are carried out. Small scale soil maps of 1:1 million are needed for macro level planning at national level for several developmental programmes. Similarly, soil maps at 1:250,000 scale are needed for state / regional level planning by various agencies such as state level Land Use Boards, Department of Agriculture, Irrigation etc. Soil maps on 1:50,000 scale could be generated through standard soil survey consisting of comprehensive data collection on soils / land in such a manner that the data could be used for a variety of purposes. Soil maps at 1:8,000 or larger scales are required for micro level planning and most of these maps are oriented to a specific purpose such as for soil conservation, reclamation, soil fertility studies, trafficability, revenue and taxation, crop suitability etc.

4.4.1. Status

The Food and Agriculture Organisation published (FAO, 1970- 78) 1:5 Million scale soil maps of the World. In western countries, soil mapping at appropriate scales is completed or nearly done and the emphasis is towards specific, project oriented surveys and innovative application. Survey of literature reveals that many countries have same kind of general soil map at very small scale usually at or smaller than 1:250,000. Soil maps at scales 1:50,000 or 1:25,000 scale, appropriate for project planning, are not available with many countries. The soil maps for operational planning at scales larger than 1:25,000 are very scares. This shows that there is a requirement for medium and large scale soil maps in most of the countries including India. At larger scales, soil information can significantly contribute to micro level land use planning and solution to problems in soil.

In India, soil survey is carried out both by central and state level organizations. However, there is no regular system of recording and periodic updating of the areas covered by soil surveys by various central and state organizations / agencies. Soil surveys done by various agencies usually lack uniformity with respect to scale of base maps and published maps, kinds of survey and intensity of observations, units of mapping and soil correlation. According to report of the Task Force (1984) the total areas surveyed in the country up to 1983 under detailed soil surveys was 33.5 million hectares and reconnaissance soil surveys was 115.0 million hectares. NBSS&LUP had prepared soil map of the entire country at 1:250,000 scale using satellite imagery and published them at 1:500,000. According to DOS (1999), the status of soil mapping at 1:50,000 scale was 119.37 million hectares for the whole country. Information on larger than 1:50,000 scale may be available for very limited area and statistical figures are not available at country level.

4.4.2. Survey Methods

General soil survey methods comprises non-systematic, grid, continuous, physiographic and free surveys. In non-systematic survey, soil boundaries are determined from published maps such as geology and physiography. Broad field checks are made to determine typical soil properties. There is no estimate of internal variability. In Grid survey, a systematic sampling scheme is designed, taking into account the expected range of spatial auto-correlation. Sample points are located in the field and characterized. Standard statistical and geo-statistical methods are used to estimate spatial variability of soil properties. Continuous survey provides very accurate estimates of internal soil variability. Remote sensing methods come under this category.

In the case of physiographic survey, interpretation of landforms with the help of aerial photographs is carried out followed by field checking of map unit composition; sometimes only in sample areas, i.e. not all the delineations are actually visited. Sampling is biased towards 'typical' landscape positions. This method is used for scales: 1:50,000 to 1:200,000. The utility of soil maps at various scales and the remote sensing data suitable are appended as Table 4.1. Free survey starts with a detailed physiographic interpretation and all boundaries are verified and possibly modified by field investigation. In areas with poor correlation of geomorphology to soils, the field observations themselves are used to locate the boundaries. There should be enough observations to obtain a fairly good estimate of internal variability. Typical scales of free surveys range from 1:12,500 to 1:25,000. Initially the surveyor analyses the soil forming factors of a given location in a top sequence and locates observations to confirm his hypothesis. Initially, a few field observations in terms of soil profile will be made to

Table 4.1: Mapping scales, sensors and levels of soil mapping

Soil Survey Scale	Sensors	Soil Classification	Useful For
1:250,000	LANDSAT-MSS, IRS-LISS-I , WIFS	Subgroups/ Families and their association	Resource Inventory at Regional Level
1:50,000	IRS-LISS-II/III LANDSAT-TM SPOT	Soil Series and their association	District/ Sub-District Level
1:25,000	IRS-IC/ID (PAN+LISS-III MERGED DATA)	Soil Series and their association	Block / Taluk / Mandal Level
1:8000 or larger	IKONOS / LISS-4 / CARTOSAT	Types and Phases	Village Level

test this hypothesis and assess the variability. Depending on requirement, more observations will be recorded, if variability is not properly addressed.

4.4.3. Geo-Pedological Approach to Soil Mapping

The 'Geo-pedological Approach' to soil survey was developed by Zinck (1988) and is essentially a systematic application of geomorphic analysis to soil mapping. This approach can be used to cover large areas rapidly, especially if the relation between geomorphology and soils is close. It is based on two hypotheses. The first one is, boundaries drawn by landscape analysis separate most of the variation in the soils. This will be the case if the three soil-forming factors (parent material, relief, time) which can be analyzed by this approach are dominant (not organisms, climate), and also if the mapper has correctly interpreted the photo / imagery and sample areas. The interpreter must form a correct model based on the geomorphology (soil-landscape relations) and apply it correctly and consistently. If sample areas are representative, soil pattern can be reliably extrapolated to unvisited map units. In addition, the geo-pedological approach has advantages in legend construction and structuring. The geo-pedological approach is a hierarchical system applied in semi-detailed studies.

4.4.4. Remote Sensing and Soil Mapping

Before the advent of remote sensing techniques, the soil surveys were conventionally carried out at reconnaissance, detailed and detailed-reconnaissance level depending upon the requirements. In all these three methods soil mapping is done after field observations. Later, aerial photographs were used as remote sensing tool in soil mapping and because of some technical limitations they could not be operationalised in soil mapping. Application of satellite remote sensing data from satellites for soil studies began with the launch of Landsat-1 in 1972. Remote sensing techniques have reduced fieldwork to a considerable extent and soil boundaries are more precisely delineated than in conventional methods. While mapping the soils using remote sensing technique, the stereo data is highly useful in identification of different landforms, which have got close relationship with the soils associated with them. The stereo data from panchromatic (PAN) cameras aboard SPOT/ IRS-1C/ Cartosat-1 enabled the delineation of physiographic units and soil maps derived there from in a better way.

4.4.5. Visual Interpretation for Soil Mapping

The approach for soil mapping using visual techniques has been summarized in Figure 4.1. The Figure 4.2 gives the schematic approach for soil mapping using satellite data. The broad methodology for mapping soils has been explained hereunder.

Satellite Data

The satellite data with minimum crop cover / vegetation better aids in the identification of soil patterns from the remote sensing imagery. The data of summer months is in generally good for soils study. However, under certain terrain conditions the data of monsoon in association with summer season helps to better extract information on soil types. The scale of soil map determines the sensor that has to be employed in the project. For example, Landsat – MSS and IRS – LISS –I sensor data with a spatial resolution of 80 m and 72.5 m were more useful for soil mapping at 1:250,000 scale or smaller scales. Similarly, for mapping soils at 1:50,000 scale remotely sensed data from Landsat – TM and IRS-LISS II / III sensors will be of greater help.

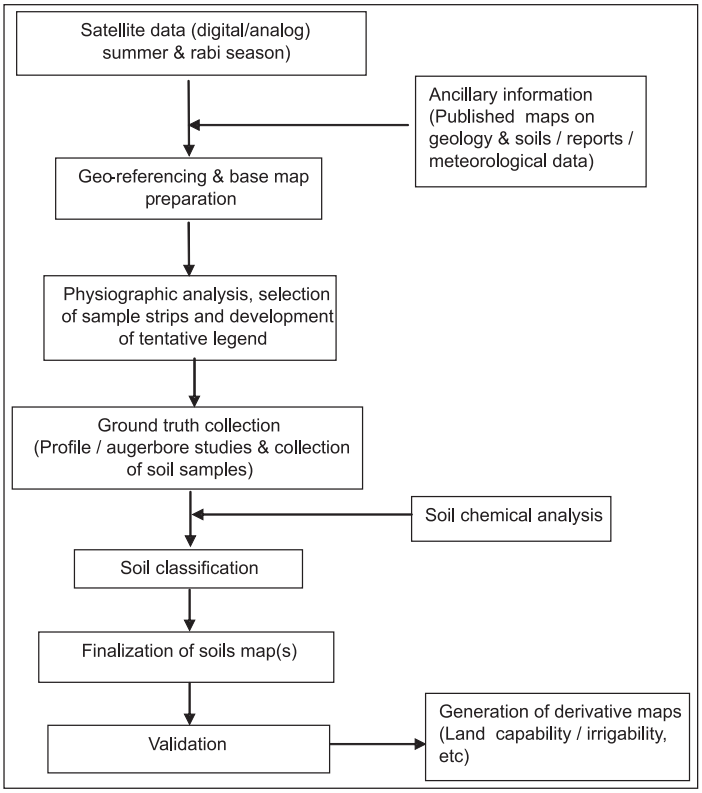

Figure 4.1: Flow chart for soil map preparation

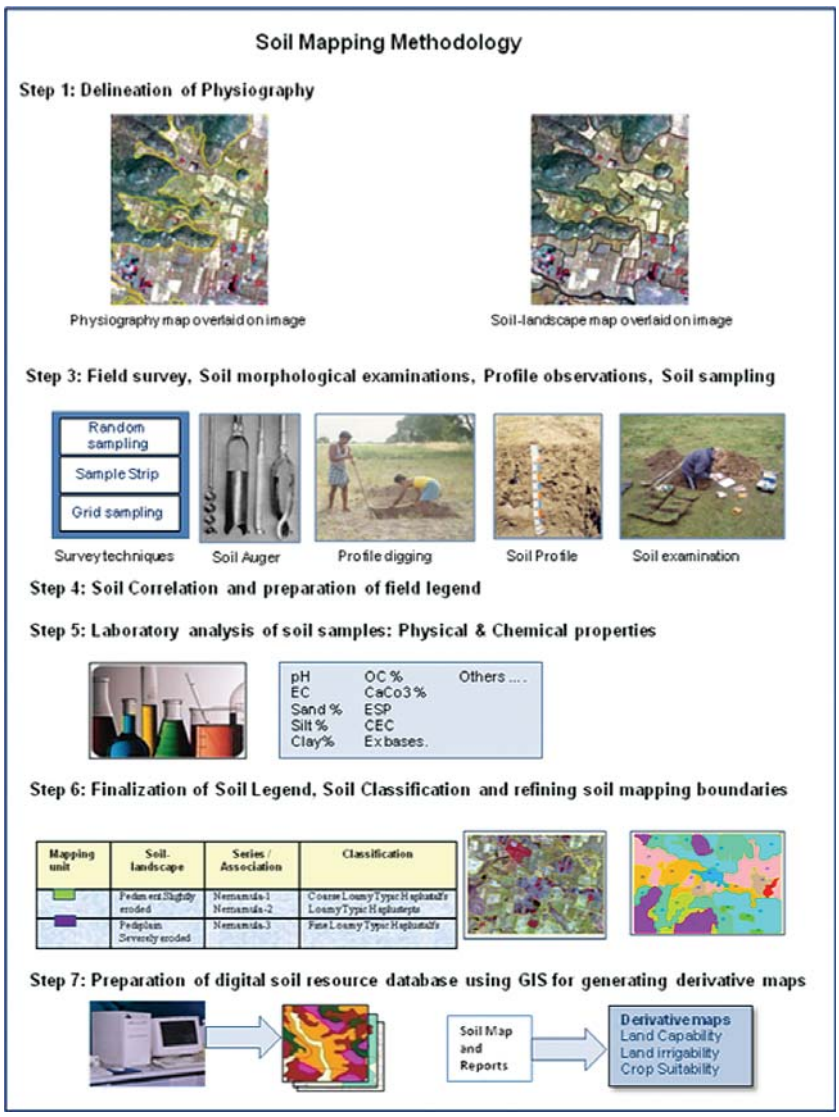

Figure 4.2: Schematic diagram of soil mapping methodology

Ancillary information

The ancillary data required for preparation of soil map consists of topographical maps, published soil maps, geological maps, reports, climatic data (rain fall, temperature etc). Topographical map sheets of the study area are required for preparation of base maps, ground truth collection, in the selection of sample stripes and geo-coding of satellite data.

Preliminary interpretation

The principle of 'geo-pedological approach' as discussed earlier is employed in preparing soil map. Initially the False Colour Composites (FCC) print of the study area will be interpreted for broad physiographic units by placing a translucent film over FCC prints under a light table or on computer screen. On the basis of available lithological information through ancillary data, the different physiographic units are attached with the geological information. The sub division of broad physiographic units will be carried out based on drainage network, erosion, land use etc., as manifested on the satellite data. A tentative legend will be developed for the preliminary interpreted map in terms of physiography, lithology and mapping units.

Selection of soil sample areas

On the basis of preliminary interpretation, sample areas covering all mapping units in the legend are selected in the form of sample strips of suitable size. The size of sample strip is usually about 2 x 5 km covering at least 2 or more mapping units. The number of sample strips may vary depending upon the variability in lithology, physiography, vegetation cover etc. Through sample strips, a minimum of 10 per cent of total study area is covered in a toposequence. This may be increased depending upon the heterogeneity in the terrain conditions. Besides, in each sample strip, random observations in the form of auger bores or mini pits are taken to account for variability in the soils within the mapping unit. The selected sample strips are transferred on to the base map for field sample collection.

Ground truth collection

Initially a rapid traverse of the entire study area is under taken to adjust the sample strips. Subsequently, in each sample strip, soil profiles, mini pits, auger bores etc., are studied along with morphological characteristics, existing land use / terrain parameters. The information recorded systematically by noting the place of observation, topographic conditions, existing land use / land cover, geology of the area, physiographic unit, natural vegetation occurring in the area and morphological characteristics of the soils. Random observations are also made in the study area to confirm the soils in different mapping units. The soil samples are collected from soil profile horizons with proper labeling to determine various soil properties later in the laboratory.

Soil sample analysis

The soil samples collected during the filed work are processed after air drying of the soils. They are pounded and grinded so that soil sample passes through 2 mm sieve. These soil samples are analysed for various physical and chemical properties like pH, EC, texture, organic carbon, exchangeable cations, CEC etc., that aid in the taxonomic classification of soils and also to identify any salinity or alkalinity like problems.

Classification of soils

The soils are classified, based on the morphological, physical and chemical properties collected in the filed work and laboratory analysis, following the Soil Taxonomy of USDA. The scale of mapping determines the level of classification of soils. For example, the soils are classified up to association of sub-group level at 1:250,000 scale or at soil series at 1:50,000 scale or up to phase level at 1:8,000 or 1:4,000 scale. For each soil mapping unit there will be association of soil taxonomic classes up to 1:12,500 scale as it is very difficult to establish a pure soil taxonomic class at small scale.

Finalisation of soil maps

The preliminarily interpreted maps with landscape units are finalized in light of ground truth collected and soil analytical data. The physiographic / landscape units are converted to soilscape units by incorporating the soil classification information into the mapping units. A final comprehensive legend showing the relationship physiography, lithology, relief, vegetation, land use along with description of soils and soil classification are developed and adopted for all soil mapping units in the study area. The final mapping units are transferred on to a suitable base map and final soil map is generated with appropriate legend.

The geo-pedological approach based on physiographic / landscape analysis work well upto 1:50,000 or 1:25,000 scale under most of the terrain situations. However, at larger than 1:25,000 scale, this may not be suitable because the micro relief or locale specific conditions or soil phases play dominant role. The conventional method of interpretation of satellite data under a light table by placing a translucent film on FCC print is almost replaced by on-screen drawing of soil polygon boundaries using PC based GIS software. This enables preparing soil digital data base for further processing of soil information. A soil map of Mohammadabad village prepared using the above approach has been appended as figure 4.3.

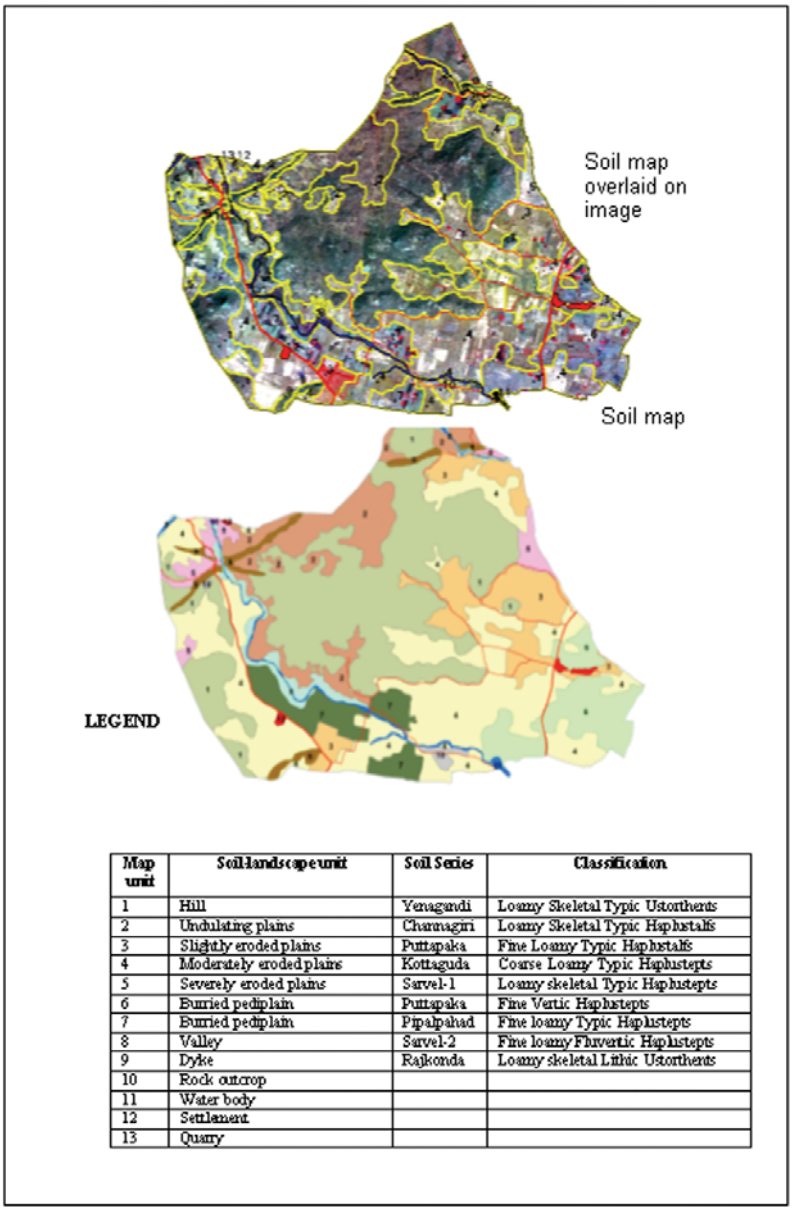

Map unit	Soil-landscape unit	Soil Series	Classification
1	Hill	Yenagandi	Loamy Skeletal Typic Ustorthents
2	Undulating plains	Channagiri	Loamy Skeletal Typic Haplustalfs
3	Slightly eroded plains	Puttapaka	Fine Loamy Typic Haplustalfs
4	Moderately eroded plains	Kottaguda	Coarse Loamy Typic Haplustepts
5	Severely eroded plains	Sarvel-1	Loamy skeletal Typic Haplustepts
6	Burried pediplain	Puttapaka	Fine Vertic Haplustepts
7	Burried pediplain	Pipalpahad	Fine loamy Typic Haplustepts
8	Valley	Sarvel-2	Fine loamy Fluvertic Haplustepts
9	Dyke	Rajkonda	Loamy skeletal Lithic Ustorthents
10	Rock outcrop		
11	Water body		
12	Settlement		
13	Quarry		

Figure 4.3: Soil map of Mohammadabad village, Nalgonda district, AP

4.4.6. Digital Techniques for Mapping Soils

Digital techniques allow exploitation of full range of image radiometry, spatial resolution and spectral channels; and thus facilitate better discrimination of soil classes and their phases of degradation. Digital analysis of satellite data solely

depends on spectral response of soil surface and the spectral signature for same type of soils was found to vary with the change of solar elevation angles, vegetation cover and moisture conditions. Many studies in literature are reported that attempted for digital classification of soils solely using spectral properties yielded poor results (Evans, 1975; Fagbami 1986; Cruickshank and Tomlinson, 1988) due to overlap of spectral signatures and lack of established procedures for extracting physiography information. Further it was also observed that more number of mapping units can be delineated by visual interpretation techniques as compared to digital techniques. Digital analysis leads to generalization of mapping units and the associated soil information. Most of these classification approaches were attempted to map soil using spectral properties alone. However attempts were also made using Digital Elevation information also.

The conventional classification techniques like maximum likelihood rely on the assumption that input data is having normal distribution. However, while using topographic information, which is generally a non-normal distribution, these classification procedures fail to deliver a satisfactory result. In such cases, the classification algorithms which do not make any assumption on data distribution and can consider the data from other discrete data will be of immense use for preparing soil maps though digital approaches. To overcome difficulties in conventional digital classification that uses the spectral characteristic of a pixel as the sole parameter in deciding to which class a pixel belongs to, new approaches like context classifiers, decision tree classifiers, neural network algorithms etc. are being employed during recent times to digital classification of soil resources.

In the contextual classification, classification is performed by considering a pixel in the context of its neighbouring pixel. Other ancillary data may also be incorporated in order to improve the classification like incorporating a digital elevation model as its derived parameters like slope and aspect. In one of the studies at NRSA (1997), digital elevation model is developed for using elevation information in generating colour coded soil map. The inclusion of slope and elevation information in digital classification of IRS-1C LISS-III data substantially improved overall classification accuracy as compared to LISS-III data alone.

In Fuzzy classification, each pixel a membership function is assigned for each class, ranging from 0 to 1, which indicate the proportions of the different classes which have contributed to the observed spectral signature. Some image processing softwares incorporate digital classification techniques which use the fuzzy logic approach to classification. A limitation to this program is that the number of end-members that can be employed must be less or equal to the number of input bands. Thus, if the six reflective Landsat TM bands are used, a maximum of six classes can be employed. However, fuzzy logic is more relevant to soil mapping to address the fuzziness across soil boundaries in spatial domain.

Neural network classification algorithms are extensively being used in remote sensing. Unlike the maximum likelihood classifier, they do not rely on the assumption that data is normally distributed. A surface class may be represented by a number of clusters in a feature space plot rather than a single cluster. At NRSA (1998a), Artificial Neural Network (ANNs) technique was attempted to classify the soils as the maximum likelihood (ML) classification algorithm was not giving satisfying results to classify various soil classes. The lithology, slope, and elevation information of the study area was incorporated along with spectral response to an ANN classification technique. The comparison of ANN classification results with ML classification revealed that the classification accuracy was improved by 7% from 88% to 95% due to integration of multi source information in ANN technique.

4.5. Land Degradation

In general, it implies temporary or permanent regression from a higher to a lower status of productivity through deterioration of physical, chemical and biological aspects The information on the extent and spatial distribution of various kinds of degraded lands is thus essential for strategic planning of development of degraded lands. Development of degraded lands in India is one of the options available to increase food production for growing population and to restore the fragile ecosystem. Land degradation has numerous environmental, economic, social and ecological consequences, such as decline in land productivity, reduced agricultural or forestry production, siltation of rivers, canals and drainage systems, decline in income of agricultural populations leading to worsening of a poverty situation, increased rural-urban migration, increased frequency of natural disasters such as floods and landslides and loss of biodiversity.

The physical processes which contribute to land degradation are mainly water and wind erosion, compaction, crusting and water logging. The chemical processes include salinisation, alkalisation, acidification, pollution and nutrient depletion. The biological processes, on the other hand are related to the reduction of organic matter content in the soil, degradation of vegetation and impairment of activities of micro-flora and fauna.

4.5.1. Status

The first quantitative spatial assessment of desertification was made on the basis of information available with UNCOD and the total area affected by desertification was estimated at 3.8 billion hectares (Mabbut, 1978). But five years later the figure reported was 4.7 billion hectares (Dregne, 1983) and the increase is being attributed to the inclusion of the areas of true hyper deserts into the total area. A study of three agencies of United Nations viz., FAO, UNDP and UNEP (1994) estimated that altogether 140 million hectares, or 43% of the South Asia's total agricultural land, is suffering from one form of degradation or more. Of this, 31 million hectares were strongly degraded and 63 million hectares moderately degraded. The worst affected country was Iran, with 94% of agricultural land degraded, followed by Bangladesh (75%), Pakistan (61%), Sri Lanka (44%), Afghanistan (33%), Nepal (26%), India (25%) and Bhutan (10%). The study also concluded that these countries are losing at least US$10 billion annually as a result of land degradation.

According to National Commission on Agriculture (1976), about 175 million hectares of land constituting 53.3 per cent of the total geographical area of 329 M ha is subject to various kinds of degradation. According to the latest reports of Department of Agriculture and Co-operation (DAC, 1994) shows 107 million hectares of land is under various types of degraded lands.

In India, the largest category is water erosion, which account for 80 percent of degraded land and the remaining categories include salinization, waterlogging, and loss of top soil due to wind erosion. Of these, reliable time series data are available only for salt affected land, which has grown from 7.18 million hectares in 1987 to over 10 million in 1993 (Annon, 2002). It may be pertinent to add here that according to NRSA / DOS project on, 'Mapping of salt affected soils of India', the area under salt affected soils in the country is 6.727 million hectares (NRSA, 2008), based on satellite remote sensing and adequate ground truth for the period 1986-'87.

For the assessment of land degradation, on a global level at 1:5 million scale FAO/UNEP/UNESCO (1979) had used direct observations, parametric methods as well as remote sensing techniques and according to this study remote sensing provides a rapid, relatively inexpensive means to gather land information where no other sources are available or where the quality of available information is low. It permits an exact delineation or clear physiographic boundaries. It gives the opportunity for repetitive, annually or seasonally multi-spectral examination.

Remote sensing data from satellites like Landsat, SPOT and IRS, were employed subsequently to derive information on the nature, extent, spatial distribution and magnitude of various types of degraded lands like salt affected soils, waterlogged areas, ravinous lands, eroded areas, shifting cultivation etc., and also to monitor them periodically (Venkataratnam and Ravisankar, 1992, Karale *et al.*, 1988, Dwivedi and Ravisankar, 1991, Dwivedi and Sreenivas, 1998). Besides, remote sensing data has been used as an input to derive the parameters required for spatial modeling of soil erosion (Sreenivas, 2000). Stereoscopy from IRS-1D PAN stereo can give perspective view of depth of ravines, which enabled improved delineation of ravines into their reclamative groups (Sreenivas and Dwivedi, 2006)

4.5.2. Land degradation processes

Land is the most valuable natural resource, which needs to be harnessed according to its potential. Due to over exploitation and mismanagement of natural resources coupled with socio-economic factors (like land shortage, inappropriate land use, severe economic pressures on farmers, poverty, population growth etc.). The problems of land degradation are on the rise. Therefore, management of land resources is essential for both continued agricultural productivity and protection for the environment. This requires inventory of degraded lands to initiate appropriate reclamation / treatment plans. The information on the extent and spatial distribution of various kinds of degradation/ degraded lands is thus essential for strategic planning of development of degraded lands.

Water Erosion

Water erosion is the most widespread form of degradation and occurs widely in all agro-climatic zones. The displacement of soil material by water can result in either loss of topsoil or terrain deformation or both. This category includes processes such as splash erosion, sheet erosion, rill and gully erosion. The result is more loss of fertile topsoil and plant nutrients. In some cases where subsoil has kankars, lime nodules, etc will get

exposed on the top there by altering the pH regime of the surface soil and subsequent nutrient holding capacity and their availability to plants. In wind erosion too, the surface soil is lost and gets deposited in other fertile areas thereby altering the fertility and nutrient as well as water holding capacities.

The off-site and downstream effects of erosion include siltation of dams and waterways, nutrients in runoff causing Eutrophication, and pesticide in runoff causing pollution of water bodies and aquatic flora and fauna.

Wind Erosion

It implies uniform displacement of topsoil by wind action. It can result in loss of topsoil and the deposition of the eroded material elsewhere leads to formation of dunes. The uniform displacement of topsoil by wind action occurs in thin layers / sheets. The uneven displacement of soil material by wind action leads to deflation hollows and dunes. The lifted medium to coarse soil particles may reduce the productivity of adjacent fertile land when they are deposited in the form of sand castings.

Water logging

Water logging is considered as physical deterioration of land. It is affected by excessive ponding / logging of water for quite some period and affects the productivity of land or reduces the choice of taking crops. Either because of topography, flooding or poor drainage condition, water logging occurs in some areas. The major consequence in these areas include lack of proper oxygen supply to plants leading to rotting, development of soil borne diseases, reduction in nutrient supply, non-availability of certain nutrients, etc. However, the magnitude of impact depends on the duration of water logging. The water logging could be surface (ponding of water) or sub-surface. While surface logging could be noticed, the sub-surface water logging mostly goes unnoticed.

Salinization / Alkalization

Salinization and alkalization are problems of semiarid and arid areas. They could be of natural or manmade. This is a major problem resulting in the desiccation of plants due to high osmotic potential exerted on plant because of high concentration of salts. Nutrient imbalance due to non-availability of essential nutrients to plants is also an associated problem. While, salinization is mostly associated with the coastal areas and younger alluvial plains, alkalization happens mostly in inlands and older alluvial plains. Generally, alkalization is associated with waterlogging due to poor permeability of soil by presence of sodium.

Salinization can result from improper management of canal irrigation water resulting in the rise of water table and consequent accumulation of salts in the root zone in arid, semi-arid and sub humid (dry) conditions and ingress of sea water in coastal regions and/or use of high-salt containing ground water.

Acidification

Any soil process or management practices which lead to buildup of hydrogen cations (also called protons) in the soil will result in soil acidification. It also occurs when base cations such as Calcium, Magnesium, Potassium and Sodium are lost from the soil leading to high hydrogen ion concentration. This results in decrease of soil pH below 6.5. Increasing acidity through selective removal of calcium cations on the exchange complex affects the balance in nutrient availability, encourages P-fixation and induces free aluminium causing severe toxic effects. It is also associated with iron toxicity at places. It generally occurs in regions of very high rainfall.

Glacial

These are the areas under perpetual snow covered areas in Himalayan region. It degrades an area by two processes namely frost heaving and frost shattering. Frost heaving is defined as a process in glacial and periglacial environment where intense frost action and freezing of water evolves peculiar forms of rock, regolith and soil. The water crystallizes to ice below the surface horizon leading to micro-relief variations on the surface. This process affects the germination and root growth of several crops there by limiting the productivity of land. Generally, these regions remain fallow during winters.

Anthropogenic

Human economic activities like mining, industries etc., have also contributed to decreased biological productivity, diversity and resilience of the land. Mining, brick kiln activities and industrial effluent affected areas are included under this type of degradation. Nutrient depletion or nutrient mining from fertile agricultural fields, without replacement through manure or fertilizer, results in nutrient deficiencies. Removing plant residues also reduces soil organic matter content. Removal of topsoil while mining for precious metals and affecting its surrounding agricultural fields is another dimension of land degradation. Hence, the top fertile soil is almost permanently lost, if properly not conserved. Chemical toxicity from industrial effluents and soil contamination with poisonous chemicals affects the plant growth significantly.

Others

Some of the degraded lands, which could not be included in the above type of land degradation, are included here. They are mass movement/ mass wastage, barren rocky / stony waste areas, riverine sand areas, sea ingression areas.

Land degradation assessment is often not a simple task. It requires continuous monitoring of the ecosystem for several parameters, which are often difficult to collect and monitor. Several indicators are in vogue to describe soil quality like pH, organic matter content, available nutrients to plant, soil depth, soil texture, bulk density / porosity, water permeability, water holding capacity, nutrient retention capacity, presence of chemicals toxic to plants or their primary consumers, and so on. Added to this, there will be several complex interactions among these properties. Thus soil quality cannot easily be described by one variable or an index.

It is the complicated interaction and cumulative effect of land degradation processes which ultimately translates to an actual decline in farm production. Only farmers' upon keen observation may recognize some of these individual processes. Reduced soil depth, exposure of sub-surface gravel / kankar, poor seed germination are often cited as changes, but rarely do farmers relate them directly to water erosion or any other land degradation process. Further, the toxicity of elements, most often, do not exhibit any perceptible visual impact on surface, such as aluminium / iron toxicity, resulting in significant crop failures. Thus the ignorance of farmers is also responsible for unnoticing the effects of land degradation.

The above-mentioned soil properties and their interactions do affect the crop yields, sometimes very significantly. Hence, some people consider crop yield as one of the proxy indicator to assess land degradation. However, crop yield is not a good indicator since human management in terms of seed variety, seed quality, water availability, fertilizer inputs, etc., also influences it. However, measuring yield trends with control on other inputs and management practices can provide an observable and credible measure of trends on land degradation.

4.5.3. Remote Sensing, GIS and Land Degradation

For the assessment of land degradation, on a global level at 1:5 million scale FAO/UNEP/UNESCO (1979) had used direct observations, parametric methods as well as remote sensing techniques and according to this study:

- Remote sensing provides a rapid, relatively inexpensive means to gather land information where no other sources are available or where the quality of available information is low
- It permits an exact delineation or clear physiographic boundaries
- It gives the opportunity for repetitive, annually or seasonally multi-spectral examination
- Interpretation of satellite imagery can be at several levels of intensity / scales

The role of remote sensing and GIS in land degradation has been summarized as Table- 4.2 (Sreenivas, 2007).

Table 4.2: Remote Sensing and GIS in land degradation studies

Theme	Geographical Representation	Attributes required	Method
Land Degradation	To show the major types of land degradation operating	• Type of land degradation • Severity / level • Cause description • Topography • Land Use type • Notes on solutions to tackle the problem	Visual interpretation of satellite imagery with adequate field verification / checks
Land degradation hotspots	Show the extents of areas, which are degraded during period range, classified according to the degree of degradation	• Degradation type • Degradation level • Major causes • Current Land Use type. • Period elapsed to reach critical threshold of degradation • Notes on solutions to tackle the problem	• Preparation of land cover and NDVI maps of a historic and current year using multi-spectral remote sensing data • Identification of land degradation hot-spots based on type and degree of land transformation and NDVI change matrix in GIS domain • Classification of areas into various type and degree of degradation based on above information • Analysis of land transformations with available livestock and human census data details • Investigation and understanding of the desertification by domain experts and suggesting solutions
Land degradation prediction	Show the extents of areas most likely to degrade in the near future and their classification according to the probability of its tendency to get degraded	• Grade of expected land degradation • Level of Confidence • Predicted period in to reach the threshold level of degradation • Current Land Use • Topography	• Main drivers of land degradation to be identified from land degradation change maps / hotspot maps • Using historical and current land degradation areas data, rate of desertification need to be studied and confidence levels will be estimated • Scope should be given to accommodate proposed alternate land utilization plans, if any, or land transformation policies to be implemented in near future • The general approach for prediction could be through spatial modeling

4.5.4. Mapping land degradation

The following section provides outlines of the procedure involved in mapping land degradation using satellite data which consists of input data, preparatory work and methodology. The methodology normally adopted for mapping at any scale consists of preparation of base map, on –line visual interpretation of satellite data, development of legend, ground truth collection, analysis of soil samples, classification of degradation classes and finalisation of maps in light of field information and analytical data. The methodology is given in the form of a flow chart (Figure 4.4). The major steps are discussed here under:

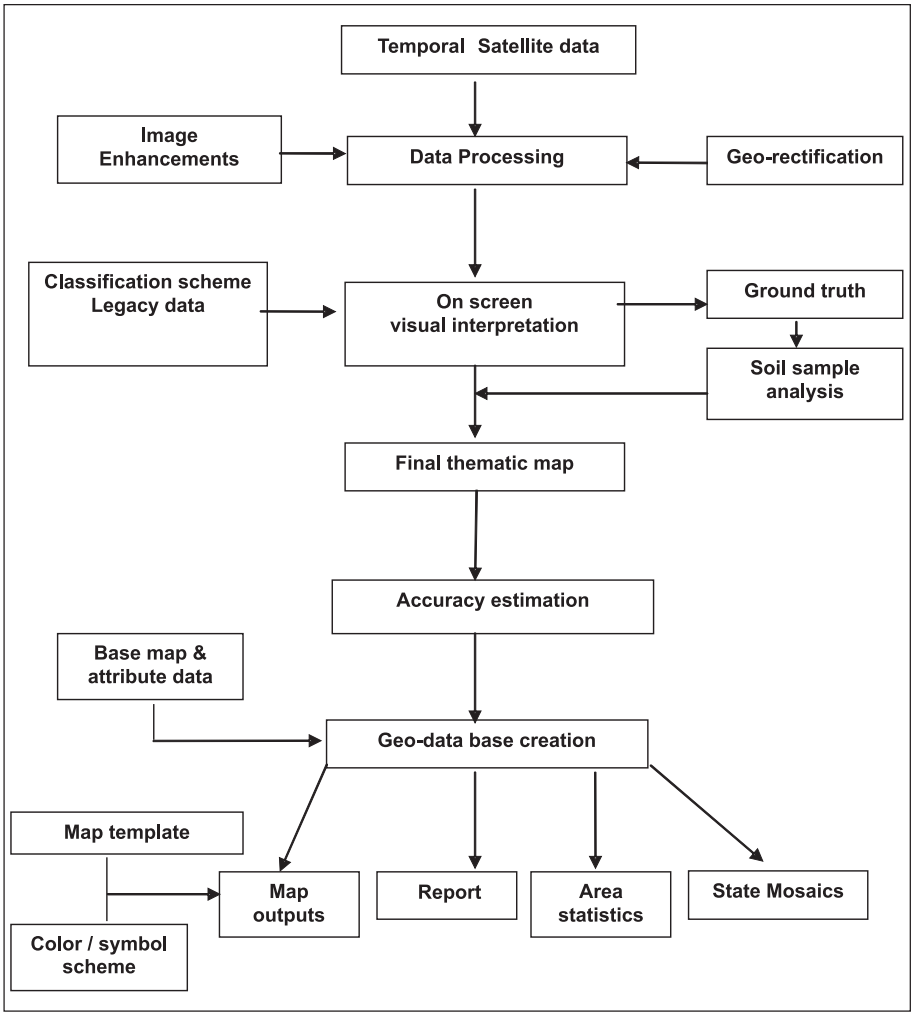

Figure 4.4: An overview of the land degradation mapping methodology

Input data and its preparation

For delineation and mapping of land degradation classes, multi-temporal geo-rectified data acquired during major cropping seasons like kharif, rabi and zaid seasons are used. Such a temporal data set helps to address the seasonal variability in intensity of problem in degraded lands. The satellite data is geometrically corrected for further processing, like visual interpretation, ground truth collection and land degradation map preparation.

Besides, while mapping land degradation, ancillary data in the form of topographic maps, existing land use land cover data, wasteland data, district and any other published relevant material are used as reference data. Survey of India digital topographic maps at suitable scale are used for identification of base features and for planning ground data collection. Any legacy data sets in the form of maps can also be used for substantiating land degradation process.

Interpretation cues

The methodology involves standard visual interpretation techniques that are followed in any other mapping exercise. The image interpretation key provides a critical reference base for advanced interpretation. It helps the interpreter in evaluating the information in an organized and consistent manner. An image interpretation key for the study area has to be designed prior to interpretation, which can be further refined in course of interpretation. A general visual interpretation keys for land degradation has been included as table 4.3. However, for delineation of severity, the interpretation cues vary with the season of data available and local processes. Using these cues the satellite data are visually interpreted either on the screen or using image prints. After preliminary interpretation of satellite data sample areas are identified for ground truth collection.

Ground truth Collection

Ground truth/ field verification is an important component in mapping and subsequent validation exercise. Utmost care and planning is required for collecting ground data and verification. To facilitate a good ground

Table 4.3: Visual interpretation cues for land degradation.

Land degradation process	**Land degradation type**	**Colour / Tone (On standard FCC)**	**Texture** (on LISS-III data)	**Pattern**	**Size**	**Shape**	**Association**	**Remarks**
Water erosion (W)	Sheet erosion (sh)	Slightly brighter than surrounding land of its class	Smooth to medium	Contiguous patches	Small to large	Irregular	Sloping cultivated / lands with poor vegetal cover during rainy season	Information need to be deduced from available soil information slope and satellite data in conjunction RUSLE can be used to quantify soil loss
	Rills (ri)	Brighter than surrounding land of its class	Medium	Discrete to contiguous patches	Small to medium	Irregular	Sloping cultivated lands	Mostly seen on ploughed land after first rains
	Gullies (gu)	Brighter than surrounding land / gray in color depending on soil colour.	Medium to slightly coarse	Discrete to contiguous patches	Small to medium	Irregular	First order streams	–
	Ravines (rs / rm)	Medium gray to dark gray	Slightly coarse for shallow ravines and coarse for deep ravines	Contiguous patches	Large to very large	Irregular	Stream / river banks	Image texture and association are to be given attention
Wind erosion (E)	Sheet erosion (sh)	Various shades of yellow and light gray combination	Smooth to medium	Contiguous / mottling (in cultivated areas)	Large to very large	Regular / Irregular	Desertic plain areas with of active sand movement	In deserted areas; with little or no vegetal protection
	Partially stabilized dunes (dp)	Light grey to medium grey with light yellowish tones	Medium	Contiguous / discrete patches	Small to medium	Regular/ irregular	Desert sandy dunal area	Sand dunes in desert areas with slight to moderate vegetal /grass cover

	Stabilized dunes (ds)	Medium grey with light yellowish tones during dry season. Pink mottles during rainy season	Medium to coarse	Discrete patches	Small to medium	Regular / Irregular	Desert sandy dunal area	Sand dunes in desert areas with good vegetal / grass cover
	Un-stabilized dunes (du)	Various shades of yellow and very light gray combination	Smooth to medium	Contiguous / discrete	Medium to large	Irregular	Desert sandy dunal area	Sand dunes in desert areas with no vegetal / grass cover
Water logging (L)	Surface ponding (sp)	Light blue to Very dark blue	Smooth	Discrete patches	Small to large	Regular / Irregular	Depressions in inland plains / coastal plains	
	Sub-surface water logging (sw)	Medium to dark gray on normal FCC; on FCC with SWIR band (R:G:B=SWIR: NIR:Red) various shades of blue	Smooth	Discrete/ contiguous patches	Medium to large	Irregular	In irrigated areas / plains with high water table	
Salinisation / Alkalisation (S)	Saline (sa)	Light gray to white	Smooth	Discrete patches	Small to medium	Irregular	Coastal plains / young alluvial plains / stream courses / irrigated canal commands	Needs very careful delineation delineation in black soils and sandy regions
	Sodic (so)	Grayish white / dull white	Smooth	Discrete patches	Small to medium	Irregular	Older alluvial plains / stream courses / irrigated canal commands.	Needs very careful delineation in black soils and sandy regions
	Saline – Sodic (ss)	Grayish white to White	Smooth	Discrete patches	Small to medium	Irregular	Young to older alluvial / stream courses / irrigated canal commands	Needs very careful delineation in black soils and sandy regions
Acidification (A)	Acidic (ac)	Various shades of green/ black	Smooth to medium	Mottled / parceling, contiguous / discrete	Small to large	Irregular	Lateritic /high rainfall regions, cultivated peats / marshes	Soil pH data is essential

Glacial (G)	Frost heaving (fh)	Light pink to grey	Smooth	Discrete / contiguous patches	Medium	Regular / Irregular	Cultivated / fallow valley areas of glacial region	Look for valleys adjacent to snow covered peaks
Anthropogenic (H)	Industrial – effluent affected areas (ie)	Various shades of blue, if ponded with water. Light grey to white patches when dries	Smooth	Discrete / contiguous	Small to medium	Irregular / regular	Adjacent to industries and its effluent discharge pathways	Association is very important
	Mining and dump areas (md)	Shades of White, yellow, red, black	Smooth to medium	Discrete	Small to medium	Irregular / regular	Hilly / plain areas	Colour varies depending on the mining stage and type of mineral explored
	Brick kiln (bk)	Dull white to light yellow	Smooth	Isolated patches giving rise to mottling pattern on its background.	Very small	Irregular / regular	Associated with urban areas and its surroundings; located along trafficable road network	Requires careful logical deduction
Others (T)	Mass movement / mass wastage (mm)	Yellowish white to very light cyan	Smooth	Discrete	Very small to small	Irregular / regular	Foot of steep sloping hilly regions	–
	Barren rocky / Stony waste (bs)	Light to medium grey / yellowish white	Smooth	Discrete / Contiguous	Medium to large	Irregular	Hilly or pediment regions	–
	Snow covered areas (sc)	Bright white to dull white; bright blue on SWIR band FCC (R:G:B=SWIR: NIR:Red)	Smooth	Contiguous patches	Large to extensive	Irregular	Very high altitude peaks & glaciers.	Use SWIR band FCC for their separation from clouds
	Miscellaneous (Riverine sands / Sea ingress areas, etc) (ms)	Generally white. Light cyan when associated with moisture	Smooth	Discrete / Contiguous	Medium to large	Irregular	River banks / old river course/coastal beach/dune sands and river bed/ natural levees	Sandy areas other than desert sands

truthing exercise identify and list all the doubtful areas for the ground verification and refer all such areas with respect to the toposheet to know their geographical location and accessibility on the ground. Then prepare field traverse plan to cover maximum doubtful areas in the field. Ensure that each traverse covers, as many land degradation classes as possible, apart from the doubtful areas. Soil samples are collected from representative areas and are analysed for chemical & physico-chemical properties.

Soil Sample Analysis

The soil samples are to be analysed for pH, EC, texture (sand, silt, clay), CEC, exchangeable cations, calcium carbonate %, organic carbon % using standard analytical procedures. These observations are required for signature extrapolation during interpretation.

Final Map Generation

The land degradation map needs to be finalized in light of the ground observations, visual interpretation keys, available ancillary and legacy data sets. Once map is finalized they need to be checked for topological and labelling errors. For mapping units having more than one problem, the associated problem need to given the mapping symbol in a separate attribute column. Map is composed using the major land degradation problem. Edge matching of the features are carried out to maintain the continuity of classes between adjoining sheets. Final map is tested for thematic accuracy. Base map features are overlaid and then map is generated on the layout consisting of theme map, legend, scale bar, north arrow, sources of data, index map, agencies involved, project name and year of publication.

Validation

Information collected during the field visit is utilised in checking the final maps for which purpose a representative samples are collected on ground covering all the thematic classes. In extreme cases, the finalised thematic maps are also be validated by verifying the mapping units in the field. A salt – affected soil map prepared using the above approach has been appended as figure 4.5.

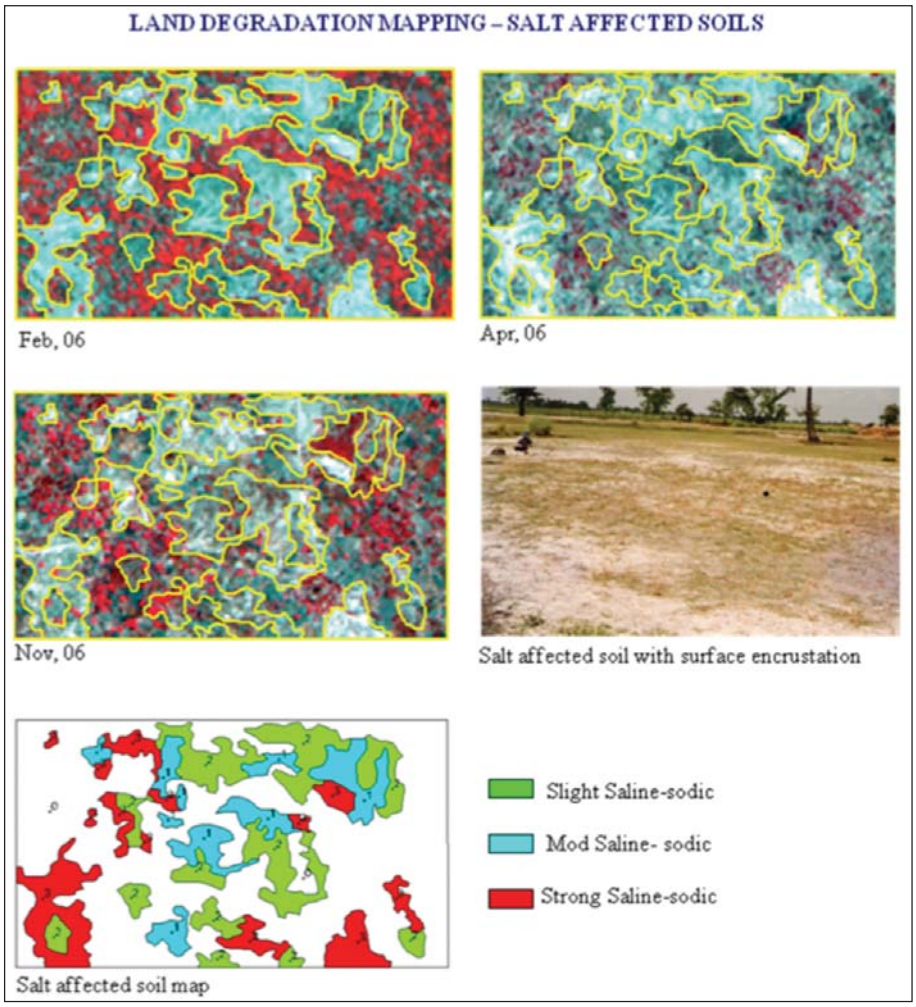

Figure 4.5: Salt-affected soil map prepared from multi-season temporal LISS-III satellite data

4.5.5. Monitoring of land degradation

Repeatitive nature of satellite data enables to monitor land degradation process over a period of time in any geographical location (figure 4.6) The methodology consists of the geometric correction of multi date satellite data. Then the satellite data is corrected for Sun elevation angle effects and atmospheric influences. Subsequently the data is normalized for their radiometric differences. Once the data set is ready, the ground truth is collected with respect to current season data

by means of studying soil profiles and surface observations. The soil samples are analysed for various chemical and physical properties. Based on the ground truth and ancillary information, the signatures are established for various land degradation classes. Using the other ancillary information and ground truth information, the signatures are extrapolated to other dates. The changes that have been observed in the satellite data are verified again on the ground. NRSC had carried out monitoring of waterlogging and salinity/alkalinity in the major command areas in various states in India like UP - Sharada Sahayak, Maharastra – Upper Tapi, Purna, Krishna, Bhima, Girna, Jayakwadi, AP – NSP Command, Karnataka – Krishnarajasagar command and Rajasthan – Chambal command at the request of Central Water Commission, New Delhi. In this project using pre-monsoon, monsoon and post-monsoon season satellite data salinity and water logging were identified with field investigations. Sample areas portraying significant changes in land degradation status has been appended as Figure 4.6.

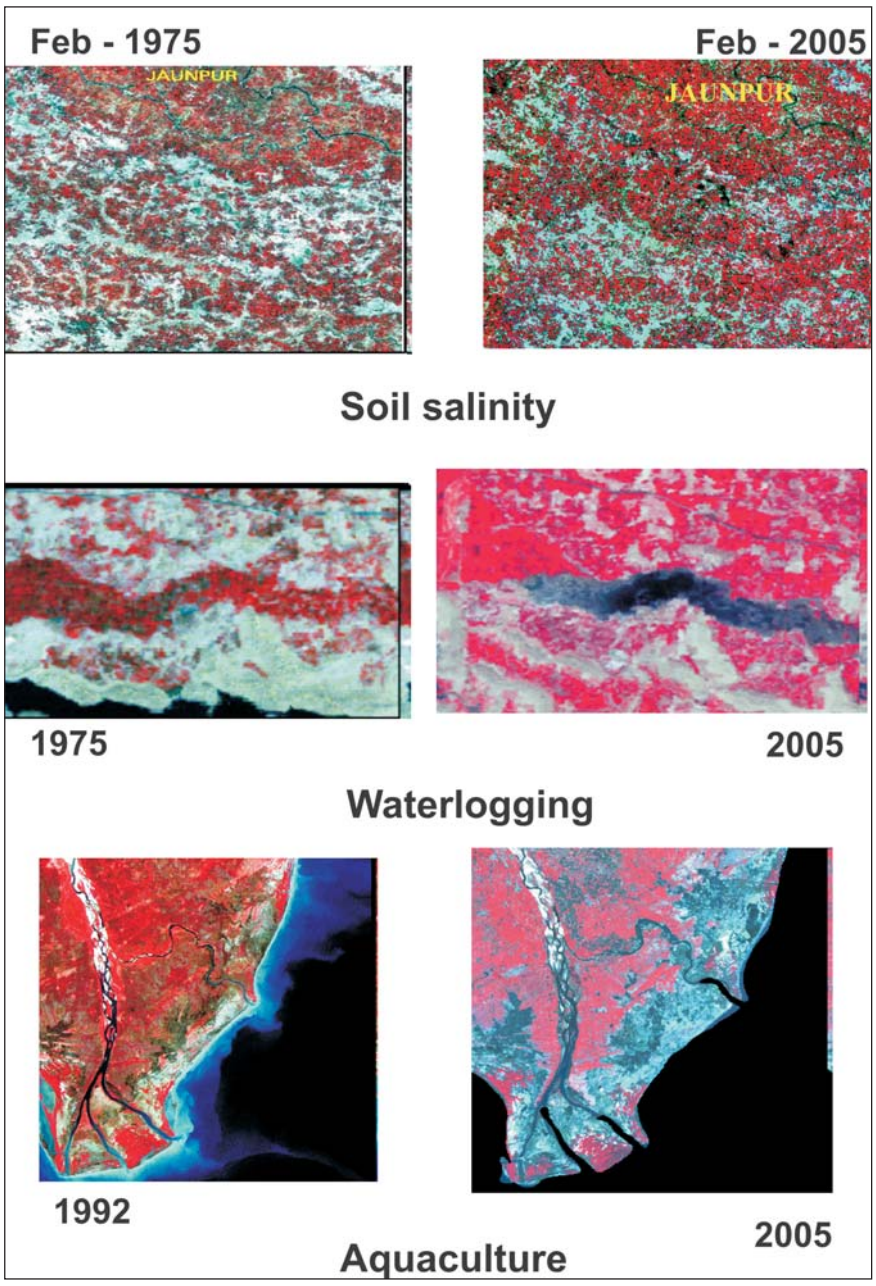

Figure 4.6: Monitoring land degradation

4.6. Soil Moisture Studies

Soil moisture is an important input parameter in number of land surface and atmospheric processes in view of its ubiquitous nature and unique thermal and electrical properties. In addition, its role in agriculture and hydrology needs no emphasis. Remote sensing techniques, by virtue of their large area coverage, frequent revisit capability enabling repeated estimates on regular basis are highly suitable for soil moisture estimation. The assessment of soil moisture was done by studying the changes in soil colour (Musick and Pelletier, 1986; Kijowski, 1988), by estimating the thermal inertia (Evans and Catt, 1987; Berge and Stroosnijder, 1987) and microwave radiometry (Schmugge and O'neill, 1986).

Moisture also greatly influences the reflection of shortwave radiation from soil surfaces in the VNIR (400–1100 nm) and SWIR (1100–2500 nm) regions of the spectrum (Bowers and Hanks, 1965; Skidmore *et al.*, 1975). In a study Lobell and Asner (2002) concluded that the SWIR region is more suitable to pickup soil moisture differences than optical wavelengths. The effect of soil type difference on soil moisture could be reduced by expressing the moisture as degree of saturation rather than volumetric soil moisture content. More pronounced decrease in reflectance was noticed at 2.2 μm irrespective of soil type. Reflected radiation in visible and Near IR regions, though sensitive to soil moisture, is not applicable due to its higher sensitivity to soil chemical composition, colour and organic

carbon and its inability to provide remote sensing data during inclement weather conditions. Thermal radiation emitted in the 8-14 μm range is highly sensitive to soil moisture variations as soil moisture content determines the thermal inertia of soils. Higher the soil moisture content higher the thermal inertia leading to smaller change in physical temperature of the soil with time. Attempts using thermal remote sensing techniques are successful to the extent of determining soil moisture qualitatively due to influence of intervening atmosphere and any ground cover.

Microwave remote sensing techniques (passive and active) are by far the most successful and widely investigated since early 70s in view of all weather capability of emitted or scattered microwave radiation and its strong sensitivity to soil moisture variations and penetration through crop cover and surface soil layers. Microwave backscattered radiation increases with increasing soil moisture content at low look angles i.e., 10 to 20 degrees. Under similar surface conditions, soil textural variations, which in turn govern the quantum of bound water fraction, modify this relationship (Schmugge, 1983; Ulaby *et al.*, 1983).

Active microwave sensors operate on the principle of radar. Magnitude of radar backscatter coefficient (a measure of reflected microwave radiation) depends on soil moisture, surface roughness and crop cover on one hand and on microwave frequency, polarization and look angle at which the terrain is viewed on the other. Though observation made at C-band (5.3GHz), HH or VV polarization and near nadir look angles of 10^{o} to 15^{o} is considered to be the ideal sensor configuration for soil moisture estimation using radar, it is proved inadequate in terms of accuracy of soil moisture retrieval due to the effects of other terrain parameters.

Passive microwave radiometers are best suitable for large area soil moisture estimation from space borne platforms such as NIMBUS, Oceansat-1 and DMSP satellites due to their coarse spatial resolution and high revisit capability of 2 days or higher. Microwave radiometers record the emitted microwave radiation in terms of brightness temperature, which is the product of emissivity and physical temperature of the target and is highly sensitive to soil moisture variations. Thus passive microwave radiometry at L-band in dual polarization mode caters to the needs of meteorologists in global circulation models. In view of its potential, ESA is planning to Soil Moisture and Ocean Salinity (SMOS) Mission in 2009 to provide soil moisture on operational mode at regular intervals with a spatial resolution of 50 km.

At NRSA, experiments with SAR data from ERS-1/2 satellites have been attempted for estimation of soil moisture under different soil and moisture conditions (NRSA, 1995). The studies enabled to understand the relation between soil moisture and back scattering coefficient of SAR data; and also the influence of surface roughness on soil moisture estimation. A study on soil moisture with IRS-P4 MSMR data was also attempted for regional level study. Efforts in the direction of root zone soil moisture modeling with remotely derived surface soil moisture content and soil profile characteristics are in progress. Subsequently experiments are also conducted with SAR data from RADARSAT.

Soil moisture estimated from remote sensing platforms would enable retrieving moisture in surface layers of the soil only. Adequate modeling techniques need to be developed using soil profile information on soil characteristics and satellite derived surface soil moisture for estimating the profile soil moisture for a wide range of applications in agriculture. The various efforts made in retrieval of soil moisture are (i) regression modeling with moisture vs. soil roughness and soil texture; and (ii) inversion of physical or quasi-physical models. Most of the inversion techniques developed includes inversion of forward physical or quasi-physical radar backscattering models which are a function of dielectric constant and surface roughness.

Assured availability of multi-dimensional SAR data with dual or quad polarizations from such future satellites as Indian Radar Imaging Satellite (RISAT), Canadian RADARSAT-2 and Japanese PALSAR in the current decade may lead to operational soil moisture estimation.

4.7. Remote Sensing of Soil Fertility

The main components of soil fertility addressed with remote sensing include organic carbon, soil nitrate levels, soil clay content and thickness, etc. Amongst plant nutrients, nitrogen is one of the most important factors in maximizing the crop yields and economic returns to farmers. The spatial variation in nitrogen content has been addressed using crop vigor as a proxy indicator, in-field referencing of point in question with a point of known nitrogen status, spatial interpolation of soil analytical data using remote sensing data as guiding force for interpolation.

In general, Nitrogen deficiency causes a decrease in leaf chlorophylls concentration, leading to an increase in leaf reflectance in the visible spectral region (400-700 nm). However, several other stresses (pest and diseases) may

also result in increased plant reflectance due to reduced amount of chlorophyll (Carter and Knapp, 2001). Diagnosing a specific nutrient deficiency with remote sensing data can be difficult when plants are subjected to deficiencies of multiple elements. Hyperspectral remote sensing was found to be an important tool for the diagnosis of plant nutrient stress which is an indicator of soil fertility as well. Osborne *et al.* (2002) showed the utility of hyperspectral data in distinguishing differences in nitrogen and phosphorus at the leaf and canopy level, but the relationships were not consistent over all plant growth stages. Spectral reflectance peaks resulted from derivative analysis of spectral reflectance spectra found to be a good technique for stress detection. The position of the inflection point in the red edge region (680 to 780 nm) of the spectral signature, termed as red edge position (REP), is affected by biochemical and biophysical parameters. Shifts in the REP to longer or shorter wavelengths has been used as a means to estimate changes in foliar chlorophyll or nitrogen content and also as an indicator of vegetation stress. Cho and Skidmore (2006) have used linear extrapolation method for extracting REP that has shown high correlations with a wide range of foliar nitrogen concentrations for both narrow and wide bandwidth spectra.

Another area of research that is fast growing is fluorescence spectrometry which was found to be good for detecting plant nutrition status. Plants contain pigments which absorb photons from sunlight that are involved in photosynthesis and other photochemical processes. The leaf pigment absorbs the photons of certain wavelengths and can emit partially or fully of this absorbed energy as fluorescence at longer wavelengths. The magnitude of the fluorescence emission is inversely related to relative efficiency of plant photosynthesis and other biochemical systems. Fluorescence can also be an indicator of the relative concentration of certain plant constituents. This technique was successfully used in corn and soybean (*Glycine max*.Mirr.) and differences between the fluorescence of healthy plants and plants deficient in the major plant nutrients N, P and K, and the minor plant nutrients Ca, Mg, S, Fe, and B have been detected (Chappelle *et al.*, 1984). Using laser-induced fluorescence (LIF) and passive reflectance measurements in the laboratory McMurtrey *et al.*, (1994) observed differences in maximum intensity of fluorescence at 440nm, 680nm, and 780nm which were found related to different levels of N fertilization in corn (*Zea mays* L.).

4.8. Application of GIS techniques in Soil Resources study

Development of computer technology, especially Geographical Information System (GIS), provides valuable support to handle voluminous data being generated through conventional and remote sensing techniques both in spatial and non-spatial format. Further, GIS also allows the integration of these data sets for deriving meaningful information and outputs in map or tabular formats. The integrated analysis of resources data at different scales, enables to study the potentials and limitations of natural resources and to generate optimal utilisation plans for land and water resources.

In recent years the applications of GIS has increased many folds in various fields. It is used widely as a standard tool in agriculture, environmental management, forestry, hazard monitoring, hydrology, watershed management, land analysis, etc. The introduction of GIS promoted interdisciplinary studies, both within the natural, environmental, social and economic sciences. GIS technology and applications have expanded rapidly in parallel with advances in remote sensing and computer technology and increasing demand for environmental information. It provides an infrastructure for the examination of complex spatial problems in new and exciting ways. The technology has developed rapidly, and has quickly been taken up by a diverse user community with very difficult and often demanding applications.

Besides digital cartography, major applications of GIS in the field of soil survey and land evaluation are land capability classification (LCC), land irrigability assessment, land suitability for different purposes, watershed management and generation of optimal land use maps.

Land evaluation provides a rational basis to analyse various soil, climate and land parameters to arrive at optimum solution to various problems of natural resources. In the land evaluation process GIS has become an important tool because it enables to integrate the complex decisions to be taken under multi-variant situations of the resource base and their dynamics. Land evaluation principle is based on matching the requirements of a land for specific use with the characteristics of inherent soil, climatic, topographic and other natural resources and is concerned with the assessment of land performance when used for a specific use.

Major GIS applications relevant to soils are:

- land capability assessment

- land irrigability assessment
- land productivity assessment
- irrigation water management in command areas
- prioritization of sub-watersheds / micro-watersheds in a given watershed
- soil suitability assessment for various purposes like specific crops, industries, forestry, etc.
- to identify critical areas in watershed / micro-watershed
- to generate optimal land use plans etc
- quantification of soil loss
- planning the urban development
- reclamation planning of degraded lands

… and so on.

4.8.1. Crop Suitability Studies

The sustainable crop production in any area depends on its climate, soil and site characteristics of the area. This can be achieved through evaluation of soils of a given area for their suitability to different crops considering the inherent soil properties, topographical features and climatic parameters independently as well as in combination. A study had been carried out at NRSA (1998b) with the objective of assessing soil suitability to groundnut crop through GIS approach. The test site for the study was Tettavai vagu watershed in Tungaturthi mandal of Nalgonda district of AP. The soil maps for the study area was prepared using IRS-1B LISS-II data at 1:50,000 scale. Suitability criteria for groundnut crop in terms of climate, soil and site parameters were developed following FAO approach and incorporated as decision rules in GIS environment. The study revealed that in the test area about 69% of the total geographical area is highly suitable for groundnut crop. Similarly studies were carried out using remote sensing and GIS for sugarcane crop suitability in Puddukottai district, Tamilnadu and upland rice in Koraput district., Orissa. Similarly larger scale soil maps of Mohammadabad village, Nalgonda (Figure 4.3) were used in similar lines as mentioned above to assess the suitability of the village for various crops (Figure 4.7).

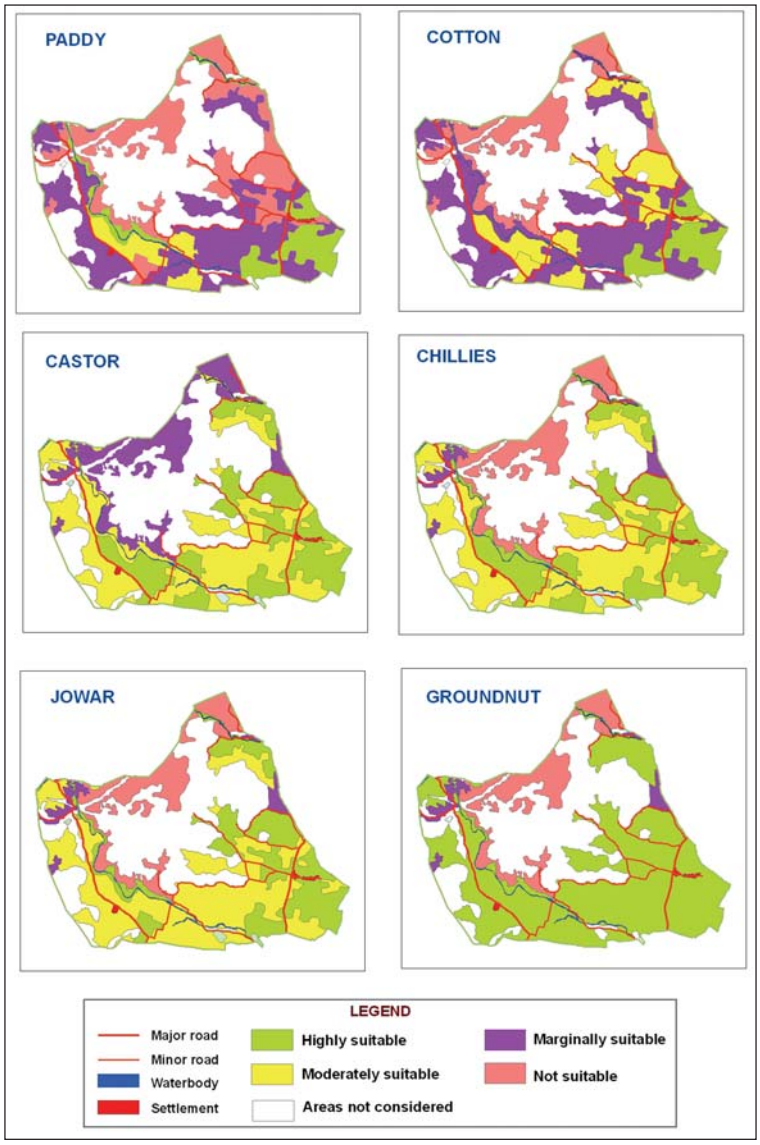

Figure 4.7: Land suitability of soils of Mohammadabad village for various crops

4.8.2. Land Irrigability Assessment

Land irrigability assessment is another important derivative map from soil map. It gives an assessment whether or not an area is suitable for irrigation. The soil depth, slope, salt problem, stoniness, waterlogging, etc are the some of the criteria used for irrigability assessment. It is more relevant before introduction of irrigation in any proposed command areas. The soil maps were overlaid on slope maps and various criteria were given

as weightages to derive mapping units in an GIS environment. Then based in irrigability criteria, the assessment of the area is made for their suitability for irrigation. This enables to prevent salinity or water logging and maximize the crop production by efficient utilization of irrigation water. An irrigability assessment made on similar lines for the Mohammadabad village has been appended as Figure 4.8. Similar exercises were carried out for various canal irrigated command areas like Sri Ram Sagar Project (SRSP) Phase-II (NRSA, 1997a) and Krishna-Pennar link canal command area.

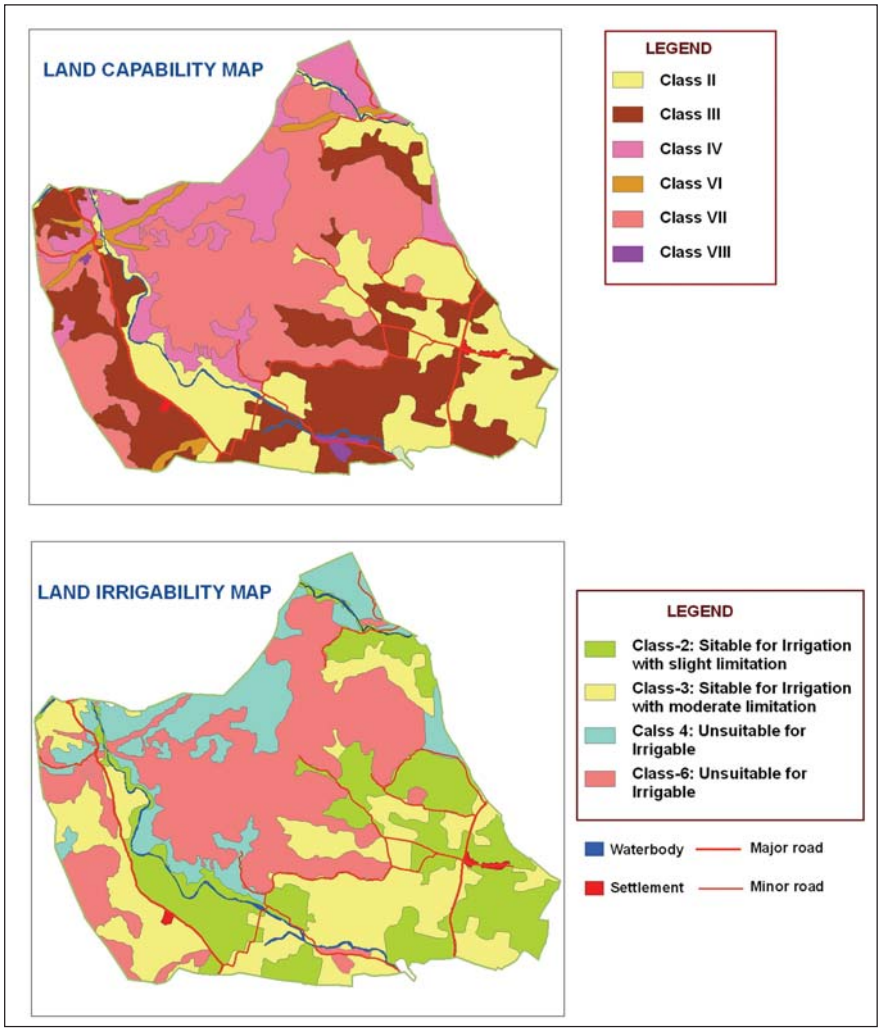

Figure 4.8: Land Capability and Land Irrigability map of village Mohammadabad

4.8.3. Land Productivity Assessment

The soil / land productivity assessment is one of the several soil survey interpretations which plays a critical role in the generation action plan for sustainable development of soil and water resources. An experiment has been carried out with the objective of assessing the land productivity using remote sensing and GIS techniques (Ravisankar, 2001). To assess the land productivity, initially soil map of the study areas are prepared at suitable scale. The land productivity index (LPI) of the area are assessed with respect to crops, pasture and forest / trees, following parametric approach of Riquire et al (1970). GIS tools were used for calculating LPI values for soil types and for deriving area weighted LPI values for soil mapping units and in the generation of Land Productivity map for the study area . The LPI varied from 8 – 65 for crops and forest / tree species and 8 – 58 for pasture for different soil mapping units. The study revealed that in the test site all soil mapping units have better coefficient of improvement with respect to crops (0.7 to 2.6) and minimum for forest / tree species (1.0 to 2.0).

4.8.4. Soil Erosion Modelling

Quantification of soil loss is an important application that several researchers attempted using GIS. The general approaches include a rule based approach where several parameters that influence the soil loss are weighted and summed to assess the final index to rate whether or not a particular area is eroded. In another approach, the absolute values of the model are derived from the maps and the soil loss is calculated using a physical or an empirical model. Unlike rating method, this method gives the physical quantity of soil loss. The important parameters that influence the soil loss are slope, cover, soil erodibility, rainfall quantity and intensity and the soil conservation or management factor that are practiced on a parcel.

4.8.5. Prioritization of Watersheds

In recent years, resources developmental planning has taken a shift towards watershed-based approach. In order to plan and manage the watersheds efficiently and use the available monitory resources judiciously,

prioritization of watersheds becomes very crucial. Remotely sensed data provides a valuable spatial information on natural resources and the information thus generated can be used in integrated analysis in Geographical Information System (GIS) to arrive at suitable solutions for complex resource problems in watersheds. The potential of these two technologies have been demonstrated in DOS projects like IMSD, IRIS-DA, Sujala, NATP etc., at watershed level to micro-watershed level. Presently a number of developmental projects are being implemented based on the watershed approach. However, when we have several such watersheds all cannot be developed at a time due to paucity of funds. Such a situation calls for prioritization of watersheds. A variety of approaches are in vogue for their prioritization. They include, resource based, economy based and socio-economic based approaches. Thus, the problem of prioritization of watershed is objective oriented and efforts are being made in the direction of development of methodologies that have more scientific rationale for development of watersheds and monitoring them in future.

NRSA (2007) had carried out a project for Ministry of Rural Development with the objective of prioritization of micro-watersheds based on wasteland information (NRSA- wasteland project), percent ST/SC population, acute shortage of drinking water, and development of knowledge base to combine the theme-wise priority maps and to ascertain the priority of sanctioned watersheds of MoRD. The study was taken up in Chhattisgarh, Maharashtra and Orissa states . The methodology of the project was established by considering the percentage distribution of waste land categories in each village, village wise drinking water status such as NC, PC, FC etc., and socio-economic data like SC/ST percentage etc. Initially individual theme-wise priority maps namely drinking water status, waste lands, and % SC/ST population were generated. The final integrated priority maps were generated based on these thematic maps on to which village boundaries were superimposed. In Orissa state it was found that 5200 (9.9%) villages fall under high integrated priority class while 9,872 (18.8 %) villages under medium priority and 30,400 (57.8%) villages under low priority. Analysis of the sanctioned watersheds / villages by MoRD revealed that out of the 601 watersheds only 79 villages were found to occur in high, 138 villages under medium and 380 watersheds under low priority integrated classes.

Issues and prospects

Even though remote sensing techniques are in vogue over a period of nearly three decades in the study of various aspects of soils, there are certain issues still to be resolved for efficient utilization of satellite data. The various issues and future prospects are discussed below:

- Soil reflectance is modified to a great extent due to the presence of vegetation cover. If the vegetation cover is sparse, a mixed response from soil and vegetation may be observed. If the density of vegetation is high, the reflected energy received at the sensor is mostly from the vegetation. Even though the soils are intimately related to the natural vegetation cover, presence of crops / plantations modifies this relationship. Consequently, the inherent and natural relationship of soils with the vegetation is disturbed
- In satellite imagery one can observe similarities in spectral reflectance of two different soil types. Example - Mollisols and Vertisols, which exhibit same spectral reflectance pattern, as both of these are darker in colour. Similarly, Vertisols and deltaic alluvium, Red and lateritic soils, as well as highly calcareous alluvial soils and salt affected soils
- Even though, the remote sensing data enables better delineation of soil mapping units, there are certain gray areas like areas covered with crops or forest vegetation where the accuracy of soil maps could be relatively less, without extensive ground truth
- Another issue is keeping of contrasting soils in the same mapping unit which diminishes the prediction of soil potentials for practical uses. For example, Lithic Ustorhents and Typic Haplustepts may be placed in the same mapping unit. To some extent scale of mapping and type of sensing spatial resolution do contribute to such situation. At times some soil properties needed for specific uses may be missing from mapping legend or soil report because most of the soil surveys are conducted for general land use planning and not for locale specific applications
- Soil maps are available at 1:250,000 scale for the whole country (NBSS & LUP) which serve the requirement of broad land use planning at regional / state level. In recent years for many of the projects concerned with conservation of natural resources or for planning the strategies to combat land degradation or to develop action plans to improve land productivity, the emphasis is on soil information at 1:50,000 scale especially for district level planning

- The existing soil maps at 1:50,000 scale with various organizations need to be checked for quality by an expert committee before using them to create database. This would also enable to identify the areas where soil surveys need to be repeated or partial surveys to be conducted to get data. Guidelines for quality auditing of soils maps should be formulated in consultation with various state / central government organizations. Even for the mapping to be done in future, quality of delineation, interpretation of remote sensing data, ground truth collection and soil chemical / physical analysis etc., has to be thoroughly standardized
- Design of a sound soil database using Geographical information System (GIS) for storage, updation, retrieval, analysis, modeling and generation of outputs is very essential. Though various soils survey organizations have developed their own data base, a national level expert committee should be formed to standardize the various aspects of creating digital base such as design, coding, GIS package to be used etc

4.9. Conclusions

The application of remotely sensed data from space borne sensors for study of soil resources is almost three decades old and its usage is increasing at a rapid pace. This potential of the remote sensing technology need to be exploited / employed on regular basis for mapping and monitoring soils / degraded lands at different scales. GIS based models for automatic land evaluation need to be developed for operational use. The utility of stereoscopic satellite data in soil mapping has not been fully exploited and greater scope is seen in this aspect. Soil informatics is still in R&D stage and high priority should be accorded for better utilization of soil information towards soil data handling and establishment of digital soil database. Ground Penetrating Radars for soil survey investigations was successfully demonstrated in various studies conducted in France and USA and used to study the presence, depth and lateral extent of soil horizons. These properties are useful for classifying the soils and estimate the taxonomic composition of soil map units. These techniques are needed to be explored. Polarimetric SAR data need to be explored for studying the spatial-temporal variations in soil moisture. The hyper spectral remote sensing data need to be explored to establish quantitative relationship between spectral reflectance and soil properties. The scope of data from remote sensing satellites with very high spatial, spectral and radiometric resolutions need to be made operational usage for micro-level (1:4000 to 1: 8000 scales) management of soil resources for sustained agricultural production.

References

Anonymous, 2002, Agriculture inputs and Soil Degradation, www.teriin.org/reports/rep02/repo2o6.html

Baumgardner MF, Silva LF, Biehl LL and Stoner ER, 1985, Reflectance properties of soils, *Advances in Agronomy,* **38** : 1-44

Ben-Dor E, Goldlshleger N, Benyamini Y, Agassi M and Blumberg DG, 2003, The Spectral Reflectance Properties of Soil Structural Crusts in the 1.2- to 2.5-m Spectral Region, *Soil Science Society of American Journal*, **67**: 289–299.

Ben-Dor E, Inbar Y and Chen Y, 1997, The reflectance spectra of organic matter in the visible near infrared and short wave infrared region (400–2500 nm) during a controlled decomposition process, *Remote Sensing of Environment*, **61**: 1–15.

Berge H Ten and Stroosnijder L, 1987, Sensitivity of surface variables to changes in physical soil properties: limitations to thermal remote sensing of bare soils, *IEEE Transactions on Geosciences and Remote Sensing,* **25**: 702-708.

Bowers SA and Hanks RJ, 1965, Reflection of radiant energy from soils, *Soil Science*, **2**: 130–138.

Carter GA and Knapp AK, 2001, Leaf optical properties in higher plants: Linking spectral characteristics to stress and chlorophyll concentration, *American Journal of Botany*, **88**: 677–684.

Chappelle EW, McMurtrey JE III,Wood FM and Newcomb WW,1984, Laser induced fluorescence (LIF) of green plants, II: LIF changes due to nutrient deficiencies in corn, *Applied Optics,* **23**: 139-142.

Chen Y and Inbar Y, 1994, Chemical and spectroscopical analysis of organic matter transformation during composting in relation to compost maturity, *Science and Engineering of Composting: Design, Environmental, Microbiology and Utilization Aspects*, HAJ Hoitink and H M Keener, eds., Renaissance Publications, Worthington, Ohio, pp. 551-600

Cho AM and Skidmore KA, 2006, A new technique for extracting the red edge position from hyperspectral data: The linear extrapolation method, *Remote Sensing of Environment*, **101(2)**: 181-193.

Clark RN, 1999, Spectroscopy of rocks and minerals, and principles of spectroscopy, 3–52. *In* N. Rencz (ed.) Remote sensing for the earth sciences: *Manual of remote sensing*, **3** , John Wiley & Sons, New York.

Cruickshank MM and Tomlinson RW, 1988, An assessment of the potential of SPOT reflectance data for soil survey in Northern Ireland, Proc. Royal Irish Academy, 88B, 45-60

DAC, 1994, Draft Report on status of Land Degradation in India, Department of Agriculture and Co-operation, Ministry of Agriculture and Co-operation, Govt. of India, New Delhi.

DOS, 1999, Application of remote sensing in soil resources mapping, Peer review document.

Dregne HE, 1983, Desertification in Arid lands, Hartwood Acad. Publishers. London.

Dwivedi RS and Ravisankar T, 1991, Monitoring shifting cultivation using space borne multispectral and multitemporal data,*International Journal of Remote Sensing*, 1**2(3)**: 427 – 233.

Dwivedi RS and Sreenivas K,1998, Delineation of salt-affected soils and waterlogged areas in the Ind-Gangetic plains using IRS 1C LISS-III data, *International Journal of Remote Sensing*, **19(14)**: 2739-2751 .

Dwivedi RS, Singh AN and Raju KK, 1981, Spectral reflectance of some typical Indian soils as affected by tillage and cover types, Journal of Photo interpretataion and Remote Sensing, **9(2)**: 33-40.

Elvidge CD, 1990, Visible and near infrared reflectance characteristics of dry plant materials, *International Journal of Remote Sensing*, **11**: 1775-1795.

Escadafal R, 1993, Remote sensing of soil colour: Principles and applications, *Remote Sensing Reviews*, **7**: 261-279.

Evans R, 1975, Multiband photography for soil survey in Breckland, East Anglia, *Photogrammetric record*, **8**: 297-308

Evans R and Catt JA, 1987, Causes of crop patterns in eastern England, *Journal of Soil Science*, **38**: 309-324.

Fagbami A, 1986, Remote sensing options for soil survey in developing countries, *ITC Journal***, 1**: pp3.

FAO,1970-78, Soil map of the world, Rome, FAO/UNESCO.

FAO, UNDP and UNEP, 1994 Land degradation in South Asia: its severity, causes and effects upon the people, Rome, FAO, 1994. www.fao.org/docrep/v9909E/v9909e02.html.

Hoffer RM, 1978, Biological and physical considerations in applying computer aided analysis techniques to remote Sensor data in *Remote Sensing: The quantitative Approach,* Ed. McGraw-Hill., 232-289.

Hunt GR, 1982, Spectroscopic properties of rocks and minerals, p 295–385, *In* R.S. Carmichael (ed.) *Handbook of physical properties of rocks,* CRC Press, Boca Raton, FL.

Irons JR, Weismiller RA and Petersen GW, 1989, *Soil reflectance Theory and Application Optical Remote Sensing*, G Asrar, ed., Wiley Ser. Remote Sensing, Wiley, New York, p 66-106.

Janik LJ, Merry RH and Skjemstad JO, 1998, Can mid infrared diffuse reflectance analysis replace soil extractions?, *Journal of Experimental Agriculture,* **38**: 681–696

Kalra NK and Joshi DC, 1994, Spectral Reflectance Characteristics of Salt-Affected Arid Soils of Rajasthan, Journal of *the Indian Society of Remote Sensing* ,**22(3**):183-193.

Karale TL, Saini KM and Narula KK, 1988, Mapping and monitoring ravines using remotely sensed data, *Journal of Soil Water Conservation India*, **31 (1,2)**, p 76.

Kijowski A, 1988, Interpretation of aerial photographs as a method of studying variations in lithology and soil moisture of the surface ground layers: detailed study of the Mosina International Study Area, *Quaestiones Geographicae*, **10**: 47-70.

Kruse FA, Thiry M and Hauff PL, 1991, Spectral identification (1.2-2.5mm) and characterization of Paris Basin kaolinite/ smectite clays using a field spectrometer in Proceedings of the 5th International Colloquium on Physical Measurements and Signatures in Remote Sensing, Courchevel, France, **1**: 181-184.

Lobell DB and Asner GP, 2002, Moisture Effects on Soil Reflectance, *Soil Science Society of American Journal*, **66**: 722–727 .

Mabbut JA, 1978, The impact of desertification as revealed by mapping, *Environmental Conservation*, **5**: 45-56.

McMurtrey JE III, Chappelle EW, Kim MS, Meisinger JJ and Corp LA,1994, *Remote Sensing of Environment*, **47**: 36-44.

Mulders MA, 1987, *Remote Sensing in Soil Science*, Development of Soil Science, 15, Elsevier, Amsterdam, p 379.

Musick HB and Pelletier RE,1986,Response of some thematic band ratios to variation in soil water content, *Photogrammetric Engineering and Remote Sensing*, **52**: 1661-1668

Myer JH, 1998, Near infra-red spectroscopy (NIRS) research in the South African sugar industry, *International Sugar Journal*, **1194**: 279–286.

NRSA, 1995, Project report on soil moisture estimation using microwave data.

NRSA, 2006, Atlas on National Agricultural Technology project, Development of regional scale watershed plans and methodologies for identification of critical areas for prioritized land treatment in the watersheds of rainfed rice, oil seeds, pulses, cotton and NCRI production systems.

NRSA, 2007, Prioritization of watersheds using RS&GIS techniques – project report.

NRSA, 1997, Evaluation of IRS-1C data for mapping soil resources and degraded lands, Project report.

NRSA, 1997a, Soil survey for Land irrigability assessment Sriram Sagar Project, Phase – II, A.P. Project Report.

NRSA, 1998a, Artificial Neural Networks for soil classification, Project Report.

NRSA, 1998b, Soil suitability to crops : A GIS approach - (A case study on groundnut), Project report.

Obukhov AI and Orlov DC, 1964, Spectral reflectance of the major soil groups and the possibility of using diffuse reflection in soil investigations, *Soviet Soil Science*, **2:** 174-184.

Osborne SL, Scheper JS, Francis DD and Schlemmer MR, 2002, Detection of Phosphorus and Nitrogen Deficiencies in Corn Using Spectral Radiance Measurements, *Agronomy Journal,* **94**: 1215-1221.

Pieters CM, 1983, Strength of mineral absorption features in the transmitted component of near-infrared reflected light: first results from RELAB I, *Geophysical Reserach*, **88**: 9534-9544.

Post DF, Horvath EH, Lucas WM, White SA , Ehasz MJ and Batchily AK, 1994, Relations between soil color and Landsat reflectance on semiarid rangelands, *Soil Science Society of American Journal*, **58**: 1809–1816.

Post DF, Bryant RB, Batchily AK, Huete AR, Levine SJ, Mays MD and Escadafal R, 1993, Correlations between field and laboratory measurements of soil color, p. 35–49. *In* JMBigham and EJ Ciolkosz (ed.) Soil color. SSSA Spec. Publ. 31. SSSA, Madison, WI.

Rao BRM, Ravisankar T, Dwivedi RS, Thammappa SS and Venkataratnam L, 1995, Spectral behavior of salt-affected soils, *International Journal of Remote Sensing*, **16**: 2125-2136.

Ravisankar T and Rao BRM, 2004, Evaluation of MODIS data for regional level studies of soil spectral reflectance, Proc. MODIS data utilization, 115-121.

Ravisankar T, 2001. Soil Information System for optimum land use planning, Ph.D.Thesis, JNTU, Hyderabad

Reeves JB, McCarty GW and Mesinger JJ,1999, Near infrared reflectance spectroscopy for the analysis of agricultural soils, *Journal of Near Infrared Spectroscopy*, **7**: 179–193.

Riquier J, Luis Bramao D and Cornet JP, 1970, A new system for soil appraisal in terms of actual and potential productivity (first approximation), F.A.O. Bulletin Agriculture Tesr. /70 /6.

Savin IYU, 1996, The effect of heavy rain on the net surface reflectivity of Cherozems, *Europian Soil Science*, **28**: 168–174.

Schmugge TJ, 1983, Remote Sensing of soil moisture: recent advances, *IEEE Transactions on Geoscience and Remote Sensing*, **21**: 336-344.

Schmugge TJ and O'neill PE,1986, Passive microwave soil moisture research, *IEEE Transactions Geoscience and Remote Sensing*, **24**: 12-22.

Sharada D, Ravikumar MV, Venkataratnam L and Malleswara Rao TCh,1993, Watershed prioritization for soil conservation - A GIS approach, *Geocarto International, 1* : 27-34.

Shepherd KD and Walsh MG, 2002, Development of reflectance spectral libraries for characterization of soil properties, *Soil Science Society of American Journal,* **66**:988-998

Sinha AK, 1986, Spectral reflectance characteristics of soils and its correlation with soils properties and surface conditions, *Journal of Indian Society of Remote Sensing*, **14(1)**, 1-9.

Skidmore EL, Dickerson JD and Shimmelpfennig H, 1975, Evaluating surface-soil water content by measuring reflectance, *Soil Science Society of American Proceedings*, **39**: 238–242.

Sreenivas K and Dwivedi RS, 2006, Ravine morphometry from Cartosat-1 stereo data, NNRMS bulletin, NNRMS(B)-31, pp: 47-51.

Sreenivas K ,2000, Quantification of soil loss using remote sensing and GIS. Ph.D Thesis, JNTU, Hyderabad.

Sreenivas K, 2007, Land degradation and soil fertility. Presented at National symposium organised by State Soil Survey Dept., Kerala.

Stoner ER and Braumgardne MF,1981,Characteristics Variation in reflectance of surface soils, *Soil Science Society of American Journal,* **45:** 1161-1165.

Sudduth, KA and Hummel JW, 1996, Geographic operating range evaluation of a NIR soil sensor, Transactions of ASAE, **39**: 1599–1604.

Task Force,1984, Report of the task force on Soils and Land Use.

Ulaby FT, Razani M and Dodson MC, 1983, Effects of vegetation cover on the microwave radiometric sensitivity to soil moisture, *IEEE Transactions on Geoscience and Remote Sensing*, **21**: 51-61

Venkataratnam L and Ravisankar T, 1992, Digital analysis of Landsat TM data for assessing degraded lands in *Remote sensing applications and Geographical Information Systems – Recent Trends*, Published by Tata McGraw Hill publishing Company Ltd., New Delhi, 87-190.

Vincent RK, 1973, An ERTS multi spectral scanner experiment for mapping iron compounds. Proceedings of the 8th International symposium on Remote Sensing of Environment. University of Michigan, Ann Arbor, pp: 1239-1247.

Zinck JA, 1988, *Physiography & Soil*s. ITC Lecture Notes SOL.41. 1988, Enschede, the Netherlands: ITC.

nrsc

Remote Sensing Applications

P. S. Roy
R. S. Dwivedi
D. Vijayan

National Remote Sensing Centre

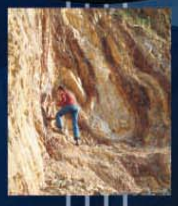

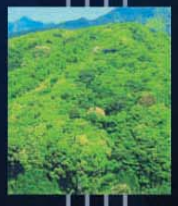

Remote Sensing Applications

Urban and Regional Planning

5.1. Introduction

Expansion of urban area due to increase in population and migration from rural areas and the impact is bound to have on Urban areas in terms of infrastructure, environment, water supply and other vital resources. For organized way of planning and monitoring the implementation of physical urban and regional plans high-resolution satellite imagery is the potential solution. Remote Sensing data is being widely used for urban and regional planning, infrastructure planning mainly telecommunication and transport network planning, highway development, accessibility to market area development in terms of catchment and population built-up area density, etc. With remote sensing it is possible to identify urban growth, which falls out side the formal planning control and remedial measures can be taken timely to provide necessary basic infrastructure to improve health and hygiene.

Remote Sensing and GIS technique combined together facilitate the planners, in making decisions, for general public and investors to have relevant data for their use in minimum time. The advantages and utilities of both the techniques are given below. Even though the initial investment is slightly higher to organize digital data base for using GIS, its utility is immense in coming years. The data can be updated at regular intervals and the data will be transparent and it will be useful for public participation in planning process. However, remote sensing data, limited use was made for resource inventory with course resolution data. Slowly with Thematic Mapper (TM) the resolution was increased to 30 mts and more details were seen on the image. This data was also used in urban and regional planning in limited way like urban sprawl mapping and land use inventory etc. IRS 1A/1B which is near equivalent to TM data was widely used in our country for resource mapping and land use mapping and same data was used in preparation of Regional plans of BMRDA and as well mapping of land use of National Capital Territory (NCT), Delhi for 1993. With SPOT satellite the resolution further improved to 10 mts and this data was used in urban planning as well in regional planning to update the land use and base details. IRS-1C/1D satellite provided 5.8 m high-resolution data, which was used in preparation/revision of development plan. This data was used in revision of development plans of Hyderabad Urban Development Authority (HUDA) planning area, for Ahmedabad Urban Development Authority (AUDA) planning area, Jammu Urban Development Authority (JUDA), Pimpri Cinchwad Municipal Corporation and other towns. Now Cartosat-1 of 2.5 meter resolution, Cartosat-2 of 1 meter resolution and Resourcesat LISS-IV of 5.8 meter resolution data being used for base & land use thematic mapping of Hyderabad Metropolitan Area and Dadra Nagar Haveli (UT) on 1:10000 and 1:5000 scales. The IRS high resolution Cartosat-1 Satellite data is being used up to class-1 towns for generating thematic information under National Urban Information System (NUIS) approved by the Ministry of Urban Development (MoUD).

5.2. Urbanization Scenario and Issues: Global and National

The world's population is quickly becoming urbanized as people migrate to the cities. Figure 5.1 shows the urban population growth between 1950 and the year 2000. In 1950, less than 30% of the world's population lived in cities which grew to 47% in the year 2000 (2.8 billion people).

According to UN reports, half of the world's 6.7 billion people are expected to live in urban areas by the end of 2008. The world population is expected to increase to 9.2 billion, by 2050. By that time, urban population is expected to rise from nearly 3.4 billion in 2008 to 6.4 billion in 2050. Also, these are global figures. When the data are disaggregated by world region, they show marked differences in the level and pace of urbanization. In the Americas, Europe, and Oceania, the proportion of people living in urban areas is already over 70%. Although the figures for Africa and Asia are currently much lower, 39% and 37%, respectively, many cities in those regions will double their populations in the next fifteen years (UN 2006).

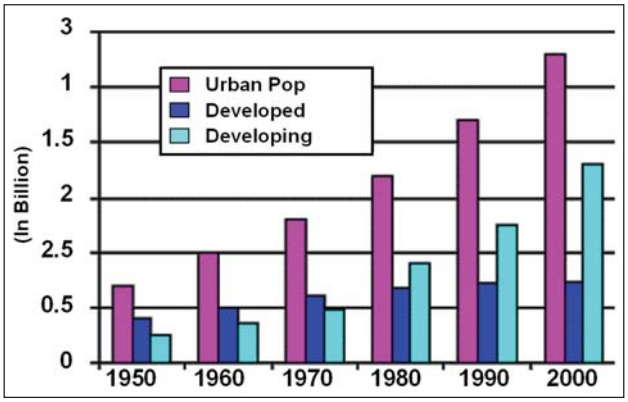

Figure 5. 1: World Urban Population Growth in Past 5 decades (Source: www.earthtrends.wri.org)

Developed nations have a higher percentage of urban residents than less developed countries. However, urbanization is occurring rapidly in many less developed countries, and it is expected that most urban growth will occur in less developed countries during the next decades.

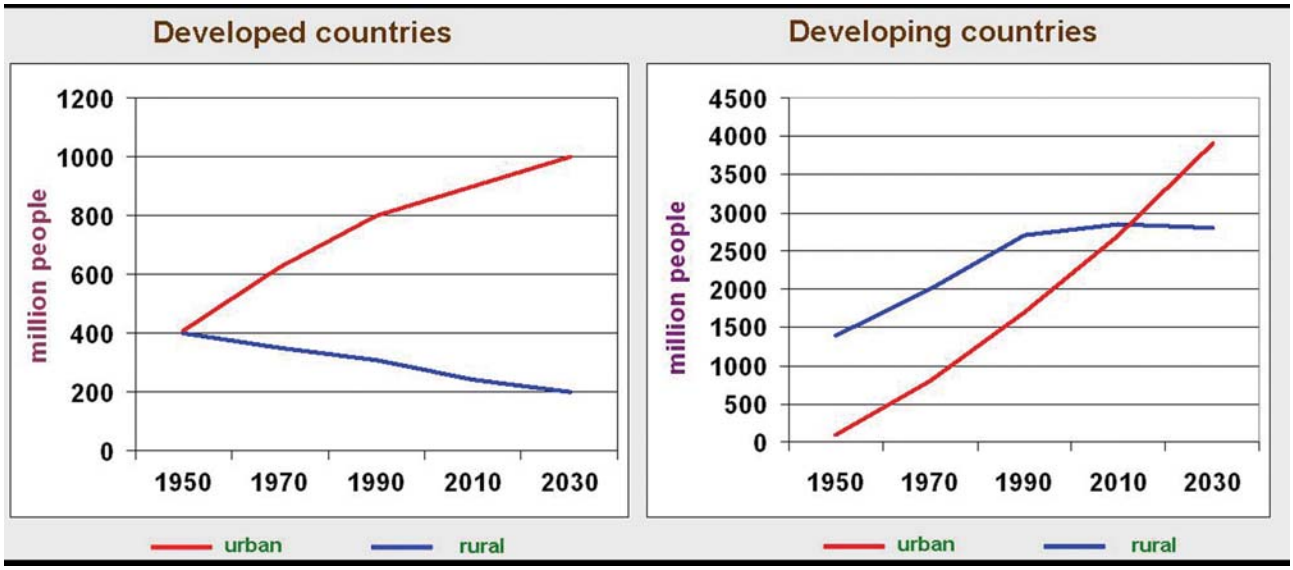

Figure 5.2: Projected Urban Rural Population in Developed and Developing Countries (Source: www.globalchange.umich.edu)

Figure 5.2 shows the projected growth of the urban and rural populations in developed and less developed countries. The urban population of India according to the population census 2001 was 285 million spread over 5161 urban agglomerations/towns. The urban population has been growing at a much higher rate than the total and the rural population as a result; its proportion in the total population has increased from around 11 % in 1901 to about 28 % in 2001. Cities with over 5 million inhabitants are known as megacities. There were 41 in the year 2000. This number is expected to grow as the population increases in the next few decades. It is predicted that by the year 2015, 50 megacities will exist, and 23 of these are expected to have over 10 million people.

In India, the Class I urban agglomerations/cities accounted for 62 percent of the urban population of the country in 2001. A further breakup of the population of cities indicates that the majority (42%) of the population of Class 1 urban agglomerations/ cities lives in 27 metropolitan urban agglomerations/cities with a population of more than a million each. Class I cities account for roughly 61% of country's urban population. Almost one-fourth of the total urban population is living in more then one million population cities (Table-5.1).

Table 5.1: Population in each size Class during 1991-2001 – INDIA

Size	Class	No of UA/Towns	Population distribution %	
	1991	**2001**	**1991**	**2001**
All Classes	4689	5161	100	100
I (> 1,00,000)	300	423	64.91	61.48
II (50,000-1,00,000)	345	498	10.95	12.30
III (20,000- 50,000)	944	1386	13.30	15.00
IV (10,000-20,000)	1170	1560	7.91	8.08
V (5000-10,000)	740	1057	2.62	2.85
VI (<5000)	198	227	0.31	0.29
Others	992*	10#	-	-
Total Urban Population	217,551,812	285,345,954	26	28

* Statutory towns and Census towns population breakup data is not available.

Gujarat towns (Anjar, Bhachu, Bhuj, Gandhidham, Kandla, Morvi, Mundra, Rapar, Wananer) population data is not available.

Source: Census of India (1991 & 2001)

The rapid growth of urban areas is the result of two factors: natural increase in population (excess of births over deaths), and migration to urban areas. Migration is defined as the long-term relocation of an individual, household or group to a new location outside the community of origin. Today, the movement of people from rural to urban areas (internal migration) is most significant. Although smaller than the movement of people within borders, international migration is also increasing. Both internal and international migration contribute to urbanization.

Urbanization refers to the process by which rural areas take on urban characteristics. It also refers to more concentration of people in human settlements. The urbanization process is much more than simple population growth; it involves changes in the economic, social and political structures of a region. While the current pace of urbanization is not unique in human history, the sheer magnitude is unprecedented, with vast implications for human well-being and the environment. Rapid urban growth is responsible for many environmental and social changes in the urban environment and its effects are strongly related to global change issues. The rapid growth of cities strains their capacity to provide services such as energy, education, health care, transportation, sanitation and physical security. Cities have become areas of massive sprawl, serious environmental problems, and widespread poverty. The intense concentration of population, industry and energy use has lead to severe local pollution and environmental degradation. Furthermore, a city's ecological footprint extends far beyond its urban boundaries to the forests, croplands, coal mines and watersheds that sustain its inhabitants.

City dwellers in developed countries, characterized by some of the highest per capita levels of consumption in the world, are largely responsible for these trends. While an American city with a population of 650,000 requires approximately 30,000 square kilometers of land to service its needs, a similar sized but less affluent city in India requires only 2,800 square kilometers (UNEP, 2005). Similarly, urban residents in the developed world generate up to six times more waste than those in developing countries.

However, developing countries are becoming wealthier and more urban, bringing their consumption levels closer to those of the developed world. As a result, they are fast becoming significant contributors to the global problems of resource depletion and climate change. In the cities of the developing world, where population growth has outpaced the ability to provide vital infrastructure and services, the worst environmental problems are experienced with severe economic and social impacts for urban residents like inadequate household water supplies, waste accumulation, unsanitary conditions etc. Developing country cities also experiencing the worst urban air pollution as a result of rapid industrialization and increased motorized transport.

Nevertheless, cities possess unparalleled potential to increase the energy efficiency and sustainability of society as a whole. They have an unrivaled capacity to absorb large population sustainably and efficiently. With proper planning and long-term vision, dense settlement patterns offer economies of scale that can actually reduce pressures on natural resources from population growth and increase energy efficiency. Because people live close together and need less space in cities, each person requires less critical infrastructure like sewers, electricity, and roads than in suburbs or other decentralized human settlements. Innovations in building construction, energy efficiency, waste management, and transportation are just a few of the ways that we can make cities mores sustainable.

Given increasing responsibilities and limited funds, city governments must make strategic choices about which environmental and social problems to tackle first. This will require balancing immediately pressing environmental problems such as water and sanitation with long-term concerns such as energy use and climate change, while also reconciling the often competing demands of economic growth and environmental protection. The choices made in cities today will help determine the extent to which urbanization will be a positive force for human development and the future of the global environment.

So, as we understand, although one of the key geographical developments over the last two centuries has been that of urbanization, it has also raised various issues and problems. It is essential for governments, planners and researchers to understand and study the urbanization process and its associated problems. Latest technologies like Remote Sensing and Geographical Information Systems (GIS) can help resolve some of the urban issues and also acquire best approaches for urban planning, governance and management.

5.3. Planning Approach

Planning is continuous process and for the planning condition of the land on which the settlement is built, its effects on the surrounding lands and the change occurred in land use determines the importance of land resource and its use by mankind. Thus, a sustainable habitat planning demands a comprehensive understanding of the

different uses of land. In order to prepare urban development plan, the planners need detailed information on the distribution of land and its use in city and its surroundings. For example, the city planners and engineers are required to plan optimum routes for transportation, construction of better utilities, pipe lines for water, gas sewerage with minimum construction cost as per different terrains. For planning these utilities in better way the availability of total information in a spatial and tabular form assumes importance. It also becomes essential to integrate both spatial and non-spatial information for perspective planning and management. With the advent of remote sensing and GIS, the city planners have begun to evaluate the resources though a multi disciplinary approach for timely results and with less preparation cost and man power support. The process of planning is political in nature in the sense that it must deal with the value of many groups of people within the area where planning is conducted. Planning is also predictive in the sense that it must identify alternative future and evaluate these in terms of goals which are based on values. The general concerns of planning are physical, man made or built environment and natural environment, economic, political, social and fiscal. Out of the stated planning activities, remote sensing is most useful for depicting information on physical component, especially the natural component of the physical environment. Under Jawaharlal Nehru National Urban Renewal Mission (JNNURM) it is mandatory to reform urban local bodies wherein one of application is e-governance using IT applications, such as GIS and MIS for various services. To carry out such application one of basic requirement is satellite/aerial data. The urban and regional development plans are of four types based on the requirement of plan implementation (Table 5.2).

Table 5.2: Mapping Scales for Various Plans

S.No.	Type of Map / Planning Exercise	Size of Planning Area		Data source
		Metropolitan Level	Small and Medium	Satellite Data
01.	Map of Regional Setting	1:250,000 1:1,000,000	1:100,000 – 1:250,000	
02.	Perspective Plan	1:100,000 1:250,000	1: 50,000 1: 100,000	Satellite Data, Census Data & Collateral Maps
03.	Development Plan	1: 25,000 1: 50,000	1: 10,000 1: 25,000	Satellite Data, Census Data, Collateral Maps & Ground truth
04.	Plan of Project / Scheme	1: 1,000 1: 5,000	1: 500 1: 2,500	Satellite Data, Aerial Data, Census Data, Collateral Maps, Ground truth & GPD Data

Source: Urban Development Plans Formulation & Implementation (UDPFI) Guide lines prepared MUD, GOI 1996.

The Perspective Plan is a long term (20-25 years) written document supported by necessary maps and diagrams providing the state government with the goals, policies, strategies and general programmes of the urban local authority regarding spatio-economic development of the settlement under its governance.

The Development Plan conceived within the framework of the approved perspective plan, is a medium term (generally five years) plan providing the people comprehensive proposals for socio-economic and spatial development of the urban centre indicating the manner in which the use of land and development therein shall be carried out by the local authority and other agencies.

Annual Plan, conceived within the framework of a development plan, is a plan containing the details of new and ongoing projects that the local authority intends to implement during the respective financial year and for which necessary fiscal resources shall be mobilized through plan funds and other sources.

Projects/schemes Conceived within the frame work of approved development plan, projects/schemes are detailed working layouts with all supporting infrastructure, and documents including cost of development, source of finance and recovery instruments for their execution by a public or private agency.

5.4. Remote Sensing & GIS Technology use in Urban and Regional Planning Information

Remote sensors may be categorized as passive sensors – which observe reflected solar radiation – or active sensors – which provide their own illumination of the sensed object. Both types of sensors may provide images or simply collect the total amount of energy in the field of view. Sensors can be located on satellites, piloted aircraft, unpiloted aerospace vehicles or in ground stations; thus, the data acquired by space-based remote sensing instruments feed into a wide array of mapping and other application services.

Remote sensing instruments provide unique views of Earth and its processes. Space – based sensors gather data from Earth's atmosphere, land and oceans that can be applied to a wide variety of resource management tasks. One of the best known of these applications is the collection of satellite images (NOAA, visible and near-infrared radiometers, for example) of the weather and storms that appear on the television and newspapers. Such images, along with sounding and other data, allow forecasters both to predict the paths of severe storms as they develop and to predict weather in advance. Government agencies with the responsibility of managing large tracts of land, or of providing information regarding land conditions, make use of data from the land remote sensing satellites. Commercial data users with interests in agriculture and forestry, land use and land cover, geological information, and mineral exploration, and many other industrial sectors also use data acquired from the land remote sensing satellite systems. In Urban and Regional planning field, IRS products are widely used for urban sprawl and land use/land cover mapping, Utility planning and management, Infrastructure planning and location of major industrial, recreational, institutional facility in context to the Region.

While most local environmental surveys still depend on manual interpretation of aerial photography, the use of digital imagery for regional and urban analysis is now commonplace and will undoubtedly increase in the future. As a source of geographical information, digital remote sensing represents more than a simple extension of conventional aerial photography, requiring fundamentally different approaches to the analysis of Earth surfaces. In GIS context, especially the important features of remotely sensed data are their sampling characteristics in the space and time domains.

Maps for centuries have been an important means for storing, analyzing and communicating information about geographic phenomena. The GIS is systematic procedures for automatically doing what maps have been doing for centuries. However, the base of the GIS is a data file from which maps can be made, whereas the map file itself is the traditional database. The data base manipulation techniques, which include various analytical functions and data processing function, which can be performed on spatial, automated data. Since Remote Sensing Satellites provides continuous images once the database is created in GIS environment, which allows updating and results can be obtained in less time and used for decision making.

The advantage of Remote Sensing data:

- It provides reliable data at regular intervals
- It provides base data that is built-up area information and location
- It provides land use land cover information
- It provides base for plan monitoring and implementation

The advantages of GIS:

The GIS is widely used in Urban/Regional Planning is wide because of following advantages over traditional system of keeping maps.

- Data is maintained in a physical compact data files
- Large amount of data can be maintained and extracted at will with great speed
- Various computerized software modules/tools allow for variety/type of manipulation, including map measurement, map overlay, transformation and geographic design and data manipulation
- Graphic and non-graphic information can be merged and manipulated simultaneously in a related manner

The limitations

- Both the techniques required trained manpower
- Investment in Hardware and Software
- Time consuming and problems in initial stages of GIS data base design and creation

- Changing data formats and software, which will create problem in merging old data with new data
- Storage environment

5.5. Retrospective

Before making any development exercise the first task, both from planning point of view and statutory requirement, is to prepare or obtain a reliable accurate and upto-date base map of respective city and its region for which plan is being prepared. Data is collected from conventional source and data was analyzed in conventional forms for preparation of Development Plan/ Regional Plan. Area estimation was done through planimeter and grid method. The conventional secondary data sources are mentioned below.

- Census of India Publications
- Tabular data from various planning agencies
- Old Municipal property maps
- Land use details from land revenue records
- Municipality/village parcel maps from Land Records office
- Old published Gazettes and other publications
- Maps prepared from other planning agencies like Public Works Department , Public health, power, etc.
- National Atlas and Thematic Mapping Organisation Maps
- City guide and tourist maps
- Specified field survey
- Topographical maps of Survey of India

The shortcoming of above data source is not upto date and survey year is different for each data source which creates complication in data compilation. Data inaccuracy is incorporated due to mechanical mode of adjustments of maps. In absence of latest survey sheets, employing the field survey to record land use or any other details for planning purpose is difficult. Thus, the task of plan preparation takes longer time. By the time plan is approved lot of development takes place, which creates problem in implementation. To speed up the process of data collection, satellite images were used from 1972. In early days the resolution was coarse and thematic details were not up to the level of users in urban planning.

The base map was prepared from available map source and land use inventory was carried by field survey method or from revenue records. The colour maps and single column area table were made for analysis. Plan document contained more of tables and less of spatial details.

For few cities one time digital data was prepared and used for preparation of Regional / Development Plan. The analysis was limited to generation of area estimates and preparation of thematic map plots.

5.5.1. Prospective

So far conventional source data have been the major input for generation of base maps for preparation of development plans. Of late the emerging techniques of aerial photography and remote sensing are being used increasingly for generation of base maps and updating of existing base maps in conjunction with conventional collateral data and limited field survey. The innovative techniques of survey are

- Conventional aerial photography and Photogrammetry
- Digital Photogrammetry
- High-resolution satellite image survey
- Use of Global Positioning Systems and Geographic Information Systems (GIS)

Now, IRS Cartosat-2 satellite provides 1-meter resolution of the panchromatic data enables planners to distinguish ground features as small as 1-meter. The accuracy and interoperability of the imagery makes ideal for mapping analysis.

With increase in spatial resolution, GIS database expected to increase many folds due to amount of information available in the image. Each Urban Development Authority/Town and Country Planning Organisation (TCPO) or Regional Planning Board expected to have advanced data processing systems. The information pertaining to development plan (DP) is expected to be on web site where citizen can interact with Development Authority for their need. This will increase citizen's participation. As per the 74th amendment, each Panchayat /Municipality will have power for preparation of Development Plan and execution. Since the town areas are small, with high-resolution data land use variation can be mapped, GIS will help in updating information and data retrieval for citizens.

To increase the public participation web based packages are expected. The web is best available mechanism for providing the general public with route for direct involvement in the planning process and access to relevant data including,

- Access to relevant spatial and non-spatial information in a multi-media format (text, graphics, maps, photographs, video, animation and sound);
- Access to relevant planning tools (including GIS) via intuitive and user-friendly interfaces such that little or no prior training is required;
- Access to problem-specific data for use with the above; and
- Formal and informal mechanisms for communication with other users for the exchange of ideas, feedback and comparison of decisions made without the social and psychological barriers normally associated with more formal channels such as open planning meetings and written/telephone correspondence

The other area will be Multimedia planning Technologies in Planning where it is possible to manipulate and display the following types of data:

- Text of infinitely variable size and structure;
- Still images, like bitmaps and raster, either generated or captured and digitized;
- Still and animated computer-generated graphics;
- Audio, whether synthesized or captured and replayed sound; and
- Video or moving frames

Multimedia software applications are computer tools based on the simultaneous display and processing of several types of multimedia data. These tools allow for interactive exploration of the data. Base information and Plan details should be translated to soft copy form. The working procedures are to be developed to adopt the new approach in planning. Although automated GIS are just beginning to have practical benefits, they have been adapted to many application areas.

5.5.2. Role of Remote Sensing

Remote sensing (RS) data depicts spatial location of various activities and analyzing the linkages between activates, regional plan, development plan and environmental plans are prepared. RS data is immensely used in creating database on following aspects and with GIS data analysis tools, information can be processed as per the planning requirements.

Perspectives Plan/ Development Plan preparation

- Present land use (statutory requirement)
- Infrastructure network (Roads, Railways, and Settlements)
- Hydrological features (River/Stream, lakes)
- Regional level landscape
- Updation of base maps
- Urban sprawl, land use change and population growth, and
- Master plan/ Regional plan proposals

Infrastructure Planning

- Road alignment
- Utility planning (Sewage treatment plant , garbage dump site selection, water works)
- Road network and connectivity planning
- Growth centre locations

Environmental Planning

Remote sensing data enables mapping of environmental parameters like green cover, surface water bodies and drainage network with other collateral data following are possible to study and to analyse the urban environment.

- Urban land use indicators and Impact assessment
- Development of Urban Information System (UIS)
- Decision Support System (DSS)
- Development of Urban Indicator Observatory (UIO)
- Municipal Information System (MIS)

5.6. Review of literature

Urbanization is an index of transformation from traditional rural economy to modern industrial one. It is progressive concentration (Daveis, 1967) of population in urban unit. In the 21st century the majority of the world's population are living in urban areas for the first time in the history (Miller, 2003). In 1892, the famous city planner Patrick Geddes had leased an observatory in Edinburgh to set up the "Civic Observatory and Laboratory" with a goal "Outlook Tower" as it came to be known – to give visitors insight into the plan, function and inner working of the city Edinburgh (Geddes, 1915). More than a century later urban historians can still learn from Geddes' idea of taking a view from above city/town for effective Urban planning (Jensen and Keys, 2003).

There has been a strong interest in using earth observation data in urban areas for several decades (Tuyahov *et al.*, 1973; Jensen, 1983; Haack *et al.*, 1997). In an early attempt to relate remotely sensed reflectance to socio-economic parameters, Forster (1983) devised a classification scheme for Landsat imagery that could be applied to urban areas to produce a residential quality index. Remote sensing data have also been used in attempts to estimate population (Lo, 1986 and 2001) and quantify urban growth and land use (Mesev *et al.*, 1995; Stehanov *et al.*, 2001). Welch (1982) conducted a resolution analysis of satellite sensors and demonstrated that 0.5 to 10 m spatial resolution is necessary to adequately characterize urban infrastructure in most of the cities/towns. Jensen and Cowen (1999) have identified a hierarchy of urban/suburban attributes that can be measured using remote sensing data. The current/near future high resolution satellite data from Cartosat-1/2, Cartosat-3, RISAT, ASTER, LANDSAT ETM in optical, microwave, infrared, thermal will begin to meet urban needs.

Remote sensing data provides reliable information on urban growth and current land use changes. Aerial photos, IKONOS and QuickBird images over a decade were used to monitor and analyze urban growth in Al-Seeb Wilayat, Oman by Al-Awadhi and Azaz (2004). For urban development in metropolitan area of Athens, multi-spectral satellites images were used to locate and identify the irregular settlements zones (Weber *et al.*, 2005) wherein indicators such as indices, Brightness Index and Normalized Difference Vegetation Index; and supervised classification methods were applied to the images. In order to locate and identify these regions, common biophysical characteristics related to the urban and sub-urban landscape structures were identified. Results were integrated within a Geographical Information System (GIS), allowing the user to check the legal situation of the classified areas. Such techniques are very fruitful to identify specific irregular settlements in organic growth. A study on urban growth in Istanbul has also been done using Landsat 5 TM and Landsat-7 ETM+ satellite data (Kaya, 2007). After the classification of the images separately, eight main land use/cover classes were obtained and the classified outputs were compared to get the extent of urban growth and land use change. In another study carried out for Shiraz city in Iran, different satellite images since 1976 to 2005, and population census of Shiraz city in this time period were used wherein the land use coverage for different dates were classified and measured (Ibrahim and Sarvestani, 2009).This was further used to calculate the built-up and vegetation per capita with respect to population which helped in estimating the reduction in natural resources due to urbanization and population increase.

Urban planners also require information related to the rate of growth, pattern and extent of sprawl to provide basic amenities such as water, sanitation, electricity, etc. In the absence of such information, most of the sprawl areas lack basic infrastructure facilities. GIS and remote sensing data along with collateral data helps in analysing the growth, pattern and extent of urban sprawl. A study on measuring urban sprawl through 'Entropy Approach' for patterns of urban growth over different time scales done by Lata *et al.,* (2000), has discussed the use of remote sensing data and GIS for quantifying the urban sprawl trends at various land use sites, viz., commercial, industrial, residential sensitive and mixed zones. IRS-1C Pan sharpened merged data was used and entropy was used to indicate the degree of urban sprawl by examining whether land development in a city is dispersed or compact. A larger value indicated occurrence of urban sprawl. With the spatial and temporal analyses along with modeling it has been possible to identify the pattern of sprawl and subsequently predict the nature of future sprawl. The work done by Sudhira *et al.*, (2004) has brought out the extent of sprawl taking place over a period of nearly three

decades in Mangalore city, India, using LISS-III satellite data and GIS techniques. The study has also attempted to describe some of the landscape metrics required for quantifying sprawl. Remote sensing and GIS provides vital tools which can be applied in the analysis of land use / land cover and change in rural fringe as well at city level. The study done by Nigam (2000) evaluated the effectiveness of High-Resolution satellite data and computer aided GIS techniques in assessing the land use change dynamics within the city as well in fringe. The methodology adopted involved the visual interpretation of land use on accurate overlays with the land use classification. The land use maps were crossed with each other to identify and quantify the land use changes types. Finally, hot links and user interface were developed so that the information could be provided to the user.

Satellite data in association with GIS provides cost effective methods for infrastructure planning and urban environment assessment studies. Landsat satellite data have been used to provide information for integrated land resources, agriculture and rural access road planning in Atacora Province, Benin (Beaumont,1992). Sriram *et al.,* (2001) in their study have used IRS LISS II data to determine the least cost alignment of highway in Panchmahal and Dahod districts, Gujarat,India. Site selection for waste disposal has been identified using IRS-1C-PAN (5.8m spatial resolution) and LISS-III (23.5m spatial resolution) satellite data for Ranchi Municipal area (Upasana and Nathawat, 2001). Rajaram *et al.*, (2001) have used Indian Remote Sensing data along with ground information on water and air quality to carry out Environmental Impact Assessment study for Konkan railway alignment in India. In another study done by Cristina *et al.,* (2003) human settlements and photosynthetic activity derived from satellite data have been used to monitor the impact of human activity on the environment in Mediterranean basin.

Quantification of green space patterns is a pre requisite to understand green space changes in urban areas and is essential for monitoring and assessing green space functions. This study (Kong *et al.*, 2005) presented a new method for quantifying and capturing changes in green space patterns supported by GIS and remote sensing, the method comprised of quantification of local area green spaces by the “moving window” technique (using FRAGSTATS), and a gradient analysis involving sampling from the urban center to the fringe. In another study by Faryadi and Taheri (2008), the direct effects of urban green space dispersal and density on quality of the environment of the regions of Tehran city have been investigated and evaluated. The measurements have been done by means of land use layers in GIS, satellite images of vegetation cover dispersal and density and calculating the normalized difference vegetation index (NDVI). Comparison of these indices, and analysis of the correlation level between them helped in identifying the regions which have the least green space area per capita. Reza *et al.*, (2009) have carried out a study for Mashad city, Iran to detect changes in extent and pattern of green areas and to analyze the results in terms of landscape ecology principles and functioning of the green spaces. Landsat TM and IRS LISS-III image were used and a post-classification comparison done to determine the changes in green space areas. Then, landscape ecology calculations were done to derive metrics that quantified pattern of the changes in the green areas.

Satellite data has lot of applications in the field of landscape archaeology also. The utility of satellite remote sensing techniques towards locating and identifying ancient ports of Gujarat in India were studied in detail by Thakker (NNRMS, 2000). High resolution satellite data has also been used to study the ruins of Hampi, Karnataka, India by UdayRaj *et al.*, (NNRMS, 2000).Interrelationship between palaeo drainage courses and sites in Saraswati Basin, India have been studied using remote sensing data by Gupta *et al.,* (NNRMS, 2000). Nalanda and other archaeological sites like Kausambi, Ahichhatra, Lumbini, Sravasti were surveyed for their ruins using satellite remote sensing techniques by Thakker (2001). A long term archaeological research project using remote sensing data has been done in Burgandy region, France wherein a 2000 year period has been analyzed to find Celtic and Roman sites (Manual of Remote Sensing, 2006). Radar data has also been used to penetrate sand in Sudanese desert and reveal watercourses. Landsat-5 TM image as well as JERS-1 SAR image has been used to determine the distribution and position of the ruins of Khmer Civilization in Cambodia, Northern Thailand (Manual of Remote Sensing, 2006). Thus Remote Sensing data has provided not only a synoptic view of the sites but also helped in identifying existing sites and also potential sites. Airborne and satellite imagery has been used to investigate

ancient Maya settlement, subsistence and landscape modification in the dense forest region of Guatemala (Manual of Remote Sensing, 2006). The remote-sensing technology has been used to investigate large seasonal swamps (*bajos*) that make up 40% of the landscape. Through the use of remote sensing, ancient Maya features such as sites, roadways, canals, and water reservoirs have been detected and verified through ground reconnaissance. Micro environmental variation within the wetlands was elucidated and the different vegetation associations were identified in the satellite imagery. More than 70 new archaeological sites within and at the edges of the *bajo* were mapped and tested. The use of Landsat Thematic Mapper (TM) and Enhanced Thematic Mapper (ETM), 1-m IKONOS satellite imagery, as well as high-resolution airborne STAR-3*i* radar imagery at 2.5 m backscatter/10 m Digital Elevation Model (DEM)—have opened new possibilities for understanding how a civilization was able to survive for centuries on a karst topographic landscape.

A lot of semi-automated and automated methods for classification and information extraction from satellite imagery in urban areas have been developed the world over. Morphological and Neural approaches have been investigated for feature extraction from high resolution satellite data (Pesaresi and Benediktson, 2000). These attempts were made on high resolution Indian Remote Sensing (IRS 1C) and IKONOS remote sensing data. A fuzzy classification approach for high-resolution multispectral data over urban areas have been investigated in detail using IKONOS Panchromatic and multispectral imagery by Shackelford and Davis (2002). Gamba and Houshmand (2001) had carried out a research work on C-band total power AIRSAR data and optical images of Santa Monica, Los Angeles, wherein a suitable neural classification algorithm, based on the use of Adaptive Resonance Theory (ART) networks has been applied to the fusion and classification of optical and SAR urban images. The interaction between the two methods lead to encouraging results in less CPU time than classification with fuzzy clustering alone or other classical approaches (ISODATA). In another research attempt done by Mena and Malpica (2004) a new technique, named Texture Progressive Analysis (TPA) has been used in order to obtain the segmented binary image from high resolution satellite image which has been further vectorised using morphological methods to derive the road network. Mayunga *et al.,* (2005) have developed a semi-automatic method to extract buildings in structured and unstructured urban settlements areas from high-spatial resolution panchromatic imagery using radial casting algorithm to initialize snakes contours and the fine measurements of building outlines were carried out using snakes model. The advent of Light Detection and Ranging (LiDAR) technique has provided a promising resource for three-dimensional building detection. A study by Meng *et al.,* (2009) presented a morphological building detecting method to identify buildings by gradually removing non-building pixels.

The government of India has taken an important initiative to strengthen municipal governance, like enactment of the 74th Constitution Amendment Act (CAA), 1992. Through this initiative, Ministry of Urban Development, Govt. of India launched a National Urban Information System (NUIS) with an objective generation of multi scale (10 K, 2 K & 1 K) hierarchical Urban Geospatial database including thematic data for various levels of Urban Planning, Infrastructure development and e-governance using satellite, Aerial and Ground Penetrating Radar (GPR) techniques for all the 5621 Urban Local Bodies (ULB's). In NUIS phase-I, 152 towns covering at least 3 to 4 cities/ towns in all states have been taken up and will be completed by July 2010 (NUIS, 2006). Because many ULBs in India or other part of world were now using IT as an administrative tool, the capacity for integrating remote sensing images and other GIS data for day-today urban e-governance applications were relatively wide spread and is beginning to be the focus of research.

5.7. Major Application Projects

5.7.1. Regional Planning

Regional plans are prepared for metro regions, city/town conurbation and special economic zones. The main objective of the plan is to provide guideline for development direction, polices of land use regulation, and land use zoning for future development considering the national / local polices. One of the vital input towards preparation of these plans is existing land use / land cover spatial information.

Regional Plan 2021 of National Capital Region (National Capital Region Planning Board (NCR-PB))

The project aim was to generate inputs on urban sprawl, existing land use, and image atlas using high resolution data. The National Capital Region (NCR) covers an area of 33578 sq km consists of National Capital Territory (NCT) of Delhi (1,483 sq km), sub-region, Haryana (13,413 sq km), sub-region, UP (10,853 sq km) and Rajasthan (7629 sq km) surrounding Delhi. Its population is expected to increase from 370 lakhs (2001) to 641 lakhs by 2021 including 138 lakhs (2001) to 235 lakhs for NCT Delhi during the same period. The project was taken up with following objectives:

- To map Urban sprawl and land use/land cover of 1999 using IRS-1C (LISS III + PAN) data on 1:50,000 scale, to create GIS layers and preparation of NCR land use mosaic
- To study land use changes between 1993 and 1999 for monitoring the urban growth and land use patterns
- To generate Image Atlas for regional and towns planning
- Creation GIS database for Regional Plan Proposals

IRS 1C (PAN & LISS-III) merged data of March/April, 1999 and land use data of 1993 & 2004 comprised the database. Based on the visual interpretation techniques feature identification, land use classification was designed and 67 sheet-wise land use/land cover maps were prepared, supported by limited ground verification. The GIS database comprises of layers of

- Administrative boundaries (State, District, Taluk & Forest)
- Land use of 1993
- Land use of 1999
- Road
- Rail
- Canal
- Drainage
- Watershed
- Ground water prospects
- Derived map of conservation areas (ground water rechargeable areas, forest & hills, streams/drainage/ Waterbodies)
- Derived map of urbanizable areas
- Proposed transportation corridor alignment based on existing land use

Sheet-wise land use colour plots were generated on 1:50,000 scale for about 75 map sheets. The satellite based analysis of NCR has revealed about 47% of area is already converted into built-up area, which include available open spaces and greenery. A GIS database is also generated for Regional Plan 2021 (RP 2021) for entire area of NCR based upon draft RP 2021 criteria for following themes.

- Proposed Land use of 2021
- Policy zones for development
- Settlement Plan of 2001 and 2021
- Transport Plan (Road and Rail) of 2001 and 2021
- Ground water rechargeable area
- Environmental sensitive and Ground water rechargeable areas

After reviewing objections and suggestions received, RP 2021 map plots were generated on 1:50,000 scale. Study maps were created using GIS database which were included in final report of RP 2021. As per the area tables generated for Controlled / Urbanizable area, total controlled area in NCR is about 25% out of which 10% is earmarked as urbanizabe area and further 3.5% is concentrated in NCT, Delhi.

Apart from the above work, land use/land cover maps were prepared on 1:50,000 scale and digital database was also created for five counter magnet town namely Bareilly in Uttar Pradesh, Gwalior in Madhya Pradesh, Kota in Rajasthan, Hissar in Haryana and Patiala in Punjab.

5.7.2. Master / Development plan

The scale of plan is large compared to regional plan. These plans are prepared as per the sate town planning act. The objective of the plan is to show future urbanizable zones, proposed land use structure, public utility network including transportation system and conservation aspects. Since the scale of plan is large, IRS high resolution images are suitable for extracting physical inputs towards preparation of plans.

A Plan for Sustainable Development, Hyderabad 2020 Draft Master Plan for Hyderabad Metropolitan area. Hyderabad Urban Development Authority (HUDA):

The Hyderabad Urban Development Authority (HUDA) planning area covers an extent of 1905.04 sq.kms inclusive of about 172.6 sq.kms. of Municipal Corporation Hyderabad (MCH) area. Outside the MCH area, it consists of 12 – Municipalities, Osmania University, 13 outgrowths and 4 other census towns of census urban agglomeration (HUA). As per census 2001, Hyderabad Urban agglomeration population was about 57.52 lakhs and projected population for Master Plan is about 136.43 lakhs The project was taken up with following objectives:

- Mapping existing land use on 1:12,500 scale
- Updating of base maps of HUDA
- Creation of land use register (proposed and existing), and
- Creation of Digital database for entire HUDA area

IRS-1C (PAN + LISS-III) merged data of Feb, 1997 and April 1998 on 1:12500 scale along with SOI map sheets on 1:25000 scale and HUDA base maps on 1:1000 scale were used as the data base in the study. Also limited ground truth was carried out for verification of updation of land use up to 2000.

The GIS database comprises of layers of

- Administrative boundaries (HUDA, Zone, Cantonment, Municipality, Village & Parcel)
- Land use 2000
- Road
- Rail
- Canal
- Drainage
- Land use proposals

Since the 1984 base maps had become out dated, in 1999 – 2000 HUDA, launched a joint project with the National Remote Sensing Agency (NRSA), Hyderabad to update not only base maps but also the land use maps for the non MCH area with the help of IRS Satellite (LISS III and PAN) as well as ground verification in 2000. The NRSA – HUDA study produced colour coded thematic land use maps (47 plates) for the non-MCH area in 1:10000 scale (approx). It was thus possible to have updated physical features and land use within a short period of time a fairly high degree of accuracy suitable for land use planning at metropolitan sale. A major benefit of this Land Use data is that is available in GIS base. The map can be further modified and additional non-geographical information incorporated as and when needed. Land Use statistics are generated.

As per the area estimate, residential area is about 12.7 % where as agriculture and vacant category is 66 % of the total study area. Residential land requirement estimated for 2020 is about 421 sq.km taking 550 persons per hectare (PPH) in MCH & 250 PPH in non MCH) and additional requirement estimated to around 132 sq.kms.

Creation of Urban Landuse database for Dadra & Nagar Haveli (UT) for Development Plan using Remote sensing & GIS techniques:

The preparation of a Development Plan of a town and its urbanisable area is based on understanding the geo-graphical location, spatial distribution pattern and composition of present landuse and socio-economic data. Preparation of development plan of a town is the statutory requirement according to the State Town Planning Act. Towards this, high resolution Cartosat-1 (PAN) ortho corrected data of 2007 was interpreted and using GIS techniques and a spatial database was prepared at 1:10000 scale. Further the database details were updated using Cartosat-2 data on 1:5000 scale. The Cartosat-2 of 2007 data was othocorrected using Cartosat-1 stereo data and by using GCPs. The study area covers an area of 490 sq.kms. and is surrounded by Valsad District of Gujarat and Thana District of Maharastra. The Census (2001) aggregated the total population of the UT at 2.2 lakhs distributed over 72 villages and two census towns Silvassa and Amli. Various thematic details such as road network, settlement nodes, built-up area footprints, water bodies, surface drainage and canals and other landuse details up to Level-III

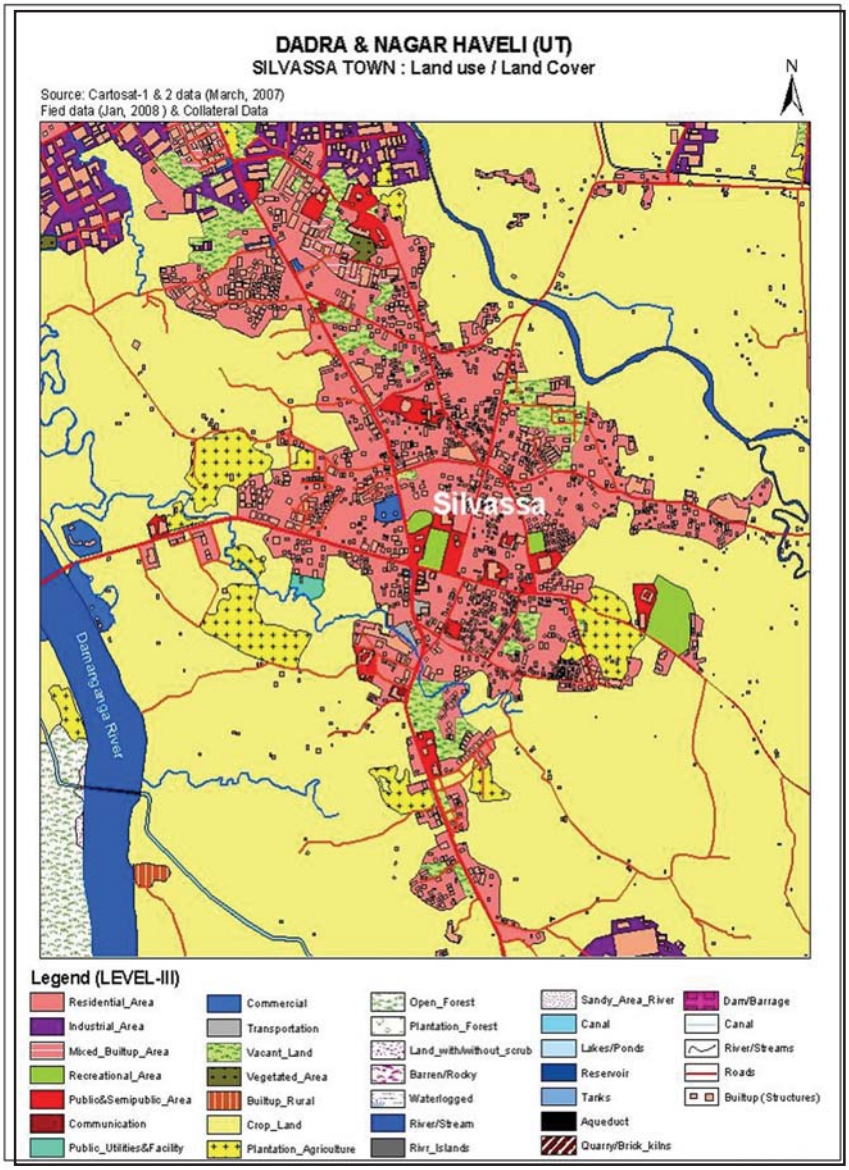

Figure 5.3: Urban Landuse Map of Silvassa

was captured and ground checked in 2008. Figure 5.3 shows urban landuse for Silvassa town. The Cartosat-2 data enabled to map the built-up area foot prints clearly due to its high resolution. The spatial land use distribution suggests distribution of settlement nodes all over UT and industries in and around Silvassa and Amli towns. The major area under landuse is covered under the agricultural use followed by forest/plantation. The GIS data base helps to prepare the Development Plan by analyzing the database for transportation, environmental sensitivity, settlement zoning, and for policy regulations on the proposed land uses by the Department of Town Planning, Govt. of UT.

5.7.3. Infrastructure Facility Mapping

These plans are prepared within the frame work of national / local development polices. Basically the aim of this plan is to develop efficient way of optimizing the infrastructure and facility network. These plans are also useful for management purpose. Data capture of existing infrastructure and location of facilities is possible with high resolution satellite imagery and aerial photos. Route alignment of infrastructure and facility location analysis is possible with GIS.

Route Alignment Study of 400kv D/C Teesta – V – HEP to New Siliguri Transmission line using IRS-Satellite Imagery and GIS techniques:

Remotely sensed satellite data offers a very useful scientific base for carrying out the route alignment corridor surveys, because it provides information on terrain features such as topography and slope, current land use, forest/vegetation cover, water bodies / drainage, built-up areas, road, rail, sanctuaries/parks and others which are the guiding factors to support the decisions during the Pre-feasibility and Feasibility studies. Further, GIS helps in carrying out the integration (spatial and non-spatial data) and the spatial analysis to support the decision process.

Under the project, the route alignment corridor survey between Teesta-V-HEP in Sikkim and New Siliguri town in West Bengal was undertaken for Powergrid Corporation of India Limited, Gurgaon, Haryana. The study was conducted using the topomap data in conjunction with other collateral maps, ground traverses to identify three alternate routes based on, 'maximum avoidance criteria' indicators. The selection of the optimal route (from the three alternate routes) was based on IRS PAN+LISS-III merged satellite data and DEM analysis using a 'semi-automated' method in a GIS environment (figure 5.4).

Thus, final route selected, covers a ground distance of 105.05 km between Teesta and New Siliguri town. Different sets of map like the base map, land cover map, flood sub-mergence maps, terrain profile map are prepared on 1:50,000 scale supported by area estimates, number of crossings and angular bends of turnings of the final route line alignment.

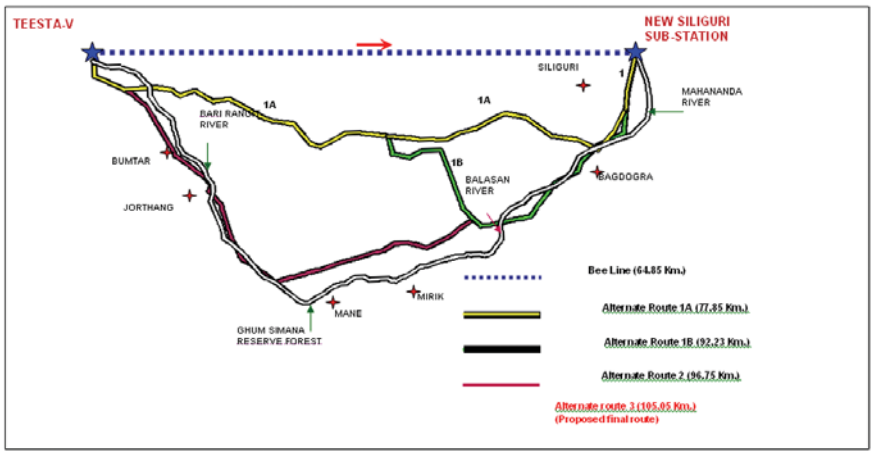

Figure 5.4: Alignment of three alternate routes for powerline between Teesta and New Siliguri

East Cost Gas Pipeline Alignment using CARTO-1 Stereo data and GIS Techniques:

M/s Reliance Gas Transportation Infrastructure Limited (RGTIL), Mumbai planned to connect Chennai and Cuttack with Kakinada through a Gas pipeline (~1200 Km) for supplying LPG. Towards this, for optimization of Route alignment and fixation of corridor, a feasibility study has been initiated using geospatial techniques.

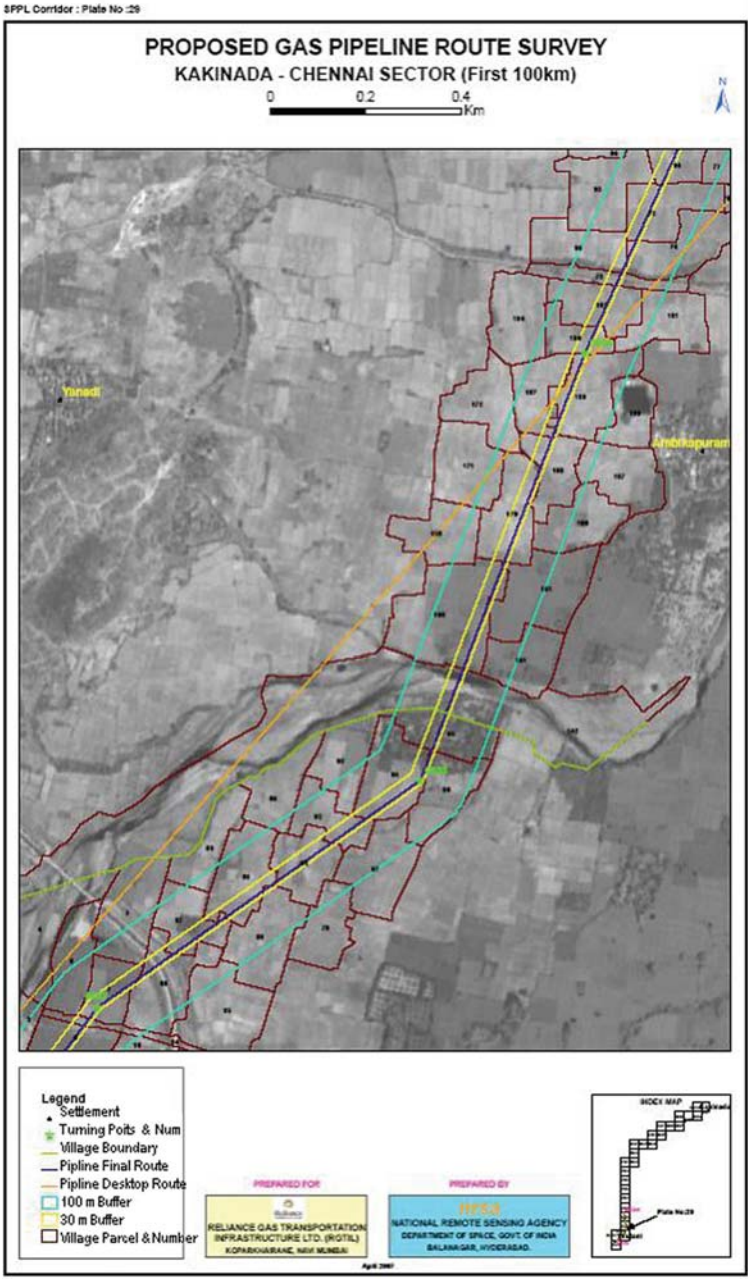

Figure 5.5: Proposed Gas Pipeline Route overlaid with parcels for Kakinada-Chennai Sector

Cartosat-1 PAN (2.5 m) stereo data (2007), orthorectified with the help of DGPS derived GCPs is used for generating the primary avoidance layers like, extent and spatial distribution of habitations, waterbodies (rivers/ streams and tanks/lakes), wetlands, wastelands, vegetation, geology, soil and disaster prone areas. Legacy data like administrative boundaries, forest boundaries, national parks / sanctuaries is collected and geospatial database is created as per the methodology developed on rule base using GIS techniques.

Desktop route is examined through overlay method to generate alternate routes between starting and end points through Maximum Avoidance Criteria, and the final alignment is optimized considering the field data. Using GIS tools, buffers of 30 m & 200 m are generated for the final route. The statistics of Turning Points (TPs), segmented distances between TP's and extent of passage of final route through the villages are generated using referenced (village) parcel vectors warped to the orthorectified Cartosat-1 PAN data. The study is initially completed for ~500 km stretch between Chennai to Kakinada covering ~220 villages and the outputs have been generated onto a spatial scale of 1:10,000. A sample of the CARTOSAT-1 imagery overlaid with the final route, village/parcel boundaries and buffers is shown in Figure 5.5.

The results of the study will enable RGTIL to decide on the cost implications and environmental considerations, based on the current pattern of land utilization and infrastructure development.

Land Use / Land Cover study of Assessment GAIL's proposed LNG pipe line Kochi-Mangalaore-Bangalore using Remote Sensing and GIS Techniques:

Liquefied Natural Gas (LNG) is assuming greater importance in the energy segment as it is used to operate Power Plants and Industrial (fertilizer) Plants. Supply of LNG from source to various destinations (located in different states) through near sub-surface pipelines is techno-economically feasible and has a definite edge over other modes of transport for bulk quantity supply covering large distances. M/s. Gas Authority of India Limited (GAIL) propose to setup a sub-surface pipeline network covering parts of Kerala, Karnataka and Tamil Nadu for transportation and distribution of LNG supplied by Petronet LNG Ltd. (PLL) through a pipeline to be commissioned between Kochi - Mangalore - Bangalore over a distance of 912 Km .

Here, using IRS-1D (LISS-III) satellite data of 2002 with ground truth data of April 2003 Land Use /Land cover mapping and assessment for the corridor of 1 km has been carried. Also, mapping covering 5 km circles at Receipt and Dispatch stations also been carried. The pipeline segments (5 km interval) passing through each land use/land cover category has been estimated along with the geographical extent of the each of the land use/land cover classes.

The study indicated 693 km length of pipeline passes through agriculture land, 119 km of wasteland, 71 km of built-up area, 23 km of water bodies, 6.4 km of forest and 0.5 km of other land use classes. The total number of crossings (road, rail, canal, river/streams) along the pipeline route is around 891 with maximum number of crossings of the pipeline along road and river/streams. Geographically, agriculture is predominantly covering an area of 663 sq km (74%) land followed by 113 sq.km (13%) wasteland, 81 sq.km (9%) built-up area, 29 sq.km (3%) water bodies, 7.33 sq.km (0.8%) forest and 3.1 sq.km (0.3%) other land uses classes along the corridor. Figure 5.6 shows one out of 38 maps prepared for the pipeline corridor study. Inputs were used in Environmental Management Plan (EMP).

5.7.4. Urban Information Systems

Urban information system includes both spatial and non spatial data for planning and management of urban settlements. To facilitate planning and management of urban settlements by Urban Local Bodies (ULBs), National Urban Information System (NUIS) project is approved by Govt. of India.

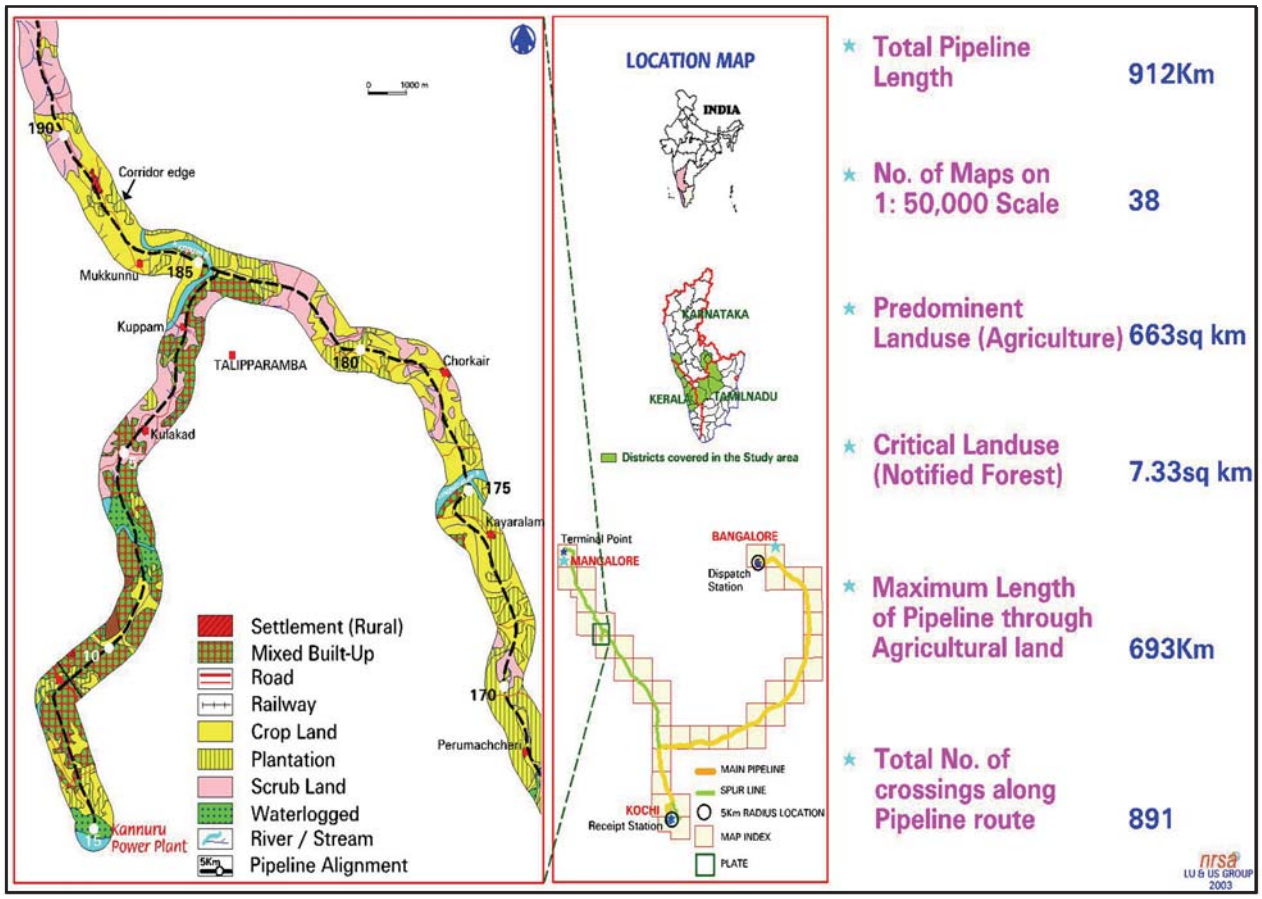

Figure 5.6: Landuse/Landcover along the proposed Gas Pipeline route for Kochi-Bangalore-Mangalore Corridor

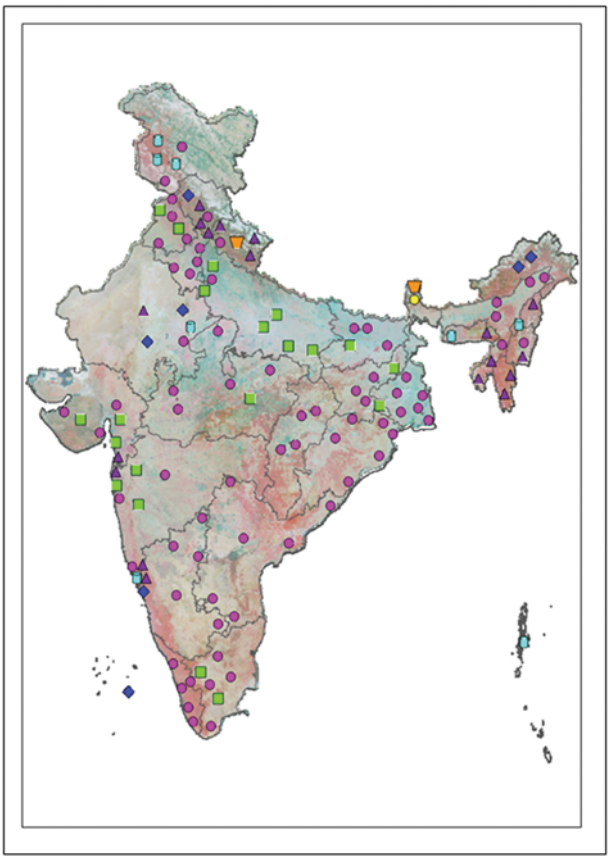

Figure 5.7: Distribution of NUIS Phase-I towns

National Urban Information System (NUIS) Scheme:

The National Urban Information System (NUIS) project was taken up on national mission mode to enable establishing town level geospatial database under a single National (Central) Scheme. Broadly it comprises two major components a) Urban Spatial Information System (USIS) to meet the spatial (base and thematic maps/image) data requirements of urban planning and management functions, and b) National Urban Data Bank and Indicators (NUDBI&I) to develop town level urban database to support development of Indices through a network of Local Urban Observatories (LUOs) under the National Urban Observatory (NUO) programme. The NUIS project envisages developing USIS and NUDBI covering all the 5161 Cities/Towns/UA's in the country in three phases. The Phase-I covers 158 towns with a geographical area approximately 55,755 sq.km. The geographical distribution of towns is given in Figure 5.7 and conceptual scheme of NUIS and is shown in Figure 5.8.

The major objective of NUIS is to generate multi-scale hierarchical Urban Geospatial and non-spatial (attribute) databases for various levels of planning and decision support to meet requirements of Urban planning, Management and Governance. Development of Urban Spatial Information System to support and strengthen the outreach of geospatial database to SNA and ULB through the use of GIS tools and techniques to assist in better urban decision making and governance.

The thematic database was prepared at 1:10000 scale using Cartosat-1 PAN and LISS-IV multi spectral Satellite data, 1:2,000 scale database prepared from aerial photographs, and for selected towns on 1:1,000 scale underground assets survey (Water supply and sewerage network) using Ground Penetrating Radar (GPR). NUIS Thematic mapping comprises of 12 primary layers and 4 incorporated layers.

Primary Layers

- Urban land use
- Physiography (outside core area)
- Geomorphology (outside core area)
- Geological Structures (outside core area)
- Lithology (outside core area)
- Soils (outside core area)
- Drainage
- Surface waterbodies
- Road
- Rail
- Canal
- Transportation Nodes

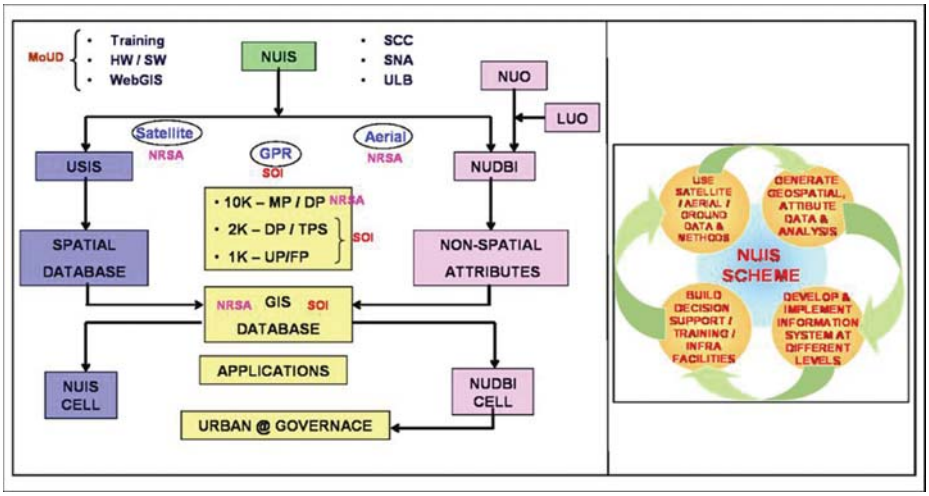

Figure 5.8: NUIS Scheme

Incorporated Layers

- Administrative Boundaries
- Forest Boundary
- Settlement & Village Locations / Names
- City / Town Boundaries

In phase-I, among 158 towns, as a priority, database for Korba town covering 276 sq.k was prepared as shown in

figure 5.9. The geospatial databases of towns would enable the preparation of urban plans to meet the requirements of different levels of urban planning. Applications/ automated integration techniques developed in GIS would provide inputs to Master/ Development/Zonal Planning and Utilities management and help to build capacity among town planning professionals at State and Local Body level on the use of remote sensing and GIS techniques.

5.7.5. Archaeological Studies

Remote Sensing being a non-destructive technique has gained lot of importance in the field of archaeological applications. It has helped in recognising and studying potential archaeological sites on the basis of signature variations on the satellite data. This relevance of this study has been mainly to use high resolution Indian satellite data, and advanced geospatial technologies towards newer applications in archaeology.

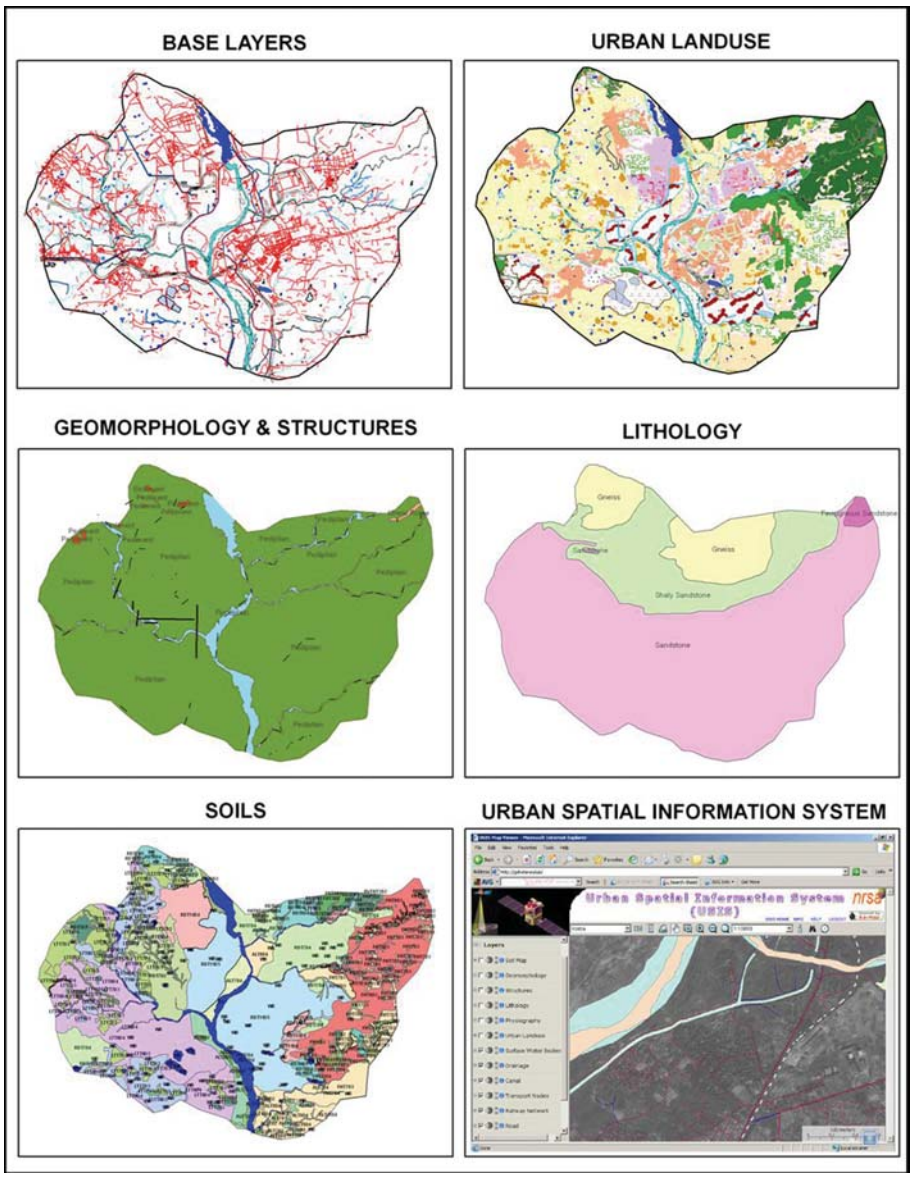

Figure 5.9: Snapshot of NUIS Database of Korba town, Chattisgarh

Satellite based Archaeological Study of Ancient Nalanda Site and Environs, Bihar:

The Objectives of the study were mainly:

- To establish the feasibility of high resolution satellite remote sensing data in archaeological reconnaissance surveys for identification, delineation and monitoring of archaeological sites
- To examine potential sites for further archaeological research and excavations

Nalanda is located at 90 km south-east of Patna, Bihar and 11 Km north of Rajgir. The study area covers 16 sq km in and around Nalanda including the 1.5 sq.km present excavated site. It is located between 25° 6' to 25° 10' and 85° 24' to 85° 30' E as shown in figure 5.10.

Nalanda, is an ancient Buddhist ruin, located close to the village Bargaon in Bihar. Nalanda has a very ancient history of being established as a Buddhist Centre of learning, going back to the days of Mahavira and Buddha in 6th & 5th century B.C. Based on the findings of Nalanda by Buchanan in 1838, General Alexander Cunningham identified the site for the first time in the year 1861-62 which was followed by A.M.Broadley, who carried out some excavations. Later, for about twenty years, beginning with 1915-16 upto 1937, the Archaeological Survey of India (ASI) excavated the site, besides its preservation and collection of antiquities. Excavations conducted in 1974-1982 and recently in 2004-2005, have revealed the existence of ruins of temple close to the Nalanda. Further, it is stated that the 2500 year old Nalanda University was spread over 16 sq.kms. However, till now only 1.5 sq.kms of the ruins has been reported to be excavated by ASI.

The following datasets were used for the study:

- Satellite data: CARTOSAT-1 PAN Aft and IRS LISS-IV images

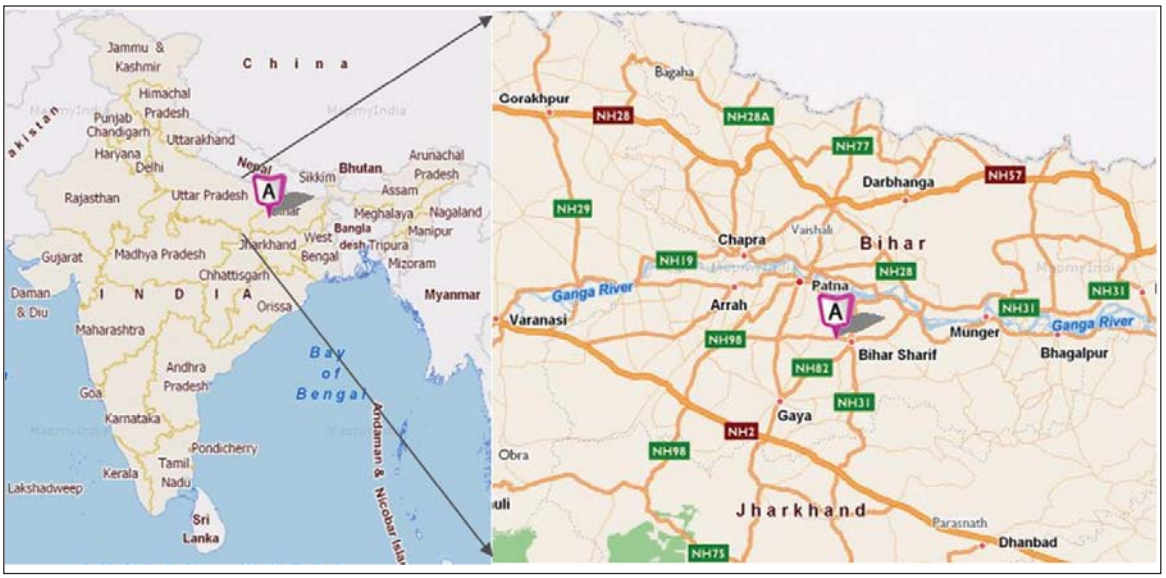

Figure 5.10: Location and regional setting of Nalanda site (source: www.mapsofindia.com)

- Field data: Ground Penetrating Radar (GPR) based ground survey for short-listed prospective sub-surface sites for detailed investigation
- Secondary Data: SOI Map / ASI Maps / Monument Plans and Literature

High resolution CARTOSAT-1 PAN data was used to locate the present site and determine its extent and precincts. Various structures present on the site were identified. IRS LISS IV multi spectral data was used in stand alone mode and also merged with CARTOSAT to observe features in vegetated areas. Since vegetation is highlighted in the multi-spectral data, it would help in the better differentiation of features especially in contrast with vegetation since historic sites are hidden under vegetation. Topomaps were used as a base for the study. The detailed land use / cover like settlements, agricultural fields, waterbodies, exposed ground, roads and canal/streams were also extracted from the imagery following heads up interpretation approach.

The already excavated site was correlated with the neighboring land use to identify its extension. The position and alignment of the structures in the site was studied with reference to existing literature. Some conspicuous features, outside the existing site were identified on the imagery and further verified during the ground truth. Ground Penetrating Radar (GPR) survey was carried out for one of the identified mound, in consultation with ASI, to know and study the sub surface structures and to assess its relation with existing site of Nalanda.

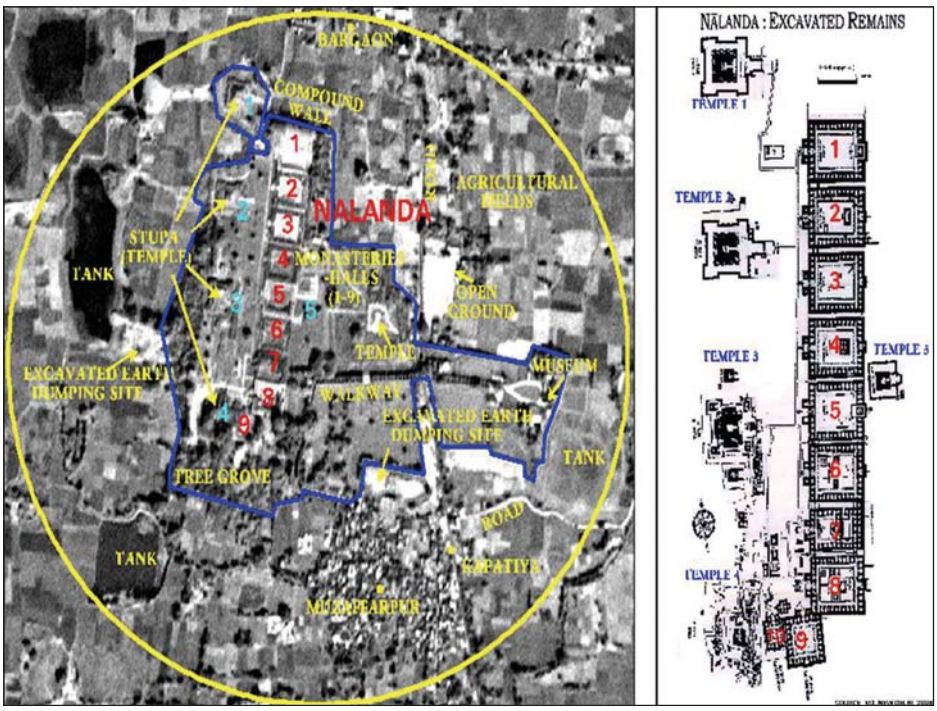

Figure 5.11: CARTOSAT-1 PAN image (03 Feb, 2006) and ASI map(2006) showing the Nalanda site

The imagery clearly showed the location, extent, pattern and layout of Nalanda. A comparison of the features in CARTOST-1 PAN image and ASI map (Figure 5.11), reveals that nine of Ten Monasteries and four out of the five temples/stupas, with their geometric shape and pattern, were distinctly visible on the image. The left out monastery (No.10) and the temple (No.4) were noticed in ruins during the ground truth visit. The monasteries 1,2

and 3 show the presence of a paved surface over the others (unpaved surface). Other details identified on the image include the compound wall, pathways, entrance to the monasteries, vegetation/trees, tanks, lakes, settlements, approach roads besides the cultivated lands with field bunds. Traces of the compound wall were also seen on the CARTOSAT-1 image. The Newly developed settlement, Muzaffarpur, was seen 200 meters to south of the site. The older settlement, Bargaon, is located at 350 m to the north of the site.

Three conspicuous features identified on the image were confirmed with ground truth as mounds of 4-5 m height. One of them was near Begumpur settlement about 1 km north of existing site and two others were near Jagdishpur settlement about 2-2.5 km south-east, as shown in Figure 5.12. The mound at Begampur was the closest to the existing site and its plan on the image resembled the plan of stupa in the already excavated site. On discussion with ASI, GPR survey was carried out for this mound, which yielded results giving the features beneath the mound upto a depth of 5 m. The results showed an almost square shaped structure with extended corners and internal cubicles made of brick.

Detailed ground investigations is required to confirm whether the mound is really a part of ancient Nalanda or just another structure, which could have existed at the same time as Nalanda and having its own archaeological importance.

The study using Indian Remote Sensing satellite data has offered a valuable insight into Nalanda site towards establishing baseline information to serve as a repository for further monitoring and archaeological investigations. This has also demonstrated the capability of Indian remote sensing data, in conjunction with ground surveys, to carry out archaeological exploration studies.

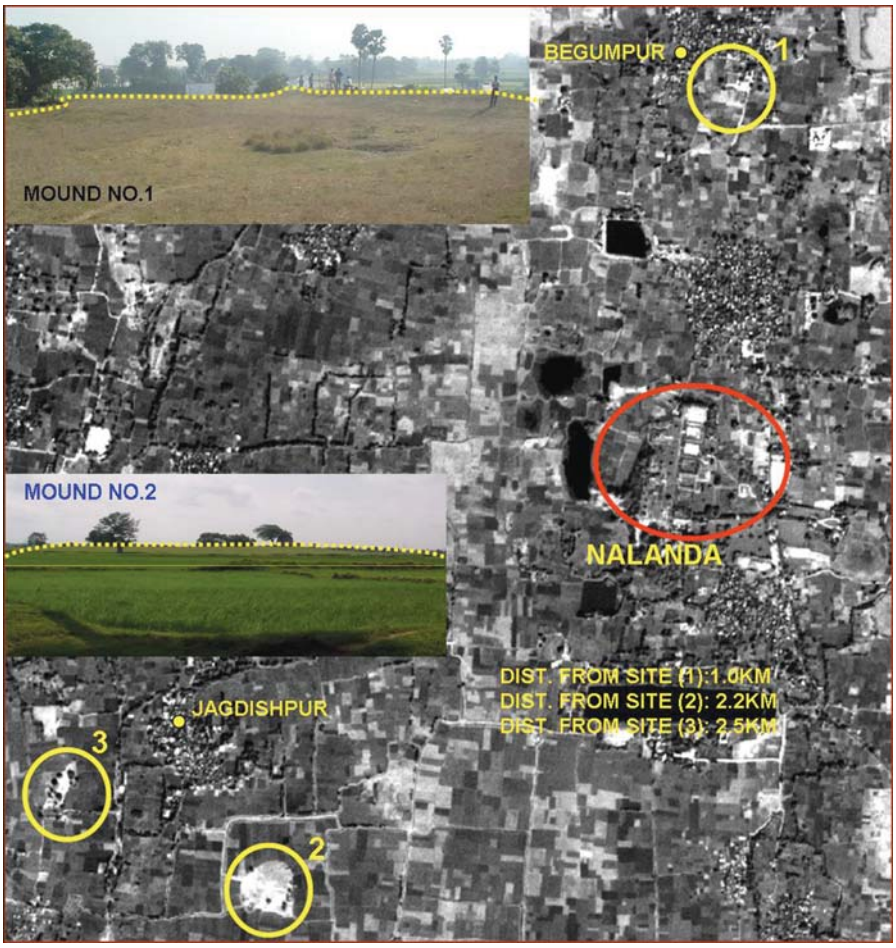

Figure 5.12: Three mounds as seen on Cartosat-1 and its ground photos

5.8. Scientific Methods

The present chapter has tried to look into the utility of remote sensing data and scientific methods in solving some of the urban problems. Applying remote sensing technology to urban areas is relatively new and with the advent of high resolution satellite data and advances in digital technology, it has gained momentum.

Some of the requirements of urban planners which remote sensing is able to provide are:

- the location and extent of urban areas
- the nature and spatial distribution of different land-use categories
- primary transportation networks and related infrastructure
- 3-D structure of urban areas
- Ability to monitor changes in these features over a time

5.8.1. Feature Extraction and Classification

One of the very basic tasks is mapping of urban/rural settlements. Landcover and land use is an obvious product of remote sensing which is the basic element for any kind of urban planning. The land use map generated by

thematic classification of a satellite sensor image can be viewed as end product as it constitutes a document showing the existing situation before any planning action. However, it is also a starting point for further analyses. Direct identification techniques like visual interpretation, feature extraction, classification etc., are widely used for image interpretation. Visual or Manual interpretation has so far been recognized as effective tool in urban mapping. But in recent times, there has been a shift to digital techniques which has been improved with the advances in spatial resolution. Traditional techniques used for image classification include unsupervised, supervised, hybrid and fuzzy classification. Various image classification techniques developed include both semi-automatic and automatic techniques and some of the latest information extraction techniques include linear feature extraction, spectral mixture modeling etc. Traditionally, image classification procedures were mainly in the spectral domain, while the latest image segmentation procedures involve spatial descriptors and make use of panchromatic data.

Another important aspect of remote sensing in urban areas is the delineation of urban areas based on the morphological variability of settlements. Urban/rural settlements can be detected through differences in spectral signatures between the built environment and vegetation and crops. Although the fundamental elements of size, color, shape, pattern, texture etc., are used for any feature identification, its shape, texture, pattern, association, contextual information are more effective in classification of urban features and characteristics.

In metropolitan and urban areas, problems relating to rapid transformations in terms of land cover and land use are very pronounced. As a result, availability of timely information on urban areas is of considerable importance. A very basic issue in urban planning has been non- availability of information/database for Master Plan Development Plan preparation for urban areas. Visual and digital techniques are used to map land use/land cover, infrastructure, utilities, topography etc which constitutes urban database at required scale. Multi-scale geospatial database can be generated in association with GIS techniques, which are useful for planning, management and governance of urban areas at various levels. GIS is a major tool in analyzing the urban spatial database and decision making process.

5.8.2. Change Detection

Change monitoring, which requires comparison of two images of different times is an important analysis technique for urban studies. The simplest way to detect change in settlements is to visually compare images at two or more different times. Spatiotemporal analysis helps in studying urban sprawl and growth process. The physical changes in distribution of urban activities can be provided. This helps in measuring and monitoring the location and extent of urbanization. Many dimensions of change can be monitored directly through optical and also microwave data. The size of a settlement is related to the areal extent of built up area which in turn is related to the size of the population. Allometric growth model and Central Place theory has been extensively used to estimate population on the basis of the built-up area extent.

Haphazard development in urban fringes can be monitored using temporal data. In this era of rapid urbanization, it is vital to have a means of monitoring on a global or regional scale. Change detection algorithms include Visual interpretive methods, Post classification comparison, knowledge based visions etc., which are mainly applied on multispectral data. Change detection is also carried out through spatial, textural and numerical analysis. eCognition is one of the very latest techniques used to delineate urban settlements which tries to imitate human visual perception and image understanding, the software generates image objects using multi resolution segmentation.

5.8.3. Fusion and Photogrammetry

Image fusion helps in producing imagery that includes best of both, especially high spatial resolution and spectral resolution which is useful for urban studies. It combines the inherent advantages of each dataset into one. This increases image clarity, allows efficient mapping and maximizing information on urban areas. Some of the existing techniques include Principal Component Analysis, IHS transform, Brovey transform and Wavelet transform being the latest. Merging can not only been attempted on multi resolution sensors but also with GIS data or DEM or ancillary data.

Photogrammetry, is one of the first techniques to have used remote sensing data for measurements. It is a 3-dimensional coordinate measuring technique that uses photographs or images as the fundamental medium for measurement. Images corrected for terrain slope are essential for urban areas so that there is a true representation of each feature and the real change is evident. Towards this process, known as orthorectification, DEM plays a very important role. DEM can also be used for rendering 3D visualizations, urban flood or drainage modeling, terrain analyses etc.

5.8.4. Environment and Transportation Analysis

The environmental impact on urbanization is an important aspect to be included in planning, design and sustainable development of urban areas, for example, slums can be easily and directly identified on satellite imagery. Remotely sensed data and observations are providing new tools for addressing environment related human health problems relevant to human settlements. It is also significant for identifying, measuring, mapping and monitoring characteristics of natural and man-made hazards or disasters. Vulnerability mapping helps in identifying the locations which are at risk from hazards. Post disaster analysis, for example, the extent of flooding and related damage can also be assessed. As the cities/ towns expand, the encroachment and impact on environment is ever increasing. Degradation of water habitats, higher storm water runoff leading to urban flooding etc are some of the environmental issue very much related to urban development. An indicator used in this regard is the impervious surface area which can be derived from satellite data. Thermal infrared data have been applied in analysis of a wide variety of ecological processes that relate directly or indirectly to urban areas. The urban heat island resulting from replacement of natural cover to urban land use can be observed and studied using thermal infrared data. This helps in understanding how urbanization and urban sprawl affect biophysical and land-atmosphere interactions

The most dynamic element of urban area is the various modes of transportation. Road patterns, its width and alignment can be directly identified and digitized from remote sensing data. A detailed feature/asset inventory of items like dividers, sidewalks, culverts, gutters etc can be prepared from high resolution imagery. Alignment of new roads/rail can be determined in conjunction with parcel and environmental data. Capacity of road intersections, turn lanes can be studied by taking images of same location over a period of time.

5.8.5. Historical sites study

Remote Sensing data can be used in detection of historical settlements or archaeological sites with respect to its position in the ancient and modern landscapes. Soil marks and crop marks clearly seen on satellite image are used to identify sites without any ground surveys. Vegetation signatures in multi spectral imagery are very good indicators of archaeological sites. The different state of vegetation on an archaeological site and the natural background gives a different spectral response which helps in easy identification of the sites. Combining DEM with satellite imagery shows a high degree of correlation between signature and elevation which strengthens historical site detection. The boundary walls of archaeological sites can be easily identified which are otherwise difficult to be seen on the ground. By incorporating ancillary layers like soil, hydrology and elevation in GIS along with remote sensing data, the historical features can be related to present existing site.

5.8.6. Urban Modeling

The thematic database/maps generated needs to be further analysed for various applications. Urban models can be used to support planning, policy and management decisions. Urban simulation is the process through which the plans, policies are tested or their efficiency and impact. Automata models and visualization in urban simulation represent the state-of-the art in modeling of human settlements. Two classes of automata which are significant are Cellular automata (CA) and Multi-agent systems (MAS). CA are generally employed for interaction between static units like buildings, parcels, infrastructure objects whereas MAS is used for more fluid like movements. Simple computer animated design models of buildings have been improved upon by virtual reality models which are capable of supporting applications such as urban design, facilities management, environmental analysis, disaster management etc.

Remote sensing analysis in conjunction with urban modeling has potential to provide information needed for planning and management decisions. Planning Support Systems (PSS) incorporate and integrate different data components such as spatial data sets, GIS, urban models etc. Possible future land development scenarios can also be prepared. The use of scenarios is one of the essential concepts in bridging urban modeling and urban planning and management. A link to planners and the public is provided and communicated via scenarios that are defined or explored within a PSS.

5.9. Economic Benefits of Remote Sensing & GIS in Urban Applications

The use of remote sensing & GIS technology in urban applications are being operationalised due its advantages in time, cost benefits, reliability over the traditional ground methods. For any urban applications such as urban planning including infrastructure as well as for municipal applications (tax, water supply etc.,) up-to-date maps/ geospatial data are required. The traditional method of preparing maps through ground survey has been time consuming and expensive. These maps require timely updation in phase as rapid development takes place in

cities like Delhi, Bombay, Hyderabad, Bangalore. Preparation of maps/geospatial databases are essential for preparing Master plans / zonal plans as ground surveys are impractical for such large areas. However, necessary attribute data such as collecting house hold data, utility data are to be carried out by ground based methods. The following table provides broad guide lines of economic benefits of using remote sensing and GIS technology from NRSC experience.

Table 5.3: Cost and time requirements for preparation of Urban thematic maps in various scales

Sl. No.	Description Project Activity	RS& GIS Methods		Traditional Ground Methods (~ estimated values)	
		~Cost per Sq.km (RS)	~Time required	~Cost per Sq.km (RS)	~Time required
1	Thematic quality Urban Landuse /Land cover mapping and GIS database creation for Delhi NRC region (34,000 sq.km) on 1:50,000 Scale. This database is being used for regional plans	1000	1 year	10,000	More than 2 years
2	Cartographic quality Large Scale Mapping on 1:10 K using High Resolution satellite data. 5000 sq.km covering 40 towns	10,000	2 years	25,000	More than 3 years
3	Thematic quality Urban Landuse / Land cover mapping and GIS database creation for Hyderabad, HUDA region on 5,000 Scale using High resolution Satellite data. These databases are being used for master/zonal plans and infrastructure plans.	5000/-	For 2000 sq.km 6 months	20,000/-	More than 2 years

The values shown in table 5.3. are only approximately estimated. The cost and time elements may vary depending upon intended use of map/geospatial database, level of information content, accuracy and time. RS& GIS technologies are effective and suitable for large areas rather than small areas. For example, to prepare a map of town covering 10 sq.km, ground based methods are recommended and for town/city covering more than 100 sq.km, RS &GIS methods are only practical solution. The economic & time benefit ranges from 30% to 60% based scale of mapping, required accuracy and information content by using RS&GIS technologies over the traditional ground methods. Presently, metropolitan urban local bodies are implementing the RS& GIS technologies for preparation of base maps/thematic maps and geospatial databases for Urban Planning.

5.10. Conclusions

Spatial maps prepared on a 1:10,000/1:5000 scales using High Resolution Satellites (CARTOSAT) data offer an important “Urban Asset” for urban planning and development. Resources information content derived from remotely sensed data has been “proved useful” for the preparation of Regional Perspective Plans, Master Plans/Development Plans and Infrastructure plan. In archeology, remote sensing data found useful in identifying archeology sites for excavation. Various visual methods and digital techniques are operationally tested for ‘data capture’ at a higher degree of accuracy and in this respect many “benchmark studies” have been carried out in the country. Urban GIS offers, application driven solutions as a “value addition” for strengthening urban planning and development scenarios. Integration and fusion of satellite derived information with available conventional/ground based data in a GIS environment offers a “valuable outreach” for the success of urban studies.

References

Batty M, 1992, Urban modeling in computer graphic and geographic information systems environment, Environment and Planning Board.

Beaumonta TE, 1992, *Advances in Space Research*, **2 (8)**: 91-96

Bracken Ian, 1981, *Urban Planning Methods, Research and Policy Analysis*, Mathew & Co., USA.

Cristina Milesi, Christopher D Elvidge, Ramakrishna R Nemani and Steven W Running, 2003, *Management of Environmental Quality*, **14(1)**: 99 - 107

Dana Tomlin C, 1990, *Geographic information system and cartographic modeling*, Published by Prentice-Hall. Inc., NewJersey.

Davies D Wayne, 1967, Centrality and the Central Place Hierarchy, *Urban Studies*,**4(1**) : 61-79.

DDA,1990, Master plan for Delhi Perspective 2001, prepared by Delhi Development Authority, Delhi.

Executive Office of Environmental Affairs Office of Geographic and Environmental Information (MassGIS), October 2002, Getting Started With GIS A Guide for Municipalities.

Forster B, 1983, Some urban measurements from Landsat data, *Photogrammetry Engineering and Remote Sensing*, **49**: 1707- 1716.

Govt. of India, 1988, *Report of National Commission on Urbanization* ,Volume- VI, Published by Govt. of India.

Govt. of India, September 2008, Ministry of Home Affairs, National Disaster Management Division, "Proposed Amendment in Town and Country Planning Legislation.

Haack B, Guptill S, Holz R, Jampoler S, Jensen J and Welch R, 1997, Urban analysis and planning, *Manual of Photographic Interpretation*, ASPRS, Bethesda.

Jensen Jens Toftgaard and Garry Keys, 2003, Mapping Urban History, International association for History and Computing's XVth Conference, Tromso, Dennmark.

Jensen JR, 1983, Urban/suburban land use analysis, *Manual of Remote Sensing*, second ed. ASP, Falls Church,1571–1666.

Jensen JR and Cowen DC, 1999, Remote sensing of urban suburban infrastructure and socio-economic attributes, *Photogrammetry Engineering and Remote Sensing,* **65(5)**: 611–622.

Kaya Sinasi, 2007, Multi-temporal Analysis of Rapid Urban growth in Istambul using Remotely Sensed data*. Environmental Engineering Science*, **24(2)**: 228-233.

Kong Fan-hua , Nobukazu Nakagoshi, Yin Hai-wei and Akira Kikuchi, 2005, *Chinese Geographical Science*, **15(3)**: 254-261.

Konstantino G, 2008,Comparison of Nine Fusion techniques for very High Resolution Data, *Photogrammetry Engineering and Remote Sensing* , **74(5)**: 647-659

Lata Madhavi K, KrishnaPrasdV, Badrinath KVS and RaghavaswamyV, 2000, www.gisdevelopment.net/application/urban/sprawl/urbans0004

Lo CP, 1986, Accuracy of population estimation from medium-scale aerial-photography, *Photogrammetry Engineering and Remote Sensensing*, **52(12)**: 1859–1869.

Lo CP, 2001, Modeling the population of China using DMSP operational linescan system nighttime data, *Photogrammetry Engineering and Remote Sensing*, **67(9)** : 1037–1047.

Maithani M and Sokhi BS, 2002, "Modeling Land Transformation using Remote Sensing and GIS –Case study, Hardware and surrounding Areas", *ITPI Journal*, **2(2)**: 181.

Manual of Remote Sensing,2006, Volume 5: "Remote Sensing of Human Settlements".

Meng Xuelian, Le Wang and Currit Nate, April 2009, *Photogrammetric Engineering and Remote Sensing*, **75(4)** : 437-442.

Mesev TV and Longley PA,1995, Morphology from imagery— detecting and measuring the density of urban land-use, *Environmental Planning,* **27(5)** : 759–780.

Miller RB, 2003, Cities for space: potential applications of remote sensing in urban environmental research policy, *Environmnetal science & Policy*, **6** : 129-137.

MUA&E, 1996m ,UDPFI guidelines, **I** :1-253.

NCRPB, 1988,Regional Plan, 2001, New Delhi.

NCRPB, 1999, "Delhi 1999 A fact sheet,New Delhi.

NCRPB, 1999, "National Capital Region Directory,New Delhi.

Nigam RK, 2000, www.gisdevelopment.net/application/urban/fringe/urbanf0001.htm

NNRMS, Training course on Remote Sensing for Archaeology, NRSA, Dept. of Space, Hyderabad, 2000.

NRSA,1994, Mapping and Monitoring urban sprawl Hyderabad city. Project report, 1-84.

Patrick Geddes, Cities in Evolution, Lodon, 1915, Chapter XIV "The Study of Cities"

Pesaresi M and Benediktsson JA, 2000, Geoscience and Remote Sensing Symposium Proceedings, **7**:3066 - 3068.

Raghavswamy V, Pathan SK, Ram Mohan P, Bhandari. RJ and Priya P,1996, IRS-1C Applications for Urban planning and development, *Current Science*, **70(7)**: 582-588.

Rajaram B, Nagarajan R and Khire MV, 2001, *International Journal of Remote Sensing*, **22 (16)**: 318 -3201.

Ramesh B, 1988,Monitoring Urban Land uses using Aerial photographs and SPOT Image data, ACRS, Bangkok.

Rateliffe John, 1981, *An introduction to Town and Country planning* , Book Published by Hutchinson company Ltd., 62-65 Chandos place, London WC 2N 4NW.

AC, Ahmedabad, 1997, Revised development plan of Ahmedabad Development Authority area –2011, Volume 1: Remote Sensing and GIS approach. Technical Report SAC/RSAG/TR/12/Aug/19997.

Srirama.B, Bhatt MR and Pathan SK, 2001, www.gisdevelopment.net/application/utility/transport/ma0557.htm

Stefanov WL, Ramsey MS and Christensen PR, 2001, Monitoring urban land cover change: an expert system approach to land cover classification of semiarid to arid urban centers, *Remote Sensing of Environment*, **77 (2)**: 173–185.

Surendra S and Aggarwal R.C, 1998, "Application of Remote Sensing & GIS Techniques for National Capital Region", Proceedings of First Workshop of Southern Region State Town Planners on " Remote Sensing and GIS in Urban Development Planning, Management and Emerging Information Needs".

Thakker PS, 2001, Remote Sensing of Cosmic cities in Ancient India. NNRMS Special issue on Archaeological Applications of Remote Sensing, Dept. of Space, Govt.of India, Bangalore, **26**: 43-54.

Tuyahov AJ, Davies CS and HolzRK, 1973, Detection of urban blight using remote sensing techniques, *Remote Sensing Earth Resources*, **2**: 213–226.

UNCHS HABITAT, 1984, Human Settlement Polices and Institutions issues, options, trends and guide lines, Published by United Nations, Center for Human Settlements, Nirobi, Kenya.

United Nations, Economic and Social Commission Asia and Pacific,UNESCAP, Manual on GIS for Planners and Decision Makers.

Upasana Srivastava and Nathawat MS, 2001, www.gisdevelopment.net/application/utility/transport/mi03203pf.htm

Weber Christiane, Chryssanthi Petropoulou and Jacky Hirsch, February 2005, *International Journal of Remote Sensing,* **26 (4)**: 785 - 796.

Welch R, 1982, Spatial resolution requirements for urban studies, *International Journal of Remote Sensing*, **3(2)** : 139–146.

Worboys M, 1995, *GIS: A computing Perspective*, London: Taylor and Francis.

http://www.earthtrends.wri.org

http://www.globalchange.umich.edu

http://www.interenvironment.org/cipa/urbanization

http://www.mapsofindia.com

nrsc

Remote Sensing Applications

P. S. Roy
R. S. Dwivedi
D. Vijayan

National Remote Sensing Centre

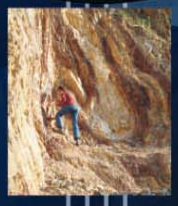

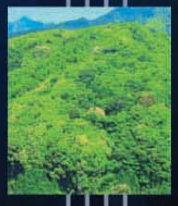

Remote Sensing Applications

Water Resources Management

6.1. Introduction

Water is a key driver of economic and social development and one of the fundamental elements in sustaining the integrity of the natural environment. It is the major renewable resource amongst the various natural resources. Water being an indispensable constituent for all life supporting processes, its assessment, conservation, development and management is of great concern for all those who manage, facilitate and utilize.

Issues related to water resources development and management are not in isolation but are inter-related with other human activities. The issues involved range from those of basic human well-being (food, security and health), economic development (industry and energy) and preservation of natural ecosystems on which ultimately we all exist and sustain. The combination of lower precipitation and higher evaporation in many regions is diminishing water quantities in rivers, lakes and groundwater storage, while increased pollution is damaging ecosystems and the health, lives and livelihoods of those without access to adequate, safe drinking water and basic sanitation. The increase in frequency of occurrences of extreme events is probably firm illustration of fundamental changes that are altering water resources worldwide, including India. Therefore the conservation and optimal utilization of this scarce resource is extremely important for sustainable development. In order to meet present/ future demands for food, the world food production is to have an annual growth rate of about 3%. Present total harvested area is about 1600 million ha and FAO assessments put the world's area of potentially suitable cropland at some 3200 million ha. The water management in the coming years is likely to have profound impact on human society with regard to its quality of life and its very existence.

6.1.1. Water Resources of India

Water resources of India are quantitatively large but significantly divergent in their occurrence, distribution and utilization. The annual precipitation aggregated as 4000 km^3 with utilizable resource of 1122 km^3 (28%). Out of which utilizable surface water resources are 690 km^3 and ground water resources are 432 km^3. According to National Commission for Integrated Water Resources Development, basins-wise average annual flow in Indian river systems is 1953 km^3. India is endorsed with a large network of 12 major river basins covering 256 M ha, 46 medium river basins covering about 25 M ha besides other water bodies like tanks and ponds covering 7 M ha, with the ultimate irrigation potential of 140 M ha. In India, since its independence, sizeable financial resources (approx. Rs. 2400 billion) were invested to harness water resources for irrigation, domestic, industrial, and other sectors. This constituted about 15% of total public sector outlay till 2001.

6.1.2. Water Requirements of India

Indian water resources utilization mostly dominated by agricultural sector nearly accounting to 428 km^3 (around 69% of total water use) with 300 km^3 from surface resources and 128 km^3 from ground water resources. To meet the increased food production requirements and to achieve food security, the agriculture sector would command a quantum jump in water utilization and is expected to be in the order of 708 km^3 by the year 2050. Domestic water requirements are around 25 km^3 at 5% of total usage, out of which surface water contributes 7 km^3 and ground water contributes 18 km^3. With the significant urbanization of population, it is expected that around 54% of population would be living in urban areas by 2050, which increases the domestic demand to 90 km^3. Industrial usage is in the order of 15 km^3 which is likely to grow up to 103 km^3 by 2050.

The total water requirements of the country are expected to be around 1450 km^3 by the year 2050, which is significantly higher than the present estimate of utilizable water resources potential of 1122 km^3. It is estimated that Indian ground water overdraft is of the order of 66% which places food and livelihood security at great risk and could lead to 25% reduction in India's harvest. The per capita availability of 1820 m^3 (2001) is fast endangered with teeming population and likely fall to 1191 m^3 by 2050 getting precariously closer to water scarce condition (FAO).

6.1.3. Gaps and Issues related to Indian water resources

The above statistics indicate the impending crisis, which Indian Nation is likely to encounter. The surface water potential developed only to an extent of 37% and that of groundwater to 38%. Significant gap exists in the ultimate irrigation potential, creation and the utilization. In addition, the water-use efficiency in the country is reported to be only 25-30 percent. While India has about 16% of the global population, it only has 4% of total water

resources, and many parts of India already face water scarcity. The problems associated with the water resources development are varied and complex. Some of them are:

- Spatial and temporal variations in availability
- Falling per capita availability of the country
- Expanding multi-sectoral demand
- Under and inefficient utilization of irrigation potential
- Loss of surface storage due to reservoir sedimentation
- Frequent floods severely affecting the flood prone area development
- Recurring drought
- Over-exploitation and depletion of the ground water resources
- Deteriorating water quality and environment
- Climate change impact on water resources

Coping and managing the above problems largely depends upon our preparedness through a well structured system. It calls for great challenges in the best use of available water resources through surface water capture and storage, long distance conveyance and inter-basin transfer, ground water exploitation, watershed management, conjunctive use of surface and ground water and de-salinization. This necessitates having relevant information at appropriate time for arriving at rational decisions which would support sustainable water utilization. New tools have to be developed to facilitate integrated water resources management. Managers have to be able to access to quality data through a well-structured data acquisition, flow and access system. Conventional data collection is a well established practice, although the convertibility between available data and readily usable information is little. They are oriented more towards archival than operational usage and in-situ observations are generally characterized by inadequacy and non-reliability. To achieve maximum water use efficiency and to cope up with varying water resources availability conditions, real time information on various aspects, which control and influence the supply & utilization regimes are to be obtained. The satellite remote sensing geo-spatial techniques promise to be potential tools to aid water management decisions. Systematic approaches and studies involving satellite remote sensing techniques have supported scientific efforts of water management.

6.2. Role of Satellite Remote Sensing For Water Resources Management

Measurements from satellite remote sensing provide a means of observing and quantifying land and hydrological variables over geographic space and support their temporal description. Remote sensing instruments capture upwelling electromagnetic radiation from earth surface features which is either reflected or emitted. The former is reflected solar radiation and the latter is in thermal infrared and microwave portions of electro-magnetic spectrum. Active microwave radars obtain reflected/returned microwave signals. The reflected solar energy is used for mapping land & water resources like land use, land cover, forests, snow & glaciers, surface water features, geologic & geomorphologic features, water quality, etc. The thermal emission in the infrared is used for surface temperature, energy fluxes and microwave for soil moisture, snow & glacier, flood, etc.

Remote sensing has several advantages over field measurements. First, measurements derived from remote sensing are objective; they are not based on opinions. Second, the information is collected in a systematic way which allows time series and comparison between schemes. Third, remote sensing covers a wide area such as entire river basin. Ground studies are often confined to a small pilot area because of the expense and logistical constraints. Fourth, information can be aggregated to give a bulk representation, or disaggregated to very fine scales to provide more detailed and explanatory information related to spatial uniformity. Fifth, information can be spatially represented through geographic information systems, revealing information that is often not apparent when information is provided in tabular form.

Towards evolving and supporting comprehensive water management strategies space technology plays a crucial role. Systematic approaches involving judicious combination of conventional ground measurements and remote sensing techniques pave way for achieving optimum planning and operations of water resources projects. Remote sensing has shown enormous promise for providing wealth of data and information that were deficient with the in-situ observations. It has also been a valuable tool in many hydrologic modeling applications due to its capability of providing unrestricted collection of information with wide spatial coverage and temporal revisit.

Earth Observation Satellite (EOS) data has been extensively used to map surface water bodies, monitor their spread and estimate the volume of water. The SWIR band of AWIFS sensor in IRS-P6 was found to be useful in better discrimination of snow and cloud, besides delineating the transition and patch in snow covered areas. Snow-melt runoff forecasts are being made using IRS-WiFS/AWiFS and NOAA/AVHRR data. These forecasts enable better planning of water resources by the respective water management boards. Monitoring reservoir spread through seasons has helped to assess the storage loss due to sedimentation, updating of rating curves. Satellite data derived spatial and temporal information on cropping pattern, crop intensity and condition forms basic inputs for developing indicators for agricultural performance of the irrigation systems and bench marking of systems. Satellite data derived geological and hydro-geomorphologic features assist in prospecting the ground water resources to plan aquifer recharging, water harvesting and drinking water sources. High resolution satellite data remarkably augmented the remote sensing services extending it to infrastructure planning & management.

The overall applications of RS & GIS in water resources sector can be broadly categorized into the following:

- Water Resources Assessment
- Water Resources Management
- Water Resources Development
- Watershed Management
- Flood Disaster Support
- Environmental Impact Assessment & Management
- Water Resources Information & Decision Support Systems

Table 6.1 provides the details of Sensors / satellites data suitable for Water Resources Management.

Table 6.1: Sensors / Satellites data suitable for Water Resources Management

Application	Satellite and sensor
• Field/Plot boundaries • Irrigation network/infrastructure • Cartographic information • Micro-scale features	Cartosat -1 & 2(PAN), Ikonos, QuickBird, SPOT (PAN)
• Land use • Land cover • Surface water resources • Crop identification • Crop yield / condition • Soil salinity • Water logging	IRS, Landsat, SPOT, ASTER, CBERS
• Evapotranspiration • Soil moisture	NOAA, Aqua, Terra, Landsat, ASTER, CBERS
• Surface roughness • Soil moisture	ERS, Radarsat, RISAT
• Flood inundation • River bank erosion • River control works	IRS, Landsat, SPOT, ERS, Radarsat, JERS, RISAT IRS, Landsat, SPOT, Cartosat-1 & 2 Cartosat-1 & 2, Ikonos, Quickbird
• Surface Water • Snow cover • Glaciers	IRS, Landsat, SPOT, ASTER, NOAA, Aqua, Terra
• Snow depth • Snow water equivalent	ERS, Radarsat, JERS, RISAT
• Water quality	IRS, Landsat, SPOT
• Precipitation	TRMM, METEOSAT

Various applications have been developed, since last 3 decades, wherein SRS data is being put into use to provide quantitative and reliable information, there by facilitating improved water resources management.

- Snow & Glacier
  - Snow cover mapping & monitoring
  - Snowmelt runoff forecasting
  - Glacier mapping & monitoring
  - Glacier Lake monitoring
  - Glacier mass balance (R&D level)
- Surface water resources
  - Water bodies
  - Wetlands
- Irrigation water management
  - Inventory of Irrigated Agriculture
  - Performance Evaluation & Bench Marking
  - Monitoring Intervention Schemes
  - Near Real-Time Monitoring
  - Surface Water Logging
  - Soil Salinity/Alkalinity
  - Irrigation Infrastructure Mapping
  - Assessment of Irrigation potential creation
  - Pre-feasibility studies
  - Actual Evapotranspiration estimation (R&D level)
  - Irrigation Information System (R&D level)
- Reservoir Sedimentation
  - Assessment of Sedimentation
  - Updation of Elevation-Area-Capacity Curve
  - Estimation of Reservoir Capacity
  - Assessment of Rate of Siltation
  - Estimation of Life of Reservoir
  - Reservoir Catchment Analysis
  - Impact of Foreshore Cultivation
- Hydro-Power generation
  - Submergence area analysis
  - Inputs for pre-feasibility assessment
  - Inputs for ranking studies
  - EIA studies
- Interlinking of rivers
  - Pre-feasibility studies
  - Canal alignment studies
  - Submergence area analysis
  - Land irrigability
  - Inputs for Detailed Project Reports
- Flood disaster monitoring and management
  - Flood inundation mapping & monitoring
  - Flood hazard zonation
  - Flood forecasting (R&D level)
  - Flood inundation simulation
  - Disaster management & support

- Watershed Management
  - Water harvesting
  - Sustainable Action plans
  - Soil erosion & Catchment's area treatment
- River engineering
  - River migration
  - River control works mapping & monitoring
- Ground Water Prospecting
- Environmental Impact Assessment and Management

6.2.1. Major Application Projects

Satellite RS applications in India evolved during mid to late 70's during which Landsat-1 & 2 data provided first insights of remote sensing capability for natural resources applications. Recognizing the potential of RS data for water resources management (WRM) a joint Indo-US workshop was organized during April, 1978 and broad strategies for extended and sustained use of satellite data for water resources management were formulated. During the period 1980-1990, the remote sensing data applications were focused on image interpretation, 3D aerial photographs, and methods of classifying and transforming digital satellite data into images or sorts of maps. The initial phase – Landsat data utilization – provided the required understanding and experience for generating geo-spatial information and water related events mapping. The advent of Indian Remote Sensing (IRS 1A/1B) series satellite data provided the much needed fillip to RS applications for water resources sector through availability of multi-spectral information at various resolutions and at affordable prices. The subsequent IRS satellites (IRS 1C/1D/P2) expanded the applications going far beyond visual interpretation/mapping to monitoring, digital data base, quantitative analysis, modeling, etc. The more recent constellation of IRS satellites, namely, Resourcesat-1, Cartosat-1 & Cartosat-2, extended the remote sensing applications to near real time monitoring, hydrological modeling, infrastructure planning, mapping & monitoring, information systems, and decision support systems and so on. The following sections provide brief account of some of the satellite remote sensing based applications in water resources sector.

6.3. Water Resources Assessment

(Snow cover, Glacier, Surface Water, Rain/Runoff, Water balance)

The rapid growth of population and urbanization resulting in steady increase in water demands for agriculture, domestic and industrial requirements. Accurate information on surface water, its existence, spatial extent, temporal changes is essential to manage this resource judiciously.

Surface water occurs in the form of liquid water in lakes, reservoirs, rivers, oceans and in its solid form as snow, glacier and lake ice. Remote sensing platforms are amenable to detect and map the spatial extent of both forms of water.

6.3.1. Snow & Glacier Studies

Snow cover and the equivalent amount of volume stored supplies at least one-third of the water that is used for irrigation and for the growth of crops world wide. Northern rivers of India receive significant inflows due to snowmelt during summer months. Snowmelt runoff feeds many multi-purpose storage reservoirs that provide irrigation, hydropower, urban/industrial water supply and recreation.

The vast difference in spectral properties of snow and other natural land cover supports its identification on satellite data. The relatively high albedo of snow reflects much higher percentage of incoming solar shortwave radiation than snow free surfaces (80% for relatively new snow whereas roughly 15% for snow-free vegetation). The snow cover can be detected and monitored from a variety of remote sensing platforms. Both reflective and thermal remote sensing is being extensively used for mapping snow cover area, its build up during winter and depletion during summer seasons. Microwave instruments are providing parameterization of snow cover physical properties such as snow water equivalent, density, grain size, depth, state (wet/dry) and age. Remote sensing images provide accurate information on the glaciers and their spatial extent. The glacier lakes are easily identifiable on multi-spectral satellite data of medium resolution (24-30 m) to fine resolution (6 m).

Snow Cover Mapping

Snow cover mapping is done using both reflective and microwave remote sensing data. Snow cover, with relatively high albedo, appears very bright on standard false colour composite (FCC) images and is easily differentiated with other land cover features. However, cloud and snow bound areas appear similar in standard FCC images, which is resolved through SWIR band response in which snow covered areas have low reflectance. Remote sensing platforms with SWIR band have been extensively used for snow cover mapping and monitoring.

Space Application Centre (SAC), Ahmedabad is involved in snowcover mapping of entire Himalayas at the request of Ministry of Environment using IRS AWiFS data. Generation of ten daily snow cover products and area-altitude distribution products to observe the snow cover variability for 28 basins of the Western Himalayan region is being executed. Using Normalised Difference Snow Index (NDSI) and IRS-P6 AWiFS data for 8 sub basins in Himalayan region snowcover maps were prepared. Snow cover Atlas of the Ganga basin for the year 2006-07 was prepared. Some of the sensors operationally used for snow cover mapping are shown in table 6.2.

Table 6.2: Some of the sensors operationally used for snow cover mapping are:

Satellite - Sensor	Snow cover mapping status
NOAA – AVHRR MODIS – Aqua/Terra	Region level snow cover area mapping on daily basis
Resourcesat 1 - AWiFS	Regional to basin level snow cover area mapping and monitoring on five daily basis
Resourcesat 1 – LISS III; Landsat – ETM; ASTER; SPOT	Basin to sub-basin level snow cover area mapping and monitoring

Snowmelt Runoff Forecasting

Accurate estimates of the volume of water stored in the basin in the form of snow in winter and its rate of release due to melting in summer are needed for many purposes. These include stream flow and flood forecasting, reservoir operation, watershed management, water supply, and the design of hydrologic and hydraulic structures. The planning of new multi-purpose projects in the Himalayan region further emphasizes the need for reliable estimates from rain, snow and glacier runoff. The variation of runoff depth can vary greatly from year to year for mountain basins because of differences in seasonal snow cover. Melting of snow cover in summer is an important source of water for many Himalayan rivers, and an increase in atmospheric temperature accentuates the melting of snow cover.

In general, snowmelt models can be divided into two types of models, namely energy balance models and index models. Broadly, energy balance models require the information on radiant energy, sensible and latent heat, energy transferred through the rainfall over the snow and heat conduction from ground to the snow pack. Several meteorological parameters are to be monitored to obtain this information over the snow pack. A thorough understanding of the basic energy transfer processes and their role in melting of snow pack helps in improving the performance of the operational snow melt models. Index models use one or more variables in an empirical expression to estimate snow cover energy exchange. Air temperature is the most commonly used index, but other variables such as net radiation, wind speed, vapour pressure and solar radiation are also used. The degree-day method is more popular because temperature represents reasonably the energy flux and at the same time, it is relatively an easy parameter to measure, extrapolate and probably to forecast. However, snowmelt prediction can be significantly improved by using vapour pressure, net radiation and wind rather than the temperature variable alone. The accumulation and recession of snow cover in a basin is found useful to quantify snowmelt runoff.

NRSC, for the last 20 years, provides advance forecast of snowmelt runoff into Bhakra reservoir to Bhakra Beas Management Board (BBMB). The forecast provided by NRSC assists BBMB to allocate water for different sectors and sharing among five northern States. Snow cover in Sutlej basin is monitored from October to June to understand the accumulation and depletion pattern of the snow pack in the season using NOAA/AVHRR satellite data. The

relative comparison of the current year recession pattern with that of previous years helps in characterizing the nature of snow pack present in the basin, rate of depletion and onset of depletion. The comparative analysis is done to identify the interval in which current year inflows are expected to be and accordingly forecast is made. The forecast of snowmelt runoff inflows into Bhakra reservoir during the period Apr-May-Jun months is provided to Bhakra Beas Management Board in 1st week of April. A revised forecast is made in last week of May. The snow accumulation and depletion in Sutlej basin during 2006-2007 season is shown in figure 6.1.

National Institute of Hydrology (NIH) used water balance approach to estimate the average contribution of snow- and glacier-melt runoff in the annual flow of the Beas River at Pandoh Dam. About 45% of the basin area is covered by snow during winter and about 15% remains covered by permanent snow and glaciers. Snow and glacier-melt contribution was estimated by computing the other components, i.e., rainfall, runoff and losses through evaporation, of the water balance equation. The results of the analysis show that the snow- and glacier-melt runoff contributes about 35% to the annual flow of the Beas River at Pandoh Dam. NIH also carried out a study on estimation of snow and glacier melt runoff in Ganga and Chenab basins using satellite data. Snow and Avalanche Study Establishment (SASE), Chandigarh carried out snow melt run-off prediction based on point energy balance method for sub-catchments of Beas Basin.

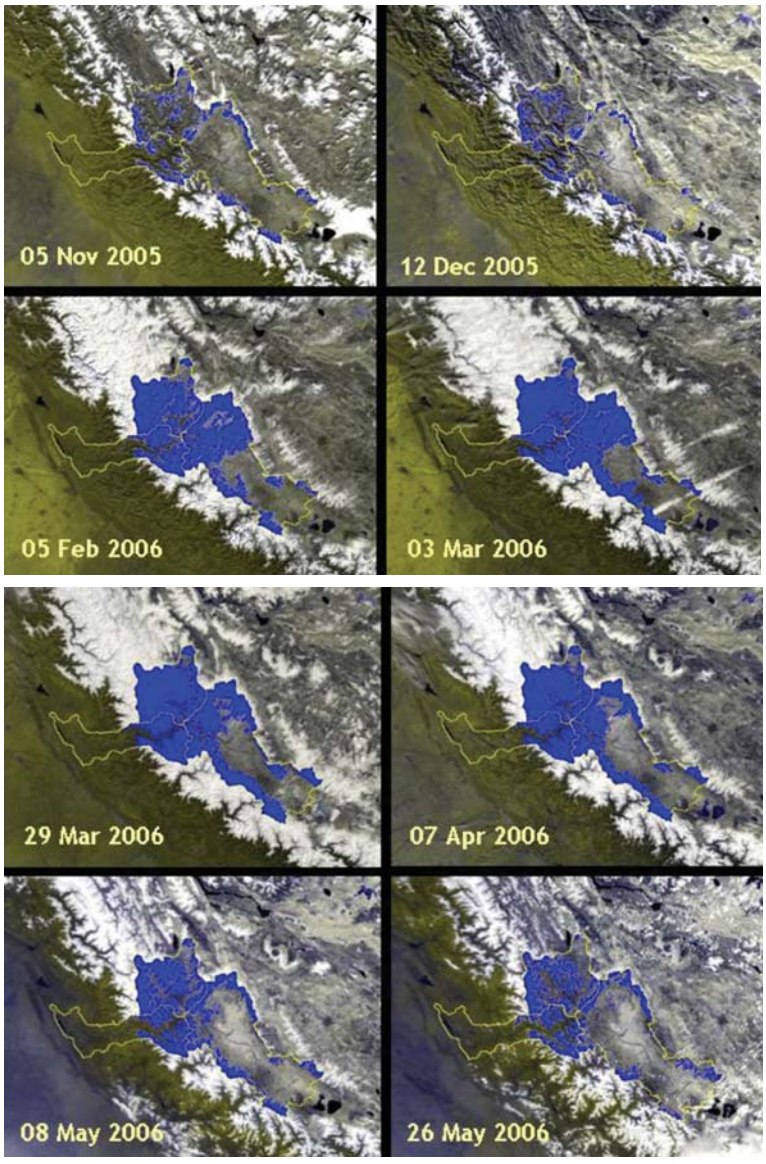

Figure 6.1: Snow cover accumulation and depletion in Sutlej basin

Inventory of glaciers, Glacial Mass Balance, and Glacial retreat

Retreat of glaciers is the cause of great concern for the perennially fed Himalayan river system. The Ganges, the Brahmaputra and the Indus rivers rely on the glacier resources like snow and ice from the Himalayas. The long-term database on glaciers and melting patterns of snow in the above river basins is expected to provide evidence of climate change impacts and consequent effect on river discharges. Glacier lakes can also result into outburst leading flooding which may cause disaster in the down stream. Therefore, monitoring their formation, status and changes is of utmost importance to safeguard down stream utilities. Satellite data forms the only source to map and inventory these natural entities as they lie in most inaccessible regions. Remote sensing images provide ample information on the status of the glaciers and dynamic changes over time. The glacier lakes are easily identifiable on multi-spectral satellite data and their spatial extent can also be measured with reasonable accuracy. Satellite data of medium resolution (24-30 m) and fine resolution (6 m) is found suitable to map these frozen entities.

Many studies have demonstrated the capabilities of satellite data for identification, mapping of glacial lakes. Inventory of glacial lakes was carried out in Dhauliganga basin, Sutluj basin up to Nathpa dam using LISS-III data shown in figure 6.2. Glacial Lakes/ water bodies greater than 2 hectares in area were identified and monitoring was done in the case of glacial lakes/water bodies which are greater than 10 hectares in area during the monsoon

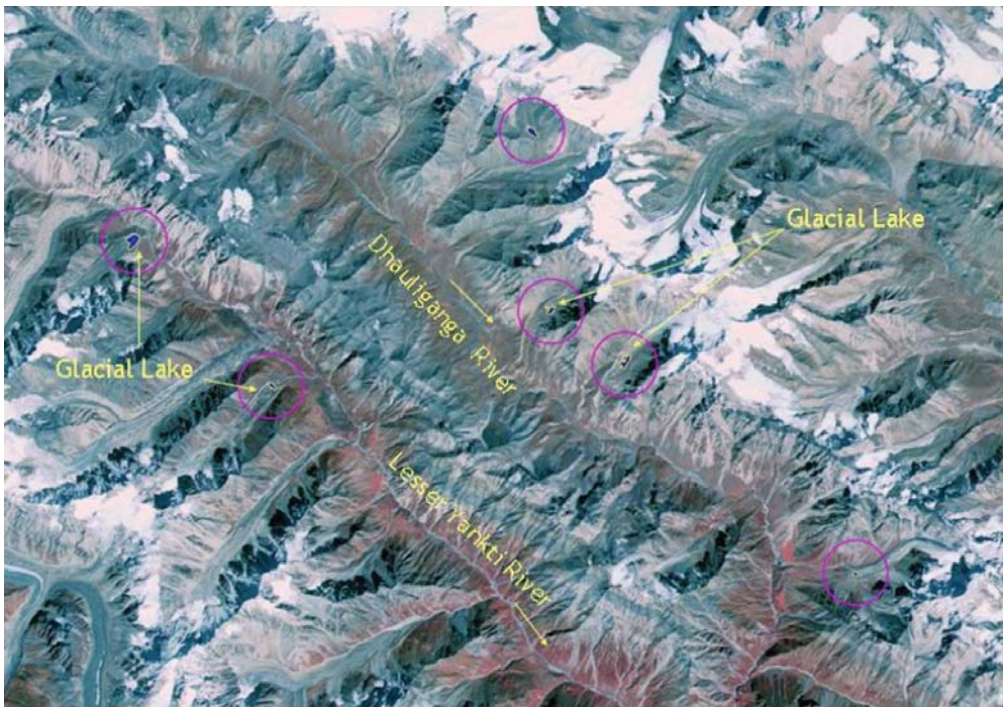

Figure 6.2: Glacial lake identification on satellite data

period. Similar effort was also done in Mangadechu basin. A major project has been launched by MOEF and DOS to study the Snow and Glaciers in the country. Glacial inventory of entire Himalayas was carried out on 1:50,000 scale and snow cover monitoring on 1:250,000 scale for every 10 days. Efforts are on to use these databases for glacier retreat & mass balance studies and for development of Himalayan Snow and Glacial information System in the country. Survey of India taken up inventory of major Glaciers in Indian Himalayas supported by the Department of Science and Technology (DST) on 1:1 Million scale.

A collaborative project between SAC, Ahmedabad and SASE, Chandigarh was executed for snow and glacier investigations and snow-pack characterization. A technique was developed to monitor seasonal snow cover using WiFS data, Weekly on-going charts were supplied to commanding officers in near real time.

Space Application Centre, Ahmedabad and Himachal Pradesh Remote Sensing Cell and Government college, Dharamsala carried out studies on change in glacier area and glacial retreat of 466 glaciers in the Chenab, the Parbati and the Baspa basins of Himalayas using data from the Indian Remote Sensing satellite and field expeditions and comparing them with the 1962 topographic surveys by the Survey of India. The study has shown an overall 21 per cent reduction in the glacier surface area. The process of deglaciation also led to the fragmentation of the larger glaciers. The mean area of glacial extent also declined from 1 sq km to 0.32 sq. km. during 1962-2004. In addition number of glaciers has increased between 1962 and 2001 due to fragmentation due to the detachment of tributary glaciers from main glaciers as a result of glacier retreat. Dokriani glacier in Garhwal Himalayan was studied in detail over the last ten years as part of Himalayan Glaciology Programme of the Department of Science and Technology (DST). Remote-sensing, radar technology and other geophysical methods are being used in the studies.

Snow Avalanches

Snow and Avalanche Study Establishment used satellite data for avalanche hazard zonation in parts of J&K, Uttaranchal and HP. Under avalanche mapping, a number of highways and lateral road axes in J&K, HP and Uttaranchal have been studied for identification and registration of snow avalanche paths, snow drift deposition and ice formation sites; frequency and severity of avalanche activity; and the extent of highway affected. Avalanche atlas was published comprising terrain data, frequency of occurrence of avalanches, magnitude of damage, proposed control measures etc.

6.3.2. Surface Water Mapping & Monitoring

Temporal fluctuations in water resources occur in different seasons of the year, with great variations in water spread area of water bodies during monsoon to summer. Capturing these variations and systematic inventorying on regular basis is operationally difficult task through conventional techniques. However, with the availability of satellite data at multiple spatial resolutions and at regular time intervals, surface water bodies can be mapped and monitored in terms of their occurrence and spatial extent. Generation of such information has many field level applications and provides continuous audit of surface water resources over space and time.

Surface Water Bodies Mapping

The typical spectral response of water facilitates its accurate identification and delineation on remotely sensed images. The time series data provides a record of changes in these storages.

The use of multi-spectral images in mapping and inventorying surface water bodies was demonstrated through many early RS studies (Thiruvengadachari, 1978; Sharma *et al.,* 1989). Water bodies were mapped up to 0.9 ha surface area in Jodhpur district, Rajasthan state using Landsat TM images which were other wise indistinguishable by Landsat Multispectral Scanner (MSS) due to the latter's poor spatial resolution. The Landsat TM data facilitated reliable and reasonable accuracy of ±10%. The comparison with Survey of India topographical maps of the year 1958 revealed reductions in the water surface and drainage basin areas up to 1.8 to 2.4 and 6.0 to 8.0 times, respectively, over a period of 28 years (1958-1986) due to the biotic interference like cultivation and urbanization resulting in desertification in the large adjoining areas.

NRSC initiated a major effort in mapping surface water bodies at national level through development of automatic feature extraction techniques using multi-spectral data from multi-date IRS LISS III/AWiFS data sets.

Wetlands Mapping

Vegetation laden swamps and wet lands form important constituents' of natural ecosystems. Both reflective and thermal infrared images are extensively used to map and monitor these water bodies. As part of inland wetland mapping by ISRO-RRSC's, integrated land use, turbidity and aquatic vegetation maps were generated using multi-season IRS LISS III data. Wetland statistics were generated for all the 65 districts in Gujarat, Bihar, J&K, MP, Rajasthan, UP, Karnataka, Tamil Nadu and AP. Field data was integrated for prioritization of wetlands towards conservation planning as part of MoEF/UNDP sponsored project.

6.3.3. Runoff and Hydrologic Modeling

The status of water availability, particularly spatial and temporal pattern at the basin level is essential for regional planning and decision making on water management. Runoff is an indication of availability of water. Thus in situ measurement of runoff is useful, however in most cases such measurements are not possible at the desired time and location as conventional techniques of runoff measurement are expensive, time-consuming and difficult. Therefore, rainfall–runoff models are commonly used for computing runoff.

Rainfall-runoff modeling has many applications:

- Basin level water resources assessment
- Flood wave run simulation
- Flood protection design to support down stream rescue and management
- Reservoir storage management
- Hydrologic balance computation
- Climate change modelling

Basic components of rainfall-runoff modeling are:

- Precipitation – (point, spatial extension)
- Runoff components – (Interception, evapotranspiration, accumulation in depressions, infiltration, percolation)
- Runoff concentration
- Channel flow

Runoff, the quantity of water volume flowing through a hydrological basin/river cross section cannot be directly measured by remote sensing techniques. However, there are two general areas where remote sensing can be used in hydrologic and runoff modeling:

- Determine watershed geometry, drainage network, and other map-type information for distributed hydrologic models and for empirical flood peak, annual runoff or low flow equations; and
- Provide input data such as soil moisture, delineated land use classes that are used to define runoff coefficients.

Topography is also basic need for any hydrologic analysis and modeling. Remote sensing can provide quantitative topographic information of suitable spatial resolution to be extremely valuable for model inputs. For example, stereo Cartosat-1 imagery can be used to develop a Digital Elevation Model (DEM) with 30 m horizontal resolution and vertical resolution of 10 m. Interferometric SAR is also capable of providing digital elevations and terrain models.

Another major input for rainfall–runoff modelling is land-cover. Satellite remote sensing is the best source of mapping this information. Using multi-date remote sensing data, both spatial and temporal patterns of the land-cover can be derived, which can be used to generate the spatio-temporal pattern of derived parameters.

Many applications of remote sensing data in hydrologic models were developed to quantify surface runoff. Most of the work on adapting remote sensing to hydrologic modeling has involved the Soil Conservation Service (SCS) runoff curve number model (US Department of Agriculture, 1972) for which remote sensing data are used as a substitute for land cover maps obtained by conventional means. Other types of runoff models that are not based only on land use are also developed (Papadaakis *et al.*, 1993).

Satellite remote sensing data can be incorporated into the system in a variety of ways: as a measure of land use and impervious surfaces, for providing initial conditions for flood forecasting, and for monitoring flooded areas (Neumann *et al.*, 1990). The GIS allows for the combining of other spatial data forms such as topography, soils maps as hydrologic variables such as rainfall distributions or soil moisture (Kouwen *et al.*, 1993). The Soil and Water Assessment Tool (SWAT) model (Arnold and Fohrer, 2005) has proven to be an effective tool for assessing water resource and non-point source pollution problems for a wide range of scales and environmental conditions across the globe.

Zade *et al.*, (2005) estimated runoff for all major basins of India using satellite data using SCS approach. The study provided analysis of intra and inter-basin runoff potential for major basins of India. The runoff in the Brahmaputra, Narmada and Mahanadi basins responded well to rainfall, i.e., high runoff coefficient, whereas low runoff coefficient was found in the Cauvery basin.

The amount and intensity of runoff on catchment scale are strongly determined by the presence of impervious land-cover types, which are the predominant cover types in urbanized areas. Chormanski *et al.*, (2008) examined the impact of different methods for estimating impervious surface cover on the prediction of peak discharges, as determined by a fully distributed rainfall-runoff model (WetSpa). The study showed that detailed information on the spatial distribution of impervious surfaces, as obtained from remotely sensed data, produces substantially different estimates of peak discharges than traditional approaches based on expert judgment of average imperviousness for different types of urban land use.

SCS Method

The model developed by the United States Department of Agriculture (USDA) Soil Conservation Society (SCS) known as curve number (CN) is popular among all rainfall–runoff models because of its simple mathematical relationships and low data requirement. The CN represents the watershed coefficient, which is the combined hydrological effect of soil, land use, agricultural land treatment class, hydrological condition and antecedent soil moisture condition (AMC). Generally, the model is well suited for small watersheds of less than 4000 ha, as it requires details of soil physical properties, land use, conservation treatment and vegetation condition. The CN method is based on the assumption of proportionality between retention and runoff. The mathematical relation for runoff is given by:

$$Q = \frac{(P - I_a)^2}{(P - I_a + S)} \quad (1)$$

where Q is the actual runoff, P the precipitation, I_a the initial abstraction which includes interception, surface storage and infiltration into soil and S the potential retention. Since I_a = 0.2, S (based on the analysis performed by SCS for the development of the rainfall–runoff relation for average condition, i.e. AMC II), AMC is determined by the sum of the last five consecutive days' rainfall. In addition, the, following relationships between initial abstraction and potential maximum retention have been developed for Indian condition.

Equation (1) can be written as:

$$Q = \frac{(P - 0.2S)^2}{(P + 0.8S)} \text{ for black soil} \quad (2)$$

$$Q = \frac{(P - 0.3S)^2}{(P + 0.7S)} \text{ for other soil groups} \quad (3)$$

where, S is determined by CN, through the following relation:

$$S = \frac{25400}{CN} - 254$$

The first step in the model was to derive a hydrological soil grouping (HSG), which is a qualitative term given by the SCS. It is categorized into A (lowest runoff potential), B (moderately low runoff), C (moderately high runoff), and D (highest runoff) using in- formation on soil texture. Ideally, a hydrological soil grouping was to be derived on the basis soil type, infiltration, soil depth and permeability. Since most of these parameters are soil texture-dependent, HSG was done on the basis of soil textural map and tentative map of hydrological soil groups. The raster theme of HSG was integrated with the land-cover theme to generate the hydrological soil cover complex (HSCC). This HSCC map was used for assigning the CN (CN ranges from 0 to 100, i.e., no runoff to runoff equating rainfall).

6.3.4. Water Balance Studies

The water balance is useful for predicting some of human impacts on the hydrologic cycle. Many models are available for computing runoff or water balance in a watershed. SCS curve number method, Soil Moisture Accounting Model, Green Ampt Model, Thornthwaite and Mather model, etc., are very popular models used for computing runoff. All these models take the information derived from the remote sensing data. Thornthwaite and Mather model is widely used for computing water balance. It is a book-keeping method, very useful for computing runoff at preliminary stage of planning of any water resources project. It can be applied for big size watersheds also. It follows the concept of energy budget.

The water balance of a small drainage basin underlain by impervious rock at depth can be represented by the equation:

P = I+AET+OF+DSM+DGWS+GWR

Where, P is precipitation, I- Interception, AET- Actual evapotranspiration, OF- Overland flow, DSM- Change in soil moisture, DGWS – Change in ground water storage, GWD- Ground water runoff.

Here, the symbols, expressed as equivalent depth of water for specified time interval, precipitation, interception, evopotranspiration, overland flow, change of soil moisture storage, change of ground water storage, and ground water runoff (figure 6.3).

To compute the climatic water balance, it is necessary to obtain data of water supply (precipitation) and climatic water need potential evapotranspiration (PET). For the computation of water balance, potential evaporation data can be calculated by using either evaporation data or empirical equation or by analytical methods.

PET is a primarily function of climatic conditions (energy from the sun) and is not a function of type of vegetation, type of soil, soil moisture content, or land management practices (Mather, 1978). PET can be calculated using different methods like Penman-Monteith method, Thornthwaite method etc.

The water storage capacity (SM), which depends upon the soil texture type, rooting depth of vegetation and land use, in the root zone of the soil must be determined. Then, from the readily available tables or graphs or by using the empirical formula for dry season months we can find how much water will be retained in the soil after various amounts of accumulated potential water loss. For the case of wet seasons soil moisture values can be determined by adding the excess precipitation to the soil moisture value of the previous month until the total storage again reaches the water-holding capacity of the soil.

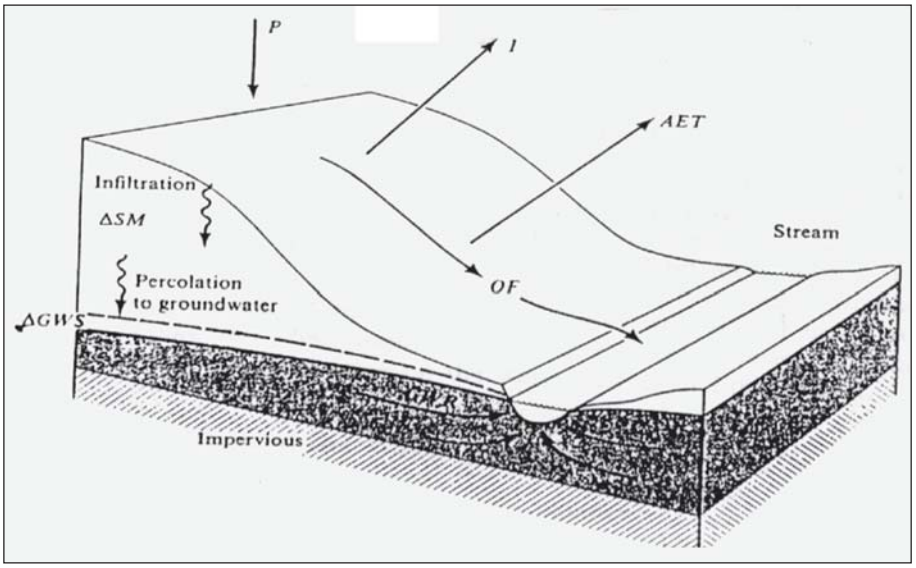

Figure 6.3: Componants of water balance on a hill or a small cachment

The ability of soil to retain water depends upon the amount of silt and clay present; higher the

amount, the greater is the soil moisture content. The change in moisture content (ΔSM) that is equal to the difference of soil moisture in a month and its proceeding month should be calculated. Actual evapotranspiration (AET) represents the actual transfer of moisture from the soil and vegetation to the atmosphere.

Ottle *et al.*, [1989] have shown how satellite derived surface temperatures can be used to estimate ET and soil moisture in a model that has been modified to use these data. Duchon *et al.*, [1992] have used Landsat TM satellite data to identify uniform land cover areas and GOES data for input insolation for a monthly water balance model.

6.4. Water Resources Management

(Irrigated Agriculture, Reservoir Management, Urban Water Supply)

6.4.1. Irrigation Water Management

Investment and development of irrigation infrastructure has been long and continued priority in India. In 1950-1951 the net irrigated area in India was 21 million ha and as a result of sustained efforts, fuelled by Nehru's call to make irrigation works the 'temples of modern India', this expanded to close to 100 million ha by 2006. The role of irrigation in India in expanding crop production, reducing output instability and providing protection against periodic drought has been a major factor in the substantial achievement of Indian agriculture over the past four decades. Programs such as Bharat Nirman/AIBP accelerate the irrigation potential creation and efforts are on for improving the performance of existing irrigation systems to bridge the gap between potential created and utilized and to improve overall water use efficiency/productivity.

With the growing competition for fresh water resources from other sectors and increasing uncertainty of water quantities due to impending climate change, irrigation water management is faced with increasing needs for more reliable, consistent and timely water resources related data flow. Data collection in irrigation systems is a well established practice, although the convertibility between available data and readily usable information is little. The conventional data acquisition is oriented more towards archival than operational usage and in-situ observations are generally characterized by inadequacy and non-reliability. To achieve maximum water use efficiency, real time information on various aspects, which control and influence the supply & utilization regimes are to be obtained.

Advances in communications and remote sensing satellites provided many new opportunities to generate and transmit information on weather, water and agriculture. Use of satellite remote sensing data for IWM has been demonstrated through many studies addressing: base line inventory, performance assessment & monitoring, providing in-season inputs, monitoring physical progress of potential creation, generating inputs for feasibility assessment of new projects, environmental impacts such as water logging & soil salinity, reservoir management, etc. This would support the field departments to cope up with water scarcity and augmenting the water use efficiency through integration of geo-spatial information with their conventional practices.

6.4.1.1. Inventory of Irrigated Agriculture

Mapping of cropping pattern and crop condition assessment using remote sensing data was carried out as early as during early 1990s after successful launch of first Indian Remote Sensing (IRS) satellite IRS-1A in 1988. Mapping of crops in irrigation command area was carried out through visual interpretation (Rao and Mohankumar, 1994) of image prints to analysis of multi-spectral optical remote sensing data using various image processing algorithms and also using microwave radar data (Saindranath *et al.*, 2000, Chakraborty *et al.*, 1997). Baseline information on cropping pattern was generated using remote sensing from basin level (Biggs *et al.*, 2006) to water course level. Multi-temporal optical (Sesha Sai and Rao, 2008) and microwave data was used to identify multiple crops in irrigated agricultural system. Murthy *et al.*, (2003) used advanced classifiers like ANN back-propagation technique for classification of irrigated crops.

Various satellite derived indices have been used to evaluate crop condition. Some of the indices like NDVI were found to be directly related to crop yield and thus were used for estimation of crop yield. Crop yield has been estimated for cereal crops like paddy (Murthy *et al.*, 1996) and wheat (Patel *et al.*, 2006). NDVI was also used for ground sampling of crop cutting experiment in irrigation system (Murthy *et al.*,1996).

NRSC has also executed various command area projects under National Water Management Project (NWMP) and Water Resources Consolidation Project (WRCP). In addition to the above, NRSC has also executed several

projects (28) for various State Irrigation and Command Area Departments. Inventory and monitoring of irrigated agriculture in Nagarjuna Sagar Project & Krishna Delta is shown in figure 6.4.

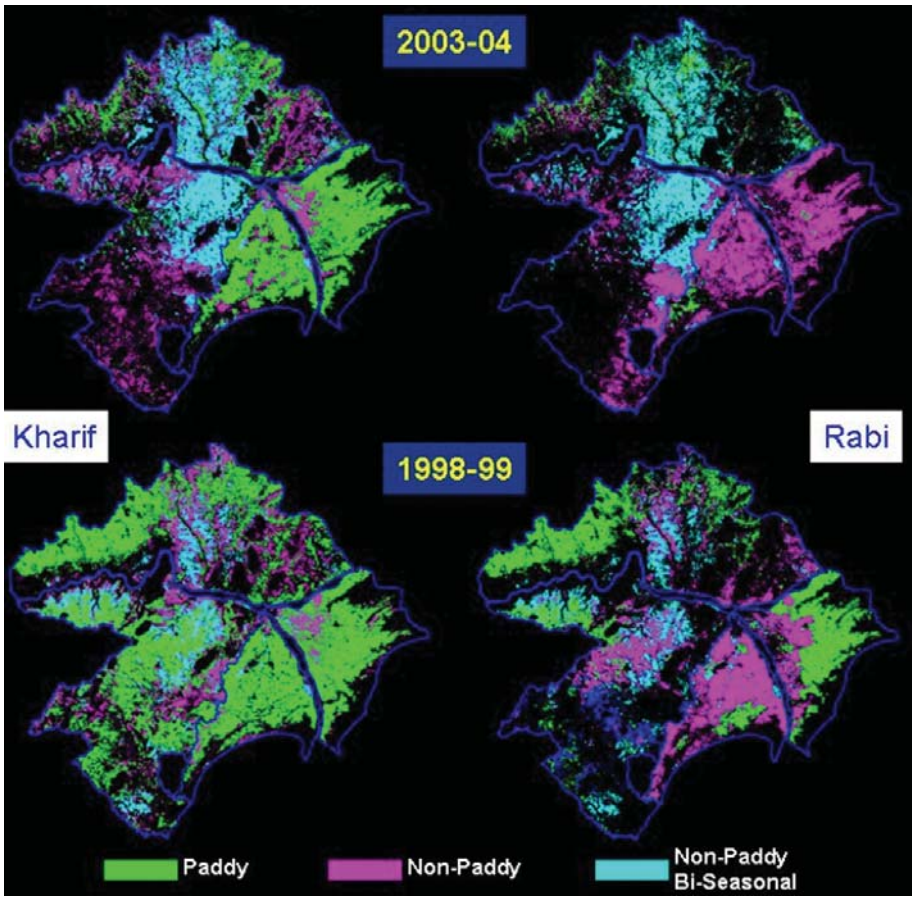

Figure 6.4: Inventory and monitoring of irrigated agriculture in Nagarjuna Sagar Project & Krishna Delta

6.4.1.2. Performance Assessment

Many Indian irrigation systems perform at a very low level and number of National efforts has been initiated to improve the performance of existing irrigation schemes. In most of the existing irrigation schemes there is a serious lack of reliable and adequate information on system performance and one of the extraordinary characteristics of irrigation projects is that a large number of projects generated revenue in far excess of the largest business corporate, there is virtually no information on the extent of which these projects are achieving the designed per-formance objectives. Before taking up any improvement measures, it is essential to evaluate the present per-formance and identify the areas/pockets whose performance is below par. Such exercise would help the irrigation man-agers to prioritize the improvement measures. Although, information of irrigation system performance can be obtained by conventional techniques, they are often subjective, inconsistent and are mostly point based measurements and extended spatially. While conventional procedures are capable of providing system performance at a gross command area level, they are in general time consuming and cost-intensive. Satellite Remote Sensing (SRS) has

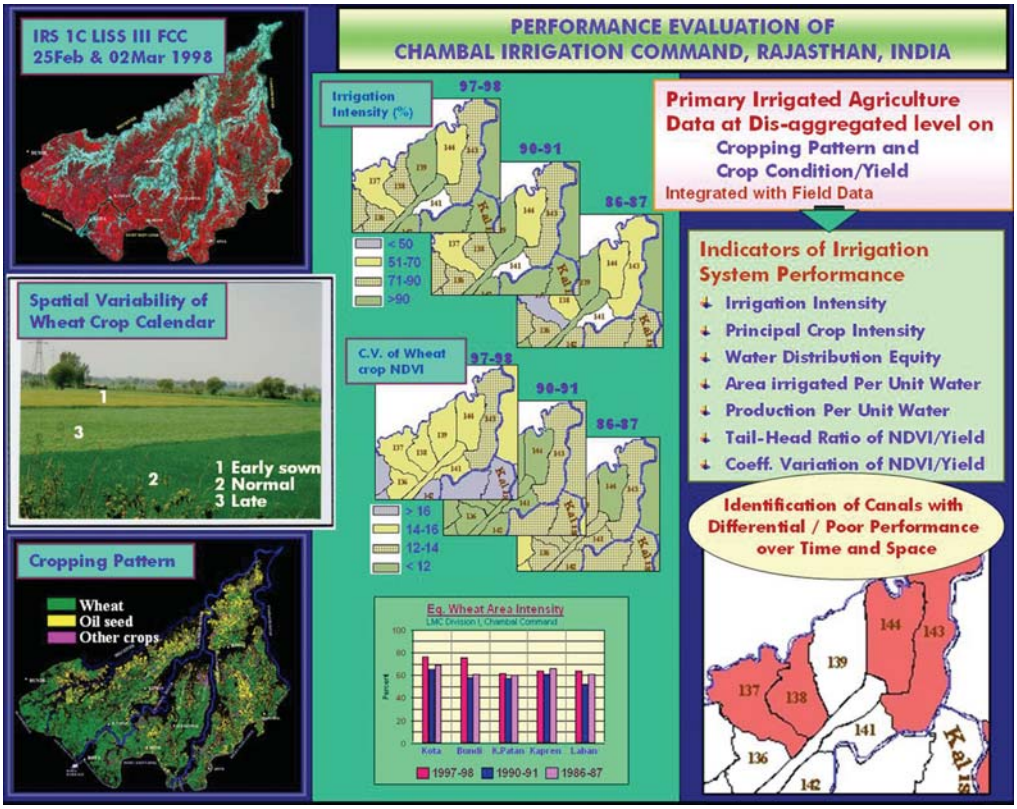

Figure 6.5: Performance evaluation and problem pockets identification

established itself as an effective and accurate tool for providing essential elements for characterizing the irrigation system performance. The accuracy of SRS derived information is significantly higher than the conventional methods. Another advantage of SRS data is to create time series- as much as 15-20 years- for monitoring the changes in time. It is being operationally used to assess the performance of irrigation systems, bench marking, identifying low performing pockets, effectiveness and sustainability of improvement schemes, etc.

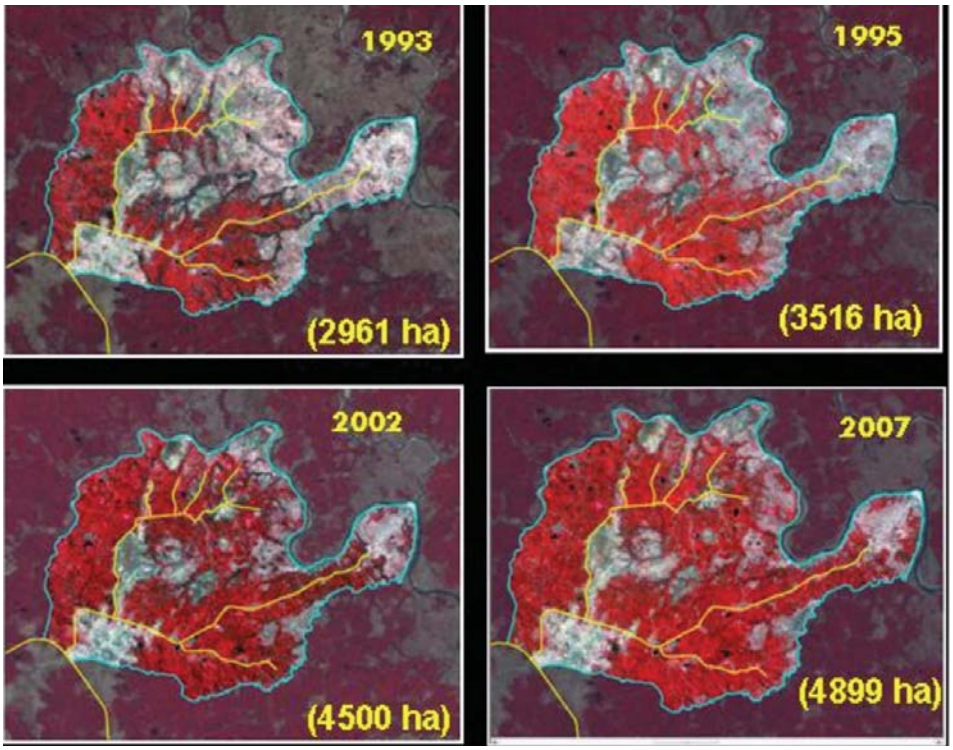

Figure 6.6: Impact and sustenance monitoring of intervention schemes

Performance evaluation of an irrigation system requires the spatial information on crop intensity, crop type, crop calendar and crop condition/productivity etc. Multi-spectral satellite data is found useful to derive primary information on cropping pattern and crop condition, which can be used to quantify the agricultural performance of the system. This spatial information can be integrated with relevant field data to generate various performance indicators to gauge the performance and compare with targeted, in order to identify and rank the pockets of poor performance. Some of the performance indicators generated from satellite data are:

- Crop Intensity
- Equivalent crop area intensity
- Principal crop intensity
- Proportionate Crop Intensity
- Crop Condition
- Coefficient of variation in crop condition
- Tail-Head ratio of cropping intensity
- Tail-Head ratio of crop condition
- Sustainability in crop intensity

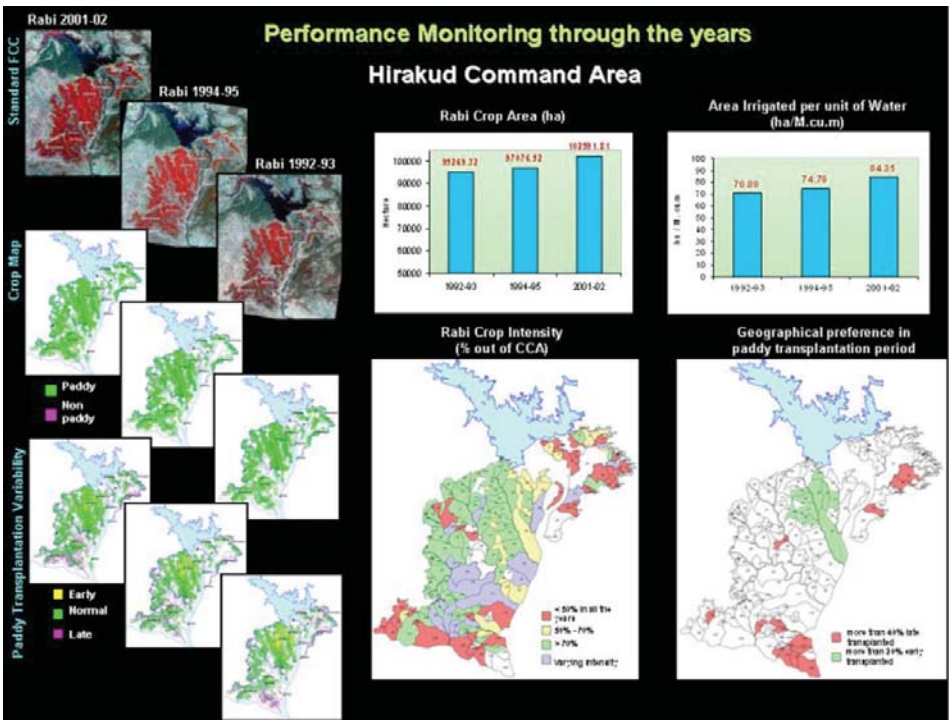

Figure 6.7: Performance monitoring through the years

Satellite data based monitoring and evaluation of irrigation command areas was initiated by NRSC in 1991-92. Initially base line inventory of irrigated crop areas and their extent was carried out at distributary group in Bhadra project command area in Karnataka state. Remote sensing based performance indicators were used for performance assessment of various irrigation systems in the country. Performance evaluation and problem

pockets identification is shown in Figure 6.5. Bastiaanssen (1998) has listed the performance indicators derived from RS algorithms supplemented by ground data. Ray et al (2002) used RS data has to compute three indices namely, adequacy (AI), equity (EI) and water use efficiency (WUE) for the evaluation of performance of distributaries in an irrigation system. Panigrahy et al (2005) attempted to derive crop indices like Multiple Cropping Index (MCI), Area Diversity Index (ADI) and Cultivated Land Utilization Index (CLUI) using satellite derived parameters such as cropping pattern, crop rotation, and crop calendar, crop type, acreage, rotation and crop duration. NRSC executed, CAD, MOWR selected 13 irrigation commands on a pilot basis to evaluate the performance of these irrigation schemes using satellite remote sensing techniques (1997-98 to 1998-99). NRSC (March, 2005) successfully organized 5 regional workshops as a part of this study. In figure 6.6, impact and sustenance monitoring of intervention schemes is shown. Per-formance monitoring of irrigation command area all through the years is shown in figure 6.7.

6.4.1.3. In-Season Inputs for Irrigation Water Distribution

To maintain control over the process of delivering water, real time information is to be obtained on various aspects, which control and influence the supply & utilization regimes. Intentional water requirements does not always meet the actual use due to changes in the field environment such as weather conditions, farm management practices, water distribution mechanism, etc. In the event of mismatch between planned and actual water requirements, distribution needs changes considering the actual demand. Irrigation managers are constrained by the lack of real time information on - to what extent irrigated agriculture is confirming with their plans and the extent of deviations, if any.

Multiple satellite observations, at high time frequency, during the irrigation season can capture the temporal changes that are taking place in an irrigated command area. AWiFS on board IRS-P6 (Resourcesat-1), can acquire images at 5-day interval and its ~56 m resolution coupled with multi-spectral information were found very useful to capture and monitor the periodical changes right up to tertiary canal level. These data sets are capable of providing near-real-time information on:

- Extent of crop area
- Progression of crop acreage
- Cropping pattern
- Variations in crop calendar
- Crop condition variations across time and space

Such information, when derived and provided during supply time, would equip the managers to make real-time decisions and to sensitize the water release pattern in accordance with demand variability and its sensitivity. Spatial and temporal variations in progression of irrigated agriculture is shown in figure 6.8.

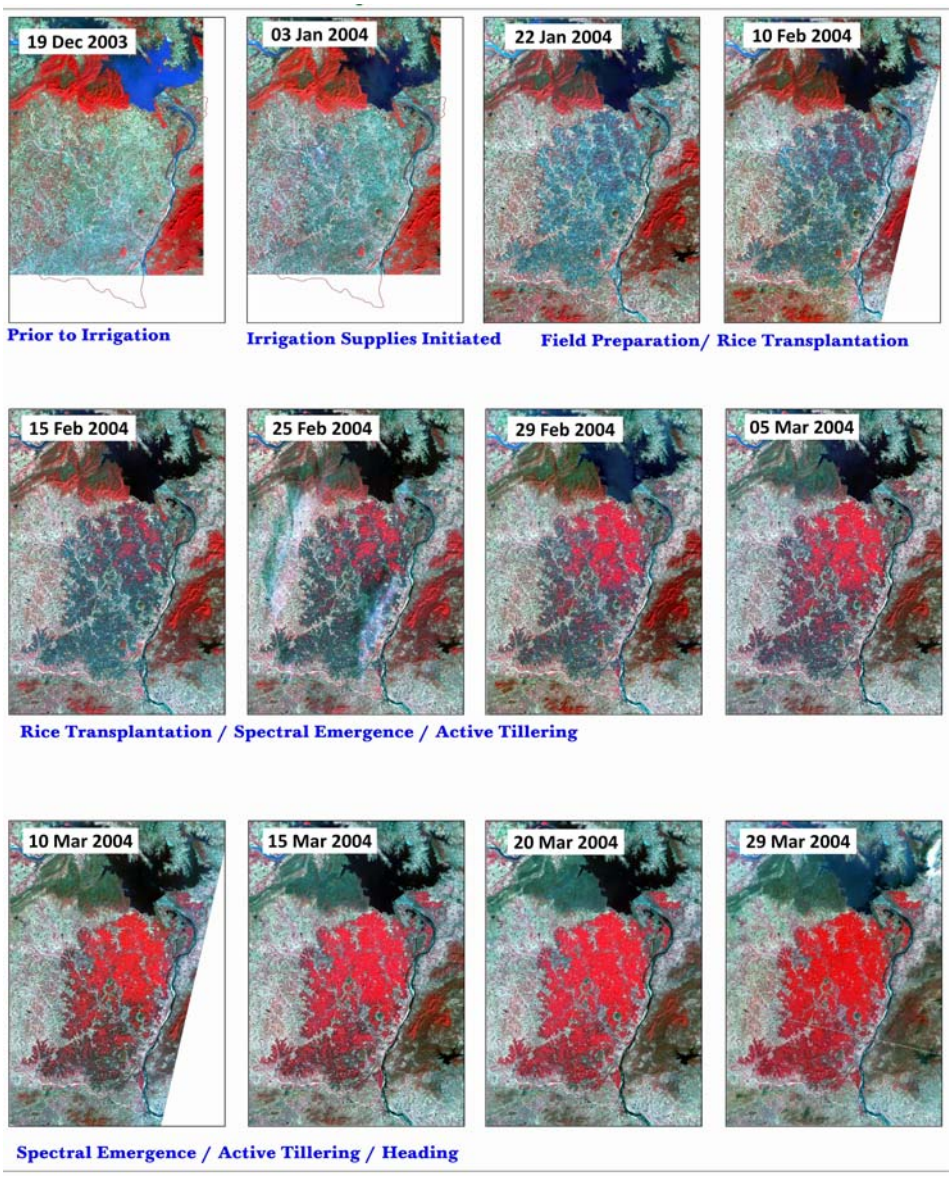

Figure 6.8: Spatial and temporal variations in progression of irrigated agriculture

6.4.1.4. Salinity and Waterlogged Area Mapping & Monitoring

Waterlogging and subsequent salinization and/alkalization are the major land degradation processes operating upon in the irrigation commands of the semiarid regions. The significant occurrence of salt affected soils lies in the arid and semiarid regions reducing considerably (7–8%) the productive capacity of the land surface in the world. Due to improper management of soil and water resources in the command areas, the problems of salinity/ alkalinity and water logging are reported to be on the increase. Information on the nature, extent, spatial distribution and temporal behaviour of areas under water logging and salinity/alkalinity is essential for proper management of irrigated lands.

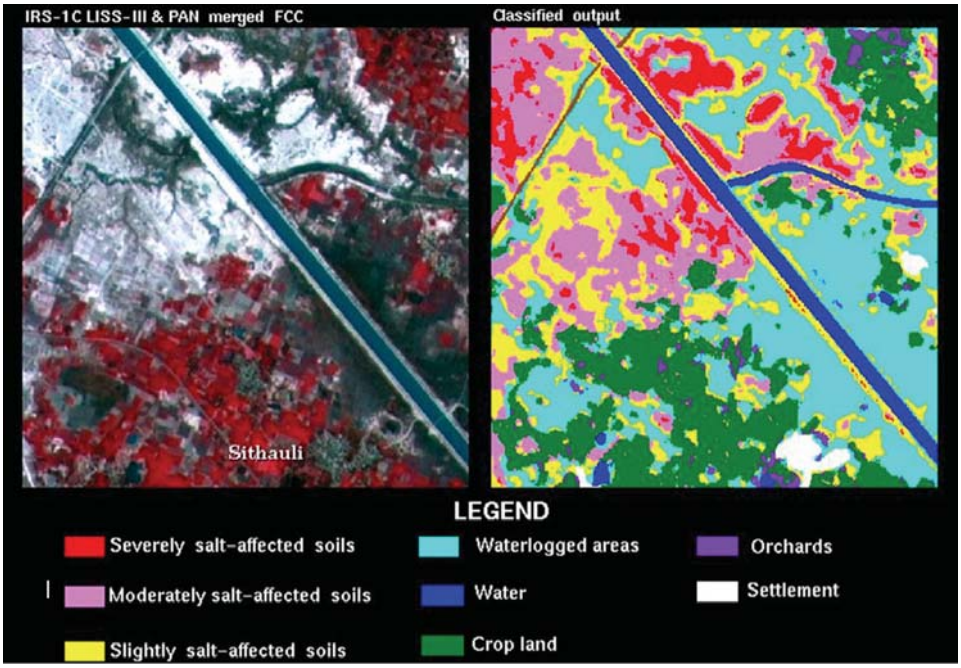

Figure 6.9: Mapping of salt affected soils and water logged areas

Until recently, information on the nature, extent, magnitude and spatial distribution which is a pre-requisite for amelioration and management of salt affected soils, has been generated through traditional soil surveys which are tedious and time-consuming apart from being cost-prohibitive. Among the new technologies developed for soil survey, remotely sensed data from space borne sensors like Landsat-MSS, TM, IRS-LISS-I/II/III, Resourcesat-1, SPOT MLA/PLA etc., proved to be valuable to map and monitor salt affected soils and water logged areas. Satellite data are being used regularly for mapping of salt affected soils (Singh & Dwivedi, 1989; NRSA, 1995; 1996)

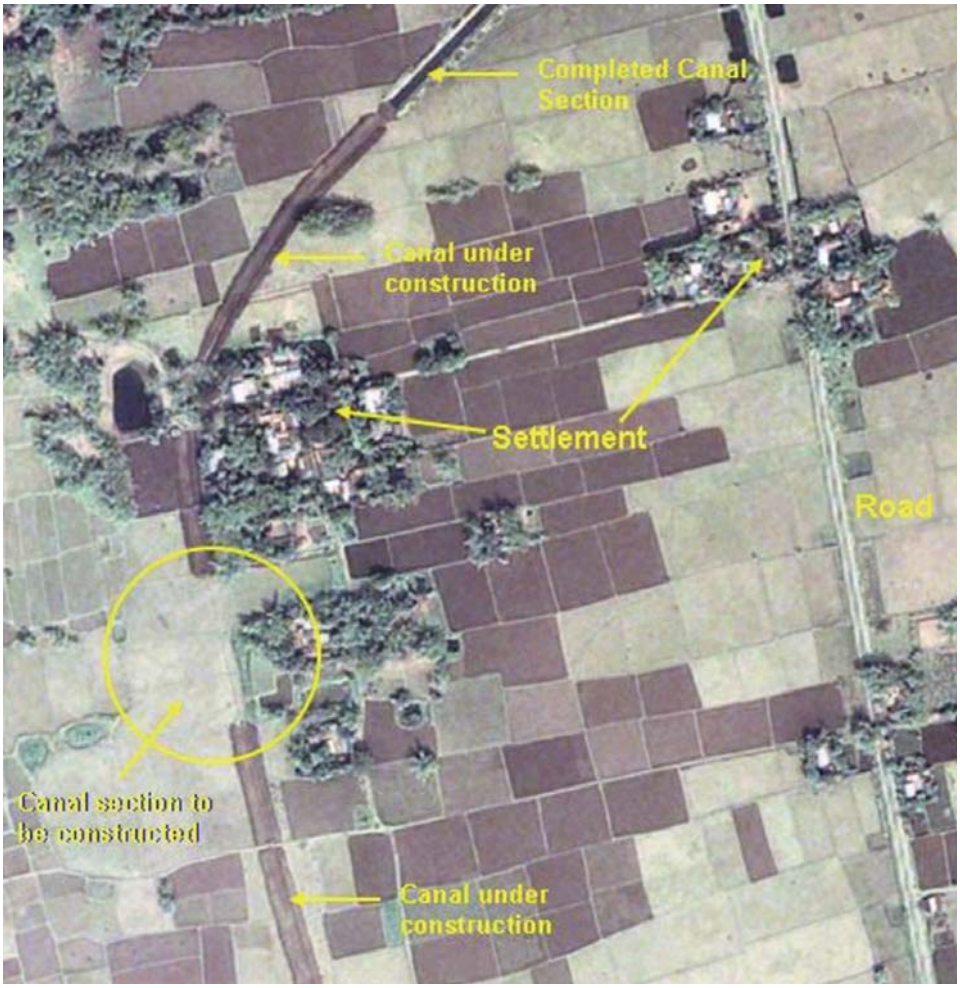

Figure 6.10: Monitoring progress and status of Irrigation network creation

and waterlogged areas (Sharma & Bhargava, 1987; Dwivedi & Deka, 1990). Command Area Development (CAD) programme, the Ministry of Water Resources, Government of India, supported a programme to apply satellite remote sensing techniques to generate distributary-wise information on the status of water logging and salinity/ alkalinity periodically during selected years of operation in selected command areas. The information on nature, extent, and spatial distribution of waterlogged area and salt-affected soils was derived through systematic visual interpretation of standard false colour composite (FCC) prints on 1:50,000 scale.

The National Remote Sensing Centre (Department of Space) Hyderabad, prepared state-wise the salt affected soils map of India on 1:250,000 scale using remote sensing data and ground truth jointly with the Central Soil Salinity Research Institute (ICAR), Karnal , National Bureau of Soil Survey and Land Use Planning (NBSS & LUP), Nagpur. The database contains maps showing physiographic features, distribution and extent of salt affected soils supported by a basemap and a descriptive dataset showing nature and degree of salinity/sodicity. Mandal and Sharma (2006) used GIS to integrate salt affected soil maps for a composite database of the Indo-Gangetic Plain in India and derived information on the extent and distribution of salt affected soils for agro-climatic regional and zonal planning. Satellite derived salt affected and soil and water logged areas is shown in figure 6.9.

6.4.1.5. Monitoring New Irrigation Potential Creation

Ultimate irrigation potential of India is 139.89 M ha and at present only 99.76 M ha is under place. Major National programs such as AIBP are expediting the new irrigation infrastructure creation. High resolution satellite data is assisting the sponsoring institutions to monitor the physical progress and status of the new potential creation. (Figure 6.10).

NRSC at the request of Ministry of water Resources, GOI, monitors the progress of irrigation infrastructure creation and potential creation in AIBP funded projects using high resolution satellite data. The pilot project in Teesta command area, West Bengal state and Upper Krishna project, Karnataka state led to National level activity for 53 projects spread over 18 states. The high resolution satellite data from the Indian satellite sensors (Cartosat-1& Cartosat-2) are extensively used for this activity. The next phase is expected to cover all the remaining projects under AIBP.

6.4.1.6. Satellite data for Evapotranspiration studies

An important step forward in hydrology for water management is the work on the evapotranspiration flux using satellite data. The available amount of water on land (Q) is determined by the amount of rainfall (P) minus the evapotranspiration (ET) (i.e. the water that returns from the land surface to the atmosphere). Thus, in its simplest form, the water balance is P – ET = Q.

Quantifying evapotranspiration in time and space facilitates determination of the amount of water resource in catchments, support characterization of irrigation scheme in terms of actual water usage, water productivity, water distribution efficiency and ground water usage. It is also one of the critical elements for carrying out both long term and short term water balance studies. At present, evapotranspiration from satellite data is confined to regional level assessment, providing basin level water balance appraisal.

Satellite data was used to derive crop-wise monthly crop coefficient data for estimation of crop evapotranspiration. Jonna et al (2007) studied spatial variation in crop surface properties like emissivity and canopy surface temperature (CST) using moderate-resolution imaging spectrometer (MODIS) satellite data and diurnal ground measurements.

6.4.2. Reservoir Management

6.4.2.1. Reservoir Sedimentation

Reservoirs lose their storage capacity due to sedimentation. The analysis of sedimentation data of Indian reservoirs show that the annual siltation rate has been generally 1.5 to 3 times more than the designed rate and the reservoirs are generally losing capacity at the rate of 0.30 to 0.92 per cent annually. The consequence of loss in storage due to sedimentation is precluding the intended usages such as flood protection/moderation, irrigation, hydro-power generation, etc. Sedimentation in reservoirs occurs not only in dead storage but also in live storage region simultaneously, which reduces the useful storage and affects the water utilization pattern of the project. Periodic assessment of sedimentation rates is essential to ascertain the current reservoir live storage capacity for

efficient and productive management of water resources. This information is also necessary to plan for the upstream catchment treatment in order to control the rate of sedimentation. Such assessment would also facilitate characterization of basins/catchments in terms of their siltation rate potential and provide realistic basis for planning new reservoir schemes. Conventionally, assessment of sediment deposition in the reservoir is carried out either by inflow-outflow measurement method or by hydrographic survey. Hydrographic survey method is in practice for quite long time in India and elsewhere.

The reduction in storage volume results from the decrease in water spread area due to sedimentation at different elevations. Therefore, capturing the water spread at various reservoir operating levels would help in estimating the current reservoir storage and a comparison with previous or original storages would provide the loss in storage due to sedimentation. In this context, satellite remote sensing plays a very useful role due to its synoptic and repetitive coverage. Water, by virtue of its typical spectral response characteristics is noticeably manifested on satellite data. Multi-spectral satellite data facilitates distinct separation between water bodies and the surrounding land-use/landcover. The water spread boundary captured by the satellite data provides water spread contour at that particular reservoir water level. By taking a series of satellite data covering various reservoir operating levels, the water spread contours can be derived for the corresponding elevations. Using mathematical formulae, the actual reservoir storage between the observed water levels can be computed. This helps in generating present area-capacity curves and a comparison with previous curves provide the changes in reservoir storage.

Multi-temporal satellite data have been used as an aid to capacity survey of many reservoirs in a cost and time effective manner in India. While this technique helps in revising capacity table between minimum and maximum draw down level observed in satellite data, loss of dead storage capacity can be obtained only through conventional hydrographic surveys. A National action plan of sedimentation survey of 124 reservoirs using remote sensing technology has been taken up in India during the 10th Five Year plan by Ministry of Water Resources.

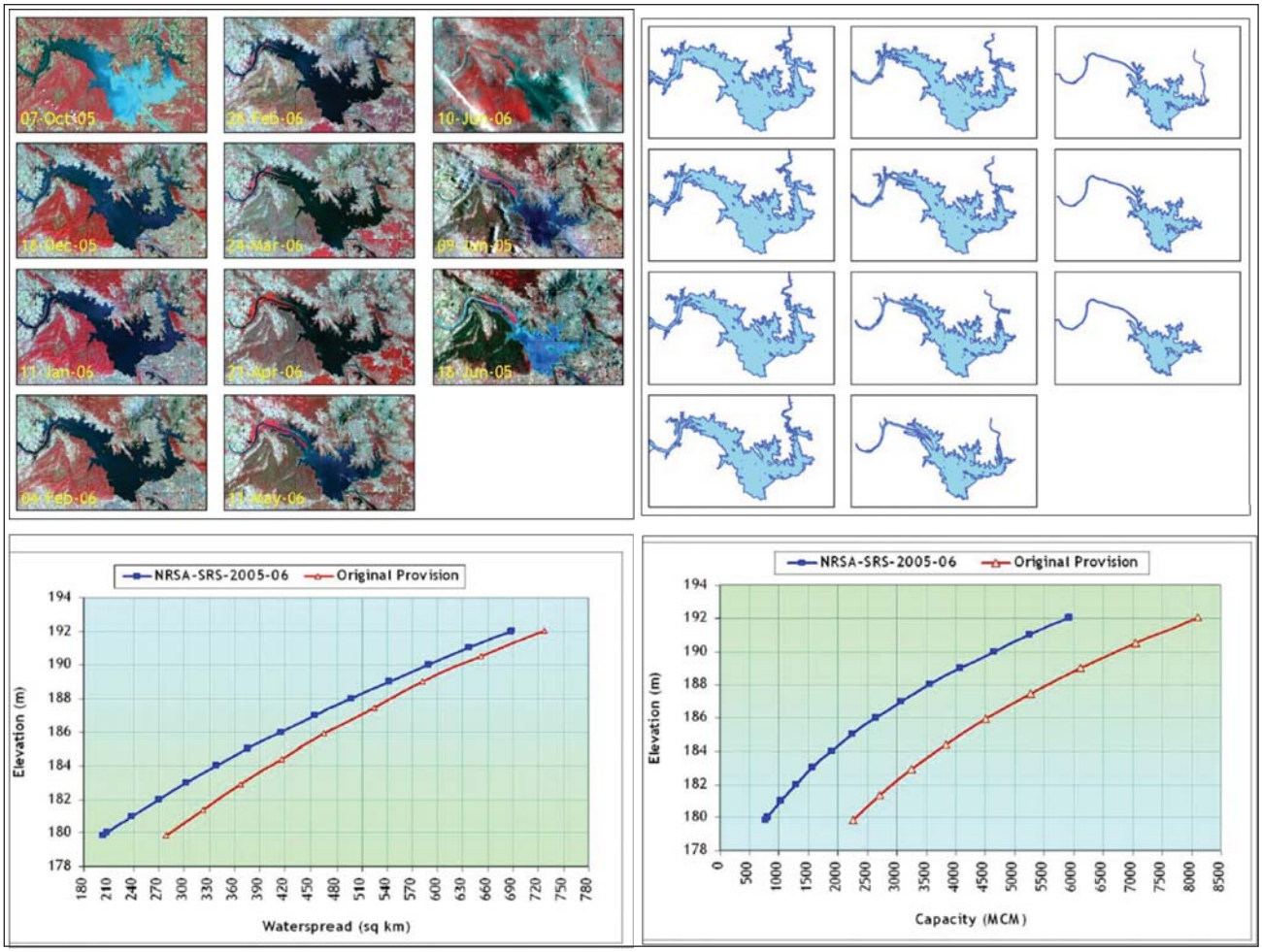

Figure 6.11: Reservoir capacity loss and sedimentation assessment

Reservoir sedimentation surveys of the balance 54 reservoirs of National Action Plan were executed by NRSC/DOS/Others. CWPRS and NRSC have jointly executed two reservoir sedimentation projects viz. Sri Ram Sagar Project reservoir in Andhra Pradesh State (2003-2004) and Ujjani reservoir sedimentation survey project in Maharashtra. NRSC recently carried out satellite data based updation of elevation-area capacity curves and sedimentation assessment of Hirakud reservoir, Orissa state for the year 2005-06, as shown in figure 6.11.

6.4.2.2. Catchment Area Treatment

Storage reservoirs structures are one of the most important infrastructure investments offer essential services: drinking water, irrigation water, flood and torrent control, hydroelectric power, fisheries, wildlife, recreation, and other environmental benefits. The catchment's behaviour and its resource capability especially in regions of soil erosion is one of the major threats to water resources storage and management. Soil erosion and sedimentation reduce the economic life of storage structures through the inflow and deposition of soil particles. In addition, sedimentation results in dramatic environmental impacts on water quality and aquatic habitat. Sustainable management and conservation of such expensive investments and their catchment is crucial for the long-term quality of resource and its utilization. The catchment behaviour is mainly affected by vegetation cover, topographic features, climatic variables, and soil characteristics. The human activities and large-scale developments alter the vegetation cover, impacting upon the behaviour. Topographic features such as ground slope, slope length, and shape affect rill and inter-rill erosion. The climatic variables such as rainfall amount and precipitation intensity, temperature are also important.

Assessing the soil erosion rate is essential for the development of adequate erosion prevention measures for sustainable management of land and water resources. Remote Sensing & Geographic Information System (RS & GIS) technologies are valuable tools in developing models through their advance features of data storage, management, analysis, display and retrieval. While soil erosion models only calculate the amount of soil erosion based on the relationships between various erosion factors, RS and GIS integrated erosion prediction models do not only estimate soil loss but also provide the spatial distributions of the erosion. Especially, generating accurate erosion risk maps in GIS environment is very important to locate the areas with high erosion risks and to develop adequate catchment area treatment plans and strategies. The most common empirical erosion prediction models, integrating with RS and GIS, are Revised Universal Soil Loss Equation (RUSLE). The RUSLE was developed to estimate the annual soil loss per unit area based on erosion factors including soil erodibility, topography, rainfall and vegetation cover. The potential soil erosion risk is calculated as a function of soil erodibility, erosivity, and topography. The vegetation cover data is very important parameter in erosion models since intensity of vegetation cover significantly affects erosion rates. Using medium to high resolution satellite imagery, image classification techniques have been used to generate accurate and reliable land use/cover data and spatial inputs for erosion modelling.

6.5. Watershed Management

(Water harvesting, Sustainable Action plans, Soil erosion)

Watershed is a natural hydrologic unit, considered as the most appropriate basis for sustainable integrated management of the land and water resources. Judicious management and conservation of soil and water resources on watershed basis is perquisite for sustaining the productivity. Characterization and prioritization of watersheds are essential steps in the integrated management of land resources. Watershed characterization involves measurement of related parameters, such as geological, hydrogeological, geomorphological, and hydrological, soil, land cover/land use etc. Remote sensing using aerial and space borne sensors can be effectively used for watershed characterization and assessing watershed priority, evaluating problems, potentials, management requirements and periodic monitoring. Remote sensing data greatly facilitates mapping of forest, vegetation cover, geology and soils over watershed, which would assist in the study of land use, watershed potential, degradation etc. This, along with ground based information, can be used for broad and reconnaissance level interpretations for land capability classes, irrigation suitability classes, potential land uses, responsive water harvesting areas, monitoring the effects of watershed conservation measures, correlation for runoff and sediment yields from different watersheds and monitoring land use changes and land degradation.

Watershed development requires delineation, characterization, prioritization, generation of development plans, monitoring their implementation and impact assessment. An essential component for preparation of watershed

development plans is the database of the natural resources. Generation of such a database by conventional means is tedious, expensive and time consuming. Information on all the natural resources of the watershed namely soils, geology, geomorphology, ground water, land use/ land cover, slope, generated from satellite data are highly efficient. Thus, space borne remote sensing data is playing a crucial role in this effort. Availability of stereo data helps in delineation of a micro-watershed and higher spatial resolution data facilities better characterization of micro-watershed in terms of its resource potential.

6.5.1. Water Harvesting

The problem of water shortage in arid and semi-arid regions is low rainfall and uneven distribution through out the season, which makes rainfed agriculture a risky enterprise. Water harvesting for dry-land agriculture is a traditional water management technology to ease future water scarcity in many arid and semi-arid regions of world. As the appropriate choice of technique depends on the amount of rainfall and its distribution, land topography, soil type and soil depth and local socio-economic factors, these systems tend to be very site specific. The water harvesting methods applied strongly depend on local conditions and include such widely differing practices as bunding, pitting, micro-catchments water harvesting, flood water and ground water harvesting.

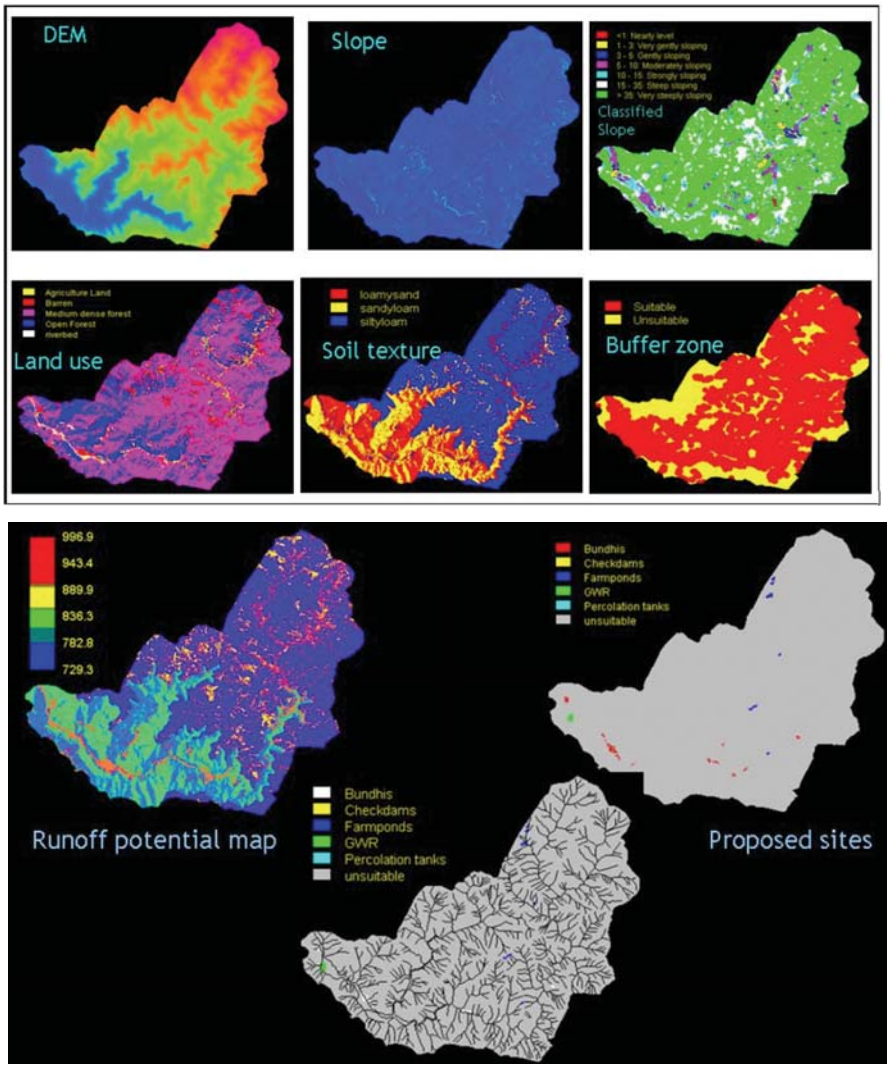

Figure 6.12: Water harvesting structures planning using geo-spatial data

Parameters for identification of suitable rain water harvesting areas are:

- Rainfall
- Land use or vegetation cover
- Topography and terrain profile
- Soil type & soil depth
- Hydrology and water resources
- Socio-economic and infrastructure conditions
- Environmental and ecological impacts

Using the above parameters in a watershed, various water harvesting structures can be identified as shown in figure 6.12.

6.5.2. Sustainable Action Plans

6.5.2.1. Integrated Mission for Sustainable Development (IMSD)

The Department of Space, Govt. of India launched project called 'Integrated Mission for Sustainable Development', for watersheds spread across the country by integrating the information on various natural resources such as land cover, soils, hydro-geo-morphology along with the slope information and provided recommendations for construction of soil and water conservation structures and in situ action plans for selection of appropriate farming systems. This

project covered 174 districts covering 84 M ha was carried out in India. In many of the watersheds, plans are being implemented by the government as well as by the voluntary agencies. Besides evolving locale-specific prescriptions for development, this project succeeded in harmonizing the local wisdom of small and marginal farmers with scientific knowledge and administrative acumen.

6.5.2.2. National Agricultural Technology Project (NATP)

Development of regional scale watershed plans and methodologies for identification of critical areas for prioritized land treatment in the watersheds of rainfed rice, oilseeds, pulses, cotton and nutritious cereals production systems was taken up under NATP.

All the natural resources were mapped in the selected watersheds at 1: 50000 scale using satellite data. A methodology was developed for identification of critical areas. A representative micro watershed of an area of 500 – 1000 ha was selected from the critical areas for preparing natural resource inventory at 1:12,500 scale using high resolution satellite data. Detailed thematic maps of soils, land use / land cover, hydro-geomorphology were prepared using satellite data. The methodology developed was applied to identify critical areas for land treatment in the selected micro watersheds. The critical areas were addressed through specific action plans for development of land and water resource in consultation with local farmers & cooperating centers. All the cooperating centers implemented action items such as construction of water harvesting structures, soil conservation measures, crop improvement techniques, etc., were identified in their respective micro watersheds. The positive impact of the implementation work was also studied using satellite data. This study revealed that by using the advanced technologies like remote sensing and GIS, critical areas could be located in the watersheds in a short time and cost effective manner, thus helping the researcher / planner to focus more on these areas while planning for watershed development following the production system approach.

6.5.2.3. Other Efforts

Monitoring and evaluation of 77 sub-watersheds (854 micro-watersheds) in 5 districts (in 3 Phases) in Karnataka State. With the establishment of monitoring and evaluation (M & E) units in all the 5 study districts, baseline survey was completed in Phase 1 & 2 watersheds and initiated in Phase 3 watersheds; Mid term evaluation for Phase 1 watershed completed; Concurrent monitoring is on in all the watersheds; Various software packages (Sujala-Mahiti, Sukria_Naksha & Sukria_Vivera) have been developed, installed and operationally being used for effective monitoring and evaluation process. The entire M&E approach evolved by ISRO has been acknowledged by World Bank review team as “a model of excellence and should be promoted widely for other projects to follow”. Monitoring and evaluation of Watersheds treated under NWDPRA, a nation wide project has been completed for all the 122 watersheds in 12 States treated under 8th & 9th Five Year Plan. This involved multi-season satellite data analysis for pre and post monitoring towards preparation of land use/ land cover and vegetation dynamics change detection to quantify the impact of watershed development programme.

Following the devastating Earthquake in Kachchh on January 26, 2001, at the initiative of the Prime Minister’s Office (PMO) and at the request from the Government of Gujarat, Indian Space Research Organisation (ISRO) with SAC, Ahmedabad as nodal agency took a project for generation of water and land resources developmental plans for Kachchh district on 1:25,000 scale using IRS IC/ID merged data. The main objective of the study was to prepare land and water resources plans for the district at 1:25,000 scale. The study led to mark the following:

- Demarcation of micro-watersheds
- Prospective sites/zones for ground water exploration, various rain water harvesting structures and artificial recharge
- Suggestion for change in land Use for agriculture resources development, grassland and wasteland development
- Suitable soil and moisture conservation measures

6.5.3. Soil Erosion

Out of 328 million ha of land area, India’s approximately 175 million ha are suffering from intense soil erosion. Soil erosion is a natural process caused by water, wind and ice. In situ soil erosion and its off-site down stream damages cause soil productivity, degradation of landscape, sedimentation of storage schemes, water quality deterioration, etc. Assessing the soil erosion rate is essential for the development of adequate erosion prevention measures for sustainable management of land and water resources. Quantifying and characterizing spatial distribution of soil erosion using conventional measurements is difficult, time consuming and expensive. The sediment load

measurements at outlet of catchments do not provide the spatial distribution. In addition to field measurements, empirical and process based models have been developed to estimate soil erosion.

Soil erosion causes both physical (gullies and rills) and visible (exposure of different soil layers) changes in the surface properties of soils on the landscape. These changes are amenable for measurement through remote sensing sensors. There have been many studies on modeling soil erosion by utilizing RS and GIS technologies. The capabilities of these technologies increase when they are integrated with empirical erosion prediction models. The relationships between various erosion factors, RS and GIS integrated erosion prediction models do not only estimate soil loss but also provide the spatial distributions of the erosion. Especially, generating accurate erosion risk maps in GIS environment is very important to locate the areas with high erosion risks and to develop adequate erosion prevention techniques (Sazbo *et al.*, 1998, Bojie *et al.*, 1995). GIS analysis provides satisfactory results in developing erosion surveys and risk maps by using GIS data layers such as DEM, slope, aspect, and land use. The most common empirical erosion prediction models, integrating with RS and GIS, are Revised Universal Soil Loss Equation (RUSLE), The Water Erosion Prediction Project (WEPP), and COoRdination of INformation on the Environment (CORINE), which can be used for soil erosion risk assessment (Yuksel *et al.*, 2008). The most widely used model is USLE (Universal Soil Loss Equation) and RUSLE (Revised) for estimating sheet and rill erosion, in spite of its limitations. The RUSLE was developed to estimate the annual soil loss per unit area based on erosion factors including soil erodibility, topography, rainfall, and vegetation cover. In the WEPP model, sediment yield and erosion rates were estimated for multiple time periods based on specific erosion factors.

Universal Soil Loss Equation

The Universal Soil Loss Equation (USLE) presented by Wischmeier (1959) in the USA. The USLE can be presented as:

$$A = R * K * L* S* C * P \quad (3)$$

Where,

- A = Average annual soil loss,
- R = Rainfall erosivity index,
- K = Soil erodibility factor,
- L = Slope length factor,
- S = Slope steepness factor,
- C = Cropping management factor, and
- P = Conservation practice factor

This equation can be modeled in GIS environment and factors can be determined by using remote sensing and GIS.

6.6. Water Resources Development

(Inter linking of rivers, Land irrigability, Ground water prospecting)

6.6.1. Interlinking of Rivers

River basins vary with their water resource availability, utilization, adequacy and surplus-ness. Interlinking of rivers was considered to be the most effective way to resolve the regional water deficit, increase food grain production, and mitigate the drought and floods. The execution of Inter Linking of Rivers (ILR) requires a vast database on hydrology and a framework that can use the data to carry out the water budgeting for each river basin in terms of their topography, geology, hydrology and environment. Space based inputs to feasibility, detailed project, implementation strategy; monitoring and evaluation studies help in harmonizing them and lead to an optimal strategies.

Remote sensing inputs for preparation of pre-feasibility report (PFR), final report (FR) and detailed project report (DPR) in the context of Interlinking of Rivers are:

- River Surveys
- Reservoir Capacity Assessment
- Reservoir Sedimentation

- Submergence Area analysis
- Rehabilitation & Reconstruction
- Link Alignment
- Canal Network Planning
- Sites for Online New Storages
- Conveyance System
- Land irrigability assessment
- Ideal Site Selection of Dam
- Land Use/Land Cover analysis
- Cropping System Analysis
- Command Area Survey

For assessing the feasibility of proposed dam sites, maps of the terrain features, at appropriate scales are necessary. This encompasses the inventory/ assessment of land use/ land cover. Space technology plays a very important role in terrain mapping and scientific assessment of the ground conditions quickly. In case of construction of new dams, satellite data provide unique inputs on the terrain, soil characteristics, agricultural practices, natural ecosystem and habitats to determine the impact of new dams. Since the interlinking of rivers project envisages creation of new storage structures, satellite data of high spatial resolution of 2.5 m from Cartosat-1 and 5.8 m data from IRS LISS IV are very useful for assessing the feasibility of proposed sites. Several large dams built to provide the head and storage to feed the canals could submerge certain stretches of fertile lands, forests, villages and towns. Satellite data would provide wealth of information as valuable inputs for preparation of Feasibility Reports and the Detailed Project Reports (DPRs) of the proposed river links.

Studies were carried out for Krishna-Pennar link between Nagarjunasagar reservoir in Krishna basin and Somasila reservoir in Pennar basin, which is one of the components of peninsular, inter- basin water transfer. Recently, NRSC provided inputs from high resolution satellite data analysis for preparing feasibility assessment of proposed irrigation projects in Upper Betwa basin as a part of Ken-Betwa river link project. Close contour DEM generated from Cartosat-1 stereo-pair data and, land use / land cover information from LISS IV MX data provided the details of submergence and command for evaluating the proposed dam sites under the project (Figure 6.13 & 6.14).

Thematic mapping of the garland canal area and runoff computations on the given alignment was undertaken for planning diversion of west flowing Netravathi river water towards east by constructing 4900 km length of garland and service canals. The survey was carried out using total length covering 1 Km on either side of the proposed alignment. There are two reservoirs in first phase which were also surveyed. The mapping of the area is completed in 1:2500 scale.

ALTM-DC is being analyzed for generating large scale (1:2500) maps and DEM for Godavari-krishna link canal project. The generation of L-sections for entire length, cross section for every 400 m on the alignment was generated as part of planning inputs.

Based on operationally demonstrated applications of remote sensing, relevant to information needs of interlinking of Rivers, important aspects of aerospace technology based supports can be summarized as below:

- 3D Terrain modeling & finer level characterization from airborne digital photogrammetry and LASER Terrain Mapper (ALTM)
- Land and Water Resource Inventory
- Hydrological characterization
- Geomorphological characterization
- Ecological characterization
- Multi-criteria Decision Making and GIS Techniques
- Modelling Framework
- Planning of New Storage Reservoirs
- Stabilizing the existing Irrigation Systems
- Information on Command area Expansion
- Establishing Water Harvesting Structures
- Environmental Impact Assessment

- Enriches the scope and content of Pre-feasibility, Feasibility, and Detailed Project Reports, Project implementation strategy
- Facilitates monitoring during execution stage and impact assessment subsequent to implementation

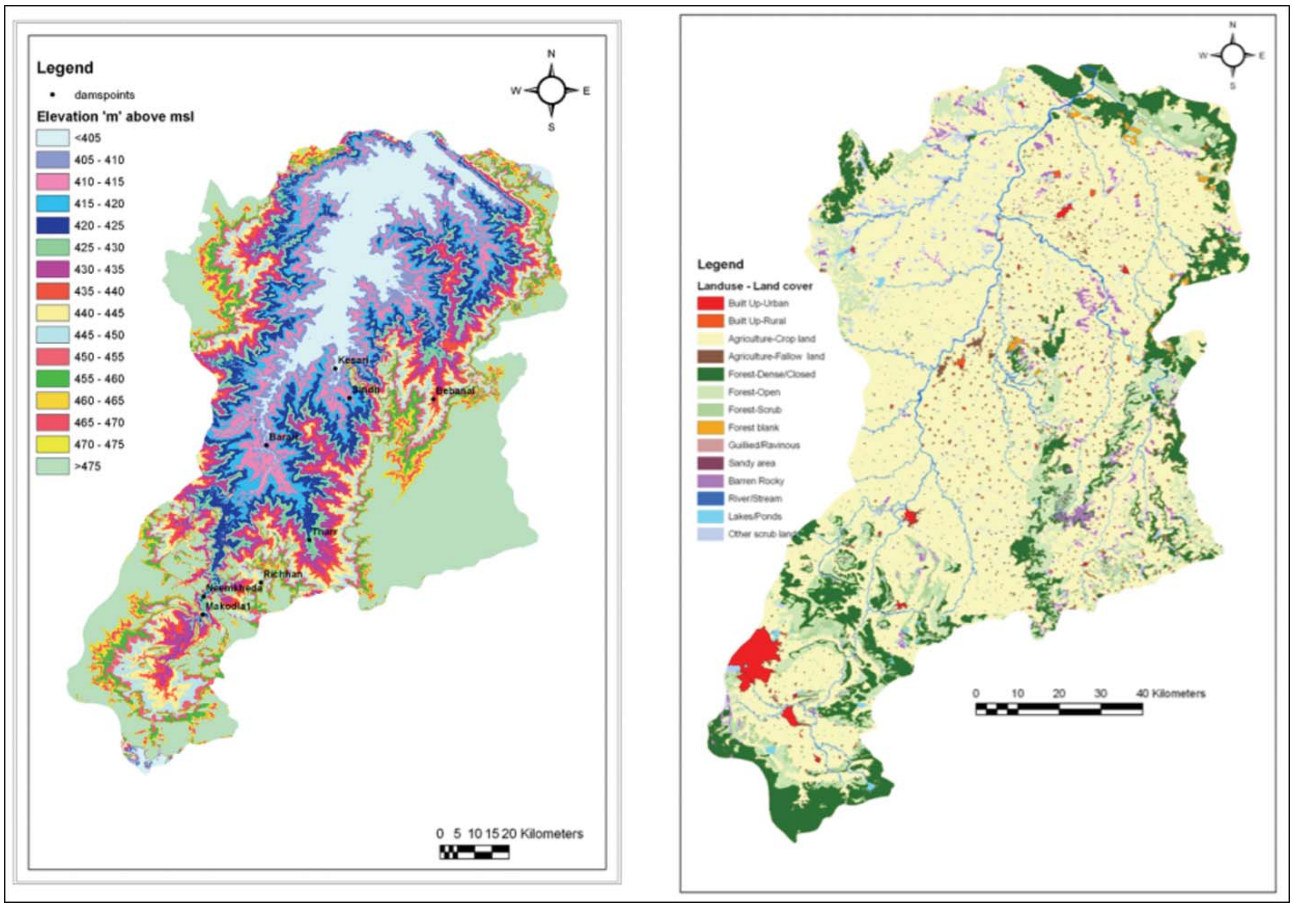

Figure 6.13: Relief Variations and Land Use/Cover of newly proposed irrigation potential

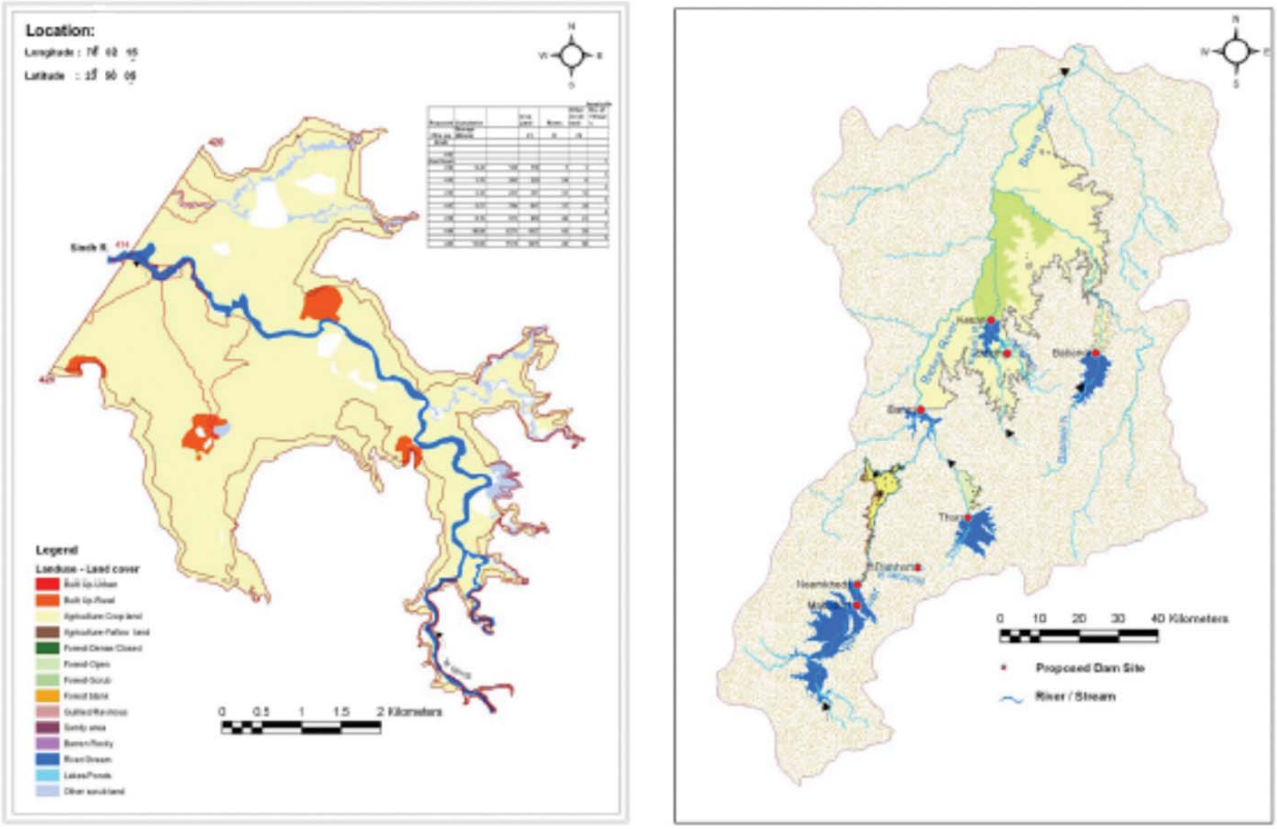

Figure 6.14: Submergence and Command area analysis

Airborne Laser Terrain Mapping (ALTM)

The 3-dimensional terrain modeling with the state-of art sensor data products from the Airborne Laser Terrain Mapper (ALTM)/ and high-resolution satellites (IKONOS/ Quick Bird/CARTOSAT-1)/ aerial photographs, is essential for precise identification of the alignment of canals and other structures. Digital elevation data derived from ALTM is effective for retrieving the close contour information towards precise canal network alignment. ALTM is a state-of-the-art tool for deriving the sub-metre level contour information of the terrain. ALTM provides accurate elevation data at cm level, and helps generating terrain maps with close (sub-metre) contours. These maps are useful in planning of the earthwork, alignment of distributaries in the commands, etc. With ALTM, digital elevation data sets can be collected at high resolution, meeting the requirements of different water resources engineering applications.

6.6.2. Ground Water Prospecting

Annually replenishable ground water in India is estimated to be 433 billion cubic metres (BCM) and Net Ground Water available for irrigation is 399 BCM and net draft for irrigation is 213 BCM. Ground Water constitutes 55% of irrigation water requirement and 50 % of water supplies of Urban and industrial areas and 85% of domestic use in rural areas. The above statistics reveal that the Ground water management is the key to combat the emerging problems of water scarcity in India. It being a hidden resource often developed without proper understanding. Therefore, there is a need for scientific planning of Ground water development in different hydrogeological set ups to evolve effective management practices.

Since ground water regime is dynamic system wherein, the framework in which the ground water occurs is as varied as that of rock types, as intricate as their structural deformation and geomorphic history, and as complex as that of the balance among the lithologic, structural, geomorphic and hydrologic parameters. The conventional hydrogeological maps are prepared mainly based on ground hydrogeological surveys provide geological unit-wise ground water prospects.

The Ground Water Prospects maps prepared under RGNDWM project contain information on 1:50000 scale on different rock types that occur in the area, various landforms that represents the terrain, dykes, linear ridges which form the barriers for ground water movement; weaker zones like fractures/lineaments which act as conduits for ground water movements etc. The maps also contain hydrological details like all stream courses, canals, water bodies (both seasonal & perennial), tank/canal irrigated areas and ground water irrigated areas etc. Each map contains information about nearly 80-100 wells collected during ground truth indicating type of the well, depth to water table, total depth of the well and its yield range with different symbols. By combining all the technical details referred above, the ground water prospects are evaluated for each hydrogeomorphic unit and the prospects are indicated on the map. In addition to the above, these maps show the locations of all the habitations indicating non-covered (NC) and partially-covered (PC) habitations in respect of sources of drinking water with different symbols. Tentative locations for planning different types of recharge structures are also shown nearer to NC/PC habitations to improve the sustainability of drinking water sources wherever required. These maps provide comprehensive information on ground water prospects indicating depth to water table, nature of aquifer, type of wells suitable, depth range of well suggested, expected yield range, success rate of wells, quality of water, type of recharge structures suitable and priority for recharge etc., with exhaustive legend. More than 2,00,000 wells have been drilled with a success rate ranging from 90-95 % and around 7500 recharge structures have been planned/ implemented by the line departments using Hydro-geomorphologic maps prepared using satellite data and collateral information under this Project. Till now 10 states, namely, Andhra Pradesh, Karnataka, Kerala, Madhya Pradesh, Chattishgarh, Rajasthan, Jharkhand, Himachal Pradesh, Orissa and Gujarat are covered under Phase-I & II. This project has successfully demonstrated the application of space technology for addressing the grass root level problem in the country and user departments are using these maps for last three years and achieved 90% success rate.

6.7. Flood/Cyclone Disaster Support

The increasing frequency of occurrence of extreme events of droughts and floods are posing great challenge to human society to absorb the consequent impacts and to get prepared to face such future events with reduced

misery. Policies and practices adopted under extreme water conditions are influenced by the causes and characteristics of the extreme conditions. It is also important to consider the nature of activity affected, as the impact varies.

Remote sensing data, both historical and near-real time provide objective and authentic information both on the behavior and response of various activities to extreme water conditions. Such information is vital to create, understand and model the effects and formulate strategies to cope up with extreme water conditions. Over the last two decades it has been established as a reliable and cost-effective tool for managing extreme water conditions such as flood and drought. The timeliness of satellite data has proved to be very critical in flood management, rescue operations, damage assessment, planning the flood plains and to formulate long term strategies. In conditions of water scarcity, satellite data is useful for monitoring and assessing the drought severity and consequent impact on agricultural production. Integration of newer technologies such as Remote Sensing & GIS in conjunction with traditional knowledge would enhance the resilience of human society in coping up with extreme water availability conditions. However, building up the resilience would largely depend on the sound knowledge of the historical adaptive process that sustained overtime and remained functional.

6.7.1. Flood Disaster Monitoring and Management

Floods are the most common and widespread among all natural disasters in India. India is the worst flood-affected country in the world after Bangladesh and accounting one fifth of global death count due to floods. About 40 million hectares (mha) or nearly 1/8th of India's geographical area is flood-prone and the country's vast coastline of 5700 Kms is exposed to tropical cyclones originating in the Bay of Bengal and Arabian Sea. The annual average area affected by floods is about 7.57 Mha and the affected crop area is about 3.5 mha. The average loss in financial terms is about Rs13,000 millions.

One of the most important elements in Flood Management is the availability of timely information for taking decisions and actions. During floods, timely and detailed situation reports are required by the authorities to locate and identify the affected areas for organizing relief operations. To obtain the information by conventional means is virtually ruled as the areas may not be accessible. In this context, the Earth Observation satellites provide comprehensive, synoptic and multi temporal coverage of large areas in near real time and at frequent intervals which enables to compare the data before and after flood disaster. Remote sensing data coupled with Geographic Information System (GIS) tool proves to be capable of overcoming some of the critical limitations that are being faced using conventional techniques. The developments in space technology offer tremendous technological potential to address the critical information needs during all the phases of disaster management, which include mitigation and preparedness, response and recovery/relief.

During monsoon season, a constant watch is kept on the flood situation in the country and all possible satellite data will be procured over flood affected areas. The procured satellite data is analyzed for delineation of flood inundation layer. The flood inundation layer was integrated with district boundaries and district-wise flood inundation area statistics were generated. The flood inundation maps along with affected area statistics were furnished to - NDMA, Min of Home affairs, Govt. of India, New Delhi, Chairman, Central Water Commission, Govt. of India, New Delhi, Relief Commissioner of the concerned States and other Departments connected with flood management in the States & Central Government. Apart from providing flood inundation information, based on the historic flood inundation observed from the satellite data was used for generation of flood hazard zone maps for planning non-structural flood management measures. Using multi-date satellite data maps pertaining to river configuration, bank erosion and flood control works were prepared and furnished to user for planning structural flood control measures. NRSC is also contributing towards generation of National Database for Emergency Management which would help in planning suitable flood control measures, relief and rescue management and to formulate long term strategies.

The flood risk zone maps are updated with high spatial resolution data and digital elevation models based on close contour information. Flood damage vulnerability analysis requires integration of the information on satellite derive physical damage and socio-economic data. Since 1987, all major flood events of the country have been mapped in near real time and statistics on crop area affected and number of marooned villages generated. Near real time flood monitoring is being carried operationally in Brahmaputra (Assam), Kosi/Ganga (Bihar), Indus (J&K), Godavari (AP) and Mahanadi (Orissa) river basins using optical and microwave data. Studies have been carried out for delineation of flood risk zones in Bramhaputra and Kosi river basins.

6.7.2. Flood Forecasting

Flood forecasting and early warning to affected areas are among the most important and cost-effective measures for flood management. The Central Water Commission has set up a network of flood forecasting and warning stations on most of the inter-State rivers in the country. Currently, 157 flood forecasting stations are in operation and nearly 5500 flood forecasts are issued using gauge correlation techniques and using hydrological models in some basins every year. But many important flood prone rivers/tributaries are yet to be covered.

Traditionally, gathering and analyzing hydraulic and hydrologic data related to floodplains and river catchments has been a time-consuming effort requiring extensive field observations and calculations. With the development of remote sensing and computer analysis techniques, now traditional techniques can be supplemented with these new methods of acquiring quantitative and qualitative flood hazard information.

Since the 1930s, numerous rainfall-runoff models have been developed to estimate streamflow on daily, monthly and seasonal basis. Remote sensing outputs are widely accepted by many of the hydrological models to compute surface runoff of the watershed. Runoff cannot be directly measured by remote sensing techniques. However, satellite remote sensing data can provide lot of real time information on landuse/landcover, soil moisture, determining watershed geometry, drainage network, and other map-type information in spatial environment for estimating surface runoff more accurately using distributed hydrologic modeling approach.

Topography of the river catchment is a basic need for flood forecasting. Remote sensing can provide quantitative topographic information of suitable spatial resolution to be extremely valuable for model inputs. For example, stereo pair of the satellite remote sensing data can be used to develop a Digital Elevation Model (DEM) with better resolution. Satellite remote sensing can play a major role in rainfall runoff modeling which is a part of the flood forecasting model. Now a day's meteorological satellites are providing valuable information on the real-time rainfall which may be used as an input in the flood forecast models.

6.7.3. River Engineering

River migration and river control works form the major elements in the flood plain management Satellite data provides accurate delineation of river configuration and the status of flood/river control works.

Most of the flood prone rivers in India change their course frequently after every flood wave attacking strategic locations at different times. Hence, it is necessary to understand the behaviour of the river and its latest configuration so as to plan the flood control measures effectively. At the same time it is equally important to monitor the existing flood control structures from time to time to avoid breaches in view of the frequent changes in river configuration. For planning flood control works, physical model studies will be conducted for which the latest configuration of the river is required. Every year the banks of the flood prone rivers are subjected to erosion, eating away the fertile land and at times villages on the bank. In order to provide bank protection works, vulnerable areas subjected to bank erosion along the rivers have to be monitored. In this regard latest and temporal information is required. Using conventional techniques to collect the information is not cost effective and time effective. Further, flood hazard zonation maps at large scale are eventually required for planning non structural measures. Hence, the data requirement for flood disaster management is quite complex and need extensive effort to collect especially using conventional techniques. In this regard satellite remote sensing provides an excellent source of information. Remote sensing data coupled with Geographic Information System (GIS) tool proves to be capable of over coming some of the critical limitations that are being faced.

Mapping of river configuration and flood control works of river Kamla Balan in Bihar using satellite remote sensing data was carried out for the years 1991, 1996 and 2001. Mapping of bank lines of Bagmati and Lalbakeya Rivers in Bihar using satellite remote sensing data was carried out for the years 1992, 1996 and 2002. Identification and estimation of River Bank Erosion along Brahmaputra and Barak Rivers in Assam was carried out for the years 1996 and 2002.

6.7.4. Urban Flood Management

The primary causes of urban flooding are: 1) extensive concrete surfaces leading to significant proportions of surface runoff with very little in situ percolation 2) inadequate channelization of natural waterways 3) surcharge due to blockage of drains and street inlets. Flooding in urban regions is an inevitable problem for many cities, particularly in cities which are old and have developed according to varying historical needs and visions. The transformation of

vegetated land to impermeable surface has gone hand-in-hand with the development of our urban areas over the past two millennia. This has led to a substantial decrease in the proportion of rainfall that infiltrates into the ground and a consequent increase in surface runoff, in terms of both volume and flow rate. One of the typical features of urban flooding is shortening the runoff travel time and making it flash event. Urbanization changed natural runoff pattern and accelerated transport of water, pollutants and sediment from the urban areas. Since urban settlements are undergoing continuous development, data on flow rates, physical and topographical settings require more periodic assessment and monitoring to cope up with storm water flooding. In India the problem of urban flooding is of increasing concern over the years.

Recent advancements in spatial resolutions have greatly enhanced the satellite remote sensing data capabilities in supplementing the data needs for management of urban flooding. High resolution data in the order of few meters provides the accurate layout of existing infrastructure, topographical settings, impervious surface mapping, and helps in preparation of master plans, planning storm water drainage channels. The temporal data sets also help to monitor the growth in urbanization and consequent impacts on storm water flooding. In the past, there are few studies that deal with modelling of urban flooding. With the development in the field of modeling software and availability of software packages like MOUSE, SOBEK, etc., it is feasible at present to model urban flooding with the vital inputs from remote sensing data and this raises new possibilities for managing urban flooding problems.

6.8. Environmental Impact Support

(Hydro-power development, Water Quality, Climate Change)

6.8.1. Hydro-Power Development

Power is a critical infrastructure for socio-economic development. Hydroelectricity is clean energy and its generation is not linked to issues concerning fuel supply, especially the price volatility of imported fuels. It enhances our energy security and is ideal for meeting peak demand. Industrialized countries harness over 80% of their economically-viable hydropower potential, in India the figure is quite low, despite the fact that the Indian electricity system is in desperate need of peaking power and the Himalayan hydropower sites are, from social and environmental perspectives, among the most benign in the world. Less than one fourth of the vast hydel potential of 1,50,000 MW has been tapped so far. In India, the share of hydro generation has gradually declined during the past 25 years. Consequently, thermal generation, which should generally be used for base load operation, is also being used to meet peaking requirements. As against the desirable hydro share of 40 per cent, the current share is only about 25 per cent in India.

Hydropower projects submerge vast areas of natural resources and satellite data is being extensively used for generating inputs for pre-feasibility analysis and also for carrying out environmental impact analysis. Space technology plays a very important role in terrain mapping and scientific assessment of the ground conditions with minimum time and manpower is ideally suitable for inaccessible mountainous regions where majority of these balance hydro-electric dam / diversion sites are located.

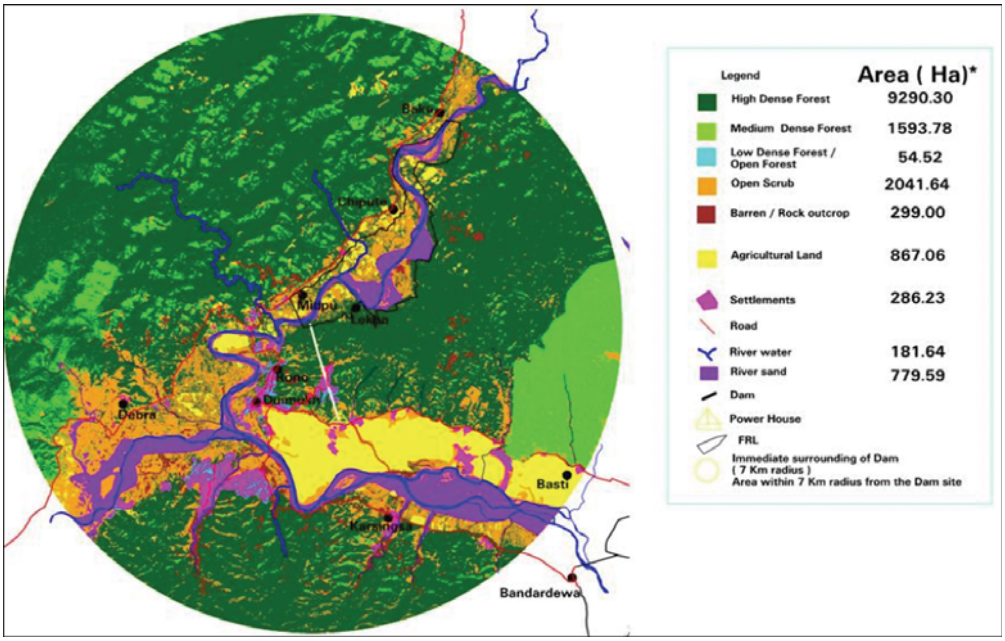

Figure 6.15: Submergence area analysis of proposed hydro-power site

The central electricity authority (CEA) in consultation with the States, Department of Space, Ministry of

Environment & Forests, CWC and Geological Survey of India, has initiated a basin wise ranking study of all the balance hydro sites with a view to identify those hydro projects which could be taken up first so that hydro power development is taken up in an appropriate sequence. The objective was to optimally utilize the potential of feasible hydro projects in the country over the next few decades.

The potential of this technology was demonstrated in the preliminary ranking study of the 81 proposed hydro- power sites located in Indus River Basin for the CEA executed by National Remote Sensing Centre in October 2001. Subsequently NRSC carried out the initial environmental assessment of 45 proposed (prioritized) hydro-power sites as part of preparation of pre-feasibility reports (PFRs) in different river basins of India during 2003 for NHPC and HPSEB. The high resolution satellite data (IRS 1C/1D PAN+LISS-III merged data) was used to estimate the Land use / Land cover area in the proposed dam submergence area and its immediate environs of hydro-power sites mostly located in inaccessible areas. Also, identification of the infrastructure details like roads, bridges, settlements etc., was carried out. Initial environmental assessment using submergence area statistics covering rehabilitation & relocation aspects and impact of proposed hydro-electric projects on national parks and sanctuaries using proximity analysis was carried out. Recently, NRSC carried out a similar study for the proposed Tamanthi hydro-electric project on Chindwin river in Myanmar, which is a bilateral project between Indian and Myanmar. A sample, Submergence area analysis of proposed hydro-power site is shown in figure 6.15.

6.8.2. Water Quality

With the rapid increase in the population of the country and the need to meet the increasing demands of irrigation, human and industrial consumption, the water resources in many parts of the country are polluted and the water quality has deteriorated. Many surface water resources are polluted due to the discharge of untreated sewage and industrial effluents. Groundwater quality problems have reached to a cause of concern throughout the country. Some of the major concerns in water pollution are due to rapid industrial revolution, over exploitation of agriculture fields with extensive usage of chemicals (i.e., pesticides and manures etc.,) and rapid growth of cities and depriving of vegetative cover over land surface in all over the world.

Water quality is a descriptor of water properties in terms of physical, chemical, thermal, and/or biological characteristics. Spectral properties of water vary with wave length not only due to molecular nature of water but also depend upon the impurities present with water body. Constituents in water influence its spectral and backscattering characteristics. Remote sensing techniques for monitoring water quality depend on the ability to measure these changes in the spectral signature backscattered from water and relate these measured changes by empirical or analytical models to water quality parameters. Major factors affecting water quality are suspended sediments, algae, chemicals, dissolved organic matter (DOM), thermal releases, aquatic vascular plants, pathogens, and oils. Some of these parameters like suspended sediments, algae, DOM, oils, aquatic vascular plants, and thermal releases directly influence the energy spectra and hence can be measured by remote sensing techniques (table 6.3). Most chemicals and pathogens do not directly affect or change the spectral or thermal properties of surface waters; they can only be inferred indirectly from measurements of other water quality parameters affected by these chemicals.

Visible and infrared (reflected) regions of EMR are useful for detecting indicators of water quality. Thermal infrared is also used for measuring water quality but it uses a direct measure of emitted energy. Microwave region is not particularly useful for determining water quality parameters but it is useful for detecting oil slicks or other surface contamination. In general, relationship between water quality parameter and the reflectance need to be established. As the reflectance changes with the modified value of water quality parameter, an empirical relationship can be established between reflectance and water quality parameter. This empirical relationship may not be valid for different times because the type of constituent in water may not remain constant. Sun elevation angle as well as composition of the atmosphere changes with time and year will also affect this relationship. Thermal infrared region 8 - 14 μm will be helpful due to its atmospheric window as well as maximum radiant emittance of most earth features in this range. Effluent dispersion patterns from industries and from other sources are easily identifiable due to varying nature of temperature differences. Point source identification calls for high resolution satellite data. Regional models of non-point source pollution loading is arrived based on remote sensing derived inputs on land use - land cover, supported by sample ground data collection. In general, remote sensing techniques can be successfully applied in all environments where there is a change in colour, temperature or turbidity of water bodies.

Table 6.3: Remote Sensing Techniques in Water Quality Monitoring

S. No.	Water Pollution/ Quality parameter	Spectral Region	Remarks
1	Total suspended solids (TSS)	Visible spectral region of EMR	Reflectance increases with the increase in sediment concentration. Empirical relationships could be developed for TSS estimation
2	Temperature	Thermal infrared and passive microwave	Infrared radiometers (8-14 μm region) based on Aircraft/satellite can be used to estimate the temperature. The temperature variation is function of nature of pollutants and effluents
3	Agriculture runoff	B&W and colour infrared photography	Change in vegetation can be identified & monitored through colour infrared. B & W IR image also can be used to identify the sources of agriculture pollution
4	Eutrophication	Colour Infrared (CIR)	Monitoring of floating algae can be done with CIR data Identification & defining of potential areas of algal blooms Water transparency, colour, chlorophyll, algal blooms, aquatic vegetation of eutrophication can be monitored
4	Oil Pollution	Ultraviolet Thermal infrared / Passive microwave	Good weather and low level flying is required to monitor oil pollution. Limited to day time monitoring Day/night capability
5	Water depth	Blue/green regions of visible spectrum Aerial /Laser profile	In clear water blue light penetrates upto 15 to 20 meters, & Green light penetrates upto 5 - 7 meters. Lidar systems can be used to be measure accurate profiling of water depths
6	Municipal & Industrial discharge	Satellite/ airborne thermal infrared	Temperature difference between the effluents and the receiving waters can be identified and monitored
7	Colour/ material insolation	Laser spectrometers	May not be possible to detect through satellite techniques. However ground based laser spectrometers are used for identification of chemical composition

6.9. Future Trends / Prospects

6.9.1. Water Resources Information system

The investments in Science & Technology, the communication facilities, the satellite technology and the computer capabilities that have increased manifold since our independence, have resulted in an explosion of the quantum of data. In a country like India adopting welfare concept in its constitution, the information that has been generated with national inputs should be used for developmental purposes for social benefits. The widely scattered large amount of information generated through various efforts have to be properly coordinated, coded and preserved using an Information system. The need of creating water data bases are imminent and we can hardly afford to delay the matter. National Resources Information System (NRIS), NR Census and (NRC) National Spatial Data Initiative (NSDI) initiatives go a long way in addressing the data related issues that emerge while preparing the road map for implementation of many water resources projects including inter linking of rivers.

The National Water Policy stipulates that the prime requisite for resource planning shall be a well developed information system consisting of scientifically designed data bases for improving both the quality of data and the

data processing capabilities. Towards this, a national level water resources information System (WARIS) is being formulated and designed using geo-spatial and conventional field data. It is essentially an interactive computer based system that incorporates capabilities for efficient data input, storage and retrieval, information processing and analysis capabilities and user friendly data (acquisition, management and processing), models (development, analysis, prediction and decision guidance) and interfacing (for interactive applications). The application package 'WARIS' will be developed by ISRO and collaborating partners and will be installed at CWC, New Delhi (Figure 6.16).

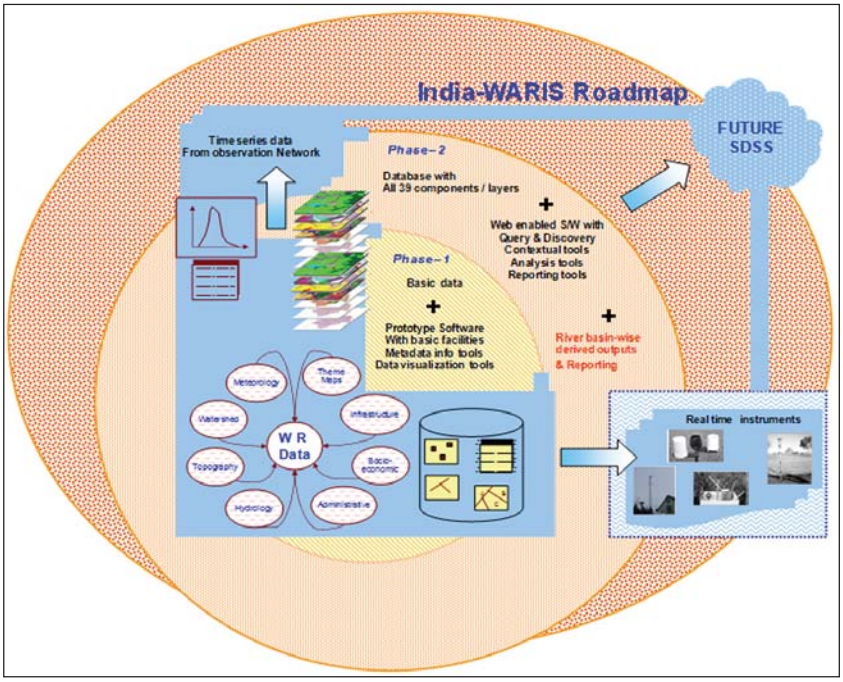

Figure 6.16: Conceptual frame work of WARIS

References

Arnold JG and Fohrer N, 2005, SWAT2000: current capabilities and research opportunities in applied watershed modeling, *Hydrological Processes*, **19**: 563–572.

Bastiaanssen WGM, 1998, *Remote Sensing in Water Resources Management: the State of the Art*, IWMI, Colombo, Sri Lanka, p 118.

Biggs T, Thenkabail PS, Krishna M, GangadharaRao P and Turral H, 2006, Vegetation Phenology and Irrigated Area Mapping Using Combined MODIS Time-series, Ground Surveys, and Agricultural Census Data in Krishna River Basin, India, *International Journal of Remote Sensing*, **27(19)**:4245-4266.

Bojie F, Xilin W and Gulinck H, 1995, Soil erosion types in the Loess Hill and Gully area of China, *Journal of Environmental Science Engineering.*, ***7:*** 266-272.

Chakraborty M, Panigrahy MS and Sharma SA, 1997, Discrimination of rice crop grown under different cultural practices using temporal ERS-1 synthetic aperture radar data, *ISPRS Journal of Photogrammetry and Remote Sensing*, **I52(4)**: 183-191.

Chormanski J, Van de Voorde T, Roeck T D, Batelaan O and Canters F, 2008, Improving Distributed Runoff Prediction in Urbanized Catchments with RS based Estimates of Impervious Surface Cover, *Sensors*, **8**: 910-932.

Duchon CE, Salisbury JM, Lee Williams TH and Nicks AD, 1992, An Example of Using Landsat and GOES Data in a Water Budget Model, *Water Resources Research*, **28(2)**: 527–538.

Dwivedi RS and Deka C, 1990, Degraded Lands in NE region as imaged by Landsat-TM, APRS Journal, 3, p. 35.

Jonna S, Badrinath KVS, Chandrasekhar G, Amminedu E and Chand TR Kiran, 2007, Crop surface temperature estimation in irrigated command areas using MODIS satellite data', *International Journal of Remote Sensing*, **28(23**): 5195-5205.

Kouwen N, Soulis ED, Pietroniro A, Donald J and Harrington RA, 1993, Grouped Response Units for Distributed Hydrologic Modelling, *Journal of Water Resources Planning & Management*, ASCE, **119(3)**: 289-305.

Mandal AK and Sharma RC, 2006, Computerized Database of Salt Affected Soils for Agro-climatic Regions in the Indo–Gangetic Plain of India Using GIS, *Geocarto International*, **21(2)**: 47 – 57.

Mather JR, 1978, The Climatic Water Budget in Environmental Analysis, Lexington Books, Lexington, USA.

Murthy CS, Thiruvengadachari S, Raju PV and Jonna S, 1996, Improved ground sampling and crop yield estimation using satellite data, *International Journal of Remote Sensing*, **17(5)**: 945–956.

Murthy CS, Raju PV and KVS Badrinath, 2003, Classification of wheat crop with multi-temporal images: Performance of maximum likelihood and artificial neural networks, *International Journal of Remote Sensing,* **24**: 4871–4890.

National Remote Sensing Agency, 1995 & 1996, Study of land degradation problems in Sharda Sahayak command area for sustainable agriculture development, Project reports, NRSA,

Neumann P, Fett W and Schultz GA, 1990, A geographical information system as data base for distributed hydrological models, In: Proc. International Symposium on Remote Sensing and Water Resources, IAH, the Netherlands, 781-791.

Ottlé C, Vidal-Madjar D and Girard G, 1989, RS applications to hydrological modeling, J*ournal of Hydrology*, **105**: 369-384.

Panigrahy S, Manjunath KR and Ray SS, 2005, Deriving cropping system performance indices using remote sensing data and GIS, *International Journal of Remote Sensing*, **26(12)**: 2595 – 2606.

Papadakis I., Napiorkowski J and Schultz GA, 1993, Monthly runoff generation by non-linear model using multispectral and multitemporal satellite imagery, *Advances in Space Research*, **13(5)** :181–186.

Patel NR, Bhattacharjee B, Mohammed AJ, Tanupriya B and Saha SK, 2006, Remote sensing of regional yield assessment of wheat in Haryana, India, *International Journal of Remote Sensing*, **27(19)**: 4071-4090.

Rao PPN and Mohan Kumar A,1994, Cropland inventory in the command area of Krishnarajasagar project using satellite data, *International Journal of Remote Sensing*, **15(6)**: 1295-1305.

Ray SS, Dadhwal VK and Navalgund RR, 2002, Performance evaluation of an irrigation command area using remote sensing: a case study of Mahi command, Gujrat,India, *Agricultural water management,* **56(2)**: 81-91.

Saindranath J, Rao PV N and Thiruvengadachari, 2000, Radarsat data analysis for monitoring and evaluation of irrigation projects in the monsoon, *International Journal of Remote Sensing,* **21(17)**: 3219 – 3226.

Sesha Sai MVR and Rao PVN, 2008, Utilization of Resourcesat-1 data for improved crop discrimination, *International Journal of Applied Earth Observation and Geoinformation,* **10(2)**: 206-210.

Sharma KD, Singh S, Singh N and Kalla AK, 1989, Role of satellite remote sensing for monitoring of surface water resources in an arid environment, *Hydrological Sciences Journal*, **34**: 531-537.

Sharma RC and Bhargawa GP, 1987, Operational use of SPOT-1 image in mapping and management of alkali soils, Proceedings of the National Symposium on RS in Land Transformation and Management, Hyderabad.

Singh AN and Dwivedi RS, 1989, Delineation of Salt-affected Soils through Digital Analysis of Landsat MSS Data, *International Journal of Remote Sensing*, **10**: 83-92.

Sazbo J, Pasztor L, Suba Z and Varallyay G, 1998, Integration of remote sensing and GIS techniques in land degradation mapping, Proc. of the 16th International Congress of Soil Science, Montpellier, France, 63-75.

Thiruvengadachari S, 1978, Surface water inventory in arid and semi arid areas, Proceedings of joint Indo-US Workshop on remote sensing of water resources, Hyderabad, India, p. 96-108.

Wischmeier WH, 1959, A rainfall erosion index for USLE. Proceedings – *Soil Science Society of America*, **23**: 246–249.

Yuksel A, Gundogan R and Akay AE, 2008, Using the Remote Sensing and GIS Technology for Erosion Risk Mapping of Kartalkaya Dam Watershed in Kahramanmaras, *Turkey Sensors*, **8**: 4851-4865.

Zade M, Ray SS, Dutta S and Panigrahy S, 2005, Analysis of runoff pattern for all major basins of India derived using remote sensing data, *Current science*, **88(8)**: 1301-1305.

nrsc

Remote Sensing Applications

P. S. Roy
R. S. Dwivedi
D. Vijayan

National Remote Sensing Centre

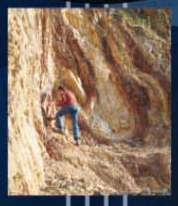

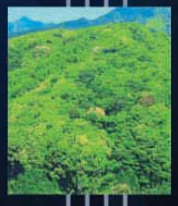

Remote Sensing Applications

Geosciences

7.1. Geological Mapping

7.1.1. Introduction

Remote Sensing is broadly defined as collecting and interpreting information about a target without being in physical contact with the object. Aircraft and satellites are the common platforms for remote sensing data collection. In general, the data collected by remote sensing system is commonly presented in the form of an image. An image is any pictorial representation, irrespective of the wavelength of imaging device used to produce it. A photograph is an image that records wavelengths of 0.3 to 0.9 μm that have interacted with light sensitive chemicals in photographic film. In initial period of remote sensing applications, aerial photographs proved useful in mapping geological structures. Images derived from multispectral sensors showed tremendous potential as an important source of application in various branches of geology- specially in geomorphology, structure and lithological mapping. These maps proved useful in different applications like Geoenvironmental appraisal projects, mineral exploration projects, geotechnical projects. But, it is to understand remote sensing images will be of little use for geological mapping if terrain is covered with forest, soil or other land use cover. Moreover, many of the time geological mapping is accomplished from the rock exposures exposed at the road-cut, river or other vertical section. Therefore map prepared from the remote sensing images is needed to be validated in the field. With the advancement of sensor technology, the applications of remote sensing has increased manifold in the field of geological mapping. Hyperspectral images collected within narrow and continuous spectral channel can detect the spectral signatures characteristic to minerals and therefore help immensely in lithological mapping based on mineralogy. Microwave sensor, on the other hand, due to its side looking imaging capability enhances the geological structures by creating shadow etc.

7.1.2. Image Interpretation

Image interpretation is the act of examining images/photographs for the purpose of identifying objects and judging their significance. The interpretation is not restricted to identifying object on the image; it also usually includes determination of their relative locations and extents. Visual interpretation of satellite image is being applied successfully in many fields, including geology, geography, agriculture, water resources, forestry, etc. A systematic study of satellite images usually involves a consideration of two basic elements, namely image elements and terrain elements

Image interpretation of terrain elements and image elements with identification of geological features based on variations in spectral signatures help in satellite based geological mapping. A broad geological knowledge about the terrain is a prerequisite for interpretation and delineation of rocks, structures and other relevant geological features from satellite image. Collateral data such as existing regional geological maps, reports guide the interpretation of satellite image to derive updated, detailed or large scale geological map. Moreover, the synoptic coverage and multispectral information provided by the remotely sensed data have proved to be advantageous over conventional methods for geological mapping. The synoptic view helps in visualizing the terrain as a whole and comprehend to the spatial relationship between different features (Reddy, 1987). These geological maps can be used in varied applications like mineral exploration, engineering geological studies, environmental geology related studies, geohazard analysis, etc.

7.1.2.1. Image Elements

Following are the eight characteristic image elements that aid image interpretation. These are: Tone/colour, Texture, Pattern, Shape, Size, Shadows, Site and Association.

Tone/Colour: Refers to relative shades of gray on black and white images or colours on normal colour composite, False Colour Composite (FCC) or images. Tone is directly related to reflectance of light from terrain features. For example, water which absorbs nearly all incident light produces black tone, whereas, a dry sand reflects a high percentage of incident radiation. Consequently it produces very light tone on the image. Tone/colour is a fundamental property of an image and conveys more information to an interpreter than any other image elements. Without tonal differences, shapes, patterns and texture of objects described below, could not be discerned.

Some of the terms often used to describe relative tonal values are light, medium, dark etc. Absolute tonal values in terms of photo density have no physical significance for interpretation purposes and practically never used. The variation in gray tones can be transformed into corresponding colours of various shades/lines on FCC. Colour imagery normally provide better thematic information than single band B/W imagery, by virtue of the more spectral information it contains.

Texture: Refers to the frequency of tonal changes in an image. Texture is produced by an aggregate of unit features, which may be too small to be clearly discernible individually on the image. It is a product of their individual shape, size, pattern, shadow and tone. By definition, texture is dependent on the scale. As the scale of the photograph is reduced the texture of a given object becomes progressively finer and eventually disappears. Some of the terms often used to describe relative texture values qualitatively are coarse, fine, medium, smooth, rough, etc., it is rather easier to distinguish various textural classes visually than in the digital-oriented techniques.

Pattern: The pattern relates to the spatial arrangement of the objects. The repetition of certain general forms or relationships is characteristic of many objects, both natural and man made, and gives objects a pattern which aids the image interpreter in recognizing them. For example, interbedded sedimentary rocks typically gives an alternating tonal pattern which aids in their identification.

Shape: Relates to the general form, configuration or out line of an individual object. Shape is one of the most important single factor for recognizing objects from images. For example, a railway line is usually readily distinguished from a highway or a kuchha road because its shape consists of long straight tangents and gentle curves as opposed to the shape of a highway. The shape of an object viewed from above may quite different from its profile view. However, the plan view of object is more important and sometimes conclusive indication of their structure, composition and function is possible.

Size: The size of an objects can be important tool for its identification. Objects can be misinterpreted if their sizes are not evaluated properly. Although, the third dimension, i.e., height of the objects, is not readily measurable on satellite images, but valuable information can be derived from the shadows of the objects. Images with stereoscopic coverages, such as those from SPOT and CARTOSAT-1 & 2 provide information on third dimension (height). For planar objects, it is easier to calculate the areal dimensions on imagery, for example-alluvial fan, flood plain, etc.

Shadows: are of importance to photo interpreters in two opposing respects (1) The outline or shape of a shadow affords a profile view of objects, which aids interpretation, and (2) objects within shadow reflect little light and are difficult to discern on photographs, which hinders interpretation.

Association: It is one of the most helpful clues in identification of land forms. For example, a flood plain is associated with several fluvial features such as terraces, meanders, ox-bow lakes, abandoned channel, etc. Similarly, a sandy plain in a desert is associated with various types of sand dunes.

7.1.2.2. Terrain Elements

In addition to the image elements described above, the terrain elements listed below are also very useful for image interpretation. The terrain elements include drainage patterns, drainage density, topography/land form and erosion status.

Drainage pattern: The drainage patterns and texture seen on images are good indicators of landform and bedrock type and also suggest soil characteristics and drainage condition. For example, dendritic drainage pattern is the most common drainage pattern found in nature. It develops under many terrain conditions, including homogeneous unconsolidated materials, rocks with uniform resistance to erosion such as horizontally bedded sedimentary rocks and granitic gneissic terrains.

Drainage Density: Drainage density refers to the drainage lines within a given unit area. In a given climatic region, coarse-textured pattern would tend to develop where the soils and rocks have good internal drainage with little surface runoff, whereas fine textured pattern would tend to develop where the soils or rocks have poor internal drainage and high surface run-off.

The following three drainage density classes have been recognized:

Fine : Average spacing between tributaries and first-order streams is less than ¼ inch in 1:50.000 scale. Fine-textured drainage is indicative of high levels of runoff, suggesting impervious bedrock type and/or fine-textured soils of low permeability.

Medium: Average spacing between first-order streams is roughly ¼ to 2 inches in 1:50000 scale. Runoff is medium in relation to fine-and coarse-textured drainages. Soil textures and underlying rock are typically neither fine not coarse but contain mixtures of particle size.

Coarse: First-order streams are greater than 2 inches apart, and they carry little runoff. Such textures are indicative of resistant, permeable bedrock materials and coarse, permeable soil materials. Shale would tend to develop fine textured drainage patterns, whereas sandstone develops coarse textured drainage patterns.

Drainage analysis is an important parameter to understand the geomorphic and structural variants of a terrain indirectly. Drainage analysis includes the study of drainage pattern, drainage texture, individual stream pattern and drainage anomalies. It provides clues to the distribution and attitude of the underlying rock formations and geologic structures, such as bedding plane, joints, fractures, faults, folds, etc. The basic drainage patterns and their significance in geologic interpretation are summarized in Table 7.1.1. Drainage texture is also an important parameter for studying the rock type distribution as it indicates the infiltration capacity of the rocks. Higher the infiltration Capacity of the rocks, coarser is the drainage texture and vice versa. Drainage anomalies, i.e., the local deviation from the regional drainage/stream pattern in the form of linear stream segments, active stream courses, appearance/disappearance of braided and meandering streams, change in drainage texture, etc., also indicate a change in underlying rock types and geologic structures. (Reeves *et al.*, 1975 ; Pandey, 1987 ; Gupta, 1991). Significance of drainage patterns in geologic interpretation is summarized in following table 7.1.1.

Table 7.1.1: Drainage pattern and Geological significance

Drainage Pattern	Geologic Significance
Dendritic	Develops in regions of rock homogeneity, shows lack of structural control; indicates horizontal to sub-horizontal bedding and gentle regional slope. Example-shales and granitic gneisses.
Rectangular	Shows structural control, develops along joints/faulty intersecting at right angles. Example-sandstone
Trellis	Shows structural control; develops in • areas having parallel fractures/faults, • tilted interbedded sedimentary rocks having differences in rock resistance and • folded sedimentary sequence.
Parallel	Develops due to pronounced regional slope or in areas having elongated geomorphic features, such as homoclinal ridges of quartzites.
Radial	Associated with domes, doubly plunging folds, volcanoes, etc.
Deranged	Indicates limestones in humid climate

Topography/Land form: The size and shape of a landform are probably most important identifying characteristics. There is often a distinct topographic change at the boundary between two landforms as can be seen in several images. Identification of landforms can help deciphering the underlying geology. Often many of the rock types have distinct topographic expressions, for example, interbedded sedimentary rocks typically exposed in the form of alternating ridge and valley topography. Similarly, basaltic flows occur in the form of mesa hills, Granitic bodies typically form hummocky topography, etc.

Erosion: In general, the deformation status and overall erosion within a given area can be assessed from the image which aids interpretation, particularly for geological mapping. For Example, a highly deformed and eroded rock unit can be considered older than the surrounding less eroded rock units. It also implies the physical competence, chemical susceptibility of underlying rocks to the weathering process.

7.1.2.3. Collateral Data

In addition to the image and terrain elements described above, collateral data in the form of published maps such as geological, soil type, topographical maps, etc., are very useful in the process of image interpretation.

Particularly, topographical maps are of immense help to an image interpreter. For example, slope and aspect information readily available on topographic maps are of great help in geomorphological studies. Similarly, topographic maps also depicts man made objects and other cultural features often useful for base maps preparation and also for transferring the interpreted details from images.

7.1.3. Spectral Signature of Rocks

The spectral signatures of rocks depend mainly on the spectral characteristics of constituent cations, anions and internal molecular structure. Spectral measurements, made in the laboratory and field, of various minerals have indicated that spectral features in visible and near infrared region (0.4-1.0 μm) are dominated by transition metals, such as Fe, Mn, Cu, Ni, Cr etc., and in short wavelength infrared region (1.0-3.0 μm) are dominated by hydroxyl ions, carbonates and water molecules. Interestingly, silicates, oxides, nitrates, nitrites and phosphates which form abundant rock forming minerals, do not have diagnostic spectral features in the reflected region (0.4-3.0 μm) of electromagnetic spectrum. However, thermal infrared region (3-14 μm) has characteristic spectral features of these constituents (Gupta, 1991; Hunt, 1977, 1979, 1980; Salisbury and Hunt, 1974; Kahle *et al*., 1986). The diagnostic spectral characteristics of various cations and anions in terms of wavelength at which the absorption peak occurs in different regions of electromagnetic spectrum are summarized in Table 7.1.2.

Table 7.1.2: Absorption peaks of various cations and anions in different regions of electromagnetic spectrum (Gupta, 2003).

Cations/Anions	Absorbtion peaks (μm)
Normal - Visible and near Infrared (VNIR) Region	
Ferric ion *	0.40, 0.50, 0.70 and 0.87
Ferrous ion*	0.43, 0.45, 0.57, 0.55, 1.00 and 1.80 – 2.00
Manganese	0.34, 0.37, 0.41, 0.45 and 0.55
Copper	0.80
Nickel	0.40, 0.74 and 1.25
Chromium	0.35, 0.45 and 0.55
Normal - Short Wavelength Infrared (SWIR) Region	
Hydroxyl ions	1.44 and 2.74 – 2.77
Al – OH	2.20
Mg – OH	2.30
Water molecules	1.40 and 1.90
Carbonates	1.90, 2.00, 2.16, 2.35 and 2.55
Thermal Infrared (TIR) Region	
Silicates	9.00 – 11.50 (depending upon the crystal structure)
Carbonates	7 (not used in remote sensing) and 11.30
Sulphates	9 and 16
Phosphates	9.25 and 10.30
Nitrates	7.20
Nitrites	8 and 11.8
Hydroxides	11

* The absorbtion features of 0.87 m (iron oxide), 1.00m (amphiboles and olivines), 0.70 m, 1.00 m and 1.80 m (pyroxenes) appear to be more common.

The spectral measurements suggest that mineral constituents display conspicuous spectral features at a particular wavelength or in a very narrow wavelength band, which require sensors having bandwidth of the order of about 10 nm or even lower. The present day multispectral sensors on-board various satellites, such as IRS-IA & IB, IRS-1C/1D, Landsat and SPOT provide data in much broader wavelength regions due to which direct identification of minerals/rocks is not possible.

7.1.4. Lithological Mapping using Remote Sensing

The important characteristics of common rock types manifested on the remotely sensed data are briefly discussed below (Reeves *et al.*, 1975; Lillesand and Kiefer, 1987; Pandey, 1987; Reddy, 1987; Gupta, 1991; Srivastav and Bhattacharya, 1991).

7.1.4.1. Sedimentary Rocks

The most conspicuous characteristic of sedimentary rocks is stratification, which exhibits banded appearance on the remotely sensed images/photographs. Commonly occurring sedimentary rocks are sandstones, shales and limestone. Horizontally bedded sandstones being resistant to weathering, form massive hills and hogback ridges. The drainage pattern varies from modified dendritic to rectangular and drainage texture is medium to coarse due to high porosity and permeability. Due to high permeability and elevation, sandstones support natural vegetation. Sandstones, if not covered with vegetation, give light tone on the image because of high silica

content and less surface moisture. Tonal banding on the image indicates the bedding of sandstones. Typically, two or three sets of joints are present in sandstones, which control the stream segments.

Shales, being incompetent rocks, form subdued topography. In humid climate, they form gently rounded hills with very gentle slopes. The drainage in shales is external and is mainly dendritic. They have fine drainage texture and badland topography develops in arid regions. Cultivation is generally practiced over shales because of the presence of moisture in soils and their low lying nature. Shales show darker tone compared to sandstones because of more surface moisture.

Limestones in humid climate show karst topography, subsidence, sink holes, caverns, etc., due to chemical weathering by water. These rocks have coarse drainage density because mainly internal drainage is present. The drainage is mainly controlled by joints / fractures / bedding planes. Deranged pattern is characteristic of limestone in humid climate. They show light tone and mottled texture on the image. Dolomitic limestone have comparatively less solution activity compared to pure limestone. In arid climate, limestone form prominent hills and ridges with steep side slopes and appear similar to sandstones.

Horizontally bedded sedimentary rocks such as sandstones, shales and limestones form terraced landscape in both humid and arid climate. In sandstone-shale sequence, sandstones form the cap rock and in limestone-shale sequence, limestone form the cap rock because of their resistant nature. The hills occur at almost the same elevations. Sandstones and limestones have steeper slopes compared to shales.

In tilted interbedded sedimentary rocks, ridge and valley type of topography having trellis type of drainage pattern is developed. In humid climate, sandstones form strike ridges, and limestones due to chemical weathering by water. Wheer as Shales form valleys. In arid climate, sandstones and limestones form strike ridges and shales form valleys. Landforms like Cuesta is common for interbedded and gently tiled sedimentary rocks.

7.1.4.2. Igneous Rocks

Igneous rocks are divided into intrusive and extrusive igneous rocks. Plutonic igneous rocks are characterized by their massive and homogeneous nature, and their discordant relationship with the country rocks. Granitic rocks are more common in nature compared to other plutonic igneous rocks, and are characterized by the presence of hummocky topography. They form dome-like hills surrounded by vast undulating plains. The drainage is dendritic to modified dendritic, however, radial and annular type of drainage are also present locally. The streams have a tendency to curve around the domes. These rocks are also characterized by the presence of crisscross jointing. Granitic rocks give light tone due to their acidic composition in contrast to gabbroic rocks having basic composition. Dolerites, which generally occur as dykes form linear to curvilinear ridges and have discordant relationship with the country rocks. However, when the surrounding rocks are more resistant, dykes form depressions. Sills are difficult to identify on the images as they are intruded parallel to the bedding of sedimentary rocks and can be misinterpreted as one of the sedimentary layers. Extrusive igneous rocks can be easily identified with the presence of volcanic land forms e.g., lava cones, lava flow and also by the presence of landforms such as cuesta, mesa/butte. Terraced landscape develops when these rocks are inter layered with non-volcanic sediments, wherein basalts have steeper slopes compared to non-volcanic rocks. Acidic extrusive rocks, such as Rhyolite, have the similar topography as that of the basic extrusive rocks, however, they have limited areal extent as the acidic lava is highly viscous in nature. Radial and annular drainage is developed in central type of eruption associated with volcanic cones and fine dendritic drainage is common in lava flows. Basic extrusive rocks give darker tone than acidic extrusive rocks due to the presence of mafic minerals. Thick black soil is developed over highly weathered basalts, which is often cultivated.

7.1.4.3. Metamorphic Rocks

Metamorphic rocks are comparatively more difficult to identify on the image/ photograph, since most of the primary features of the original rocks are lost because of the metamorphism. Commonly occurring metamorphic rocks are gneisses, schists, phyllites, slates and quartzites. These rocks, except quartzite, have subdued undulating topography and manifest regional foliation / schistosity / cleavage in the form of thin parallel lineations, called trend lines, on the images. Quartzites owing to their resistant nature form linear to curvilinear ridges. Metamorphic rocks give banded appearance on the image. However, the bandings in metamorphic rocks are short, irregular and numerous compared to long, sedimentary rocks. These rocks have trellis, rectangular, dendritic and mixed drainage pattern.

7.1.4.4. Steps in interpreting lithology from satellite image

Satellite data is preprocessed (co registered, mosaiced) and enhanced using different image processing techniques. Best image products in terms of delineation of all the lithological units are used for image processing. Figure 7.1.1 shows flow chart describing steps to be followed for updating/preparing lithological map through satellite data interpretation.

7.1.5. Criteria for Structural Mapping

The structural features that can be identified on remotely sensed imagery may be divided into two categories – (i) associated with or internal to specific rocks known as rock structures and (ii) those which cut, deform and otherwise affect the rock units themselves known as geologic structures (Reeves *et al.*, 1975). The basic criteria for the identification and mapping of geologic structures are given below (Reeves *et al.*, 1975; Pandey, 1987; Gupta, 1991; Srivastav and Bhattacharya, 1991).

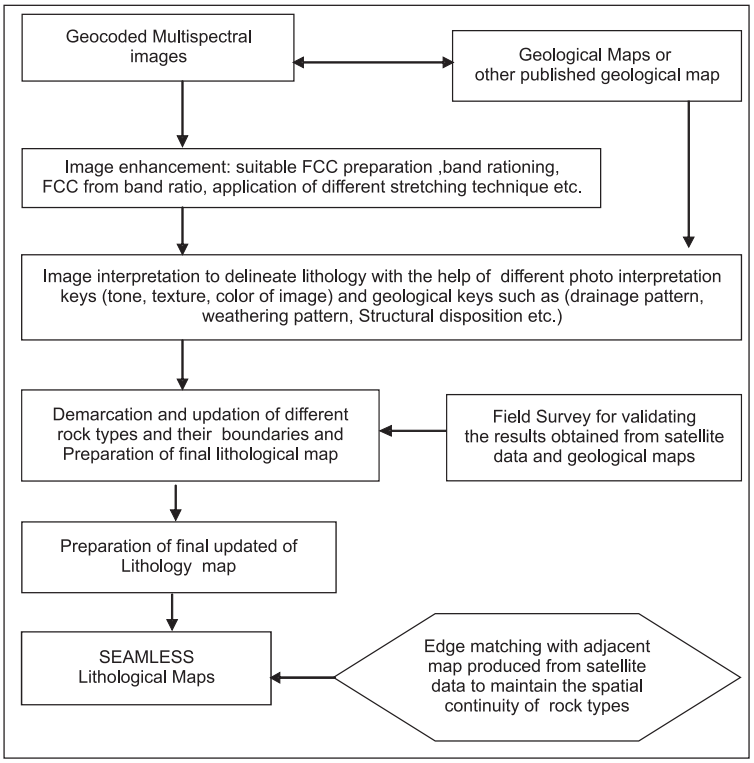

Figure 7.1.1: Flow chart describing steps for preparation/updation of Lithological map from Satellite image

7.1.5.1. Attitude of Beds

The strike and dip direction, and amount of dip constitute the attitude of beds. By visual interpretation of satellite image, amount of dip can be estimated broadly by studying the slope asymmenty (i.e., the amount of inclination of slopes on opposite sides), land form, drainage characteristics, etc., Some of the important characteristics of horizontal to sub-horizontal and inclined beds are the following:

A) **Horizontal and sub-Horizontal beds**

- Show tonal/colour bands parallel to contour
- Show mesa/butte type of landform
- Show dendritic drainage pattern

B) **Inclined beds**

- Show elongated ridges and valleys due to differential weathering
- Low dipping or gently dipping beds (5° to 25°) form cuesta hills having pronounced gentle dip slope and steep obsequent slope
- Moderately dipping beds (>25° and <35°) develop homoclinal ridges
- Steeply dipping beds (>35°) develop hogback ridges
- Vertical beds show narrow, long, continuous and evenly spaced narrow bands running parallel to the strike of the formation. Triangular dip facets develop wherever interbedding of hard and soft rocks exists. The open end of the dip facets points towards down-dip direction

7.1.5.2. Folds

Plunging, non-plunging and refolded folds can be identified on the aerospace data by mapping the marker horizons. The criteria for the recognition of folds are given below:

- Non-Plunging folds produce outcropping in parallel beds
- Plunging folds have v-or U-shaped outcrop pattern. Further classification into plunging anticline or syncline can be made on the basis of dip direction of beds. The nose of a plunging anticline is typically V-shaped

in outcrop pattern and the plunge is in the direction of outcrop convergence. Whereas, a plunging syncline generally shows U-shaped nose and plunge is towards the open end of the outcrop convergence

- Doubly plunging folds produce oval shaped outcrop patterns
- Major streams curve around the nose of the plunging folds

7.1.5.3. Linear Features

Remotely sensed data offer enough scope for the mapping of linear features of geological interest, called lineaments, representing joints, fractures, faults, etc., the lineaments on the remote sensing data can be identified mainly based on their linear nature, presence of moisture, alignment of vegetation, alignment of ponds, straight stream segments, etc., however, the interpretation of fault is complex, but a few general principles apply as given below:

- Rocks on opposite sides of a fault line fail to match each other in type or attitude or both
- Abrupt termination of geological structures, land forms, drainage pattern, etc.
- Lateral offset of the topographical features
- Modified drainage patterns and alignment of vegetation, alluvial fans, springs etc.
- Presence of scarps, nick points or local steepening of streams

7.1.5.4. Unconformities

Angular unconformity can be easily recognized on the image by seeing the angular disposition of rock types on opposite side of the contact. Similarly, non-confirmity in which the older rock is of plutonic origin is easily recognizable. Unconformable contacts are mainly irregular and can be easily differentiated from faulted contacts of straight or slightly curvilinear nature.

7.1.5.5. Methodology for extracting structural information

Several image processing methods are useful in enhancing geological structures. Various spatial domain filters especially Highpass, edge detector, etc., may be attempted for enhancing the structures. Most of the structures are highlighted in a standard FCC with a suitable radiometric enhancement. Microwave data also can be used in conjunction with visible data for highlighting the structures. High pass filters are generally suitable for enhancing linear geological structure;. During Fourier transformation, images are converted from spatial domain to frequency domain. A flow chart (figure 7.1.2) is given to show the steps demonstrating the sequential methods generally followed to delineate geological structure from satellite imageries.

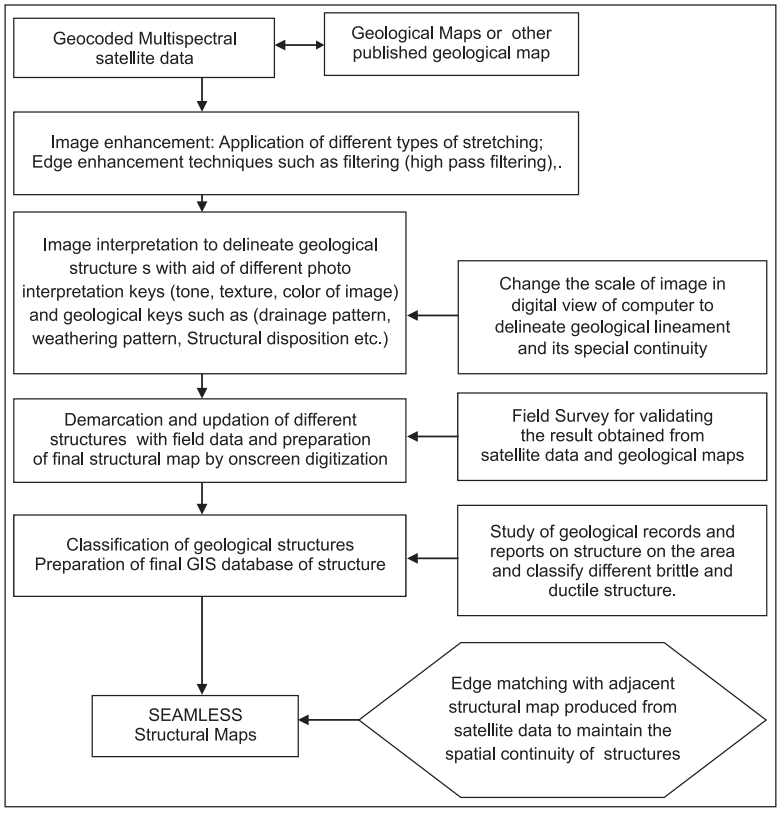

Figure 7.1.2: Flow chart describing steps for delineating Structural features from Satellite Image

7.1.6. Criteria for Geomorphological Mapping

Geomorphology is a complex subject with multiple approaches to its analysis and multiple scales of mapping. In earlier days, ground surveys were the only source of information for geomorphological mapping supplemented by information from topographic maps. But such type field based geomorphology mapping used to be local and demand more time. From the 1970s aerial photographs have played a key role in such surveys (van Zuidam 1985, 1986). But with arrival of digital photogrammetric technique and high computing facilities, the old aerial

photographs are scanned and used to generate 3D for landform analysis (Schiefer and Gilbert, 2007). Areal photographs provide also an opportunity to view the terrain 3 dimensionally and thereby aid in landform interpretation. One has to analyse more number of aerial photographs (unlike few scenes in satellite imagery), when geomorphology mapping has to be carried out for a large area. Major drawback of aerial photographs are its high cost and non repetitive nature to capture the dynamic morphological changes.

Subsequently with advent of new satellites, geomorphology mapping has taken a new dimension as it provides direct perspective of large regions. Useful sources of satellite data for geomorphologic applications are images from the Landsat Multispectral Scanner (MSS) and Thematic Mapper (TM), SPOT HRV, and other higher resolution sensors, such as IRS-LISS, MOMS, and the camera systems of KFA-200, KFA-1000, and SPOT HRV and other higher resolution sensors provide images with more spatial detail that may also allow stereoviewing of the terrain. Landsat TM and MSS data have been extensively used for geomorphology mapping by many workers because of narrower spectral bands, particularly suitable for the mapping of bathemetry (bands 1 and 2), vegetation (bands 2, 3, 4, and 5), soil (band 6) and rock (band 7). Microwave data such as ERS and Radarsat have cloud penetrating capability and are sometimes useful for geomorphological mapping. Van Zuidam *et al.*, (1994) used image fusion technique and GIS for mapping coastal landforms. They have used ERS-1 SAR, Landsat TM, SPOT XS and PAN and DTM to find out the tidal changes along the coast of The Netherlands.Use of Digital Elevation Model (DEM) in geomorphology study is not uncommon. Recently DEM has been derived from LiDAR, Stereoscopic satellite data is emerging as a new tool for both quantitative and qualitative geomorphological mapping. Terrain visualisation using DEM provides an opportunity to map the area 3 dimensionally. Mason *et al.*, (2006) have automatically extracted the tidal stream network from LiDAR data. Smith and Clark (2005) analysed different visualisation technique using DEM and observed that curvature visualisation is better than relief shaded visualisation as it provides a non illuminated image.

The nature of the geomorphic unit is controlled by the model of analysis chosen and the scale of mapping required. The basic geomorphic unit is not a single feature or entity, but must be carefully selected to be essentially homogeneous and indivisible at the scale chosen. Although all generally agree that the basic geomorphic unit should be a homogeneous entity, it can be defined in terms of genetic or structural pattern. The approach followed by the International Geomorphology Union (IGU) and most European geomorphologists are in terms of location and dimensions of geometric elements, along the lines of the British system. In India very few attempts have been made to bring out a regional classification system addressing all the aspect of the landform evolution. Of late with advent of remote sensing technology especially in the late 70, geomorphology has gained importance in the entire mapping project. Nevertheless all the study has been of local in coverage catering to theme-specific objectives. Most of the geomorphological mapping has been carried out for geo-environmental appraisal, mineral exploration, geo-engineering, geo-hazards and ground water targeting. Geological Survey of India has carried out geomorphological mapping for the entire country on 1:2,000,000 scale using Landsat MSS data. Department of Space has carried out many nationwide resource mapping projects in which geomorphology is one of the important inputs. Under Natural Resources Cencus(NRC) a renewed attempt has been made by Department of Space with National Remote Sensing Centre (NRSC) as the nodal agency for systematic classification and mapping of geomorphic units in a nation wide mission on 1:50,000 scale.

In nutshell, remote sensing data products (aerial photographs and satellite images) give direct information on the landscape-the surface features of the earth. Therefore geomorphological investigations are most easy to carry out based on such data. Moreover, landscape features can be better studied on regional scale using synoptic coverage provided by the remote sensing data, rather than in the field (Gupta, 2003).

7.1.6.1. Identification of different types of Landform/Geomorphic Units

Landforms are characteristic to the processes which operated to develop their sculpture. Landforms can be broadly subdivided in broad seven categories based on the processes or medium played role in their formations. These are: Aeolian Landform, Coastal Landform, Denudational Landform, Fluvial Landform, Glacier Landform, Tectonic Landform and Volcanic landform.

Aeolian Landform: Aeolian landform is a feature of the Earth's surface produced by either the erosive or constructive action of the wind. The word derives from Aeolus, the Greek god of the winds. Wind erosion processes consist of abrasion, the scouring of exposed surfaces by the sand-blasting action of wind-borne material; and deflation, the removal of sand-sized and smaller particles by the wind. Sand is transported short distances as individual grains

or by saltation (a form of movement in short leaps) to form distinct constructional bed forms at various scales: aeolian ripple ridges (a few centimeters in width), meso-dune forms (a few meters in diameter), dunes (several tens to a hundred metres in size), and, finally, ergs (several square kilometers or more). The finer silt-sized particles are transported by airflow turbulence in suspension over much greater distances to form loess. Wind transportation causes attrition of the moving particles, which rub one another and develop characteristic surface frosting and pitting.

Coastal Landform: Coastal landforms are those which are influenced or controlled by the proximity to the Sea. There are two broad types of coastal Landforms: erosional coastal land forms and depositional coastal landform. Most prominent among erosional coastal landforms are those which are cliffs, terraces, benches, shelves, caves etc and significant depositional landforms are beaches ,spit, bars, tidal flats and deltas.

Denudational Landform: Denudational landforms are formed by the continued process of erosion of original landscapes by repeated action of denudational agents like river, wind and climate components like rainfall, temperature etc., Few major denudational landforms are pediplain, pediment, denudational hill etc.

Fluvial Landform: Fluvial landforms are created by the action of rivers or streams and the processes associated with them. This is one of most widely distributed landforms on the earth surface. The landform associated with fluvial erosions are gorges, canyons, V-shaped valleys, steep hill slopes, water falls etc. Typical depositional landforms include alluvial fans, cones, alluvial plain, flood plain, natural levees, river terraces, meander scars, channel fills, point bars and delta.

Glacial Landform: Glaciers are stream-like features of ice and snow, which move down slopes under gravity. Glaciers occur at high altitudes and latitudes and about 10% of earth surface is covered by ice. Areal extent of glacier is difficult to measure by field method and remote sensing data images provide information of much practical utility in this regard (Gupta,2003). Typical erosional landforms of glaciers are U shaped valley, hanging valleys, cirques etc. Main depositional landform of glaciers is moraine. Below streamline, glaciers melt down and form streams. Typical glacio-fluvial landforms are outwash plan, end morain, eskers, etc.

Tectonic Landform: Tectonic landform may be defined as structural landforms of regional extent. Davis in 1899 considered that structure, processes and time constitute the three most significant factors shaping the morphology of a land. Scarp, shutter ridge, structural hill, monocline, etc are few noteworthy tectonic landform.

Volcanic Landform: Volcanic Landforms are mainly constructional and are resulted from extrusion of magma along the vents or fracture of the earth's surface. Cinder cones, crater lava ropes etc are few noteworthy volcanic landform. The definition of major landforms formed under all seven categories of landforms is appended as annexure at end of this chapter.

7.1.6.2. Methodology for extracting Geomorphological information

Satellite data /aerial photographs are most suitable to identify and demarcate the boundaries of different landform as it gives the synoptic coverages. Some times, collateral data like toposheet maps, digital elevation models (DEM) are used to pick up the subtle variations of landscape and also to detect the intraunit variations. All the landforms are demarcated with the help of onscreen digitization process to prepare the geomorphology map. Field work is carried out to validate the map produced from satellite image interpretation. A flow chart (figure 7.1.3) is given to show the steps demonstrating the sequential methods generally followed to prepare a geomorphological map by satellite based method.

7.1.7. Thermal and Microwave data in Geological Mapping

7.1.7.1. Thermal Remote sensing data in Geological Mapping

In thermal infrared (TIR) region, energy emitted by the objects is measured. This emitted energy depends upon the temperature and emissivity of the objects. For geological mapping, thermal response of the rocks to temperature changes is the fundamental property used for discrimination of rock types. Higher the thermal inertia of the rocks, warmer (or brighter) the signature in the night-time image and vice versa. For example, dolomite, which is difficult to distinguish from limestone on optical image, appears warmer (or brighter) on the

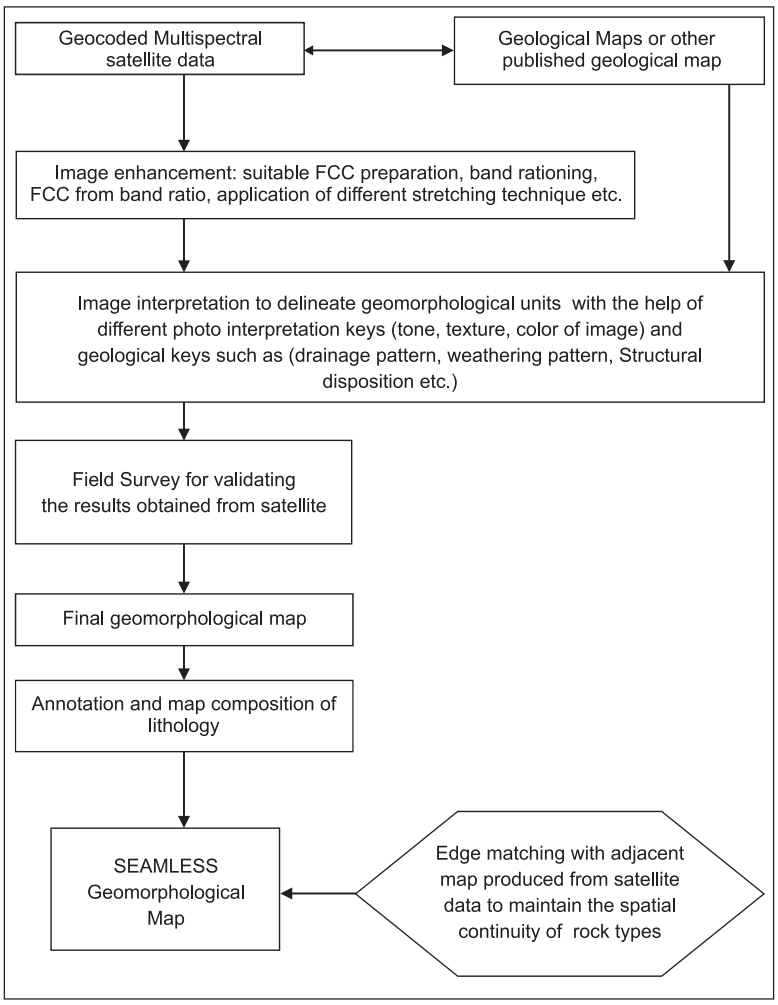

Figure 7.1.3: Flow chart showing steps followed in preparation of Geomorphological Map from satellite Imag

night- time thermal image because of higher thermal inertia. Geological structures such as plunging anticlines and synclines show a distinctive pattern of warmer and cooler signatures due to differences in thermal inertia of rocks. The weak zones, such as faults and fractures give cool linear anomalies in both the day-and night-time thermal images (Sabins, 1987).

7.1.7.2 Microwave remote sensing data in Geological Mapping

Imaging radars are operated in the microwave range of the electromagnetic spectrum at wavelengths from about 1 cm to 1m (Henderson, 1998). The Synthetic Aperture Radar (SAR) has unique capabilities to provide information on surface geometry i.e., shape, orientation, surface roughness and complex dielectric constant. Therefore SAR provides valuable information on surface roughness, soil moisture, topography, and drainage pattern of geologic terrain (Gupta, 1991). SAR also has the limited capabilities to penetrate through the soil cover and thereby can provide valuable information about in-situ rock type and sub-surface structure and SAR techniques have the efficiency to provide relatively coarser resolution where minor details and variations are suppressed. Owing to this fact, SAR images are very helpful in regional landform studies, especially if the variations in landform units are manifested in terms of differences in surface roughness, relief, moisture, etc. Lineaments are well manifested in radar images. Lineaments give the information about the strikes or trends of geological structures like fault, joints, shear planes, fractures, gneissosity plane etc. It must be emphasized that often geological features are better observed on SAR images than on corresponding VNIR or photograph images (Gupta, 1998). Singhroy *et al.*, (1993) have given a brief account of applications of microwave remote sensing in geological applications. Rivard *et al.*, (1999) demonstrated how radar data could be used with Landsat TM images for structural reconnaissance study of deep structural organs. The detailed work of Sharma *et al.*, (in Greenville Greenstone belt, Canada) has manifested the capabilities of radar data in enhancing regional geological structure. In this study, it has been demonstrated as to how radar data helped in the identification of structural dome and nappe in Greenville Province. In a sedimentary terrain, morphological characteristics such as dip slope-asymmetry, flatiron and v shaped pattern of outcrops develops on the images. The manifestation and patterns of these features depends on illumination geometry of microwave sensor (Henderson, 1998).

SAR is also useful in delineating different lithologies based on indirect criteria like surface roughness, soil moisture, drainage, relief, geomorphological features like sink holes, solution ridge, etc., Texture of SAR image is another important criterion as investigations have revealed appreciable correlation between radar return and surface roughness of different types of lithologies, which produce distinct texture in image. Further there is also a possibility of distinguishing various lithologies using multi-channel, cross and like polarized radar images (Daily, 1978, Dellwig, 1969, Bloom *et al.*, 1987). Their study revealed that the shorter wavelengths and small incident angle are best for Lava flows while for the sedimentary rocks the longer wavelengths and somewhat larger incident angle are preferred.

7.1.8. Review of Literature

Remote sensing has been effectively used for broad lithological mapping primarily based on principle and techniques of photo interpretation. Faults, fractures and contacts often provide a conduit for depositional environment for hydrothermal or magmatic fluids in regions of known mineralization, and thus make excellent targets for further investigation. Landsat ETM has been used to map large scale lithological information in different parts of world (Macias, 1995; Rencz *et al.*, 1996; Glikson & Creasey, 1995). With the advancement in sensor technology, new sensors with better spectral resolution like ASTER (12 channels covering visible, SWIR and TIR), Hyperion (242 channels covering visible and SWIR) are being used for lithological mapping. A significant increase in the spectral resolution has led to increase in narrow spectral band to generate hyperspectral images. The narrow spectral channels of an imaging spectrometer forms a continuous reflectance spectrum of the earth surface in comparison to the narrow channels of multi-spectral. In particular, images that represent the effects of diagnostic absorption bands can be produced to show specific variability of certain material features. Absorption bands play a key role in defining the spectral curves of the different terrain parameters. There are various issues in the processing of such sensor data especially calibrating for reflectance with suitable atmospheric correction models, improving the Signal to Noise Ratio (SNR), reducing the redundancy, separating the spectrally pure end member and finally mapping using pixel and sub-pixel techniques. Airborne /satellite hyperspectral data has been used for mapping mineral abundance by various researchers (Boardman *et al.*, 1994; Kruse *et al.*, 2003; Vinod, 2006). This technique is rapidly gaining importance for lithological discrimination.

Satellite based remote sensing approach is best suited for geomorphological mapping. Philip *et al.*, (1989) used aerial photographs and Landsat MSS and TM imagery for the detection of palaeofeatures that have helped to establish the migratory trend of the Ganga and Burhi Gandak rivers. Jones (1986) demonstrated the applicability of suitably processed TM imagery for geomorphologic investigations in arid and semi-arid environments. Updation of geomorphological maps is of great importance for environmental monitoring and sustainable development. Yang *et al.*, 1999 have demonstrated the use of satellite image in deltaic environment updating the dynamic landforms. Sgavetti and Ferrari (1988) used TM data to study the deltaic depositional systems of the Po and Adige rivers.

The ability of radar polarimetry to obtain information about physical properties of the surface has led to many innovative applications in Geoscientific research and concerning environmental issues. Dierking and Haack (1998) demonstrated the capability of polarimetric L-band data acquired by the Danish airborne sensor EMISAR in August, 1997 in delineating the different lava flow and surrounding terrain as well as the identification of different lava facies within one flow. Singhroy *et al.*,(2004) has provided interesting information of polarimetric signatures collected from CV-80 high resolution airborne SAR data. It is found that copolarised polarimetric signatures are significantly different for different surface material type such as sand-silt alluvium, clayey till, deltaic sediment and sedimentary textures played important role in generating different polarimetric signatures. Evan's *et al.*,(1998) described an interesting account of how polarimetric signatures changes with the flow age in consistent with the physical mechanism of lava flow weathering in arid region. These processes, such as rubbling and filling, smoothen the surface of lava flows over time. The important visible difference was in the height of the pedestal, which seems to generally decrease with age, which is consistent with decreasing roughness with age. Guha *et al.*,(2007) evaluated the role of look angle, look direction, microwave frequency and polarisation in enhancing geological element of Kurnool Super Group of rocks, Andhra Pradesh. The future of geological microwave remote sensing would emphasize more on evaluating the role of polarimetry in delineating geological element and also to successfully use the satellite based microwave data in geodynamics. The future missions, namely first Indian microwave remote sensing satellite RISAT scheduled to be launched in 2009 and Radarsat-2 by Canadian space agency would enable detection of certain geological features otherwise indiscernible by virtue of polarimetric observation fulfill the requirement of satellite based polarimetric microwave data for such applications.

7.1.9. Gap Areas

Remote sensing sensors only helps in deriving the geological information impressed on the surface of the earth. Moreover, broadband multispectral sensors are, generally not suitable for delineation of different rocks type based on spectral signatures as no rock has characteristic spectral signatures under broad spectral band. Therefore, geological mapping from satellite data entirely depends on indirect criteria like geomorphic, weathering and geotectonic signatures. Moreover, geological structure specially brittle tectonic structures are only mappable on surface. Low angle brittle structures or ductile structures which do not have characteristic surface information such as recumbent

fold, non plunging fold are difficult to be delineated from satellite data. It is therefore always difficult to prepare a conclusive geological map based on satellite data. However, satellite data can be used to prepare detail and updated geological map if satellite data analysis is compounded with the informations from existing regional geological map in small scale and complementary field work.

7.1.10. Case Study

Geological mapping was carried out in parts of Jaipur area in Rajasthan for preparation of geological database for urban information system of Jaipur city. The informations on geology and geomorphology and geological structures are important element for any urban information system because these components guide the urban planner to get the answers of many questions like where one would get better groundwater or what are the places that would be more suitable for rain water harvesting or which are the places with compact basement rock suitable for large scale engineering structures or what are the places that can be used for amusement park or tourist place etc.

7.1.10.1. Geological Description

The relevant information on aforesaid themes are discussed below:

Lithology: The geological sequence of the area is highly varied and complex, revealing the co-existence of the most ancient rocks of Proterozoic age and the most recent alluvium as well as wind- blown sand. Delhi super group are older rocks and are deposited at the central portion of Aravalli range and deposited in synclorium. The exposures of Delhi super group of rocks are restricted in eastern, north-eastern and south-eastern part of the area but in the west and the south-west, they are often engulfed in sandy alluvium and desert sands.

Delhi super group is divided into lower Ralio group, middle Alwar group and upper Ajabgarh group. Ralio group is rich in crystalline limestone, grits, schistose rocks and quartzites. The famous marble of Makrana (Nagaur district) belongs to this group. Alwar group and Ajabgarh group consist mostly of calc-silicates, quartzites, grits and schistose rocks. Thick-bedded quartzite, shiest/phyllite and other lower grade metasediments are exposed here (Figure 7.1.4). In the western part, recent wind blown deposits have covered the metamorphics of Delhi super group. Thickness of the wind blown deposit varies from few centimeters to few meters and at places stabilized dunes are formed. Stabilized dunes are formed if sand is deposited in a depression and moisture and vegetation around the sand body have restricted its further transportation. In places, especially at the margin of drainages or along a trend where palaeo channels existed early, sand and cohesive of alluvial origin are deposited.

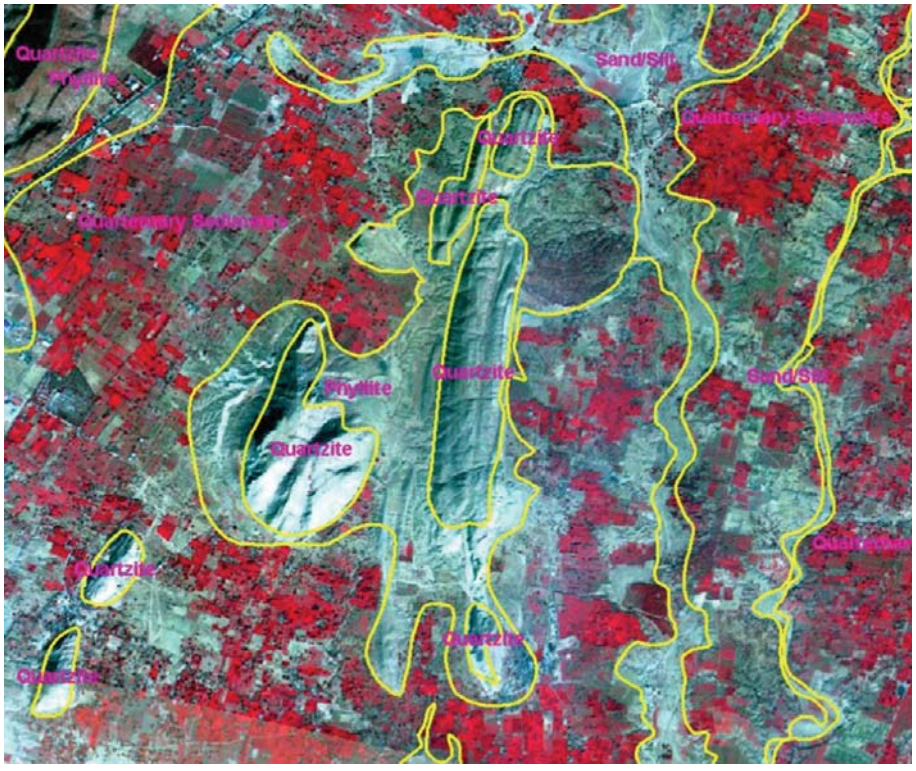

Figure 7.1.4: Lithological map of parts of Jaipur

Structures: The Delhi super groups of rocks are deposited in a synclorium and the trend of Delhi fold belt is NW-SE. The fold axis or orogeny of Delhi fold belt or Delhi orogeny is well depicted in the satellite data. Moreover, many fault and fractures are also delineated in Delhi group of rocks; which represent the pattern of brittle deformation in the area (Figure 7.1.5).

Geomorphology: The geomorphology of this area is very conspicuous and guided by the competence of the rocks. There are four major divisions in geomorphology. These are structural hill, denudation hill, pediment, alluvial plain and aeolian plan (Figure 7.1.6). Structural hills are formed as the result of regional deformation and their pattern and trend is guided by the regional deformation. These hills are very useful to map the regional fold belt of the Delhi Super group with the help of satellite data. Structural hill is subdivided in four categories e.g., highly dissected, moderately dissected, least dissected and linear ridge.

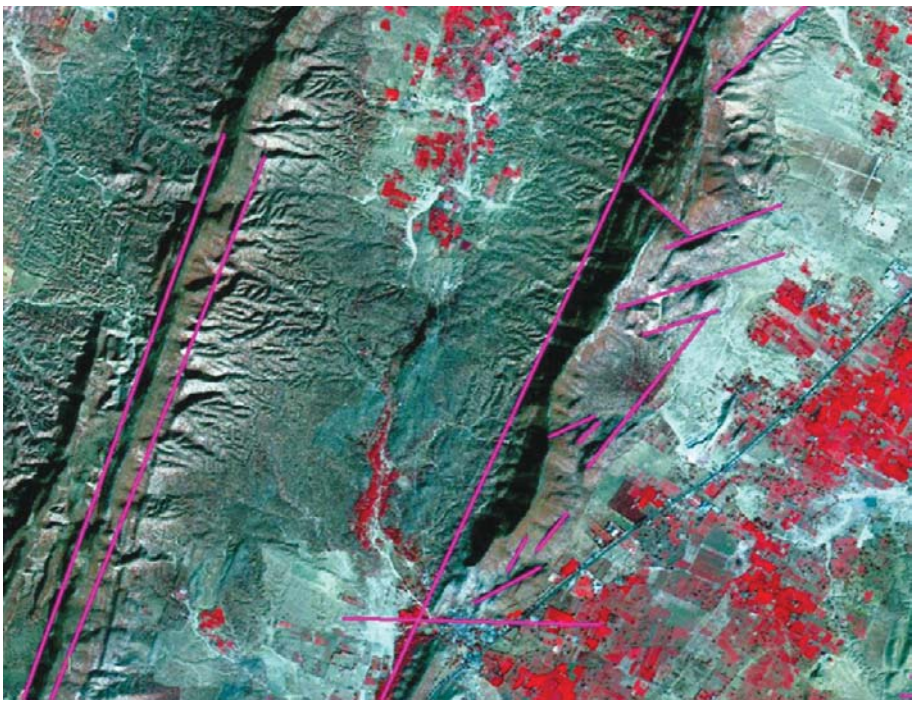

Figure 7.1.5: Lineament map of parts of Jaipur

These divisions are based on the trend of the structural hill and the amount of dissections is made by the fault, fracture and drainages. Similar subdivisions are possible in denudational hills but only two categories - least dissected denudational hill and moderately dissected denudational hills are present in this area. Denudational hills are remnant hills; which may be formed by the same orogeny; which has created the structural hill but amount of denudation is more over these hills. Aeolian plain has been divided into two categories based on the thickness of accumulated sand and its pattern. Isolated thick patches of sands are mapped as stabilsed sand dunes whereas the remaining area where veneer of thin sand deposition has taken place has been categorized as aeolian plain. In geology, any relatively flat surface of bedrock (exposed or veneered with alluvial soil or gravel) that occurs at the base of a mountain or as a plain having no associated mountain. Pediments are erosional surface of weaker rocks and inundated by lower order drainages and the weathered material of gully erosion of these lower order drainages moves downward and a thin or moderately thick weathered materials are accumulated at the base of pediment. Sometime weathered residue of each lower order drainages coalesces to form Bajada. Pediments are developed on lower grade metamorphic rocks like phyllite and schist. Alluvial plain are formed in the vicinity of present day drainage systems and also along the trend of older and buried drainage course.

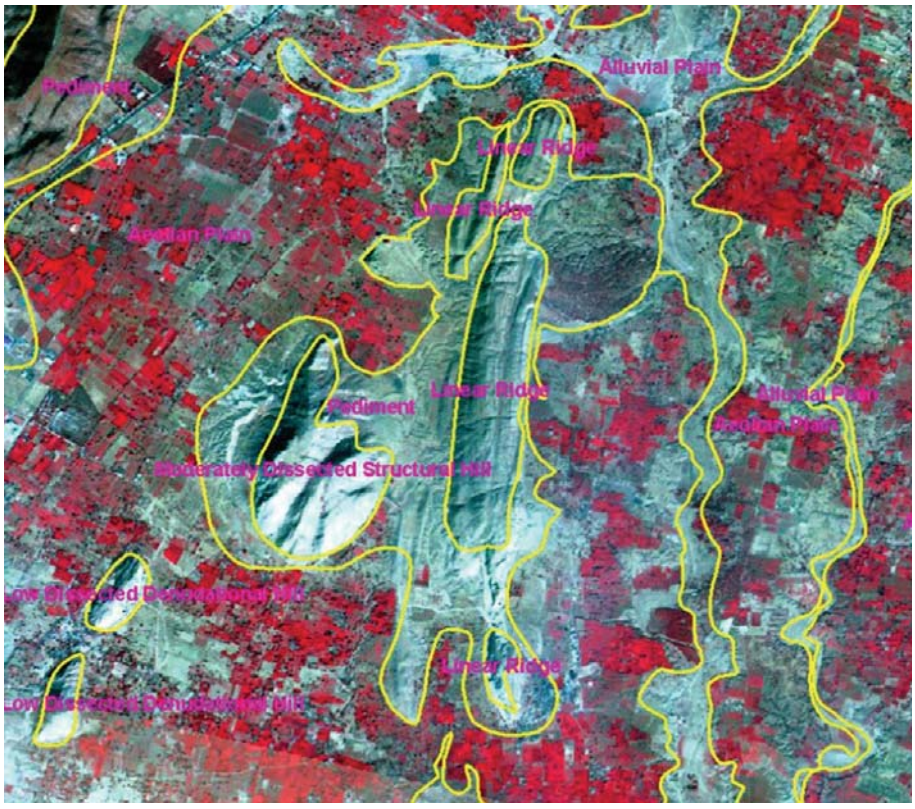

Figure 7.1.6: Geomorphological map of parts of Jaipur

7.1.10.2 Methodology

The geological informations were derived by on-screen or heads up interpretation followed by onscreen digitization process. IRS P6 LISS-IV data is used for the purpose of geological mapping. Geological map of the area at 1:250,000 scale was used as a reference for onscreen interpretation of units for lithology and structure. Geomorphological map on the other hand is entirely based on onscreen interpretation of landform. Photo-geologic elements and terrain elements were used to delineate various geological elements namely lithology, structure and geomorphology.

7.1.11. Summary

Remote sensing has given a big thrust to field of mapping. Remote sensing data analysis helped in updating the field-based lithological maps of regional structural analysis and geomorphological mapping. Synoptic coverage of satellite data facilitates faster and accurate mapping of landforms and therefore allowed to give better understanding between landform and processes.

7.2. Mineral Exploration

7.2.1. Introduction

The various mineral deposits occur in a vast variety of genetic associations. However, the commercial deposits of minerals are limited in genetic type and mode of occurrence (Gupta, 2003). This forms basic concept of mineral prospecting. Mineral exploration is the process; which is an endeavour of finding ore (commercially viable concentrations of minerals) to mine. Mineral exploration is a much more intensive, organized and professional form of mineral prospecting, though it frequently uses the services of prospecting, the process of mineral exploration on the whole is much more involved. Remote sensing data, by virtue of its synoptic overview, multispectral and multi-temporal coverage, can help in rapidly delineating the metallogenic province/belts/sites thereby cutting down the cost.

Remote sensing enables mapping the location of altered areas and regions of hydrothermal upwelling and outflow zones related to mineralization. The increased spatial and spectral resolution of satellite and airborne sensors provide powerful tool to exploration, evaluation and understanding of the genesis of mineral deposits. The use of remote sensing in mineral exploration began some 60 years ago with hand-held cameras being pointed out of aircraft windows and has since evolved through stereoscopic aerial photography to sophisticated space age technology, with satellite and airborne multispectral and hyperspectral digital imaging systems. The advent of sensor technology facilitates the generation of spectral signatures within very narrow spectral bands. These signatures help in identifying alternation minerals associated with significant mineral deposits. Moreover, the narrow spectral channels of an imaging spectrometer form a continuous reflectance spectrum of the earth surface in comparison to the broad channels of multi-spectral data. The critical aspect of the hyperspectral data processing lies in separating diagnostic spectral feature components from the background both in the pixel and sub-pixel domain and in assigning a meaningful class. There are various issues in the processing of such sensor data especially calibrating for reflectance with suitable atmospheric correction models, improving the Signal to Noise Ratio (SNR), reducing the redundancy, separating the spectrally pure end member and finally mapping them using pixel and sub-pixel based techniques. Spatial zones, relative abundances and assemblages of these minerals allow geologists to reconstruct the mineralogical, chemical and sometimes thermal disposition of ancient hydrothermal systems in their search for optimal drilling targets. Airborne hyperpspectral data has been successfully used for mapping mineral abundance in arid terrain (Boardman *et al.*,1995).

To maintain our economic growth we must continue mining for minerals, which requires rigorous exploration strategies for new deposits of all types. Mineral exploration is like looking for a needle in a haystack, so it is important to keep on exploring by integrating various technologies. New mineral prognosis models need to be developed with the emphasis on mineral paragenesis rather than its spatial occurrences.

7.2.2. Global, National Issues, Scenario Development

When the Landsat multispectral scanner (MSS) began operations in the early 1970's, remote sensing mineral exploration took an enormous leap forward but still functioned largely by way of photogeological interpretation of hard copy. Since then, the Landsat Thematic Mapper (TM) has provided the geologists with information relating to specific groups of minerals, specifically the iron oxides and clays.

In the 1980's, airborne remote sensing began with the development of the Airborne Thematic Mapper by Daedalus, the Geoscan instruments (MKI and MKII) by Australian Carr Boyd Minerals Ltd., the Collins' imaging spectrometers developed by Geophysical and Environmental Research Corporation of Millbrook, New York and the Airborne Visible Infrared Imaging Spectrometer (AVIRIS) developed by the Jet Propulsion Laboratory, Pasadena, California. All the instruments offered improved spectral and spatial resolution over their satellite borne predecessors and the AVIRIS instrument in particular, provided geologists with a means of discriminating and mapping individual mineral species and alteration assemblages. However, in the 1990's that the means of processing this data has become available to the average geologists through the development of low cost, commercial image processing and analysis software for desktop computer. The rapid growth in computing power and storage capacity in desktop computer has allowed the very large data files captured by the airborne instruments to be handled in a time frame compatible with the needs of mineral exploration.

The biggest challenge before geoscientists today is to locate new mineral deposits. Remote sensing techniques have emerged as powerful tools in recent times for isolating the favourable areas from unfavorable areas at regional level. Remote sensing data are mainly used to provide the reconnaissance level lithological, geomorphic and structural guide for any exploration programme. Geographic Information System (GIS) on the other hand, is used to integrate and analyze different types of spatial datasets, such as geological, geophysical and geochemical maps to derive mineral potential maps based on knowledge based integration of themes.

In India, several mineral exploration projects using remote sensing technology have been taken up in isolation. Mineral targeting has been attempted under the project like Vasundhara for southern Indian peninsular shield, Pur-Banera and Rajpura area for base metals, Diamond Exploration in Chattisgarh, Gold Exploration in Hutti- Maski Schist belt, Uranium Exploration in Umra area in Rajashthan, etc., (Krishnamurthy, 1999). In all these projects remote sensing data was integrated with the ground and geophysical data for narrowing down the target zones. Suitable prognostic models were developed for interpolating the results from know to unknown. A significant finding was the discovery of new kimberlite pipe in Tokapal, Chattisgarh using this technique. Faults, fractures and contacts often provide a conduit for depositional environment for hydrothermal or magmatic fluids in regions of known mineralization, and thus make excellent targets for further investigation. NASA's GRACE mission improved our knowledge of Earth's gravity field by more than 100 times and is helping to revolutionize our understanding of Earth's climate The unique design of the satellite-based GRACE mission, launched in the year 2002 with twin-satellites flying in formation is expected to lead to an improvement of several orders of magnitude in these gravity measurements and allow much improved resolution of the broad to finer-scale features of Earth's gravitational field over both land and sea. The Magsat project is another important satellite mission by NASA/USGS effort to measure near-earth magnetic fields on a global basis. Objectives include obtaining an accurate description of the earth's magnetic field, obtaining data for use in the update and refinement of world magnetic models. All these satellite-based geophysical observation would contribute to geoscientifc data pool and would form important scientific data sets for future exploration strategies. The synopticity of these satellite observations would provide the first hand information in hitherto unexplored zones.

7.2.3. Conventional and Scientific Methods in Practice

7.2.3.1. Methods/approaches for utilization of Remote Sensing data for Mineral Exploration

Primary rock-forming minerals as well as many secondary weathering and alteration minerals exhibit wavelength dependent (spectral) absorption features throughout the visible and infrared wavelength ranges of the electromagnetic spectrum. These features result from the selective absorption of photons with discrete energy levels and are dependent on the elemental composition, crystal structure, and chemical bonding characteristics of a mineral, and are therefore diagnostic of mineralogy (Burns, 1993; Clark, 1999;). In silicate, carbonate and sulfate minerals fundamental molecular vibrations cause strong spectral features that appear as emissivity minima (reflectance maxima) in the 8–12 µm region (Hook *et al.*, 1999; Salisbury *et al.*, 1991). This region coincides with a window where Earth's atmosphere is relatively transparent to TIR (Thermal infrared radiation) and is also the region of maximum emission from a 300 K temperature bearing body (e.g., Earth), making it ideal for terrestrial geologic remote sensing applications (Kahle *et al.*,1993). For silicate minerals the wavelength position of the emissivity minima (''reststrahlen bands'') shifts to longer wavelengths with the increasing isolation (decreasing polymerization) of tetrahedral SiO_4 molecules in the crystal structure (Hook *et al.*, 1999).

The steps involved in mineral exploration include area selection, target definition, resource evaluation, reserve definition and extraction. Remote sensing plays an important role in the first two stages of mineral exploration.

Spaceborne multispectral sensors/ hyperspectral sensors can detect the spectral signatures characteristic to the alternation zone associated with a mineral deposit. These features can easily be detected specially in airborne hyperspectral scanner. The detection of alteration zone, favourable geological structures prospective for mineral deposits or suitable host rock of any particular mineral helps in area selection and target delineation phase of the mineral exploration. Other collateral data, namely geological map, geochemical data, and geophysical data is required along with remote sensing data to model the reserve potential. Since remote sensing helps deriving information on surface feature, it is not suitable for modeling a target for exploring a deep seated mineral deposit. A schematic diagram at Figure 7.2.1 is given below to show the steps generally followed when remote sensing data is used in integrated manner with other geoscientific data.

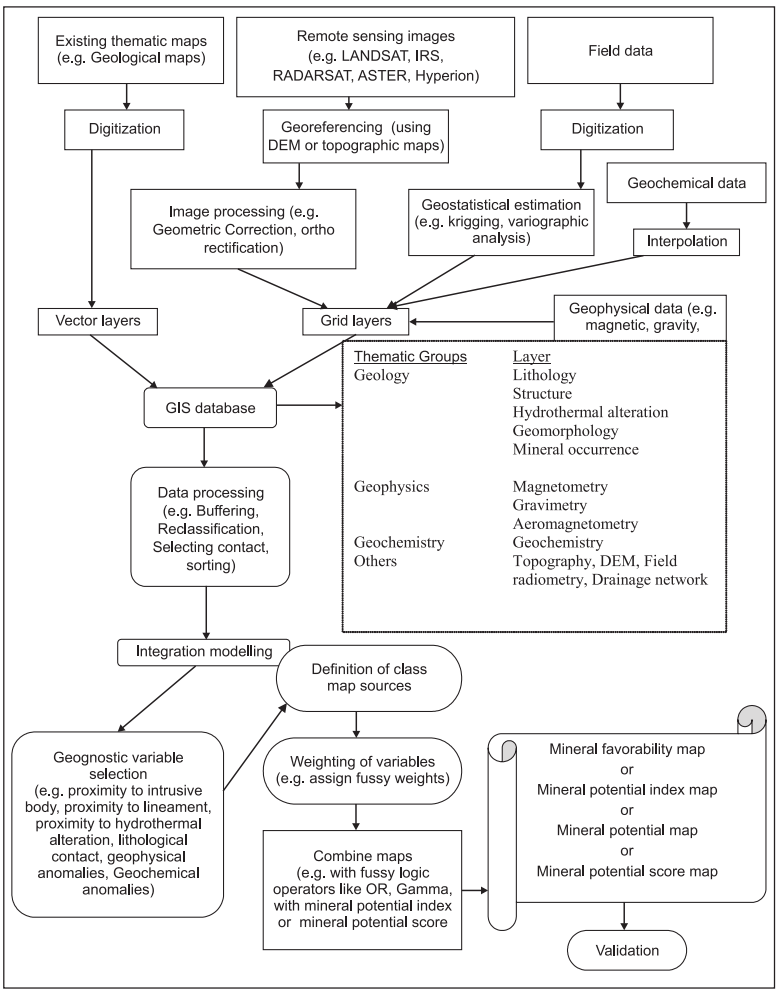

Figure 7.2.1: Steps used in Integration of Remote Sensing data with other Geoscientific data for Minaral Exploration

7.2.3.2. Methods for Oil field Detection through Remote Sensing

The primary source material for the origin of petroleum is generally considered as organic but theories on inorganic origin also exist. Early ideas and theories leaned towards the inorganic source whereas the modern theories consider organic matter as the only potential source, which occurs in a wide variety of both animals and plants. Petroleum occurs at considerable depths below the surface in sedimentary basins. It is formed in specific geological environment represented by source rock for the formation of oil from organic debris under particular pressure and temperature conditions, ultimately migrated, entrapped and accumulated in reservoir rock. A petroleum bearing basin must exhibit several important characteristics including-

- Source rock from which petroleum is generated and a thermal history which provides suitable thermodynamic conditions for the evaluation and release of the petroleum from rock
- Rocks with adequate porosity and permeability to allow migration and become a reservoir and a cap rock to seal further migration
- Structural and stratigraphic traps in which petroleum can accumulate
- Timing factors, which bring all of the geological and geochemical factors together at the right time in such a way that generated hydrocarbons are entrapped and preserved

The other factors that control petroleum accumulation is the sequence of the earth's movements, release of internal pressure and compaction of source rocks, all taking place over geological time scale. Thus, petroleum accumulation is controlled by structural changes which at any given time can be visualized by the study of folds, faults, domes, unconformities, etc.

7.2.3.2.2. State of the-art techniques for Petroleum Exploration

Remote Sensing: The remote sensing plays a major role in regional geological mapping. It is the basis for reconstructing the geologic history of a region and for locating areas having the greatest promise for buried petroleum deposits. Remote sensing data helps in identifying the following four basic terrain elements important for oil exploration.

- Structural Mapping: Folds, faults, fractures and joints

- Rock type mapping : Rock types can be recognized on the basis of colour, texture, landform pattern, thermal inertia etc
- Geomorphic Analysis: In areas where the bedrock is obscured by surfacial deposits or vegetation, evidences of underlying geologic conditions are reflected at the surface but are only suggestively revealed through detailed geomorphic analysis. Drainage patterns, landforms, fracture patterns, and tonal or colour anomalies are valuable clues in this analysis
- Surface indications of hydrocarbons: The hydrocarbons escaping from the traps can alter the surface rocks to produce colour, mineralogic and vegetation anomalies, which can be detected by remote sensing techniques. The primary objective of using remote sensing technique for onshore exploration is to detect anomalies indicating possible presence of petroleum bearing structures at depth. Some of the anomalies which manifest on remote sensing data include:
  - High heat flow associated with hydrocarbon bearing structure (thermal IR data)
  - Vegetation or soil anomalies and subtle tonal anomalies resulting due to interaction between soil/ vegetation (SWIR) and
  - Chemical alteration zones caused by vertical migration (thermal inertia mapping)

7.2.4. Literature Review

Several noteworthy works have been carried out on mineral exploration at global level. Several examples of this type of application are known in the literature. For example, using Landsat MSS data and supervised classification, Halbouty (1976) located the likely extension of strata-bound copper deposits in the Tertiary Totra sandstones of Bolivia, into adjoining territory of Peru. Guild (1972) reviewed the relationship between mineral exploration and global tectonics. Offield *et al.*,(1977) using satellite data discovered a significant ore controlling linear feature in South America. Bowers (1996) integrated lineament structures derived from Landsat TM and SAR data with a database for known occurrences in GIS for more fruitful interpretation of lineaments for mineral exploration.

Alteration zones often accompany mineral deposits and constitute one of the most important guides for mineral exploration. These are very important for hydrothermal deposits, which include metals such as copper, lead, zinc, cobalt, molybdenum, etc. This type of alteration zones with phyllosilicates has been delineated in satellite based mineral exploration study (Abrams *et al.*, 1977). Spectral characteristics of limonite have been successfully used for mapping and exploration of hydrothermal deposits (Conradson and Harpoth,1984). Fraser (1991) adopted Directed Principle Component Technique (DPCT) for discriminating ferric oxide (hematite and goethite) from vegetation. Rowan *et al.*,(1974) demonstrated the utility of ASTER data for mapping the hydrothermally altered areas from regional rocks and soil units in Pakistan.

Suitable sites for placer deposits i.e., diamond, gold, monazite, etc., also can be better located on the remote sensing data. For example fluvial placers also can be identified by delineating buried channels, abandoned meander scars, scrolls etc (Gupta, 2003). Geological structure plays a major role in locating an ore deposits in metallogenic provinces.

In geobotanical remote sensing, several contributions have been made to demonstrate the capability of spectral behaviour of geobotanical elements in mineral exploration. For the purposes of mineral exploration, the geobotanical changes are of three types: structural, taxonomic and spectral (Mouat, 1982). These changes can easily be studied using remote sensing data. It is reported that the red band absorption (0.67 micrometer) is more characteristics of concentrated heavy metals in soil, rather than red edge, the absorption band being regularly shallower and narrower over mineralized areas (Singhroy and Kruse, 1991). Mathematically, modeling for mineral exploration was attempted in Rajpura- Dariba – Lunera mineralized belt. A number of favorability index maps based on unweighted, weighted and logical models were generated (Bhattacharya *et al.*,1993). Nasipuri *et al.*,2006 has shown the utility of day and consecutive nighttime Advanced Spaceborne Thermal Emission and Reflection Radiometer (ASTER) data over a part of the Cambay basin, Gujarat, India in generating thermal inertia images. The thermal inertia map has been utilized for exploration of petroliferous basins.

A significant improvements in the spectral resolution has led to increase in narrow spectral band to generate hyperspectral images. The narrow spectral channels of an imaging spectrometer forms a continuous reflectance spectrum of the earth surface in comparison to the narrow channels of multi-spectral. Imaging spectroscopy resolves the narrow absorption bands in the spectrum which can be used to identify specific parameters. In

particular, images that represent the effects of diagnostic absorption bands can be produced to show specific variability of certain material features. Absorption bands play a key role in defining the spectral curves of the different terrain parameters. The critical aspect of the data processing involves separating this component from the background both in the pixel and sub-pixel domain and assigns a meaningful class. There are various issues in the processing of such sensor data especially calibrating for reflectance with suitable atmospheric correction models, improving the Signal to Noise ratio (SNR), reducing the redundancy, separating the spectrally pure end member and finally mapping them using pixel and sub-pixel techniques Spatial zones, relative abundances and assemblages of these minerals allow geologists to reconstruct the mineralogical, chemical and sometimes thermal disposition of ancient hydrothermal systems in their search for optimal drilling targets. Airborne hyperpsectral data has been used for mapping mineral abundance in arid terrain (Boardman *et al.*,1995). The EO-1 Hyperion sensor launched by NASA covers the 0.4 to 2.5 microns spectral range with 242 spectral bands with 10 nm band width.

Aeromagnetic surveys are widely used to aid in the production of geological maps and are also commonly used during mineral exploration (Bhan *et al.*,1991, Hegde *et al.*,1983). Some mineral deposits are associated with an increase in the abundance of magnetic minerals. The integration of remote sensing data with aeromagnetic data seems as important tool for mineral exploration. Regional aeromagnetic surveys have been undertaken by National Remote Sensing Centre (NRSC) since 1981 under National Aeromagnetic Project sponsored by Airborne Mineral Surveys and Exploration Wing (AMSE) of the Geological Survey of India (GSI). Under this programme states of Tamil Nadu, Karnataka, Kerala and parts of Andhra Pradesh, Maharashtra, Madhya Pradesh, Orissa, Bihar and Gujarat, Upper Assam shelf covering parts of Arunachal Pradesh, Assam, Meghalaya & Nagaland and the entire Vindhyan basin was covered. So far, NRSC(National Remote sensing Centre) has acquired, the aeromagnetic data for about 5.00 lakh line kms and prepared about 2, 200 maps on 1:50,000, 1:250,000 and 1:500,000 scales.. These maps and the data are being utilized in the ongoing exploration programmes of GSI, ONGC and DGH for planning detailed ground geoscientific investigations and also utilized in the project Vasundhara (geoscientific database creation for mineral exploration), which was taken up jointly by the Department of Mines and the Department of Space, GOI. Recently High Resolution Aeromagnetic (HRAM) surveys was carried over Ganga basin for Directorate of Hydrocarbon with the state-of-the-art survey and data processing procedures for identifying oil bearing structures in the basement as well as within the sediments.

7.2.5. Gap Areas

Since many of the unexplored mineral deposits occur at considerable depths below the surface, exploration techniques for those minerals is geologically more complex and uncertain. In such cases, for mineral target delineation would not be possible by remote sensing method unless indirect geologic signatures indicative of mineral deposit are present on the surface. Hence, the detection of mineral zones depends mainly on the geological, geophysical, geothermal, geochemical and geobotanical parameters of the area. An integrated approach utilizing a wide range of remote sensing devices which measure spectral signature from the space and aerial platforms and the geophysical techniques; which measure various physical properties of the subsurface rocks would certainly define potential target areas. Aerogeophysical data can provide supplementary information that is useful for targeting shallow subsurface deposits. Aeromagnetic survey is a potential reconnaissance tool in mapping the regional surface and subsurface structures. Measurements of variations in the earth's magnetic field are used to determine the configuration of crystalline basement rocks that commonly influence the development of hydrocarbon trapping structures in overlying sedimentary rocks. Another important geophysical technique is gamma ray spectrometer survey. Uranium, thorium and potassium concentrations have been found to be related to gamma field intensity of surfacial geologic materials, and the measured concentrations being a product of radio-active mineral fixation. It can also help in oil field detection. The processes of fixation are known to be influenced by oil/gas habitat and, therefore can represent surface manifestation of possible hydrocarbon occurrence at depth. A low activity area, characterized by gamma field sink, and rimmed by 10-15% increased activity is observed generally over oil/gas bearing structures. These geophysical techniques are needed to be integrated with remotely sensed data to delineate potential zones for detailed exploration. Without such integration, remote sensing data would be of little use for mineral exploration surveys.

Availability of spaceborne sensors extracting different geophysical/geochemical signatures would be more useful in mineral exploration. For example, aerogeophysical/ aeromagnetic signatures and remote sensing based spectral informations, received from a mineral prospective terrain will help more realistic identification of mineral potential zone.

7.2.6. Case Study

Conjuctive use of remote sensing and geophysical data over parts of Deccan Syneclise for hydrocarbon exploration

7.2.6.1. Introduction

With the increase in demand for the petroleum products and diminishing indigenous production, it has become necessary to look for probable potential zones even in locales that were hitherto known as areas with bleak prospects. The study area consists of series of basaltic lava flows presumed to have been erupted on to the surface during Cretaceous – Tertiary period, blanketing all pre-existing rocks ranging in age from pre-Cambrian to Cretaceous. Deccan Syneclise is a super order negative platform structure with appreciable thickness of sediments below the Trap. The mesozoic sediments, throughout the world, are known sources for hydrocarbons and are potential source rocks for more than 50 % of the world's hydrocarbon reserves. These sediments are expected to be present below the northwestern, northeastern and middle parts of the Deccan Syneclise. The discovery of hydrocarbons in the Mesozoic sediments in Jaisalmer basin (Goru & Pariwar formations) and East Godawari sub-basin (Narsapur & Mandapeta structures) indicated the significance of looking for structures entrapping hydrocarbons in Mesozoic sediments in Cambay basin and adjoining trap covered areas. The hydrocarbon prospects of the Deccan Syneclise are still poorly understood, as the studies are based only on the sparse sedimentary exposures. The evaluation of the basin for the Mesozoic prospects is a challenging job in the absence of adequate geophysical data. The study area is bound between the 73º 00' to 75º 05' E and latitudes 20º 50' to 22º 00'N and covered by six topographic sheets (46 G, 46 H, 46 K, 46 L, 46 O and 46 P) of Survey of India on 1:250,000 scale and form north western parts of Deccan syneclise.

The study area of about 40,000 sq. km. has been covered by 6000 gravity stations and the gravity data was acquired along roads and tracks at approximately 2 km spacing using Lacoste Romberg G-type gravimeters (LRG) with an accuracy of 0.01mGals. The data was processed and modeled. Comparison of the elevation, free air and regional and residual Bouguer anomaly maps clearly indicate the crustal density distribution of the region. The broad gravity low over the Cambay basin is due to the known Tertiary filling. The residual gravity low over the Shirpur and the semi-circular Residual gravity low encompassing the Navapur may be interesting for the subtrappean Mesozoic sediments. The Bouguer anomaly map of the gravity data was interpreted for major regional faults. Magnetotelluric (MT) method is considered to be one of the effective techniques in delineation of sediments buried below the trap covered layers, since it has a marked resistivity contrast with the underlying basement and also with the overlying volcanic cover. This technique is one of the well-known geophysical techniques to probe the earth into much deeper crustal layers. This study provides a detailed electrical structure, which in turn could be interpreted in terms of lithology, and geological structure over a range of depths extending from very shallow levels to as deep as few tens of kms. A total of 511 MT soundings were carried out in the study area. A major sedimentary basin is delineated from this study between Narmada – Tapti rivers towards eastern part of the study area. The thickness of the Mesozoic sediments below Deccan traps is of the order of 2.5 to 3 km and also possesses relatively low resistivity as compared to the sediments delineated in other parts of the region. Over the study area 50 DRS stations were carried out, which could successfully delineate a major sedimentary basin covered under trap in the eastern part of the area. The DRS results are found to be very consistent with the results from other studies such as MT, Gravity and Seismics. The total thickness of the Tertiary and Quaternary sediments in the deepest part of the basin is expected to be of the order of 5000 m resting on the Deccan Trap floor. In the Narmada valley and adjoining areas, the trap thickness is about 700 – 800 m. In the area south of the Narmada River, a few gravity-magnetic computations did earlier indicate the traps to be thicker than 1500 m. Thus the older works have revealed that the Cambay – Narmada – Tapti rift zone holds potential Mesozoic sediments for hydrocarbon exploration. The geophysical investigations in the trap covered areas of Kutch and Saurashtra by NRSC and NGRI (NRSC, 1998; NGRI, 1998, 2000) respectively was a proved and fruitful effort in delineation of the structures. The gravity, DRS, MT and seismic data was acquired and processed by NGRI, Hyderabad .

7.2.6.2. Methodology

The IRS P6 - AWiFS geocoded digital data of the area was co-registered with the geophysical data. The profiles along which the geoelectrical sections have been constructed based on DRS stations and the gravity and resistivity profiles along which the actual field observations were collected, were scanned, digitized and registered on to the satellite image. The geo-referenced satellite data was interpreted for the geological structures namely faults /

lineaments based on the 'length-based classification' and 'geomorphic anomalies' using digital image processing techniques. Some of the required geophysical observations were coded as separate vectors into this attribute. This was used to understand the inter-layer relationship and also to confirm the satellite-derived information.

A regional geological structure assessment of the basin was carried out to understand the manifestation of any sub-surface geological structure for hydrocarbon exploration. The basic geological information like lithology and the stratigraphic details were taken from published geological quadrangle maps of Geological Survey of India on 1: 2 million scales. Figure 7.2.2 demonstrates the steps followed to prepare structural map and associated geomorphic anomaly to indicative of favorable zone of oil accumulation (Figure 7.2.3).

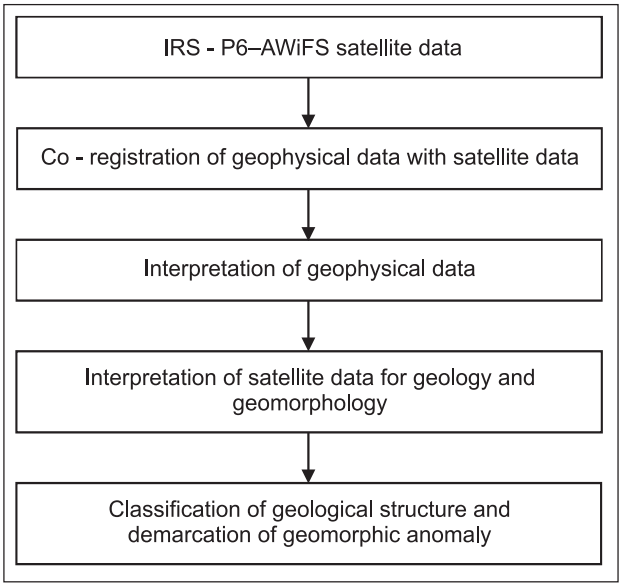

Figure 7.2.2: Schematic diagram of the approach

There are basically three major trends of lineaments and faults in this area i.e., NW-SE, NE-SW and ENE-WSW. The NW-SE trend is the oldest one corresponding to the Pre-cambrian trend. The mega fault has prominent ENE-WSW trend, which corresponds to the Mesozoic group. Prominent geomorphic anomalies are observed in the area, coinciding probably with the subsurface basement high. Two areas of tectonic activity, one in the north-western part around Dediapada village and the other in the eastern part around Shirpur village were also identified by the integrated analysis of remote sensing and geophysical data interpretation. These may be the potential zones for oil bearing formations.

7.3. Geoenvironmental Studies

7.3.1. Introduction

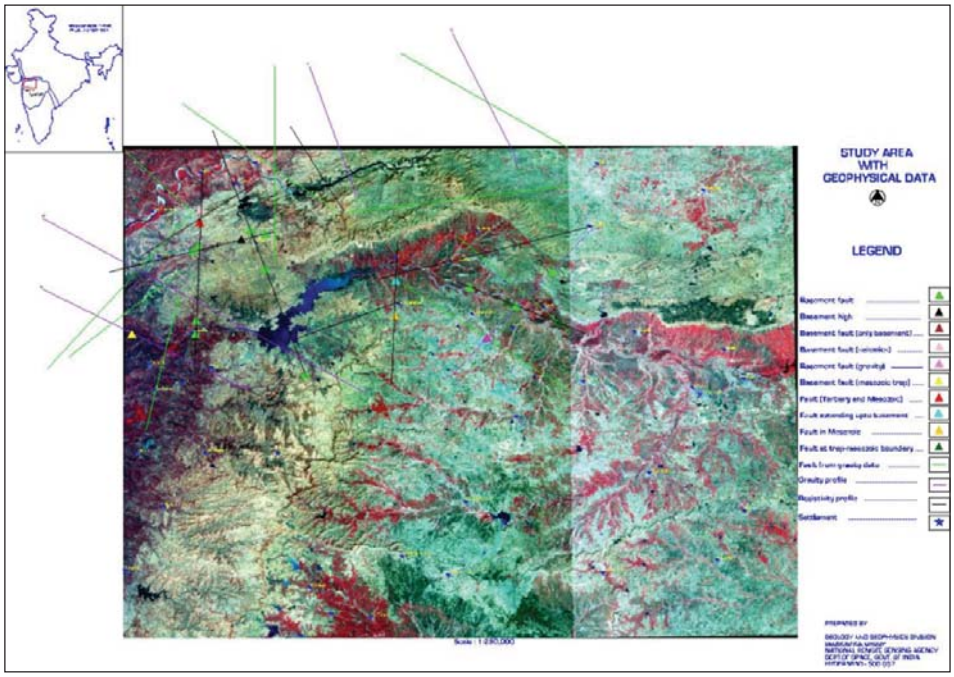

Figure 7.2.3: Geophysical interpreted map of Narmada Tapti Region

Environmental geoscience is a highly interdisciplinary in nature with offshoots extending to almost all scientific disciplines. The application potential of remote sensing techniques for environmental surveillance stem from their unique advantages: a multispectral approach, synoptic overview and repetitive coverage i.e., the possibility of examining objects in different spectral ranges, in the perspective of regional setting and repetitively at certain time intervals. Broadly, various genenvirornmental problems can be related to changes or degradation of land, water, air or vegetation resources. Following geoenvironmental studies can be taken up using remotely sensed data.

- Land-use changes associated with open – cast strip mining

- After-effects of underground mining, such as subsidence etc
- Evolution of dumping grounds
- Spread and dispersion of smoke plumes from industries and power plants
- Discharge of thermal plumes from power plants and industries in rivers and lakes
- Deforestation and erosion in river catchments and sediment load studies
- General warming of the environment in industrial areas
- Discharge from nuclear power plants and associated environmental hazards
- Degradation in quality of vegetation, due to atmospheric pollution in industrial areas and metropolitan cities

In addition, investigations into many other specific problems are also possible.

The presence of an oil film on a water surface leads to a lower emissivity. Although the kinetic temperature for a oil film and the clear water is same, the difference in the emissivity produces a differences in radiant temperature of the order of 1.5^{0} C. As most thermal detectors have a temperature sensitivity of the order of 0.1^{0} C, this difference between oil slick and surrounding water can easily be measured. Coal fire is one of the major environmental problem specially in the coal field area in countries like China, India, South Africa, USA, Venezuela and other countries. Coal fires burn out valuable energy and also create environmental pollution. Satellite and airborne thermal infra red surveys play an important role in mapping coal fires in timely and cost-effective manner.

7.3.2. National and Global Scenario

The applicability of remote sensing in monitoring the environmental impacts of human activity is immense. Several environmental hazards like coal-fire, subsidence due to mining activity are being monitored from satellite data. Satellite based thermal data from medium resolution thermal channel like ASTER can help in periodic monitoring of coal fires in coalfields on India, China, Africa. Microwave data (ERS data, Radarsat-2) with tandem acquisition can help in determining the subsidence associated with the mining activity. Moreover, in microwave data (ERS data, Envisat ASAR, Radarsat-1&2) are of great use in monitoring natural and artificial oil-slick mapping.

7.3.3. Literature Survey

Remote sensing is an important tool for understanding the dynamics of earth surface processes. Remote sensing technology is an important tool in delineating high temperature earth features such as coal mine fire, surface fire, volcano etc. In the electromagnetic (EM) spectrum the thermal infrared region with the wavelength domain 3-5 µm and 8-12 µm is actually used in remote sensing for delineating high temperature bodies because atmosphere acts almost transparent to the EM spectrum in above mentioned range. With the advent of thermal remote sensing several algorithms have been developed and proved to calculate the emissivity of thermal pixel in domain of thermal remote sensing with an effort to accurately calculate the temperature of thermal pixels. The major applications of thermal remote sensing was confined to delineating coal fires and estimating the spatial extent and temperatures of coal fires. During 1960s, when air borne thermal sensor data and later when satellite borne thermal scanner data became available, remote sensing-based coal fire detection and monitoring became operational (Gangopadhyay *et al.*, 2005). Most of the researchers used broadband thermal channel of Landsat TM/ETM+ to monitor and model the coal fire zones in earlier phase of geological thermal remote sensing (Reddy *et al.*, 1993). In these studies most researchers applied an average emissivity value (0.96) to represent all land cover. At the later stage of research, pixel integrated NDVI value obtained from medium to high resolution space borne sensors like TM/ETM, IRS/LISS, etc. have been found appropriate to derive average emissivity of land surface classes (Chatterjee,2006). It is found that NDVI has empirical relationship between average value of thermal emissivity and normalized difference vegetation index (NDVI) for different surface covers (Van de Griend and Owe,1993). This empirical relationship has been proved from the field measurement of the both the parameter.

Prakash *et al.*,(1995) and Saraf *et al.*,(1995) have contributed to the mapping coal fires and to estimate the depth of coal fires. But the depth modeling of subsurface hot features (such as subsurface coal fires) from satellite remote sensing data is still in infancy since many parameters are required for the depth of subsurface coal fires. Moreover, coarse spatial resolution of thermal satellite data precludes monitoring and mapping coal fires with very

small spatial extent and moderate temperatures. In India, Landsat TM and ETM thermal data have been used to delineate the coal fire zones in coalfields in the last decade of twentieth century. The coal fires in Jharia coalfield were studied in detail and efforts also were made to map the subsurface coal fires with little success. Recently, NRSC has produced coal fire map of Jharia (October 2006) and Raniganj coal field (December, 2006) of India with the help of night time ASTER data. Guha (2007) delineated major coal fire zones in the western portion of the Raniganj coalfield and localized along the open cast mines of the coalfield. Vinod Kumar *et al.*,(2006) have evaluated the dynamics of the coal fire in Jharia coalfield . Another important utility of thermal remote sensing is monitoring very high temperature features such as volcano with the help of thermal channel of satellite data. Researchers are using the thermal data for monitoring the volcanic eruptions in different part of the world. Thermal channels of Landsat TM data have been used to monitor the Barren Island Volcanic eruption (Reddy *et al.*, 1993) Moreover, very high temperature phenomenon also can be monitored in visible domain of electromagnetic spectrum. Eruption in Barren Island was delineated using IRS P6 AWiFS sensor images (Vinodkumar *et al.*, 2006).

7.3.4. Case Study

7.3.4.1. Introduction

Coal fire is a serious problem in Indian coal field such as Jharia coal field, where high ranking coals are burning due to this hazard. The combined act of surface and sub-surface fires and subsidence has endangered the environmental stability of Jharia coal field. Coupled with the ecological damage done by open cast mining, this has made parts of Jharia resemble moonscapes with dark rolling hills and deep smoking ravines. Remote sensing data have immense potential in coal fire studies. In the present study, delineation of coal fire, which is a major environmental problem in coal mining areas, is addressed using Landsat-7 ETM+ (60 m resolution) and ASTER (90 m resolution) thermal infrared images to demarcate the coal mine fire areas from non fire areas. For this study, Landsat-7 ETM+ data of 29th March, 2003 and ASTER data of 9th October, 2006 were used. Landsat-7 ETM+ data have the best spatial resolution in thermal band among many of available commercial satellites operating in thermal region. The kinetic temperature was calculated from Landsat ETM+ satellite data using NDVI derived emissivity models whereas band 13 of ASTER nighttime data was used with fixed emissivity value to derive kinetic temperature. The study reflects that eastern part of the Jharia coalfield is most affected by the coalmine fire in comparison to western part. The collieries affected by coalmine fire are Kusunda, Kujama, Bararee, Ena etc. Amongst all the colliery areas, Kusunda area is most affected (29% of total area) by coalmine fire. It also shows significant increase (28%) in fire from 2003 to 2006. The coalmine fire and non-fire areas were further verified on the ground and fire temperature on the ground was measured using the handheld infrared thermometer. The final coal mine fire map of Jharia coalfield was prepared by using density-slicing techniques with the information collected from the ground. The surface features map prepared using IRS-P6 LISS-III data shows the distribution of land use / land cover units such as forest land, built-up area, agricultural land and mining area etc. An estimated 6.9% of the total area in Jharia coal field is occupied by mining related activities, which depicts the vulnerability of the area for environmental degradation.

7.3.4.2. Remote Sensing Data Analysis: Principles of thermal remote sensing

All matter at temperature above absolute zero (0º Kelvin) emits electromagnetic radiation continuously. The temperature of the earth materials and high temperature phenomena can be estimated based on the thermal emission from these materials. Max Planck, using his quantum theory, developed a relation between spectral radiance, wavelength of the emitted radiation and temperature for the blackbody. The Planck's equation for black body is given in equation -1.

$$L_\lambda = \frac{2\pi hc^2}{\lambda^5} * \frac{1}{e^{hc/\lambda\kappa T_{rad}} - 1} \qquad (1)$$

Where

L_λ = Spectral radiance in band-6 ($W/m^2/Sr$) of Landsat-TM
λ = Wavelength (μm) in band-6 of Landsat-TM
T_{rad} = Radiant Temperature (°K)
h = Planck's constant (6.63×10^{-34} joule sec)
c = Speed of light (3.0×10^8 m/sec)
k = Boltzmann constant (1.38×10^{-23} joules/k)

Equation (1) can be rearranged as follows

$$T_{rad} = \frac{C_2}{\lambda \ln(\in C_1/\pi L_\lambda \lambda^5 + 1)} \qquad (2)$$

Where,
C1 = $2\pi hc^2 = 3.742 \times 10^{-16}$ Wm^2
C2 = hc/k = 0.0144 mK
$\in$ = Emissivity

In equation - 2, wavelength may be considered as the mean wavelength of the spectral region under investigation. Once the corrected spectral radiance (L_λ) is known for a pixel, it can be substituted to equation – 2 to compute radiant temperature value. The radiant temperature is defined as the equivalent temperature of a black body which would give the same amount of radiation, as obtained from a real body. The radiant temperature (TR) depends on actual temperature of surface element i.e., kinetic temperature (TK), emissivity (ε) and transmissivity of atmosphere (Gupta, 2003). Emissivity (ε) for a blackbody is 1 and for most materials it is less than 1 ranging generally between 0.7 and 0.96. So the kinetic temperature of natural materials is always higher than the radiant temperature.

In the present study, coal fires were mapped on the basis of their temperature from the back ground non fire zone. Coal fires not only occurs due to different causes (man-made, lightning strike, accidental fire, forest fire or spontaneous combustion) worldwide, but also have a along history (Zhang 2004). Coal fires are very high temperature surface elements and emit high thermal flux. Coal fires are very close to black body in terms of their thermal behaviour but emissivity of fire zones are dependant on several factors such as presence of moisture in coal, the total carbon concentration in coal, etc. Coal fires with high thermal flux are restricted in terms of surface extent. Therefore total thermal flux of pixel area of 3600 m^2 (in case of Landsat-7 ETM+) and 8100m^2 (in case of ASTER Data) represent the average thermal flux emanating from both coal fire zones and non coal fire area of given pixel. The emissivity and radiant temperature of a pixel containing fire depends on the entire contributing element within the pixel. If pixel averaged radiant temperature remains quite higher than the pixel containing no fire, then only coal fire zones can be delineated.

7.3.4.3. Methodology

A. Processing of Landsat-7 ETM+ data

Landsat-7 ETM + thermal band (band no. 6). Landsat-7 ETM+ data is acquired in .hdf (hierarchical data format) format and scene specific radiance value is calculated from raw digital values by using by Markham and Barkar equation (Markham and Barkar, 1986).

$$L_\lambda = L_{min\,(\lambda)} + [(L_{max\,(\lambda)} - L_{min\,(\lambda)})/Q_{calmax}] * Q_{cal} \qquad (3)$$

Where

L_λ = spectral radiance,
$L_{min\,(\lambda)}$ = minimum detected spectral radiance for the scene,
$L_{max\,(\lambda)}$ = maximum detected spectral radiance for the scene,
Q_{cal} = Grey level for analysed pixel,
Q_{calmax} = Maximum grey level,

Once the spectral radiance (L_λ) for ETM+ band 6 data is computed, it is possible to calculate radiant temperature directly using equation – 4 provided in the Landsat-7 users' handbook.

$$T_R = K_2 / \ln((K_1 / L_\lambda) + 1) \qquad (4)$$

Where

T_R = Radiant temperature,
K_1 = Calibration constant (1260.56 K),
K_2 = Calibration constant (666.09 watts/(meter squared*ster*μm)),
L_λ = Spectral radiance

Once the radiant temperature is obtained it is possible to calculate kinetic temperature provided emissivity is known using equation - 6.

In the case of single band thermal data, a possible option to extract land surface emissivity could be a classified image, in which an emissivity value for each class is assumed (Gangopadhyay, 2003). The methodology to extract land surface emissivity from NDVI has already been described by many researchers (van de Griend and Owe, 1993). The method of NDVI gives three classes of emissivity.

- NDVI < 0.2 – bare soil
- NDVI > 0.5 - vegetation
- NDVI between 0.2 - 0.5 - comes under the pixel of category of mixed pixel, which contains combination of vegetation, soil and rock etc. An empirical relationship between the average values of thermal emissivity and normalized difference vegetation index (NDVI) for different surface covers was established from the field measurements of both parameters and the relationship is as follows

$$\varepsilon = a + b * \ln (NDVI) \qquad (5)$$

Where, ε and NDVI are average thermal emissivity and average normalized difference vegetation index for individual surface covers respectively, 'a' and 'b' are two constants (a=1.0094 and b= 0.047 for a correlation coefficient of 0.941 at 0.01 level of significance). Satellite-based measurements of NDVI have been found helpful in making close approximation of real estimates of thermal emissivity (van de Griend and Owe, 1993).

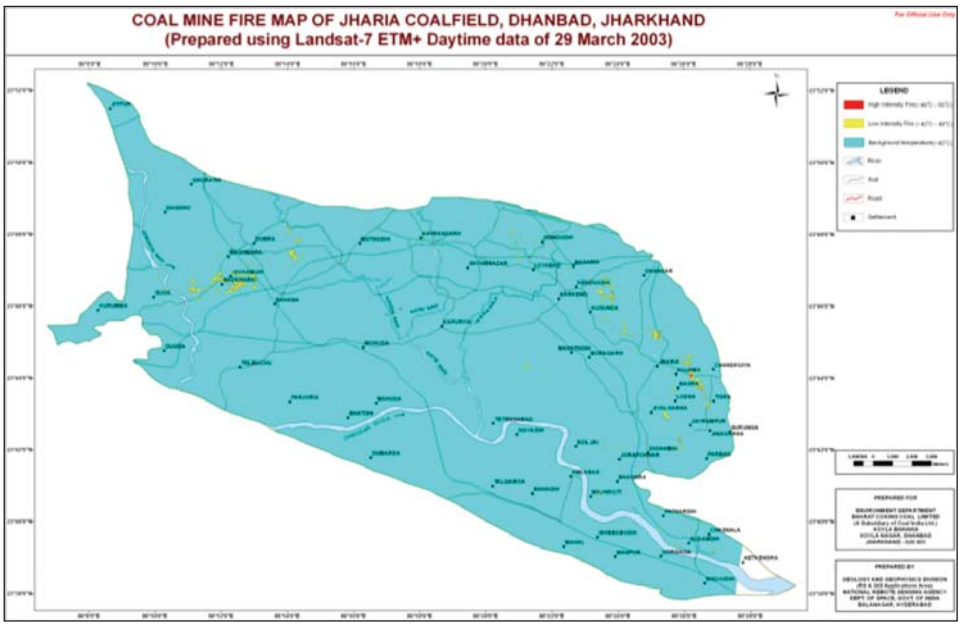

Figure 7.3.1: Coal mine fire map of Jharia coal field, Dhanbad, Jharkhand

Pixel-integrated NDVI values from medium resolution satellite sensors like Landsat-7 ETM+, MSS are appropriate for this purpose owing to their pixel size comparable with respect to thermal data (Chatterjee, 2005). In this work Landsat-7 ETM+ data was used to compute the NDVI.

Once the NDVI is derived, emissivity is calculated using equation - 5. The emissivity was subsequently resampled to the spatial resolution of thermal data i.e., 60 m. Once emissivity is derived, it is used to extract kinetic temperature using following equation.

$$T_K = T_R / \varepsilon^{1/4} \qquad (6)$$

The kinetic temperature computed from the satellite data by using above mentioned procedure was further classified into three classes as given in Table 7.3.1 to prepare the coal mine fire map of the Jharia Coal field (Figure 7.3.1).

Table 7.3.1: Temperature class used in the preparation of coal mine fire map from Landsat-7 ETM+ data

Sl No.	Temperature Class	Remark
1	< 43º C	Background temperature
2	43º C - 49º C	Low intensity coal mine fire
3	> 49º C - 55º C	High intensity coal mine fire

All the data are processed by using standard image processing softwares such as ERDAS 9.1 and ENVI 4.2 to generate the requisite outputs

B. Some vital aspects and limitations in calculation of fire temperature from landsat-7 ETM+ data

- Landsat-7 ETM+ Data is the best in thermal bands in terms of spatial resolution but by 31st May, 2003 a problem encountered in the sensor. So, ETM+ data was not available for mapping the latest coal fires
- Here NDVI approach was used to derive the emissivity of surface features in the study area. The role of topography for controlling the emissivity of surface features was subdued in present terrain, as the terrain is almost flat with some occasional monadnocks / undulation present sporadically in the area. Therefore, the assumption of deriving emissivity from NDVI values (van de Griend and Owe, 1993) holds good to get the kinetic temperature of surface pixel
- Atmosphere also plays a role in attenuating or enhancing the thermal wave emanating from surface. During daytime, upwelling thermal wave from the hot atmospheric layer also changes the kinetic temperature of the pixel. Path radiance of thermal wave is very less but has some effect, which also reduces the amount of thermal flux that reaches the sensor. The disturbance and movement at the upper part of atmosphere also play a dampening role in subduing the temperature of a pixel manifesting the coal fire
- From satellite-based study, kinetic temperature of a pixel, which could be a mixed pixel containing features from background earth surface as well as coal fire is measured. Coal fire generates very high temperature but it is sometimes spatially restricted to a smaller area (one third to one fourth pixel or even less) and the background subdues the fire temperature when temperature is measured for a pixel (60 m x 60 m) instead of smaller active coal fire area
- Thermal data for 6th channel is recorded in two gain setting e.g., low gain and high gain. For thermal band data, both low and high gain data are available by default in Landsat-7 ETM+ data. The low gain setting measures a greater radiance range but with decreased sensor sensitivity, while high gain measures a lesser radiance range but with increased sensitivity. Coal fire is a high temperature phenomenon, which gets subdued by adjacent background when pixel containing coal fire is measured for kinetic temperature. Low gain setting measures high radiances for coal fire and therefore it help to separate the pixel containing the coal fire from the adjacent pixel and makes coal fire

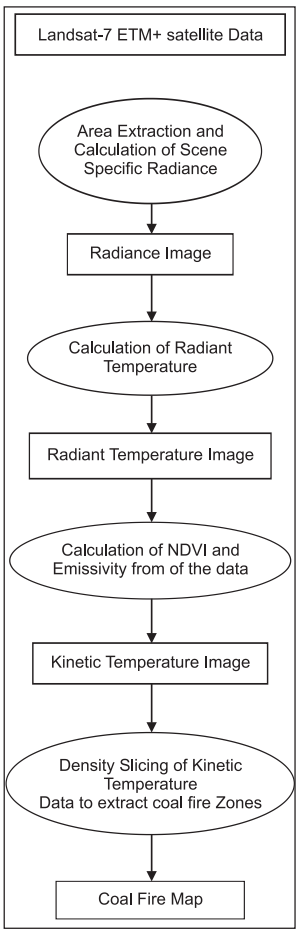

Figure 7.3.2: Steps for calculating Kinetic temperature from Landsat ETM data

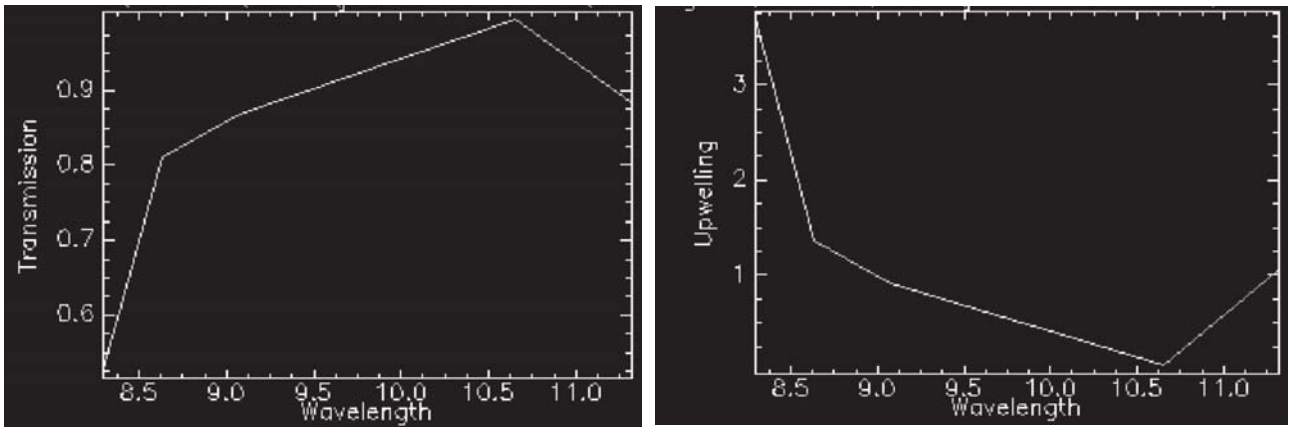

Figure 7.3.3 & 4: Transmission profile, welling Profile in ASTER thermal channel

demarcation better. The entire image processing methodology for extracting the coal fire for Landsat-7 ETM+ data is given below in the figure 7.3.2**.**

C. Processing of ASTER data

In the present study, Multispectral Advanced Thermal Emission and Reflection Radiometer (ASTER) night time data dated 9th October, 2006 was acquired for coal fire mapping. ASTER provides five thermal channels in the thermal region within 8.125 -11.65 µm wavelength domain. Multi channel ASTER data is very useful to

derive emissivity by using temperature emissivity algorithm and thereby allows to see the thermal anomaly within the range of entire thermal domain of ASTER. However, band 13 (10.25-10.95 µm) is considered here to delineate the coal mine fire zones as transmission of thermal wave is highest in this channel and upwelling (generated by the additive radiance of atmosphere) appear lowest in this particular thermal channel (Figures 7.3.3 & 4). Emissivity varies within the short range between 0.93 and 0.96 in this channel and therefore for present study, emissivity is assumed constant (0.96) to calculate the surface kinetic temperature from the radiant temperature. The emissivity of NDVI was not calculated from night time data since there was no channel in visible wavelength region for night time data.

Thermally emitted radiance from any surface depends on two major factors.

Table 7.3.2: Temperature class used in the preparation of coal mine fire map from ASTER data

Sl No.	Temperature Class	Remark
1	< 29º C	Background temperature
2	29º C – 32º C	Coal mine fire
3	> 32º C – 34º C	
4	> 34º C – 37º C	
5	> 37º C – 40º C	

- Surface temperature, which is the expression of state of heat energy budget on the surface and also indicate the equilibrium thermodynamic state of incident and emitted thermal energy fluxes and
- The surface emissivity, which determines the efficiency of surface for transmitting the radiant energy (Schmugge, 2002)

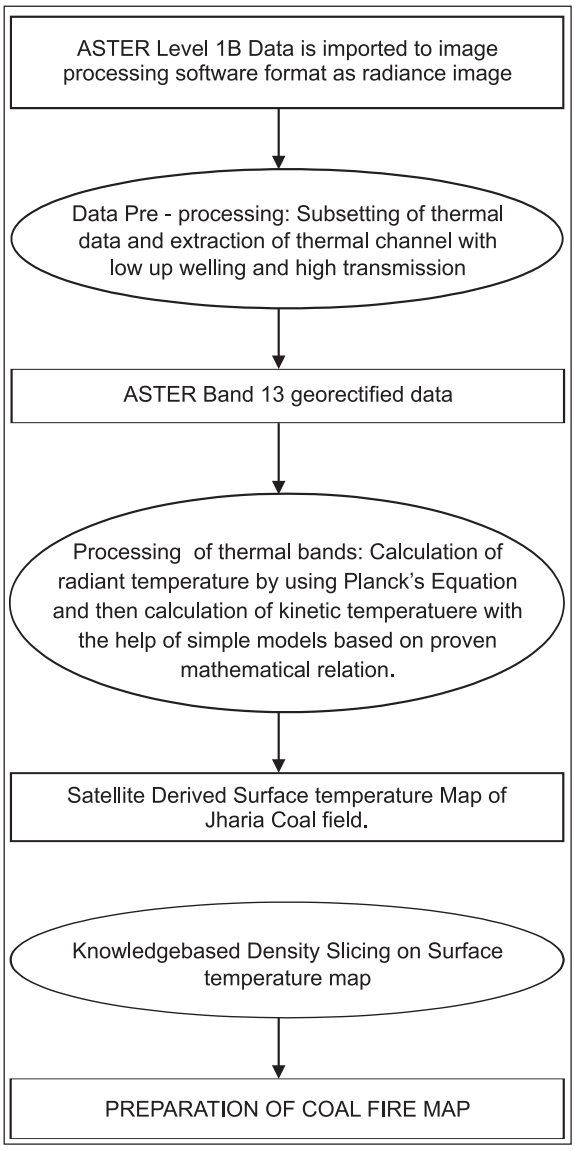

Figure 7.3.5: Steps for calculating Kinetic temperature (Coal fire map) from ASTER Data

Nighttime data provides better equilibrium state of surface heat energy budget as it has negligible solar flux contribution. Therefore nighttime band 13 data appears as the best available combination to derive the coal fire map for Jharia coalfield.

ASTER data was received as geocoded level 1B format from ERSDAC, Japan. This data was imported in ERDAS 9.1 software after converting in radiance by using facility module available for radiance conversion while importing. The georectified radiance data for 13th thermal channel was then used in a model for calculating the radiant temperature from the radiance values using equation – 2. After deriving the radiant temperature image from the radiance image, kinetic temperature image was derived by simple model created in ERDAS platform implementing equation – 6. Procedure for calculating Kinetic Temperature from ASTER data is shown in figure 7.3.5.

Emissivity is assumed to be 0.96 in the thermal domain of 10.25-10.95 µm. Density slicing technique was used on the kinetic temperature image to differentiate the fire pixels from the background. The kinetic temperature computed from the satellite data by using above mentioned procedure was further grouped into five classes (Table 7.3.2) to prepare the coal mine fire map of the Jharia Coal field (Figure 7.3.6). Isothermal map is also prepared from kinetic temperature image using same methodology applied to Landsat – 7 ETM+ data (Figure 7.3.1).

D. Some vital aspects and limitations in calculation of fire temperature from aster night time data

- Determination of threshold temperature to delineate the fire from non-fire area is an important aspect of present study and appears critical. The satellite derived temperature of fire pixel is less as compared to

ETM+ data and hence, the threshold is fixed 29º C. The method of selection of the threshold temperature is fully based on knowledge-based iterative technique, which keeps on separating the non-fire zone where probability of fire is nil. In this case field information is very useful in iteratively isolating the fire pixel from non-fire pixel

- Satellite-derived temperature for fire pixel depends on the temperature of fire zone and the back ground. It is also influenced by the proportion of area of fire pixel occupied by the background
- Temperature of fire pixel derived from satellite data is dependant on the density of cracks emanating fire and the fire temperature. Increment in any of the variables increases the temperature of the fire pixel
- Nighttime data in the month of October keeps background temperature reasonably lower and the temperature of pixel containing fire does not seem to increase too much. Field study revealed that there are very few pixels where density of cracks with high fire temperature was present and back ground reasonably had a lower temperature. The month of September – October in 2006 received good rain in the area and this also reduced the temperature of fire cracks. These parameters contribute to the reduction in the satellite-derived temperature of a fire pixel

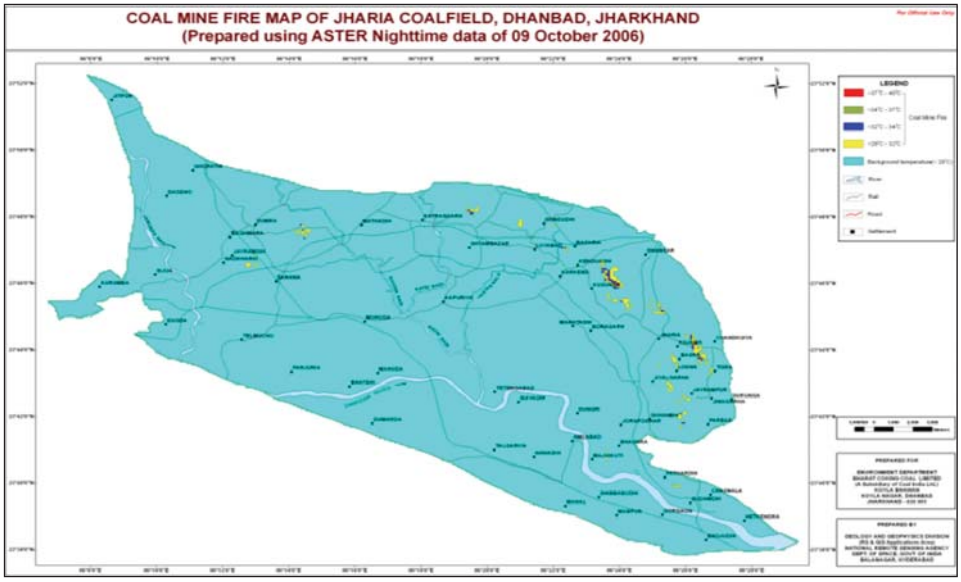

Figure 7.3.6: Coal mine fire map of Jharia coal field, Dhanbad, Jharkhand (prepared using ASTER Night time data of 09 October, 2006)

7.3.4.4. Results

The study was aimed at providing the status of coal fire in the Jharia coalfield in the period of 2003 and 2006. Landsat-7 ETM+ daytime data of 29th March 2003 was used to derive the coal mine fire map for the year 2003 (Figure 7.3.2). Similarly ASTER nighttime data of 9th October 2006 was used to prepare the coalmine fire map (Figure 7.3.6) for the year 2006. These data were used to prepare the coal fire maps on 1:50,000 scale. These two datasets are 60 m and 90 m spatial resolution in the thermal bands, respectively and they are the best thermal satellite data available on respective dates. The highest temperature computed for the year 2003 by Landsat-7 ETM+ is 55^0 C and for the year 2006 by ASTER is 40^0 C. The difference in the highest temperature is due to the time of satellite observation i.e., Daytime (March) for ETM+ and Nighttime (October) for ASTER and also for the difference in the spatial and spectral resolution between the two satellites. Coal fire map produced in different year depicts the pattern of dynamics of coal fire.

7.4. Geoengineering Studies

7.4.1. Introduction

Modern geology has been multi-disciplinary in nature since its origins more than 200 years ago. Multi-spectral remote sensing and Geographical Information Systems (GIS) together offer a new geological tool for different geological applications. Engineering geology is one of such disciplines where remote sensing has contributed significantly. Engineering geology is the application of the geologic sciences to engineering practice for the purpose of assuring that the geologic factors affecting the location, design, construction, operation and maintenance of engineering works are recognized and adequately addressed. Engineering geologists investigate and provide geologic and geotechnical recommendations, analysis, and design. Engineering geologic studies may be performed during the planning, environmental impact analysis, civil engineering design, value engineering

and construction phases of public and private works projects, and during post-construction and forensic phases of projects.

Works completed by engineering geologists include; geologic hazards, geotechnical, material properties, landslide and slope stability, erosion, flooding, dewatering, and seismic investigations, etc.

Engineering geologic studies are performed by a geologist or engineering geologist educated, professionally trained and skilled at the recognition and analysis of geologic hazards and adverse geologic conditions. The overall objective of the study is the protection of life and property against damage and the solution of geologic problems. Analysis and interpretation of multi-spectral remote sensing data helps in delineating lithology, geological structures of a terrain .This information along with the information on topography, land use when integrated in GIS platform helps in identifying suitable area for dam or tunnel or any crucial engineering structure and also help in analyzing the feasibility of developing engineering structures in already identified area. High resolution stereo pair satellite data helps in generating DEM (digital elevation model) of higher accuracy for rugged terrain with the help of only few field-based point height collected by differential global positioning surveys (DGPS). These models are very useful to assess the stability of a engineering structure and also would help to simulate the effect of engineering structure such as dam over a terrain. The geological informations collected from satellite data also helps in modeling the impact of any large-scale engineering structure to surrounding natural resources.

7.4.2. National and Global Scenario

The advent of sensor technology especially high-resolution mono/stereo pair satellite data (such as Cartosat-1, Cartosat-2, Ikonos, etc.,) helps in mapping geological structures in details. Geological structure plays important role in governing the stability, environmental suitability of a large engineering structure. Moreover, stereo pair satellite data helps in constructing very accurate digital elevation model (DEM); which is important input information for finalizing the place for Dam or tunnel or similar engineering structure. Moreover, high-resolution operational multispectral satellite (ASTER, IRS P6-LISS-IV) help in lithological mapping more accurately helps that accurate identification of sites.

7.4.3. Cost- Benefit Analysis

Remote sensing based mapping of lithology, geological structure and topography reduces the time and cost for feasibility analysis for developing engineering structure in a particular area. Moreover, remote sensing based monitoring of engineering structure after its construction helps in understanding the impact of engineering structure.

7.4.4. Methodology

Building a hydropower station or stations in a rugged terrain such as in the Himalayas requires thorough understanding of geological lithologies, water drainage patterns, surface and subsurface structures. If hydropower is to be generated from dam water then selecting suitable dam sites requires careful consideration of environmental impacts. Image processing technology can play a vital role in the studies of the categories mentioned. Detailed field studies can be followed, once image processing accomplishes the initial stage of the studies. Processing of satellite data and its interpretation helps in identifying information on following themes; which are essential for feasibility analysis of any large engineering structure or monitoring the environmental impact of large-scale engineering structures.

In any geoengineering studies, the role of satellite data is reconniasnce mapping. Data like IRS/ASTER/LANDSAT ETM for liuthological contacts and classifying rocks as per rock mass strength. Following are the broad steps.

- Updation of existing geological map
- Preparation of structural map especially faults, lineaments, fractures, drainage etc for understanding the rock strength and vulnerability to tectonic forces
- Integrating all the above layers with field information for site suitability analysis
- Validation and report generation

Geomorphology map preparation using satellite data to understand ruggedness of terrain, weathering, landslides and any other terrain related information.

7.4.5. Summary

Remote sensing technology is a boon for suitability analysis studies for large engineering structures for its effectiveness in cost and time. Feasibility analysis projects for developing engineering structures are often time bound and the structures are made over rugged terrain. Therefore remote sensing has a bigger role in generate geological information required for site suitability analysis and impact analysis of such large engineering structure such as dam, tunnel, national highways within a fixed time period. Moreover, remote sensing also gives information on resource availability required for such large structures. For example, information on near source of exposures building material such as gneiss, quartzite, etc., helps in identifying the nearest resources for availing the raw materials for such projects.

References

Abrams MJ, Ashley RP, Rowan LC, Goetz AFH and Kahle AB, 1977, Mapping of hydrothermal alteration in the Cuprite Mining District, Neveda, using scanner images for the spectral region 0.46 to 2.36 mm, *Geology*, **5**: 713-718.

Bhan SK, Bhattacharya A, Guha PK and Ravindran KV,1991, Applications in geology and mineral resources, *Current Science*, **61(3&4)**: 247-251.

Bhattacharya AK, Kamaraju,MVVV, Mehta DS,Shirmal AK and Reddy GS,1993, Mathematical modeling for mineral exploration: a case study from Rajpura-Dariba-Lunera mineralised belt, Rajasthan, India, *ITC Journal*, **4**: 360-366

Boardman JW and Kruse FA,1994, Automated spectral analysis: A geologic example using AVIRIS data, North Grapevine Mountains, Nevada, Proceedings of tenth thematic conference on geologic remote sensing, Environmental Research Institute of Michigan, I407–I418.

Boardman JW and Kruse FA, 1995, Mapping target signature via partial unmixing of AVRIS data: in summaries, Fifth JPL Airborne Earth Science Workshop, *JPL Publication*, **95(1)**: 23-26.

Bowers TL and Rowan LC,1996, Remote mineralogic and lithologic mapping of the Ice river alkaline complex, British Columbia, Canada, using AVIRS Data, *Photogrammetry Engineering and Remote Sensing*, **62(12)**:1379-1385

Burns RG, 1993, Origin of electronic spectra of minerals in the visible to near-infrared region, In C. M. Pieters, & P. A. J. Englert (Eds.), Topics in *remote sensing* 4– remote geochemical analysis: Elemental and mineralogical composition, Cambridge University Press.

Clark RN, 1999, Spectroscopy of rocks and minerals and principles of spectroscopy, In A. N. Rencz (Ed.), Remote sensing for the earth sciences: Manual of remote sensing, vol. 3 3rd edition), New York' John Wiley and Sons.

Conradsen K and Harpoth O, 1984, Use of Landsat multispectral scanner data for detection and reconnaissance mapping of iron oxide staining in mineral exploration, Central Eat Greenland, *Economic Geology*, **79**: 1229-1244

Daily MI, Elachi C, Farr TG and Schaber G,1978, Discrimination of Geologic units in Death Valley using dual frequency and polarization imaging radar data, *Geophysical Research Letters*, **5**: 889 – 892.

Dierking W and Haack H, 1998, L band polarimetric SAR- signatures of Lava flows in the northern volcanic zone, Iceland, *IEEE Transaction on Geoscience and Remote Sensing* , **3**: 1339-1341

Evans DL, Farr TG, Ford JP, Thompson TW and Werner CL, 1986, Multipolarisation radar images for gelogical mapping and vegetation discrimination, *IEEE Transaction on Geociences and Remote Sensing*, **24**: 246-257.

Fraser SJ, 1991, Discrimination and identification of ferric oxides using satellite thematic Mapper data: A Newman Case study, *International Journal of Remote Sensing*, **9**: 635-641

Gangopadhyay PK, Malthuis B and Van Dijk P, 2005, Aster Derived emissivity and coal-fire related surface temperature anomaly a case study in Wuda, North China, *Internation Journal of Remote Sensing,* **26**: 5555-5571.

Glikson AY and Creasey JW, 1985, Application of Landsat- 5 TM imagery to mapping of the Giles Complex and associated granulites, Tomkinso nranges Western Musghaves Block, Central Australia, *Journal of Australian Geology and Geophysics,* **16**: 173-193

Guha A, Vinod Kumar K and Kamarju MVV, 2007, Potential of Envisat ASAR data in geological studies in Kurnool Group of rocks, Kurnool, Andhrapradesh, Conference of Joint Experiment project towards Microwave Remote Sensing Data utilization (JEP-MW), Conference papers (Space Application Centre), ISRO,5-26-5-57.

Guha A, 2007, Coal mine fire mapping along Haldia-Barauni pipeline using satellite data in Raniganj coal field, West Bengal, NRSA-IOCL report (unpublished), p-14.

Guild PW, 1972, Metallogeny and the new global tectonics, Proc. 24th Int. Geol Cong Sect 4, mineral deposits, p 17-24.

Gupta RP, 2003, *Remote Sensing Geology*, Springer-Verlag,2nd Ed., p 498-524.

Gupta RP, 2003, *Remote Sensing Geology*, Springer Verlag Publication, Germany

Halbouty MT, 1976, Application of Landsat Imagery to petroleum and mineral exploration, *American Association of petrolium Geology*, **60** : 745-793

Hegde VS, Suryanarayan M and Bhan SK, 1983, Utility of Landsat data in aeromagnetic surveys-a case study from Manipur, Remote sensing in subsurface exploration, Association of Exploration Geophysicist, Hyderabad, p 48-72

Hook SJ, Abbott EA, Grove C, Kahle AB and Palluconi FD, 1999, Use of multispectral thermal infrared data in geological studies. In A. N. Rencz (Ed.), Remote sensing for the earth sciences: *Manual of remote sensing*, vol. 3 (3rd ed.) p. 59– 110, John Wiley and Sons, New York.

Hunt GR, 1977, Spectral Signatures of Particulate Minerals in the Visible and Near Infrared, *Geophysics*, **42**: 501-513

Hunt GR, 1980, Electromagnetic Radiation: The Communication Link in Remote Sensing" in Siegal BS and Gillespie (eds.), *Remote Sensing in Geology*, Wiley, New York, p 5-45.

Hunt GR, 1979, Near Infrared (1.3 – 2.4 um) Spectra of Alteration Minerals Potential for use in Remote Sensing, Geophysics, **44** : 1974-1986.

Jones AR, 1986, *An evaluation of satellite thematic mapper imagery for geomorphological mapping in arid and semi-arid environment*, International Geomorphology, edited by Gardiner V, (Chichester: Wiley), p 343-357.

Kahle AB and Rowan LC, 1980, Evaluation of multispectral middle infrared aircraft images for lithologic mapping in the East Tintic Mountains Utah, *Geology*, **8**: 234– 239.

Kahle AB, Christiansen P, Crawford M., Cuddapah P, Malia W, Polluconi F, Powysocki M., Salisbuey J and Vincent R, 1986, Geology Panel Report. Commercial Applications and Scientific Research Requirements for TIR Observations of Terrestrial Surface, EOSAT – NASA Thermal IR working group – Aug. 1986, p 34-72.

Krishnamurthy J,1999, Status of remote sensing applications to geological studies in india, NNRMS, ISRO.

Kruse FA, Boardman JW and Huntington JF, 2003, Comparison of airborne hyperspectral data and EO-1 hyperion for mineral mapping. *IEEE Transactions on Geoscience and Remote Sensing,* (Special Issue), **41(6)**:1388–1400.

Lillesand, TM and Kiefer RW, 1987, Remote Sensing and Image Interpretation, John Wiley & Sons, New York.

Macias LF, 1995, Remote Sensing of Mafic – Ultramafic rocks; Examples from Australian Precambrian terrain, *Journal of Australian Geology and Geophysics*, **16**: 163-171

Mason DC, Scott TR and Wang HJ, 2006, Extraction of tidal channel networks from airborne scanning laser altimetry, *ISPRS Journal of Photogrammetry and Remote Sensing*, **61**: 67-83.

Mouat DA,1982, The response of vegetation to geochemical conditions. Proc. International Symposium Remote Sensing Environ,2nd Thematic Conference Remote Sensing Exploration Geology, Fort Worth, Texas, p 75-84

Nasipuri P, Majumdar TJ and Mitra DS, 2006, Study of high-resolution thermal inertia over western India oil fields using ASTER data, International Journal of Applied Earth Observation and Geoinformation, **7**: 129–139

Offield TW, Abbott EA, Gillespie AR and Loguerciao RO,1977, Structure mapping on enhanced Landsat images of southern Brazil: tectonic control of mineralisation and speculation on mettalogeny, Geophysics, **42**: 482-500

Pandey SN, 1987, Principles and Applications of PhotoGeology, Wiley Eastern Limited, New Delhi.

Philip G, Gupta RP and Bhattacharya A, 1989, Channel migration studies in the middle ganga basin, India, using remote sensing data, *International Journal of Remote Sensing*, **10**: 1141-1149.

Prakash A, Sastry RGS, Gupta RP and Saraf AK, 1995, Estimating depth of buried hot features form thermal remote sensing data: a conceptual approach, *International Journal of Remote Sensing*, **16(3)**: 2105-109

Reddy CSS and Srivastav SK, 1993, Application of thematic mapper short wavelength infrared data for the detection and monitoring of high temperature related geoenvironmental features, *International Journal of Remote Sensing*, **14(17)**: 3125 - 3132.

Reddy PR, 1987, Geological and Geomorphological Studies through Remote Sensing, presented at the workshop on Remote Sensing technologies, Malaysia.

Reeves RG, Anson A and Landen D, 1975, *Manual of Remote Sensing*, Volume II, American Society of Photogrammetry, Falls Church, Virginia, USA.

Rencz AL, Bowie C and Ward B,1996, Application of thermal imagery for identification of Kimberlietes, Lac de Gras area,

District of Mackenzi, NWT.In; LeChaimant AN , Richardson DG, Dilabio RNW Richardson KA, (eds.), Searching for Diamonds in Canada, *Geological Suvey Canada*, 255-258.

Rivard B, Corriveau L and Harris LB, 1999, Structural reconnaissance Of a deep crustal orogen using Radarsat and Landsat imagery and airborne Geophysics, *Canadian Journal of Remote Sensing*, **25(3)**: 258 –268.

Rowan, Lawrence C, Schmidt, Robert G Mars and John C, 2006, Distribution of hydrothermally altered rocks in the Reko Diq, Pakistan mineralized area based on spectral analysis of ASTER data, *Remote Sensing of Environment*, **104**: 74-87

Salisbury JW, Walter LS, Vergo N and D'Aria DM, 1991, *Infrared (2.1– 25 lm) spectra of minerals*, Baltimore, MD' Johns Hopkins University Press.

Salisbury JW and Hunt GR, 1974, Remote Sensing of Rock Types in the visible and near Infrared, Proceedings, 9th Intl. Symp, *Remote Sensing of Environment*, Ann Arbor, MI, Vol. III, 1953-1958.

Schiefer E and Gilbert R, 2007, Reconstructing morphometric change in a proglacial landscape using historical aerial photography and automated DEM generation, *Geomorphology*, **67**: 167-178.

Sharma KNM, Singhroy VH, Modore L, Hebert E, Hinse M and Levesque C, 1999, Use of Radar images in the identification of major regional structures in the Greenville province, Western Quebec, *Canadian Journal of Remote Sensing*, **25(4)**: 221 –228.

Singhroy VH and Kruse FA, 1991, Detection of metal stress in boreal forest facies using the 0.67 mm chlorophyll absorption band. Proc. 8th Thematic Conference Geol Remote Sensing.

Singhroy V and Katrin M, 2004, Geological case studies related to Radarsat –2, *Canadian Journal of Remote Sensing*, **30 (6)**: 893 – 902.

Singhroy V, Slaney R, Lowman P, Haris J and Moor W, 1993, Radarsat and Radar Geology in Canada, *Canadian Journal of Remote Sensing*, **19(4)**: 338 –349.

Smith MJ and Clark CD, 2005, Methods for the visualization of digital elevation models for landform mapping, *Earth Surface Processes and Landforms*, **30**: 885-900.

Srivastav SK and Bhattacharya A, 1991, "Remote Sensing and Lithological and Structural Mapping, Presented at National Workshop on Role and Status of Remote Sensing and Groundwater Prospecting, NRSA, Hyderabad.

Van de Griend AA and Owe M, 1993, On the relationship between thermal emissivity and the normalized difference vegetation index for natural surfaces, *International Journal of Remote Sensing,* **14(14)**: 1119–1131.

Van Zuidam RA, 1985, *Aerial Photo Interpretation in Terrain Analysis and Geomorphological Mapping*, Smits, The Hague.

Van Zuidam RA, Pohl C and van Genderen JL, 1994, Synergy of remotely sensed data for coastal environmental studies: The Ameland-Waddensea example, Northern Netherlands, Second thematic conference on remote sensing for marine and coastal environments, New Orleans, Louisiana, USA, I-323 – I-334.

Vinod Kumar K, Martha TR and Roy PS, 2006, Detection of volcanic eruption in Barren Island using IRS P6 AWiFS data, *Current Science*, **91(6)**: 752-753.

Glossary:

Alluvial fan: A low, outspread, relatively flat to gently sloping mass of loose rock material; shaped like an open fan or a segment of a cone, deposited by a stream (esp. in a semiarid region) at the place where it issues from a narrow mountain valley upon a plain or broad valley, or where a tributary stream is near or at its junction with the main stream, or wherever a constriction in a valley abruptly ceases or the gradient of the stream suddenly decreases.

Alluvial plain: A level or gently sloping tract or a slightly undulating land surface produced by extensive deposition of alluvium, usually adjacent to a river that periodically overflows its banks; it may be situated on a flood plain, a delta, or alluvial fan.

Alluvial terrace: A stream terrace composed of unconsolidated alluvium (including gravel), produced by renewed down cutting of the flood plain or the valley floor by a rejuvenated stream, or by the later covering of a terrace with alluvium.

Anticline: A fold, the core of which contains the stratigraphically older rocks.

Antiform / Anticline: A breached/unbreached uplift, where the structure is shown directly in the topography and perhaps by drainage pattern. In case of the presence of older rock in the core of the uplift the antiform is called as anticline.

Arete: The knife edge caused by the intersection of two adjacent cirque walls or indeed at sharp mountain ridge.

Avalanche Chute / Track: These are distinct channels in bedrock formed due to repeated debris avalanches.

Bajada: A broad, continuous alluvial slope or gently inclined detrital surface extending along and from the base of a mountain range out into and around an inland basin, formed by the lateral coalescence of a series of separate but confluent alluvial fans, and having an undulating character due to the convexities of the component fans; it occurs most commonly in semiarid and desert regions.

Barchan: A moving, isolated crescent shaped sand dune lying transverse to the direction of the prevailing wind, with a gently sloping convex side facing the wind so that the wings or horns of the crescent point downward (leeward) and an abrupt or steeply sloping concave or leeward side inside the horns.

Barrier beach: A single, narrow, elongate sand ridge slightly above the high-tide level and extending generally parallel with the shore, but separated from it by a lagoon or marsh; it is extended by long shore drifting and is rarely more than several kilometres long.

Barrier island: A detached portion of a barrier beach between two inlets.

Basin: A general term for a depressed, sediment filled area. It may be an elongate, fault-bordered intermontane basin within an orogenic belt.

Beach: A gently sloping zone, typically with a concave profile, of unconsolidated material that extends landward from the low-water line to the place where there is a definite change in material or physiographic form (such as a cliff) or to the line of permanent vegetation (usually of the effective limit of the highest storm waves).

Beach ridge: A low, essentially continuous mound of beach or beach and dune material (sand, gravel, shingle) heaped up by the action of waves and currents on the backshore of a beach beyond the present limit of storm waves or the reach of ordinary tides, and occurring singly or as one of a series of approximately parallel deposits. The ridges are roughly parallel to the shoreline and represent successive positions of an advancing shoreline.

Bornhardt: A residual peak having the characteristics of an inselberg; specifically a large granite-gneiss inselberg associated with the second cycle of erosion in a rejuvenated desert region.

Braided stream: A stream that divides into or follows an interlacing or tangled network of several, small, branching and reuniting shallow channels separated from each other by branch islands or channel bars, resembling in plan the strands of a complex braid. Such a system is generally believed to indicate the inability to carry its entire load such as an overloaded and aggrading stream flowing in a wide channel on a flood plain. Syn: an anastomosing stream.

Buried / Palaeo Channel: Deep valleys cut in the bedrock terrain and today filled largely with alluvium, glacial otwash gravels and sands or with tills. These are good source for underground water.

Butte: A conspicuous, usually isolated generally flat-topped hill or small mountain with relatively steep slopes or precipitous cliffs, often capped with a resistant layer of rock and bordered by talus, and representing an erosion remnant carved from flat-lying rocks; the summit is smaller in extent than that of a mesa.

Channel bar: An elongate deposit of sand and gravel located in the course of a stream, especially of a braided stream.

Cirque: A deep, steep walled, flat or gently floored half bowl like recess or hollow, variously described as horseshoe or crescent shaped or semicircular in plan, situated high on the side of a mountain and commonly at the head of a glacial valley and produced by the erosive activity (frost action, nivation or ice plucking) of mountain glaciers. It often contains a small round lake, and it may or may not be occupied by ice or snow.

Coastal plain: A low, generally broad but sometimes narrow plain that has its margin on the shore of a large body of water (esp. the ocean) and its strata either horizontal or very gently sloping toward the water, and that generally represents a strip of recently emerged sea floor or continental shelf.

Colluvial fan: If the fan material consists of accumulation of heterogeneous material of ant particle size which accumulates on the lower part of the base of slopes. The material is mostly transported by gravity.

Complex dune: A dune formed by multidirectional winds resulting in the intersection of two or more dunes.

Crater: Any geological process that involves the effusion of materials from beneath the earth's surface via some sort of vertical pipe or vent usually develops a cone, collar or ring of deposits around the exit. This opening to the vent is the crater.

Cuesta: A hill or ridge with a gentle slope on one side and a steep slope on the other; specifically and asymmetric ridge with one face (dip slope) long and gentle and conforming with the dip of the resistant bed or beds that form it, and the opposite face (scarp slope) steep or even cliff-like and formed by the out crop of the resistant rocks, the formation of the ridge being controlled by the differential erosion of the gently inclined strata.

Deflation Plain: The planar surface in the desert exposed due to the removal of solid particles by wind action.

Delta: The low, nearly flat, alluvial tract of land deposited at or near the mouth of a river, commonly forming a triangular or fanshaped plain of considerable area enclosed and crossed by many distributaries of the main river, perhaps extending beyond the general trend of the coast, and resulting from the accumulation in a wider body of water (usually a sea or lake) of sediment supplied by a river in such quantities that it is not removed by tides, waves and currents.

Delta plain: The level or nearly level surface comprising the landward part of a large delta; strictly and alluvial plain characterized by repeated channel bifurcation and divergence, multiple distributary channels, and interdistributary flood basins.

Desert Pavement : It is a surface feature that may develop on the desert flat, on fans and bajadas and consist of rounded or sub-rounded angular pebbles. These are developed by the removal of fine sediments with resulting concentration of pebbles.

Dike: A tabular igneous intrusion that cuts across the planar structures of the surrounding rock. Also spelled as dyke.

Dissected Dune Complex : It is basically a dune complex which are dissected.

Dolines: Any basin or closed depression in a karst affected limesrone, of larger dimensions than a sinkhole, often enlarged by the collapse of caverns. The shape may vary from round to oval to elongate. Its floor is generally flat, often partly filled with alluvium.

Dome: A general term for any dome shaped landform or rock mass, such as a smoothly rounded rock-capped mountain summit, roughly resembling the dome of a building.

Dune: A low mound, ridge, bank, or hill of loose, wind blown granular material (generally sand, sometimes volcanic ash), either bare or covered with vegetation, capable of movement from place to place but always retaining its own characteristic shape.

Dune Complex: Two or more dune complex combined to form a large dune or dune field or a distinct group pattern.

Esker: An Esker is a sinuous low ridge composed of sand and gravel which formed by deposition from melt waters running through a channel way beneath glacial ice. Eskers vary in height from several feet to over 100 feet and vary in length from hundreds of feet up to many miles. The course of many eskers is similar to that of a stream. The cross lamination in eskers indicated downward flow.

Flood plain: The surface or strip of relatively smooth land adjacent to a river channel constructed (or in the process of being constructed) by the present river in its existing regimen and covered with water when the river overflows its banks at times of high water. It is built of alluvium carried by the river during floods and deposited in the sluggish water beyond the influence of the swiftest current.

Glacial valley: A 'U' shaped, steep sided valley showing signs of glacial erosion; a glacial valley, or one that has been modified by a glacier.

Glacial Stairway / Crevasse: Glaciers, ice shelves, snow fields and sea ice are subjected to stresses which are relieved by fissures and cracks called crevasses. In cross section crevasses are V shaped and often bridged by snow which makes them difficult to see on the surface.

Hanging valley (glacial): A glacial valley whose mouth is at a relatively high level on the steep side of a larger glacial valley. The larger valley was eroded by a trunk glacier and the smaller one by a tributary glacier and the discordance of level of their floors, as well as their difference in size is due to the greater erosive power of the trunk glacier.

Hanging valley (streams): A tributary valley whose floor at the lower end is notably higher than the floor of the main valley in the area of junction, produced where the more rapid depending of the main valley results in the creation of a cliff or steep slope over which a water fall may develop.

Highly Dissected Structural Hills and Valleys: Hills and valleys which are originated due to tectonic process and are highly dissected by the drainage lines. Here the drainage density is very high.

Hogback: It is a long narrow ridge or series of hills, structurally controlled by the presence of homoclinal sedimentary strata that dip steeply (over 50^0). Hogbacks develop best in sediments that are in hard and soft layers of marked contrast. Because of their steep dips, hogbacks remain more or less fixed in the landscape, and do not retreat as will a cuesta.

Homocline: Uniform regional tilting of the strata in the Physiography. The expression is a function, among other things, of the amount of tilt which is considered to be recorded in the dip of the rocks.

Horn: When more than two adjacent cirque walls intersect at a common point, it results in a sharp mountain peak called as horn.

Inselberg A prominent, isolated, steep-sided, usually smoothed and rounded, residual knob, hill or small mountain of circumdenudation rising abruptly form and surrounded by an extensive and nearly level, lowland erosion surface in a hot, dry region (as in the deserts of southern Africa or Arabia), generally bare and rocky although partly buried by the debris derived from and overlapping its slopes; it is characteristic of an arid or semiarid landscape in a late stage of the erosion cycle.

Interdunal Depression: The depression between the two consecutive dunes.

Intermontane Valley: The valley between the mountains.

Island: A tract of land, smaller than a continent, completely surrounded by water, under normal condition, in an ocean, sea, lake, or stream. An elevated piece of land surrounded by a swamp, marsh, or alluvial land, or isolated at high water or during floods.

Kame Terrace: Kames are mounds of poorly sorted sand and gravel deposited from running water in close association stagnant glacial ice. A kame terrace forms as an ice contact deposit when waters flowing from a glacier find a course between the ice mass and a valley wall. The character of the sediments within a kame terrace is intermediate in complexity between that of an esker and that of a kame.

Lake: Lakes formed by glacial action i.e., cirque lake formed at about snow line in glaciated valleys, lakes by glacial deposits.

Lapies: It refers to a rill like erosional form of lime stone solution in the karst landscape.

Lateral Moraine: This is debris shoved together or melted out from the advancing glacier along its sides.

Lava flow: The lava coming out from the vent during active volcanism and flowing down the flank of volcano.

Levee / Natural levee: An artificial embankment, usually of random earth fill, built along the bank of a watercourse or an arm of the sea and designed to protect land from inundation or to confine stream flow to its channel.

Loess: It is largely homogeneous, unstratified silt. It is usually permeable, porous, unconsolidated sediment apt to form vertical cliffs or bluffs. It is commonly yellow or buff in colour owing to its content of finely dispersed limonite, though sometimes it is grey.

Longitudinal dune: A long, narrow, usually symmetrical (in profile) sand dune oriented parallel with the direction of the prevailing wind responsible for its construction, being wider and steeper on the wind ward side but tapering to a point on the leeward side, and commonly forming behind obstacles in an area where sand is abundant and the wind is strong and constant.

Meander: One of a series of some what regular, sharp, freely developing, and sinuous curves, bends, loops, turns, or windings in the course of a stream.

Meander scar: A crescentic, concave mark on the face of a bluff or valley wall, produced by the lateral planation of a meandering stream which undercut the lateral planation of a meandering stream which undercut the bluff, and indicating the abandoned root of the stream. An abandoned meander often filled in by deposition and vegetation, but still discernible (esp. from the air).

Meander scroll: One of a series of long, closely fitting, arcuate ridges and troughs formed along the inner bank of a stream meander as the channel migrated laterally down-valley and toward the outer bank.

Medial Moraine: It lies between two ice streams and is formed upon intersection of two lateral moraines.

Mesa: An isolated nearly level land mass standing distinctly above the surrounding country bounded by abrupt or steeply sloping erosion scarps on all sided, and capped by layers of resistant, nearly horizontal rocks (usually lavas). Less strictly, a very broad, flat-topped, usually isolated hill or mountain of moderate height bounded on at least one side by a steep cliff or slope and representing an erosion remnant.

Monocline: A unit of strata that dips or flexes form the horizontal in one direction only, and is not part of an anticline or syncline. It is generally a large feature of gentle dip.

Monadnocks: A monadnock is an isolated mountain representing an erosional residual (peak or knob).

Nunatak: An isolated hill, knob, ridge, or peak of bedrock that projects prominently above the surface of a glacier and is completely surrounded by glacier ice.

Outwash Plain: These are proglacial landforms that are built by streams extending beyond an ice front. Outwash plains are produced by merging of a series of outwash fans.

Oxbow lake: The crescent-shaped, often ephemeral, body of standing water situated by the side of a stream in the abandoned channel (oxbow) of a meander after the stream formed a neck cutoff and the ends of the original bend were silted up.

Parabolic dune: A sand dune with a long, scoop-shaped form, convexly bend in the downwind direction so that its horns point upwind (windward), and whose ground plan (when perfectly developed) approximates the form of a parabola. It is characteristically covered with sparse vegetation and is often found along the coast where strong onshore winds are supplied with abundant sand.

Pediment: A broad, flat or gently sloping, rock floored erosion surface or plain of low relief, typically developed by sub aerial agents (including running water) in an arid or semiarid region at the base of an abrupt and receeding mountain front or plateau escarpment, and underlain by bedrock (occasionally by older alluvial deposits) that may be bare but more often partly mantled with a and discontinuous veneer of alluvium derived form the upland masses and in transit across the surface.

Pediment-Inselberg Complex: The pediments dotted by numerous inselbergs of small size, which makes it difficult to distinguish from the pediments. Hence it is called as a complex of pediment and inselbergs.

Pediplain: An extensive, multiconcave, thinly alluviate rockcut erosion surface formed in a desert region by the coalescence of two or more adjacent pediments and occasional desert domes, and representing the end result (the “peneplain”) of the mature stage of the arid erosion cycle.

Piedmont slope: A small, low cliff occurring in alluvium on a piedmont slope at the foot of, and essentially parallel, to, a steep mountain range, resulting from dislocation of the surface, esp. by faulting.

Plateau: Broadly, any comparatively flat area of great extent and elevation specif. and extensive land region considerably elevated (more than 150-300m in altitude) above the adjacent country or above sea level and commonly limited on at least one side by and abrupt descent, having a flat or nearly smooth surface but often dissected by deep valleys or canyons and surmounted by ranges of high hills or mountains, and having a large part of its total surface at or near the summit level. A plateau is usually higher and has more noticeable relief than a plain (it often represents an elevated plain). And is usually higher and more extensive that a mesa; it may be tectonic, residual, or volcanic in origin.

Plateau Top: It is the flat or relatively flat portion of the Plateau on the topmost part.

Playa : It is essentially the dray lake remnant of a former base level of erosion which may be presently active. The name playa can be loosely applied to a dry lake filled periodically with a sheet of water regardless of whether or not the playa depression is a sedimentary/volcanic basin or a basement rock surface partially covered by a thin sheet of clastic sediments.

Point bar: One of a series of low, arcuate ridges of sand and gravel developed on the inside of a growing meander by the slow addition of sediments.

Residual Hill: A small remnant hill which has witnessed all forms of denudation.

Rift Valley: Valleys of subsidence with long steep parallel walls. The valley consists of a graben in the middle and horsts on both the sides. These are formed in regions of extension tectonics e.g., in East Africa.

Ridge: A long narrow naturally elevated topography. This created either by structural processes or due to the exposure of hard rock to erosion activities.

Sand dune: A dune consisting of loose sand piled or heaped up by the wind, commonly found along the low-lying seashores above high-tide level, more rarely on the border of a large lake or river valley, as well as in various desert regions and generally where there is abundant, dry surface sand during some part of the year.

Sand Sheet: Thin layer of sand spread over a horizon.

Scarp: Also known as escarpment is defined as a cliff or steep rock face of great length. The development of a scarp could be due to structural or erosional processes.

Scree: A heap of broken angular rock fragments greater than 10cm in diameter on the slope of a hill.

Seif Dune: Longitudinal dunes are also known as seif dunes.

Shield Volcano: These are very flat cones of moderate size with summit craters usually so small as not to interfere appreciably with conical shape.

Sinkhole: A general term for a closed depression in an area of karst topography that is formed either by solution of the surfacial limestone or by collapse of underlying caves.

Spit: A small point or low tongue or narrow embankment of land commonly consisting of sand or gravel deposited by longshore drifting and having one end attached to the mainland and the other terminating in open water usually the sea; a finger-like extension of the beach.

Star Dune : A dune with the shape of a star is called as star dune.

Strath Terrace: The terraces developed in wide flat floored valley because of the continuous deep cutting of the stream or crustal upliftment.

Strato Volcano: Symmetrical volcanic cone mountains with alternate layers of mixed ash and lava flows.

Structural origin: The landforms which are originated due to the structural/tectonic movements. The influence of geologic structures on the development and appearance of landscapes is prominent. The influence of geologic

structures ranges from large features which exert a dominant influence on the form of an entire landscape, to small features which affect an individual landform and the geomorphic processes operating on it. The structural control could be active structures whose form is directly impressed on the modern landscape or ancient structural features whose influence on a modern landscape is due primarily to differential erosion.

Synform / Syncline: A breached/unbreached depression, where the structure is shown directly in the topography and perhaps by drainage pattern. In case of the presence of younger rock in the core of the depression the synform is called as syncline.

Talus cone: A small, cone shaped or apron like landform at the base of a cliff and consisting of poorly sorted talus that has accumulated episodically by mass-wasting.

Terminal moraine: An end moraine, extending across a glacial valley as an arcuate or crescentic ridge that marks the farthest advance or maximum extent of a glacier; the outermost end moraine of a glacier. It is formed at or near a more or less stationary edge, or at a place marking the cessation of an important glacial advance.

Tidal flat: An extensive, nearly horizontal, marshy or barren tract of land that is alternately covered and uncovered by the rise and fall of the tide, and consisting of unconsolidated sediment (mostly mud and sand). It may form the top surface of a deltaic deposit.

Till: It is glacial debris ranging from clay to large block size and of heterogeneous origin. By diagenesis or metamorphism tillites are formed from this.

Tor: A bare rock mass surmounted and surrounded by blocks and boulders. They display marked structural control and are delineated by joint planes, which are commonly near vertical and quasi horizontal.

Transverse Dune : Dunes that are developed across the direction of the wind.

Uvala: The uvala comprises a series of joined or coalescent dolines, often elongate and marking a former subterranean stream channel or series of collapsed sinkhole.

Valley: It is typically a low lying area of land surrounded by higher areas such as mountains or hills.

Valley fill: The unconsolidated sediment deposited by any agent so as to fill or partly fill a valley.

Volcanic cone: The cone shape mountain created due to volcanic eruption surrounding the vent. It has relatively homogeneous strata showing radial drainage pattern.

Wadies: Small tributaries.

nrsc

Remote Sensing Applications

P. S. Roy
R. S. Dwivedi
D. Vijayan

National Remote Sensing Centre

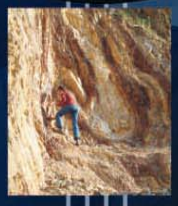

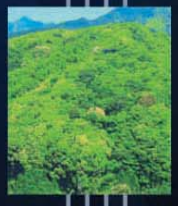

Remote Sensing Applications

Groundwater

8.1. Introduction

The distribution of groundwater is not uniform throughout the country. The spatio-temporal variations in rainfall and regional/local differences in geology and geomorphology have led to uneven distribution of groundwater in different regions across the country. Unplanned and haphazard development of groundwater in some areas has further compounded the problem and has led to a sharp decline in groundwater levels. As a result, a large number of shallow wells have gone dry, resulting in a huge loss and shortage of drinking water in 20 to 25% of the habitation in the country. Similarly, along the coastal zones also the delicate balance between sea water and the groundwater has been disturbed leading to sea water intrusion into the fresh water aquifers causing irreparable damage and environmental degradation. Systematic estimation and budgeting of groundwater resource based on its spatio-temporal distribution, its allocation for meeting the competing demands for irrigation, industrial and domestic usage, and conjunctive use of surface and a groundwater resource are, therefore, pre-requisite for optimal utilization of available groundwater on a sustained basis.

Groundwater study of an area requires the knowledge of the nature of lithological units occurring in the area, their structural disposition, geomorphic set up, surface water conditions and climate. These had been studied by the conventional method of extensive field work till recent past. With the development of remote sensing sensors accompanied with improvement of interpretation techniques of the remotely sensed data, focus has turned to this technique. World wide professional organizations involved with groundwater investigation in an area commence their work with analysis of remotely sensed data. Although remote sensing data can't directly detect subsurface resources, its importance lies in providing indirect but reliable inferences about the groundwater potentiality of the region. Analysis and interpretation of remote sensing data followed by selective ground check is important to obtain an idea about the probable groundwater potential areas. This should be substantiated through surface and subsurface geophysical methods best suited for groundwater exploration.

8.2. Background

Timely and reliable information on the occurrence and movement of groundwater is a prerequisite for meeting its growing demand for drinking, domestic and industrial sector. Being a sub-surface feature, the detection of groundwater relies heavily on the controlling factors, namely lithology, geomorphology, structures and precipitation, run-off, surface water and the extent of irrigated lands that control its occurrence and movement. Spaceborne spectral measurements hold a great promise in providing such information in timely, reliable and cost-effective manner. In India, initially the coarse resolution data from Indian Remote Sensing Satellite (IRS-1A/-1B LISS-II) & Landsat-TM have been operationally used by the Department of Space Govt. of India mainly for identifying and mapping groundwater potential zones for entire country (447 districts) on 1:250,000 scale under National Drinking Water Technology Mission. Mapping of the groundwater prospects on 1:50,000 scale using IRS-1C/-ID LISS-III data for entire country under Rajiv Gandhi Drinking Water Technology Mission is in progress and till now ten states have been completed successfully.

Conventional surveys are tedious, time consuming apart from being impractical in the inaccessible and inhospitable terrain. Moreover, many features of regional nature could not be mapped precisely owing to lack of regional perspective. Earlier, the aerial photographs have been used for deriving information on lithology, geomorphology and structures. By virtue of providing synoptic view of the terrain at regular intervals, space borne multi-spectral measurements offer immense potential in generating the information on parameters required for groundwater exploration, exploitation and development.

8.2.1. Factors Controlling Groundwater Regime

The groundwater regime is a dynamic system wherein water is absorbed at the surface of the earth and eventually recycled back to the surface through the geological strata. In this process, various elements like relief, slope, ruggedness, depth and nature of weathering, thickness and nature of deposited material, distribution of surface water bodies, river / stream network, precipitation, canal command areas, groundwater, irrigated areas, etc., also influence the groundwater regime, besides the geologic framework. Thus, the framework in which the groundwater occurs is as varied as that of rock types, as intricate as their structural deformation and geomorphic history, and as complex as that of the balance among the lithologic, structural, geomorphic and hydrologic parameters (Jasrotia *et al.*, 2007; Chowdhury *et al.*, 2009). The possible combinations of variety and intricacy are virtually infinite

leading to the unavoidable conclusion that the groundwater conditions at a given site are unique and not completely amenable to scientific understanding. Some of the conditions are often obscured and not readily apparent even from the field observations. However, factor-wise analysis, systematic mapping, data integration and interpretation based on conceptual understanding will help in overcoming this problem to some extent.

Though, there are a large number of variables that are important in understanding the groundwater conditions of an area, it is not possible to separately map and study all the variables individually during the course of the investigation. Rarely is it possible for an investigator to complete all the examinations to eliminate uncertainties and provide quantitative information about the type, thickness and depth of aquifer, its yield potential, success rate, etc with complete confidence. Varying degrees of uncertainty and inconsistency are inherent in the present methodology (conventional hydrogeological mapping). Hence, the entire procedure of mapping has to be made more systematic and simpler with well defined units based on which better inferences can be made. For this purpose, all the variables that control the groundwater regime have been grouped into the following 4 factors -

- Geology / Lithology
- Geological Structures
- Geomorphology / Landforms
- Recharge conditions

Once, information on these 4 factors is precisely known, it is possible to understand the groundwater regime better by visualizing the gross aquifer characteristics of each unit. Systematic visual interpretation of satellite imagery in conjunction with existing geological / hydrogeological / geomorphological maps and data supported by limited field checks / observations provide the information related to these 4 factors. By integrating the lithological, structural, landform and hydrological information, the groundwater prospects map can be prepared which provide better understanding of groundwater regime as compared to the conventional hydrogeological map.

8.3. Role of Space Technology in Groundwater Studies

The launch of Earth Resources Technology Satellite (ERTS-1), later renamed as Landsat-1 with the Multispectral Scanner System in 1972 ushered in a new era in mapping and updating of geological, geomorphological and structural features using the optical sensors data. Subsequently, Landsat-Thematic Mapper and the India Remote Sensing Satellite (IRS-1A LISS-II) sensors have been operationally used in India to generate groundwater potential maps at 1:250,000 scale. Remote sensing data have been widely used in groundwater prospecting (Sreedevi *et al.*, 2005; Dinesh *et al.*, 2007; Chandra *et al.*, 2006; Per Sander, 2007). The LISS-III multispectral data from IRS-1C and 1D satellites have been used later for preparing groundwater potential maps at 1:50,000 scale.

In addition to optical sensors data, microwave data have also been used at experimental level for deriving information on lithology, landforms and structures (Ghoneim and El-Baz, 2007). Microwave (Synthetic Aperture Radar) data have a very limited capability for direct measurement of groundwater because the depth of penetration is limited to a few centimeters except in extremely dry sand covered areas. Imaging radar data has proven to be very useful in discrimination of surface lithology buried palaeo-channels, dykes, sand-covered bed rock to a depth ranging from 1.5 to 6.0 m (Drury 1990; Jensen 1995; Sabins 1987; Shankar *et al.*, 2001).

Apart from optical and microwave data thermal infrared sensor data have also been used for identification of groundwater potential zones under certain conditions. Heilman et al (1982) found a correlation between Heat Capacity Mapping Mission-derived radiometric temperatures and groundwater depth when the effect of vegetation on the surface thermal region was considered. Similarly, a correlation between predawn radiometric temperature and thickness of aquifer was also observed (Moore, 1982). In-spite of encouraging results, insufficient ground spatial resolution and lack of repetitive global calibrated thermal data precludes the usage of thermal infrared data for groundwater studies. Thus, the satellite data provide supporting information for recharge estimation, draft estimation, mapping of prospective zones, identification of over exploited and under developed/undeveloped areas and prioritization of areas for recharge structures which conjunctively facilitate systematic planning, development and management of groundwater resources on a sustainable basis.

Geophysical measurements, namely geo-electrical, seismic refraction and electromagnetic systems, have also been commonly used for groundwater exploration. Besides, Ground Penetrating Radar (GPR) operating in low frequency (100 to 500MHZ), nuclear magnetic resonance, magnetic and gamma ray spectrometric techniques

have been tried out at experimental level for detection of shallow groundwater table, phreatic surface, crustal structures and bedrock profile (Bahuguna *et al.*, 2003; Gupta, 1991).

8.4. Groundwater Prospects Mapping

Groundwater targeting and prospects mapping is one of the thrust areas in groundwater studies since it forms the base for groundwater exploration and development. It involves identification and mapping of prospective zones for groundwater exploitation. The methodology for preparing groundwater maps using satellite imagery has undergone rapid changes during the last two decades. Initially, the remote sensing data, namely aerial photographs and satellite images were used mainly to update and refine the conventional hydrogeological maps prepared from ground surveys. Subsequently, many organizations in the country including National Remote Sensing Centre (NRSC) /Department of Space (DOS), Central Ground Water Board (CGWB), Groundwater Departments of different states, research laboratories and academic institutions have also started preparing the groundwater maps through a systematic visual interpretation of satellite data with limited field checks. These maps, with different titles, vary greatly in their quality and information content. The operational utilization of satellite data for groundwater studies in India has taken a firm footing in the year 1985 when the Department of Space prepared the groundwater potential zone maps at 1:250,000 scale for two states, namely Maharashtra and Karnataka during the period 1985 –1986 followed by a nation-wide mapping of groundwater potential zone at 1:250,000 scale using the Landsat-TM and the Indian Remote Sensing Satellite - IRS-1A Linear Imaging Self-scanning Sensor (LISS-II) data under National Drinking Water Technology Mission during the period 1987 to 1992 using a common legend (Baldev *et al.*, 1991).

These maps formed the regional database for groundwater exploration for entire country. Subsequently, the Department of Space in collaboration with the State Remote Sensing Centres and concerned State Departments has prepared, apart from other thematic maps, the hydrogeomorphological maps on 1:50,000 scale for 84.0 million hectares covering 175 districts under major national level project Integrated Mission for Sustainable Development (IMSD) project.

For providing safe drinking water to 4.4 lakhs villages in the country a nation-wide project titled “Rajiv Gandhi National Drinking Water Mission (RGNDWM): has been taken up by NRSC/DOS to prepare groundwater prospects maps on 1:50,000 scale through visual interpretation of IRS-1C/-1D LISS-III geo-coded images in conjunction with the existing geological, hydrogeological and hydrological information with the limited field checks. In order to achieve the objective of the project, a new methodology has been developed and the manual has been brought out. In this approach, the information on lithology, landform, geological structure and hydrology are generated and by integrating them subsequently the groundwater prospects map is prepared. Thus, by taking input parameters, namely lithology, landform, geological structures, recharge conditions, depth to water table, and yield information, the groundwater prospects are evaluated and defined in terms of following output parameters i) Aquifer material (ii) Type of wells suitable (iii) Depth range of wells (iv) Yield factor (v) Heterogeneity of the aquifer/the failure rate of wells (vi) priority for planning recharge structure and the type of recharge structures suitable and (vii) Quality/ problems/limitation. In the first phase, Rajasthan, Madhya Pradesh, Andhra Pradesh, Karnataka and Kerala States have been taken up. These maps are generated as digital outputs in GIS environment (Burrough 1986) containing information on several layers covering different parameters. Thus, these maps provide much more information as compared to the conventional hydrogeological maps and are quite useful in narrowing down the target zones for detailed geophysical/ground hydrogeological studies (Bhattacharya and Patra 1968) for selection of sites for drilling as well as for planning recharge structures.

8.4.1. Lithology

The synoptic view and multispectral nature of the satellite imagery help in discrimination and mapping of different lithologic units. Geological mapping is carried out mainly based on visual interpretation of satellite images (Figure 8.1) adopting deductive approach by studying image characteristics and terrain information in conjunction with a prior knowledge of general geological setting of the area. The tone (colour) and landform characteristics combined with relative erodibility, drainage, soil type, land use/ land cover and other contextual information observable on the satellite image are useful in differentiating different rock groups / types.

The direct clue for interpretation of rock type / lithologic unit comes from the tone (colour) of the image. For example, the acidic and arenaceous rocks appear in lighter tone as compared to the basic / argillaceous rocks. Similarly, coarse grained rocks having higher porosity and permeability appear brighter on the image as compared to fine-grained rocks having higher moisture retaining capacity. The highly resistant rock formations occur as

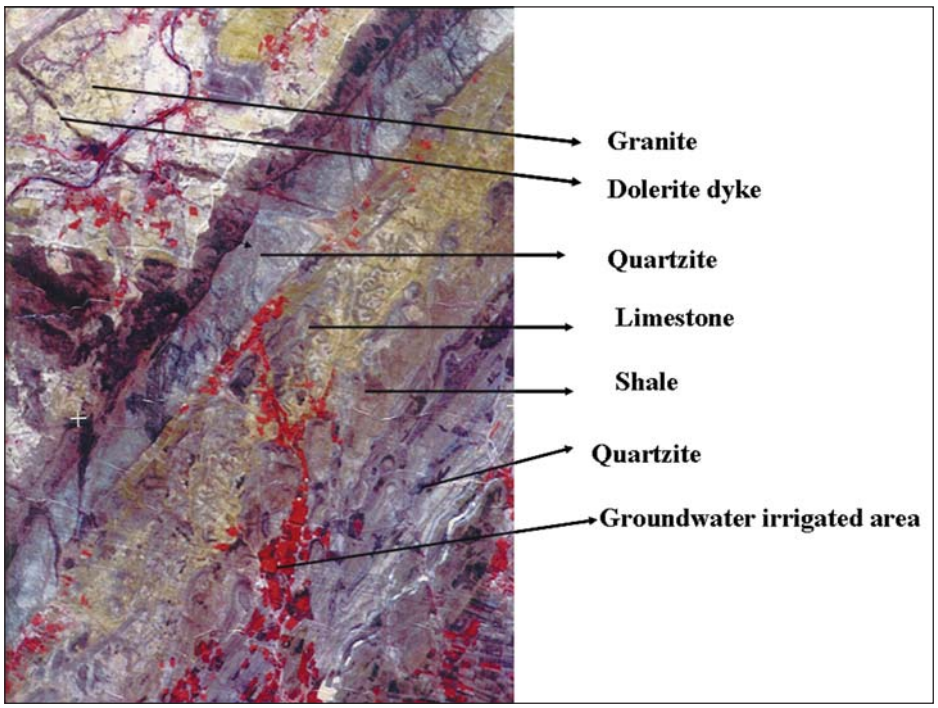

Figure 8.1: Interpretation of Lithology from satellite imagery

different types of hills depending upon their texture and internal structure; whereas, the easily erodible rocks occur as different types of plains and valleys. While dendritic drainage indicates homogeneous rocks, the trellis, rectangular and parallel drainage patterns indicate structural and lithological controls. The coarse drainage texture indicates highly porous and permeable rock formations; whereas, fine drainage texture is more common in less pervious formations. The coarse textured and light coloured soils indicate the acidic / arenaceous rocks rich in quartz and felspars; whereas, the fine textured and dark coloured soils indicate basic / argillaceous rocks. Thus, by combining all these evidences, it is possible to interpret different rock groups / formations. Though, one or two recognition elements, mentioned above, may be diagnostic for the identification of a particular rock type, the convergence of evidences must be considered by studying all the recognition elements conjunctively (figure 8.1). However, limited field checks are a must to identify the rock types and to make necessary corrections in the interpreted map based on field evidences. Once, the rock types are identified, the contacts can be extended over large areas with minimum ground control. The identification, correlation and extrapolation of rock types are possible based on similar spectral and morphological characters.

For preparation of lithological map overlay (Figure 8.2'b'), information from the following sources is required:

- Consultation of existing geological / hydrogeological maps or literature
- Interpretation of satellite imagery (figure 8.2 'a')
- Field visits / surveys

8.4.2. Geological Structure

Various workers have emphasized the utility of satellite imagery for mapping the geological structures. The synoptic coverage provided by the satellite imagery enable mapping regional structures which is difficult in conventional

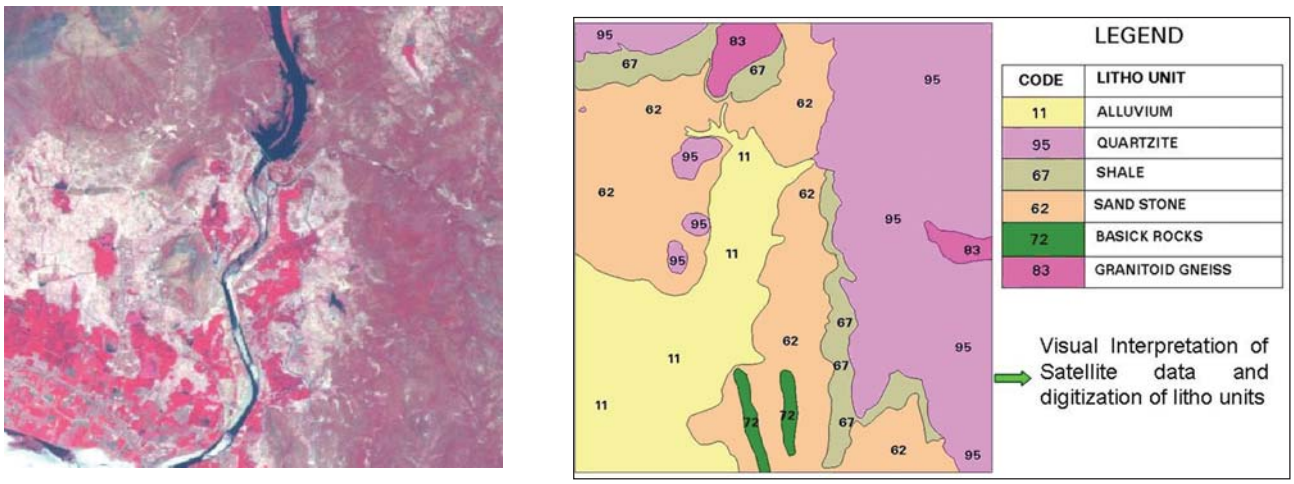

Figure 8.2: (a) Satellite imagery of the study area and (b) Preparation of lithological map

ground surveys due to scanty rock exposures, soil cover, lack of continuous observations, etc. The different types of primary and secondary geological structures (attitude of beds, schistosity / foliation, folds, lineaments etc.) can be interpreted from satellite imagery by studying the landforms, slope asymmetry, outcrop pattern, drainage pattern, individual stream / river courses, etc.

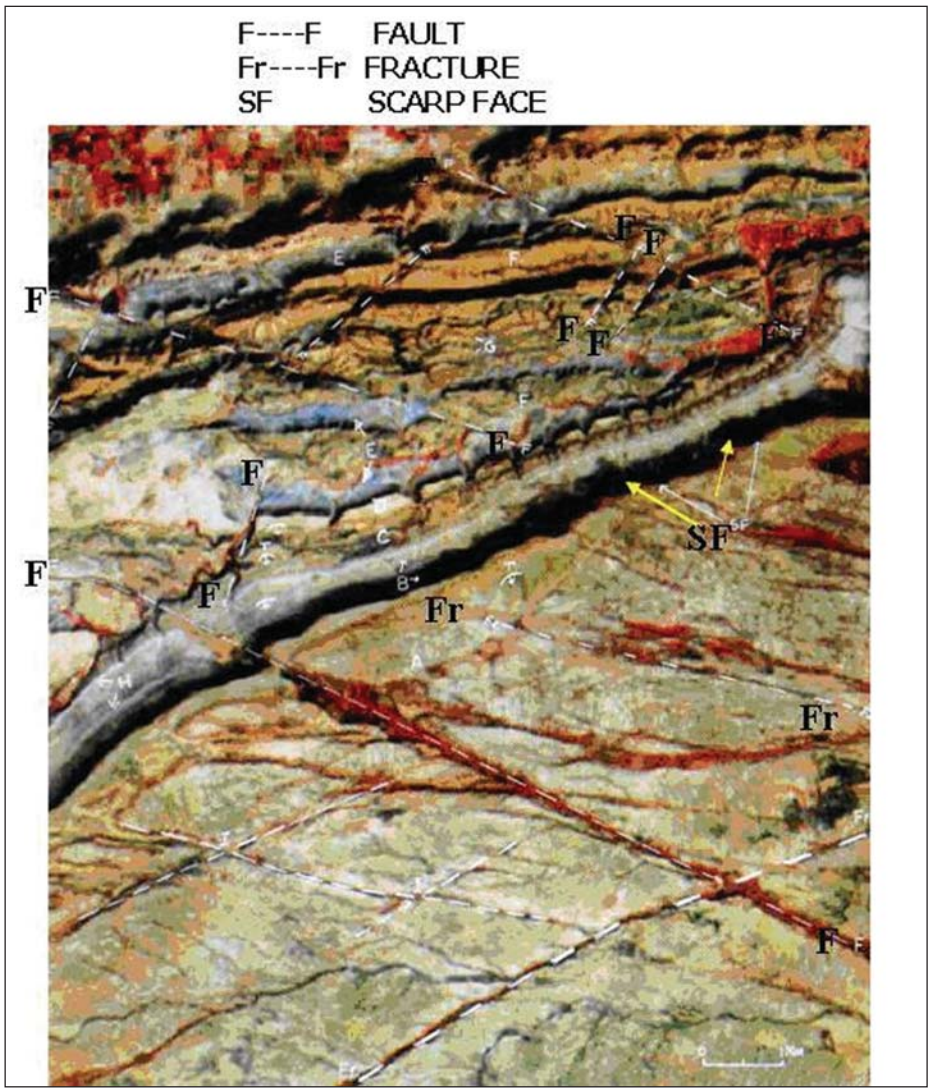

Figure 8.3: Interpretation of structural features from satellite imagery

Lineaments representing the faults, fractures, shear zones, etc., are the most obvious structural features interpretable on the satellite imagery (Figure 8.3). They control the occurrence and movement of groundwater in hard rock terrain and their significance in groundwater exploration has been proved beyond doubt. They occur in parallel sets in different directions indicating different tectonic events. They appear as linear to curvilinear lines on the satellite imagery and are often marked by the presence of moisture, alignment of vegetation, straight stream / river courses, alignment of tanks / ponds, etc. These lineaments can be further subdivided into faults, fractures and shear based on their image characters and geological evidences.

The attitude of beds (strike and dip) can be estimated broadly by studying the slope asymmetry, landform, drainage characteristics, etc. For example, horizontal to sub-horizontal beds show mesa / butte type of landform, dendritic drainage pattern and tonal / colour banding parallel to the contour lines. Inclined beds show triangular dip facets, cuestas, homoclines and hogbacks. The schistosity / foliation of the rocks are depicted on the satellite imagery by numerous thin, wavy and discontinuous lines. Folds can be identified on the satellite imagery by mapping the marker horizons. Further classification into anticline or syncline can be made on the basis of dip direction of beds.

For preparation of structural overlay, information from the following sources is required:

- Existing geological / hydrogeological maps and literature
- Interpretation of satellite imagery
- Field visits / surveys

8.4.3. Geomorphology

The synoptic view of satellite imagery facilitates better appreciation of geomorphology and helps in mapping of different landforms and their assemblage. The photo-interpretation criteria, such as tone, texture, shape, size,

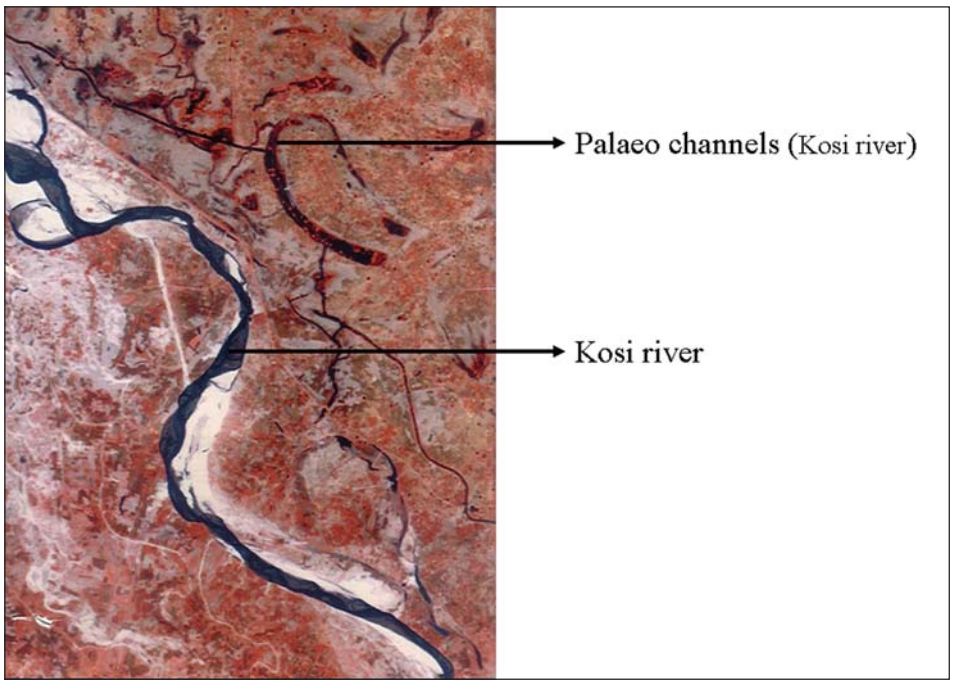

Figure 8.4: Interpretation of Lithology from satellite imagery

location, association, physiography, genesis of the landforms, nature of rocks / sediments, associated geological structures, etc., are to be used for identification of different landforms / geomorphic units (Figure 8.4). Initially, the entire image has to be classified into 3 major zones, i.e. Hills & Plateaus, Piedmont Zones, and Plains considering the physiography and relief as the criteria. Then, within each zone, different geomorphic units have to be mapped based on the landform characteristics, their aerial extent, depth of weathering, thickness of deposition etc., as discussed earlier. Subsequently, within the alluvial, deltaic, coastal, eolian and flood plains, individual landforms have to be mapped and represented on the map using the standard alphabetic codes.

These geomorphic units / landforms interpreted from the satellite imagery have to be verified on the ground during the field visit to collect the information on the depth of weathering, nature of weathered material, thickness of deposition and nature of deposited material, etc. For this purpose, nala / stream cuttings, existing wells, lithologs of the wells drilled have to be examined. By incorporating these details in the pre-field interpretation map, the final geomorphic map overlay has to be prepared.

For preparation of geomorphic map overlay, information from the following sources is required:

- Lithological map overlays
- Interpretation of satellite imagery
- Field visits / surveys

If previous maps / literature are available, the job becomes easier; even otherwise also, a good geomorphological map showing assemblage of different landforms can be prepared based on the above sources of information (Figure 8.5). The satellite image along with the interpreted lithological map overlay should be kept on the light table. A fresh transparent overlay should be kept on the top and each rock type should be classified into different geomorphic units / landforms as per the

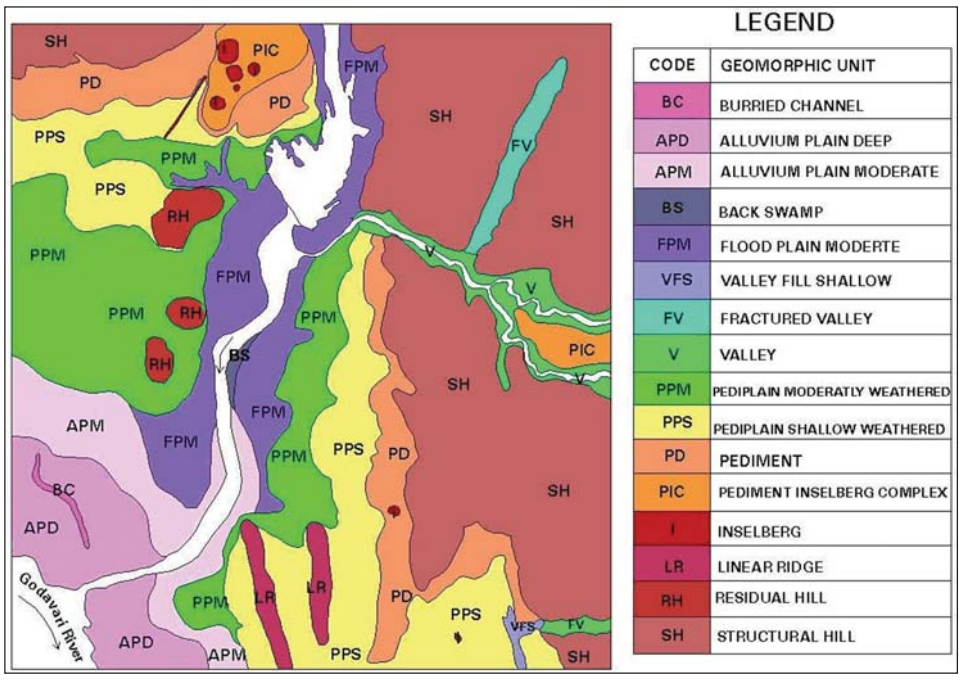

Figure 8.5: Preparation of Geomorphological map from satellite imagery

classification system suggested. Sometimes one lithologic unit may be classified into 2 or more geomorphic units / landforms and vice versa. This is to note that wherever the lithologic/ geomorphic boundaries are common, they should be made co-terminus. All the geomorphic units / landforms should be labeled with alphabetic annotation as RH, PPS, VFD, etc.

8.4.4. Hydrological Mapping

Satellite imagery provide excellent information on hydrologic aspects like stream/river courses, canals, major reservoirs, lakes, tanks, springs / seepages, canal commands, groundwater irrigated areas, etc. Based on visual interpretation of satellite data, all the above information can be derived and mapped.

The hydrologic information, derived from satellite imagery in conjunction with collateral data has to be shown on a separate map overlay in a classified manner with appropriate symbols. Further, the observation wells of State and Central Groundwater Departments and the wells inventoried during field visit have to be marked on this map overlay in a classified manner with appropriate symbols.

For preparation of hydrological map overlay, the following sources of information are required -

- Interpretation of satellite imagery
- Field visits / surveys
- Observation well data and
- Meteorological data

The following details are shown in the hydrological map overlay (Figure 8.6) -

- Canal / tank commands
- Groundwater irrigated areas
- Well observation data collected in the field and Govt. Depts
- Rain gauge stations indicating average annual rainfall. In case of absence of rain gauge station in a Toposheet, average annual rainfall in mm shall be given in the legend. Source of rainfall data shall be either IMD or District Gazetteer.

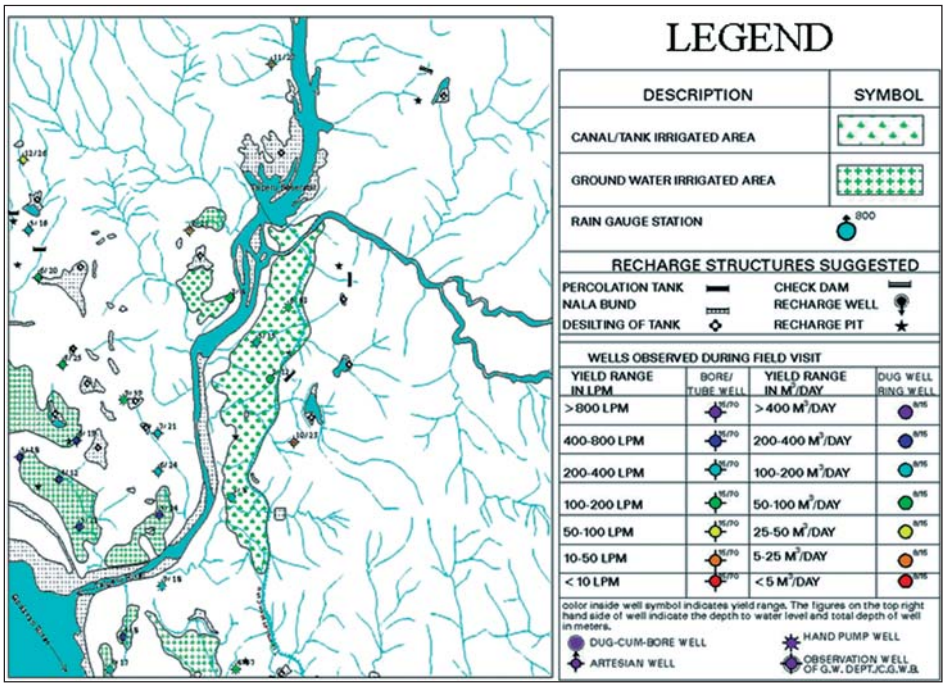

Figure 8.6: Preparation of Hydrological map from satellite imagery

8.4.5. Groundwater Prospects

For preparing the groundwater prospects map first integrate manually the lithological, structural, geomorphological and hydrological map overlays in the following manner:

Integrate lithologic-geomorphic units by superimposing the lithological and geomorphological map overlays. These integrated lithologic-geomorphic units are the 'hydrogeomorphic units' and have to be annotated with alphanumeric codes, e.g. PPS-71, PPD-81, UPM-32, etc. wherein the alphabetic code represents the geomorphic unit and the numeric code represents the lithologic unit. Transfer the geological structures from the structural map overlay on to the integrated lithologic-landform map. The geological structures, which act as conduits and barriers for groundwater movement, should be drawn.

Transfer the hydrological information including all the drainages and water bodies from the hydrological map overlay on to the integrated lithologic-landform -structure map. In addition to above, some of the rivers/streams, major water bodies and metalled roads (including NH & SH) have also to be transferred on the integrated map for control. To avoid the confusion in identification of features, rivers/stream/water bodies have to be drawn in cyan colour and roads in brown colour.

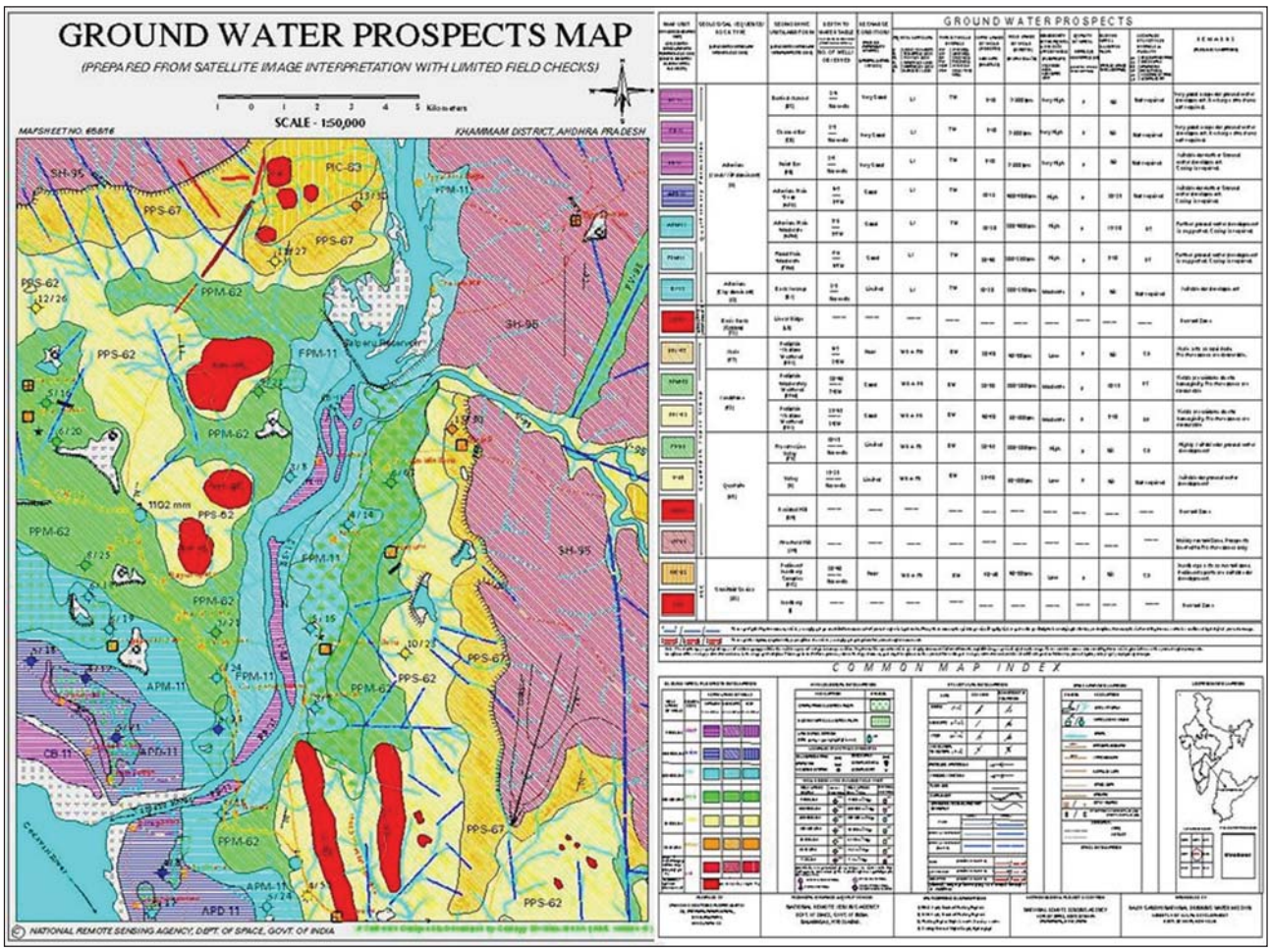

Figure 8.7: Preparation of Groundwater prospects map

All the hydrogeomorphic units occurring in the area have to be listed in the legend following the geological sequence. Then, the groundwater prospects of each hydrogeomorphic unit have to be evaluated by considering the lithological, structural, geomorphological and hydrological information (Figure 8.7). The details of the columns are mentioned in Figure 8.8.

Map Unit	Column- 1	Geological sequence/rock type
	Column- 2	Geomorphic unit/Landform
	Column- 3	Depth of water table/No. of wells observed
	Column- 4	Recharge conditions (rainfall &other sources)
	Column- 5	Nature of aquifer material
	Column- 6	Type of wells suitable
	Column- 7	Depth range of wells (suggested)
	Column- 8	Yield range of wells (expected)
	Column- 9	Aquifer homogeneity & success rate of wells
	Column-10	Quality of water (potable/non-potable)
	Column-11	Ground water irrig. Area (exploration status)
	Column-12	Recharge structures suitability & priority
	Column-13	Remarks (problems/limitations)

Figure 8.8: Details of the columns as listed in Figure 8.7

8.4.6. Groundwater Quality Mapping

There are many dissolved minerals and organic constituents present in groundwater in various concentrations. Among them the most common dissolved mineral substances are sodium,calcium, magnesium,

potassium, chloride, bicarbonate, and sulphate. In water chemistry, these substances are called common constituents. They are not harmful if they are within permissible limits. Few elements are highly toxic and hazardous to health of both human and animals. Groundwater is less susceptible to bacterial pollution than surface water because the soil and rocks through which groundwater flows screen out most of the bacteria. Bacteria, however, occasionally find their way into groundwater, sometimes in dangerous concentrations. But the bacterial pollution is not considered for the present study.

Water typically is not considered desirable for drinking if the quantity of dissolved minerals exceeds 500 mg/l (milligrams per liter). Water with > 500 mg/l of dissolved minerals is classed as slightly saline, but it is sometimes used in areas where less-mineralized water is not available. Water from some wells and springs contains very large concentrations of dissolved minerals and cannot be consumed by humans and other animals or plants. Many parts of the nation are underlain at depth by highly saline groundwater that has only very limited uses. Water that contains a lot of calcium and magnesium is said to be hard. The hardness of water is expressed in terms of the amount of calcium carbonate-the principal constituent of limestone or equivalent minerals that would be formed if the water is evaporated. Groundwater, especially if it is acidic, in many places contains excessive amounts of Iron. Iron causes reddish stains on plumbing fixtures and clothing. Like hardness, excessive iron content can be reduced by treatment. A test of the acidity of water is pH, which is a measure of the hydrogen-ion concentration. The pH scale ranges from 0 to 14. A pH of 7 indicates neutral water; greater than 7, the water is basic; less than 7, it is acidic.

The important toxic elements like fluoride and arsenic are creating more hazardous in many parts of the country. Fluoride is a major, naturally occurring contaminant in drinking water in many regions. At low levels, say 1 mg/l, it is found to be beneficial and high levels can cause structural tooth damage and at a high enough level can cause skeletal damage. The arsenic contamination invariably arises from natural geological and environmental conditions. Arsenic arises in many ores and minerals and is frequently present in combination with iron and manganese oxides; under various natural conditions it can be rendered soluble and released into the groundwater. The problem is especially acute in the Ganges delta region, where the arsenic is believed to be associated with the iron and manganese oxides in the alluvial sediments.

8.5. Groundwater Recharge Estimation

Since the groundwater is a replenishable resource, the quantity of water recharged every year from rainfall and other sources to a particular aquifer/basin/area is an important element in planning various developmental activities. The groundwater recharge estimation in the country is carried out using one of the following methods as recommended by Groundwater Resource Estimation Committee (GEC,1997) constituted by the Government of India.

8.5.1. Water Level Fluctuation Method

In this method, the gross groundwater recharge is worked out by multiplying the aquifer thickness (T) with specific yield (S) of the formation and the area (A) occupied by the unit. The thickness of aquifer (T) is determined based on water table fluctuations recorded from the observation wells. The specific yield (S) of each aquifer/formation is calculated by conducting pump tests. The Groundwater Estimation Committee (GEC, 1997) has suggested certain (S) values for different rock formations but recommended to use the actual (S) values calculated from the pumping tests in the concerned areas. In hard rock areas, variations in specific yield values are so common within the same rock formation, which lead to either over-estimation or under-estimation of the resource. The studies carried out at NRSC have proved that the satellite imagery by way of providing additional information on landforms, weathering and fracturing of the rocks which account for variations in specific yield values within the same rock formation, could help in more realistic estimation of the recharge. The individual rock formation could be sub-divided into more homogeneous hydrogeomorphic units taking into account the lithology, landform, fracturing and weathering characteristics derived from satellite data which further minimizes the error of averaging the aquifer parameters over large areas leading to more realistic and accurate estimation of the groundwater recharge.

Even for estimation of rechargeable area (A), satellite data provide the information on certain landforms like different types of hills, inselbergs, pediments, pediment-inselberg complexes and other rocky areas which are note favourable for groundwater recharge. Thus, it leads to more precise estimation of groundwater resource.

8.5.2. Rainfall Infiltration Method

The method involves the estimation of groundwater recharge by taking certain percentage of the rainfall as infiltration to groundwater depending upon the type of rock formation. By multiplying the average annual rainfall with the rainfall infiltration factor (RF) and the rechargeable area (A), the gross groundwater resource is estimated. The GEC (1997) has recommended different rainfall infiltration factors for different rock types. But in reality, the rainfall infiltration values are not constant for a given rock type and vary significantly with the variation in geomorphology, fracturing, weathering, type of soil, land use/land cover, etc., within the same rock type. Thus, the satellite data provide information on all the above mentioned factors which help in determining the rainfall infiltration values more accurately leading thereby to improved estimation of groundwater resource.

Further, like in the previous method, here also the satellite imagery enables identifying the landforms unfavourable for groundwater recharge. Satellite images also help driving precise estimation of the spatial extent of surface water bodies in different zones during different seasons which helps in the precise estimation of seepage to groundwater. Another important input that could be derived from satellite imagery is the spatial extent of irrigated croplands based on which the return flow of water from the irrigated fields could be worked out more precisely.

8.5.3. Groundwater Draft Estimation

Groundwater draft refers to the quantity of water that is being withdrawn from the aquifer. It is a key input in estimating groundwater balance available in a given area/basin which in turn governs all its developmental activities. Over-estimation of groundwater balance has resulted in a significant loss to the industrial and agricultural activities in many parts of the country and the under-estimation has restricted the planning of developmental activities in some parts. Hence, precise estimation of groundwater draft assumes greater significance.

Conventionally, the groundwater draft is estimated by unit draft method using mainly well census data. The number of wells of different types available in the area are multiplied with the unit draft fixed for each type of well to estimate the groundwater draft. But, upto-date well census and average withdrawal for each type of well are not precisely known. In some parts of the country, the groundwater draft is estimated based on the electricity consumed by the agricultural pump sets multiplied with the quantity of water discharged per unit power approximately gives the quantity of groundwater withdrawn. However, the power consumed by pump sets is not always proportional to the groundwater withdrawal and it depends mainly on the depth of the water table and efficiently of the pump sets. Further, misuse of power for other agricultural purposes and the groundwater draft from non-energized wells is also not taken into account in this method. Thus, by and large, the scientific community involved in groundwater budgeting in the country has been looking for a more realistic and appropriate method for groundwater draft estimation.

Satellite data provide reliable information of the extent of groundwater irrigated crops and their spatial distribution which helps in estimating the groundwater draft. Due to the presence of chlorophyll, the irrigated crops have maximum absorption in 0.63-0.69 micrometer region and high reflection in the infrared (0.77 to 0.86 micrometer) region of the electromagnetic (EM) spectrum. Because of characteristic absorption and reflection in different spectral bands, irrigated areas can be easily mapped by digital analysis of satellite data. From the total irrigated area, the area irrigated by major and minor irrigation sources can be excluded based on the association of such areas with surface water bodies and canal systems. Using multi-temporal satellite data and crop calendar supported by limited ground truth, the spatial extent of different crops irrigated by groundwater could be mapped. By multiplying the acreage of different crop types obtained from satellite data with the crop water requirement with respect to crop, the groundwater draft could be estimated more accurately.

This approach has been successfully demonstrated by NRSC, through an R&D study in Moinabad mandal of Ranga Reddy district, Andhra Pradesh. In this study, 100% well inventory was conducted for entire mandal in terms of total number of wells of different type, number of hours of pumping for each well and the number of days of pumping, acreage and crops cultivated, etc., under each well during the same period. Spatial distribution of groundwater irrigated areas within the mandal was derived from satellite data. The potential of remote sensing data for groundwater draft estimation and identification of over-exploited zones has been presented to the Groundwater Resources Estimation Committee (CGWB, 1991). Based on the suggestion made by GEC (1996), a pilot study was taken up in Rolla mandal of Ananthapur district A.P. in collaboration with the State Groundwater Department, Govt. of A. P. and the potential of remote sensing for groundwater draft estimation has been established.

8.5.4. Groundwater Balance and Stage of Development

The concept of groundwater balance was introduced by the World Bank for clearance of minor irrigation schemes

under ARDC phase-III programme. The groundwater balance refers to the net groundwater resource available for development in a given basin/area which is estimated by subtracting the net groundwater draft from the new recoverable recharge. Based on the balance, the stage of development is assessed and the areas are categorized into white, gray and dark zones. Thus, the groundwater balance and the stage of development are the two important factors governing the development of groundwater in a given area.

The inputs for realitistic estimation of groundwater resource and the draft derived from satellite data, as mentioned earlier, enable estimation of its balance more accurately which ultimately helps in the assessment of the stage of development. The demonstrative studies carried out at NRSC have shown that some of the areas which were categorized earlier as white through conventional approach have been re-categorized into gray or dark areas when refinements were made in the recharge and draft estimation based on inputs derived from satellite data. In many cases in the conventional approach it has been observed that the recharge is over estimated and draft is under estimated. Use of satellite image –derived inputs can rectify such anomalies and help in proper categorization of the areas in terms of development.

8.5.5. Identification and Mapping of Over-exploited Areas

In many parts of the country, the groundwater levels have started declining and in some cases even the existing wells have dried up due to lowering of water table. Rough estimates made so far put the loss due to drying up of old wells so far in the country at around Rupees 1000 crores. Studies conducted at NRSA have proved that satellite data by providing the information on distribution of groundwater irrigated areas, helps in mapping of groundwater over-exploited zones. On satellite image, the over exploited zones appear as large clusters of groundwater irrigated crops in different shades of red colour. Multitemporal satellite images are useful in continuous monitoring of groundwater utilisation in gray and dark areas.

8.6. Systematic Planning and Development

Systematic planning and development involves a scientific rationale for planning and development of groundwater. As mentioned earlier, using inputs derived from remote sensing data, it is possible to know more precisely where and how much of groundwater is available, how much of it is already utilized along with its spatial distribution, the net balance available for planning and prioritization of the areas based on the prospects, the demand and above all the rational development. Thus, the satellite data facilitate in the systematic planning and development of groundwater resource.

Augmentation of the Resource:

The demand for groundwater in our country is more than the resource available. Wherever the demand is higher than its availability augmentation of the resource by way constructing the percolation tanks, check dams and other water harvesting structures is required. The watershed management programme also helps improving the groundwater recharge resulting thereby in its augmentation.

Though the augmentation of the resource is possible everywhere, except in a few hydrogeologically unfavourable zones, covering entire country at a time during a given period with the available resources may not be feasible. Hence, the prioritization of zones is essential. In this endeavor too, the satellite data is useful in selection of areas based on the purpose for which water is required and the suitability of the site conditions. The problem villages having shortage of drinking water get first priority followed by and over exploited zones where crops are suffering from water or industrial production is affected due to shortage of water. Besides, satellite data help in the selection of suitable sites for construction of water harvesting structures. In our country, the IRS-1A/1B LISS-II data have been operationally used for identifying sites for construction of water harvesting structures apart from other soil and water conservation measures under a major nation wide project titled “Integrated Mission for Sustainable Development (IMSD) “covering 84 million ha and spread over in 175 districts.

Identification of Problem Areas for Conservation of Resource:

In spite of employing all the resource augmentation measures, in some parts, there may be a large gap between the demand and the resource that can be realized. Satellite data help in identifying and mapping of such hydrogeologically unfavourable zones/problem areas where conservation of the resource need to be taken up on a priority. Besides, satellite data are useful in suggesting the necessary changes in land use, cropping pattern and irrigation practices, etc., for conservation of the resource.

Conjunctive Use of Surface and Groundwater:

By providing information on surface and groundwater, the satellite data help in planning conjunctive use of surface and groundwater. Satellite data, as pointed out earlier, enable mapping of surface water bodies like minor, medium and major irrigation tanks/reservoirs; prospective groundwater zones, and canal and groundwater irrigated areas; and planning of new reservoirs/tanks. By suing such information, conjunctive use and management of surface and groundwater resources can be planned and implemented.

Optimum utilization and Management of Groundwater:

In the areas where resource potential is less than the demand and there is no scope for its augmentation optimal use of water for most beneficial purpose is the only solution. To avoid indiscriminate use of the scarce resource in such critical zones, certain regulations/ restrictions are essential. In this context, high spatial resolution IRS-1C LISS-III data have been found useful in demarcation of critical zones where groundwater resource is limited/scarce requiring regulated use, identification of alternative surface and groundwater sources around the problem areas and potential and prospective zones for establishing groundwater sanctuaries, and continuous monitoring to detect the unauthorized/indiscriminate use of groundwater for irrigation in the prohibited and restricted zones.

Monitoring Groundwater Development and Utilization:

The development of groundwater resource and its utilization is a dynamic phenomenon which requires frequent monitoring. Multi-temporal satellite images help in periodic monitoring of groundwater development which in turn helps in controlling the overexploitation and indiscriminate use of groundwater in some pockets leading thereby to scarcity of water for drinking and other essential uses. Proper monitoring of groundwater for projecting the drinking water sources assumes greater significance for a semi-arid country like India with competing demands for water. Due to continuous pumping of water for irrigation, the drinking water sources may get dried up. Some of the state Governments have already brought legislation to protect the drinking water sources. In this endeavor too, satellite data form a very valuable tool in monitoring the groundwater utilization for irrigation closer to the drinking water sources and also in the over-exploited zones.

8.7. Conclusions and Future Perspective

Satellite data provide information on rock types, landforms, geological structures, namely faults, folds, fractures, dykes, weathering, soil types, erosion, land use/land cover and surface water bodies (lakes, tanks, and reservoirs), distribution of groundwater irrigated areas and their acreage. Such information when integrated in a Geographic Information System (GIS) environment enable groundwater recharge estimation, draft estimation, calculating the balance, categorization of areas into highly developed, under developed and undeveloped, identification and mapping of prospective groundwater zones, systematic planning and development of groundwater, identification of over-exploited zones, prioritization of areas for resource augmentation, conservation and optimal use of water, conjunctive use of surface and groundwater, and continuous monitoring of groundwater development and its utilization. Polarimetric SAR, radar interferometry, Ground Penetrating Radar (GPR) and nuclear magnetic resonance techniques along with the stereoscopic measurements in the optical region may help further refinement in the level of information generated on groundwater using remote sensing data. The development of Groundwater Information System based on information derived from in situ, and air and space borne observation help in judicious planning, effective management and sustainable development of groundwater resource in the country.

Lot of progress is being made in groundwater prospects mapping, however full potential of total groundwater balance and its quality is yet to be realized. National Remote Sensing Centre (NRSC) has started work on preparation of groundwater quality layer in collaboration with states remote sensing centres under RGNDWM project. Detailed hydrogeological units have been extracted from remote sensing data from interpolating point locations (wells) of groundwater samples to prepare groundwater quality layer.

References

Bahuguna IM, Nayak S, Tamilarsan V and Moses J, 2003, Groundwater prospective zones in Basaltic terrain using Remote Sensing, *Journal of the Indian Society of Remote Sensing*, **31(2)** : 107–118.

Baldev S, Bhattacharya A and Hegde VS, 1991, IRS-1A application for groundwater targeting, *Current Science*, **61**: 171–179.

Bhattacharya PK and Patra HP, 1968. *Direct Current Geoelectrical sounding: Principles and Interpretation*, Elsevier Scientific Pub. Co., Amsterdam, The Netherlands,p 135.

Burrough PA, 1986, *Principles of Geographical Information Systems for Land Resources Assessment*. Glarendon Press, Oxford, U.K., p 194.

Central Ground Water Board (CGWB), 1991, Groundwater Resources and development Potential of Sambalpur District, Orissa, (South eastern region, Bhubaneswar), p 74.

Chandra S, Rao VA, Krishnamurthy NS, Dutta S and Ahmed S, 2006, Integrated studies for characterization of lineaments used to locate groundwater potential zones in a hard rock region of Karnataka, *Indian Hydrogeology Journal*,**14(6)**: 1042–1051

Chowdhury A, Jha MK, Chowdary VM and Mal BC, 2009, Integrated remote sensing and GIS-based approach for assessing groundwater potential in West Medinipur district, West Bengal, India, *International Journal of Remote Sensing*, **30(1)**: 231 – 250

Das SN, Narula KK and Laurin R, 1992, Run-off estimation potential indices of watersheds in Tilaiya Catchment, Bihar (India) through use of remote sensing and implementation of GIS, *Journal of the Indian Society of Remote Sensing*, **20**: 207–221.

Dinesh PK, Gopinath G and Seralathan P, 2007, Application of remote sensing and GIS for the demarcation of groundwater potential zones of a river basin in Kerala, southwest coast of India, *International Journal of Remote Sensing*, **28 (24)**: 5583–5601.

Drury SA, 1990, *A guide to remote sensing, interpreting images of the earth*. Oxford University Press, Oxford, United Kingdom, p. 126.

Ghoneim E and El-Baz F, 2007, DEM-optical-radar data integration for palaeohydrological mapping in the northern Darfur, Sudan: implication for groundwater exploration, *International Journal of Remote Sensing*, **28(22)**: 5001 – 5018.

Gupta RP, 1991, *Remote Sensing Geology,* Berlin ; New York : Springer-Verlag.

Heilman JL and DG Moore, 1982, Evaluating depth to shallow groundwater using Heat-Capacity Mapping Mission (HCMM) data, *Photogrammetric Engineering and Remote Sensing*, **48(12)**: 1903–1906.

Huntley D, 1978, Detection of shallow aquifers using thermal infrared imagery, *Water Resources Research*, **14(6)**: 1075–1083.

Jaiswal RK, Mukherjee S, Krishnamurthy J and Saxena R, 2003, Role of remote sensing and GIS techniques for generation of groundwater prospect zones toward rural development – an approach, *International Journal of Remote Sensing*, **24**: 993–1008.

Jasrotia AS, Kumar R and Saraf AK, 2007, Delineation of groundwater recharge sites using integrated remote sensing and GIS in Jammu district, India, *International Journal of Remote Sensing,* **28(22)**: 5019 – 5036

Jensen JR, 1986, *Introductory digital image processing*. Prentice Halls, Englewood Cliffs, NJ, p 339.

Jensen JR, 1995, *Introductory Digital Image Processing: A Remote Sensing Perspective* (2nd Edition), Prentice Hall, Englewood Cliffs, New Jersey, USA, p 316.

Moore GK, 1982, Ground-water applications of remote sensing, USGS Open File Report 82-240, US Geological Survey, Reston, Virginia.

Moran MS, Jackson RD, Slater PN and Teillet PM, 1992, Evaluation of simplified procedures for retrieval of land surface reflectance factors from satellite sensor output, *Remote Sensing of Environment*, **41**: 169-184.

Per Sander, 2007, Lineaments in groundwater exploration: a review of applications and limitations, *Hydrogeology Journal,* **15**: 71–74

Sabins FF Jr., 1987, Remote Sensing : Principles and Interpretation. W. H. Freeman and Co., San Frascisco, California, USA, p 429.

Shankar JG, Jagannadha Rao M, Rao BSP and Jugran DK, 2001, Hydrogeomorphology and Remote Sensing applications for groundwater exploration of Agnigundala Mineralised Belt, Andhra Pradesh, India, *Journal of the Indian Society of Remote Sensing,* **29 (3)**: 165–174.

Sreedevi PD, Subrahmanyam PD and Shakeel Ahmed, 2005, Integrated approach for delineating potential zones to explore for groundwater in the Pageru river basin, Cuddaph District, Andhrapradesh, India, *Hydrography Journal*, **13**: 534–543.

nrsc

Remote Sensing Applications

P. S. Roy
R. S. Dwivedi
D. Vijayan

National Remote Sensing Centre

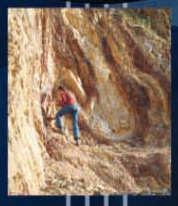

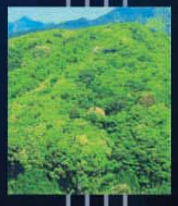

Remote Sensing Applications

Oceans

9.1. Introduction

Oceanography is the systematic scientific study of the Earth's oceans with the goal of understanding its processes and phenomena. Such a study requires an integrated view of the oceans and their relationships with other aspects of the Earth's overall environment. Surface of the earth is 70.8% water-covered. In the zonal direction, there is no land between 85-90 degrees N and between 55-60 degrees S. At meridional direction, 45-70N, there is more land than water and 70-90 S there is only land (Antarctica).

The average earth's radius is approximately 6371 km and the average depth of the ocean is about 3795 m. Thus the ocean is a thin skin on the outside of the earth. The average height of land is 245 m. Compared to the maximum elevation of about 9,000 m (Mt. Everest) over land, the maximum ocean depth is about 11,500 m (Mindanao Trench).

9.1.1. The need for Ocean Studies

Understanding the oceans is required for pure scientific curiosity, global climate change issues, fisheries/ aquaculture conservation, minerals/energy resource (both renewable and non-renewable) exploitation, coastal zone management, transportation/recreation, marine pollution hazards and submarine communication and acoustic propagation for strategic planning. There are several complementary approaches to studying the ocean: (1) observations, (2) process models, including pure theory and simplified numerical models, (3) simulations of the flow using complex numerical models, (4) combined observational/numerical modeling simulations (data assimilation) and (5) statistical approaches/soft computing techniques like multiple regression, genetic algorithm or artificial neural networks. The boundaries between these are not firm - observational analysis often includes modeling, process models are usually based on observations, complex numerical models are often exploited to understand general processes.

9.1.2. Broad disciplines of Ocean Sciences

The study of oceanography can be broadly classified in to three disciplines of physical, biological, and geological oceangraphy, though a clear demarcation is not possible. For example, ocean colour, which is primarily considered to be a biological parameter, has potential applications in physical and geological oceanography.

- Physical Oceanography - The study of waves, currents, tides, physical water properties, air-sea interaction and the physical forces that cause them.
- Biological Oceanography - The study of marine life and its productivity, life cycles, and ecosystems.
- Geological Oceanography - The study of plate tectonics, the geology of the ocean basins, the geologic history of the oceans and coastal processes erosion, sedimentation.

9.2. Physical Oceanography

Physical oceanography is the study of the physical properties of the oceans. Its goal is to understand the processes at all time and space scales, to simulate these processes, and to make predictions if possible. Some investigators consider dynamical oceanography, dealing with purely dynamics of the oceans, as a separate subject from physical oceanography. This deals with surface and internal waves, air-sea exchanges, turbulence and mixing, acoustics, heating and cooling, wave and wind-induced currents, tides, tsunamis, storm surges, large-scale waves affected by earth's rotation, large-scale eddies, general circulation and its changes, coupled ocean-atmosphere dynamics for weather and climate research/predictions.

9.2.1. Forces acting on Oceans

The external forces that act on the oceans are wind stress, wind-waves, swell-waves, turbulence, circulation, short and longwave radiation, evaporation, sensible and latent heat fluxes, precipitation and tidal oscillations. Solar radiation is the main source of heat energy to the oceans, though only 73% reaches 1 cm depth, 45% 1 m depth, 22% 10 m depth and 0.5% 100 m depth. These parameters consist of the heat budget of the oceans. The internal forces acting on the oceans are pressure/density gradients and viscosity or friction. In studying the ocean dynamics, the concept of scale analysis is very important that is summarized below.

9.2.2. Scale Analysis

A very small set of five equations governs all the motions of fluids from nearly-molecular scale to capillary waves to global circulation. This set of equations is nonlinear, which means that many terms are products of two things that vary. Since we can not possibly solve for all ranges of motion at the same time, direct solutions of the complete governing equations are impossible and computational power to cover all possible motions is simply not enough. The nonlinearities make theoretical solutions difficult. As a result we resort to the science of fluid mechanics, which is a science of approximation that differs from the traditional physics and mathematics with precise answers and proofs. Advanced applied mathematics includes the rigorous, justified approximation methods used in fluid mechanics. Approximations must be justified. Much of the debate about validity of a particular numerical model centers on justifying either the physical approximation or the numerical resolution (time and space scales that are resolved). As a first and necessary step, we evaluate the scales (approximate sizes) of the motion that we wish to resolve. We then perform a rigorous analysis of the governing equations, based on this scale analysis.

For oceanic flows, the aspect ratio, which is the ratio of height/length, is small (order 0.1 or 0.01 or smaller). In this case, motion in the vertical direction will be very different (smaller) than motion in the horizontal direction. For example, in case of general circulation, the horizontal scales are of the order of 100 to 1000 km whereas the vertical motions are of the order of 1-5 km, thus making the aspect ration very small.

Another very useful ratio is that of the earth's rotation time scale to the time scale of the actual motion in the oceans. For surface waves, this is a large number, and earth's rotation is not important. For internal waves, tides, this is of the order of 1, where rotation and changing motion are both important. For the ocean circulation, this ratio is very small, and time dependence is much less important than rotation.

9.2.3. Physical Oceanographic Parameters

The major physical oceanographic parameters include waves (both surface, internal and tsunamis), currents/ circulation, sea surface temperature (SST), sea surface height (SSH), and temperature/salinity/current profiles. SST can either be measured from instruments or estimated from the satellite thermal sensors. The profiles of temperature and salinity are generally measured from conductivity, temperature and depth (CTD) or expendable CTD observations. Expendable bathy thermographs (XBTs) provide only temperature profiles. Estimation of these profiles is possible from statistical or soft computing techniques using surface parameters affecting these profiles (Ali *et al.* 2004). Remote sensing of physical oceanographic parameters is discussed in the section on remote sensing observations. Ocean currents can be broadly divided into surface currents, comprising of 10% of waters and thermohaline currents comprising of 90%. Surface currents are mainly wind driven while the thermohaline circulation is due the temperature and salinity, as the name itself indicates. Surface currents are possible from in situ measurements from current meters, ship drifts. Thermohaline circulation is slow compared to the surface circulation. Using temperature and salinity profiles, dynamic topography can be estimated from which geostrophic velocities can be computed at different depths with respect to a depth of no motion. SSH observations from altimeters are also useful in estimating the geostrophic currents. Similarly, waves can be either measured from instruments like thermo-salinograph, wave recorders of bottom pressure recorder or from satellite sensors like synthetic aperture radar and altimeters. All these parameters are also possible to be estimated through ocean models forced by atmospheric parameters.

9.2.3.1. Ocean waves

Waves are periodic deformations of an interface. Surface waves in oceanography are deformations of the sea surface, i.e., the atmosphere-ocean interface. The deformations propagate with the wave speed, while the particles describe orbital or oscillatory motions at particle speed and remain at the same position on average.

In deep water, particle paths are circles. In shallow water, the particle paths flatten to ellipses. The change from deep to shallow water waves is observed when the wavelength λ becomes larger than twice the water depth h. A change in wave properties occurs also at $\lambda = 20h$. It is therefore useful to distinguish between deep water waves, transitional waves and shallow water waves or long waves. The distinction between deep and shallow water waves has little to do with absolute water depth but is determined by the *ratio* of water depth to wave length. The deep ocean can be shallow with respect to waves provided the wave length exceeds twice the ocean depth. This is the case for example with tides and tsunamis. Tsunamis are long waves generated by any disturbance generating vertical motion in the water column, generally, the submarine earthquakes.

9.2.3.2. Ocean currents

Ocean currents are due to the movement of water in the oceans. These currents could be due to the wind forcing, thermohaline gradients or tidal forcing. These currents are influenced by the earth's rotation through Corriolis deflection. Geostrophic currents are due to a balance between the pressure gradient force and the corriolis force. Geostrophic currents obtained through altimeter SSHA observations or through dynamic height computation using temperature and salinity profiles can be considered as actual currents over a spatial scale of 2 degrees and temporal scales of 2 days. Ocean currents play a very prominent role in transporting heat from equatorial to the polar regions.

9.2.3.3. Sea surface temperature

SST is the water temperature close to the surface. In practical terms, the exact meaning of *surface* varies according to the measurement method. A satellite infrared radiometer indirectly measures the temperature of a very thin layer of about 10 micrometres thick (referred to as the *skin*) of the ocean which leads to the phrase *skin temperature* (because infrared radiation is emitted from this layer). A microwave instrument measures subskin temperature at about 1 mm. A thermometer attached to a moored or drifting buoy in the ocean would measure the temperature at a specific depth, (e.g., at 1 m below the sea surface). The measurements routinely made from ships are often from the bucket temperatures and may be at various depths in the upper few meters of the ocean. In fact, this temperature is often called sea surface temperature.

9.2.3.4. Sea surface height

SSH is the height of the sea surface above the reference ellipsoid. The height above the geoid is termed as dynamic topography. SSH above a reference datum can be measured from tide gauges, whereas sea surface height anomalies (SSHAs) from the satellite altimeter observations. Since we do not have accurate estimations of the geoid, we cannot have absolute height measurements from altimeters. SSH variations are causes by the changes in the heat content of the oceans, currents and tidal oscillations. This is one of the very useful parameter of the oceans as it gives the integrated picture right from the bottom to the surface.

9.2.3.5. Radiation

Radiation coming from the sun is the main source of energy to the oceans. Since the atmosphere is transparent to the short wave radiation, energy reaches the ocean surface in the visible shortwave radiation. The radiation budget comprises of insolation, reflected shortwave radiation, out going longwave radiation. Besides radiation budget parameters, sensible and latent heat fluxes are the components of the heat budget of the oceans. Most of the dynamic phenomena taking place in the oceans are due to this net heat. Even the winds that drive the surface ocean currents are caused by the pressure difference due to the differences in the net heat at different places.

9.2.4. Applications of Physical Oceanographic Parameters and Processes

The physical oceanographic parameters like SST and processes like mixed layer dynamics, upwelling and currents have many applications in day to day life. Some of these aspects are discussed below. Identification of potential fishing zone that uses physical parameters like SST/SSHA is described under Biological Oceanography section.

9.2.4.1. Influence of oceans on weather and climate

Physical oceanographic parameters/processes, through air-sea interaction, play a very prominent role in cyclones, monsoons and climate change. The influence of land-sea breeze in moderating the coastal climate and the impact of El Nino or La Nina phenomenon on the global climate, particularly, on the Indian summer monsoon are the two well known examples.

Using a coupled ocean-atmospheric model, *Mao et al.,* [2000] reported that the rate of intensification and final intensity of cyclones are sensitive to the initial spatial distribution of the mixed layer. *Shay et al.,* [2000] described details of the response of the hurricane to a warm core eddy. Thus, a well-mixed upper ocean layer, due either to the mixing processes or to eddies, may be a more effective means of assessing oceanic regimes for tropical cyclone studies.

Water has amazing property of high thermal inertia, which helps to control our climate and make life on Earth possible. Ocean waters continuously move around the globe as if they were on a huge conveyor belt (Figure 9.1), moving from the surface waters to the deep and back again. Wind, salinity and temperature control this movement. This ocean circulation helps to spread the heat from the Sun throughout the Earth. This circulation also helps in transporting the heat received at the tropical regions to the polar regions.

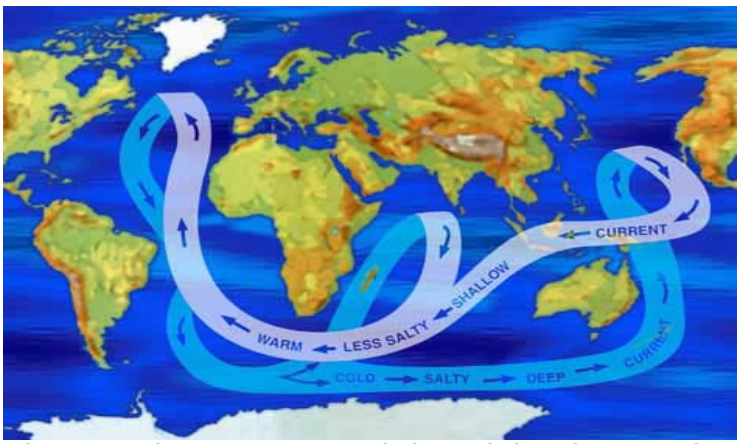

Figure 9.1: The ocean conveyor belt consisting of warm surface and cool deep water circulation (Source: http:// climatechange.wikispace.com)

9.2.4.2. Optimum ship route planning

Information on wind, currents, waves and swell help deciding on the optimum ship route planning through models, by which both time and fuel can be saved. Optimum ship route planning involves providing a vessel with a route recommendation prior to sailing and thereafter closely monitoring the progress of the vessel en route and updating the Master to ensure the vessel achieves either the earliest possible safe arrival or arrives safely at the required time. In case of the latter a clam sea speed setting will be suggested taking into account the weather, sea and current forecast ahead and an allowance for any variation in the expected speed loss. This service can also be of great use on "coastal" routes, by providing the master with advance warning of heavy weather conditions which might be encountered, for example, Tropical Storm conditions. Standard Ship Routing services can also be provided in combination with an onboard voyage planning system. Routing advice will be provided in addition to the regular weather data when sailing any cross ocean passage or in vicinity to severe weather events.

The provision of ship routing services should only be provided by those who have a wealth of experience and can be relied upon 24 hours a day, seven days a week, and are soley dedicated to ship routing. Only through complete dedication, extensive experience and high professional standards can any operator or owner rest easy knowing the best service is being provided. Any company can purport to provide ship routing but the recommendations and results can be entirely different and with disastrous results.

9.2.4.3. Strategic Applications

Acoustic signals that can travel great distances in the ocean are used in a wide range of scientific strategic applications. The important applications of sound propagation are in the detection of underwater targets and acoustic communication. Extremely complicated acoustic feature of the oceanic medium due to its inhomogeneous nature hampers the application of this important property. Speed of sound that is about four times faster than that in air varies with the characteristics of the medium through which it travels. Since the sound speed increases with increasing temperature, pressure and salinity, variations in these parameters control changes in sound speed profiles (SSP).

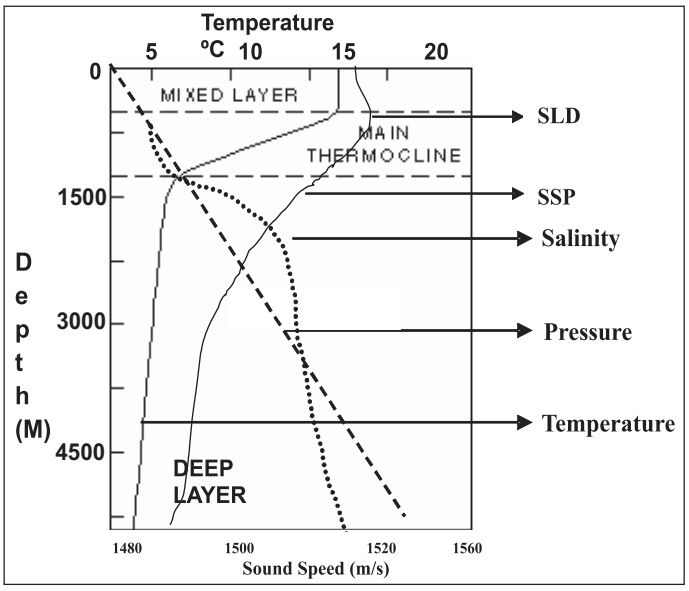

Figure 9.2: Vertical distribution of temperature, salinity, pressure and sound speed

Within the mixed layer, the temperature in the ocean remains almost constant and the pressure increases with depth. Hence, the sound speed also increases with increasing pressure/depth. On the other hand, in the thermocline region, effect of decreasing

temperature dominates over the effect of increasing pressure. In this region temperature decreases sharply with increasing depth and hence, sound speed decreases even though the pressure increases (Figure 9.2).

Under favourable conditions, shadow zones that have important bearing on the strategic applications are created below the mixed layer by this property of sound propagation. The vertical gradient of sound speed determines the direction that sound wave propagate that has both regional and temporal variations. Conventionally, SSPs are obtained either by a velocimeter that measures sound speed directly or by using the *in situ* temperature and salinity (T/S) profiles that control the sound speed. Since *in situ* observations of these parameters at all locations in the ocean are difficult to obtain due to the limitations of measurements, it is worthwhile to estimate SSP from surface parameters obtainable from remote sensing platforms. An application of SSPs is the estimation of sonic layer depth (SLD), which is the near surface maximum sound speed in the ocean, knowledge of which is used to reduce errors in sonar surveys.

Other physical oceanographic applications dealing with the biological and geological oceanographic parameters are discussed in their respective sections.

9.3. Biological Oceanography

Biological Oceanography concerns the biology and ecology of oceanic, marine, coastal and estuarine organisms. These range from viruses and bacteria to microbes and phytoplankton, from zooplankton and benthic invertebrates to shellfish, fish and marine mammals. The organisms live in a dynamic fluid easily described as a chemical soup that covers ~71% of the earth's surface and is intimately coupled to the atmosphere, the seafloor and the land. Thus, to determine how organisms are influenced by their environment, biological oceanographers must function across many sub-disciplines such as biochemistry, genetics, physiology, behaviour, population dynamics and community ecology.

Besides ocean colour, an important biological oceanographic parameter, the physical parameters also influence the biological processes.

9.3.1. Ocean Colour

Information on ocean colour is critical for some of the following applications:

- To identify the Potential Fishing Zones(PFZ) for improving catch efficiency
- To provide an accurate and detailed understanding of the oceanographic environment for offshore platform design - reducing the risks
- Provide timely information on strong currents, eddies, fronts, sediment plumes and mixing zones, for ocean environmental monitoring
- Synoptic maps of ocean colour (chlorophyll), spatial structure of pelagic ecosystem at synoptic scales

Ocean colour sensors provides valuable information for the understanding of some of the key scientific issues like

- Determine the spatial and temporal distribution of phytoplankton blooms with the magnitude and variability of primary production on global scale
- To compute regional and basin scale marine primary production
- To quantify the oceans role in global carbon cycle and other bio-geochemical cycles
- Identify and quantify the relationship between ocean physics and large scale patterns of productivity
- Elucidate the complex mechanism between upwelling and large scale circulation patterns in ocean basins
- Provides a better understanding of the processes associated with mixing along the edge of coastal currents, eddies, western boundary currents and fronts

9.3.2. Applications of Ocean Colour

Since the upwelling brings nutrient rich bottom cool waters to the surface, information on ocean colour can be used in identifying the upwelling regions (other parameters that help in locating the upwelling zones are SST and SSH). These upwelling areas attract fish and are the potential fishing grounds.

9.3.2.1. Coastal Upwelling

Vertical movement or upwelling of deep, cold, nutrient rich water is an important process in the marine ecosystem. Upwelling areas tend to be highly productive and are often the site of important fisheries. Upwelling is largely caused by wind stress and may occur in the coastal ocean and deep ocean. When winds are favourable this varies on time scales of 3 to 5 days and on length scales from a few tens to several hundred of Km. Arabian sea one of the worlds most productive regions of the ocean during summer monsoon, June-September. The coastal upwelling along Somalia and Arabia (Morrison *et al.*, 1998) and along the southwest coast of India (Shetye *et al.*, 1990) turns the coastal waters into a region of high biological productivity. The Open ocean upwelling (Bauer, *et al.*,1991), wind driven mixing (Lee *et al.*,2000) and lateral advection (Prasanna Kumar *et al.*,2001) makes the open ocean waters of central Arabian Sea more productive. Whereas in the Bay of Bengal upwelling reported is mainly confined very close to the coast along the southwestern boundary seems to be episodic (Murthy and Varadachari, 1968 , Shetye *et al.*, 1991). Extensive work has been carried out by many researchers in identification and monitoring of coastal and open ocean upwelling in the Arabian sea using ocean colour sensors data like CZCS and SeaWiFS. Vinayachandran *et al.*, (2004) studied the increased chlorophyll concentration in the waters around Sri Lanka during July 1999 using IRS-P4 OCM images and attributed the enhanced chlorophyll due to the coastal upwelling driven by monsoon winds causing the nutrient enrichment in the surface layer.

9.3.2.2. Coastal currents using sequential ocean colour images

Having 360 meters spatial resolution (high among ocean colour sensors), IRS-P4 OCM data has been used for computing sea surface velocities along North Orissa coast. The patterns of ocean colour images are used as tracers to measure the displacement of surface waters. Surface velocities can be computed using the sequential OCM images. Computed velocities were compared with simultaneous in-situ measurements along the coast using current meter observations with careful navigation of the OCM images with respect to in-situ measurements using ground location measurements provided by ship GPS locations. The pair of OCM images co-registered within an error limit of one pixel. Prasad *et al.*, (2002) found that the measured and retrieved surface velocities using OCM sequential images are highly comparable (R^2=0.99) for both magnitude and direction using the maximum cross-correlation technique for OCM sequential images. Also retrieved the suspended sediment concentration along North Orissa coast for January 2000 using OCM.

9.3.2.3. Seasonal Phytoplankton Blooms

Many researchers studied the seasonality of chlorophyll and phytoplankton blooms in the Arabian sea. Joint Global Ocean Flux Study (GOFS) identified the Arabian Sea as one of the areas for biogeochemical processes study. Under the Indian JGOFS programme studied are confined to the central and eastern Arabian Sea, whereas other countries extensively studied the western Arabian Sea. Arabian Sea experiences significant temporal and spatial variations with respect to biogeochemical properties. During this period due to strong vertical mixing processes, deep rich nutrient water are well mixed with near-surface waters that are depleted of nutrients. The net effect is fertilization of the upper layers of the ocean and stimulation of rapid phytoplankton growth as the daily sunlight increases during spring. Ocean colour measurement provides information on large scale distribution and timing of spring blooms in the global ocean. In the Arabian Sea, the general occurrence of the sub-surface chlorophyll maximum at around 40-60 meters during May (Bhattathiri et.al., 1996). The addition of nutrients into the surface layer leads to the growth of phytoplankton blooms. Banse and English (2000) reviewed the seasonal distribution of chlorophyll-a and phytoplankton blooms in the Arabian Sea. Sarangi *et al.*, (2001a, 2001b) studied the phytoplankton distribution using IRS-P4 Ocean Colour Monitor (OCM) data and observed very high concentrations of chlorophyll-a in the range of 2-5 mg/m^3 in the bloom. Chauhan *et al.*, (2001) studied the surface chlorophyll distribution in the Arabian Sea using OCM data. Vinayachandran *et al.*, (2003) used the satellite derived chlorophyll images to study the phytoplankton blooms in the Bay of Bengal during northeast monsoon (November- February). OCTS (1996) and SeaWiFS (1997-2000) chlorophyll images shows the presence of a phytoplankton bloom in the southwestern Bay of Bengal during November- January. The chlorophyll concentration in the bloom is as high as 2.0 mg/m^3 compared to near zero values before the bloom. Using IRS-P4, OCM chlorophyll maps Vinayachandran *et al.*, (2004) studied the increased chlorophyll concentration in the waters around Sri Lanka during July 1999 and explained the physical processes which lead to the phytoplankton bloom using upper ocean temperature profiles, satellite derived winds, sea surface temperature (SST) and sea level anomalies (SLA).

9.3.2.4. Study of potential fishing zones

One of major applications of ocean colour is in delineating the potential fishing zones by combining the information obtained from SST. It is established that, most of the very good fishing grounds of the world oceans are located in the areas, where upwelling is found to occur. Nearly 50% of the estimated global potential annual fish production comes from the upwelling areas. Modern fishermen require timely, reliable and accurate information on meteorological and oceanographic parameters, such as ocean colour, sea surface temperature, winds, waves, circulation etc. Several researchers have made use of Advanced Very High Resolution Radiometer (AVHRR) thermal infrared data from the NOAA Satellite series to identify the potential fishing zones. Since more than two decades, advanced countries and some of the developing countries have been using sea surface temperature (SST) information to detect thermal fronts, upwelling zones, currents and large scale oceanic eddies to aid the fishermen at sea on an operational basis (Laurs *et al.*, 1981, Gower 1982, Laurs and Brucks 1985).

India has a very long coast line of about 7500 kilometre, spread in 10 maritime states comprising of 3100 fishing villages with 1588 fish landing centres (CMFRI, bulletin). The Potential Fishing Zone (PFZ) forecast information from NOAA-AVHRR thermal infrared data (SST) has been made available to the fishing industry in India since late 1991 on an experimental basis and was made operational from late 1992 (Deekshatulu *et al.*, 1992, Nath *et al.*, 1992). The validation results show that on an average the Catch Per Unit Effort (CPUE) is more along the thermal boundaries in comparison to the catch obtained from other areas. The feedback on the utilisation of potential fishing zone information inferred from SST manifested surface features, revealed that they are highly useful and aid to the fishermen in saving the fuel and search time. Other than physical processes which inferred from SST, chlorophyll/ phytoplankton biomass is another indicator for locations of fish schools in tropical oceans where SST gradients are weak.

With the availability of real-time data from Ocean Colour Sensors and thermal sensors synergistic analysis of IRS-P4 OCM chlorophyll and AVHRR SST was carried out to understand the patterns of variability of oceanic features along the Indian coast at some selected stretches. Chlorophyll and SST features were found coincided at many locations indicating that the biological and physical processes are strongly and closely coupled. Achieved fish catch locations were plotted on the SST and chlorophyll images to understand the relationship with oceanic features and fish catch. High catches were found in the vicinity of matching oceanic features in both the images. Dwivedi *et al.*, (2002) developed an experimental PFZ forecasts integrating chlorophyll with SST off Gujarat and Kerala coast and forecasts were generated during 1999-2000, 2000-01 and 2001-2002. From the composite image only matching features from chlorophyll and SST were demarcated as PFZs and communicated to Fishery Survey of India (FSI), Veraval (Gujarat) and Gujarat Fishery Department for validating these forecasts along Gujarat coast and also communicated to CIFT for validation along Kerala coast. About two folds increase in catch was reported in the pelagic catch during validation phase of 1999-2000 (Solanki *et al.*, 2001). Validation experiments continued for the fishing seasons 2000-2001 & 2001-2002 along Gujarat and Kerala coasts. Catch Per unit Effort (CPUE) with high catch were found in fishing hauls taken in the vicinity of features and comparatively low catch were reported away from the features.

A joint programme was undertaken for the generation of potential fishing zones (PFZ) along East coast of India using the composite of SST and chlorophyll image during the years 2002, 2003 and 2004. Flow chart (Figure 9.3) explains the processing methodology for the retrieval of SST (AVHRR), Chlorophyll (IRS-P4, OCM), and generation of integrated PFZ(IPFZ) chart.

Validation experiments were conducted along North Andhra by National Remote Sensing Agency (NRSA) and Fishery Survey of India (FSI), Viskapatnam base during November 2002, April 2003, December 2003 through - February 2004. Observed that chlorophyll gradients are prominent (moderate to strong) compare to SST (feeble) gradients along the

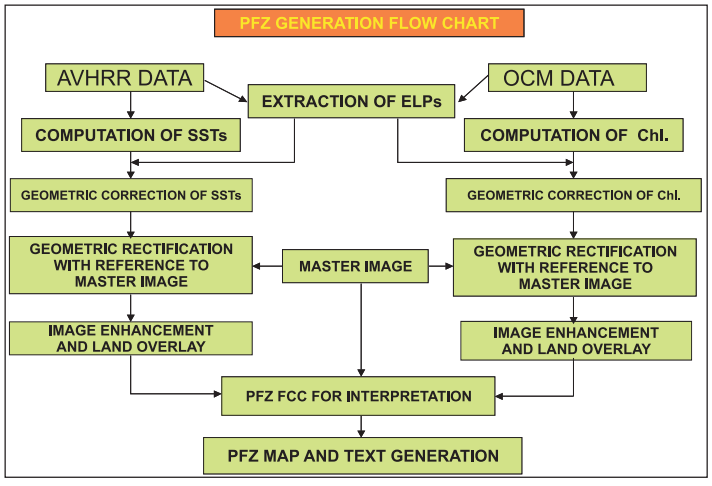

Figure 9.3: Showing the processing steps for generation of PFZ chart using AVHRR and IRS-P4 OCM data

North Andhra and Orissa coast. All the times it is observed that fish catches are more in the areas where SST and chlorophyll features are strongly coupled. Figure 9.4 shows the SST and Chlorophyll images for the period 14-17th November 2002 and integrated PFZ(IPFZ) chart generated using SST and Chlorophyll image depicting the potential fishing areas valid up to 22nd November 2002 along north Andhra and Orissa coast. In these areas fish catches are about 150- 400 kg for hall and other areas catches are only 10-100 kg.

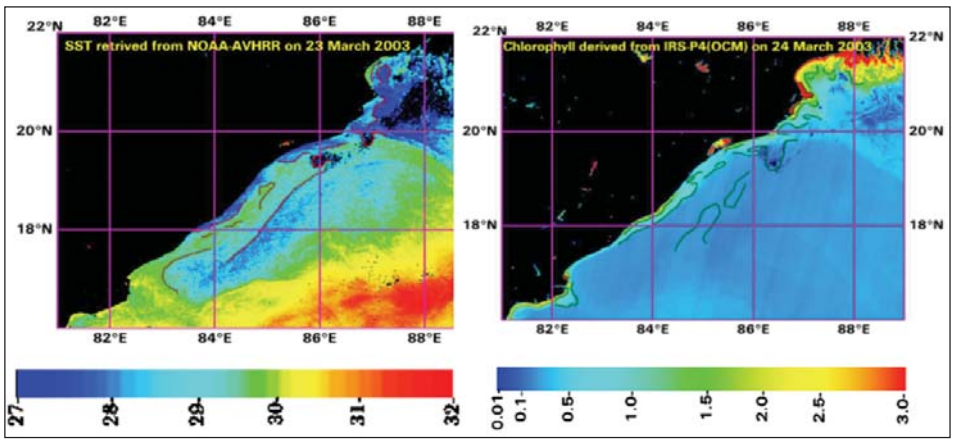

Figure 9.4: Synergy of SST and Chlorophyll derived from NOAA and OCM respectively

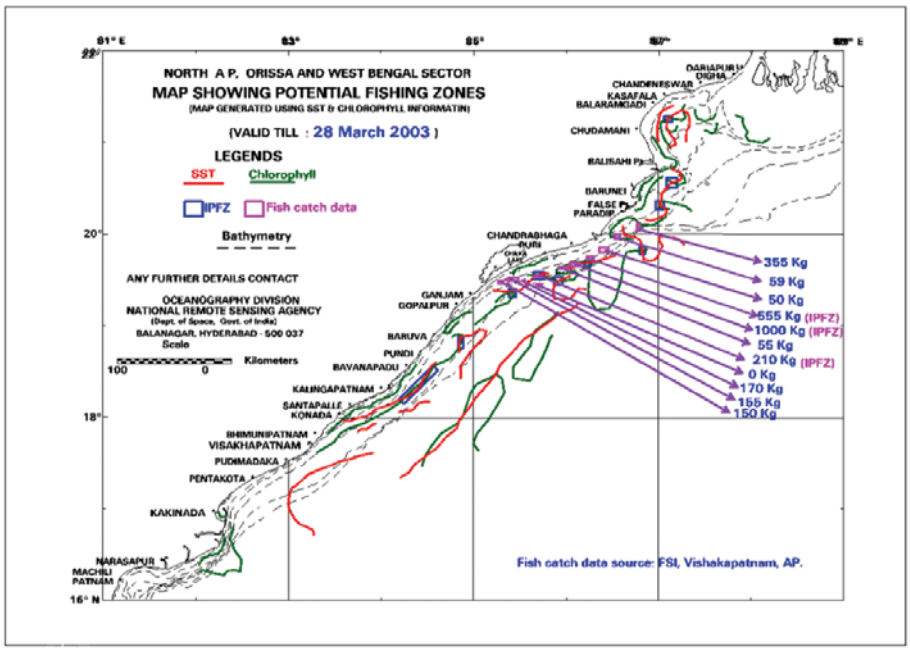

Figure 9.5: IPFZ Validation Experiment (Source: FSI, Visakhapatnam) Map showing Fish Catch data with respect to IPFZ forecast

A comprehensive validation programme was conducted in collaboration with FSI & INCOIS during the 2004 fishing season along North Andhra and Orissa coast. Figure 9.5 shows IPFZ forecast during 21-24th March 2004 (valid till 28th March 2003) along Orissa and Andhra coast. Plotted fish catches on IPFZ chart observed high catches 100-450 kg in the integrated fishing zones and minimum to nil catches in other areas. Validation is only from the FSI fishing vessels covering a limited areas, depicting the exact fishing locations and actual fish catches.

9.3.2.5. Impact of tropical cyclones on ocean colour

Tropical cyclones are a major hazard in tropical coastal regions, both in terms of loss of life and economic damage. The effect of the tropical cyclone to the cooling of Sea Surface Temperature (SST) is widely known (Gopalakrishna *et al.*, 1993; Murthy *et al.*, 1983, Premkumar *et al.*, 2000), its effect on the distribution of phytoplankton and chlorophyll in the open waters is yet to be documented. In the open sea, tropical cyclones may deepen the mixed layer by 20-30 m (Malone *et al.*, 1993). The nutrients injected to the well-lit euphotic zone in such events trigger the growth of the plankton. Shortly after a cyclone event an increase in phytoplankton biomass and productivity is observed by Delesalle *et al.*,(1993). Satellite ocean-color for chlorophyll concentrations is a new approach for understanding the influence of tropical cyclones on biology, such as phytoplankton blooms, and oceanic physical processes, such as eddies.

Detailed study of tropical cyclone-generated phytoplankton bloom in the eastern Arabian Sea during 19 May – 5 June 2001 using the IRS-P4 Ocean color data was well documented by Subrahmanyam *et al.*, 2002. Processed OCM data using an operational scheme available at NRSA developed by Ramana *et al.*,.(2000). Retrieved chlorophyll from OCM using operational OC2.V.4 algorithm developed by O'Reilly *et al.*, (2000) after applying the atmospheric corrections. Cyclone formed and developed in the eastern Arabian Sea during

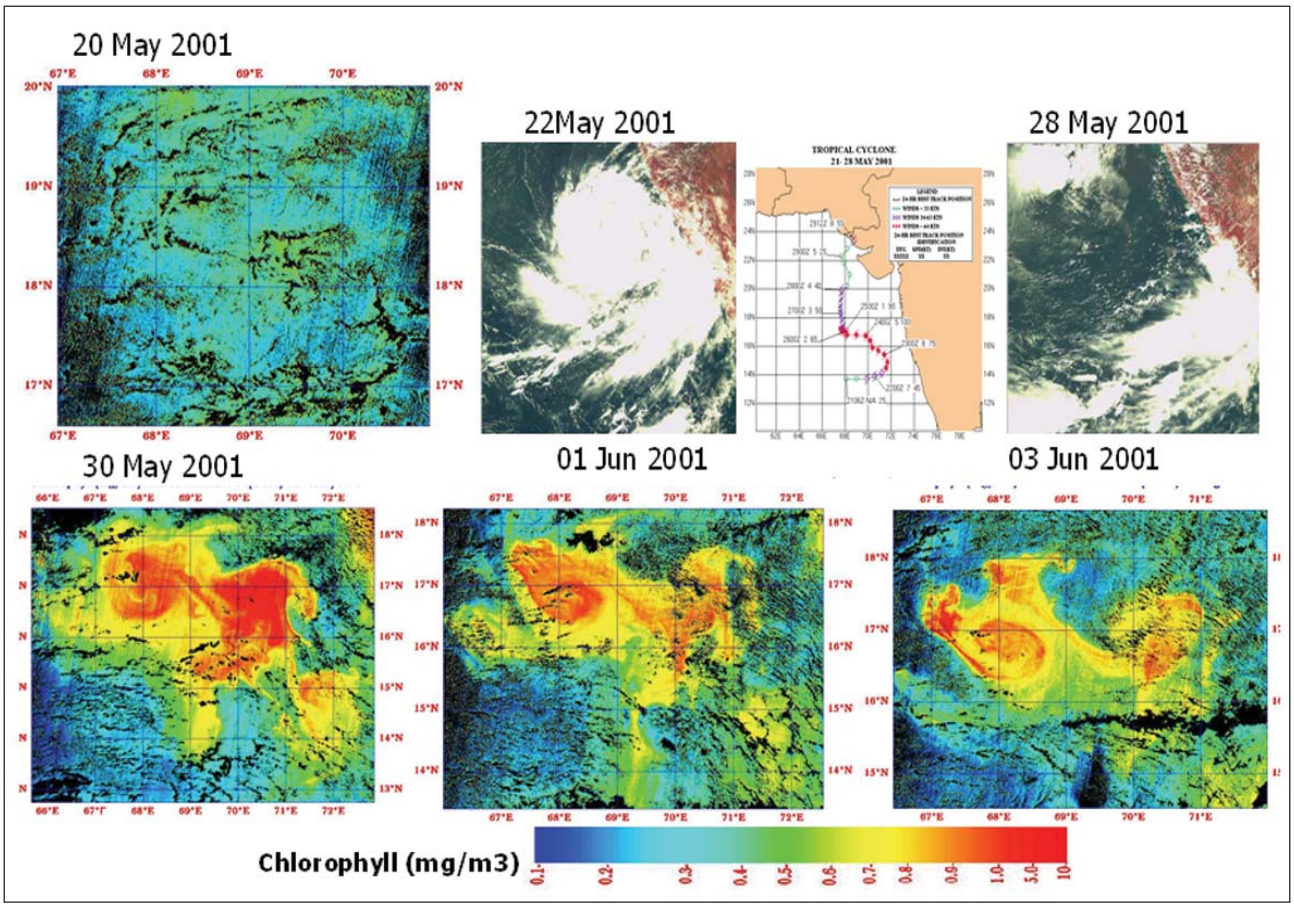

Figure 9.6: Enhanced Chlorophyll for the Tropical Cyclone during 21-28th May, 2001 in the Arabian sea

21-28 May 2001, system intensified and further moved in a north-westerly direction from 14°N, 71.8°E on 22 May to 17°N, 68°E on 26 May, 2001. After 26 May, the cyclone weakened and moved towards north. While processing the OCM images for this area it was noticed intensive phytoplankton blooms with high chlorophyll values (> 5.0 mg m^{-3}) at the centre of the blooms located along 17°N from 67°E to 71°E. Owing to overcast skies a cloud-free OCM data could not be obtained during the period of cyclone (23-28 May 2001) figure 9.6. Prior to the cyclone, the chlorophyll levels were minimum ranging between (0.1 to 0.4 mg m^{-3}) which is in agreement with the reported values in literature, exhibiting the oligotrophic (nutrient depleted) conditions during the period of intense heating (May) in the Arabian Sea (Bhattathiri *et al.*, 1996, Prasannakumar *et al.*, 2000). After the cyclone is fully intensified and moved towards north, higher concentrations of chlorophyll appear as blooms in the region influenced by the cyclone. The blooms look like round-shaped cyclonic eddies of 250-300 km diameter on 30 May between 16° and 18°N. These blooms persist with gradually reduced intensity till 3rd June 2001. It is also noticed that the blooms with decrease of chlorophyll concentration persisted for another one week, after the cyclone vanished from the Arabian Sea.

Another case study was carried out using OCM data in the Bay of Bengal tropical cyclone during December 2000. A depression formed about 800 km southeast of Pondicherry at 11.00deg N, 90.00deg E on 26 November, 2000. It further intensified into a cyclonic storm about 300 km east of Pondichery/ Cuddlore stretch by 29 November, intensified and remained stationary for a day at 12.00N and 82.13E on 30th November and then moved to west and crossed the land on 1st December 2000, further moved to the Arabian sea crossed the west coast with less intensity of 30 knots and gain intensified along 11.0 N and further weekend. During 16-23 November, 2000 the Chlorophyll concentration in the Southwest Bay of Bengal is around 0.25 mg/m^3. After the passage of cyclone there is an increase in the chlorophyll concentration, which reached to 0.55 mg/m^3. Maximum increase in chlorophyll concentration is located around 11.0^0N lat. and $81.0^07'$ E long. where the values increased from 0.35 mg/m^3 to 0.70 mg/m^3 for a few pixels. Study also has been carried for another cyclone in the Bay of Bengal during 5-19th May 2003. Maximum cyclonic winds are on 11th May 2003 around 86.5^0 E.Lon.,12.0^0 N. Lat. Processed OCM data for 5th May (before) and 19th May (after) 2003 and retrieved chlorophyll. These are the only images (partially cloudy) available during this period. Observed enhanced chlorophyll concentration after the cyclone. Chlorophyll increased from 0.35 to 0.85mg/m^3 due to the cyclonic wind mixing.

9.3.2.6. Studies of small scale eddies/gyres

Variability of ocean health can be assessed through the small scale features like oceanic eddies and small scale gyres. Oceanic eddies scoops nutrient rich water from sub surface depths to surface layer in different spatio-temporal dimensions. Indian ocean eddies are transitional in nature, reverse its direction and changes its intensity with the reversal of monsoon. The cyclonic eddies are generally considered as biologically rich with high nutrients and cold temperatures. The dimensions of these small-scale features are clearly visible in satellite imagery. OCM images dated 26-27th February 2000 showing the small scale gyres and spiral eddies in the western Arabian Sea. A strong anticyclonic (AC) spiral eddy with a size of 100 km with high chlorophyll concentration is clearly seen on the image centered around 61.0^{0}E.Lon, 24.^{0}N.Lat. Derived chlorophyll values from OCM clearly indicates the location of high chlorophyll eddy, appears to be entraining upwelled water from the Oman coast. West of the Anticyclonic eddy a small cyclonic eddy is seen on the image centred at 57.0^{0}E.Lon, 25.^{0}N.Lat. The presence of two gyre system is confirmed in the chlorophyll image (Figure 9.7). The position of these gyres are similar to that reported by Reynolds during 1992 NE monsoon. Several small spiral eddies are also seen on OCM image in Northern Arabian Sea with high concentration of chlorophyll during last week of February 2000. Contrary to this image OCM derived chlorophyll during January 2003 has shown a large cyclonic eddy centred at 24.0^0 N. Lat, 61.0^0 E. Long. OCM chlorophyll images clearly shown the presence of cyclonic & anticyclonic eddies in this region. OCM data clearly demonstrated the spatial extent (size, area) and the seasonal occurrence of these small scale features and its importance for the study of increased chlorophyll distribution in the northern Arabian Sea.

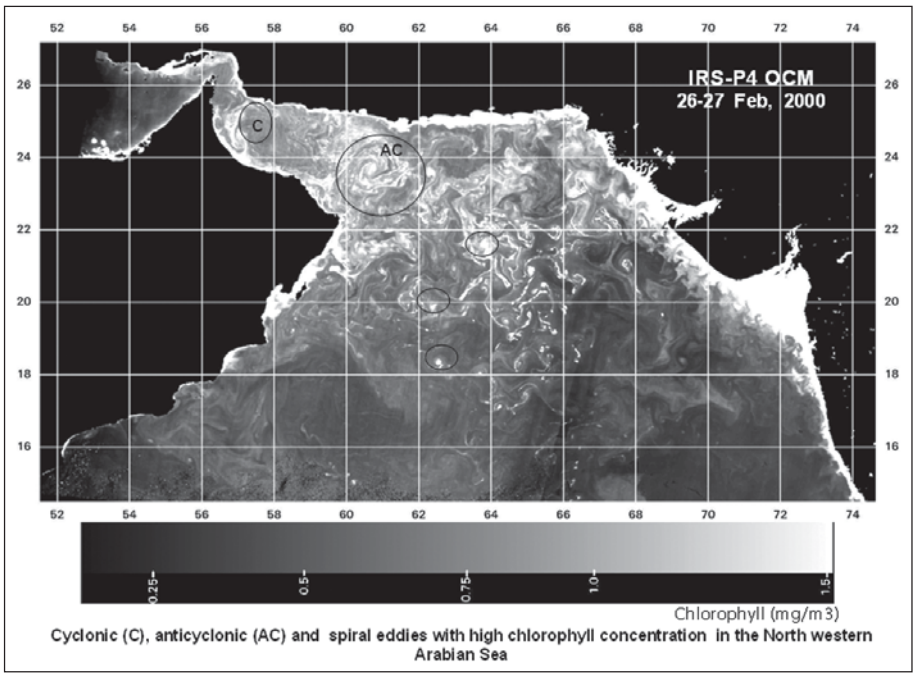

Figure 9.7: OCM chlorophyll images showing the Cyclonic & Anticyclonic eddies in Arabian Sea during 26-27 th February 2000

9.3.2.7. River Plumes

Riverine and estuarine plumes contain relatively high concentration of suspended organic and inorganic material which are highly reflective in the visible spectrum. This high reflectance is easily observed by satellite borne ocean -colour sensors. To understand the fate of fluvial nutrients and their possible effects on carbon budget requires an understanding of the sedimentation and circulation processes that control the exchange of material across the continental shelf. The river plumes spread 100 of km across the shelf. The sediment flow towards the equator confirming the earlier flow patterns along this coast during this season. Ocean colour data provides plume information and its dissipation on continental shelves and insight into other processes that effect the rate at which river and ocean water intermix.

9.4. Geological Oceanography

Marine Geology is concerned with the earth beneath the sea including the near shore zones (beaches, marshes, lagoons, and reefs), the shelf seas and -margins. Adjacent to these shallow water areas continental and island slopes connect the shallow water regions with the deep-sea basins that occupy around 80% of the sub sea-surface. Other aspects of marine geology addressed here include ocean circulation, plate tectonics, and critical events in present past global oceanography like sea-level changes. Geological processes at work in the sea are responsible for various marine environments ranging from the near shore estuarine and coastal environments to those of the deep ocean basins.

The shoreline is in a dynamic state, constantly adjusting to the combined effects of natural processes. Winds, waves, tides, and currents are the major agents active in the depositional and erosional processes. Coastal zone has been fastest emerging region in the globe for developing port, harbour cities and became gateway to the global population. Many thickly populated cities such as Mumbai, Shanghai, Seoul, Karachi, Istanbul, Jakarta, and New York are located on the coast. Considering the total global population about twenty percent of the population lives within 30 Km and twice within 100 Km (Cohen *et al.*, 1997). More than 75% of the human population lives within 60 km of a coast by 2000 (Michener *et al.*, 1997). Human pursuit for food, habitation, commerce, recreations, and defense expanded beyond coast into sea for centuries. Growing population demands for more land, this ultimately leads to fast depletion of coastal land cover and loss of coastal habitats. Many coastal wetlands and sandy beaches are reclaimed for settlements and infrastructure developments. Global warming, increased land and seas surface temperature and decreased global ice cover resulting rise in sea level. Frequent storm and wave energy increase flood, erosion, and sedimentation in some areas of the coast (Ericson, 2006). More land habitations are under inundation by sea and hydrochemistry of ground and seawater, ecosystems characteristic, biodiversity, and human health are also been affected. The responses of the coastal system to climatic changes and anthropogenic impact are well recognized. Hence, oceans become more energetic and complex than expected. Understanding of changing physical, biological and biogeochemistry characteristics of the coastal system and their dynamics are insufficient due to time lag between process and system response.

The marine ecosystem is the largest aquatic system on the earth which receives light and heat energy from sun, mixed by the wind, mechanical energy from the tides (Nixon, 1988) and hence more dynamic. It is intrinsically linked global climate changes in many ways as it covers 70% of the earth's surface and act as a huge reservoir for both heat and carbon dioxide. Ocean plays very active role in climate conditions by releasing heat and carbon dioxide from ocean surface or takes it to atmosphere (Bryan and Manabe, 1985).

The coast is a transitional zone between land and sea and integration of marine and terrestrial ecosystems. Human needs mounting force on the coastal ecosystem to a new changing environment. Both industrialization and urbanization have claimed more coastal land areas. Industrial and urban waste contaminations over a long period jeopardize the coastal ecosystem integrity including stability, sustainability, biodiversity, community composition, etc. (Burke *et al.*, 2001[a]). The changing and dynamic nature of the coast and coastal zone mean that it rarely fits within the static human boundaries often used for administrative and planning purposes (King, 1998).

Integrated Coastal Management (ICM) is a dynamic process by which decisions are taken for the use, development, and protection of coastal/marine areas and resources. Most often-coastal zone management approaches are integrated, adaptive, and experimental (Burbridge, 1999; Walter, 1997) evolved within traditional sectoral, political, socioeconomic boundaries. It recognizes the distinctive character of the coastal zone itself a valuable resource for current and future generations (World Bank, 1996). An effective coastal management plans for sustainable coastal development need thorough knowledge on short and long-term processes, its response to natural disaster and anthropogenic hazards. ICM analyzes conflicting coastal and ocean usages, interrelationships and implications between physical processes and multisectoral human developments. A successful coastal management ensures sustainable development of coastal area, protect marine resources, reduce vulnerability of coastal habitats from natural hazards and conserve biodiversity by maintaining ecological balance sufficiently among all support systems. The adaptive management is a conceptual approach and an implementation strategy to cope the uncertainties. Adaptive management provides effective approach to tackle uncertain complexities in natural resource system and its processes. It has capacity to adapt by learning from their surroundings and incorporate timely information from system itself (Lee and Lawrence, 1986). This procedure can be carried out at all levels from planning, designing to implementation and extend beyond at regular intervals for midcourse corrections. The following sections provide a comprehensive detail to the readers on various coastal issues related to coastal ecosystem functions, vulnerability and ecosystem health and coastal processes including the highlights on application potential of remote sensing data and Geographical Information System tool (Sridhar, 2008).

9.4.1. Geological Processes

Coastal changes have different order of magnitude and dimensions and also varies from site to site. Climatic changes, sea surface warming, polar ice melting and sea level oscillations are long-term processes that have impact on the global coastal zone. Relative sea-level rise, due to whatever cause, has a number of biogeophysical impacts such as increased erosion and flood potential. These processes could modify the coastal physiography

at a steady and slow pace. Short-term processes such as tsunami run up, storm surges, cyclone and floods devastate coast through beach erosion, inundation, and saline water intrusion and sedimentation. The fluctuating biogeochemistry can stress coast and marine systems (Michener *et al.*, 1997[b]); thus, resilient systems can survive and rest succumbs. This has direct or indirect effect on coastal environment and socio-economics of the coastal people (Nicholls, 2003). Both long and short-term coastal processes have unique and common causes and effects with regional and global scale implications. At large, an effective coastal management looks into long and short-term processes and their responses to natural and man made changes.

9.4.1.1. Long-term changes

The current prediction of global sea level estimates a rise between 0.1 and 0.9 meters by 2100 (IPCC, 1998). The potential impact of sea level rise on the coastal zone has drawn much attention in the recent years. Impacts of global warming and sea level rise are inundation of low lying and loss of coastal wetlands, shoreline erosion, flooding due to frequent cyclonic storms, salt water intrusion into freshwater aquifers, change in sedimentation pattern and salt water mixing into estuaries, rivers, bays due to altered tidal range, change in water quality and marine productivity (Tsyban *et al.*, 1990). Climate changes have significant impact on river basin sedimentation and sediment flux. Raising sea level floods the river mouths, this can reduce the sediment transport to the sea. Nicholls *et al.* (1999) estimated that as much as 22% of the coastal wetlands could be lost throughout the world by the 2080 due to sea-level rise. Corals and mangrove ecosystems may suffer due to sedimentation or hypersalination. Sea level rise is likely to accelerate coastal erosion at the seaward margins and wetlands or add new areas that are now retreating and initiate erosion on new beaches that are presently stable or accreting (Bird, 1987). Sea level rise tends to move waves further closer to the shore and increases the capacity of alongshore transport. Higher sea level, can allow waves to attack untouched coastal and enhance alongshore transport (Sorensen, 1978). Enhanced long shore transports render new areas to erosion or accelerate erosion at one area and propagate to nearshore waters. Nutrient rich sediment flux enhances productivity and blooming. Blooming in coastal waters could leads to fall in dissolved oxygen (eutrophication) and marine mortality. Nevertheless, high turbidity can also control light penetration and decrease primary production.

The estimation of coastal evolutionary tendency, however, is a difficult science due to the variety of spatial and temporal scales over which coastal changes occur, and the inter-dependence between different components of the coastal system (Nicholas and Jay, 2001). Both long and short-term processes contribute to morphodynamics and evolution of the shoreline. However, knowledge on the response of coastal system to both long and short term processes at various stages of project implementation enhance understanding of coastal engineering and resource management problems for successful coastal resource management.

9.4.1.2. Short-term changes

Both natural and human-induced factors are responsible for shoreline variability and evolution. Tides, wind, waves, currents, and storm surges are the major forces responsible for shoreline dynamics. The study of coastal morphodynamics reveals the dynamic evolution of shoreline owing to forced mechanism over a wide range of spatial and temporal scales. Tides have predicted cycles and generate current to move sediments in and out of the coast. The combined action of low tides and strong shoreward winds can transport huge sediments from beach into dune in a short period.

Waves and currents can act locally to move suspended as well as bed load within and to near shore as well as arrange beach sediments to shape the coast. A single storm event can remove the entire stretch of large coast within few hours and alter the coastal morphology considerably. The magnitude of such changes depends on intensity and duration of the storm. Waves and wave-derived currents are responsible for seashore sediment transport. The wave propagated from deep ocean to shallow water break obliquely to generate alongshore currents. The convergence of wave rays due to refraction on small-scale changes in bathymetry concentrates wave energy along the coast and is a probable cause of erosion. The alongshore currents move sediments through length of the coast. Construction of coastal protection structures such as jetties or breakwaters in one location can disturb the entire coastal system altering the existing sediment budget. This upset the mechanism of coastal morphology and hydrodynamics. Sediment budget finds net sediment loss and gain by accounting the rate of sediment supply from all sources and the rate of sediment loss to all sinks from an area of coastline. Sediment exchange between the beach and the shelf is regulated by fluvial, tidal, coastal and ocean currents and is an integral part of the seashore sediment budget. Sediment budget quantifies the effects of changing sediment supply on the coastal system necessary for large-scale morphological responses of the coastal system and shoreline behavior.

Human intervention in natural processes is accelerating erosion rates, perhaps by a factor of about two on a global scale (Vitousek *et al.*, 1997). Much of the problem of managing beaches and dunes in developed areas relates to the conflict between the human desire for a system that is stabilized to make it safe, maintain property rights or simplify management and the tendency for a healthy natural coastal system to be dynamic (Nordstrom, 2003[a] & 2003[b]).

9.4.1.3. Coastal changes due to shoreline development

Coastal zone is highly sought by human for residential, commercial, recreational and defence usage. Overexploitation of living and non-living resources has caused irreparable damage to the coast and its habitat. Frequent natural disasters and man made hazards like indiscriminate conversion of beaches and dunes to built-up areas, mangroves and wetlands to aquaculture sites, foreshore to ports and harbours, estuaries and tidal inlet to navigation channels have aggravated the coastal processes, specifically coastal erosion and accretion. Hence, construction of shoreline protection measures along the eroding coasts has become unavoidable. Aggravating calamities like global warming, sea-level rise, deep-sea earthquake, tsunami, hurricane, tropical storm and flood have caused concern to costal zone management world over. The problems related to coastal processes other than human induced erosion and accretion are frequent storms, heavy rainfall, flooding, river breaching, and inundation of deltaic flood plains above the intertidal regions. Nicholls (1998) has indicated that the accelerated sea level rise in coming decades to makes general erosion of sandy shore and more likely to change the local coastal conditions particularly in sediment supply. The reduction of sediment delivery, lack of beach nourishment into bays end up in increased overwash and creation of new inlets, inundation of marsh habitat and increase in open water habitat. The changing environmental scenario has forced dedicated restoration of coastal marine habitats such as estuaries, wetlands, mangroves, beaches, dunes, barrier islands and corals and conservation of their biodiversity to preserve socio-economic and environmental quality of mankind.

9.4.1.4. Physical forcing and sedimentation process

Movement of sediment in the coastal region is a natural phenomenon. Current forces mass transfer and conservation of sediment along shoreline. Currents are result of forcing mechanism driven by wind, wave or thermohaline. The currents move loose sediments from source to sink within the transporting cycle as the result, tidal inlet channels generally suffer heavy sedimentation from long shore input of sediments induced by waves. The natural sedimentation areas are known as shoals, flats, banks, sheets, bars, etc. These areas reduce the navigability of the channel due to shoaling. In a wave dominated coast, the sediment transporting capacity of the hydraulic system is reduced due to the decrease of the steady flow (currents) and oscillatory (waves) flow velocities and related turbulent motions that result in sedimentation problems. Areas, where wave energy is relatively low, tidal conditions dominate due to restricted fetch or offshore conditions trap or deflect incident wave energy, as the results the inlets at low energy regime are greatly affected by erosion related problems. A shoreline said to be in equilibrium, when the sediment input volume is balanced by outgoing volume. The estimation of sediment transport in given a cell (defined space) over a period is called sediment budget. A sediment budget balances sources and sinks of sediment. Such budgets are often formulated at a regional scale together with the resultant morphology change for a particular area and time period. But in a classical sediment budget approach, the dynamics of the processes underlying the transport gradients responsible for the sources and sinks is not resolved. However, Oceansat- I, Ocean Colour Monitor (OCM) is a high resolution ocean colour

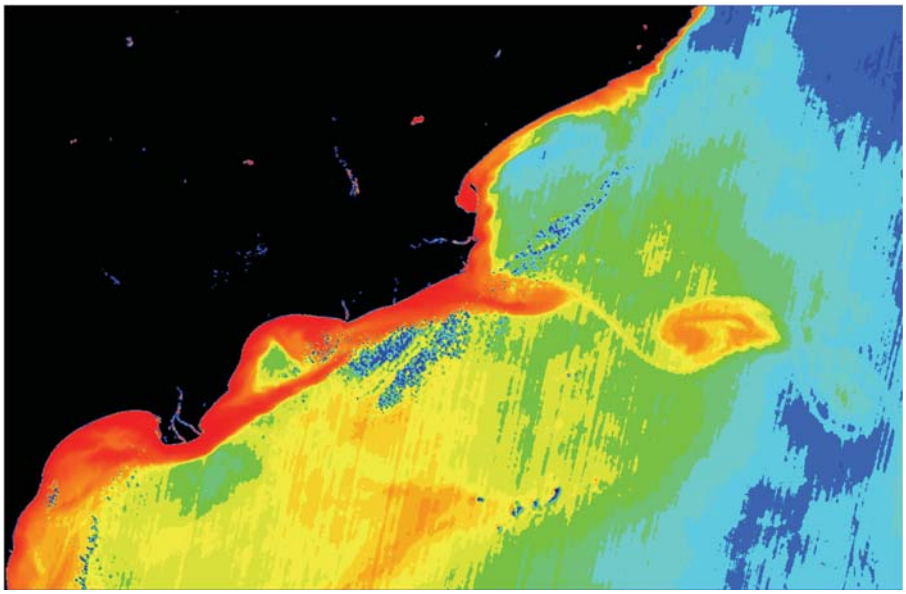

Figure 9.8: Oceansat –I, OCM SCC data showing sediment plume off KGB

data useful mapping surface sediment concentration and sediment dynamics like littoral transport, river flux and sediment plumes (Figure 9.8).

9.4.2. Coastal Ecosystem functionality and vulnerability

The functional significance of coastal ecosystems is environmental, esthetical, and economical. Coastal wetlands and tidal flats regulate nutrients, filter sediments, toxins, and pollutants to safe marine lives (Burke *et al.*, 2001[b]). Estuaries, lagoons, and salt marshes provide feeding, spawning, nursing ground, and shelter for many marine animals and their juveniles (Lean and Hinrichsen, 1992). Costal ecosystems are also a vital source for food and recreation. Coast zone provides gamut of services as ports of commerce, primary producers of fish, shellfish, and weeds, source of industrial, household products, and construction materials. The beaches, dunes, and mangroves buffer hinterland and protect from storm, high waves including tsunamis. Coastal areas are highly vulnerable to environmental impact from anthropogenic pressures and climatic changes. Over the past 30 years, destructive nature of cyclone is increasing to cause damage and loss of lives (Emanuel, 2005). Increasing land and sea surface temperatures and high sediment and nutrient loads brought by rivers into coastal waters severely alters the coastal water quality and health of aquatic systems. Changing wind and wave pattern manipulates coastal productivity and fisheries by varying temperature, coastal upwelling, and nutrient cycle. The coastal margins are prone to erosion, intrusion seawater into freshwater and flooding and inundation of low-lying areas. Slight sea-level rise substantially inundate coastal wetlands, where tidal excursions are at large (Harvey and Caton, 2003). Periodic fluctuations in sea surface temperature resulting coral bleaching and mortality (Montgomery and Strong, 1994). Frequent temperature and rainfall fluctuations have disturbed mangrove species biological diversity. Depending on local topography adaptable mangrove species have moved landward during past sea level rise (Alongi, 2002). Overall, the status of coastal ecosystem health is under extreme stress and requires monitoring mechanisms and management solutions for ecosystems protection and conservation.

9.4.3. Role of Spatial data in coastal ocean studies

Ecosystem-based management requires integration of multiple system components for identifying and striving sustainable outcomes, precaution in avoiding deleterious actions, and adaptation based on experience to achieve effective solutions (Boesch, 2006). Over the past few decades, remote sensing and GIS techniques have been increasingly used to support the environmental monitoring and assessment of estuarine ecosystems because of their cost-effectiveness and technological soundness. The remote sensing and GIS forms a powerful tool for multi-scale spatial data acquisition and analysis in continuum of a complex ecosystem.

Satellite remote sensing had undergone a tremendous development since 1972 especially in mapping, monitoring coastal zone by overcoming limitations in accessibility. Several land and ocean sensors onboard satellites with 1 m to 1 km spatial resolution provide an excellent scope for mapping and monitoring coastal habitats at desired scales. Remote estimates of coastal water quality indicators, such as dissolved organic and inorganic substances, suspended particulates matter, temperature, salinity, turbidity, oil and thermal pollutants have been under development for almost two decades (Xiaojun Yang, 2005). Ocean colour sensors are having high radiometry to measure water quality with reasonable accuracy and precision. Thermal infrared sensors provide sea surface temperatures (SST) and features with varying sea surface temperatures. Large-scale regional pollution (oil) and land discharge are monitored with ocean colour and thermal data. Transient nature of the dynamic coastal system exposes inadequacy of passive sensors to monitor short-term processes or events during night and cloudy days. Microwave sensors have overcome these limitations but normally available in course spatial resolutions. However, microwave sensors have large footprint of several kilometers with short-term acquisition capability. Some of the important microwave sensors are microwave radiometers (0.3 cm to 100 cm), scatterometers, altimeter, Profiling Radar and Synthetic Aperture Radar (SAR). The scatterometer infers sea surface wind by measuring backscatter from ocean surface. The altimeter helps ranging and sea surface height measurements where as SAR measures the surface ice, wind, sea state, marine pollution including oil slicks.

Geographic Information System (GIS) is a powerful tool for spatial data base management and modeling. The combine power of 1) Remote Sensing, 2) GIS, and 3) Global Positioning System (GPS) provide precision mapping, timely monitoring, and evolution of ecosystems vulnerability. Coming sections provides a brief account of different coastal ecosystems, their status and vulnerability studied using satellite data under GIS environment.

9.4.3.1. Ecosystem Assessment

India has been identified as one amongst 27 countries, which are most vulnerable to the impacts of global warming related accelerated sea level rise (UNEP, 1989). The ecosystem distresses are widely prevalent in both aquatic and terrestrial ecosystems. Ecosystem health assessments require analysis of linkages between human pressures on ecosystems and landscapes, altered ecosystem structure and function, alteration in ecosystem services, and societal response. The assessment of ecosystem integrity is concerning biodiversity, ecosystem functions, and stressors. Effective diagnosis requires exploring and identifying the most critical of these links (Costanza, 1992). A healthy ecosystem is being stable and sustainable, maintaining its organization and autonomy over time and its resilience to stress. Linking ecosystem health to the provision of ecosystem services and determining how ecosystem dysfunction relates to these, services are major challenges (Rapport, 1998). Ecosystem health is as much about implementing strategies in environmental management.

The existence of diverse faunal and floral communities over centuries suggests that ecosystems are adapted to cyclic natural phenomena such as seasonal storms and climatic fluctuations. In contrast, status of ecosystem health and extinction of many florae and fauna show human disturbances are generally continuous, non-cyclic events for which organisms are not adapted as the frequency of these activities and their impact increases with increasing human populations and human use of the ecosystem. The following sections describe the processes of environmental transformation leading to degradation in three coastal ecosystems of India viz. Kadmat coral reef, Pichavaram mangrove forest, and Pulicat lagoon.

9.4.3.2. Coral Reefs Ecosystem

Corals are sedentary marine animals in the tropics. The corals play an active role in the global climatic changes by acting as carbon dioxide sink and marine productivity. Coral are colonial animals, thrive on firm substratum with a temperature range of 25 to 29^{o} C, salinity of > 28 psu and sufficient light for symbiotic algal production. Elevated water temperature, fall in salinity, increase in sedimentation and nutrients can cause coral bleaching (Bell, 1992; Brown, 1997). Under physical stress, corals expel brown-green algae from within their body and become pale called *'coral bleaching'*. Bleaching exposes coral to more solar radiation and mortality and this is an indicator of environmental change.

Recent years, Lakshadeweep corals in the Arabian Sea experience frequent bleaching and mortality (Figure 9.9) and this is attributed to worldwide sea surface warming due to El Nino (Arthur, 2000[a]). During 1997-98, the under water survey by remotely operated vehicle mounted with underwater camera showed less than 1% of live corals in the reef slope Kadamat coral reef. The SST anomalies derived from TRMM/TMI (Tropical Rainfall Measuring Mission/Microwave Imager) and NOAA AVHRR data of period 1997 - 2003 have showed two different trends e.g., 1) December 1997 to June 1998. (2) July 1998 to December 2003. During first part, the average mean SST was ranged from 28.51 to 31.89°C. From December 97 to March 98, the SST was estimated around 29°C. Later it suddenly rose to 31.89 °C by May 98, which is 3.38°C above previous months. Succeeding months, SST fell from 31.89 to 27.9°C by July 1998 and gradually rose to 30°C till March 2002 and the highest temperature was 31.5°C during May 2002. Both maximum SSTs are corresponding to EL Nino in the central Pacific Ocean (Arthur, 2000[b]; Mc Phaden, 2003). However, bleaching was severe during the first phase. During winter months (December -February) the south west coast of India experience warm *pool*, an event of elevated SST (>2°C at 30°C) without significant coral bleaching suggest that coral can withstand fluctuation of 2-3°C up to 32°C. This suggests Lampshade coral have been experienced a temperature fluctuation of 2 -3°C with a maximum of ~ 32°C. However, in the May 1998, the SST reached a maximum of 31.89°C with a deviation of 3.38°C during that period several bleaching of corals have recorded/reported. These observations confirm that corals are susceptible to climatic changes can withstand high SST up to 32°C, but sudden increase in temperature will stress the corals.

9.4.3.3. Estuarine Mangroves Ecosystem

Mangroves are morphologically adaptive coastal vegetation found in tropical and subtropical climatic conditions. Generally, significant changes in environmental conditions alter the vigor or zonations of vegetation (Jimenez *et al.*, 1985). Worldwide mangroves are under going degradation due to change in sedimentation rates, soil subsidence, insufficient freshwater mixing, lack of tidal forces, and sea level rise.

Pichavaram mangrove forest in the east coast of India is located in between Vellar, Chennavaikal, and Collidam

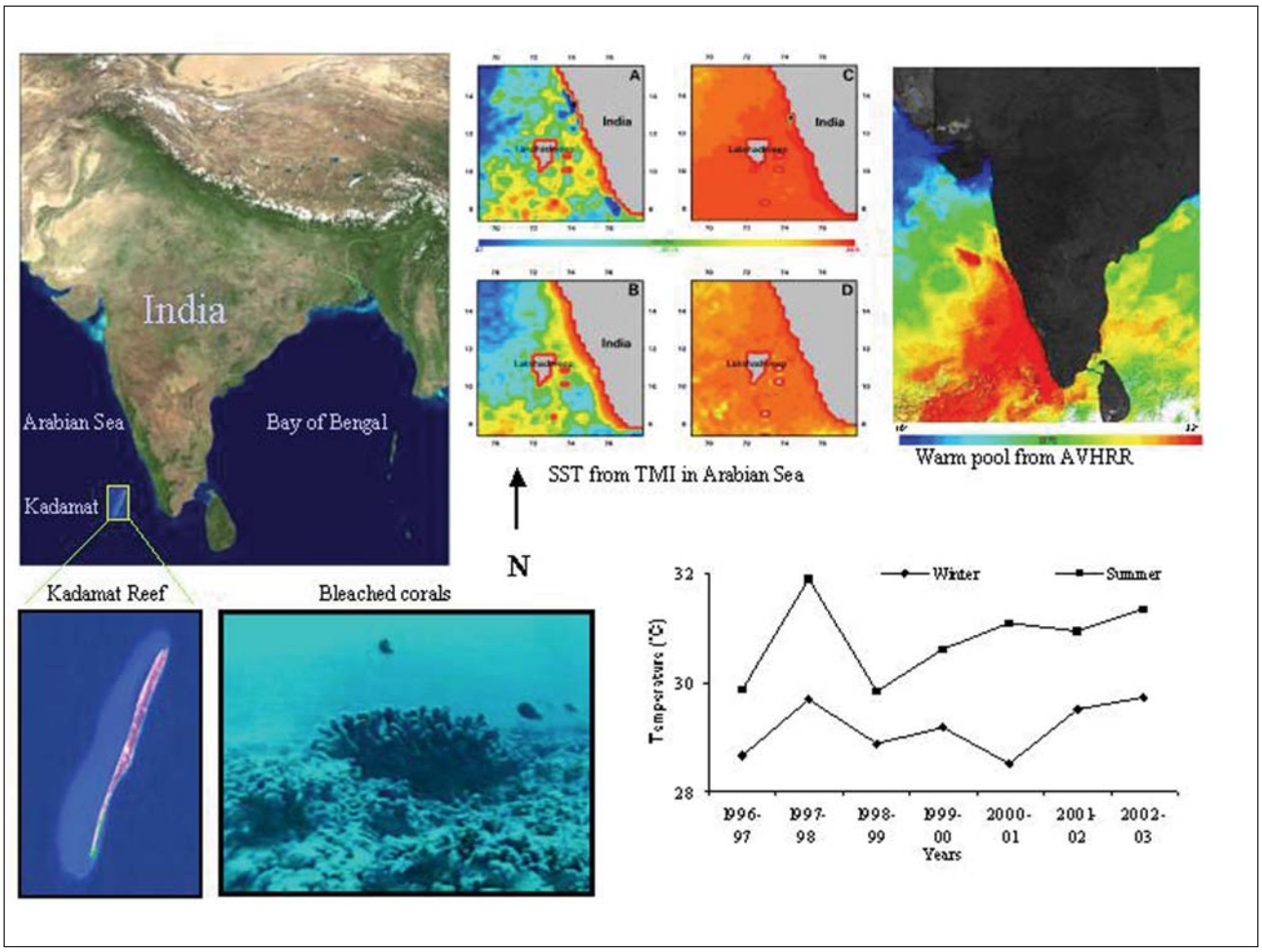

Figure 9.9: TMI and AVHRR data showing peak SSTs during 1998, 2001 and 2003 summer Seasons with a maximum of 31.89° C, rise of 3.38°C during severe bleaching event.

estuaries (Figure 9.10). Three distinct zones are found in this forest namely 1). Core mangrove dominated by *Avicennia* in high intertidal region, 2). Fringe mangroves are predominantly with *Rhizophora* and *Suaeda* found on the banks of creeks and narrow channels, and 3). Peripheral mangroves found in high tide wetlands with mixed mangrove species including *Avicennia marina, Arthrocnemum indicum, Salicornia brachiata, Suaeda maritima* and *Suaeda monoica*. *Avicennia marina*. Over three decades Pichavaram mangroves are undergoing degradation in all the three zones. Several conservation and restoration measure are being taken to keep this estuarine mangroves intact. However, ecosystem based management solution unique to each zones is appropriate for conservation and restoration of this ecosystem health. GIS based decision support was attempted primarily based on the analysis of TM (1987) and Indian Remote Sensing (IRS) satellite LISS (Linear Image Scanning Spectrometer sensors) III & IV of 1998. This study results show that the Pichavaram mangroves are affected by both natural (direct and indirect) and human impacts. Direct and indirect natural impacts are on changes hydrological regime and plant disease. The sedimentation in inlets and poor tidal circulation condition within the estuary combined with and poor rainfall are direct impacts. Pichavaram estuaries are exposed to hydrological venialities due to damming of upstream water (Purvaja and Ramesh, 2000) that can deprive essential sediment and freshwater supply to mangroves is an indirect impact. Cutting and felling of mangroves for timber, fodder, and fuel, conversion mangrove wetlands to aquaculture and agriculture developments are impacts due to human activities.

The GIS analysis results show that the fringe and core mangrove areas are prone to both direct and indirect natural impacts. The fringe mangroves are inaccessible to human and animal and hence the degradation of fringe mangroves is largely due to hydrological changes. Apart from the reduced flow of freshwater and sediment supply, large mangrove seedlings are immobilized and prevented from regeneration in lieu of old degraded mangroves. The core groups of mangroves occur in high tidal flats have become hyper-saline due to evaporation, poor runoff, and tidal mixing. In course time, even saline tolerant species like *Avicennia* have succumbed to hyper salinity. The peripheral mangroves have been used as a source of fodder, fuel, timber, and accessibility to human and cattle and fall into third category. Therefore, conservation and restoration measure for each zone should be unique and species specific.

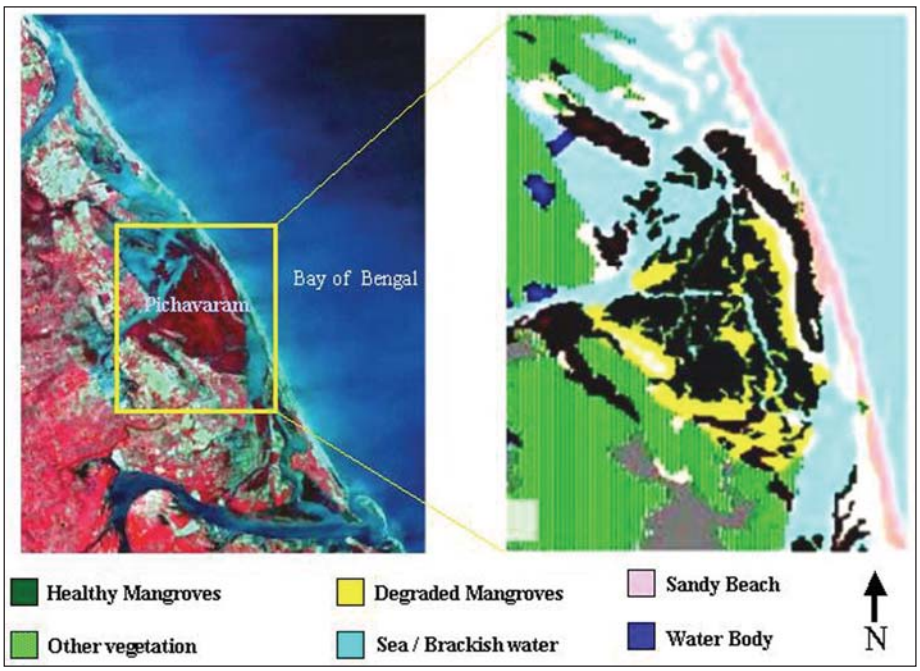

Figure 9.10: Pichavaram estuary with healthy and degraded mangrove forest in IRS LISS III data under GIS environment

9.4.3.4. Coastal Wetlands Ecosystem

The coastal ecosystem functions, health, and services are linked to adjacent marine, freshwater, and terrestrial systems. Uncontrolled developments in any one system have greatest threat to habitats and services. Over exploitation of anyone, undermine subsistence of rest. Wetlands are the most threatened coastal ecosystem. One the most severe impact to this ecosystem in futurity is interference with hydrology and freshwater flow to the coast (Pringles, 2000). Recent days, Pulicat lagoon in the east coast of India, which is the second largest brackish water lagoon and designated Ramsar site having water spread area of 600 Sq Km has declined in biodiversity and productivity. This has lead to the fall in fishery potential and livelihood of local fishing communities. Laterally, Nanda Kumar *et al.*, (2001) have reported poor water quality due to land-based effluents. Water quality of semi-enclosed coastal lagoon depends on hydrological variability like freshwater flow and seawater mixing by tidal circulation. The inlet tidal prism, bathymetry, and nearshore wave energy are the three major factors of inlet circulation. Poor flushing and land-derived pollutants can also affect the water quality of enclosed coastal water bodies (Vieira, 2000).

The study of Pulicat inlet morphodynamics using IRS-LISS III and PAN shows that the two inlets, (one in north and the other in south of Sriharikotta Island) were prone to inlet sedimentation during 1997- 2004. In general, seasonal rainfall and flooding free the sand bars at the inlet. However, the construction of two breakwaters at the southern part of Pulicat i.e., at Ennore Port had accelerated long shore sediment drift towards north that is to Pulicat inlet mouth. As a result, development of well defined sand spit at the southern headland trending towards north is

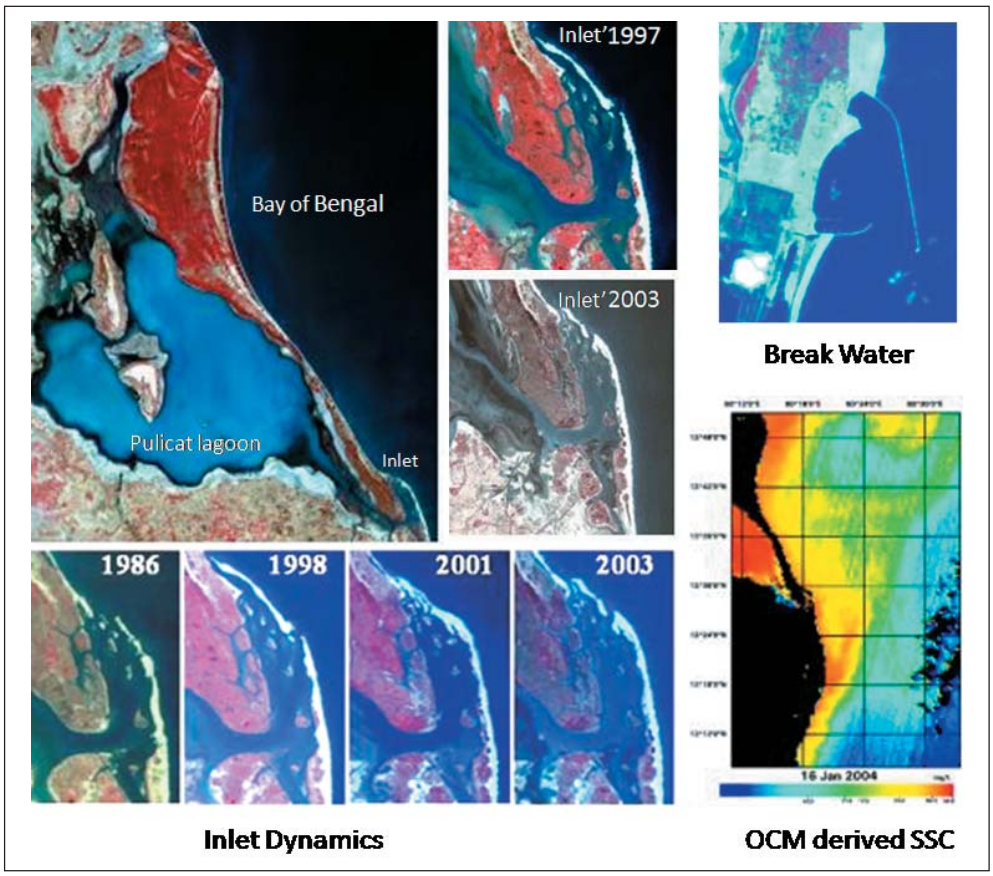

Figure 9.11: Pulicat Lagoon and its inlet dynamics at different development stages as observed from IRS LISS III and OCM data

observed in the satellite data. OCEANSAT-Ocean Colour Monitor (COM) data have showed high sediment transport from Ennore coast in the south as shown in Figure 9.11. The net alongshore drift towards north has been estimated around 0.6 million m^3 (Pranesh, 2000). Increased sediment flux from south, development of channel bars under micro tidal regime, poor surface water flow into the lagoon have resulted complete closure of the inlets during the year 2001. In-situ observations on the water salinity in Pulicat lagoon show hyper saline condition (> 45 PSU) during this period. High salinity in brackish water ecosystem is detrimental to the productivity and biodiversity and biodiversity *per se* can influence human health in many ways (Dobson and Carper, 1993). Whether impact on the coastal ecosystem may be natural or human induced, direct or indirect the resultant effect is irrevocable.

9.4.3.5. Coastal Zone Management and Solutions

Wave-induced alongshore currents provide vital energy for the flow of sand for beach development and shoreline equilibrium profile. The revetment, bulkhead, seawall, breakwater and groins are the most common structures at the approach of harbour entrance to protect it from waves and coastal currents. Some protective structures trap sand and allow beaches to expand up in the up drift direction, but interrupt the flow of sand to other beaches. Coastal structures have both positive and negative affects on sand movements along shoreline. Some structures could accumulate sediment around one segment at the expense of destabilizing other as happening at Kadamat Island coast (Figure 9.12). Structures located too close to the ocean are vulnerable to severe damage during cyclonic storm. Other practical difficulties of the coastal structures are cost effective maintenance and operations. Beaches are natural shore protection structures; when maintained at proper dimensions it can effectively dissipate wave energy. When beaches have narrowed because of long-term erosion trends or severe storms, beach restoration is often proposed (Anonymous, 1989). Beach nourishment technique directly increases the beach width by depositing sand and cost effective. Some of the advantages of beach nourishment are it provides 1) a wider recreational beach, 2) its protection to shoreline structures, 3) dredged material can be nearby sources and 4) reclaimed to other beach management methods in the future. Beach nourishment can also protect threatened or endangered plants in the dune area, and restore habitat for sea turtles, shore birds, and other transient or permanent beach organisms (Greene, 2002). Still, the technique could be detrimental to marine lives both in source and drop

Figure 9.12: Concrete revetments to control the wave run up disturb the natural beach profile at Kadamat Island reef area located in the Arabian Sea

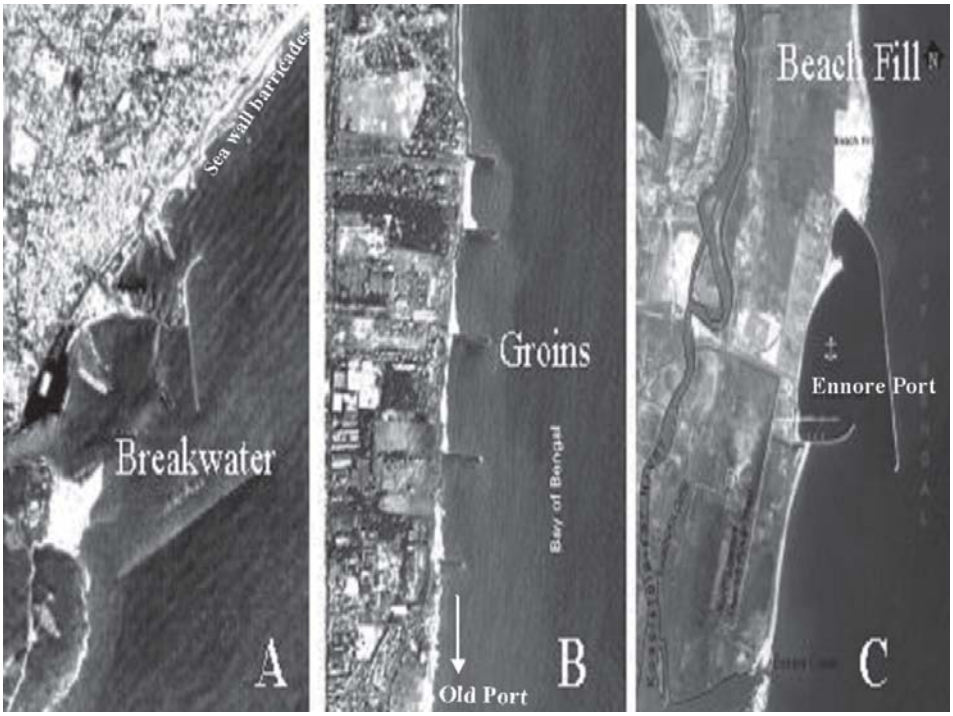

Figure 9.13: Coastal structures irrespectively cause adverse effects on the coast, classic examples are A- Vishakapatnam, Sea wall constructed to control erosion in the beach north of port break waters, b-Progressive groin at Chennai cost north of Chennai Port, C- Beach filling north of Ennore Port, Chennai, all these areas erosion is on the down drift direction of predominant long shore movement

areas due to sand extraction method. Setting buffer zone to natural processes remain active with in the buffer zone and regulate coastal activities beyond the buffer zone is the most effective coastal zone management practice is to allow the natural process remains unrestricted. Satellite data of panchromatic (PAN) mode with high spatial resolution are found to be an important tool especially to monitor the developmental activities as well as the changes in coastline configuration (Figures 9.13 and 14). The technique that it preserves aesthetic values of natural environment and decreases the need for backshore protections. Relocating threatened structures to safer ground potential erosion could another solution but there is a possible conflict between stakeholder (shareholder of coastal enterprise) and government since investor expects financial commitment by government or from insurance.

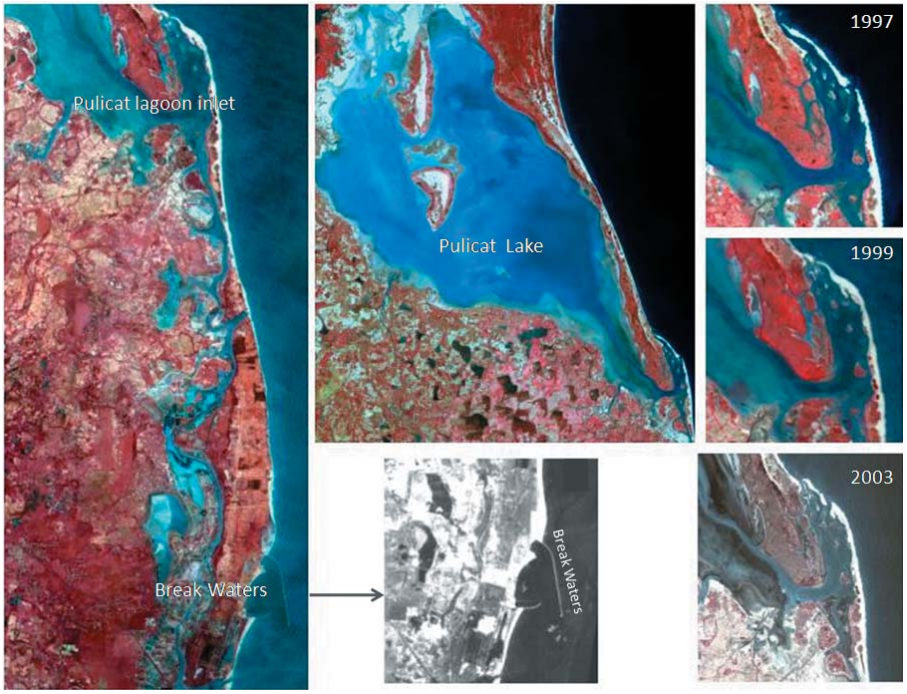

Figure 9.14: Indian Remote Sensing Satellite (IRS-LISS III) data showing Pulicat inlet dynamics before (1997) during (1999) and after to 2003 the construction of Ennore break water in the south

9.5. Remote Sensing Observations

The satellite sensors useful to observe physical oceanographic parameters are a) altimeters b) scatterometers c) synthetic aperture radar and d) radiometers.

9.5.1. Altimeter

The satellite altimeters provide information on significant wave height, wind magnitude and the sea surface height above the geoid or reference ellipsoid. The altimeters in orbit as of today are Jason-1&2, ERS-2, Geosat Follow On (GFO) and Envisat. Indian Space Research Organisation, in collaboration with CNES is going to launch for the first time a ka-band altimeter with a smaller foot print that can provide information closer to the coast.

Satellite altimeter is a remote sensing sensor providing an integrated picture of the atmosphere and the oceans over large spatial and temporal extents. A satellite altimeter is a nadir pointing active microwave sensor designed to measure characteristics of the surface of the Earth. The return signals from oceanic regions provide information on significant wave height, surface wind speed and a range measurement from the satellite to the sea surface immediately below. A radar altimeter operates by timing the delay between emission of a short microwave pulse and the subsequent detection of the returned echo, recording the time and distortion of the returned signal.

The first requirement for any remote sensing instrument designed to observe the Earth's surface is that atmospheric attenuation of the electromagnetic signal be sufficiently small that detection of the return pulse is possible. Through most of the infra-red region, signal attenuation is large due to atmospheric water vapour and gases such as carbon dioxide and oxygen. In the microwave region between 100 MHz and 10000 MHz, however, signal attenuation is small; but certainly of considerable magnitude.

Emission of electromagnetic radiation by an aperture results in diffraction, the width of which is determined by the wavelength of the radiation and the size of the aperture. A uniformly and coherently illuminated circular aperture will produce a diffraction limited beam width defined by Fraunhoffer diffraction theory. At 13 GHz (wavelength ~2.3cm), Ku-band microwave signals emitted by a 1 m antenna will have a beam width of 28 mrad or 1.6 degrees, which from an altitude of 800 km covers a disk of diameter 22 km. For higher frequencies or large antennas, this figure is correspondingly reduced (the latter being the basis for the resolution of Synthetic Aperture Radar techniques).

There is a second problem associated with the frequency of microwave radiation used: when a surface such as the ocean is illuminated by a coherent single frequency source, differences in optical path length cause constructive and destructive interference which can radically distort the signal received by the instrument. For a perfect single frequency transmitter, this produces an infinitely coherent source. In reality, all transmitters have a spectral width, and it is partly to avoid the problems of interference (known as fading) that radar signals are 'chirped', giving them a limited coherence length which is small enough to avoid fading for all but the flattest of reflectors. Bandwidth is defined as frequency spread of the emitted radiation. For ERS-1, the altimeter bandwidth is 330 MHz, resulting in a coherence length of around 90 cm.

A spot size of 20 km is too great for many applications of the data (for example high resolution geoid determination). There is therefore a need for a large antenna, a higher frequency or some other refinement to the emitted radiation. A large antenna on board the satellite is impractical while at higher frequencies, there is greater atmospheric attenuation of the returned signal; therefore the only alternative is the use of pulse limited altimetry. In this way, the leading edge of the return pulse provides sufficient information for an accurate estimate of the ocean height over a significantly smaller area. This is the second reason for chirping the emitted signal as this can simulate a short but sharply modulated pulse, the distortion of which is analysed on its return.

Besides these technical problems, the measurements from the altimeter have to be corrected for the instrumental, atmospheric and media errors which are discussed in the following sections.

9.5.1.1 Errors involved in Altimeter Measurements

The principle of obtaining the height of the altimeter above the sea surface is simple – it is computed as

$$D=Ct/2$$

where, D is the distance between the satellite and the sea surface, C is velocity of light and t is the round-trip travel time taken by the microwave radar pulse to travel from the satellite to ocean surface and back. But obtaining the sea surface height (SSH) or the dynamic topography is complicated. In order to realize the full potential of satellite radar altimeter data, it is necessary to take into account a number of error sources and apply their associated corrections with an accuracy that is compatible with the proposed measurement precision. The two classes of altimeter errors playing significant roles in signal processing are:

(a) Errors that influence the measurement of the height of the ocean surface, (b) Errors that influence the interpretation of the measurements

The origin of these discrepancies and their corresponding rectifications can be separated into the following five categories:

- Instrument Errors
- Propagation Medium Corrections
- Geoid Modelling Errors
- Effects of Temporal Variations in Ocean Surface (Tides, Barometric Pressure)
- Space Craft Orbit Determination Errors

A] Instrument Error

The instrument errors consist of a random part and a systematic long wave part. The random component refers to the precision of the instrument. This precision for the first altimeter flown on Skylab in 1973 was 60 cm which could hardly deduce the sea surface slope across the Gulf stream. This was gradually improved and the present precision for the Topex/Poisodon and Jason-1 is 2-3 cm which is sufficient to detect even small amplitude eddies. The different instrument errors that have to be accounted for are the following:

Tracker Bias: This correction arises from the calibration bias in the discrete samples of the return waveform used in the onboard tracking algorithm which is designed to accommodate linear changes in the height (constant velocity) of the altimeter. When there is a rapid acceleration in height, for example when the altimeter passes over a narrow ocean trench, there is a corresponding induced height error which must be compensated for.

Waveform Sampler Gain Calibration Bias: This correction occurs due to the fact that the amplitude of the received signal varies with the cross section of the monitored surface. An automatic gain controller is used for this signal

attenuation adjustment, but rapid changes in echo strength mislead the circuit that tracks the position of the leading edge of the pulse, thereby producing a calibration error.

Pointing Errors: Actually a combined effect of the satellite antenna gain pattern in relation to the antenna off-nadir pointing error on the shape of the return waveform correction occurs when the sub-satellite point is near the edge of the area illuminated by the altimeter. The resulting radar echo distortion produces an unwanted error bias.

Average Pulse Shape Uncertainty and Time Tag Bias: The error in return pulse shape stems from the uncertainty due to random variability of the pulses used to calculate the mean echo. The residuals associated with averaging, say, 1,000 pulses, therefore contribute noise to the measurement. Also, the aging of microwave parts and long term clock drifts can induce height errors. Clock drifts can be accounted for by comparing the altimeter clock with some reference. Drifts in the height measurement induced by aging can be partially compensated for with the altimeter's internal calibration mode.

Propagation Medium Corrections: Two types of errors are included in this category: (a) Total sea state bias of the onboard tracker estimate of mean sea level, and (b) resultant decrease in the local speed of light due to index of refraction changes as the altimeter's signal travels through earth's atmosphere.

Sea state Bias: Two effects contribute to the discrepancy between the electromagnetic (EM) sea level estimated by the onboard tracking algorithm from averaged return waveforms and that of true mean sea level:

Electromagnetic Bias: This correction arises because of the height difference between mean sea level and the mean scattering surface. The way this occurs is through the differential backscattering of power per unit surface area between wave troughs and that of wave crests. This deviation results from the fact that the power backscattered from a small wave facet is proportional to the local radius of curvature of the long-wavelength portion of the wave spectrum. In general, ocean troughs have a large radius of curvature than wave crests; thereby creating a bias in backscattered power towards wave troughs. A greater prominence of small scale "wavelets" super-imposed on wave crests creates an increased roughness which further scatters the altimeter pulse in directions away from the incident radiation; effectively enhancing the bias. The backscattered power measured by the altimeter is therefore greater from wave troughs than from wave crests, thus inducing an EM sea level bias towards wave troughs. A direct correlation between significant wave height (SWH) growth and EM bias increase allows researchers to estimate the required correction.

Skewness Bias: This error occurs because of the height difference between the mean height of specular scatterers and the median scattering surface that is actually measured by the onboard tracker. This is a direct result of the non-gaussian distribution of the sea surface height which shifts the median from the mean sea level toward wave troughs; which in turn also contributes to the EM bias towards wave troughs.

B] The atmospheric effects

The atmospheric errors are introduced into the altimeter measurements because the speed of electromagnetic propagation in the real atmosphere differs from that in vacuum basing on which the altimeter range is estimated. The two major sources of errors are from ionosphere and the troposphere.

(a) Ionospheric Correction: This correction takes into account the variation in the number of free electrons present in the sub-satellite ionosphere location. Typically, the electron content varies from day to night (very few free electrons at night), from summer to winter (fewer during the summer), and as a function of the solar cycle (fewer during the solar minimum). The signal delay encountered is inversely proportional to the altimeter monitoring frequency squared. Topex/Poseidon is the first satellite which carried a dual frequency altimeter to obtain an accurate estimate of the ionospheric effect basing on this property.

(b) Tropospheric Correction: This correction is related to water vapor content and other gases present in the path of the signal. There is both a wet & dry tropospheric delay which must be accounted for. The dry correction can be modeled via surface pressure measurements. The wet portion is typically adjusted from measurements made by an onboard radiometer. It is significant to note that the dry term includes the weight of the water molecules while the wet term accounts for their additional influence on the index of refraction.

C] Geoid Modeling Errors

To obtain ocean dynamics information from sea surface height measurements a detailed knowledge of the geoid is required. This necessity arises from having to refer the acquired surface height and slope data to the ellipsoid/ geoid reference frame (due to the non availability of exact geoid information) in order to yield sea surface topography. The deviations of the geoid from the reference ellipsoid range from -100 m (South of India) to +64 m (near New Guinea). The spatial variability can be large. For example, the geoid can vary by several meters over a few kilometers in areas where there are ocean trenches or ridges. This is in contrast to the variability of sea surface topography which is typically +/- 1.5 m. In order to determine the ocean surface topography accurately it is necessary to know the geoid shape to an accuracy that is required by a feature over length scales of the order of the ocean phenomenon being monitored. There are essentially three ways in which to measure the earth's geoid: 1)Satellite orbit tracking, 2) Direct measurements of gravity, and 3) Satellite altimetry. Gravity fields deduced from satellite orbit tracking data include spherical harmonic expansion terms of rather low degree and order (typically less than 50). Discrepancies in the spherical harmonic coefficients and truncation of the spherical harmonic expansion produce errors in these models, the majority of which are due to inadequate global observation information at the short spatial scales referred previously.

D] Effects of Temporal Variations in the Ocean Surface

These include solid earth and ocean tides and the inverse barometric effects. The gravitational perturbations induced by the moon and sun are the primary factors controlling influence of earth's solid & ocean tides. Although third body effects from the other planets contribute, their magnitudes are negligible in comparison. Since the relative interaction/orientation of the earth-moon- sun system is known very accurately, its effect on the tide-generating potential at any point on earth can be determined rather precisely. This potential can be closely approximated by only the six constituents with the largest amplitude, all of which are diurnal (one cycle per day) or semi-diurnal (two cycles per day). The problem arises from the presence of continental boundaries and complex ocean floor topography and the effects of earth's rotation which introduce large errors in equilibrium predictions of these semi-diurnal and diurnal tides (not to mention the parameterization of friction in these models). Sophisticated models must take into account the time-varying motion of the solid earth, the time invariant latitudinally dependent portion of the deformation, and that portion due to ocean loading forces on the solid earth. However, since the tidal estimations are not very accurate closer to the coast, the altimeter SSH values are not generally considered wherever the ocean depth is less than about 100 m.

The inverse barometer correction is based on a direct proportionality of about 1 cm change in the sea surface height to a change of 1 hpa in the sea surface atmospheric pressure. That is, the ocean surface is depressed in response to the increased atmospheric pressure. Problems can arise in this relationship near storms or near shore where other effects such as wind setup are correlated with pressure. For example, the decrease in SSH due to the anticlockwise rotation of water under the influence of cyclonic winds dominates over the rise due to the pressure drop. Also, while the assumptions hold for weekly and longer periods, there is doubt as to short period ocean response to pressure changes having the same type of characterization.

E] Spacecraft Orbit Determination Errors

The forces, in order of their significance, that contribute to perturbations in the satellite orbit error are parameterized as: a) Gravity, b) Radiation Pressure, c) Atmospheric Pressure, d) Geoid Modeling, e) Solid Earth & Ocean Tides, f) Troposphere, and g) Station Location.

Gravity: The fact that the earth is not perfectly spherical in nature but rather shaped as an oblate spheroid creates an asymmetric potential in earth's gravitational field. The cyclical characterization of this perturbation requires rather a high level of degree and order in the spherical harmonic expansion representation in order to predict precise effects on the satellite orbit.

Radiation Pressure/Spacecraft Radiation: Solar radiation, albedo and infrared emissions are the three external radiative fluxes acting on a spacecraft. The two separate types of flux influencing a spacecraft's temperature are internal and external. Internally the equipment dissipates heat. Externally, the solar radiation, albedo, and infrared fluxes cause surface heating. These types of forces vary with spacecraft shape, orientation and reflectivity during the different phase events of orbit such as, 1) occultation effects, 2) oblique illumination, and 3) the spacecraft's thermal inertia changes.

Atmospheric Drag: The effect of earth's atmosphere at orbit altitude creates a resistance. This is calculated using empirical relationships for air density, together with the known shape and orientation of the satellite which may be different from reality.

Geoid Model: As indicated previously, current geoid models have relatively low orders of degree and order upon which their spherical harmonic expansions are based. These discrepancies combine to perturb the satellite's estimated orbit away from the true orbit.

Solid Earth & Ocean Tides: As noted above, both oceanic and solid earth tides perturb the gravitational potential. Their influence on satellite orbits is calculated from a spherical harmonic expansion involving terms to a relatively low degree and order calculated from hydrodynamic models. It is meaningful to note that the largest amplitude M2 tide constituent is not the dominant contributor to satellite orbit anomalies. However, this same factor plays a significant role in tide frequency vs. altimeter signal aliasing and thus requires highly accurate tracking data in order to best define an adequate representation. Thus, the two most important tide modeling strategies are, 1) to improve the long wavelength tide terms which are in resonance with near-earth satellites and have distinctly large long period orbital effects, and 2) to produce as many as feasibly practical tidal coefficients which encompass many tide lines for inclusion in models thereby creating a whole category of short period perturbations.

F] Troposphere:

As discussed in propagation medium corrections above, the signal delay caused by water vapor content and other gases present in the troposphere must be accounted for in satellite tracking theory and perturbation analysis. Typically, satellite laser ranging (SLR) techniques are involved which use frequencies in the visible portion of the electromagnetic spectrum and thus are not as susceptible as the radio frequency ranging methods to the delays listed.

Station Location: Station position error, i.e. the inability to know the precise location of the tracking stations relative to the center of the earth, used to be the dominant problem in this category. However, with SLR, extremely accurate measurements are now possible. Station distribution is also a significant hindrance, with most SLRs concentrated in the northern hemisphere and on continents rather than being evenly dispersed around the globe. The advent of the DORIS tracking system considerably reduced this problem. Another, smaller in magnitude yet still present, discrepancy is that the coordinate system used to determine the station position is not precisely known because of polar motion and the variations in the length of the day.

9.5.1.2. Applications

Sea level change :

Since a large segment of the population lives in a coastal zone, sea level change is of considerable importance in terms of the socio economic consequences. In addition, the rate of sea level rise is expected to increase in response to the green house warming. Thus, the sea level changes obtained from altimeters can be used to validate the predictions from the climate models (Houghton *et al.*, 1996). Two fundamental problems are encountered in using tide gauge measurement for long term sea level changes. First, the crustal reference point over which the tide gauge measurements are referred, itself may move vertically at rates comparable to the sea level signals (Douglas 1995). Second, because of the limited availability of the tide gauges, they provide poor spatial sampling of the oceans.

Though the current satellite altimeter record is too short to arrive at any definite conclusion, altimeter data was used to study the long term sea level changes. Tapley *et al.*(1992) obtained a sea level change of 5 mm/year using 2 years of Geosat altimeter data. Sea level is the barometer for environmental change. Anthropogenic induced climate change, while likely to increase the global sea level, will actually cause sea level to decline at some locations and rise in others (Nerem & Mitchum, 2001). The true power of satellite altimetry lies in its ability to map the geographic variation of sea level change. Leuliette and Wahr (1999) used the coupled pattern analysis technique and found that most of the long term sea level change signal observed by Topex is caused by changes in sea surface temperature related to ENSO phenomena.

Ocean Circulation:

Because of the ocean's vastness and inaccessibility and the limitations of the insitu measurements, understanding ocean circulation has been a slow process. With the limited data the results were interpreted in the climatological

fashion with the assumption that the ocean did not change much with time and space. The capability of satellite altimetry to measure SSH above geoid, known as the dynamic height, gave an opportunity to study the variability of the oceanic processes not only at the surface but at depths as well. Water movements having spatial scales greater than about 30 km and time scales longer than about a day are in geostrophic balance to a first degree of approximation (Stewart *et al.*, 1986). Hence, over large temporal and spatial scales ocean circulation can be conveniently estimated from:

$$U = - g/f \ \partial\eta/\partial y$$

$$V = g/f \ \partial\eta/\partial x$$

Where, U and V are the zonal and meridional components of the current vector, g is the gravitational attraction of the earth, f is the Coriolis parameter and ∂y and ∂x are the distances in the zonal and meridional directions over which SSH, h, is estimated. However, ocean differs from geostrophic balance in a number of ways. For example, in the high core of the Gulf Stream, the downstream balance tends to be measurably non-geostrophic. Evaluation of the velocity fields with time, implying missing time dependent terms in momentum equations is another situation where actual flow deviates from geostrophy. Since absolute SSH cannot be estimated due to the lack of precise geoid information, only the current variability can be estimated. Even from the dynamic height estimations from the in situ measurements current variability alone can be estimated. However, satellite altimetry has an added advantage in the sense that if the SSH observations are referred with respect to a long time period average, the circulation estimated from the altimeter measurements can be regarded as the absolute ones with the assumption that the current vectors average out over longer time scale. This assumption is not, however, valid in regions like Somalia where the currents are towards northeast for about four months and in the opposite direction for the rest of the seasons. Obtaining the SSH to the required accuracy is a big challenge. Wunch and Stammer (1997) showed that for an ocean of 4000 m deep at 24 degree latitude, a one centimeter tilt in the ocean topography is associated with a mass transport of 7 Sv (1 Sv = 1 million tons per second, roughly the transport of all rivers combined), if the entire water column moves with the same velocity. The actual transport varies with latitude and the vertical distribution of the velocity. Measuring SSH from space with an accuracy of 1 cm is a tremendous effort. The present accuracy of 4 cm (rms value at 1/sec data rate) is achieved after two decades of untiring efforts. After spatial and temporal smoothing the accuracy is close to 2 cm on monthly time scales (Cheney *et al.*, 1994).

Ocean Tides:

Ocean tides, the most fascinating natural events, is caused by the gravitational attraction of the sun and the moon. Tides have many impacts in geophysics and oceanography. Knowledge of total dissipation in tides is required in earth rotation studies. In geodesy, tidal loading of the lithosphere has to be considered. For all these studies a good tidal model, which is lacking till the advent of satellite altimetry, is required. Any in situ measurement approach to map ocean tides at global scales is not possible because of the complexity of the tides and the difficulties involved in the installation and maintainance of the instruments. In these two contexts the advent of satellite altimetry, offering to estimate tides all over the globe, has been totally revolutionary. Obtaining SSH observations from altimeter range measurements and correcting these SSH values for the tides obtained from the same range is complicated. Repeat passes or cross-over points are used to solve for the higher frequencies assuming oceanography as noise. Due to this estimated/predicted tides over high energetic regions or coastal regions are relatively inaccurate. Since tidal variations represent more than 80% of the SSH variations, tides must be removed from the altimeter observations to study the ocean circulation. Careful and accurate removal of the tidal information from the altimeter observations is very critical as different altimeter tracks observe different phases of the tides and if not properly removed the results from SSH variations can be interpreted as propagating signals.

Ocean Surface Wind Wave Studies:

Surface waves are the most important oceanic parameters as they provide the spectacular manifestation of the sea state. The slope of the altimeter return pulse is stretched in time because of the delay between reflections from the wave crests and troughs. This information is used to estimate the significant wave height which in turn is useful in correcting SSH observations for electromagnetic bias. The strength of the return pulse gives an estimate of the wind magnitude. Even though it is often difficult to have altimeter observations at the location of the hurricane at a time close to the passage, altimeter is the only instrument that can provide this information over the oceans.

Thus altimeter allows the assessment of the meteorological forecast, based on independent data, enabling the corrections for the improvement of the models. The possibility of having real time sea state information from several altimeters in future will further enhance our ability to monitor and forecast waves generated by hurricanes and cyclones. Altimeter data is also useful for wave climate studies (Vethamany *et al.*, 1999) which otherwise would be difficult from the conventional data collection platforms.

Wind speeds obtained from altimeters over oceans provide an useful information for many applications. Although it is difficult to estimate wind speed greater than 25 m/s with reliable accuracy, this data can provide information on the structure of the cyclones, the degree of symmetry and the spatial extent along the track.

El Nino Studies:

El Nino-related climate variations often have widespread and devastating impacts. Prior to El Nino surface water piles up at the eastern end of the equatorial Pacific Ocean. Satellite altimetry helps to monitor this phenomenon in all weather conditions. Besides, SSH observations offer a part of the solution to the problem of coupled ocean-atmosphere models which have attained significant forecast skill during the past decade, but they continue to be limited by an ocean observing system. In particular, an operational flow of altimeter data has long been desired by the modeling community as a means of estimating changes in upper ocean heat content to first order approximation. But even though altimeters have flown nearly continuously since 1985, two challenges have stood in the way of progress: (1) The altimeter data must be made available fast enough (within 1-2 days) and with sufficient accuracy (a few cm) to track changes in the ocean within a tolerance that is useful for the ocean model; (2) The assimilation method must be capable of using a single parameter, sea level, to correct the model temperature as a function of depth. Using Topex/Poseidon altimeter data, both of these problems have been solved. A phenomena similar to the Pacific Ocean was also observed in the Indian Ocean by Ali and Sharma (1996) using Geosat SSH observations and SST patterns.

Cyclone/Hurricane Studies:

The intensification of cyclones or hurricanes involves a combination of different favorable atmospheric conditions such as atmospheric trough interactions and vertical shear, which lead to good outflow conditions aloft. As a result of this, inflow conditions in the near-surface layer are enhanced. Clearly, as this process continues over the scale of the storm, the upper ocean provides the heat to the atmospheric boundary layer and to the deepening process. In this scenario, the upper ocean thermal structure has been thought to be a parameter that only played a marginal role in hurricane intensification. However, after a series of events where the sudden intensification of hurricanes occurred when their path passed over oceanic warm features, it is now being realised that it could be otherwise. While the investigation of the role of these rings and eddies is a topic of research in a very early stage, preliminary results have shown their importance in the intensification of hurricane Opal (Shay *et al.*, 2000). Therefore, the monitoring of the upper ocean thermal structure has become a key element in the study of hurricane-ocean interaction with respect to the prediction of sudden hurricane intensification. These warm features, mainly anticyclonic rings and eddies shed by the Loop Current or developed due to the wind stress curl, are characterized by high SST at the elevated center, a deepening of several tens of meters of the isotherms towards their centers and with different temperature and salinity structure compared to the surrounding waters. Similarly, cyclonic features have low SST, depressed centre and shallow mixed layer. They can be easily located and identified from satellite altimeters. Ali *et al.*, (1998) prepared an atlas of the North Indian Ocean eddies giving information of the eddies during 1993 to 1997 for every 10 day interval.

Oceanic features such as warm core rings (WCR), and the currents represent a source of enhanced air-sea fluxes to the atmospheric boundary layer that may cause strengthening of atmospheric disturbances. Warm layers exceeding 26°C extend to at least 100 m beneath the surface in these oceanic features, and represent high hurricane heat potential water. Satellite altimeter data from TOPEX is a useful tool to study oceanic mesoscale dynamic processes from of the sea surface height anomaly, and provides information on the vertical ocean structure when complemented by hydrographic data. Gopalan *et al.*, (2001) have shown that cyclonic/anticyclonic eddies can give an integrated picture of the subsurface thermal features in a broader sense.

Based on historical hydrographic measurements placed within the context of a two layer model, TOPEX derived upper layer thickness fields indicated the presence of two WCRs in the Gulf of Mexico during September and October 1995. Hurricane Opal passed directly over one of these WCRs where the wind field increased from 35 m/s to 65 m/s, and the radius of maximum wind decreased from 40 km to 25 km. Pre-Opal sea surface height

anomaly in the WCR exceeded 30 cm where the estimated depth of the 20° C isotherm was located between 175 to 200 m. Thus on 4 Oct 1995, Hurricane Opal deepened from 965 hPa to 916 hPa in the Gulf of Mexico over a 14 hour period upon encountering a warm ocean ring during an upper level atmospheric trough interaction. Subsequent to Opal's passage, this depth decreased approximately to 50 m, which suggests upwelling underneath the storm track due to Ekman divergence. The maximum heat loss of approximately 24 Kcal/cm^2 relative to depth of the 26° C isotherm was a factor of six times the threshold to sustain a hurricane (Shay *et al.*, 2000). Composite AVHRR derived SSTs indicated a 2 to 3° C cooling associated with vertical mixing in the along-track direction of Opal except over the WCR where AVHRR derived and buoy derived SSTs decreased only by about 1°C. Thus, the WCR's effect was to provide a regime of positive feedback to the atmosphere rather than negative feedback induced by cooler waters due to upwelling and vertical mixing as observed over the Bay of Campeche and north of the WCR.

Similarly, during August 1999, Hurricane Bret intensified twice in the western Gulf of Mexico over two regions associated with very high (values larger than 90 KJ/cm^2) hurricane heat potential. Thus, it can be concluded that warm core eddies are the sources for the intensification of the cylones. On the other hand, when the cyclone/ hurricane passes over a cold core eddy where the temperatures are less and the mixed layer is shallow, it is likely to dissipate or suffer a reduced intensity.

The close relationship that exists between the dynamic height and the ocean mass field allows these two parameters to be used within a two-layer reduced gravity ocean model to monitor the upper layer thickness (Goni *et al.*, 1996), defined in this study to go from the sea surface to the depth of the 20^o C isotherm. This isotherm was chosen because it lies within the center of the main thermocline and is often used as an indicator of the upper layer flow in the western tropical Atlantic and Gulf of Mexico waters. Although there are other factors controlling the SSH anomaly, it is assumed here that most of its variability is due to changes in the depth of the main thermocline and is of barotropic origin. The hurricane heat potential, Q, is defined here as a measure of the integrated vertical temperature from the sea surface to the depth of the 26^o C isotherm. This parameter is computed from the altimeter derived vertical temperature profiles estimated in the upper ocean. The temperature profiles are estimated using: (a) the sea surface temperature obtained from the Reynolds near real time weekly fields, (b) the altimeter estimates of the 20^o C isotherm within a two layer reduced gravity scheme (Goni *et al.*, 1996), (c) the depth of the 26 ^{o} C isotherm from a climatological relationship between the depths of the 20^o C and 26^o C isotherm, (d) climatological estimates of the mixed layer depth. The hurricane heat potential, is a measure of the integrated vertical temperature between the sea surface and the estimate of the 26^o C isotherm (Shay *et al.*, 2000).

Rainfall Studies:

As mentioned earlier when the altimeter signal passes through a rain cell it is considered as noise to the SSH measurements and such points are discarded for oceanographic studies. On the other hand it is a signal for the estimation of rainfall. Besides, dual frequency radar altimeter observations are useful in estimating the rain rate. Topex and Jason have altimeters operating at C-band along with the nominal Ku-band. The primary objective of the C-band altimeter is to provide collocated ranging measurements to correct for atmospheric path delay in the Ku range estimates. This dual frequency altimeters have two more capabilities: to study the oceanic rainfall and to correct the surface wind speeds. Ku and C band signals are differentially attenuated by the atmospheric precipitaion. Bhandari and Varma (1996) used this property to identify rain events associated with the southwest monsoon. Quartly *et al.*, (1999) studied the seasonal changes of rain rate using Topex dual frequency altimeter data.

9.5.2. Scatterometer

A scatterometer works on the principle that electromagnetic radiation transmitted toward the sea surface is scattered back towards the emitting antenna. The intensity of the backscatter is largely dependent on the centimeter-scale roughness at the sea surface, where the scale of the roughness elements is commensurate with the emitted radar wavelength. These small-scale waves are generated by the local wind stress on the sea. For a given wind speed, the backscattered power varies as a function of cos 2M, where M is the azimuth angle between the look direction and the wind direction, often with some ambiguity in the solution. Thus, by measuring the backscattered power from the ocean surface at several azimuth angles, the wind speed and direction may be retrieved.

9.5.2.1 Principles of Scatterometers

Spaceborne scatterometers transmit microwave pulses to the ocean surface and measure the backscattered

power received at the instrument. Since the atmospheric motions themselves do not substantially affect the radiation emitted and received by the radar, scatterometers use an indirect technique to measure wind velocity over the ocean. Wind stress over the ocean generates ripples and small waves, which roughen the sea surface. These waves modify the radar cross section (sigma-0) of the ocean surface and hence the magnitude of backscattered power. In order to extract wind velocity from these measurements, one must understand the relationship between sigma-0 and near-surface winds. This relationship is known as the geophysical model function and model function are used to obtain the ocean wind vectors.

The geophysical product retrieved from QuikSCAT observations is the equivalent of neutral winds at 10-m height (Liu and Tang, 1996), from which the surface wind stress (or momentum flux) can be derived independent of the atmospheric density stratification.

The principle underlying scatterometry remote sensing is expressed as the "radar equation":

$$P_r=(P_tG_t / 4\pi R^2)\sigma_{rt}(A_r/4\pi R^2)$$

where:

- P_r = received power,
- P_t = transmitted power,
- G_t = gain of the transmitting antenna in the direction of the target,
- R = distance between the target and the antenna,
- σ_{rt} = radar cross-section: the area of the target intercepting the transmitted pulse that produces a return pulse equal to the received power,
- A_r = effective receiving area of the receiving antenna aperture.

Of these parameters, P_t, G, and A are all known quantities associated with the radar system, while R is related to the location of the target and can be determined from the duration it takes for the transmitted pulse to return to the antenna. Of greatest interest to scatterometry, then, is the quantity, σ_{rt}, which is a function of the way the transmitted electromagnetic energy interacts with the surface. When this quantity is integrated over a number of pulses, it is referred to as the "scattering coefficient," or "backscattering coefficient," and is commonly denoted as σ°. The quantity σ°, then, which is expressed in decibels (dB), is used to derive geophysical parameters and is the primary variable that scientists work with when using scatterometry data.

There are two physical properties of surfaces and surface volumes that determine the value of σ°: its roughness and its dielectric properties. A perfectly smooth surface will reflect an incident radar pulse like a mirror—90° in the opposite direction from which it arrived - thus, no energy is scattered back into the direction that the pulse came from. A surface must therefore be rough enough that some amount of energy is backscattered to the radar antenna. As a result, rougher surfaces have higher values of σ°. A surface is "rough" from the perspective of a radar pulse depending on the height of the roughness features on the surface relative to the radar's wavelength. This is expressed in the Rayleigh roughness criterion, which considers a surface to be rough if:

$$h>(\lambda/(8 \sin\gamma))$$

where:

- h = vertical relief of the surface roughness features,
- λ = radar wavelength,
- γ = depression angle of the radar pulse.

Based on this criterion, a radar of 2-cm wavelength (or 15 GHz frequency) at a 50° depression angle would only be backscattered if the surface had features with a minimum vertical relief of about 3 mm.

Another result of surface roughness is the impact it has on σ° over a range of illumination angles, or "incident angles." Because smooth surfaces have a mirror-like, or "specular," reflection, a radar satellite will only measure a return signal at nadir, when it is directly above the target (an incident angle of 0°). At the other extreme, an extremely rough surface scatters the signal so much that the antenna receives a relatively equal amount of power regardless of incident angle. This kind of surface is referred to as "isotropic," and the return signal is considered "noncoherent" as opposed to specular, or coherent. Intermediate rough surfaces vary in their angular response of σ° between the specular and isotropic examples. This change in angular backscatter response is important in identifying snow vs. ice surfaces and old, rough sea ice surfaces vs. new, smooth sea ice surfaces. Radar pulses penetrate snow surfaces and scatter multiple times within a volume of snow so that the return response is strongly noncoherent. In contrast, smooth ice is strongly specular while rough ice is less specular.

9.5.2.2. Applications of Scatterometry

Data derived from ocean scatterometers is vital for the studies of air-sea interaction and ocean circulation, and their effects on weather patterns and global climate. These data are also useful in the study of unusual weather phenomena such as El Niño, the long-term effects of deforestation on our rain forests, and changes in the sea-ice masses around the polar regions. These all play a central role in regulating global climate. Computer modeling of global atmospheric dynamics for the purpose of weather forecasting has become an increasingly important tool to meteorologists. Scatterometer data, with wide swath coverage, have been shown to significantly improve the forecast accuracy of these models. By combining scatterometer data of ocean-surface wind speed and direction with measurements from other scientific instruments, scientists gather information to help us better understand the mechanisms of global climate change and weather patterns.

Wind velocity requirements:

Knowledge of wind velocity is very critical for understanding and predicting ocean phenomenon, meteorology and climate. Wind stress is the single largest source of momentum to the upper ocean and drives oceanic motion on scales ranging from surface waves to basin wide currents. Wind velocity is being assimilated in to regional and global numerical weather prediction models. Present available wind vectors data coverage is not sufficient and accurate. Data from moored buoys are highly accurate but a few in numbers. Satellite borne radars are the only systems currently capable of providing accurate, frequent high resolution measurements of near surface winds speed and direction in clear and cloudy conditions. Scatterometer measurements are indirect, requires highlevel processing and suitable model functions to retrieve wind vectors from backscattered power.

Weather Forecasting: Data from ocean scatterometers greatly enhances overall weather-forecasting capabilities. Most of the weather over the west coast of the United States, and some over the east coast, is generated over the oceans. The measurements derived from ocean scatterometers are assimilated into numerical models (computer programs that represent natural processes in terms of equations), which can be used to predict global and regional weather patterns. The data are delivered to the National Oceanic and Atmospheric Administration (NOAA) within two hours, where they are used for timely, accurate weather forecasting.

Storm Detection: The ocean scatterometer data can determine the location, direction, structure and strength of storms at sea. Severe marine storms hurricanes near the Americas, typhoons in Asian waters, and mid-latitude cyclones worldwide are among the most destructive of all natural phenomena. In recent years, our ability to detect and track severe storms has been dramatically enhanced by the advent of weather satellites. Cloud images from space are now routine on weather reports. Data from ocean scatterometers augment these familiar images by providing direct measurements of surface winds to compare with the observed cloud patterns. These wind data help meteorologists to more accurately identify the extent of gale force winds associated with a storm, and provide inputs to numerical models that provide advanced warning of high waves and flooding.

Ship Routing: Wind-observation data from ocean scatterometers is of particular significance in ship routing. Prior knowledge of wind behavior will enable ship masters to choose routes that avoid heavy seas, or high headwinds that may slow ships' progress, increase fuel consumption, or possibly cause damage to vessels and loss of life. In the past, ship captains relied on widely spaced measurements from buoys and sporadic, sometimes unreliable reports from other ships. Data from satellite-based scatterometers are much more regular, extensive and dependable.

Oil Production: Oil and gas production is already on-going at numerous offshore sites around the world the Gulf of Mexico, the North Sea, the Persian Gulf, and other areas. Thorough knowledge of the historical wind and wave conditions at any specific location is crucial to the design of drilling platforms. Safe, efficient drilling operations depend on an accurate understanding of the current sea state and warning of impending storms. In the event of an oil spill, surface-wind information is key to determining how the oil will spread. Ocean scatterometer data could help clean-up and containment crews to minimize the environmental effects of such a disaster.

Food Production: Perhaps the oldest use of the ocean is in the harvesting of food. Today, ocean fishing is a highly systematic activity that makes extensive use of advanced technology to reduce the cost and to increase the value of every "catch". Detailed wind data from the scatterometers can aid in the management of commercial seafood crops. The annual US shrimp harvest in the Gulf of Mexico, for example, depends on favorable on-shore winds that transport offshore, plankton larvae to estuaries where the larvae can develop into adult shrimp. NSCAT and SeaWinds data would be invaluable in the prediction of winds on which such endeavors depend.

9.5.3. Radiometers

Radiometers are the instruments to measure radiation emitted from a source. These instruments can be broadly classified as optical radiometers and microwave radiometers, besides polarimetric radiometers. The thermal microwave radiation of our natural and man-made environment contains many objects with fully polarimetric information. Based on this assumption a quasi-optical imaging radiometer system was designed and realized for the determination of the complete Stokes vector. To demonstrate the system performance, the beam quality was verified by measurements and a polarimetric calibration procedure was developed. Measurements on selected objects have been carried out to demonstrate the polarimetric effects primarily of the third and fourth component of the Stokes vector. The measured results indicate new possible applications for remote sensing and material testing.

The present invention teaches a unique laser radiometer capable of accurately measuring the radiation temperature of a radiant surface and independently measuring the surface's emissivity. A narrow-band radiometer is combined with a laser reflectometer to measure concurrently radiance and emissivity of a remote, hot surface. Together, radiance and emissivity yield the true surface temperature of the remote target. A narrow receiver bandwidth is attained by one of two methods; (a) heterodyne detection or (b) optical filtering. A direct measurement of emissivity is used to adjust the value obtained for the thermal radiation signal to substantially enhance the accuracy of the temperature measurement for a given subject surface. The technique provides substantially high detection sensitivity over a very narrow spectral bandwidth.

A radiometer is a device for measuring the radiant flux (power) of electromagnetic radiation. Radiometers are used to measure SST, wind speed, salinity, soil moisture, sea ice, precipitation, integrated water vapour and liquid water content of the atmosphere. The radiometers can be broadly classified as visible, infrared and microwave radiometers. The radiometer in the visible range measures visible light energy emitted in the visible range. With a spectral sensitivity from 395-465 nm (visible portion of the spectrum), a specially designed photo sensor assembly protects the photo sensor from the high temperatures sometimes associated with today's high-intensity spot lamps.

The very high resolution scanning radiometer is an imaging remote sensing instrument by means of opto-mechanical scan. The mirror conducts line scan which enables the field of view cross over the flight trace and the movement of the satellite around the earth pushes scan line forward, forming two dimensional image of the earth. The primary optical system consists of co-axial and co-focal paraboloids with a diameter of the primary mirror of 200 mm the beam splitters of the visible/IR channels divide the incident beam into infrared, near IR and visible beams.

A Microwave Radiometer (MWR) is a radiometer that measures energy emitted at sub-millimetre-to-centimetre wavelengths (at frequencies of 1-1000 GHz) known as microwaves. Their primary application has been onboard spacecraft measuring atmospheric and terrestrial radiation and are almost solely used for meteorological or oceanographic remote-sensing. Examples of microwave radiometers on meteorological satellites include the Special Sensor Microwave/Imager, Scanning Multichannel Microwave Radiometer and Microwave Sounding Unit. Yet to be launched the Microwave Imaging Radiometer with Aperture Synthesis is an interferometer/imaging radiometer with the capability of resolving soil moisture and salinity over small regions of surface.

Those sensors, which use lenses in the visible and infrared region, are called optical sensors. Cameras and Scanners comes under this category of sensors. OCM (Ocean Color Monitor) on board IRS-P4-OCEANSAT-1, CZCS(Coastal Zone Color Scanner) on board NIMBUS-7 satellite, Landsat-Thematic Mapper, SPOT-PLA/MLA, LISS-I & LISS-II on board IRS-1A/1B and PAN & LISS-III on board IRS-1C/1D are some of the examples of optical sensors. ESA and NASA have made special efforts to develop sensor systems for ocean applications to achieve better accuracies in the retrieval of ocean color information (Example; MERIS on board of ENVISAT-1. SeaWiFS on board OrbView-2 satellites).

9.5.3.1. Thermal Infrared Remote Sensing through Thermal Radiometers

The intensity of emission of electromagnetic radiation at each wavelength and the general shape of the emission curve, particularly the location of the maximum intensity depends on the temperature of the body. The sun emits almost as a black body with a surface equivalent temperature of about 6000^{o} K while the earth emits as a black body with temperature of about 300^{o} K. It may be seen from the sun and earth emission curves that the higher the

temperature, the greater the emissive power. The curves have their maxima at short wave lengths. The earth emission is at maximum in the infra-red part around 10 μm.

AVHRR (Advanced Very High Resolution Radiometer) on board NOAA satellite and ATSR (Along Track Scanning Radiometer) ATSR on board ERS-1, ATSR-2 on board ERS-2 sate, AATSR on board ENVSAT, MODIS on board Terra/Aqua satellites are some of the thermal sensors operationally available today. Currently the measurements of sea surface temperatures are available from these sensors.

9.5.3.2. Microwave Remote Sensing Radiometers

Radiometers measure the intensity of radiation emitted or reflected by targets. They operate in the visible, infra-red and microwave ranges. In the microwave range they are passive sensors in that they measure electro-magnetic thermal radiation emitted by the objects. The microwave sensors can 'see through' clouds unlike visible or infrared sensors.

Electrically Scanned Microwave Radiometer (ESMR) on board METEOSAT, SMMR Scanning Multi-Channel Microwave Radiometers (SMMR) flown on Nimbus – 7, Special Sensor Microwave/Imager (SSM/I) on the DMSP series of Dept. of Defense, USA, TMI on board TRMM satellite, MSMR on board IRS-P4 are the examples of passive microwave sensors. These sensors play important role in Meteorology, Hydrology, and Oceanography.

9.5.3.3. MSMR – Multi-frequency Scanning Microwave Radiometer

MSMR on board IRS-P4 – OCEANSAT-1 satellite was launched in May 1999. MSMR, operating in four frequencies in both vertical and horizontal polarizations in the microwave domain, has the advantage of penetrating clouds and hence has all-weather capability. The radiation emitted by the ocean surface passes through the earth's atmosphere, gets modified before getting detected by MSMR. Using a combination of these frequency and polarization, geo-physical parameters like atmospheric water vapour, sea surface temperature, and precipitation over oceans, ocean surface winds and cloud liquid water, among others, could be derived. MSMR is a unique sensor in the international context as no other passive microwave radiometer is operating in the civilian domain today.

Finally it is concluded that the radiometers available starting from optical sensors to Microwave radiometers onboard the satellites are highly useful in the field of Oceanography to study the varied applications in coastal, ocean and atmospheric sciences.

9.5.4. Synthetic Aperture Radar

Synthetic Aperture Radars were developed as a means of overcoming the limitations of real aperture radars. These systems achieve good azimuth resolution that is independent of the slant range to the target, yet use small antennae and relatively long wavelengths to achieve the results. A synthetic aperture is produced by using the forward motion of the radar. As it passes a given scatterer, many pulses are reflected in sequence. By recording and then combining these individual signals, a "synthetic aperture" is created in the computer providing a much improved azimuth resolution.

It is important to note that some details of the structure of the echoes produced by a given target change during the time the radar passes by. This change is explained also by the Doppler effect which among others is used to focus the signals in the azimuth processor.

References

Alongi DM, 2002, Present state and future of the world's mangrove forests, *Environmental Conservation*, **29:** 331–349.

Annonymous, 1989, Shore Protection Manual, *Environmental Engineering for Coastal Shore Protection*, EM 1110-2-1204.

Arthur R, 2000, Coral bleaching and mortality in three Indian reef regions during an El Nino Southern Oscillation Event, *Current Science*, **79 (12)** : 1723-1729.

Banse K and DC English, 2000, Geographical differences in seasonality of CZCS- derived phytoplankton pigments in the Arabian Sea for 1978-86. *Deep-Sea Research II*, **47**: 1623.

Bell PRF,1992, Eutrophication and coral reefs some examples in the Great Barrier Reef lagoon, *Water Research,* **26(5)** : 553-568.

Bhattathiri PMA, Pant A, Sawant S, Gauns MU, Matondkar SGP and Mahanraju R, 1996, Phytoplankton production and chlorophyll distribution in the eastern and central Arabian Sea in 1994-95, *Current Science,* **71**: *857-862*.

Bird E, 1987, Physiographic indications of a rising sea level. Discussion paper circulated on behalf of the International Geographical Union Commission on the Coastal Environment. Parkville, Victoria: Department of Geography, University of Melbourne.

Boesch DF, 2006, Scientific requirements for ecosystem-based management in the restoration of Chesapeake Bay and Coastal Louisiana, *Ecological Engineering*, **26**: 6–26.

Brown BE, 1997, Coral bleaching: causes and consequences, *Coral Reefs*, **16** : S129-S138.

Bryan Kirk and Syukuro Manabe, 1985, A coupled ocean-atmosphere and the response to increasing atmospheric Co2; JCJ Nihoul (Editor), *Coupled Ocean-Atmosphere Models*, Elsevier Science Publishers, BV, Amsterdam, 1-6 .

Burbridge PR, 1999, The challenge of demonstrating socio-economic benefits of integrated coastal management, *Perspectives on Integrated Coastal Zone Management*, eds. Salomons, W, Turner RK., de Lacerda LD and Ramachandran S, 35-53. Springer, Berlin, Heidelberg.

Burke L, KuraY, Kassem K, Revenga C, Spalding M and Mcallister D, 2001[a,b], Pilot analysis of global ecosystem, Coastal Ecosystem, World Resources Institute, 1-77, [on-line] http://newton.nap.edu/html/coast/summary.html: Priorities for Coastal Ecosystem Science, 2006.

Chauhan, Nagur P, Mohan CRC, Nayak MSR and Navalgund RR, 2001, Surface chlorophyll distribution in the Arabian Sea and Bay of Bengal using IRS-P4 OCM satellite data. *Current Science,* **80** : 40-41.

Cohen JE, Small C, Mellinger A, Gallup J and Sachs J, 1997, Estimates of coastal populations, *Science,* **278**: 1211–1212.

Costanza R, 1992, Toward an operational definition of ecosystem health, in *Ecosystem Health: New Goals for Environmental Management* (Costanza, R., Norton, B.G. and Haskell, B.D., (eds), 239–256, Island Press.

Deekshatulu BL, Nath AN and Rao MV, 1992, Satellite derived sea surface temperature applications for Indian Ocean Resources Development, *Proceedings of the PORSEC-92*, Okinawa, Japan, 76-82.

Delesalle B, Pichon M, Frankignoulle M and Gattuso JP,1993, Effects of a cyclone on coral reef phytoplankton biomass, primary production and composition (Moorea Island, French Polynesia), *Journal of Plankton Research, **15**: 1413-1423*

Dobson A and Carper R, 1993, Health and climate change, *Biodiversity Lancet* , **342**: 1096–1099.

Dwivedi RM, Solanki HU, Gulati D, John ME, Somavanshi VS and Nayak SR, 2002, Exploration of living marine resources in the Arabian Sea through integration of ocean colour with SST. In Proceedings of ISPRS&SIS, Vol.34,Part 7, “Resource and Environment Monitoring, edited by Navalgund RR, Nayak SR and Sudarshana R , Hyderabad, India, 1404-1409.

Emanuel Kerry, 2005, Increasing destructiveness of tropical cyclone over past 30 years, Letters, *Nature*, **436(4)**: 686-688.

Ericson JP, Vörösmarty CJ, Dingman SL, Ward LG, Meybeck M , 2006, Effective sea-level rise and deltas: Causes of change and human dimension implications, *Global and Planetary Change*, **50**: 63–82.

Gopalakrishna VV, Murty VSN, Sarma MSS and Sastry JS,1993, Thermal response of upper layers of Bay of Bengal to forcing of a severe cyclonic storm – A case study, *Indian Journal of Marine Sciences*, **22**: 8-11.

Gower JFR, 1982, General overview fo the nature and use of satellite remote sensing data for fisheries application, *Science Council Studies*, **4**: 7-19.

Greene K, 2002, *Beach Nourishment: A Review of the Biological and Physical Impacts*, ASMFC Habitat Management Series # 7, Atlantic States Marine Fisheries Commission, p 179.

Harvey N and Caton B, 2003, *Coastal Management in Australia*, Oxford, p 342.

IPCC ,1998, The Regional Impacts of Climate Change: An Assessment of Vulnerability, Special Report of IPCC Working Group II [Watson RT, MC Zinyowera and RH Moss (eds.)], Intergovernmental Panel on Climate Change, Cambridge University Press, Cambridge, United Kingdom and New York, NY, USA, p 517.

Jimenez AE, Lugo AE and Clintron G, 1985, Tree mortality in Mangrove Forests, *Biotropica*, **17(3)**: 177-185.

John Perneeta, 1993, Marine Protected Area Needs in the South Asian Seas Region, Vol.2, IUCN, Gland Switzerland.

King SD, 1998, Remote Sensing as an Information Source for Better Coastal Zone Management, Unpublished Masters Thesis, University of Aberdeen, Aberdeen.

Laurs RM, Lynn RJ, Nishimoto R and Dotson R, 1981, Albacore trolling and longline exploration in eastern North Pacific waters during midwinter, NOAA-TM NMFS-SWFC, 10, p 52.

Laurs RM and Brucks JT, 1985, Living marine resource applications, *Advances in Geophysics*, **27**: 419-452.

Lean G and Hinrichsen D, 1992, Atlas of the Environment. 2nd ed. Harper Perennial, New York.

Lee KN and Lawrence J, 1986, Restoration under the Northwest Power Act, *Environmental Law,* **16**: 431-460.

Malone TC, Pike SE and Conley DJ, 1993, Transient variations in phytoplankton productivity at the JGOFS Bermuda time series station, *Deep Sea Research*, **40**: 903-924.

McPhaden MJ, 2003, Evolution of the 2002-03 El Nino, *UCLA Tropical Meterology and Climate*, Newsletter, **57**: 1-10.

Michener WK, Blood ER, Bildstein KL, Brinson MM and Gardner LR, 1997, Climate change, hurricanes and tropical storms and rising sea level in coastal wetlands (review). Ecological Adaptations, **7**: 770–801.

Montgomery RS and Strong AE, 1994, Coral bleaching threatens ocean life, *EOS Transaction*, *American Geophysical Union, 75* **(13)**: 145-147.

Mouillota D, Gaillarda S, Aliaumea C, Verlaqueb M, Belsherc T, Trousselliera M and Do Chia T, 2005, Ability of taxonomic diversity indices to discriminate coastal lagoon environments based on macrophyte communities, *Ecological Indicators*, **5(1)**: 1-17.

Murthy CS and Varadachari VVR,1968, Upwelling along the east coast of India, *Bulletin of National Institute of Sciences India*, **36**: 80-86.

Murty VSN, Rao DP and Sastry JS, 1983, The lowering of sea surface temperature in the east central Arabian Sea associated with a cyclone, Mahasagar – *Bulletin of National Institute of Oceanography,* **16**: 67-71.

Nanda Kumar NV, Saritha K, Rajasekhar M and Ameer Basha S (Div Environ Bio, Dept Zoo, SV University, Tirupati 517502, AP), 2001, Aquaculture effluent effect on physico chemical characteristics and zooplankton of Pulicat lake bird sanctuary. *Ecology and Environmental Conservation*, **7(1)**: 25-29.

Nath AN, Ramana TV, Nathaniel DE, RaoMV, Sasmal SK, Mishra AK, Gopal GV, Nath DJ, Suhasini TD and Prasad VS, 1992, Application of thermal regime information to Potential Fishing Zones identification in near realtime forecasting, Proceedings of the 28th annual convention of IGU and seminar on Geophysics for Rural development, NGRI, Hyderabad, 28-32.

Nayak Shailesh, Solanki HU and Dwivedi RS, 2003, Utilization of IRS-P4 Ocean Colour data for potential fishing zones –a cost benefit analysis, *Indian Journal of Marine Sciences*, **29**: 244-248.

Nicholas J Cooper and Helen Jay, 2001, Predictions of large-scale coastal tendency: development and application of a qualitative behaviour-based methodology, *Journal of Coastal Research*, **36**: 173-181.

Nicholls RJ, 2003, Case study on Sea-Level Rise Impacts, Organisation for Economic Co-operation and Development, ENV/EPOC/GSP (2003) 9/FINAL, 32.

Nicholls RJ, 1998, Assessing erosion of sandy beaches due to sea-level rise, *Geohazard in Engineering Geology* [Maund JG and M. Eddleston (eds.)], *Engineering Geology Special Publications, Geological Society*, London, United Kingdom, **15**: 71–76.

Nicholls RJ, Hoozemans FMJ and Marchand M, 1999, Increasing flood risk and wetland losses due to sea-level rise: regional and global analyses, *Global Environmental Change*, **9**: S69–S87.

Nixon SW, 1988, Physical energy input and comparative ecology of lake and marine systems, *Limnology and Oceanogaraphy,* **33(4)**: 1005-1025.

Nordstrom KF and Jackson NL, September 2005, Bay Shoreline Physical Processes (Fire Island National Seashore Science Synthesis Paper). Technical Report NPS/NER/NRTR-2005/020, National Park Service, Boston, MA.

O'Reilly JE, Maritorena S and 20 others, 2000, Ocean colour chlorophyll algorithms for SeaWifs, OC2 and OC4: Version 4. In S.B. Hooker & E.R. Firestone(Eds). SeaWifs Post launch Calibration and validation Analyses. Part 3. *NASA* Technical Memorandum, 2000-206892, Vol. II(pp.9-27). Greenbelt, MD: NASA Goddard Space Flight Center.

Pranesh MR, 2000, Dredging Activities along the coastal zone and its impact on the coastal morphology, Symposium on

Management problems in coastal areas, Ocean Engineering Centre, IIT Madras, 217-281.

Prasad JS, Rajawat AS, PradhanY, Chauhan P and Nayak SR, 2002, Retrieval of sea surface velocities using sequential ocean colour monitor (OCM)data. In Proceedings, *Indian Acadamy of Sciences* (Earth Planet Sci), **111(3)**: 189-195

Prasanna Kumar S, Madhupratap M, Dileep Kumar M, Muraleedharan PM, de Souza SN, Gauns M and Sarma VVSS, 2001, High biological productivity in the central Arabian Sea during summer monsoon driven by Ekman pumping and lateral advection, *Current Science*, **81**: 1633-1638.

Premkumar K, Ravichandran M, Kalsi SR, Sengupta D and Gadgil S, 2000, First results from a new observational system over the Indian Seas. *Current Science*, **78**: 323-330, 2000

Pringle CM, 2000, Threats to US public lands from cumulative hydrologic alterations outside of their boundaries, *Ecological Applications*, **10(4)**: 971–989.

Purvaja R and Ramesh R, Mangrove Ecosystem and Climate change, Global Dialogue Session, EXPO 2000, Hanover, Germany.

Ramana IV, Rao KH, Rao MV, Dash SK and Bhan SK, 2000, Data processing schem for the retrieval of oceanic parameters using IRS-P4 OCM data. Proceedings of the 5Th Pacific Ocean Remote Sensing Conference (PORSEC 2000), Published by: PORSEC 2000 Secretariat, National Institute of Oceanography, Goa, India, Vol. II, 765-769.

Ramaswamy V, Rao PS, Rao KH, Swe Thwin, Rao NS and Raiker V, 2004, Tidal influence on suspended sediment distribution and dispersal in the Northern Andaman Sea and Gulf of Martaban, *Marine Geology*, 208: 33-42.

Rapport, Costanza DJR and McMichael AJ, 1998, Assessing ecosystem health, *TREE*, **13**: 399-40.

Reynolds RM,1993, Physical oceanography of strait of Hormuz and the Gulf of Oman- results from the Mt.Mitchel expedition, *Marine pollution Bulletin*, **27**: 35-39.

Sarangi, RK, Chauhan P, Mohan M, Nayak SR and Navalgund RR, 2001a, Phytoplankton distribution in the Arabian Sea using IRS-P4 OCM satellite data, *International Jourrnal of Remote Sensing*, **22**: 2863-2866.

Sarangi RK, Chauhan P and Nayak SR, 2001b, Phytoplankton bloom monitoring in the offshore watersof northern Arabian Sea using IRS-P4 OCM satellite data, *Indian Journal of Marine Sciences*, **30**: 214-221.

Shetye SR, Shenoi SSC, Gouveia AD, Michael GS, Sunder D and Nampoorthiri G,1991, Wind driven coastal upwelling along the western boundary of the Bay of Bengal during the southwest monsoon, *Continental Shelf Research*, **11**: 1397-1408.

Shetye SR, Gouveia AD, Shankar D, Shenoi SSC, Vinayachandran PN, Sunder D, Michael GS and Nampoorthiri G, 1996, Hydrography and circulation in the western Bay of Bengal during the northeast monsoon, *Journal of Geophysical Research*, **101**: 14,011-14,025.

Shetye SR, Gouveia AD, Shenoi SSC, Sunder D, Michael GS and Nampoorthiri G, 1993, The western boundary current of the seasonal sub-tropical gyre in the Bay of Bengal, *Journal of Geophysical Research*, **98**: 945-954.

Solanki HU, Dwivedi RM and Nayak SR, 2001, Application of OCM chlorophyll and AVHRR SST for fishery forecast: Preliminary results off Gujarat Coast, *Indian Journal of Marine Sciences*, **30** :132-138.

Sorensen RM, 1978, *Basic Coastal Engineering*. New York: John Wiley & Sons.

Sridhar PN, 2008, Application of remote sensing data and GIS tool in coastal ocean studies, Integrated Coastal Zone Management, The Global Challenge, (Editors) RR Krishnamurthy, Bruce Glavovic, Andreas Kannen, David R. Green, AL Ramanathan, Zengcui Han, Stefano Tinti and Tundi S Agardy, Research Publishing, Singapore, 643-658.

Subranhmanyam Bulusu S, Rao KH, Srinivasa Rao N, Murthy VSN and Ryan Sharp J, 2002, Influence of a tropical cyclone on Chlorophyll-a in the Arabian Sea, *Geophysical Research Letters*, **20(22)**: 2065-2069.

Tsyban AV, Everett JT and Titus JG , 1990, World oceans and coastal zones. In: Climate Change: The IPCC Impacts Assessment. Contribution of Working Group II to the First Assessment Report of the Intergovernmental Panel on Climate Change [Tegart WJMcG, GW Sheldon and DC Griffiths (eds.)], Australian Government.

UNEP, 1989, Criteria for Assessing Vulnerability to Sea Level Rise: A Global inventory to High Risk Area, Delft Hydraulics, Delft, The Netherlands, p 51.

Vieira Mario EC, 2000, The Long-Term Residual Circulation in Long Island Sound, *Estuaries*, **23 (2)** : 199–207.

Vinayachandran PN and Mathew S, 2003, Phytoplankton bloom in the Bay of Bengal during northeast monsoon and its intensification by cyclones, *Geophysical Research Letters*, **30(11)**, doi: 10,1029/2002GL016717.

Vinayachandran PN, Chauhan P, Mohan M and Nayak SR, 2004, Biological response of the sea around Sri Lanka to

summer monsoon, *Geophysical Research Letters*, **31(1)**, doi:10,1029/2003 GL018533.

Vitousek PM, Mooney HA, Lubchenco and Melillo JM, 1997, Human domination of Earth's ecosystems, *Science* , **277:** 494–499.

Walters C, 1997, Challenges in adaptive management of riparian and coastal ecosystems, *Ecology and Society*, **1(2)**: 1-15.

World Bank, 1996, *World Development Report 1996: From Plan to Market*, New York: Oxford University Press.

Xiaojun Yang, 2005, Remote sensing and GIS applications for estuarine ecosystem analysis: an overview, *International Journal of Remote Sensing,* **26(23)**: 5347-5346.

http://climatechange.wikispace.com

nrsc

Remote Sensing Applications

P. S. Roy
R. S. Dwivedi
D. Vijayan

National Remote Sensing Centre

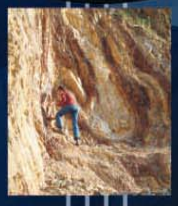

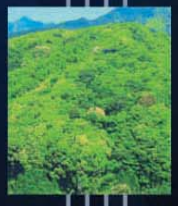

Remote Sensing Applications

Atmosphere

10.1. Introduction

The earth's surface and its near envelope, the atmosphere have provided a unique environment for the evolution and sustenance of plant and animal life on this planet. The present composition of the earth's atmosphere and its surface temperature are the result of an evolutionary process which has involved both the "Geosphere" which includes the land, oceans and the atmosphere and the biologically active region which includes plants and animals, the "Biosphere". The Geosphere Biosphere system is, therefore, a strongly interacting and self regulating system with solar radiation as an external input and a number of internal feed back interactions between its different components make the earth habitable for life. Climate is an important characteristics of the earth system influencing and being influenced by different components the atmosphere, hydrosphere and the biosphere, which determine habitability.

There has been a realization in recent times that the equilibrium of this earth system is being disturbed by a number of natural and anthropogenic factors. Some of them are evolutionary in nature and these are, generally, induced by natural causes e.g., changes in solar radiation flux, changes in earth's orbital parameters etc. But others are of a more short term nature with time scales of decades to centuries and these are largely induced by anthropogenic factors.

The International Geosphere Biosphere Programme (IGBP) launched in 1987 is a programme on global change studies with special reference to climate and environment and is aimed at a detailed study of highly interacting earth system. The scientific objectives of IGBP are: to describe and understand the interactive physical, chemical and biological processes that regulate the total earth system, including the land, oceans and the atmosphere, changes occurring in it and the manner in which they are influenced by human activities.

The main components and drivers of global change are: (i) Changes in land use and land cover; (ii) Global decline in biodiversity; and (iii) Changes in atmospheric composition-CO_2 and other greenhouse gases especially – ozone depletion. The major indicators of global change vis-a-vis human impact are global warming and ozone depletion which have been extensively studied in recent decades.

10.1.1. Greenhouse Effect and Global Warming

The greenhouse effect is a natural phenomenon that occurs when certain gases in the atmosphere, especially water vapor, carbon dioxide and methane, cause the Earth's surface to heat up more than it otherwise would, thereby maintaining a global average temperature warm enough to support life as we know it. Global warming, also called global climate change, occurs when the amounts of carbon dioxide and other trace gases in the atmosphere increase beyond natural levels, thereby intensifying the greenhouse effect. Increased carbon dioxide levels can result from human activities such as the burning of coal, oil and gas and the clearing of forests without replanting.

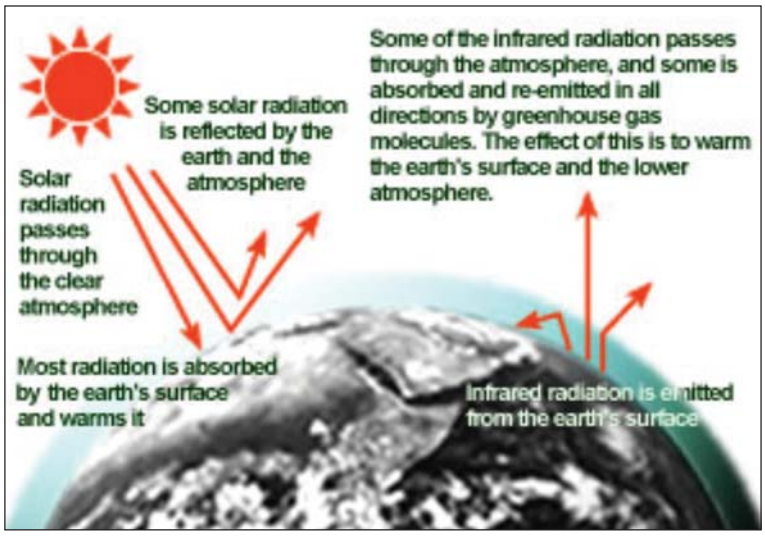

Figure 10.1: Greenhouse effect (source: http://www.gsfc.nasa.gov/gsfc/service/gallery/fact_sheets/earthsci/green.htm; http: //earthobservatory.nasa.gov/Features/Aerosols/)

Greenhouse effect (figure 10.1) is the increase in temperature of the surface of a planet due to the presence of an atmosphere. In the absence of atmosphere, the surface temperature of a planet is determined by the equilibrium between the incident solar radiation flux and the black body emission from the planet surface.

In the presence of an atmosphere, part of the reflected radiation is absorbed by the atmospheric constitutes and re-emitted part of which again reaches the surface thereby increasing the energy available for heating the surface. The result is an increase in the surface temperature and the lower regions of the atmosphere of the planet. The energy balance in the atmosphere is shown here:

The main components in figure 10.2 are the following: Short wavelength (optical wavelengths) radiation from the Sun reaches the top of the atmosphere and clouds reflect ~17% back into space. If the earth gets cloudier, as some climate models predict, more radiation will be reflected back and less will reach the surface. 8% is scattered backwards by air molecules: 6% is actually directly reflected off the surface back into space hence the total reflectivity of the earth is ~31% and this is technically called as albedo. During Ice Ages, Albedo of the earth increased as more of its surface is reflective. The remaining 69% of the incoming radiation that doesn't get reflected back undergoes the following transitions:

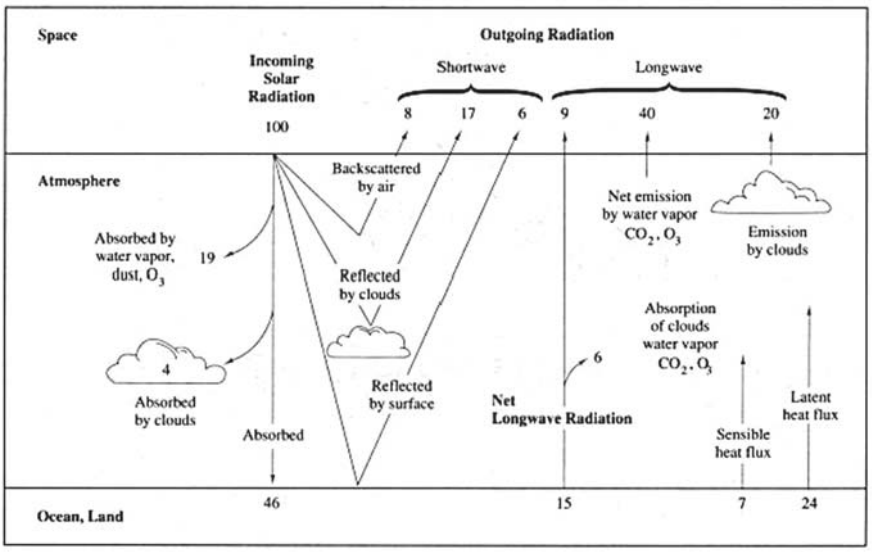

Figure 10.2: The energy balance in the atmosphere(source: http://www.gsfc.nasa.gov/gsfc/service/gallery/fact_sheets/earthsci/green.htm)

- 19% gets absorbed directly by dust, ozone and water vapor in the upper atmosphere. This region is called the stratosphere and is heated by this absorbed radiation. Loss of stratospheric ozone is causing the stratosphere to cool with time, which, of course, greatly confuses the issue of global warming
- 4% gets absorbed by clouds located in the troposphere. This is the lower part of the earth's atmosphere which defines the weather
- The remaining 47% of the sunlight that is incident on top of the earth's atmosphere reaches the surface

This short wavelength radiation absorbed by the earth heats the earth to a finite temperature, it must re-radiate this energy to stay in thermal equilibrium. The earth has an equilibrium temperature of about 300^{o}K. At this temperature, the wavelength of the emitted radiation is mostly in the thermal infrared region. If all the radiation emitted by earth goes directly back into space, the earth would be a significantly colder place than it is. 15% of the long wave radiation is directly radiated back by the cloud-free land surface: 6% of that is absorbed by the atmosphere and 9% goes directly back into space. 60% is re-radiated back into space by the net emission of the atmosphere and the clouds. The total radiated back into space is 69% meaning that 31% is temporarily stored as energy and emitted back later. Of this 31%, 24% is used to facilitate evaporation. This heat is later released through condensation. This process is called latent heat. 7% is stored by the earth's crust and then re-radiated at later through a complicated heat exchange network of convection and conduction. Due to industrial revolution, anthropogenic disturbances caused by human activities increased the ability for the earth's atmosphere to absorb IR radiation causing a net warming of the atmosphere over a period of time. This is the *Enhanced* Greenhouse effect:

Global warming is one of the most serious consequences of development, a major example of environmental degradation over large and temporal scales. It impacts all the components of our environment and the atmosphere, the hydrosphere and the biosphere. The major consequences of global warming are Climate change (Atmosphere); Sea level rise (Hydrosphere) and altered conditions for agriculture (Biosphere).

In addition to these direct effects, there are several indirect effects such as changes in ocean currents and their impact on marine ecosystem, effects on carbon fixing in the oceans and on the land, coral bleaching, changes in ecosystem composition, etc.

10.1.2. Atmospheric Composition

Table 10.1 lists the eleven most abundant gases found in the Earth's lower atmosphere. Of these gases, nitrogen, oxygen, water vapor, carbon dioxide, methane, nitrous oxide and ozone are extremely important to the health of the Earth's biosphere. As evident from the table that nitrogen and oxygen are the main components

of the atmosphere by volume. Together these two gases make up approximately 99% of the dry atmosphere and have very important associations with life. Nitrogen is removed from the atmosphere and deposited at the Earth's surface mainly by nitrogen fixing bacteria, and by way of lightning through precipitation. The addition of this nitrogen to the Earth's surface soils and various water bodies supplies much needed nutrition for plant growth. Nitrogen returns to the atmosphere primarily through biomass combustion and denitrification.

Oxygen is exchanged between the atmosphere and life through the processes of photosynthesis and respiration. Photosynthesis produces oxygen when carbon dioxide and water are chemically converted into glucose in the presence of sunlight. Respiration is the opposite process of photosynthesis. In respiration, oxygen is combined with glucose to chemically release energy for metabolism. The products of this reaction are water and carbon dioxide.

The next most abundant gas is water vapor. Water vapor varies in concentration in the atmosphere both spatially and temporally. The highest concentrations of water vapor are found near the equator over the oceans and tropical rain forests. Cold polar areas and subtropical continental deserts are locations where the volume of water vapor can approach zero percent. Water vapor has several important functional roles on our planet:

- It redistributes heat energy on the Earth through latent heat energy exchange
- The condensation of water vapor creates precipitation that falls on to the Earth's surface providing fresh water for plants and animals
- It helps warm the Earth's atmosphere through the greenhouse effect

The fifth most abundant gas in the atmosphere is carbon dioxide. The volume of this gas has increased by over 35% in the last three hundred years (Table-10.1). This increase is primarily due to human induced burning from fossil fuels, deforestation, and other forms of land-use change. Carbon dioxide is an important greenhouse gas. The human-caused increase in its concentration in the atmosphere has strengthened the greenhouse effect and has definitely contributed to global warming over the last 100 years. Carbon dioxide is also naturally exchanged between the atmosphere and life through the processes of photosynthesis and respiration.

Table 10.1: Average composition of the atmosphere upto an altitude of 25 km.

Gas Name	Chemical Formula	Percent Volume
Nitrogen	N_2	78.08%
Oxygen	O_2	20.95%
*Water	H_2O	0 to 4%
Argon	Ar	0.93%
*Carbon Dioxide	CO_2	0.0360%
Neon	Ne	0.0018%
Helium	He	0.0005%
*Methane	CH_4	0.00017%
Hydrogen	H_2	0.00005%
*Nitrous Oxide	N_2O	0.00003%
*Ozone	O_3	0.000004%

* variable gases

Methane is a very strong greenhouse gas. Since 1750, methane concentrations in the atmosphere have increased by more than 150%. The primary sources for the additional methane added to the atmosphere (in order of importance) are: rice cultivation; domestic grazing animals; termites; landfills; coal mining; and oil and gas extraction. Anaerobic conditions associated with rice paddy flooding results in the formation of methane gas. However, an accurate estimate of how much methane is being produced from rice paddies has been difficult to ascertain. More than 60% of all rice paddies are found in India and China where scientific data concerning emission rates are not available. Nevertheless, scientists believe that the contribution of rice paddies is large because this form of crop production has more than doubled since 1950. Grazing animals release methane to the environment as a result of herbaceous digestion. Some researchers believe the addition of methane from this source has more than quadrupled over the last century. Termites also release methane through similar processes. Land-use change in the tropics, due to deforestation, ranching, and farming, may be causing termite numbers to expand. If this assumption is correct, the contribution from these insects may be important. Methane is also released from landfills, coal mines, and gas and oil drilling. Landfills produce methane as organic wastes decompose over time. Coal, oil, and natural gas deposits release methane to the atmosphere when these deposits are excavated or drilled.

The average concentration of the nitrous oxide is now increasing at a rate of 0.2 to 0.3% per year. Its contribution in the enhancement of the greenhouse effect is minor relative to the other greenhouse gases already mentioned.

However, it does have an important role in the artificial fertilization of ecosystems. In extreme cases, this fertilization can lead to the death of forests, eutrophication of aquatic habitats, and species exclusion. Sources for the increase of nitrous oxide in the atmosphere include: land-use conversion; fossil fuel combustion; biomass burning; and soil fertilization. Most of the nitrous oxide added to the atmosphere each year comes from deforestation and the conversion of forest, savanna and grassland ecosystems into agricultural fields and rangeland. Both of these processes reduce the amount of nitrogen stored in living vegetation and soil through the decomposition of organic matter. Nitrous oxide is also released into the atmosphere when fossil fuels and biomass are burned. However, the combined contribution to the increase of this gas in the atmosphere is thought to be minor. The use of nitrate and ammonium fertilizers to enhance plant growth is another source of nitrous oxide. How much is released from this process has been difficult to quantify. Estimates suggest that the contribution from this source represents from 50% to 0.2% of nitrous oxide added to the atmosphere annually.

Ozone's role in the enhancement of the greenhouse effect has been difficult to determine. Accurate measurements of past long-term (more than 25 years in the past) levels of this gas in the atmosphere are currently unavailable. Moreover, concentrations of ozone gas are found in two different regions of the Earth's atmosphere. The majority of the ozone (about 97%) found in the atmosphere is concentrated in the stratosphere at an altitude of 15 to 55 kilometers above the Earth's surface. This stratospheric ozone provides an important service to life on the Earth as it absorbs harmful ultraviolet radiation. In recent years, levels of stratospheric ozone have been decreasing due to the buildup of human created chlorofluorocarbons in the atmosphere. Since the late 1970s, scientists have noticed the development of severe holes in the ozone layer over Antarctica. Satellite measurements have indicated that the zone from 65° North to 65° South latitude has had a 3% decrease in stratospheric ozone since 1978.

Ozone is also highly concentrated at the Earth's surface in and around cities. Most of this ozone is created as a by product of human created photochemical smog. This buildup of ozone is toxic to organisms living at the Earth's surface.

10.1.3. Atmospheric Structure

Atmospheric layers (figure 10.3) are characterized by variations in temperature resulting primarily from the absorption of solar radiation; visible light at the surface, near ultraviolet radiation in the middle atmosphere, and far ultraviolet radiation in the upper atmosphere.

Troposphere

The troposphere is the atmospheric layer closest to the planet and contains the largest percentage (around 80%) of the mass of the total atmosphere. Temperature and water vapor content in the troposphere decrease rapidly with altitude. Water vapor plays a major role in regulating air temperature because it absorbs solar energy and thermal radiation from the planet's surface. The troposphere contains 99 % of the water vapor in the atmosphere.

All weather phenomena occur within the troposphere, although turbulence may extend into the lower portion of the stratosphere. Troposphere means "region of mixing" and is so named because of vigorous convective air currents within the layer.

The upper boundary of the layer, known as the tropopause, ranges in

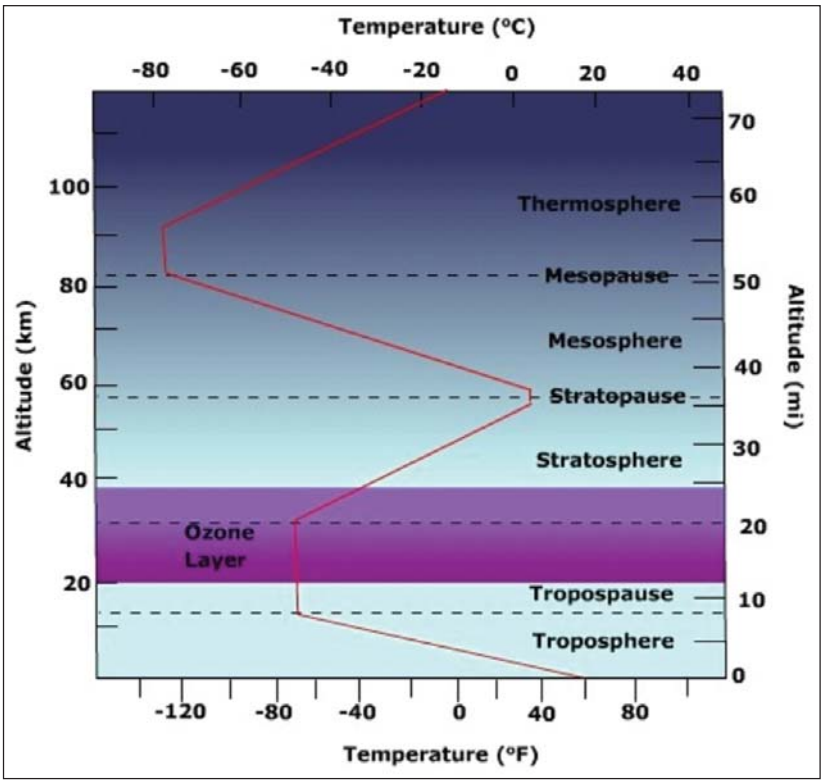

Figure 10.3: Various components of atmosphere (source: http://www.gsfc.nasa.gov/gsfc/service/gallery/fact_sheets/earthsci)

height from 5 miles (8 km) near the poles up to 11 miles (18 km) above the equator. Its height also varies with the seasons; highest in the summer and lowest in the winter.

Stratosphere

The stratosphere is the second major strata of air in the atmosphere. It extends above the tropopause to an altitude of about 30 miles (50 km) above the planet's surface. The air temperature in the stratosphere remains relatively constant up to an altitude of 15 miles (25 km). Then it increases gradually up to the stratopause. Because the air temperature in the stratosphere increases with altitude, it does not cause convection and has a stabilizing effect on atmospheric conditions in the region. Ozone plays the major role in regulating the thermal regime of the stratosphere, as water vapor content within the layer is very low. Temperature increases with ozone concentration. Solar energy is converted to kinetic energy when ozone molecules absorb ultraviolet radiation, resulting in heating of the stratosphere.

The ozone layer is centered at an altitude between 10-15 miles (15-25 km). Approximately 90 % of the ozone in the atmosphere resides in the stratosphere. Ozone concentration in this region is about 10 parts per million by volume (ppmv) as compared to approximately 0.04 ppmv in the troposphere. Ozone absorbs the bulk of solar ultraviolet radiation in wavelengths from 290 nm - 320 nm (UV-B radiation). These wavelengths are harmful to life because they can be absorbed by the nucleic acid in cells. Increased penetration of ultraviolet radiation to the planet's surface would damage plant life and have harmful environmental consequences. Appreciably large amounts of solar ultraviolet radiation would result in a host of biological effects, such as a dramatic increase in cancers.

Mesosphere

The mesosphere, a layer extending from approximately 30 to 50 miles (50 to 85 km) above the surface, is characterized by decreasing temperatures. The coldest temperatures in Earth's atmosphere occur at the top of this layer, the mesopause, especially in the summer near the pole. The mesosphere has sometimes jocularly been referred to as the "ignorosphere" because it had been probably the least studied of the atmospheric layers. The stratosphere and mesosphere together are sometimes referred to as the middle atmosphere.

Thermosphere

The thermosphere is located above the mesosphere. The temperature in the thermosphere generally increases with altitude reaching 600 to 3000 F (600-2000 K) depending on solar activity. This increase in temperature is due to the absorption of intense solar radiation by the limited amount of remaining molecular oxygen. At this extreme altitude gas molecules are widely separated. Above 60 miles (100 km) from Earth's surface the chemical composition of air becomes strongly dependent on altitude and the atmosphere becomes enriched with lighter gases (atomic oxygen, helium and hydrogen). Above about 100 miles (160 km) altitude the major atmospheric component becomes atomic oxygen. At very high altitudes, the residual gases begin to stratify according to molecular mass, because of gravitational separation.

Exosphere

The exosphere is the most distant atmospheric region from Earth's surface. In the exosphere, an upward traveling molecule can escape to space (if it is moving fast enough) or be pulled back to Earth by gravity (if it isn't) with little probability of colliding with another molecule. The altitude of its lower boundary, known as the thermopause or exobase, ranges from about 150 to 300 miles (250-500 km) depending on solar activity. The upper boundary can be defined theoretically by the altitude (about 120,000 miles, half the distance to the Moon) at which the influence of solar radiation pressure on atomic hydrogen velocities exceeds that of the Earth's gravitational pull. The exosphere observable from space as the geocorona is seen to extend to at least 60,000 miles from the surface of the Earth. The exosphere is a transitional zone between Earth's atmosphere and interplanetary space.

10.2. Platforms for measuring atmospheric constituents

Satellites have played an increasingly important role in making remote observations and measurements of global environmental parameters. Satellite motions are governed by the balance between the force of gravity and the centrifugal force due to the satellite's orbital velocity. There are two basic types of meteorological satellites: geostationary and polar orbiting.

Geostationary weather satellites orbit the Earth above the equator at altitudes of 35,880 km (22,300 miles). Because of this orbit, they remain stationary with respect to the rotating Earth and thus can record or transmit images of the entire hemisphere below continuously with their visible-light and infrared sensors. The news media use the geostationary photos in their daily weather presentation as single images or made into movie loops.

Several geostationary meteorological spacecraft are in operation. The United States has two in operation; GOES-11 and GOES-12. GOES-12 is designated GOES-East, over the Amazon River and provides most of the U.S. weather information. GOES-11 is GOES-West over the eastern Pacific Ocean. The Japanese have one in operation; MTSAT-1R over the mid Pacific at 140°E. The Europeans have Meteosat-8 (3.5°W) and Meteosat-9 (0°) over the Atlantic Ocean and have Meteosat-6 (63°E) and Meteosat-7 (57.5°E) over the Indian Ocean. The Russians operate the GOMS over the equator south of Moscow. India also operates geostationary satellites which carry instruments for meteorological purposes. China operates the Feng-Yun geostationary satellites, FY-2C at 105°E and FY-2D at 86.5°E.

Polar orbiting weather satellites circle the Earth at a typical altitude of 850 km (530 miles) in a north to south (or vice versa) path, passing over the poles in their continuous flight. Polar satellites are in sun-synchronous orbits, which means they are able to observe any place on Earth and will view every location twice each day with the same general lighting conditions due to the near-constant local solar time. Polar orbiting weather satellites offer a much better resolution than their geostationary counterparts due to their closeness to the Earth.

Several countries now have satellites in operation (Conway *et al.*, 1997). Russia operates a series of polar orbiting satellites known as Sich / OKEAN (with the Ukraine), the METEOR series, Resors, and MIR -Priroda. Russia also operates a geostationary satellite known as GOMS that transmits infrared images and standard weather maps. China operates the Feng Yun polar orbiter that transmits imagery from both visible and infrared sensors. Japan operates the geostationary meteorological satellite (GMS) which provides visible and infrared images over the western Pacific Ocean, East Asia, and Australia. Japan also has a Marine Observation Satellite (MOS) and, jointly with the US, measures rainfall remotely with the Tropical Rainfall Measuring Mission (TRMM). India operates a geostationary satellite (INSAT) providing distribution of weather maps. The METEOSAT series of geostationary satellites operated by the European Space Agency provide imagery and weather map distribution over Europe and Africa. The Europeans also have the ERS series and ENVISAT. Canada operates RADARSAT, synthetic aperture radar (SAR), which is a powerful microwave instrument that transmits and receives signals to “see” through clouds, haze, smoke, and darkness, and obtain high quality images of the Earth in all weather at any time.

Visible-light images from weather satellites during local daylight hours are easy to interpret even by the average person; clouds, cloud systems such as fronts and tropical storms, lakes, forests, mountains, snow ice, fires, and pollution such as smoke, smog, dust and haze are readily apparent. Even wind can be determined by cloud patterns, alignments and movement from successive photos.

The thermal or infrared images recorded by sensors called scanning radiometers enable a trained analyst to determine cloud heights and types, to calculate land and surface water temperatures, and to locate ocean surface features. These infrared pictures depict ocean eddies or vortices and map currents such as the Gulf stream which are valuable to the shipping industry. Fishermen and farmers are interested in knowing land and water temperatures to protect their crops against frost or increase their catch from the sea. Even El Niño phenomena can be spotted and pollution whether it’s natural or man-made can be pinpointed. The visual and infrared images show the effects of pollution from their respective areas over the entire earth. Aircraft and rocket pollution, as well as condensation trails, can also be spotted. The ocean current and low level wind information gleaned from the space photos can help predict oceanic oil spill coverage and movement.

Almost every summer, sand and dust from the Sahara Desert in Africa drifts across the equatorial regions of the Atlantic Ocean. GOES-EAST images enable meteorologists to observe, track and forecast this sand cloud. In addition to reducing visibilities and causing respiratory problems, sand clouds suppress hurricane formation by modifying the solar radiation balance of the tropics. Other dust storms in Asia and mainland China are common and easy to spot and monitor, with recent examples of dust moving across the Pacific Ocean and reaching North America.

10.3. Remote Sensing of Atmospheric Parameters

The concept of observing system for atmospheric parameters dates back to mid 1960's when planning for combining satellite cloud pictures with radiosondes, aircraft and surface observations were initiated for improved weather forecasting. Satellites have been part of observing system for stratospheric composition related to ozone and its changes for more than 30 years. The new satellite systems can make global observations of key atmospheric constituents in the troposphere. With the advent of new computational and observational capabilities, understanding and predicting global atmospheric composition is becoming more of a reality. Earth system is undergoing rapid changes due to anthropogenic activities. Satellite based observing system is needed to develop understanding of atmospheric composition, the processes that drive the dynamics and to provide the capability to interactions between atmospheric constituents and changes in Earth system due to anthropogenic activities. The observing system for atmospheric composition consists of instruments, models and research. This chapter covers different aspects related to remote sensing of atmospheric constituents such as aerosols, trace gases, temperature, relative humidity and their importance.

The energetic involved in the earth atmosphere system as discussed earlier are shown in Figure10.4. Sun is the natural source of energy and constituents of the earth/atmosphere system reflect/transmit/ absorb the incoming solar energy in different proportions, leading to temperature differences and related dynamics.

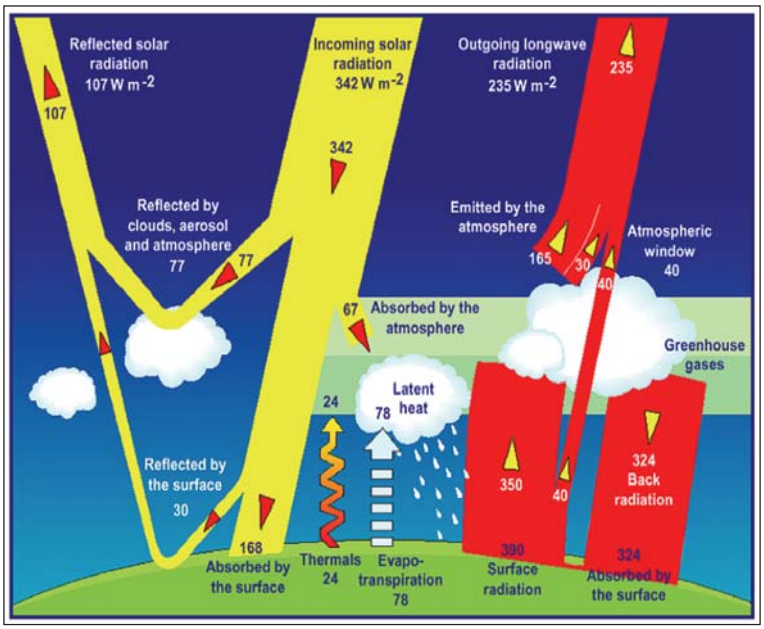

Figure 10.4: Climate system energy balance (source: http://www.gsfc.nasa.gov/gsfc/service/gallery/fact_sheets/earthsci)

The atmospheric constituents determine the air Quality, Earth's radiative balance and the cascading effects such as global warming. The schematic of issues involved in atmospheric composition are shown in Figure 10.5.

Global scale winds move pollutants from one region to another and there is growing awareness that in the Northern Hemisphere, pollution outflow from one continent is reaching the next continent downwind to the east. Thus pollution from the United States gets to Europe; pollution from Europe gets to Asia; and pollution in Asia gets to the United States.

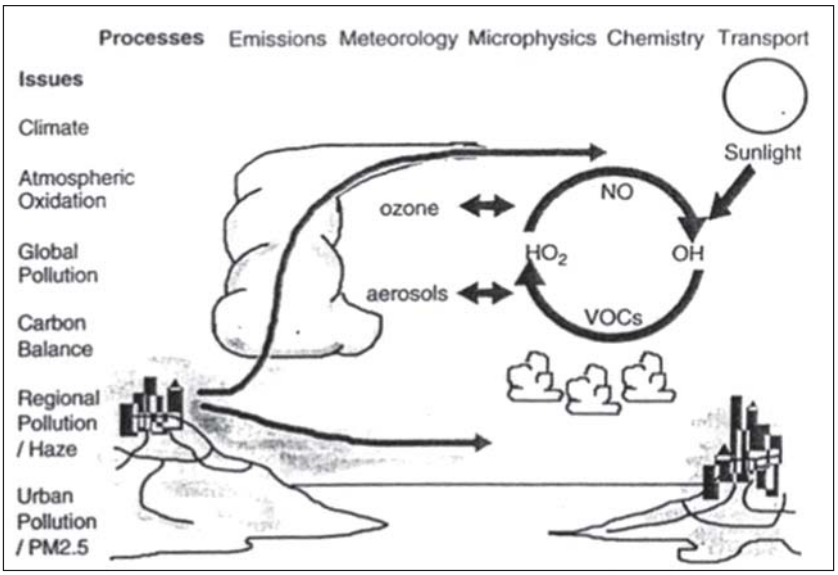

Figure 10.5: Processes and issues related to greenhouse effect (source: http://www.gsfc.nasa.gov/gsfc/service/gallery/fact_sheets/earthsci/green.htm)

Meteorology on all scales influences the atmospheric composition and air quality has become a global issue in recent times. We need to learn how to combine measurements from satellites, ground networks, intensive field campaigns and models on several scales to build an integrated system for creating understanding and predictive capability.

Particulate matter less than 2.5 μm, sulfur dioxide (SO_2), nitrogen dioxide (NO_2), carbon monoxide (CO), aerosols and ozone determine the air quality. There are serious health and environmental effects associated with high concentrations of aerosols and Ozone (O_3). Small size particles can enter the lung causing respiratory problems and enhance the

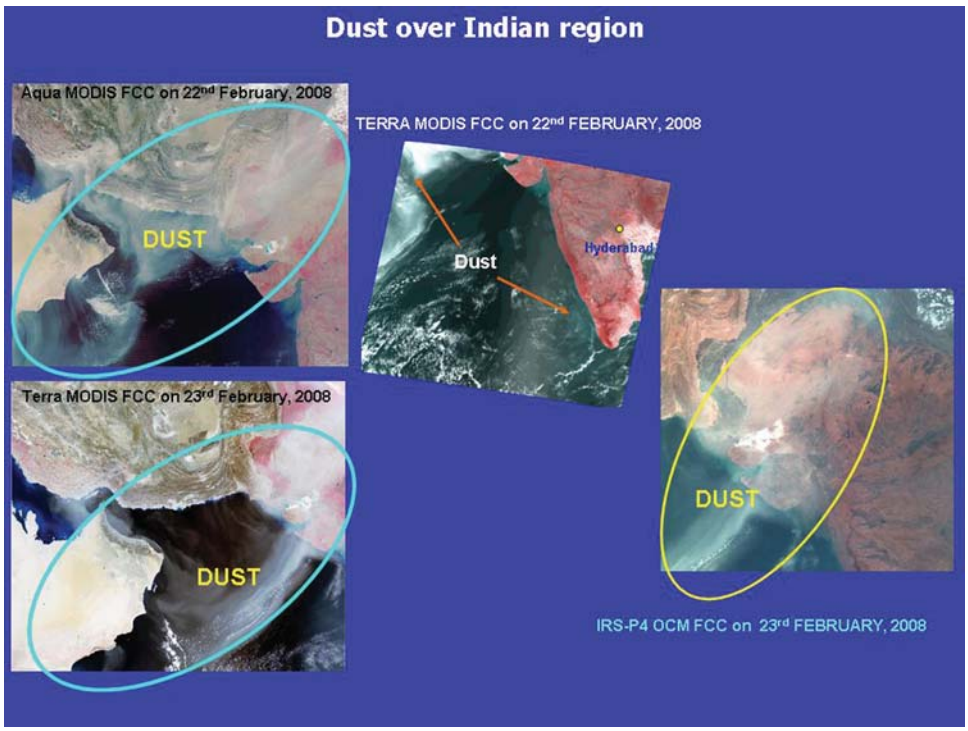

Figure 10.6: Dust storms over Indian region(Badarinath et al., 2010)

concentrations of Ozone, which can affect the immune system and decrease agricultural productivity. It is not possible to control these emissions by reducing the local emission of source gases, such as CO and O_3, as they can be transported to large distances. For example, dust aerosols from Gulf regions is transported over Indian region during pre-monsoon and monsoon period as shown in the TERRA MODIS / IRS-P4 OCM Satellite imagery in Figure 10.6.

The nadir viewing techniques employed by satellite instruments measure the pollutants in the lower troposphere using reflected/scattered sunlight in UV, visible, and near-IR wavelengths (0.3 – 2.5 µm) in figure 10.7. TOMS, GOME and SCIAMACHY are some of the sensors that employ this technique.

10.3.1. Role of aerosols and clouds

Aerosols and clouds tend to counteract the effects of greenhouse gases. Aerosols both absorb and scatter radiation and decrease the energy viable for green house effect. Aerosols are of both natural and anthropogenic origin. Model estimates of radiative forcing of aerosols vary widely between 0 and 2.5 watts/m^2. At the upper limit it is equal to the magnitude but opposite in sign to the greenhouse gas effect of ±2.4watts/m^2. Similarly clouds counteract greenhouse gas effects. Increasing surface temperature increases evaporation from the seas thereby give rise to an increase in cloud cover which can to some extent counteract the greenhouse gas induced global warming. Further the presence of aerosols affects the cloud process. An increase in aerosol content in the atmosphere will increase the cloud forming capacity of the atmosphere which serves as a positive feed back on global warming.

The air quality studies require information on surface concentration and size distribution of aerosols in addition to their vertical distribution and absorptive properties. Atmospheric aerosols are particles of solid or liquid phase dispersed in the atmosphere. These aerosols are produced either by the mechanical disintegration processes occurring over land (such as lifting of dust) and ocean (e.g. sea-spray) or by chemical reactions occurring in the atmosphere. The aerosols at one location are often carried to locations far away from their sources.

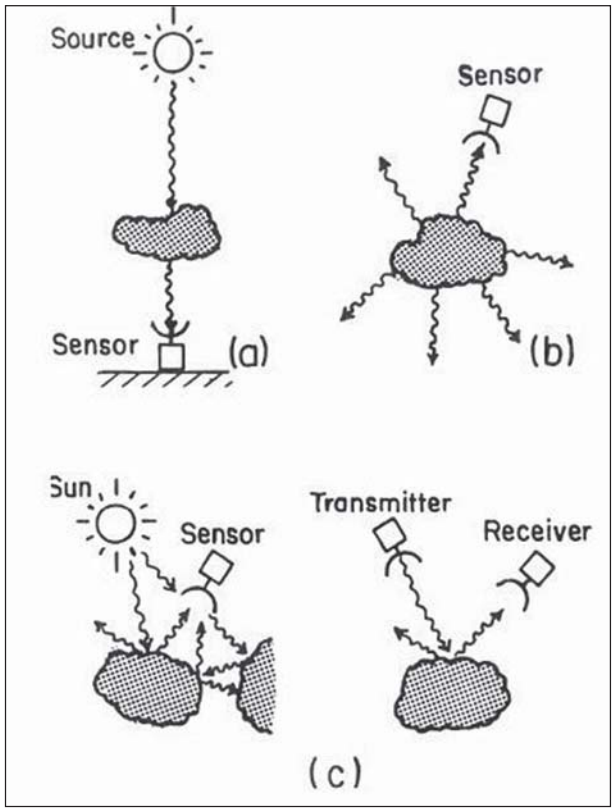

Figure 10.7: Possible receiver / transmitter configurations for remote sensing of atmosphere (source: http: //earthobservatory.nasa.gov/Features/Aerosols/)

Aerosols can vary in size from 10^{-3} to 10^{2} µm depending on the source and production mechanism. Aerosol optical depth (AOD) is quantity which defines the combined effect of scattering and absorption in a vertical column of atmosphere. The optical depth due to aerosols, i.e., "Aerosol Optical Depth (AOD)" is obtained by subtracting the contribution due to air molecules from total optical depth. AOD (t) is derived from the satellite measurement of top of the atmosphere reflectance (TOA) in the visible wavelength bands. The method for estimating aerosol optical depth is described below.

10.3.2. Physical principles of aerosol retrieval from space

One component of the satellite-observed radiance carries information about aerosol, and this component can be isolated as.

$$L(\mu, \varphi) = L_o(\mu, \varphi) + \frac{a}{1 - aR_s} \mu_0, F_0 T\, d(\mu_0) T_u(\mu)$$

For isotropic surface reflection the satellite observed L, after separation of Rayleigh and gaseous components, the same equation holds for aerosol alone. For $\tau < 1$, in single- scattering approximation L_0 is:

$$L_0(\mu, \varphi) \approx \frac{F_0}{4\mu} \omega P(\mu, \varphi, -\mu_0, \varphi_0)\tau$$

Where,

L = satellite observed radiance; L_0 = Atmospheric path radiance; T_d = Total transmittance for downward radiation; T_u = Total transmittance for upward radiation; R_s = Spherical reflectance of atmosphere; a = Surface albedo; F_0 = Normal solar irradiance at TOA; μ_0 = Cosine of solar zenith angle; µ, φ = Cosine of view angle and relative azimuth angle; τ = Optical thickness; ρ = Scattering phase function; ω = Single scattering albedo

The Moderate Resolution Imaging Spectrometer (MODIS) aboard EOS Terra and Aqua satellites makes multi - spectral measurements of top of the atmosphere reflectance (r) to determine the size distribution of aerosols in fine or coarse mode. This helps in the determination of aerosol scattering phase function, "P". Figure 10.8 shows the MODIS derived aerosol optical depth on two dates over Indian region. The increased values of aerosol optical depth over Indo-Gangetic Plains can be observed in the Figure 10.8. The accuracy of MODIS AOD over land regions is not good due to heterogeneity in land surface reflectance. Recently, a new algorithm, called the "deep blue" algorithm has been developed to improve the estimation over land. This algorithm uses the 412 and 419 nm MODIS channels, where the land is darker at the longer wavelengths.

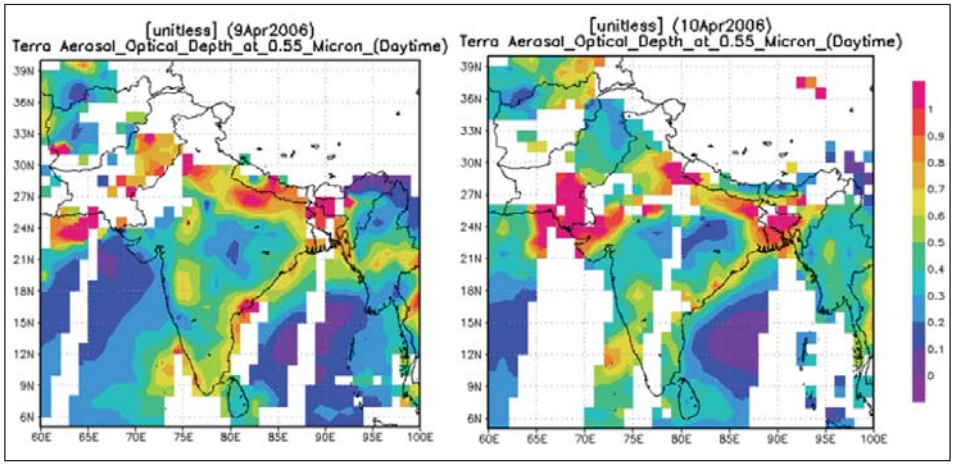

Figure 10.8: TERRA MODIS derived aerosol optical depth(Badarinath et al., 2007)

In addition to satellite based estimation of AOD in visible region of the electromagnetic spectrum (EMR), methods exist to estimate aerosol absorption optical depth t_a using ultraviolet wavelengths. Aerosol index (AI), a measure of the absorbing aerosol concentration in atmosphere, is regularly estimated from 1978, using Total Ozone Monitoring Instrument (TOMS) on board Earth Probe (EP) and was recently replaced by AURA-OMI. In the ultraviolet wavelengths, land is opaque, and the wavelength of top of the atmosphere reflectance provides information on the absorbing aerosols in the atmosphere. It is possible to make quantitative estimates of t_a and t_s from measurements of top of atmosphere reflectance (ñ) at two ultraviolet wavelengths (Torres *et al.*, 1998). By combining the deep blue, visible and the UV methods, estimation of both the scattering and absorption optical depths of aerosols over

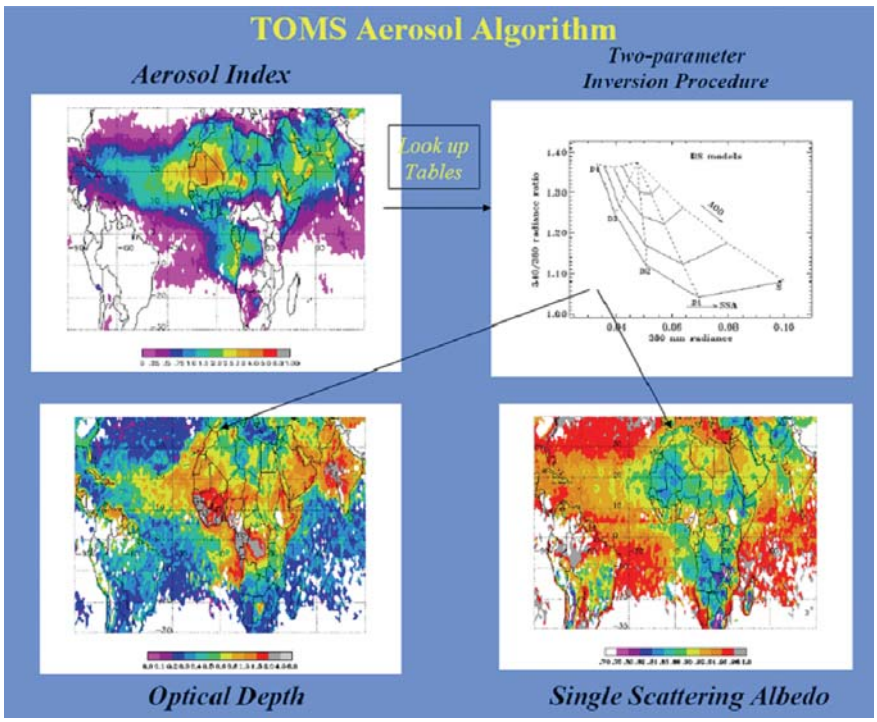

Figure 10.9: TOMS Aerosol algorithm(Torres et al., 1998)

land and ocean can be made (figure 10.9).

Estimation of tropospheric Ozone (O_3) remains a challenge for satellite measurements, as radiation sensitive to tropospheric ozone has to pass through the stratosphere before reaching to the satellite. The satellite measurements are so far able to achieve estimation of tropospheric ozone from total columnar ozone by subtracting the stratosphere overburden. There are several methods available, including the use of limb viewing instruments, such as Microwave Limb Sounder (MLS) and The Stratospheric Aerosol and Gas Experiment (SAGE) that can measure down to the tropopause to estimate stratospheric Ozone overburden.

Nitrogen Dioxide (NO_2) is a byproduct of combustion produced by automobiles and biomass burning besides it is also produced by lightning. Scanning Imaging Absorption Spectrometer for Atmospheric Cartography (SCIAMACHY) onboard ENVISAT satellite makes measurement of NO_2. Since NO_2 occurs mostly in the planetary boundary layer, the accuracy of these products requires careful scrutiny.

10.3.3. Physical basis of TOMS aerosol retrieval approach

Neglecting particle multiple scattering effects, the upwelling reflectance as measured by a satellite, is approximately given by:

Since I_0 depends on pressure, then

Aerosol single scattering contribution

Attenuation of Rayleigh and surface components by aerosol absorption

$$I \approx \frac{\omega_0 P(\Theta)\pi F}{4\pi} \frac{\mu_0}{\mu_0+\mu}\left[1-e^{-\tau(1/\mu+1/\mu_0)}\right]+[I_s+I_0]e^{-(1-\omega_0)\tau(1/\mu+1/\mu_0)}$$

$$I \approx \frac{\omega_0 P(\Theta)\pi F_0}{4\pi} \frac{\mu_0}{\mu_0+\mu}\left[1-e^{-\tau(1/\mu+1\mu_0)}\right]+\left[\frac{(\rho_s \rho_a) I_0}{\rho_s}+I_s\right]e^{-(1-\omega_0)\tau(1/\mu+1/\mu_0)}+\frac{\rho_a}{\rho_s}+I_s$$

ρ_s and ρ_a are surface and aerosol layer height pressure levels. The net aerosol contribution to the measured reflectance is-

Where,

πF_0 = Solar flux; ω_0 = Single scattering albedo; τ = Aerosol optical depth; μ, μ_0 = Cosines of satellite and solar zenith angles; b (Θ) = Aerosol scattering phase function,

The principle used for measuring carbon monoxide (CO) employs 2.3 µm absorption bands, where there is still a sufficient amount of sunlight to measure the reflected radiation. Satellite measurement of CO mainly comes from

the 4.6 µm thermal emission band, which provides CO in the middle troposphere. Recent results have come out from the MOPITT instrument onboard EOS Terra and the AIRS instrument onboard EOS Aqua satellite. Sulfur Dioxide (SO_2) mainly comes from both natural sources such as fuming volcanoes and anthropogenic sources such as burning of sulfur rich coal. Satellite base instruments such as GOME, SCIAMACHY and OMI with spectral bands in UV region provide global maps of SO_2 (Figure10.10a & 10b).

Sensor	TOMS/ TRIANA	AVHRR/ SEAWIFS	GOME	MOPITT	MODIS	SCIA MACHY	MIPAS	SAGE III	TES	HRDLS	OMI	MLS
Launch	1979		1995	1999	1999	2002	2002	2004	2004	2004	2004	2004
O_3	col		col			col/limb	limb	limb	nadir/limb	limb	col	limb
H_2O	col					col/limb	limb	limb	nadir/limb	limb		limb
CO				nadir		col/limb	limb		nadir/limb			limb
NO									limb			
NO_2			col			col/limb					col	
HNO_3							limb		limb	limb		
CH_4				col		col/limb			col	limb		
CH_2O			col			col/limb					col	
SO_2						col			col		col	
CO_2						col/limb						
BrO			col			col					col	
HCN												limb
Aerosol	col	col			col	col/limb		limb		limb	col	

Figure 10.10a: Present Satellite Measurements for Tropospheric Chemistry (source: www.esa.int)

Precipitation is one of the most variable quantities in space and time. Precipitation also has a direct impact on human life that other atmospheric phenomena seldom have: an example is represented by heavy rain events and flash floods.

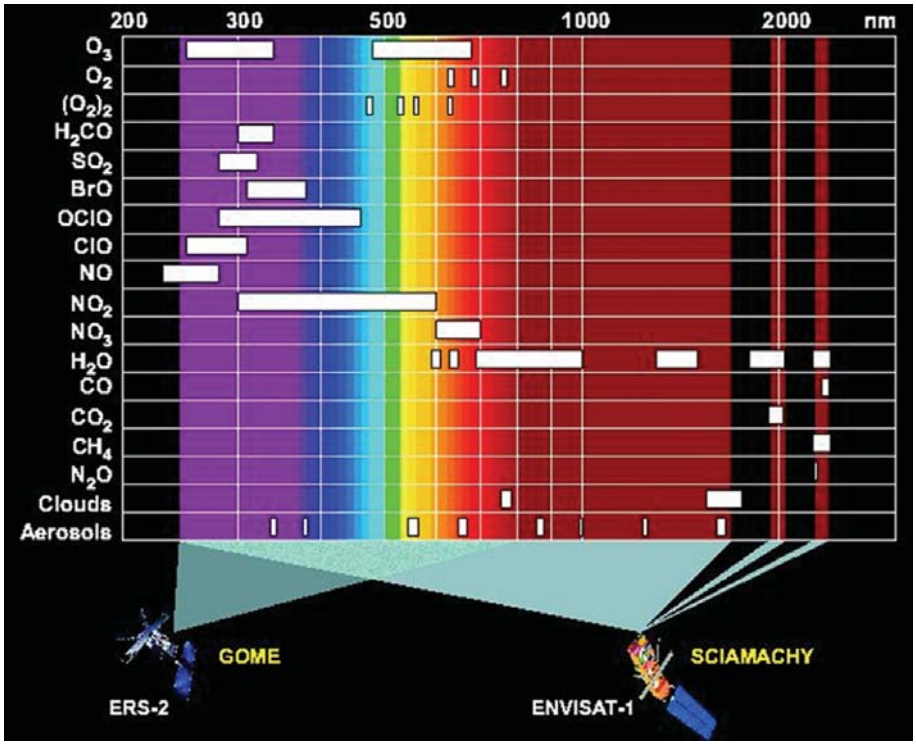

Figure 10.10b: Different spectral bands used in Satellite observation of trance gases and aerosols (source: www.esa.int)

Satellite remote sensing is an efficient tool for measuring rainfall on various spatial and temporal scales that has many applications in meteorology, hydrology and climate studies. Over India and adjoining oceans, the reliable ground based radars and dense network of rain gauge information is available but only for limited areas. Although geostationary satellite IR measurements benefit from high temporal sampling, IR radiances from cloud tops have only an indirect relationship with surface rainfall which so far resulted in weak statistical relationships between rainfall and cloudiness. The most common GOES Precipitation Index (GPI) technique (Arkin and Meisner 1987) based on simple IR-TB threshold algorithm have been in operation to produce tropical and subtropical precipitation products for various climatological studies (Arkin and Xie 1994). Satellite microwave measurements on the other hand have a very good physical connection with the rain and hydrometeors. There are many satellite microwave based techniques for rainfall estimation over land and oceans (Ferraro and Marks 1995, Wilheit *et al.*, 2003, Kummerow *et al.*, 1996, Liu and Curry 1992).

Rainfall estimation from IR and visible observations from geostationary and low orbiting satellites basically depends on combining multi-spectral measurements to estimate precipitation. One of the principal innovations of these

methods relative to earlier simpler temperature threshold based algorithms is that, it optimally combines several cloud properties used in a variety of techniques in a single and comprehensive rainfall algorithms. For example, the GOES Multi-Spectral Rainfall Algorithm (GMSRA) (Ba and Gruber 2001), Hydro-Estimator (H-E) (Scofield and Kuligowski 2003.) techniques from NOAA uses many such cloud property in VIS and IR regions. The GMSRA uses the cloud top temperature as a basis of rain estimation (e.g., Arkin and Meisner; 1987, Ba *et al.*, 1995; Vicente *et al.*, 1998) and utilizes the effective radii of cloud particles, i.e., the cloud microphysics (e.g., Rosenfield and Gutman 1994) and spatial and temporal gradients (e.g., Adler and Negri 1988; Vicente *et al.*, 1998) to screen out non-raining clouds and humidity.

The development of hybrid techniques using the strengths of both microwave and IR is highly desirable based on their proper inter-calibration over the common areas of overlap. One such algorithm was developed by Vicente *et al.*, (1998) called auto-estimator, using GOES (IR) and surface microwave radar-rainfall. Adler *et al.* (1994) developed a technique called Adjusted GPI (AGPI) in which a correction factor is derived from the comparison of passive microwave and GPI estimates for coincident time slots (from 3 hourly to one month). Gairola *et al.*, 2004; Gairola and Krishnamurthy 1992; Joyce *et al.*, 2004 developed techniques in which the IR channel is used as a means to spatially and temporally transport the rainfall features in conjunction with satellite passive microwave observations.

The inherent limitations of optical channels remain persistent for rainfall retrieval as the rainfall in the ground is inferred by cloud top signatures only. There is no direct physical connection between the rain/cloud and ice hydrometeors within the clouds with radiance emanating from cloud tops to the sensor. The accuracy of rainfall estimate improves marginally even with significant new efforts. However, the high spatial and temporal coverage of geostationary optical measurements is the very strong point along with the resolution capabilities of the sensors. At the same time microwaves have direct physical connections with vertical structure of rainfall and thus with the cloud, rain and ice hydrometeors. But the non-portability of microwave sensors to the geostationary platforms till date due to technological constraints is a limitation and thus only low earth orbiting satellites can provide the rainfall information for land, ocean and atmosphere. With the advent of active and passive radar and radiometric sensors onboard a single satellite (e.g., Tropical Rainfall Measuring Mission-TRMM) we envisage that a technique like GMSRA can be further improved for Indian tropical regions and more reliable rainfall information can be retrieved. We henceforth call this technique as INSAT Multispectral Rainfall Algorithm (IMSRA), as a specific technique for Indian Tropical regions. Our objectives for both the techniques (GPI and IMSRA) here are based on these premises and are outlined below (mainly in cases of IMSRA).

King (1956) was first to suggest that atmospheric temperature profiles could be inferred from satellite observations of thermal infrared emission and explained the feasibility of retrieving the temperature profile from the satellite intensity scan measurements. Further advances were made for the temperature sounding concept by Kaplan (1959) demonstrated that vertical profile of temperature could be inferred from the spectral distribution of emission by atmospheric gases. He suggested that observations in the wings of a spectral band sense deeper regions of the atmosphere, whereas observations in the band center see only the very top layer of the atmosphere, since the radiation mean free path is small. Thus by properly selecting a set of sounding spectral channels at different wavelengths in the absorption band, the observed radiances could be used to estimate the vertical temperature profile in the atmosphere.

Following a proposal by Wark (1961) for satellite vertical sounding program to measure atmospheric temperature profiles, the first satellite with sounding instrument (SIRS-A) was launched on NIMBUS-3 in 1969 (Wark *et al.*, 1970). NOAA launched the TIROS Operational Vertical Sounder in 1978 (TOVS, Smith *et al.* 1979), consisting of High resolution Infrared Radiation Sounder (HIRS), Microwave Sounding Unit (MSU), and the Stratospheric Sounding Unit (SSU) onboard satellites NOAA-6 to NOAA-14. HIRS provides 17 km spatial resolution at nadir with 19 infrared sounding channels (4-15 μm), whereas MSU provides 109 km resolution at nadir with 4 microwave channels (~50 GHz). SSU has 3 channels in the far IR (~15 μm) for stratospheric measurements. Current NOAA series satellites NOAA-15 and NOAA-16 (and future satellite in the NOAA series) have ATOVS with HIRS/3, and MSU and SSU have been replaced by AMSU-A and AMSU-B to improve the temperature and humidity sounding. HIRS/3 has the same spectral bands as the HIRS/2. AMSU-A uses 15 microwave channels around 23, 30, 50 and 90 GHz of oxygen absorption bands with resolution of 50 km at nadir. AMSU-B uses 5 microwave channels around 90, 150 and 190 GHz with a horizontal resolution of 17 km at nadir.

New generation of infrared atmospheric sounders are hyper-spectral sounder with thousands of channels instead of few tens of infrared bands. Atmospheric Infra-Red Sounder (AIRS) onboard EOS-Aqua satellite was launched on May 4, 2002 providing a wealth of highly accurate atmospheric and surface information using 2378 high spectral-

resolution infrared (3.7 – 15.4 µm) channels with horizontal resolution of 10 km at nadir. AIRS along with AMSU forms a state-of-art atmospheric sounding tool for temperature profiles with accuracy of 1° C in a 1 km thick layer and humidity profile with an accuracy of 20% in 2 km thick layer in the troposphere. Aqua satellite also has MODIS with very high spatial resolution of 1 km and is providing the vertical profiles of temperature and humidity. Recently, METOP satellite was launched carrying a hyper spectral sounder IASI onboard with >8400 channels and mission objectives were to achieve the temperature and humidity profiles accuracy of 1° C and 10% in 1 km and 2km layers, respectively. The first sounding instrument in geostationary orbit was the GOES VISSR Atmospheric Sounder (VAS, Smith *et al.* 1981) launched in 1980. This was followed by GOES-8 Sounder (Menzel and Purdom, 1994) that provides 8 km spatial resolution with 18 infrared sounding channels. Current satellite of this series, GOES-13, was launched recently in May 2006. Future satellite of this series GOES-R is to be launched in 2012 and it will have a Hyperspectral Environmental Suite (HES) to provide high spectral resolution in the infrared and a high spatial resolution mode for mesoscale sounding capability. Advanced Baseline Imager (ABI) onboard GOES-R will be similar to the current polar orbiting EOS-MODIS. NASA and NOAA are planning to launch Geostationary Imaging Fourier Transform Spectrometer (GIFTS) that will revolutionize our ability to measure, understand and predict the earth-atmosphere system. India is planning to launch a meteorological satellite INSAT-3D in geostationary orbit towards the end of 2010. INSAT-3D will carry an 18-channel infrared Sounder (in addition to visible channel) along with a 6 channel Imager. The algorithm for retrieving vertical profiles of atmospheric temperature and moisture along with ozone from INSAT-3D Sounder observations of clear sky infrared radiances in different absorption bands. INSAT-3D Sounder channels are similar to those in GOES-12 Sounder and many of the spectral bands are similar to High resolution Infrared Radiation Sounder (HIRS) onboard NOAA- ATOVS. Observations in these Sounder channels can be used to retrieve profiles of temperature and moisture as well as total column estimates of ozone. INSAT-3D Sounder observations will provide vertical profiles of temperature and humidity in clear-sky conditions besides total column ozone and various other derived products.

Atmospheric profile retrieval algorithm for INSAT-3D Sounder is a two-step approach. The first step includes generation of accurate hybrid first guess profiles using combination of statistical regression retrieved profiles and model forecast profiles. The second step is nonlinear physical retrieval to improve the resulting first guess profile using Newtonian iterative method. The retrievals will be performed using clear sky radiances measured by Sounder within a 5x5 field of view (approximately 50 km resolution) over land and ocean for both day and night. Separate regression coefficients will be generated for land and ocean for day and night conditions using a training dataset comprising historical radiosonde observations representing atmospheric conditions over INSAT-3D observation region. INSAT-3D Sounder has 18 infrared channel and a visible channel to help cloud detection during daytime. The normal mode of Sounder operation covers 6000km x 6000km field of view and takes approximately 160 minutes. In addition, the instrument is designed with flexible modes of operation for fast and repetitive coverage.

INSAT- 3D Sounder retrieval scheme involves two-step approach, with first step as regression retrieval combined with model forecast to prepare the temperature and humidity profile, followed by the second step as physical retrieval procedure that uses non-linear Newtonian iterative method to adjust the first guess to obtain accurate retrieval of temperature, and humidity profile. Ozone profile and integrated amount is retrieved using regression retrieval and used as first guess for the physical retrieval routine. Atmospheric sounding is one of the most important applications of satellite measurements in meteorology, which involves retrieving vertical profiles of temperature and trace-gas concentrations, especially water vapor and ozone. This is done by making observations at wavelengths that have significant attenuation in atmosphere (figure 10.11 and 12). For this we need to know the variation of temperature with altitude, and the variation of the density of atmospheric gases with altitude, such as carbon-dioxide, water vapour and ozone. Water vapor is important because of its

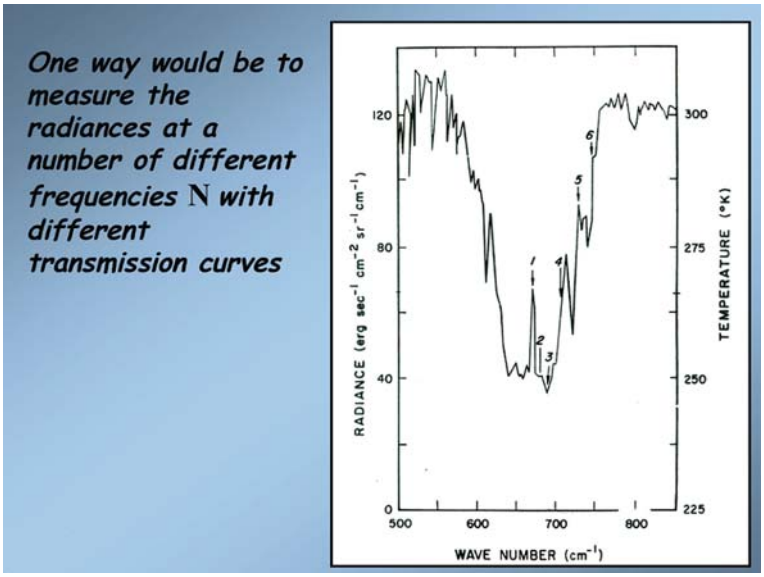

Figure 10.11: Atmospheric sounding of atmosphere at different wavelengths for deriving temperature (source: http: // earthobservatory.nasa.gov/Features/Aerosols/)

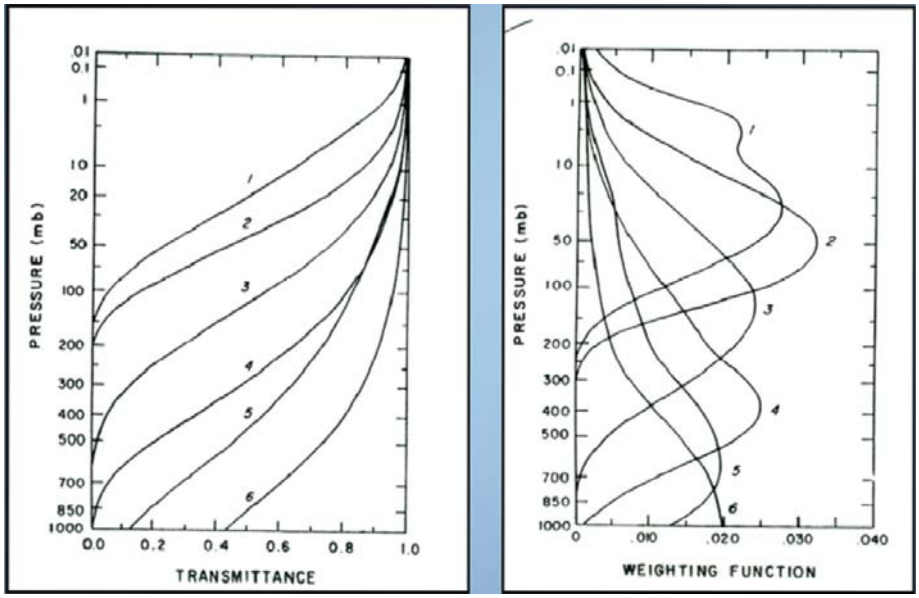

Figure 10.12: Transmission and weighting functions (source: http://www.ua.nws.noaa.gov/factsheet.htm)

meteorological impact and its importance for atmospheric correction in thermal infrared measure-ments.

Atmospheric sounding techniques exploit all three phenomena that play important role in radiative transfer processes: namely absorption, scattering and thermal emission. Most observations are made in the thermal infrared and microwave bands. At infrared wavelengths scattering due to atmospheric gases is negligible, and is not considered in the radiative transfer process. For nadir IR earth radiance methods the RT problem is more complicated and non-linear.

The upwelling 'Earth' radiance at wavelength l, or frequency (wave number) õ, observed looking down, is given by:

$$\tau_{\nu}(a,b) = \exp\left(-\int_{z=a}^{z=b} n(z)\sigma_{\nu} dz\right)$$

$$L_{\nu}(Z^{*}) = \varepsilon_{surf} B_{\nu}(T_{surf})\tau_{\nu}(0,Z^{*}) + \int_{z=0}^{z^{*}} B_{\nu}(T_{z})\, n(Z)\sigma_{\nu}\tau_{\nu}(Z,Z^{*})\, dz$$

$$L_{\nu}(Z^{*}) = \varepsilon_{surf} B_{\nu}(T_{surf})\tau_{\nu}(0,Z^{*}) + \int_{z=0}^{z^{*}} B_{\nu}(T_{z})[\, d\tau_{\nu}(Z,Z^{*})/dZ\,]\, dZ$$

For vertical sounding theory at infrared wavelengths, the significant terms in the radiative transfer equation (RTE) are absorption and thermal emission. This simplification is called Schwartzchild's equation. Here, we consider only cloud-free conditions. If a sensor views vertically downwards into the atmosphere at a wavelength at which the atmosphere is optically thick, the brightness temperature/radiances that is received by sensor will be characteristic of the atmosphere at a depth below the sensor that is of the order of the absorption length. Thus, the greater the absorption coefficient, the smaller the absorption length, and hence the greater the altitude from which the temperature signal is received. So by making observations at a number of wavelengths near a broad absorption line, different altitudes in the atmosphere can be investigated. Thermal infrared temperature profilers normally employ the broad and deep CO_2 lines near 15 µm wavelengths.

10.4. Present and Future Missions

10.4.1. INSAT Series

INSAT or the Indian National Satellite System is a series of multipurpose geo-Stationary satellites launched by ISRO for the telecommunications, broadcasting, meteorology, and "search and rescue" needs of India. Commissioned in 1983, INSAT is the largest domestic communication system in the Asia-Pacific Region. It is a joint venture of the Department of Space, Department of Telecommunications, India Meteorological Department, All India Radio and Doordarshan. The overall coordination and management of INSAT system rests with the Secretary-level INSAT Coordination Committee.

INSAT satellites provide 199 transponders in various bands (C, S, Extended C and Ku) to serve the television and communication needs of India. Some of the satellites of the INSAT series also carry the Very High Resolution Radiometer (VHRR), CCD cameras for meterological imaging. The satellites also incorporate transponders for receiving distress alert signals for search and rescue missions in the South Asian and Indian Ocean Region, as ISRO is a member of the Cospas-Sarsat programme.

INSAT system

The Indian National Satellite (INSAT) system was commissioned with the launch of INSAT-1B in August 1983 (INSAT-1A), the first satellite was launched in April 1982 but could not fulfill the mission. INSAT system ushered in a revolution in India's television and radio broadcasting, telecommunications and meteorological sectors. It enabled the rapid expansion of TV and modern telecommunication facilities to even the remote areas and off-shore islands. Today, INSAT has become the largest domestic communication satellite system in the Asia-Pacific region with ten satellites in service - INSAT-2E, INSAT-3A, INSAT-3B, INSAT-3C, INSAT-3E, KALPANA-1, GSAT-2, EDUSAT, INSAT-4A and INSAT-4B (table 10.2). Together, the system provides 199 transponders in C, Extended C and Ku bands for a variety of communication services. Some of the INSATs also carry instruments for meteorological observations and data relay for providing meteorological services. KALPANA-1 is an exclusive meteorological satellite. The satellites are monitored and controlled by Master Control Facilities that exist in Hassan and Bhopal.

Satellites in service

There are currently 11 satellites in service out of 21 which have ever been part of INSAT system.

Table 10.2: INSAT satellites

Sl. No.	Satellite	Launch Date	Mission Status
1	INSAT-1A	10 April 1982	Deactivated on 6 September 1982
2	INSAT-1B	30 August 1983	Completed mission life
3	INSAT-1C	22 July 1988	Abandoned in November 1989
4	INSAT-1D	12 June 1990	Completed mission life
5	INSAT-2A	10 July 1992	India's First Indegenious communication Satellite. Completed mission life
6	INSAT-2B	23 July 1993	Completed mission life
7	INSAT-2C	7 December 1997	Completed mission life
8	INSAT-2D	4 June 1997	Became inoperable on 4 October 1997
9	INSAT-2DT	In-orbit procurement	Completed mission life
10	INSAT-2E	3 April 1999	In service
11	INSAT-3A	10 April 2003	In service
12	INSAT-3B	22 May 2000	In service
13	INSAT-3C	24 January 2002	In service
14	KALPANA-1	12 September 2002	In service
15	GSAT-2	8 May 2003	In service
16	INSAT-3E	28 September 2003	In service
17	EDUSAT	20 September 2004	In service
18	INSAT-4A	22 December 2005	In service
19	INSAT-4B	12 March 2007	In service
20	INSAT-4CR	2 September 2007	in geo-synchronous orbit

INSAT-2E

It is the last of the five satellites in INSAT-2 series. It carries seventeen C-band and lower extended C-band transponders providing zonal and global coverage with an Effective Isotropic Radiated Power (EIRP) of 36 dBW. It also carries a Very High Resolution Radiometer (VHRR) with imaging capacity in the visible (0.55-0.75 µm), thermal infrared (10.5-12.5 µm) and water vapour (5.7-7.1 µm) channels and provides 2x2 km, 8x8 km and 8x8 km ground resolution, respectively. In addition to the above two payloads it has with it a Charge Coupled Device (CCD) camera providing 1x1 km ground resolution in the Visible (0.63-0.69 µm), Near Infrared (0.77-0.86 µm) and Shortwave Infrared (1.55-1.70 µm) bands.

INSAT-3 Series

INSAT-3A

The multipurpose satellite, INSAT-3A, was launched by Ariane in April 2003. It is located at 93.5 degree East longitude. The payloads on INSAT-3A are as follows:

- 12 Normal C-band transponders (9 channels provide expanded coverage from Middle East to South East Asia with an EIRP of 38 dBW, 3 channels provide India coverage with an EIRP of 36 dBW and 6 Extended C-band transponders provide India coverage with an EIRP of 36 dBW)
- 6 Ku-band transponders provide India coverage with EIRP of 48 dBW
- A Very High Resolution Radiometer (VHRR) with imaging capacity in the visible (0.55-0.75 µm), thermal infrared (10.5-12.5 µm) and Water Vapour (5.7-7.1 µm) channels, provide 2x2 km, 8x8 km and 8x8 km ground resolutions respectively
- A CCD camera provides 1x1 km ground resolution, in the visible (0.63-0.69 µm), near infrared (0.77-0.86 µm) and shortwave infrared (1.55-1.70 µm) bands
- A Data Relay Transponder (DRT) having global receive coverage with a 400 MHz uplink and 4500 MHz downlink for relay of meteorological, hydrological and oceanographic data from unattended land and ocean-based automatic data collection-cum-transmission platforms
- A Satellite Aided Search and Rescue (SAS&R) SARP payload having global receive coverage with 406 MHz uplink and 4500 MHz downlink with India coverage, for relay of signals from distress beacons in sea, air or land.

INSAT-3B

Launched in March 2000, INSAT-3B is collocated with INSAT-2E at 83 degree East longitude. It carries 12 Extended C-band transponders and three Ku-band transponders that have coverage over the Indian region. INSAT-3B also incorporates a Mobile Satellite Services (MSS) payload with forward link between the hub and mobile station operating in CxS band and return link between the mobile station and the hub operating in SxC band.

INSAT-3C

Launched in January 2002, INSAT-3C is positioned at 74 degree East longitude. INSAT-3C payloads include 24 Normal C-band transponders providing an EIRP of 37 dBW, six Extended C-band transponders with EIRP of 37 dBW, two S-band transponders to provide BSS services with 42 dBW EIRP and an MSS payload similar to that on INSAT-3B. All the transponders provide coverage over India.

INSAT-3E

Launched in September 2003, INSAT-3E is positioned at 55 degree East longitude and carries 24 Normal C-band transponders provide an edge of coverage EIRP of 37 dBW over India and 12 Extended C-band transponders provide an edge of coverage EIRP of 38 dBW over India.

KALPANA-1

KALPANA-1 is an exclusive meteorological satellite launched by PSLV in September 2002. It carries VHRR and DRT payloads to provide meteorological services. It is located at 74 degree East longitude.

GSAT-2

Launched by the second flight of GSLV in May 2003, GSAT-2 is located at 48 degree East longitude and carries four Normal C-band transponders to provide 36 dBW EIRP with India coverage, two Ku-band transponders with 42 dBW EIRP over India and an MSS payload similar to those on INSAT-3B and INSAT-3C.

EDUSAT

Configured for audio-visual medium employing digital interactive classroom lessons and multimedia content, EDUSAT was launched by GSLV in September 2004. Its transponders and their ground coverage are specially configured to cater to the educational requirements. The satellite carries a Ku-band transponder covering the Indian mainland region with 50 dBW EIRP, five Ku-band spot beam transponders for South, West, Central, North and North East regional coverage with 55 dBW EIRP and six Extended C-band transponders with India coverage with 37 dBW EIRP. EDUSAT is positioned at 74 degree East longitude and is collocated with KALPANA-1 and INSAT-3.

INSAT-4 Series

INSAT-4A

Launched in December 2005 by the European Ariane launch vehicle, INSAT-4A is positioned at 83 degree East longitude along with INSAT-2E and INSAT-3B. It carries 12 Ku-band 36 MHz bandwidth transponders employing 140 W TWTAs to provide an EIRP of 52 dBW at the edge of coverage polygon with footprint covering Indian main land and 12 C-band 36 MHz bandwidth transponders provide an EIRP of 39 dBW at the edge of coverage with expanded radiation patterns encompassing Indian geographical boundary, area beyond India in southeast and northwest regions. Tata Sky, a joint venture between the TATA Group and Star uses INSAT-4A for distributing their Direct To Home Digital Television services across India.

INSAT-4B

It was launched in March 2007 by the European Ariane launch vehicle. Configured with payloads identical to that of INSAT-4A, INSAT-4B carries 12 Ku-band and 12 C-band transponders to provide EIRP of 52 dBW and 39 dBW respectively. Two Tx/Rx dual grid offset fed shaped beam reflectors of 2.2 m diameter for Ku-band and 2 m diameter for C-band are used. INSAT-4B augments the high power transponder capacity over India in Ku-band and over a wider region in C-band. It is co-located with INSAT-3A at 93.5 degree E longitude.

INSAT-4CR

INSAT-4CR was launched on 2 September 2007 by GSLV-F04. It carries 12 Ku-band 36 MHz bandwidth transponders employing 140 W TWTAs to provide an Effective Isotropic Radiated Power of 51.5 dBW at Edge of Coverage with footprint covering Indian mainland. It also incorporates a Ku-band Beacon as an aid to tracking the satellite. The satellite is designed for a mission life in excess of ten years.

In addition to measurements of atmospheric constituents, satellite data from polar orbiting and geostationary satellites are been used to understand cloud properties, vertical profiles of temperature, humidity etc. In the Indian context, data from INSAT series are being used to study winds, OLR, water vapour etc. India is planning to launch a meteorological satellite INSAT-3D in geostationary orbit towards the end of 2010. INSAT-3D will carry an 18-channel infrared Sounder (plus a visible channel) along

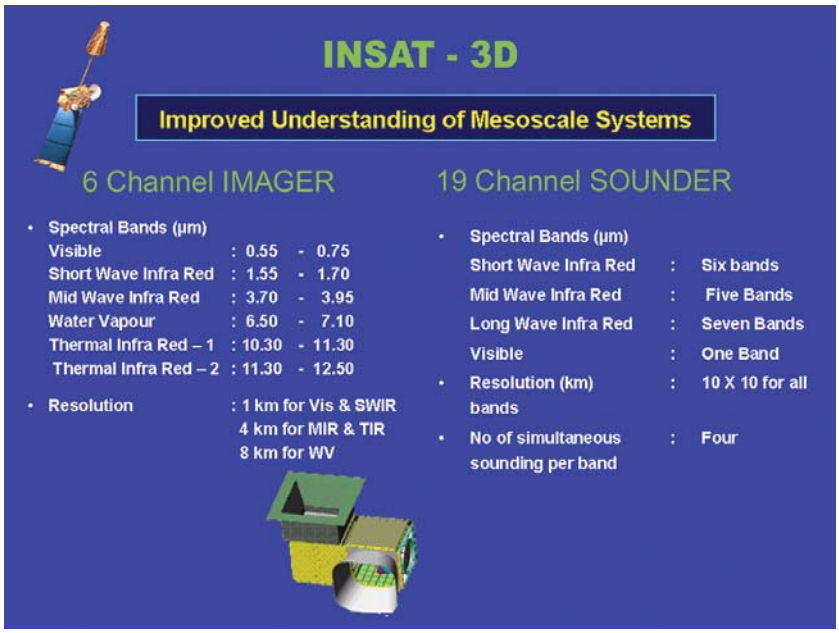

Figure 10.13: Characteristics of INSAT-3D sensors (source: www.isro.org)

with a 6 channel Imager (figure 10.13). INSAT-3D Sounder channels are similar to those in GOES-12 Sounder and many of the spectral bands are similar to High resolution Infrared Radiation Sounder (HIRS) onboard NOAA-ATOVS. Observation in these Sounder channels can be used to retrieve profiles of temperature and moisture as well as total column estimates of ozone. Present algorithm for INSAT-3D Sounder is adapted from the operational HIRS and GOES algorithms developed by Cooperative Institute for Meteorological Satellite Studies (CIMSS), University of Wisconsin.

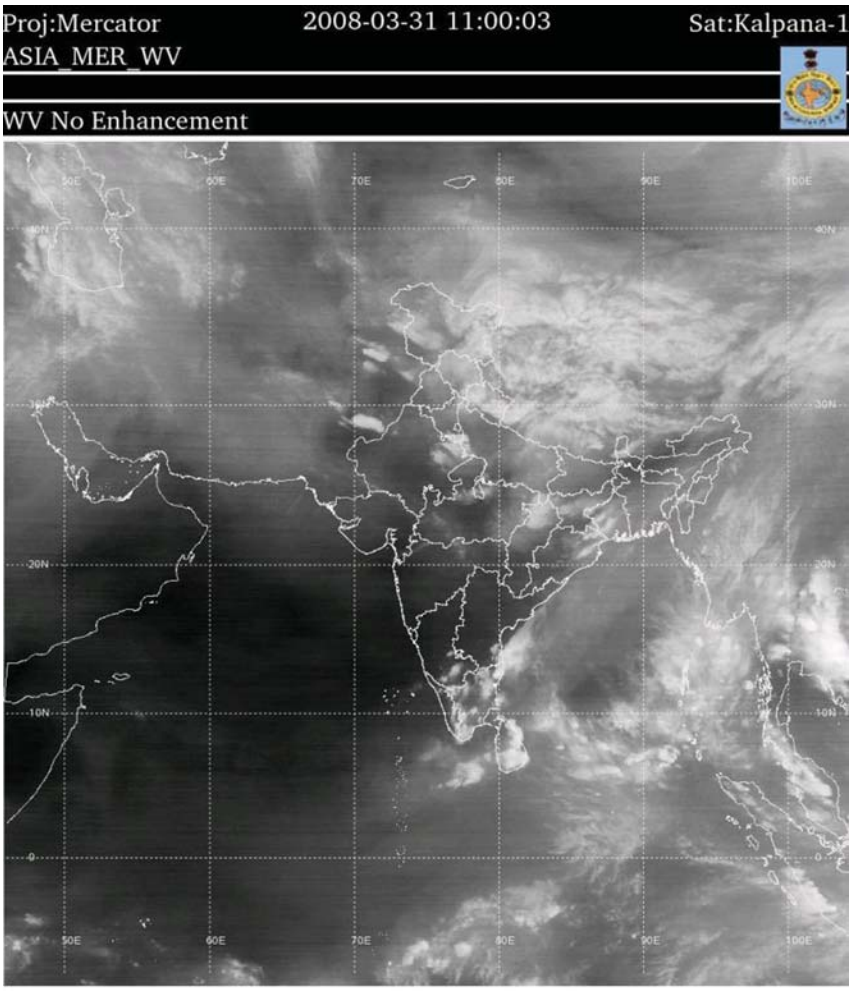

Figure 10.14: Water Vapour image from Kalpana-1 Satellite(source:www.imd.gov.in)

The use of geo-stationary water vapor imagery has allowed the determination of upper-level moisture content and determination of winds in cloud-free regions. The extraction of atmospheric motion vectors from satellite images (like IR & WV) has become most important component for operational numerical weather prediction (NWP). Satellite wind products are then assimilated in both regional and global-scale model and revealed its positive impacts on weather forecast (Kelly, 2004; Bedka and Mecikalski, 2005), especially over tropics. The availability of infrared window channel (10.5-12.5 µm) and water vapor channel (6.3 –7.1 µm) on-board KALPANA- VHRR, enabled us to derive cloud-tracked winds (900-100 hPa) and water vapor winds (500-100 hPa) from Indian geo-stationary satellites. The horizontal resolution of KALPANA- IR and WV channel is 8 Km (figure 10.14). Infrared images are used for detection and movement of clouds and for estimation of winds at different levels. The estimation of cloud motion vector (CMVs) wind is based on the assumption that clouds at different levels follow the atmospheric motion as rigid bodies. Three consecutive KALPANA-IR images at 30-minute interval are needed to determine the CMVs. The steps involved in these estimations are: i) Image Thresholding, ii) Feature Selection and Tracking, iii) Quality control and iv) Height assignment.

NASA's Mission to Planet Earth involves a variety of satellite and satellite sensors. Satellites presently in operation under this program are as follows:

Earth Radiation Budget Satellite (ERBS)

This satellite is primarily used for measuring visible radiation reflected by the earth and infrared energy emitted by the earth, including oceans, atmosphere and clouds. The principal experiments with ERBS include the Earth Radiation Budget Experiment (ERBE) and the Stratospheric Aerosol and Gas Experiment (SAGE).

Upper Atmosphere Research Satellite (UARS)

The UARS will carry out the first systematic, comprehensive study of the stratosphere and furnish important new data on the mesosphere and thermosphere. UARS chemistry and dynamics sensors will measure temperature, pressure, wind velocity, and concentrations of trace gas species in altitudes ranging from 15 to over 100 km. The UARS Data System Home Page gives an overview of the sensors, and more information can be obtained from

- The Halogen Occultation Experiment (HALOE)
- Microwave Limb Sounder (MLS)

- The Cryogenic Limb Array Etalon Spectrometer (CLAES)
- The Improved Stratospheric and Mesospheric Sounder (ISAMS)
- High Resolution Doppler Imager (HRDI)
- WINDII
- SOLSTICE
- The Solar Ultraviolet Spectral Irradiance Monitor (SUSIM)
- The Particle Environment Monitor (PEM)
- Active Cavity Radiometer Irradiance Monitor (ACRIM II)

TOPEX/Poseidon

Data from this satellite have been viewed in the unit on El Nino, since the TOPEX/Poseidon satellite is the key platform for ocean measurements such as ocean circulation (currents and tides), wave heights, and sea-surface height anomalies as well as atmospheric wind speed and water-vapor content over ocean areas.

The A-train satellite constellation (Figure 10.15), named after Aqua and Aura satellite has an orbit at an altitude of 705 km and inclination of ~98^{o}. Aqua leads the constellation with an equatorial crossing time of approximately 1:30 PM and data from these satellites provides a host of opportunity to understand aerosol cloud interactions.

10.5. MEGHA-TROPIQUES

Climate research on a global scale is a topic of worldwide interest and a necessity for general meteorological applications, weather prediction and ultimately useful in regional and global monitoring and protection of the earth's environment.

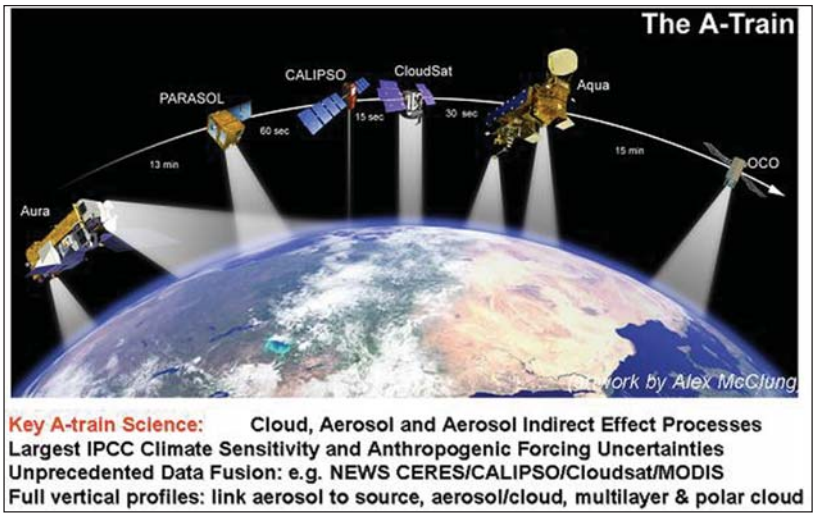

Figure 10.15: The EOS afternoon satellite constellation(source:http://www.gsfc.nasa.gov/gsfc/service/gallery/fact_sheets/earthsci)

Several satellite missions in the last three decades have demonstrated their potential utilization aspects in terms of instrument capabilities, accomplishment of science and application goals, and their merits for applying the data in weather forecasting and climate research. The currently operational space borne microwave imagers such as SSM/I, TMI (TRMM Microwave imager) and Oceansat-1 are a few examples of the keen interest and conviction on the capability, technology and performance of the passive microwave instruments for the atmospheric and oceanographic applications.

The Megha-Tropiques is a joint ISRO-CNES collaborative effort of developing and launching a small satellite and utilization of the data. This mission encompasses the development of three high technology payloads, viz. MADRAS (Microwave Analysis and detection of rain and atmospheric structure), SAPHIR (a 6-channel millimetrewave humidity sounder at 183.3GHz) and a scanner for radiation budget (ScaRaB). Prediction of the large scale variations in the tropical atmosphere is a very important aspect for climate research and meteorological applications. Particularly, measurements related to the Earth radiation budget, latent heat flux, water vapour, cloud liquid water and rainfall along with other parameters are of immense value for the climate models. High temporal frequency and large spatial coverage has been the emphasis in these applications.

The Megha-Tropiques mission is a joint ISRO-CNES programme for developing a small satellite carrying appropriate sensors for measuring the cloud and atmospheric parameters. Primarily, it carries three payloads: a microwave imager at 18, 23, 36, 89 and 157GHz, a millimetrewave sounder at 183.3GHz and a scanner for radiation budget measurements. The satellite is configured around the French Proteus bus and launched using the ISRO's PSLV launcher. The ISTRAC ground station at Bangalore is used for receiving and processing the science data.

Main objectives of the Megha-Tropiques mission:

The main objective of the Megha-Tropiques mission is to study the convective systems that influence the tropical weather and climate. The tropical region is the domain of monsoons, squall lines and tropical cyclones. It is also characterized by large intraseasonal, interseasonal and interannual variations, which may lead to catastrophic

events such as droughts and floods and change in energy and water budget of the Land-Ocean-Atmosphere system in the tropics has its influence on global climate.

The MEGHA- TROPIQUES mission aims to:

- provide simultaneous measurements of several elements of the atmospheric water cycle: water vapour, clouds, condensed water in clouds, precipitation and evaporation,
- Measure the corresponding radiative budget at the top of the atmosphere,
- Ensure high temporal sampling in order to characterize the life cycle of the convective systems and to obtain significant statistics

The main parameters to be measured by Megha-Tropiques are cloud cover, cloud top height, cloud albedo, cloud condensed water content, cloud ice content, rain rate, latent heat release, integrated water vapour content, profile of water vapour content, radiant fluxes at the top of the atmosphere, sea surface winds, sea surface temperature, sea surface evaporation fluxes, temperature profiles and 3D wind field.

The Megha-Tropiques satellite will be launched into an inclined orbit of 20 degrees and an altitude of 867 Km. The payloads are designed to provide large swahs with a high repetitively of three to six times a day depending on the latitudes. The frequency of observation is quite high in the inter-tropical zone between 10^0- 20^0 latitudes.

Mission Space Segment

The primary specifications of the satellite are highlighted below.

Spacecraft Bus	:	PROTEUS (French)
ORBIT	:	867 Km
Power available for payloads	:	~220 W
Onboard dat storage	:	2 GHz
Mission Life	:	3 Years (Design life: 5Years)
Inclination	:	20 deg
Launcher	:	PSLV (Dual satellite configuration)

The Megha-Tropiques mission envisages development of the three payloads, to measure the dynamic atmospheric variables which are

- A microwave imager: MADRAS (Microwave Analysis and Detection of Rain and Atmospheric Structure)
- A humidity sounder at 183.31GHz and
- ScaRaB (scanner for Radiation Budget:4 channels)

MADRAS

MADRAS is a five- frequency, 9-chanel mechanically scanning microwave imaging radiometric system. It has a mechanically scanning offset reflector, which scans the earth at a conical scan angle of ± 65 degrees resulting in

Table 10.3: Salient features of MADRAS

Frequencies	Polarization	Spatial Resolution	NE∆T(K) sensitivity at 300K	Absolute calibration	Inter Channel calibration (K)	Mission
18.7GHz	H+V	40±10%Km	0.7 K	±1 K	0.5 K	Rain Above Oceans
23.8GHz	V	40±10%Km	0.7 K	±1 K	0.5 K	Integrated water vapour
36.5GHz	H+V	40±10%Km	0.7 K	±1 K	0.5 K	Liquid water in clouds, rain above sea
89GHz	H+V	10±10%Km	1.1 K	±1 K	0.5 K	Convective rain areas over land and sea
157GHz (TBC)	H+V	6±10%Km	2K (TBC)	(TBC)	(TBC)	Ice at cloud tops

a ground swath of more then 1700 Km. The three low frequency channels at 18, 23 and 36 GHz have a coincident footprint of 40 Km. The 89 and 157 GHz have a resolution of 10 and 6 Km respectively.

The major specification of MADRAS are shown in table 10.3

SAPHIR

SAPHIR is mechanically scanning millimeter wave humidity sounder. It scans the earth in a nadir plane symmetrically with respect to the local vertical with a scan angle of $\pm 45^0$. The instrument has six channels in the water vapour line at 183 GHz with a footprint diameter of about 10 Km. The major specifications of SAPHIR are shown in table 10.4.

SCARAB

Table 10.4: Major specifications of SAPHIR

Central nominal frequencies (GHz)	Spatial Resolution	NEΔT(K) sensitivity requirement	NEΔT sensitivity goal	Polarisation
183.31±0.2	10 Km	2 K	1 K	V
183.31±1.1	10 Km	1.8 K	1 K	V
183.31±2.7	10 Km	1.8 K	1 K	V
183.31±4.2	10 Km	1.5 K	1 K	V
183.31±6.6	10 Km	1.5 K	1 K	V
183.31±11	10 Km	1.2 K	1 K	V

The SCARAB is a cross track scanning radiometer. This sensor has four channels operation in the 0.5 to 0.7μm, 0.2 to 4 μm, 0.2 to 200 μm and 10.5 to 12.5 μm spectral bands. SCARAB consists of two modules viz. the optical sensor module, which includes the scanner, and the calibration devices and the electronic module. Table 10.5 shows the specification of ScaRaB.

Table 10.5 : Major specifications of SCARAB

Channel	0.5 to 0.7 μm
SC1 - Visible	0.2 to 4 μm
SC2 -Solar	0.5 to 200 μm
SC3 -Total	0.5 to 0.7 μm
SC4 –IR Window	10.5 to 12.5 μm

Ground segment

The Megha-Tropiques spacecraft will be launched by PSLV in an 867 Km circular orbit having an inclination of 20^0. The spacecraft collects data from three major scientific payloads, namely MADRAS, ScaRaB and SAPHIR. The global scientific data from these payloads will be collected mainly from ISTRAC Bangalore.

The telemetry channel of the Proteus bus consists of a QPSK modulated single telemetry downlink having a bit rate of 727 kbps. The telemetry data consists of real time house keeping data of spacecraft and instrument health, stored house keeping and health data and the stored payload data.

References

Adler RF and Negri AJ, 1988, A satellite infrared technique to estimate tropical convective and stratiform rainfall, *Journal of Applied Meteorology*, **27**: 30-51.

Arkin PA, 1979, The relationship between fractional coverage of high cloud and rainfall accumulations during GATE over the B-scale array, *Monthly Weather Review*, **106**: 1153-1171.

Arkin PA and Xie P, 1994, The Global Precipitation Climatology Project: First algorithm intercomparison project, *Bulletin of American Meteorological Society,* **75**: 401–419.

Arkin PA and Meisner BN, 1987, The relationship between large-scale convective rainfall and cold cloud over the western hemisphere during 1982 - 1984, *Monthly Weather Review*, **115**: 51-74.

Ba MB and Gruber A, 2001, GOES Multispectral Rainfall Algorithm (GMSRA), *Journal of Applied Meteorology,* **40**:1500-1514.

Badarinath KVS, Kharol SK, Kaskaoutis DG, Sharma AR, Ramaswamy V and Kambezidis HD, 2010, Long-range transport of dust aerosols over the Arabian Sea and Indian region – a case study using satellite data and ground-based measurements, *Global and Planetary Change*, doi:10.1016/j.gloplacha.2010.02.003 (in Press).

Badarinath KVS, Kharol SK, Kaskaoutis DG and Kambezidis HD, 2007, Case study of a dust storm over Hyderabad area, India: Its impact on solar radiation using satellite data and ground measurements, *Science of the Total Environment*, **384**: 316-332.

Bedka KM and Mecikalski JR, 2005, Application of satellite-derived atmospheric motion vectors for estimating meso-scale flows, *Journal of Applied Meteorology*, **44**: 1761-1772.

Ferraro RR and Marks GF, 1995, The development of SSM/I rain-rate retrieval algorithms using ground-based radar measurements, *Journal of Atmospheric and Oceanic Technology,* **12**: 755–770.

Gairola RM and Krishnamurti TN, 1992, Rain rates based on OLR, SSM/I and rain gauge data sets, *Meteorology and Atmospheric Physics*, **50**: 165-174.

Gairola RM, Varma AK, Pokhrel S and Agarwal VK, 2004, Integrated satellite microwave and infrared measurements of precipitation during a Bay of Bengal cyclone, *Indian Journal of Radio & Space physics*, **33**: 115-124.

Kaplan LD, 1959, Inference of atmospheric structure from remote radiation measurements, *Journal of the Optical Society of America*, **49**: 1004.

Kelly G, 2004, Observing system experiments of all main data types in the ECMWF operational system, 3rd WMO Numerical Weather Prediction OSE Workshop, Alpbach, Austria, WMO, *Technical Report*, **1228**: 32-36.

King JIF, 1956, The radiative heat transfer of planet earth, *Scientific Use of Earth Satellites*, University of Michigan Press, Ann Arbor, Michigan, 133-136.

Kummerow C and Giglio, 1996, A simplified scheme for obtaining precipitation and vertical hydrometeor profiles from passive microwave sensors, *IEEE Transactions of Geosciences & Remote Sensing,* **34**: 1213-1232.

Liu G and Curry JA, 1992, Retrieval of precipitation from satellite microwave measurement using both emission and scattering, *Journal of Geophysical Research*, **97(9)**: 9959– 9974.

Menzel WP and Purdom JFW, 1994, Introducing GOES-I: The first of a new generation of geostationary operational environmental satellites, *Bulletin of American Meteorological Society,* **75**: 757-781.

Scofield RA and Kuligowski RJ, 2003, Status and outlook of operational satellite precipitation algorithms for extreme precipitation events, *Weather Forecasting*, **18**: 1037-1051.

Smith WL, Suomi VE, Menzel WP, Woolf HM, Sromovsky LA, Revercomb HE, Hayden CM, Erickson DN and Mosher FR, 1981, First sounding results from VAS-D, *Bulletin of American Meteorological Society,* **62**: 232-236.

Smith WL, Woolf HM, Hayden CM, Wark DQ and McMillin LM, 1979, The TIROS-N operational vertical sounder, *Bulletin on American Meteorological Society,* **60**: 1177-1187.

Torres O, Bhartia PK, Herman JR, Ahmad Z and Gleason J,1998, Derivation of aerosol properties from satellite measurements of backscattered ultraviolet radiation: Theoretical basis, *Journal of Geophysical Research*, **103** : 17099–17110

Vicente GA, Scofield RA and Menzel WP, 1998, The operational GOES infrared rainfall estimation technique, *Bulletin on American Meteorological Society*, **79**: 1883-1898.

Wark DQ, 1961, On indirect temperature soundings of the stratosphere from satellites, *Journal of Geophysical Research*, **66 (1)**: 77.

Wark DQ, Hilleary DT, Anderson SP and Fisher JC, 1970, Nimbus satellite infrared spectrometer experiments, *IEEE Transactions on Geosciences Electronics,* **8**: 264-270.

Wilheit T, Kummerow CD and Ferrao R, 2003, Rainfall algorithms for AMSR-E, *IEEE Transactions of Geosciences & Remote Sensing*, **41(2)**: 204-214.

http://www.gsfc.nasa.gov/gsfc/service/gallery/fact_sheets/earthsci/green.htm

http: //earthobservatory.nasa.gov/Features/Aerosols/

http://www.gsfc.nasa.gov/gsfc/service/gallery/fact_sheets/earthsci/green.htm

http://www.gsfc.nasa.gov/gsfc/service/gallery/fact_sheets/earthsci

http://www.esa.int

http://www.isro.org

http://www.imd.gov.in

nrsc

Remote Sensing Applications

P. S. Roy
R. S. Dwivedi
D. Vijayan

National Remote Sensing Centre

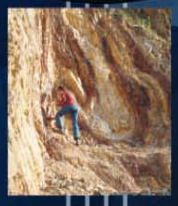

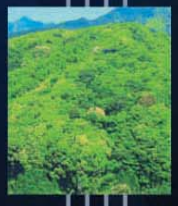

Remote Sensing Applications

Cyclones

11.1. Introduction

A cyclone is a low pressure area in the atmosphere in which winds spiral upward. A cyclone can cover an area as large as half of the United States. All cyclones are characterized by: (1) low pressure at the centre, and (2) winds spiraling toward the center. The direction of the spiral is unique because in the northern hemisphere the winds blow counter-clockwise and in the southern hemisphere they blow clockwise. Cyclones are formed from simple thunderstorms. However, these thunderstorms can only grow to cyclone strength with cooperation from both the ocean and the atmosphere. First of all, the ocean water itself must be warmer than a threshold say, 28 °C. The heat and moisture from this warm water is the source of energy for cyclones. Cyclones will weaken rapidly when they travel over land or colder ocean waters — locations where their heat and/or moisture sources do not exist. High relative humidities in the lower and middle troposphere are also required for cyclone development. These high humidities reduce the amount of evaporation in clouds and maximizes the latent heat released because there is more precipitation. The vertical wind shear in a tropical cyclone's environment is also important. Wind shear is defined as the amount of change in the wind's direction or speed with increasing altitude. When the wind shear is weak, the storms that are part of the cyclone grow vertically, and the latent heat from condensation is released into the air directly above the storm, aiding in development. When there is stronger wind shear, the storms become more slanted and the latent heat release is dispersed over a much larger area.

Cyclones are characterized as tornadoes, hurricanes and typhoons. A tornado is a smaller kind of cyclone. When a cyclone forms over tropical waters in the North Atlantic or eastern North Pacific oceans and has winds of 119 km/hr or more it is called a Hurricane. If the cyclone forms in the western Pacific with winds of 119 km/hr or more it is called a Typhoon. All of these storms are generally accompanied by high winds, heavy rains, severe thunder, and lightening. In the north Indian Ocean they are simply called as tropical cyclones.

A typical mature tropical cyclone is a warm core vortex in the atmosphere (anti-clockwise vortex rotation in the Northern Hemisphere and clockwise in the southern), cyclonic in the lower troposphere and anti-cyclonic in the upper troposphere. The circulation extends horizontally to some 1000 kilometers from the centre and vertically to about 15 km above sea level. There is an 'eye' at the centre of the cyclone of radius 5 to 50 kilometers. The eye is rain-free with light winds. It is surrounded by a 'wall cloud' made up of tall cumulo-nimbus clouds rising upto an altitude of 15-18 km, the wall cloud thickness being about 10-15 km radially. Below the wall cloud are found the strongest surface winds of the cyclone (V_{max}) with heaviest rain. Beyond the wall cloud, surface wind speeds decrease gradually with the radial distance from the centre and rainfall is confined to the regions covered by the inward spiraling cloud-bands (composed of cumulo-nimbus clouds and some cumulus clouds at large distances from the centre) that are seen within a radial distance of about 400 km from the centre of the cyclone.

As one moves from the periphery to the centre of the cyclone, the sea level atmospheric pressure falls continuously, the largest radial pressure gradients of 2-4 hPa/km, occurring in the wall cloud region. Under the influence of frictional forces, the low-level wind direction, which is almost tangential to the nearly circular isobars of the cyclone field at about 1-km above sea level, cuts the isobars at about 25° towards low pressure at sea level. The low level winds rich in moisture thus possess strong tangential and radial component causing the air parcels to spiral inwards from the peripheral regions of the cyclone towards its centre. In consequence, their rotational velocity (tangential wind) increases rapidly due to partial conservation of its angular momentum. The radial component of the wind converges large amounts of moisture to the central regions of the cyclone, which ascends and condenses in cloud formations there, keeping the central regions warmer than the surrounding tropical atmosphere. This warm anomaly which reaches a maximum of about 15°C at 300-200 hPa level (9-12 km altitude) reduces the radial pressure gradients at these high altitudes. The cyclically rotating air parcels rising up in the central regions of the cyclone move outwards in the upper troposphere, under the action of unbalanced centrifugal forces (with reduced pressure gradients) and conserving angular momentum, begin to reverse their cyclonic rotation as they move further away from the centre. Satellite pictures of tropical cyclones indeed show both the inward spiralling (anti-clockwise) low level clouds and the outward moving (clock-wise) cirrus clouds at the upper levels in the northern hemisphere.

Our current knowledge of the structure of tropical cyclones has come from studies made over a hundred years of different cyclone-prone regions of the world. Early studies using ship reports and measurements from coastal

and island observatories gave a reasonably good picture of the surface level features of the cyclone, but that of their three dimensional structure has been derived mainly from reconnaissance flights using specially equipped aircrafts that were flown into the cyclone at various levels, measuring winds, temperatures, humidity and pressure. Direct sensing as well as remote sensing methods were used. Compositing of data from routine balloon soundings of the atmosphere has also yielded a wealth of information. Details regarding the eye, wall cloud and the spiral cloud bands were obtained from satellite pictures (polar orbiting and geo-stationary) as well as cyclone detection radar systems installed at coastal and island .

11.2. Life Cycle of Tropical Cyclones

Cyclones evolve through a life cycle of stages from genesis to dissipation. A tropical disturbance in time can grow to a more intense stage by attaining a specified sustained wind speed. Cyclones can often live for a long period of time — as much as two to three weeks. They may initiate as a cluster of thunderstorms over the tropical ocean waters. Once a disturbance has become a tropical depression, the amount of time it takes to achieve the next stage, tropical storm, can take as little as half a day up to a couple of days. The same may occur for the amount of time a tropical storm needs to intensify into a cyclone. Atmospheric and oceanic conditions play the major role in determining these events.

There are several schemes that describe the life-cycle of an average TC. The four stages shown below are not really discrete entities, rather they represent a continuous process. Individual stages may even occur more than once during the life-cycle of a particular storm.

Formation or Genesis Stage:

Since the nature of Tropical Cyclone (TC) development is continuous, features associated with earliest stages of the TC life-cycle can overlap. To complicate the issue, there is no standard language for these initial stages. For example, some meteorologists prefer the term “genesis” to describe both the earliest stages of the life-cycle and progression to a mature hurricane or typhoon. Others use the term “genesis” to describe the earliest stages and “formation” to somewhat later stages in the life-cycle.

Intensification or Deepening Stage:

In this stage, the TC central pressure falls and the maximum surface wind speed increases. An eye may develop at the center of the TC if the stage continues.

Mature Stage:

The mature stage of a TC is usually associated with the period in which the TC reaches maximum intensity. The central pressure has reached a minimum, and the surface winds have reached a maximum.

Decay Stage:

When a TC decays, the central pressure increases and the maximum surface winds weaken. Usually, the decaying process is the result of a TC moving over land, moving over cool water, recurving and assuming extratropical characteristics, or a combination of these processes. Even though the TC is decaying, it can produce high winds and heavy rains.

11.3. Classification of Cyclonic Disturbances

Tropical cyclones have great socio-economic concern for the Indian subcontinent that is the only region in the world having two cyclone seasons within a year. A vast coastline of India with high density of population is exposed to these natural threats, making it one of the worst cyclone-affected regions in the world in terms of the loss of lives. Due to the varying coastal bathymetry of the Indian coast, the severity of the storm surge created by the cyclones vary from place to place for the same intensity of the cyclone. Classifications of cyclonic disturbances for the Bay of Bengal and the Arabian Sea region for the exchange of messages among the panel countries are given below:

Weather system	**Maximum wind speed**
• Low pressure area	Wind speed less than 17 kt (31 km/h)
• Depression	Wind speed between 17 and 33 kt (31 and 61 km/h)

- Cyclonic storm — Wind speed between 34 and 47 kt (62 and 88 km/h)
- Severe cyclonic storm — Wind speed between 48 and 63 kt (89 and 118 km/h)
- Severe cyclonic storm — Wind speed 64 kt (119 km/h) or more with a core of hurricane winds
- Very severe cyclonic storm — Wind speed 64 and 119 kt (119 and 221 km/h)
- Super cyclonic storm — Wind speed 120 kt and above (222 km/h)

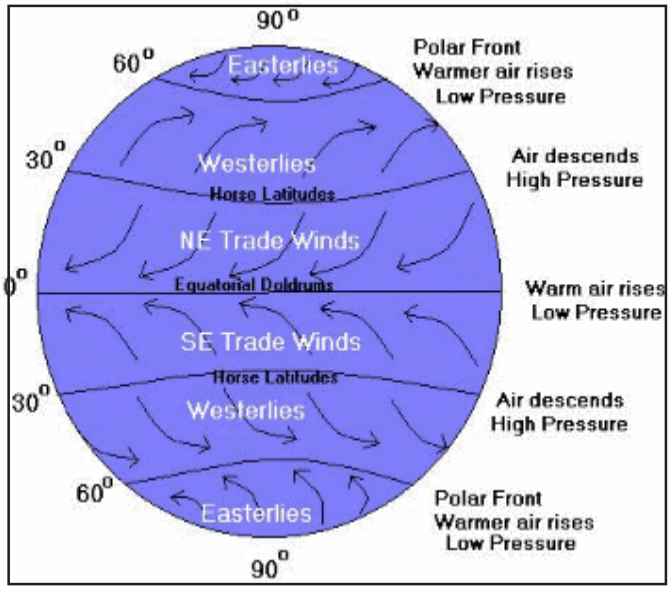

Figure 11.1: Global wind patterns (source: www.weatherwizkids.com/weather-winds.html)

11.4. Movement of Cyclones

Winds steer the cyclones. The global wind pattern is also known as the "general circulation" and the surface winds of each hemisphere are divided into three wind belts (figure 11.1).

Polar Easterlies: from 60-90 degrees latitude, prevailing westerlies: from 30-60 degrees latitude, tropical easterlies: from 0-30 degrees latitude. The easterly trade winds of both hemispheres converge at an area near the equator called the "Intertropical Convergence Zone (ITCZ)", producing a narrow band of clouds and thunderstorms that encircle portions of the globe. The path of a cyclone greatly depends upon the wind belt in which it is located. A cyclone originating in the eastern tropical Pacific, for example, is driven westward by easterly trade winds in the tropics. Eventually, these storms turn northwestward around the subtropical high and migrate into higher latitudes. Some times the local steering winds may not exactly follow this pattern.

11.5. Cyclone Intensity

Many of the physical processes associated with TC intensification and decay are difficult to observe and poorly understood. Hence, cyclone intensity prediction is a relatively difficult problem compared to the track prediction. Some of the factors that influence the TC intensities are:

11.5.1. Upper Tropospheric Anticyclones

As viewed by satellites (and satellite cloud-tracked winds and water-vapor-tracked winds), upper-troposphere circulation patterns associated with intensification are the easiest to identify because the upper tropospheric clouds usually obscure shallower clouds. These upper-troposphere patterns can define the outflow at the top of the TC, which indicates mass removal from the center of the storm (figure 11.2).

Figure 11.2: Mechanism of Tropical cyclone formation (Source: http://www.mspsofworld.com/hurricane/machanism-of-tropical-cyclone-formation.html)

In general, a mesoscale anticyclone is located directly over or near the center of the TC. This represents the location in the upper wind field where there is a buildup of mass from rising convective motion within the center of the cyclone. On the other hand, another larger, synoptic scale anticyclone is often found that pre-existed within the vicinity of the intensifying TC. The location of this larger anticyclone can vary depending upon many environmental factors, including the lower-level forcing mechanisms that are helping to create the cyclone. The relative location of this

large-scale anticyclone with respect to the TC will help dictate the direction of outflow patterns around the cyclone. These outflow patterns can be identified from satellite infrared cloud imagery, especially when the imagery is animated. These outflow patterns can be classified into one of three basic categories depending on the number of channels:

- Single-channel Outflow. The single-channel outflow may be divided into two subcategories based on direction of the outflow channel. Tropical cyclones with single-channel poleward outflow pattern generally intensify at an average maximum rate of 15 to 20 kt/6 hr. Tropical cyclones with single-channel equatorward outflow pattern generally intensify at an average maximum rate of 25 to 28 kt/6 hr
- Dual-channel Outflow. Tropical cyclones with a dual-channel outflow pattern generally intensify at an average maximum rate of 35 kt/6 hr
- No Outflow Channel. Tropical cyclones with little outflow generally intensify at a very slow rate as they are unable to evacuate mass

11.5.2. Tropical Upper Tropospheric Trough

A strong upper level (250-200 hPa) cyclonic circulation to the north or northwest of a TC, namely the tropical upper tropospheric trough (TUTT or TUTT Cell), is a common occurrence during July and August in the northern Pacific. This type of upper-level circulation pattern is favorable for vigorous outflow to the north. In addition, this pattern generally occurs as the cyclone nears the western edge of the subtropical ridge where enhanced equatorward outflow is common. The combined effects of the northward and southward outflow often lead to rapid deepening.

11.5.3. Other Factors Affecting Intensity

There are a few other observable phenomena that can affect TC intensity:

- Cumulus convection. Satellite cloud imagery can show whether convection is increasing or decreasing, and whether the TC cloud patterns become more or less organized. The convective activity implies the stage of TC development. Therefore, cumulus convection should be monitored continuously by the forecaster
- Sea surface temperature (SST): A SST of 26.5 °C is generally considered to be the minimum for TC formation. Anomalously high SST can cause more heat and moisture flux from the ocean to the atmosphere. This condition favors further development of the TC. Rapid deepening is more likely once the SST is higher than 28.5 °C
- Vertical wind shear: Weak vertical wind shear aids TC intensification while strong vertical wind shear inhibits TC intensification
- Low-level circulations: Low-level cyclonic circulations are favorable regions for TC intensification. The summer monsoon trough in the western North Pacific is an area where low level cyclonic circulations are abundant. The Earth's rotation (i.e., Coriolis effect) can also contribute to cyclonic circulation
- Low-level convergence: Low-level convergence zones such as the Inter-Tropical Convergence Zone (ITCZ), are suitable areas for TC intensification
- Land, coast, and mountain effects: These effects can be quite complex. In general, a TC that moves over land decays. A TC decays much faster when it passes over mountainous regions, such as Taiwan or Luzon, than it does over flat land. Also, a TC often re-intensifies when it re-enters a marine area
- Tropical cyclone transformation: A TC that enters into the mid-latitudes either decays rapidly or transforms into an extratropical cyclone. A decaying TC may still produce heavy rain, especially when it moves over mountainous areas. When a transformation from TC to extratropical cyclone occurs, forecast responsibility is transferred from the TC forecast center to another forecast office
- Oceanic heat content: While a threshold SST is required for the cyclogenesis, oceanic heat content plays a prominent role in the intensification or dissipation of the cyclones

11.6. Cyclone Track Prediction

Predicting the tropical cyclones has been a challenging problem. Several models and methods have been developed to predict the position of the cyclone accurately so that appropriate warning can be issued for disaster management. Mohanty and Gupta (1977) and Gupta (2006) described in detail different track prediction techniques. The most

devastating impact of the tropical cyclone, particularly, for the Indian coastal regions is the storm surge. Because of the highly varying bathymetry of the Indian region, even a slight error in the prediction of landfall point can lead to a totally different storm surge height. The objective track prediction of tropical cyclones may be grouped into four categories (Elsberry 1995): (i) empirical, e.g., climatology, persistence of past motion, climatology and persistence (CLIPER), and analogue techniques, (ii) statistical-synoptic, in which additional meteorological information is incorporated, usually via statistical regression using grid-point values from synoptic analysis available at the forecast time, (iii) statistical-dynamic, in which grid-point values from synoptic predictions are also incorporated, and (iv) dynamic, in which a global or regional numerical weather prediction (NWP) model is integrated as an initial value problem to provide a track forecast. The empirical track forecasts are easy to understand given the simple inputs. On the other hand, the statistical models have additional complexity and are not easy to interpret because the grid-point predictions are generally not available to the forecaster. The dynamical models are even more complex and difficult in which steering influences at many levels and various physical processes such as advective, diabatic and frictional effects may be contributing to TC motion.

Traditionally, modeling a dynamical system requires one to derive the equations of motion from first principles, to measure initial conditions and, finally, to integrate the equations of motion forward in time. Alternatively, when such an approach is not feasible due to some reasons, e.g., the model may be far from perfect, and initial conditions may be erroneous or even the required computing resources are not available, empirical laws governing the physical processes can be obtained by model-fitting approaches based on the observed variability of the system evolution. Nowadays, it is known that not all random-looking behavior is the product of complicated physics but it may result from the chaotic nature of a nonlinear and deterministic dynamics involving few degrees of freedom. In such cases, it is possible to exploit this determinism to make short-term forecasts that are more accurate than those obtained employing a linear stochastic model. Deterministic models directly built from observations of the system evolution carry out these forecasts. If we assume that random movement of the cyclone can be modeled from the chaotic nature of a nonlinear and deterministic dynamics, forecasting of the cyclone track is possible. These forecasts use deterministic models directly built from observations of the system evolution. Using the chaos theory, Pal (1991) suggested the possibility of predicting the position of the cyclone from the past six positions. One of the main requirements of a robust statistical technique is its ability to predict the correct track within a short time. Ali *et al.*, (2007) used 31 years (1971-2001) cyclone positions at 6 hourly intervals for developing and validating the artificial neural network model.

11.7. Cyclone Intensity Prediction

Various dynamical and statistical models have different rates of success for cyclone intensity prediction. In addition to atmospheric parameters and sea surface temperature (SST), another important parameter that enhances the understanding of the intensification of the cyclones is the upper ocean heat storage that is generally reflected in the oceanic eddies and dynamic topography. Sea surface height anomalies (SSHAs) from radar altimeters can provide information on this parameter. The relationship between the SSHAs and the associated hydrographic structure, particularly of eddies, is discussed by *Ali et al.,* (1998), *Gopalan et al.,* (2000) and *Gopalakrishna et al.,* (2003). Because of these changes in hydrographic features caused by SSHAs, warm (cold) core oceanic eddies have more (less) heat content compared with their surroundings.

The importance of SST in the formation and maintenance of tropical cyclones has long been known. *Palmen* (1948) showed that hurricanes cannot form unless the SST is greater than 26º C, though this is not the only necessary condition. Latent heat release through evaporation fuels the cyclone system. After the passage of a cyclone, SST reduces due primarily to the cyclone-induced mixing. While this negative feedback regime tends to decrease the storm intensity, pre-existing mesoscale features like warm core eddies and the deeper mixed layer provide the heat source for intensification of cyclones.

Patterns of lower atmospheric anomalies are more consistent with the upper ocean thermal structure variability than just with SSTs (*Namias and Canyan,* 1981). Using a coupled ocean-atmospheric model, *Mao et al.,* (2000) reported that the rate of intensification and final intensity of cyclones are sensitive to the initial spatial distribution of the mixed layer. *Shay et al.,* (2000) described details of the response of the hurricane to a warm core eddy. Thus, a well-mixed upper ocean layer, due either to the mixing processes or to eddies, may be a more effective means of assessing oceanic regimes for tropical cyclone studies.

Sudden unexpected intensification of Hurricane Opal from 965 to 916 hectopascals in the Gulf of Mexico over a 14-hour period (*Shay et al.,* 2000) after passing over a warm core eddy is a classic example of the influence of oceanic features on cyclones. Ali *et al.*, (2007) have demonstrated impact of SSHAs on the intensity of the Bay of Bengal cyclones.

11.8. Satellite Technologies

New technologies have been employed to grasp each of these factors when attempting to make an intensity or track forecast. The earliest attempts aimed at tropical cyclone prediction began with the development of a 2-dimensional axi-symmetric cyclone models at Space Applications Centre (SAC), Ahmedabad (Narayanan and Kishtawal, 1984). Although these models had limited or no applicability for real-time forecasting needs, they provided the basic insight into the physical processes within a tropical cyclone and helped in interpreting the satellite observations. The advent of next-generation satellite observations, mainly the wind scatterometer onboard first European Remote Sensing (ERS-1) satellite provided a boost to tropical cyclone studies (Rao *et al.*, 1994). Some of earliest attempts to demonstrate the impact of assimilation of scatterometer surface wind observations on the prediction of cyclone tracks was carried out jointly between SAC and NCMRWF (National Centre for Medium Range Weather Forecasting) (Joshi *et al.*, 1998). The period during the late nineties was very significant for the development of tropical cyclone studies with the advent of the most important international satellite missions like Tropical Rainfall Measuring Mission (TRMM) that provided much awaited insight into the tropical cyclone structure (Falguni *et al.*, 2004). This, added with the availability of larger computing resources and also the development and availability of more sophisticated meso-scale numerical weather prediction models like MM-5, and WRF, helped the tropical cyclone research community. Active use of satellite observations has always been the prime concern for all the modeling activities. Some of the early applications of satellite observations in tropical cyclone forecasting experiments based on mesoscale models is by use of a synthetic vortex in model initial conditions (Singh *et al.*, 2007) where the tropical cyclones were relocated in model fields in consistence with the satellite observations. Later, more sophisticated data assimilation techniques like 3-D variational (3D-VAR) approaches were applied to optimally assimilate the satellite derived information for improving tropical cyclone prediction (Singh *et al.*, 2008). Initially, these experiments were based on satellite observations like cyclone location and intensity, ocean surface and upper level winds, and atmospheric water vapor were obtained from international satellite missions like TRMM, DMSP, Meteosat and the data assimilation experiments clearly proved the value of these observations in improving the track and intensity prediction of tropical cyclones. Since the retrieval of geophysical parameters from Indian satellites is one of the most significant scientific activities, there was a logical concern to use these data in numerical models for improving tropical cyclone predictions. The latest development in data assimilation research includes the assimilation of INSAT-derived cloud motion winds, and the radiances from imaging sensors. Considerable impetus in tropical cyclone related data assimilation research can be expected in coming few years with the order of magnitude enhancement of satellite data from state-of-the art Indian satellite missions (e.g., atmospheric sounder onboard INSAT-3D, SAPHIR onboard Megha-Tropique, and a wind scatterometer onboard Oceansat-2). At present only existing INSAT data is being used for cyclone studies. During MSMR (Multifrequency Scanning Microwave Radiometer) time frame, the geophysical parameters from Oceansat-1 were also used in

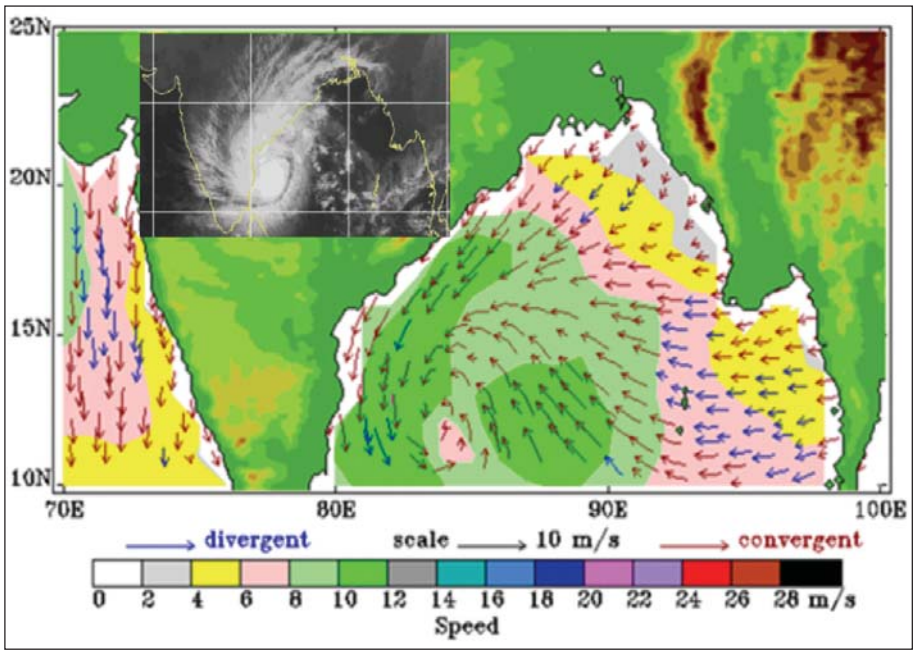

Figure 11.3: Quickscat derived wind vectors over a Bay of Bengal cyclone (inset: cloud imagery form INSAT)

numerical weather forecasting models. The wind magnitude for MSMR was found to be in good agreement with ERS-1 observations (Falguni *et al.*, 2005).

TRMM Microwave Imager (TMI) data has emerged as an exceptional tool for measuring atmospheric water vapor content, liquid cloud water, and precipitation rates in the tropics. Clouds are transparent at 10.7 GHz - one of the frequencies used by TRMM - and so it is a useful tool for monitoring SST on a daily basis even when clouds normally obscure the view. Although SST and atmospheric relative humidity have been used in idealized models to study the Maximum Potential Intensity (MPI) in the past, they have not been used to examine the interactive nature of tropical cyclones with SST and moisture variability. Kishtawal *et al.*, (2005) used genetic algorithm technique to estimate the cyclone intensity using multichannel TMI data. Since the cyclones are greatly influenced by the upper ocean heat content or the cyclonic heat potential (Goni and Trainanes, 2003), SSHAs representing this parameter have the potential towards a better forecasting of the cyclone track and intensity. INSAT visible channel is used to locate and track the cylones. Scatterometer wind vectors have shown great impact on cyclone studies, particularly, in cyclone models. A typical picture of the Bay of Bengal cyclone observed from INSAT visible imagery and Quickscat scatterometer winds is shown in figure 11.3.

11.9. Operational Scenario

India Meteorological Department (IMD) is the nodal agency to provide operational cyclone forecast to Bangladesh, India, Maldives, Myanmar, Pakistan, Sri Lanka, Sultanate of Oman and Thailand. INSAT imagery is used to identify and locate the various stages of the cyclone and to estimate the intensity and position using objective Dvorak Technique. The Dvorak technique is based on the analysis of cloud patterns in visible and infrared imagery. The cloud patterns obtained from INSAT for the Orissa Super Cyclone is shown in Figure 11.4 wherein the eye of the cyclone is clearly seen. A quasi-lagrangian model (QLM) is used by IMD for cyclone track prediction. The model provides track forecast up to 72 hours in advance. The initial analysis and the lateral boundary conditions are generated at 00 and 12 UTC from global T-80/T-254 model sigma fields operationally run at NCMRWF.

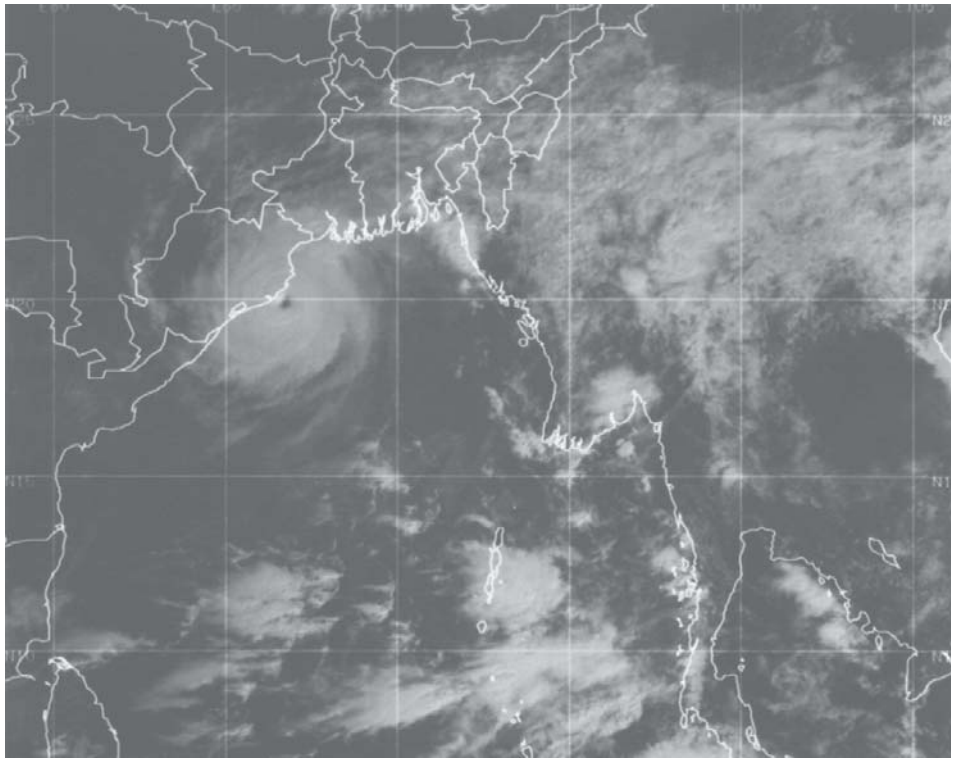

Figure 11.4: October 1999 Orissa Super Cyclone as viewed by INSAT

Operational cyclone forecasts are also available from Joint Typhoon Warning Centre, US Department of Defence, Hawaii, USA, though these forecasts are primarily meant for the US government agencies. Although not an official member or participant in the United Nations World Meteorological Organization (WMO), JTWC continually attempts to maintain cordial relations with WMO tropical cyclone forecast centers to minimize the issuance of conflicting information. JTWC monitors, analyzes, and forecasts tropical cyclone genesis, development, and movement across more than 110 million square miles of the Pacific and Indian Oceans from the west coast of the Americas to the east coast of Africa. This area of responsibility encompasses more than 90% of the world's tropical cyclone activity. JTWC uses the 1-minute mean wind speed to determine maximum sustained surface winds, as required by the US National Hurricane Operations Plan. Other countries, however, use the 10-minute mean wind speed to determine maximum sustained surface wind speeds. The difference generally means that JTWC will report higher maximum sustained surface wind speeds than non-U.S. TCWCs for the same cyclone. Besides the forecasts out to 120 hours, JTWC

provides historical data on its site. From the current cyclone season, National Remote Sensing Center (NRSC) has initiated the prediction of cyclones in the Arabian Sea and the Bay of Bengal, primarily, for the Disaster Support Centre of ISRO. Soft-computing techniques developed at SAC and NRSC are being used for the purpose.

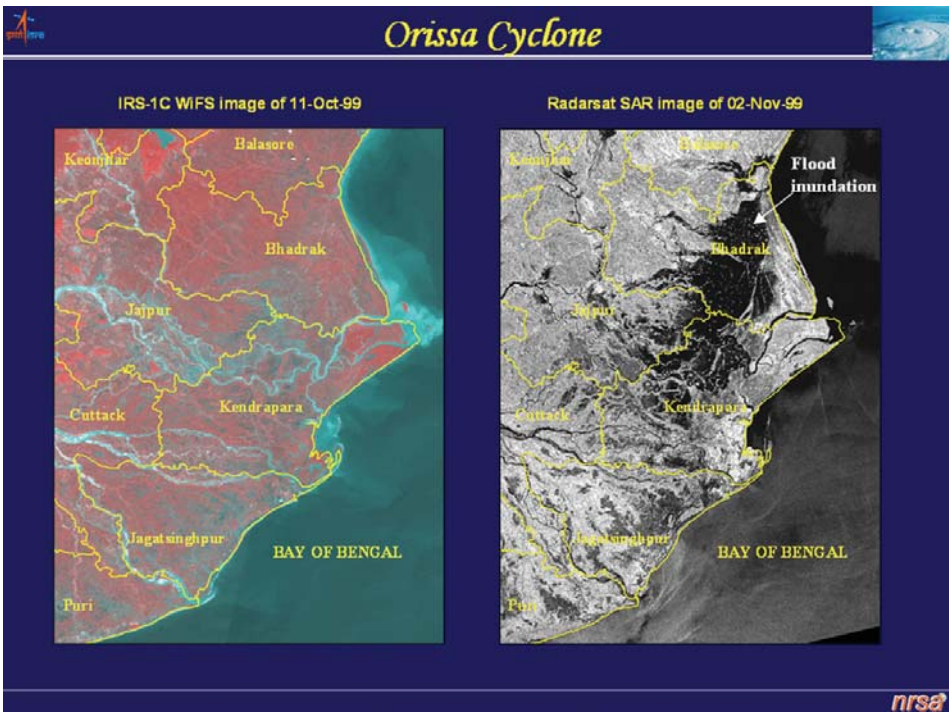

Figure 11.5: Damage assessment created for the Orissa Super Cycone using IRS-1C and Radarsat data

NRSC also plays a major role in cyclone damage assessment using Indian Remote Sensing Satellites and Radarsat data. An example of the damage assessment created using IRS-1C and Radarsat data due to the Orissa Super Cyclone is given in Figure 11.5. The procedure adopted is similar to the one for flood inundation map creation, the details of which are given at chapter 12.

11.10. The Future

Observations from Doppler weather radar systems (DWRS) are very critical, particularly, when the system reaches closer to the land. IMD plans to have a total of 55 DWRS under its modernization plan, in comparison to the existing 5 DWRS. Procurement of the cyclone probing aircrafts under the umbrella of National Disaster Management Authority will give an insight into the understanding of the physics of cyclones. Launching of Indian satellites like INSAT-3D with vertical sounders, Meghatropiques providing radiation budget, temperature and humidity profiles, Oceansat-2 providing wind vectors from a scatterometer and temperature and humidity profiles using radio occultation techniques, would certainly enhance the cyclone modeling capabilities towards a better forecasts. Compared to the track prediction intensity prediction has been more challenging. Incorporation of ocean subsurface thermal information that can be indirectly inferred from remote sensing platforms is likely to reduce this problem, particularly, in the Arabian Sea and Bay of Bengal.

Acknowledgements: Most of the material is taken from different websites. Inputs from Dr. CM Kishtawal, SAC are gratefully acknowledged. Figure 11.5 was provided by Mr. V. Bhanumurthy, NRSC.

References

Ali MM, Jagadeesh PSV and Sarika Jain, 2007, Effects of Eddies on Bay of Bengal Cyclone Intensity, *Earth Observations System*, **88**: 93-95.

Ali MM, Sharma R and Cheney R,1998, An atlas of the North Indian Ocean eddies from TOPEX altimeter derived sea surface heights, Special Publication, ISRO-SAC-SP-69-98, p 47.

Ali MM, Kishtawal CM and Sarika Jain, 2007, Predicting Cyclone Tracks in the North Indian Ocean: An Artificial Neural Network Approach, *Geophysical Research Letters*, **34**, doi: 10.1029/2006GL028353.

Elsberry R, 1995, *Global perspectives on tropical cyclones*, World Meteorological Organisation, p 289.

Falguni Patadia, Kishtawal CM, Pal PK and Joshi PC, 2004,Geolocation of Indian Ocean Tropical Cyclones using TMI observations: *Current Science*, **87**: 504-509.

Falguni Patadia, Sharma R and Ali MM, 2005, A comparison of the wind magnitudes obtained from the microwave

radiometer onboard IRS-P4 Satellite and the ERS-2 scatterometer, *International Journal of Remote Sensing*, **26** : 2479-2485.

Goni GJ and Trinanes JA, 2003, Ocean thermal structure monitoring could aid in the intensity forecast of tropical cyclones, *Earth Observation system*, **84**: 573-580.

Gopalakirhsna VV, Ali MM, Araligidad N, Shenoy S, Shum CK and Yi Y, 2003, An atlas of the XBT thermal structures and TOPEX/POSEIDON sea surface heights in the North Indian Ocean. National Institute of Oceanography, Special Publication, NIO-NRSA-SP-01-03, p 125.

Gopalan AKS, Gopala Krishna VV, Ali MM and Rashmi Sharma, 2000, Detection of Bay of Bengal eddies from TOPEX and in situ observations, *Journal of Marine Research*, **58**: 721–734.

Gupta Akhilesh, 2006, Current status of tropical cyclone track prediction techniques and forecast errors, *Mausam*, **57(1)**: 151-158.

Joshi PC, CM Kishtawal, Simon B and Narayanan MS, 1998 , Impact of ERS-1 scatterometer data in medium range forecasting (Cyclone and Monsoon), ISRO Scientific Report, ISRO-SAC-SR-43-98.

Kishtawal CM., Falguni Patadia, Basu S, Joshi PC and Narayanan MS, 2005, Automatic Intensity estimation of tropical cyclones using TMI observations : A Genetic Algorithm approach, *Geophysical Research Letters*, **32**, doi10.209.

Kishtawal CM, Patadia F, R Singh R, Basu S, Narayanan MS and Joshi PC, 2005, Automatic estimation of tropical cyclone intensity using multichannel TMI data: A genetic algorithm approach, *Journal of Geohysical Research Letter*, **32 (11)**: doi:10.1029/2004GL022045.

Mao Q, Ghang SW and Pfeffer RL, 2000, Influence of large-scale initial oceanic mixed layer depth on tropical cyclones, *American Meteorological Society*, **128**: 4058-4070.

Mohanty UC and Gupta Akhilesh, 1997, Deterministic methods for prediction of Tropical cyclone tracks, *Mausam*, **48(2)**: 257-272.

Namias J and Canyan DR,1981, Large air-sea interaction and short period climatic fluctuations, *Science*, **214**: 869-876.

Narayanan MS and CM Kishtawal, 1984, Preliminary results from an axisymmetric tropical cyclone model, *Vayumandal*, **7(1)**: 71-74.

Pal PK, 1991, Cyclone Track Prediction over the Northern Indian Ocean, *Monsoon Weather Review*, **119**: 3095-3098.

Palmen E, 1948, On the formation and structure of tropical cyclones, *Geophysics*, **3**: 26-38.

Rao BM, Kishtawal CM, Pal PK and Narayanan MS,1994, ERS-1 surface wind observations over a cyclone system in Bay of Bengal during November 1992, *International Journal of Remote Sensing,* **16(2)**: 351-357.

Shay LK, Goni GJ and Black PG , 2000, Effects of a warm oceanic feature on hurricane opal, *American Meteorological Society*, 1**28**: 1366-1383.

Singh R, Pal PK, Kishtawal CM and Joshi PC, 2007, Impact of bogus vortex for track and intensity prediction of tropical cyclone, *Journal of Earth System Science*, **114(4)**: 427-436.

Singh R, Pal PK, Kishtawal CM and Joshi PC, 2008, The impact of variational assimilation of SSM/I and Quikscat satellite observations on the numerical simulation of Indian Ocean tropical cyclones, *Waether and Forecasting*, **23**: 460-476.

http://www.mspsofworld.com/hurricane/machanism-of-tropical-cyclone-formation.html

http://www.weatherwizkids.com/weather-winds.html

used for laying models for conducting river behavior studies. Information derived from remote sensing can be used for other river morphological application studies like monitoring the existing flood control works and identification of vulnerable reaches, planning bank protection works, planning drainage improvement works etc. The changes in the river configuration can be monitored at regular intervals of time.

12.4.2. Case Study- Brahmaputra River Bank Erosion, Assam

For studying the erosion problem in Marigaon district post flood satellite data sets of 1987-91 and 1990-1998 were selected since high floods have occurred during 1988 and 1998. All the satellite data were geometrically rectified to the master map base for positional accuracy. Image enhancement techniques were applied on all the individual satellite data scenes to obtain better contrast among the features especially between land and water. The river configuration along with bank lines was delineated consisting of active river channel, sand and island. The bank lines were intersected to identify and estimate the amount of erosion and deposition at different pockets along the main Brahmaputra in Marigaon district in GIS environment. Figure 12.24

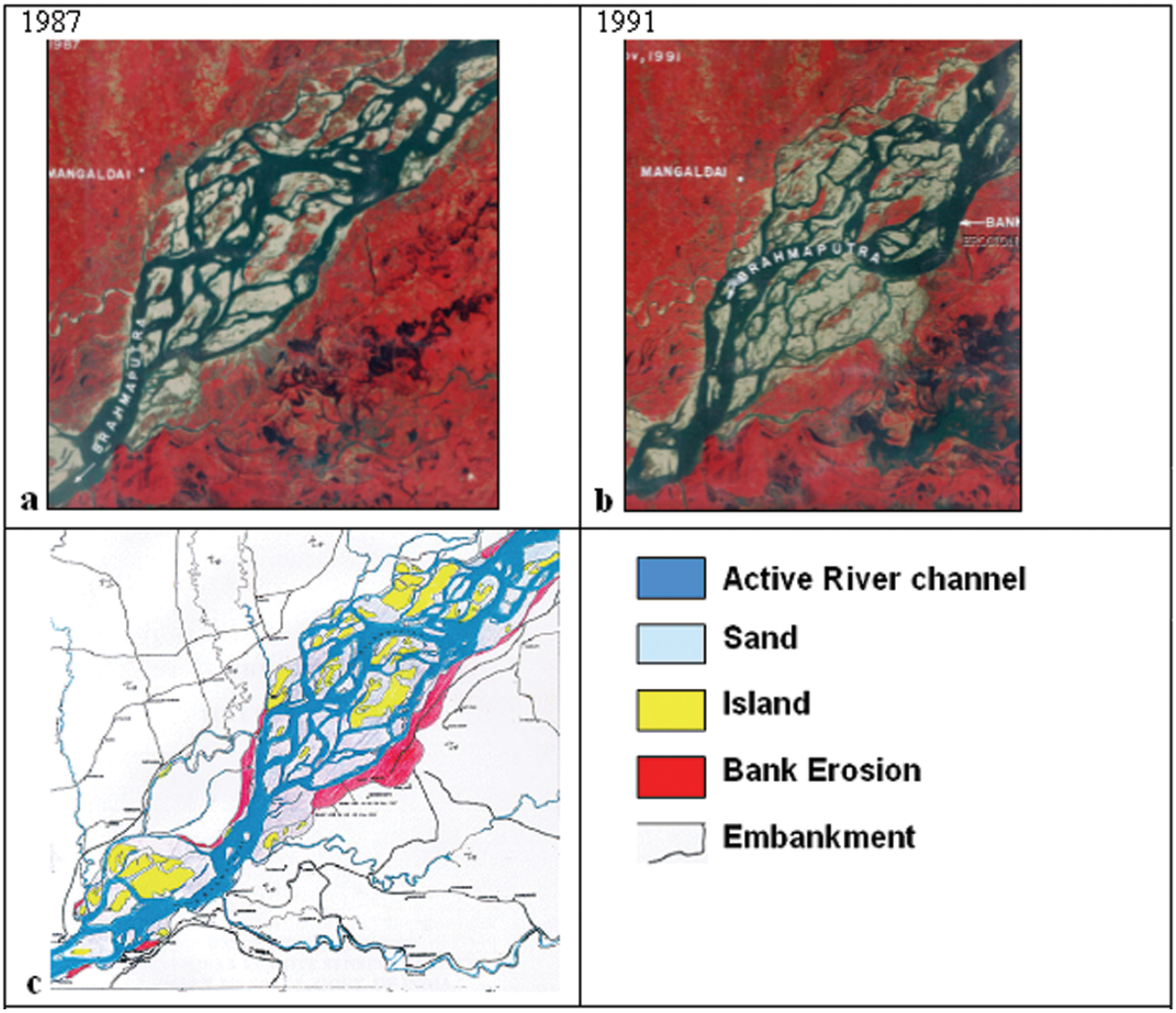

Figure 12.24: (a) Landsat –TM satellite image of 1987, (b) Landsat –TM satellite image of 1991 and (c) Bank erosion maps derived from 1987 & 1991 satellite data

shows post flood satellite data of 1987 and 1991 and the corresponding bank erosion map derived from the data set.

The post flood satellite dataset of 1990 and 1998 were analysed and the active river channel and river bank lines were delineated. These bank lines were intesected and the extent of erosion and deposition was estimated as shown in the figure 12.25.

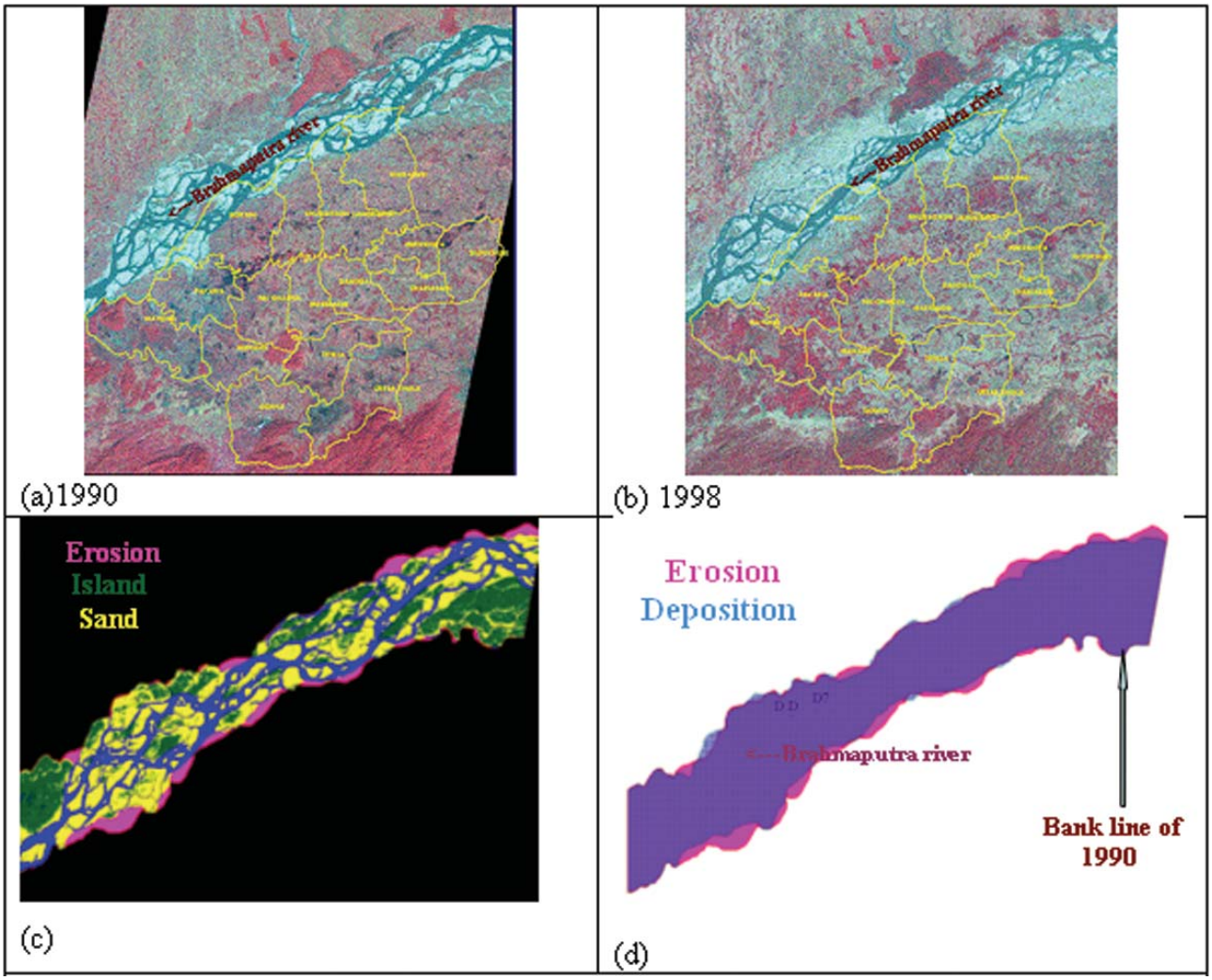

Figure 12.25: (a) Post flood satellite Images of 1990 (b) Post flood satellite Images of 1998, (c) Bank erosion and 1990 channel configuration and (d) Bank erosion map

12.5. Future Scope

12.5.1. Gap Areas

12.5.1.1. Optical

The presence of cloud in the satellite image would mask the flood affected area and it is not possible to provide the complete flood scenario. If minimum/partial cloud cover persists in the image, it is possible to delineate flood using spectral models. Therefore microwave SAR data may complement the optical data as an alternative. With the launch of RISAT, the first microwave satellite of ISRO and DMSAR, the dedicated disaster Airborne SAR, which has also got onboard processing, there is a possibility of availability of more microwave data for flood mapping and monitoring.

Sometimes, there is a chance of missing a flood event, in particular a flash flood in nature, if there is no satellite coverage immediately, may be due to longer revisit periods. In the worst case, if a flood occurs just after the satellite's overpass and the water recedes before the next satellite's overpass, from the satellite point of view, there is no flood. The spatial resolution of each image pixel may also be a constraint when identifying small areas or small patches of flooded areas in vegetated areas, agriculture fields, commercial and residential areas etc. In order to cover entire flood affected areas, particularly in India, large swaths are essential. Therefore, a constellation of Low Earth Orbiting satellites (LEOs) covering an area at regular intervals with different resolutions and swath may be a possible solution.

12.5.1.2. Microwave

In the microwave data, care should be taken in the shadow areas, smooth regions and areas disturbed by wind waves. Shadow areas do not yield any backscatter and are thus similar to ideal, smooth water surfaces. Flood in shadow areas can easily be remedied by masking out steep areas derived from the digital elevation model (DEM).

In addition to water, other surfaces like large roads, parking lots and especially airfields and runways can be smooth at radar wavelengths, and thus there is little or no backscatter. Using runways and roads from GIS database, we can be aware of potentially problematic areas and double check the likeliness of these structures being flooded.

The backscattered intensity of water bodies in SAR images increases with increasing wind speed. Thus, if the wind roughens the water surface enough to exhibit backscattering values equivalent to those on land, there will be no contrast between land and water. Therefore, large incidence angles are preferred to steep ones. But this parameter cannot be decided in a real situation, as the incidence angle depends on the location of the area of interest relative to nadir.

Today's space-borne SAR systems are polar orbiting, which yields global coverage, but with relatively long repeat cycles of 24 and 35 days for Radarsat and Envisat, respectively. By using variable incidence angles, Radarsat and Envisat are capable of acquire images from a given location with shorter intervals than the orbit repeat cycles. The frequency of how often a satellite SAR can cover a given area is dependent on the geographic location (latitude). Our experience is that it is generally impossible to get daily coverage with just one satellite, even with variable incidence angles.

12.5.2. Flood Modelling using LIDAR data

Digital Elevation Model of flood affected regions is a very important parameter in flood studies. With various limitations in optical and microwave data as discussed above, it is possible to overcome these with fine DEM.

12.5.2.1. River Forecasting

Introduction of remote sensing inputs such as satellite based rainfall estimates, landuse/landcover, soil texture etc., in the rainfall runoff models and integration of these databases in GIS environment considerably improves the flood forecasting capabilities.

A project on "Development of Flood Forecast Model and Spatial Decision Support System for Damage Mitigation" is initiated on R&D mode. The Godavari Basin is selected as a study area in the project as the Godavari Basin is one of the largest Indian River basins and floods are very frequent phenomenon in this river. The main objectives of the project are, Development of Flood Forecast Model, Flood Inundation Simulation using close contour DEM from ALTM DEM, and Development of Spatial Decision Support System for Flood Damage Mitigation. In total the project gives the end to end solution on flood disaster studies.

Spatial flood inundation simulation will be done using high resolution DEM and the output from the flood forecast model using MIKE software. Inundation simulations will be carried out for different flood scenarios in 2D modelling environment. A spatial decision support system will be developed for flood rescue and relief operations to mitigate flood damage. The process chain is shown in Figure 12.26.

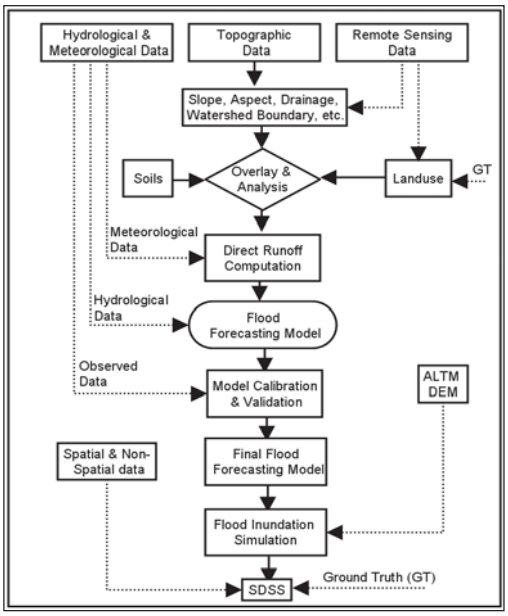

Figure 12.26: Flow chart showing the methodology

12.5.2.2. Urban Flood Modelling

Urban flooding has become a very severe problem in recent years worldwide. Urbanization has altered the timing and magnitude of flood peaks (Hazell & Bales, 1997). Hydrologic studies suggest doubling of flood peak magnitudes due to urbanization effects for a short duration and moderate intensity storms (Smith *et al.*, 2002).

As a watershed develops and rapid urbanization takes place, the land is covered with impervious surfaces like roads, roofs, parking lots, driveways, built-up areas etc., preventing rainfall entering into the ground. The result is that interflow is halted and now 80 to 90 percent of rainfall appears as direct runoff at the drainage inlets. Thus, runoff rates respond much more directly to the rainfall intensities, both in time and magnitude. A given rainstorm now produces significantly more runoff volume and more flow peaks causing severe stream channel erosion and flooding. With rapid urbanization across the globe and increased climate variability, urban flooding has been identified as a research priority (Wheater, 2002). Due to rapid urbanization, almost all major cities in India are frequently flooding even for high intensity small duration rainfall events in the recent years. The experience of floods in Mumbai and Chennai in 2005 has been one of the worst in the recent years (Saini, 2006). The management of urban flooding needs to be treated holistically in a multi-disciplinary manner. It becomes even more urgent with the fact that the migration to urban areas and an on-going development activities continue to be a threat causing an increase in the pressure on the various infrastructure and services provided. The risk of urban flooding disaster can be reduced by better town planning activities, hazard mitigation and prevention, improved preparedness and warning systems, well organized pre-emptive action and emergency response to minimize damages. Modeling of urban flooding by setting up different scenarios and analyzing their occurrence within a reliable modeling framework can help decision makers to identify the most effective actions.

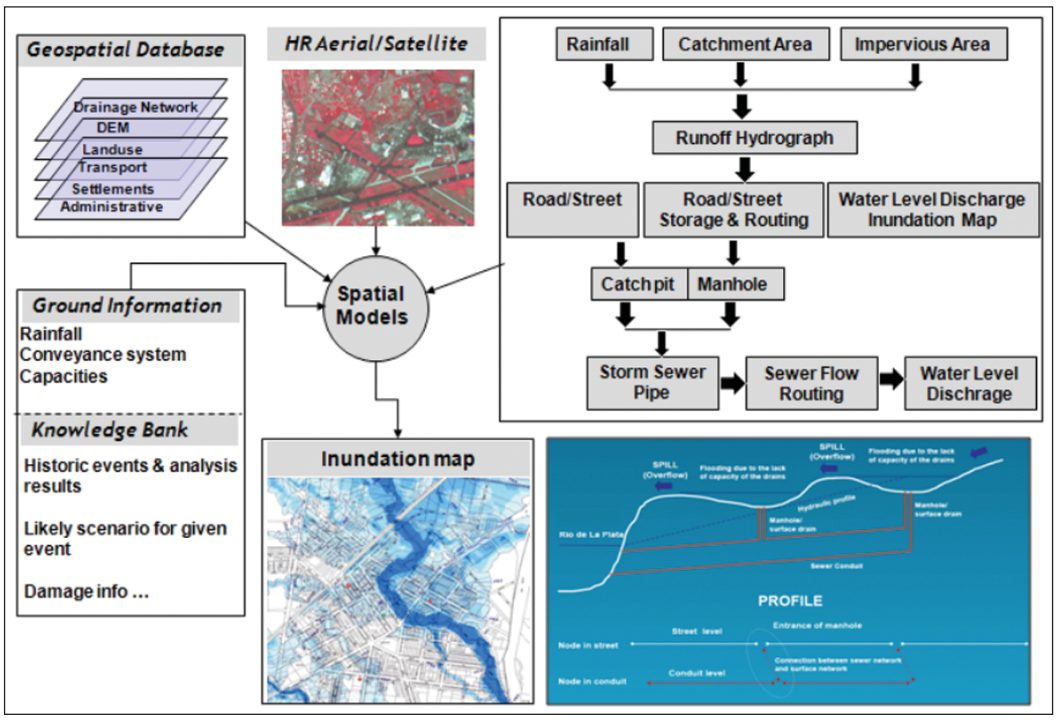

Figure 12.27: Geospatial approach for generating flood inundation maps for urban areas

High resolution terrain height data and landuse information are the two important inputs required to realistically budget floodplain storage and conveyance and the spatial distribution of resistance parameters. Rational formula / SCS curve number can be used to estimate the surface runoff from the urban catchments. Using the DEM generated from Lidar/ground survey, slopes of the study area can calculated. Delineation of suitable sub-catchments of basin can be carried out using the DEM. Distribution of the peak flow rates along the drainage network at different nodes can be estimated. The estimated peak runoff rate shall be compared with carrying capacity of storm water drains to judge whether estimated runoff will flood the area or not. The extent of flooding can be estimated using two-dimensional hydrodynamic modeling. For inundation simulation information on drainage

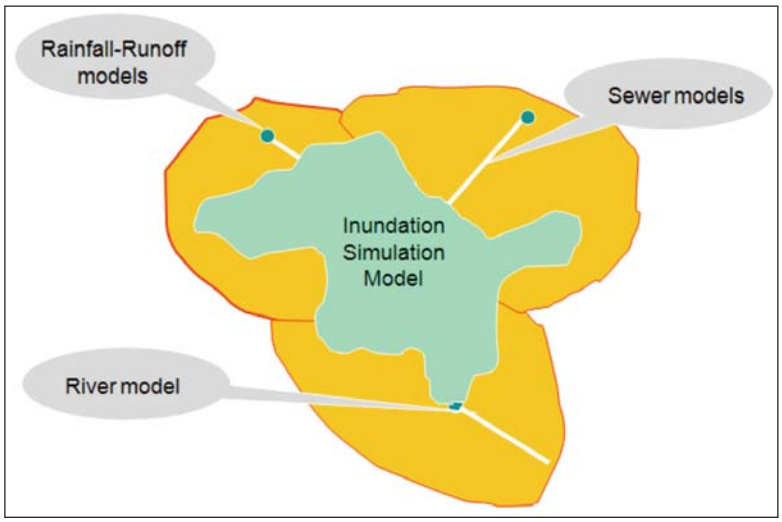

Figure 12.28: Integration of different models is required for modeling of urban floods (Source: http://www.coastms.co.uk/Conferences/Outputs.pdf)

characteristics like dimensions of the inlets, levels of the inlets and outlets, information on closed drains, open drains, type of drains etc., is required. Models like MIKE-MOUSE, SOBEK, UFDSM, etc., are being used for urban flood modeling. Figures 12.27& 28 shows the geospatial approach for generating flood inundation maps and integration of different models required for modeling of urban floods.

Figure 12.29 shows the early warning system installed for mitigating urban flooding in Mumbai, under Mumbai's urban flood disaster management and mitigation programme.

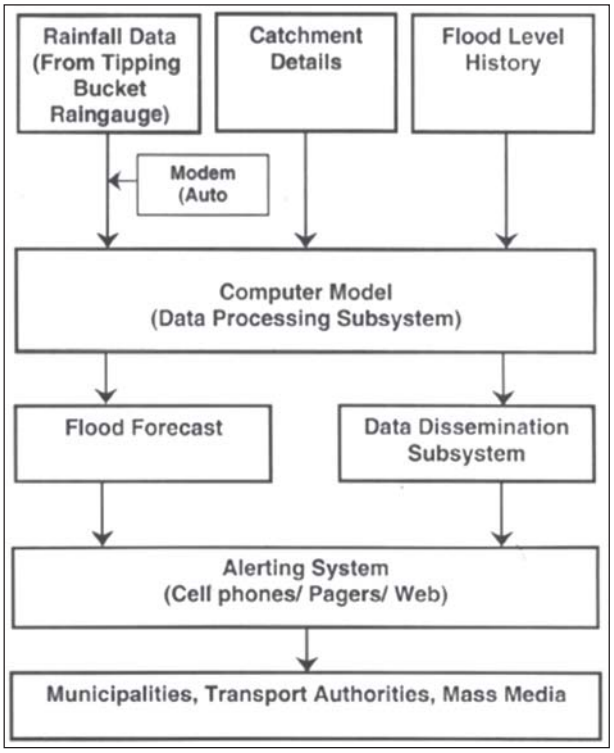

Figure 12.29: An early warning system installed for mitigating urban flooding in Mumbai (Source:http://nidm.gov.in/idmc/Proceedings/Flood/B2-%207.pdf)

12.5.3. Decision Support System

Geospatial database plays a major role in the flood management since it provides timely inputs meeting the user needs in terms of information content, format and multiple thematic layers integration and analysis. For this, a related Geo-spatial data with proper data standards formats and data access mechanism is essential. To achieve flood preparedness, mitigation, relief and rescue, Decision Support Systems (DSS) are effective tools for decision-making using available geospatial data sets in centralized data server. DSS is an intelligent information system for flood management and relief. It will be evolved through participation of knowledge institutions at user end using spatial datasets. It is also an electronic-based correspondence system and report generator that can be designed according to the user. SDSS will have two major modules 1) generic display & query module to facilitate display of spatial & non-spatial data, identification of attribute information, overlays, simple thematic queries etc., 2) analysis module catering to the specific needs pertaining to various phases of emergency management viz., early warning, damage assessment & statistics, risk prediction, evacuation plans & alternate optimal routes, proximity analysis, etc., using geospatial technologies.

12.5.3.1 Flood Management Information System (FMIS)

A prototype for flood management information system is planned to be developed for Government of Bihar to meet the operational requirements of different users involved in flood relief and rescue. It is planned to develop a standalone system on Desktop based architecture and it will have provision to view, access, update and create required outputs for flood management. A secured access to database is ensured and the users can run simple and complex queries on the data. The information system will also have Map / report generation. Figure 12.30 shows some of the sample utilities designed for FMIS.

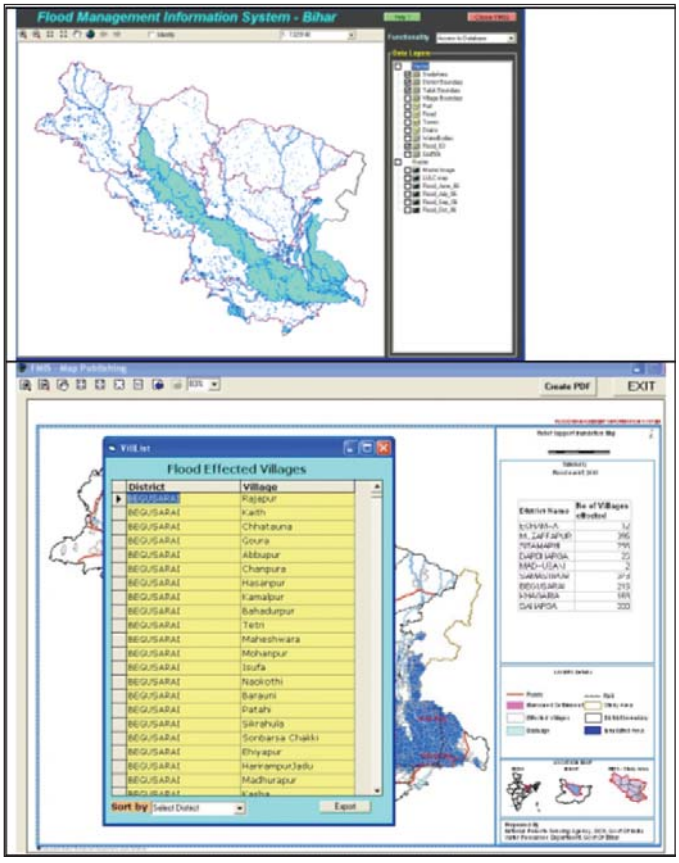

Figure 12.30: Sample utility displays designed for FMIS, Bihar

References

Bhanumurthy V, Srinivasa Rao G, Simhari Rao B and Manjusree P, 2003, A System for Survival, *Geospatial Today*, **2(2)**: 30-33.

Hazell WF and Bales JD, 1997, Real-time rainfall measurements in the City of Charlotte and Mecklenburg County, North Carolina, US Geological Survey Fact Sheet FS-052-97.

Saini HS, 2006, Urban flooding: Can it be ignored any further?, *Current Science*, **91(10)**: 1303-1304.

Smith JA, Baeck ML, Morrison JE, Sturdevant-Rees P, Turner-Gillespie DF and Bates PD, 2002, The regional hydrology of extreme floods in an urbanizing drainage basin, *Journal of Hydrometeorology*, **3(3)**: 267–82.

Srinivasa Rao G, Brinda V and Manjusree P, 2006, Advantage of Multi-polarized SAR data for Flood Extent Delineation, *Proceedings of SPIE*, Volume **6411**.

Srinivasulu J, Sasi Kumar D, SaiBaba J and Prasada Raju PVSP, 2005, Development of a Variable Threshold Method for Automatic Delineation of Flood Inundation using Radarsat SAR Data, Proceedings of the National Workshop on "Geo-informatics in Water Sector", organized jointly by the NWA, IWRS, and ISG, held at Pune,**I** :115-125.

Stian Solbo and Inger Solheim, 2004, Towards Operational Flood Mapping with Satellite SAR, Envisat & ERS Symposium, Norut Information Technology AS. Tromsø Science Park, N-9291 Tromso, Norway.

Wheater HS, 2002, Progress in and prospects for fluvial flood modelling, *Philos Trans Roy Soc A: Math Phys Eng Sci*, ***360 (1796)***:1409–31.

http://www.imd.ernet.in

http://disc2.nascom.nasa.gov/Giovanni/tovas/realtime.3B42RT.2.shtml#description

http://gs.mdacorporation.com/products/sensor/radarsat/radarsat1.asp

http://nidm.gov.in/idmc/Proceedings/Flood/B2-%207.pdf.

http://www.coastms.co.uk/Conferences/Outputs%20and%20Reports/IUD%20May%202006/IUD%20May%202006%20Crowder.pdf

nrsc

Remote Sensing Applications

P. S. Roy
R. S. Dwivedi
D. Vijayan

National Remote Sensing Centre

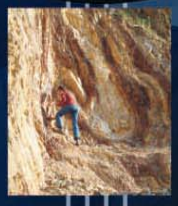

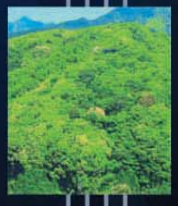

Remote Sensing Applications

Flood Disaster Management

12.1. Introduction

12.1.1. Floods in India

India, on account of its geographical position, climate and geological setting, is the worst affected centre of disaster in the South Asian region, making it vulnerable to natural hazards such as cyclone, drought, floods, earthquakes, fire, landslides and avalanches. India is the worst flood-affected country in the world after Bangladesh and accounts for one fifth of global death count due to floods. Around 40 million hectares of land in the country are subject to floods according to National Flood Commission, and an average of 18.6 million hectares of land is affected annually. The annual average cropped area affected is approximately 3.7 million hectares. The most flood-prone areas in India are the Brahmaputra and Ganga River basins in the Indo-Gangetic-Brahmaputra plains in North and Northeast India, which carry 60 per cent of the nation's total river flow. The other flood prone areas are the north-west region of west flowing rivers such as the Narmada and Tapti, Central India and the Deccan region with major east flowing rivers like Mahanadi, Krishna and Cauvery.

Nearly 75 per cent of the total Indian rainfall is concentrated over a short monsoon season of four months (June-September). As a result the rivers witness a heavy discharge during these months, leading to widespread floods in Uttar Pradesh, Bihar, West Bengal and Assam. The Himalayan Rivers also carry a large amount of sediment, causing erosion of the banks in the upper reaches and over-topping in the lower segments. Drainage problems also arise concurrently if floods are prolonged and the outfalls of major drainage arteries are blocked. One of the major reasons for the floods is the massive indiscriminate deforestation, which leads to large amounts of topsoil coming loose in the rains. Thus, the soil, instead of soaking up the rainfall, flows down into the river and in turn causes the riverbeds and its tributaries to rise.

12.1.2. Flood Management

Though floods cannot be stopped, its damages can be minimized by proper management measures. Flood disaster management demands efficient planning measures, implementation and policy making decisions, application of modern scientific and communication tools for smooth functioning of the system. For effective flood management, the concerned flood control departments require information at different phases of the flood disaster cycle as shown in Table 12.1. Relief and rescue operations need to be carried out immediately during the flood to provide emergency help to the affected people and reduce the likelihood of secondary damage. One of the most important elements in Flood Management is the availability of timely information on the spatial extent of the affected area for taking decisions and actions in the form of a map. A flood inundation map helps the decision-maker to make a scientific assessment for better management of relief activities. This spatial information about the flood situation needs to be continuously updated for the successful execution of the operations. Hence an identified system has to be developed to address the various information needs and to provide an operational service with its framework.

Table 12.1: Information requirements for a disaster manager

S.No	Phase	Required Information
1	Flood preparedness (Before Flood)	– Chronically flood prone areas – Prior information on probable flood affected areas with considerable lead time – Optimum evacuation plans
2	Relief and Rescue (During flood)	– Flood affected areas – Flood damage statistics – Updation of the flood condition in terms of flood recedence and persistence etc.
3	Flood Mitigation (After Flood)	– Changes in the river course – The status of flood control works – River bank erosion – Drainage congestion – Flood Risk zones

12.1.3. Role of Space Technology

Role of space applications in disaster management lies in its criticality to produce as well as disseminate the

information on real/near real time basis. The developments in space technology offer tremendous technological potential to address the crucial information needs during mitigation and preparedness, response and recovery/ relief phases of a disaster. Earth observation satellites enable continuous monitoring of atmospheric as well as surface parameters attributing to the phenomena. The operational role of satellite communications viz., satellite phones, point-to-point networking solutions routed through the arrays of Very Small Aperture Terminals (VSATs) deployment in remote and inaccessible areas, Cyclone Warning and Dissemination Systems (CWDS), Data Collection Platforms (DCP) and Satellite Aided Search & Rescue (SAS&R) are very critical during a disaster.

Satellite remote sensing data provides information on spatial flood extent, flood damage statistics and also in river engineering studies in a cost effective manner as discussed below. The utilization of each product is shown in Table 12.2.

Table 12.2: Utilization of the flood products

S.No	Deliverables	Utilization
1	Flood map	To map inundated areas for organizing relief operations
2	Flood damages – Extent of inundation – Crop area submerged – Number of Villages marooned – Length of Road/ railway network affected/submerged	Quick assessment of flood damages, for providing relief & Rehabilitation
3	Flood control works and River configuration	Strengthening of existing & planning of future flood control works
4	River Bank erosion	Planning anti erosion works
5	Identification of chronic flood prone areas and Floodplain zoning	Hazard zonation & floodplain regulation, planning flood control works

During preparation phase,

- Using historic satellite remote sensing data acquired during floods, it is possible to provide the chronically flood prone areas in the form of a map showing severely affected, occasionally affected, etc.
- Prior information on probable flood affected areas using hydrological models can be provided
- Using flood inundation models in GIS environment, optimum evacuation plans can be generated for carrying out rescue operations

During floods,

- A flood map showing the spatial extent of the flood affected areas
- Flood damage statistics like district-wise flood affected area, submerged crop, marooned villages and length of submerged road/rail can be provided
- Satellite data can be used at regular intervals for updation of the flood condition on the ground in terms of flood progression, recedence and persistence

During mitigation phase,

- Using high resolution historic and present satellite data, mapping of river configuration and flood control works, changes in the river configuration, and studies on bank erosion/deposition can be carried out
- Using multi-date satellite data it is possible to demarcate the drainage congestion areas in the chronic flood prone areas
- Flood hazard and risk zone maps can be generated using multi-year satellite data acquired during floods

12.1.4. Initiatives of Department of Space

In order to provide vital inputs and support in the event of a flood disaster, Department Of Space (DOS) has been developing techniques and methodology by integrating space based systems and services for disaster management. DOS had executed a Disaster Management Support Programme (DMSP) for integrating operationally the space technology inputs and services on a reliable and timely basis for strengthening India's resolve towards disaster

management. DMS Programme addresses five issues mainly (i) creation of digital databases at appropriate scales for facilitating hazard zonation, damage assessment etc., in perennially disaster prone areas, (ii) development of appropriate Remote Sensing & Geographical Information System (GIS) based decision support tools and techniques and demonstrations catering to the information needs at different levels, (iii) acquisition of close contour information for priority areas, (iv) strengthening the communications backbone for addressing the real time / near real time information transfer needs and (v) networking of scientific institutions for exchange of data, information and knowledge. Towards enabling the operational services, a Decision Support Centre (DSC) is established at National Remote Sensing Centre, (NRSC) as a single window provider, interfacing with the National / State disaster management agencies. The important components of the DSC include satellite/ aerial data acquisition strategy, user required information and formats, output generation, dissemination of information generated to the users through networking, support functions such as digital database, hazard zonation, network modelling, query shells, etc.

For the last one and half decade, NRSC has been extensively using satellite remote sensing data for flood mapping and monitoring activity operationally in near real-time besides in other river mapping studies. Optical satellite data from the series of Indian Remote Sensing satellites (IRS) and microwave data from Canadian satellite RADARSAT are used to map the flood-inundated areas in near real-time and estimate the flood damages. The flood maps and damage statistics are disseminated to central and concerned state government departments by digital and surface means. A flood map provides the spatial extent of flood inundation in the entire state, at an instant of time and helps to identify the worst flood affected areas and acts like a guide for better planning of rescue operations and allocation of resources for relief (Bhanumurthy *et al*., 2003). It can also be used as an information layer to integrate with other related available ground information. It can be used to validate / crosscheck with the information collected from other sources and helps as evidence in explaining the flood impact. This type of information is quite difficult to generate by conventional means since some of the areas may not be accessible (Srinivasa Rao *et al.*, 2006). The flood damages are based on scientific assessment and hence reliable and accurate.

12.2. Approach

The main components of flood mapping and monitoring are shown in Figure 12.1. They are

- Flood watch
- Satellite data planning and acquisition
- Satellite data analysis
- Product Dissemination

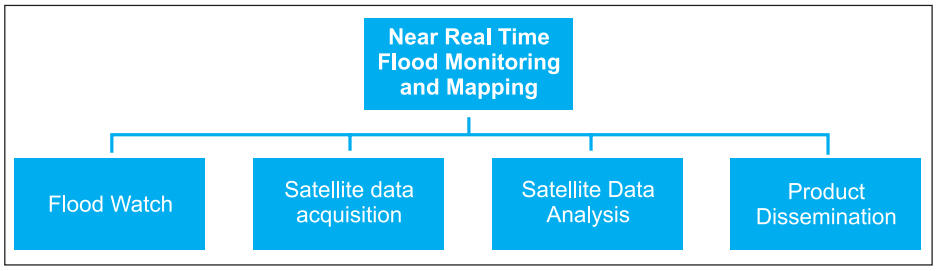

Figure 12.1: Components of the Near Real Time Flood Mapping and Monitoring Activity

12.2.1. Flood Watch

Flood watch is one of the preparedness activities where a constant watch is kept on the flood situation in the country through different sources of information. It is the most important activity and is a triggering tool for the next chain of activities.

12.2.1.1. Flood News

The flood related information is collected daily from web news/television/ newspapers/state ground departments. The local web news sites of the respective states are scanned for the latest information on the flood condition.

12.2.1.2. Meteorological Satellite Data

Meteorological satellite KALPANA-1 images over the country were collected to understand the cloud cover pattern. The cloud cover over the country from 18-21 August, 2008 through a series of INSAT images, is shown in Figure 12.2. Persistence of thick cloud cover over the country can be observed from the images during 18-21 August, which led to heavy rains and subsequent flooding in some parts of the country.

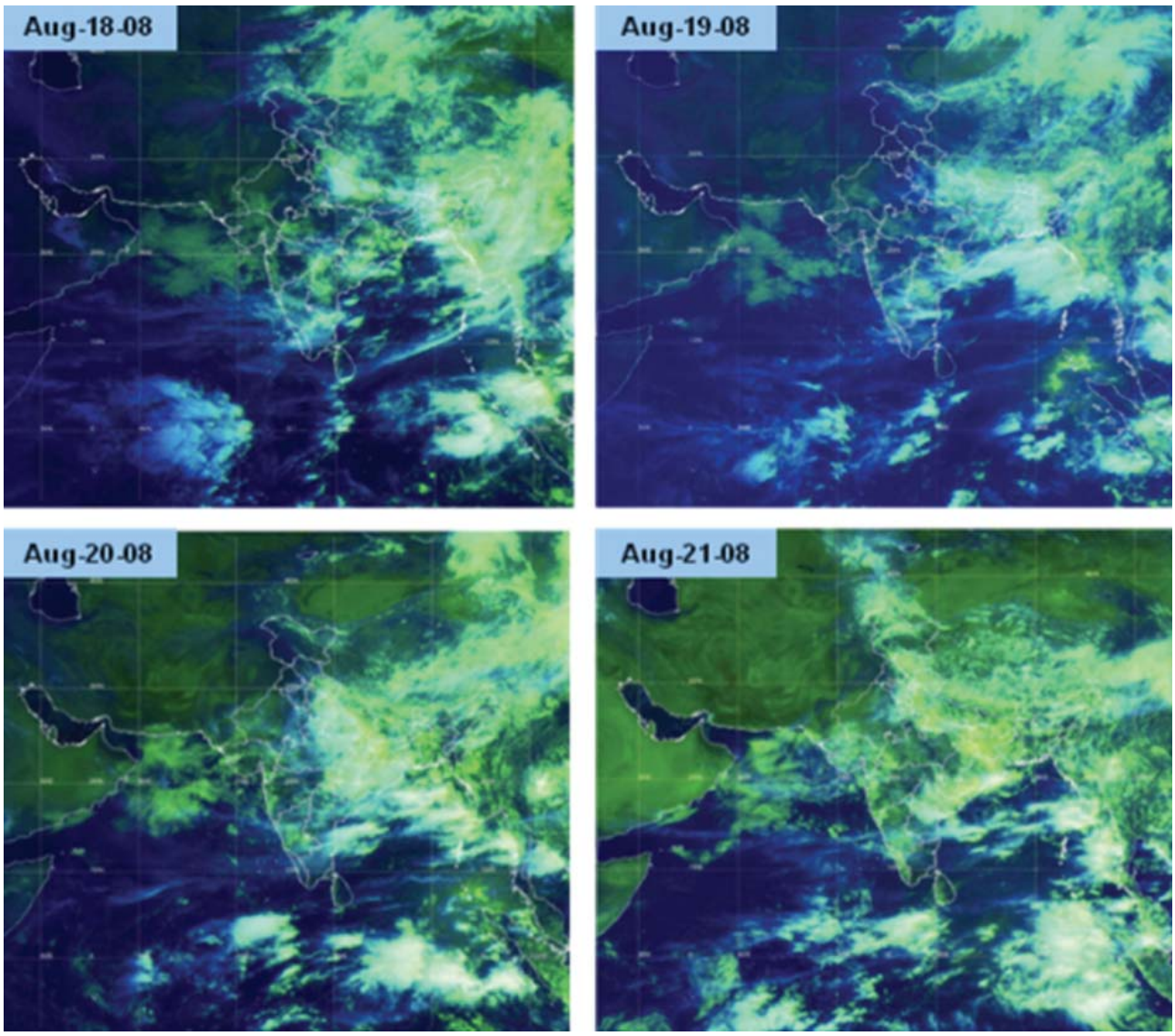

Figure 12.2: KALPANA-1 images showing cloud cover during 18-21 August 2008 (Source: www.imd.ernet.in)

12.2.1.3. Rainfall Data

The rainfall data measured at various rain gauge stations across the country by Indian Meteorological Department (IMD) and Central Water Commission (CWC) is collected and related to the cloud pattern in Kalpana-1 images. The rainfall distribution from Tropical Rainfall Measuring Mission (TRMM) merged products which are available on their website are also downloaded. Figure 12.3a shows the rainfall distribution as on 15th and 20th September 2006 from IMD and Figure 12.3b shows TRMM image showing the accumulated rain over India during September 2006. It is observed that during 15th and 20th September 2006, vigorous

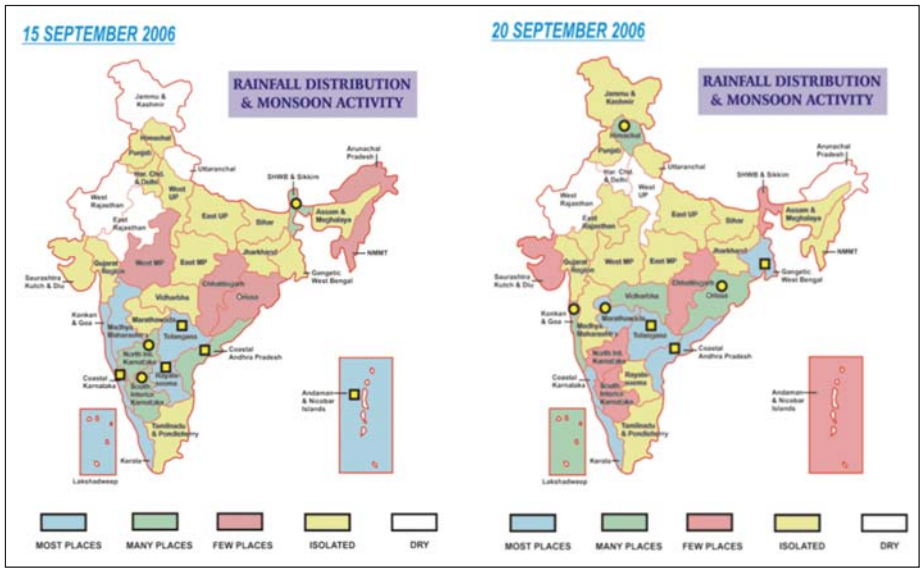

Figure 12.3a: Rainfall distribution as on 15th and 20th September 2006 (source: www.imd.ernet.in)

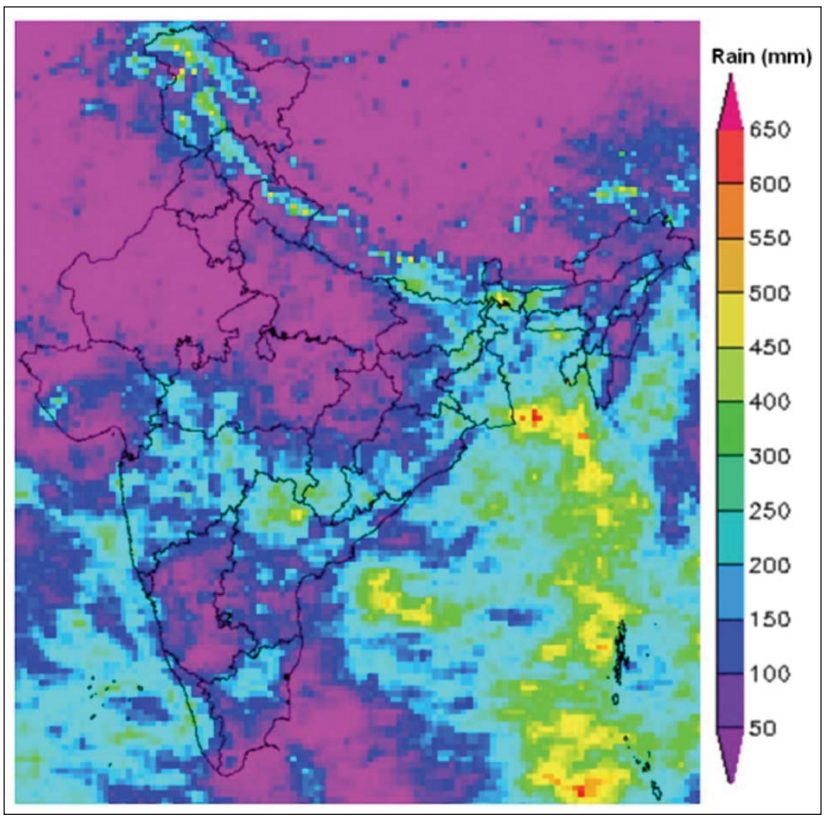

Figure 12.3b: Rainfall distribution maps from TRMM merged product (source:http://disc2.nascom.nasa.gov/Giovanni/tovas/realtime.3B42RT.2.shtml#description)

rainfall activity was over South and South East India respectively. The TRMM accumulated rainfall map shows that about 300-450 mm of rainfall occurred during September 2006 on this region.

12.2.1.4. Water Level Data

The water level data of rivers and its tributaries at various gauge recording stations is obtained from CWC on daily basis. The water levels of Ganga River and their tributaries in part of Bihar, the water levels of Brahmaputra, Barak Rivers and their tributaries in Assam are received from CWC. River gauge hydrographs are prepared using the water level data. The trend of the flood wave is monitored through these hydrographs.

Figure 12.4 shows the location of six rain gauge stations along river Brahmaputra for which the water level data is supplied by CWC. The gauge hydrograph prepared for river Brahmaputra along Dibrugarh shows that the river was flowing above the danger level mark throughout the month, whereas at Dhubri it crossed the danger level during the third week of August 2008 (Figures 12.5 a&b).

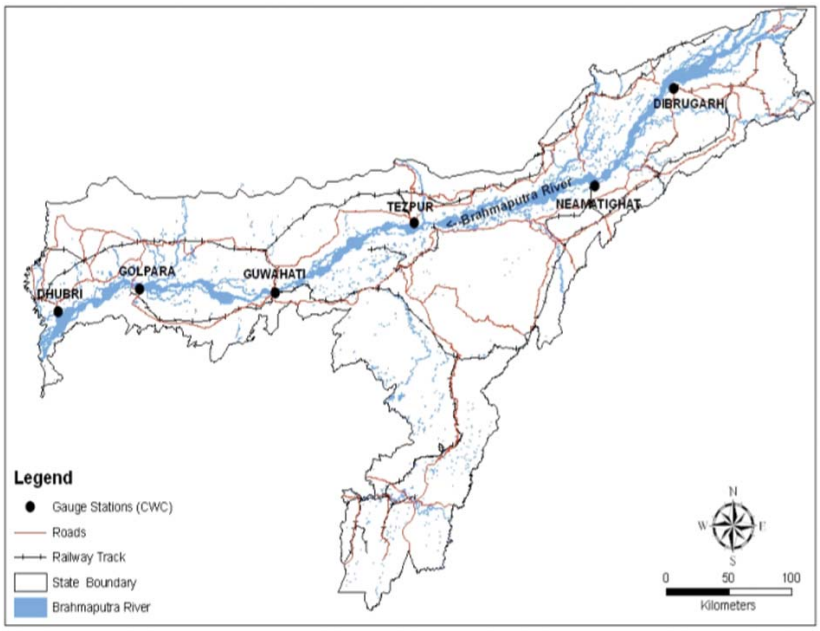

Figure 12.4: Location of gauge stations along river Brahmaputra in Assam

12.2.2. Satellite Data Acquisition

After the flood watch, the affected regions are identified and all the available satellites onboard covering the affected area are earmarked and coverage charts are prepared. Continuous meticulous planning is required to acquire satellite data during rising of flood wave, at the peak and falling of the flood wave to help the flood disaster manager for successful relief and rescue operations.

Presently, optical satellite data from IRS-P6, IRS-P4, NOAA and TERRA/AQUA satellites is being used. Based on the trend of the flood wave, microwave data from RADARSAT/ERS SAR/ ENVISAT satellites are programmed. RADARSAT-1 operates at C-band with HH polarisation and has the flexibility to acquire images at different incidence angles, resolutions and swath modes. Figure 12.6 shows the different beam modes of Radarsat satellite. ERS operates at C-band with VV polarization with a resolution of 25 m and a swath of 100 km. Presently, RSI/Canada requires minimum 48 hrs advance intimation for programming the RADARSAT-1 satellite to acquire data over any area. Emergency Programming mode with 'near real time' data supply option is selected so that the acquired raw Radarsat data will be placed on the *ftp site* of RADARSAT. Table 12.3 shows the satellites and sensors that are used for flood mapping activity.

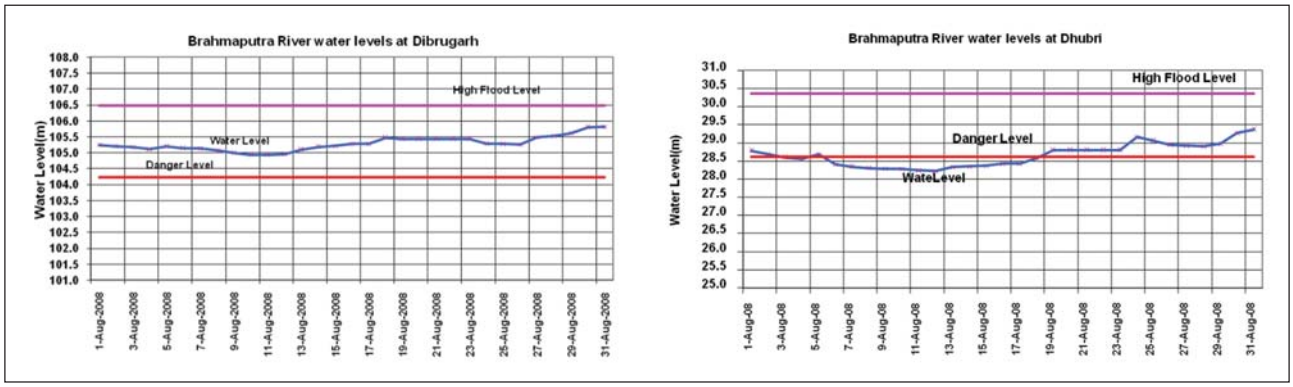

Figure 12.5: Gauge hydrograph of river Brahmaputra at (a) Dibrugarh in Assam and (b) at Dhubri in Assam

Table 12.3: Satellites and their Sensors used for flood mapping

S.No	Satellite	Sensor/ Mode	Spatial Res(m)	Spectral Res (µm)	Swath (km)	Used For
1	IRS-P6	AWiFS	56	B2: 0.52-0.59 B3: 0.62-0.68 B4:0.77-0.86 B5: 1.55-1.70	740	Regional level flood mapping
2	IRS-P6	LISS-III	23.5	B2: 0.52-0.59 B3: 0.62-0.68 B4:0.77-0.86 B5: 1.55-1.70	141	District-level flood mapping
3	IRS-P6	LISS-IV	5.8 at nadir	B2: 0.52-0.59 B3: 0.62-0.68 B4:0.77-0.86	23.9	Detailed level Mapping
4	IRS-1D	WiFS	188	B3: 0.62-0.68 B4:0.77-0.86	810	Regional level flood mapping
5	IRS-1D	LISS-III	23.5	B2: 0.52-0.59 B3: 0.62-0.68 B4:0.77-0.86 B5: 1.55-1.70	141	Detailed level Mapping
6	Aqua/ Terra	MODIS	250	36 in visible, NIR & thermal	2330	Regional level Mapping
7	IRS-P4	OCM	360	Eight narrow bands in visible & NIR	1420	Regional level Mapping
8	Cartosat-1	PAN	2.5	0.5- 0.85	30	Detailed level Mapping
9	Cartosat-2	PAN	1	0.45-0.85	9.6	Detailed level Mapping
10	Radarsat-1	SAR/ ScanSAR Wide	100	C-band (5.3 cm) HH Polarization	500	Regional level mapping
11	Radarsat-1	SAR/ ScanSAR Narrow	50	C-band (5.3 cm)	300	District-level mapping
12	Radarsat-1	Standard	25	C-band	100	District-level mapping
13	Radarsat-1	Fine beam	8	C-band (5.3 cm)	50	Detailed level mapping
14	ERS	SAR	25	C-band VV Polarization	100	District-level mapping

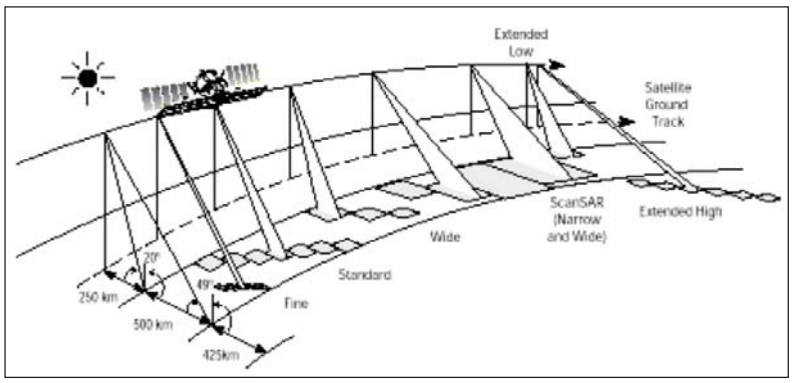

Figure 12.6: Beam modes of Radarsat satellite (Source:http://gs.mdacorporation.com/products/sensor/radarsat/radarsat1.asp)

"Data acquisition planner" application tool which is developed by ADRIN, DOS is used for determining the ideal sensor of IRS series that cover the flood affected region in a specific period of time. This software has a user-friendly GUI and is developed with Visual Basic 6.0 and MapObjects 2.0 in the front end and C-program in the backend.

In this tool, satellite and sensor characteristics are maintained in a database. Existing satellite sensor properties can be edited and new satellites and sensors can be added, as and when required. Satellite orbits are predicted using the satellites' Two Line Element sets (TLE) and the ground coverage is predicted using the viewing geometry parameters of the respective sensors. With this application, all possible coverages of the user-defined area by satellites of our interest during the specified time period can be determined. Figure 12.7a shows the path coverage of IRS-P6 AWiFS sensor over Assam region on 5th June 2006.

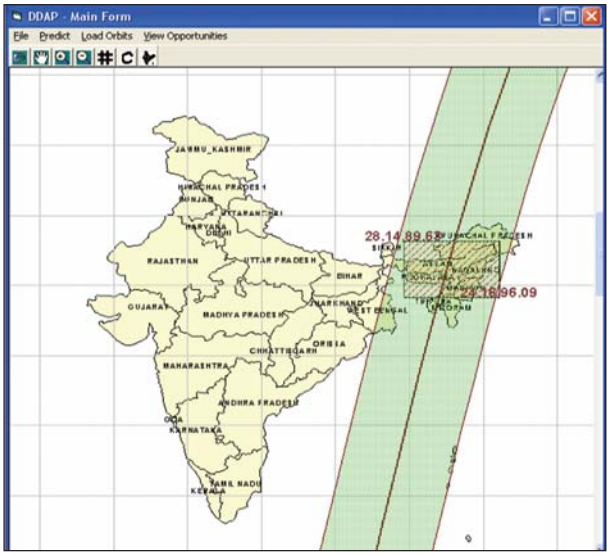

Figure 12.7a: Path coverage of IRS-P6 AWiFS over Assam region on 5th June, 2006

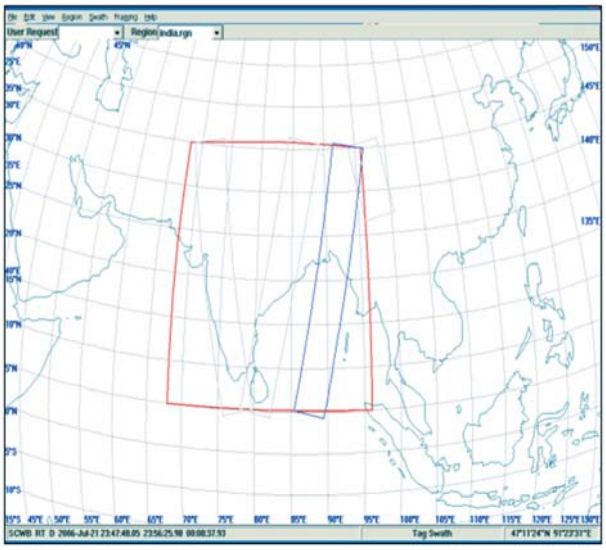

Figure 12.7b: Scan SAR Wide Beam coverage over Assam on 21 Jul., 2006 at 23:47:48.05

For Radarsat SAR data, "Swath Planner" application tool which is provided by RSI, Canada is used to identify the possible coverages over the affected area for different beam modes. Figure 12.7b shows the Scan SAR Wide Beam coverage over Assam on 21-Jul-2006. All the above information are compiled and a consolidated flood disaster watch report is prepared on daily basis, highlighting the incidence of the flood event, its trend, damages reported, along with details of satellite data planning and status of acquisition. Figure 12.8 show the elements of disaster watch report activity.

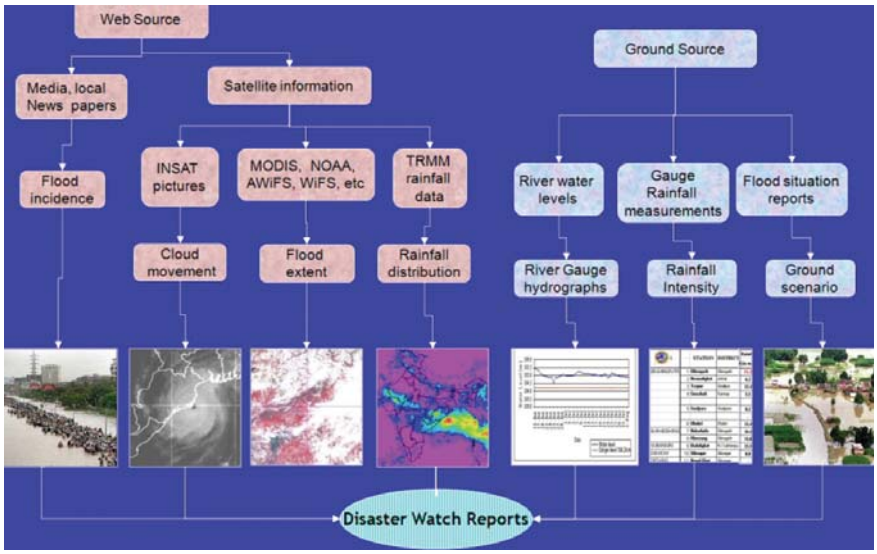

Figure 12.8: Elements for satellite data planning and acquisition

12.2.3. Satellite Data Analysis

12.2.3.1. Optical Data

Optical remote sensors measure the reflectance from objects on the ground. Pure and deep-water bodies absorb most of the electro-magnetic energy and reflect very little energy. Flood water, because of different sediment concentrations, reflects considerable energy in different bands, including near infra red (NIR) region. Figure 12.9 shows IRS-P6 image of 30-Aug-2005 with variations in flood signatures.

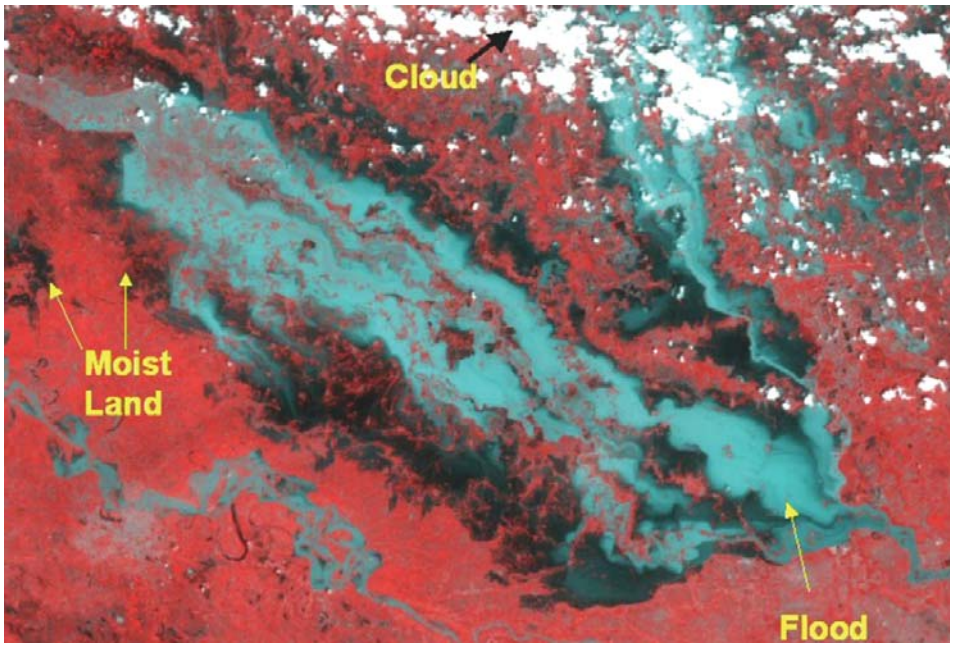

Figure 12.9: IRS-P6 AWiFS image of 30 Aug., 2005

Red Band

	Minimum	Maximum	Mean	S D
	5.81	6.367	6.191	0.153
	6.128	6.845	6.634	0.126
	6.248	6.487	6.419	0.054
	6.805	8.954	8.275	0.421

Infra Red Band

	Minimum	Maximum	Mean	S D
	4.608	5.135	4.826	0.118
	3.026	4.192	3.672	0.239
	2.665	2.804	2.748	0.036
	3.47	5.496	4.246	0.306

Table 12.4: (a) Radiance values of flood waters in (a) red band and (b) infra red band

Tables 12.4a & 4b shows the variations in radiance values of flooded areas derived from IRS-P6 AWiFS image, both in Red and Infra red bands. It is possible to delineate the flood extent from optical data even with two bands, i.e., red and infra-red bands. Figure 12.10 shows the scatter-plot between Red and Infrared bands which provides a fair view of the separation of various classes for delineating flood extent. Though delineation of flood extent is not a trivial exercise, the presence of cloud cover makes the classification process very difficult.

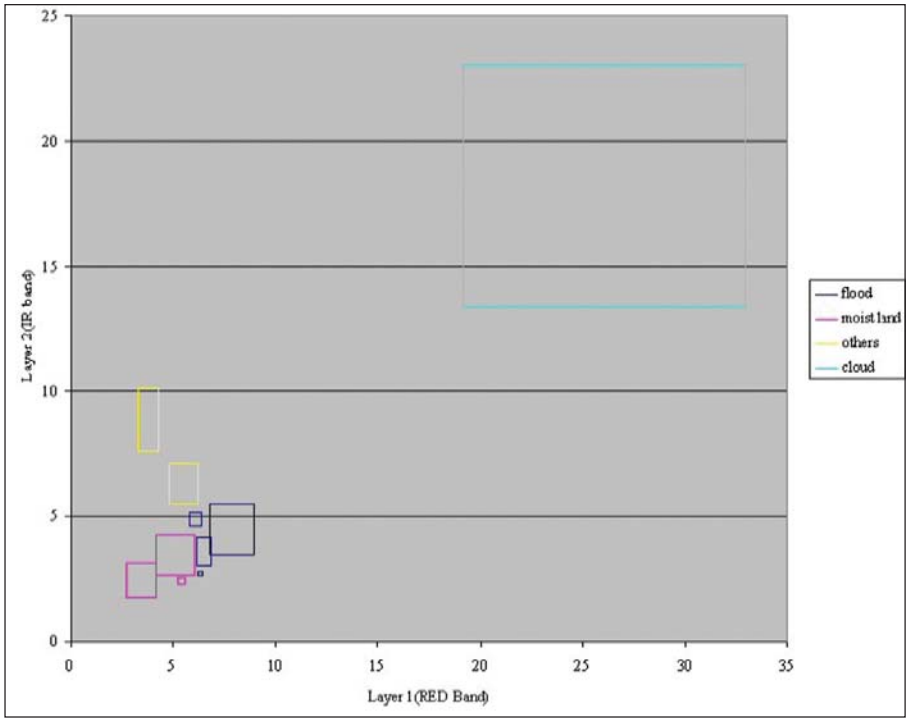

Figure 12.10: Scatter plot of Red and Infra red bands (IRS-P6 AWiFS image)

The flood water signature generally mixes with cloud shadow and also with mixed pixels of cloud and cloud shadow. In some cases, it mixes with large urban areas / built-up lands.

12.2.3.2. Microwave Data

The advantage of using radar data over the optical data is its ability to penetrate cloud cover and also data acquisition during day and night. Water surfaces are generally smooth at radar wavelengths and can be regarded as specular reflectors which yield small backscatter. The surrounding terrain is assumed to be rough at radar wavelengths which exhibits diffuse scattering with moderate backscatter, as shown in Figure 12.11. Hence, water is regarded as low intensity areas whereas the surrounding terrain corresponds to brighter intensities.

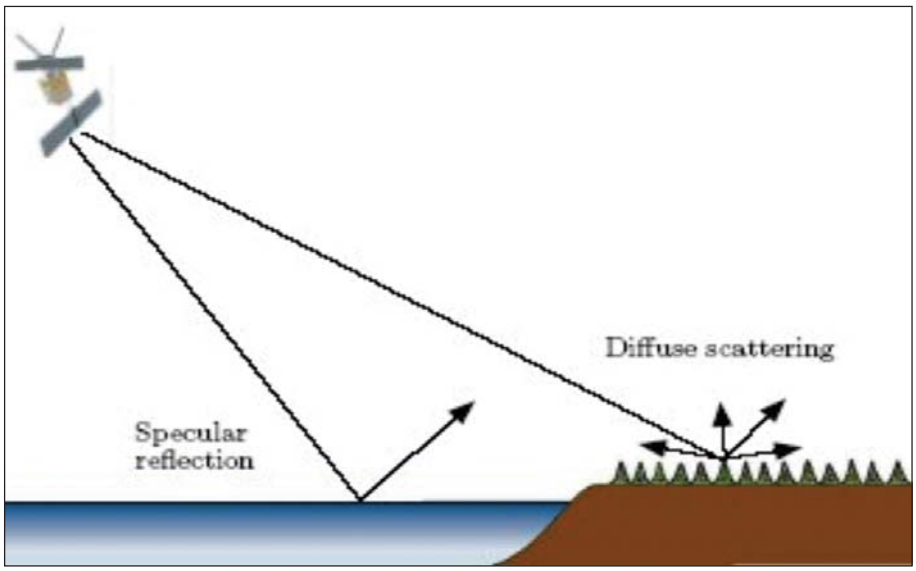

Figure 12.11: Scattering mechanisms of water bodies and dry land (source: Stian and Inger,2004)

The backscatter depends on the frequency, incidence angle, polarization and is sensitive to the ripples on the water surface induced by wind waves. Thresholding is the traditional method of detecting flooding in open areas. Intensities below the threshold are regarded as flood or open water, whereas pixels with intensities above the threshold are regarded as dry land. The threshold will depend on the contrast between the land and water classes, and generally needs to be set for each SAR scene.

Example:

We observe that for the 45º incidence angle case the water and land modes are easily separable with the proposed threshold, whereas the proposed threshold at 23º incidence angle introduce classification errors (Figure 12.12). This is because the contrast decreases with decreasing incidence angle, and the two modes of the histogram merge together (Stain and Inger, 2004).

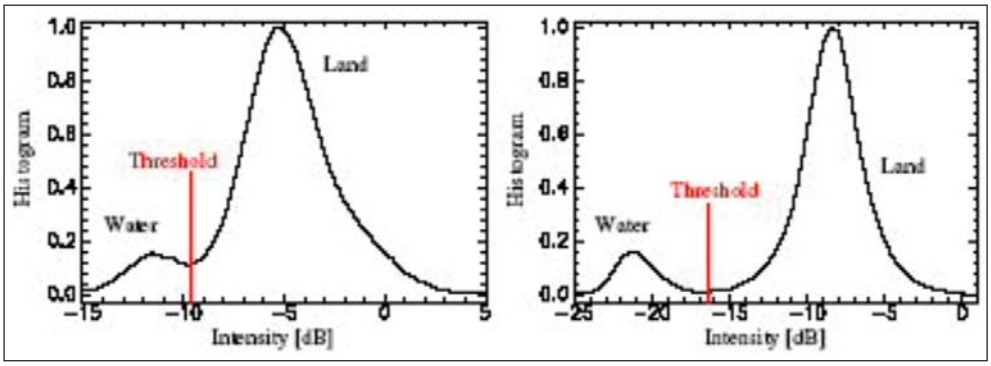

Figure 12.12: Histograms of two SAR images covering same area with different incidence angles (Left: 23⁰ & Right: 45⁰), (source: Stian and Inger,2004)

12.2.3.3. Methodology

Before the onset of flood season, pre-flood satellite data over flood prone states are acquired and analysed. River banklines, permanent water bodies and active river channel are extracted using digitization tools. These datasets and layers will be used as master data sets for further analysis.

Such pre-flood master layers are prepared every year for all the flood prone rivers in the country. The procedure is shown diagrammatically in Figures 12.13 and 14 for analysis of optical and microwave data respectively. The satellite data acquired during floods is geocoded with the respective master data sets. In case of optical data, supervised classification is performed using the infra red band by providing about 10 training classes in water at

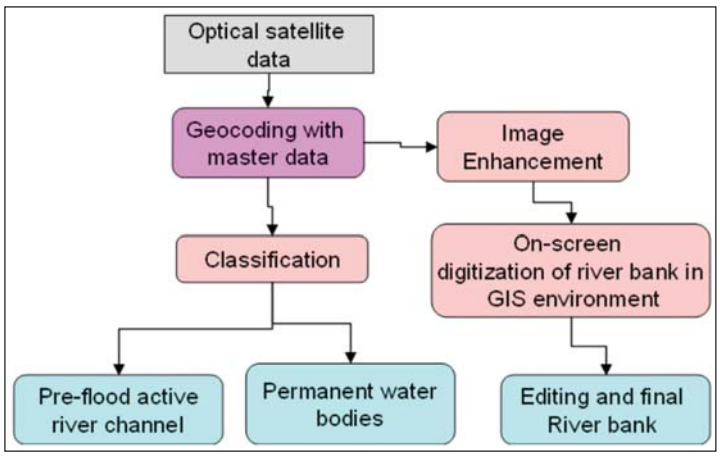

Figure 12.13: Flow chart for pre-flood analysis of optical data

river bank. The flood inundation layer is prepared in 2-bit consisting of the pre-flood river bank, permanent water bodies, active river channel as one theme and flood layer as the second theme. A single-bit flood inundation layer is also generated for estimation of damage statistics. The final flood inundation layer is converted from raster to vector format for composition of a flood map and generation of damage statistics.

12.2.4. Flood Inundation Products

The satellite data analysis and extraction of flood inundation layer is carried out using imaging software package and flood products are generated in ARCINFO environment using ARC GIS software.

12.2.4.1. Flood Maps

A database consisting of base layers like administrative boundaries (state, district, taluk, mandal), roads, railways and settlements, airport locations, district headquarters,

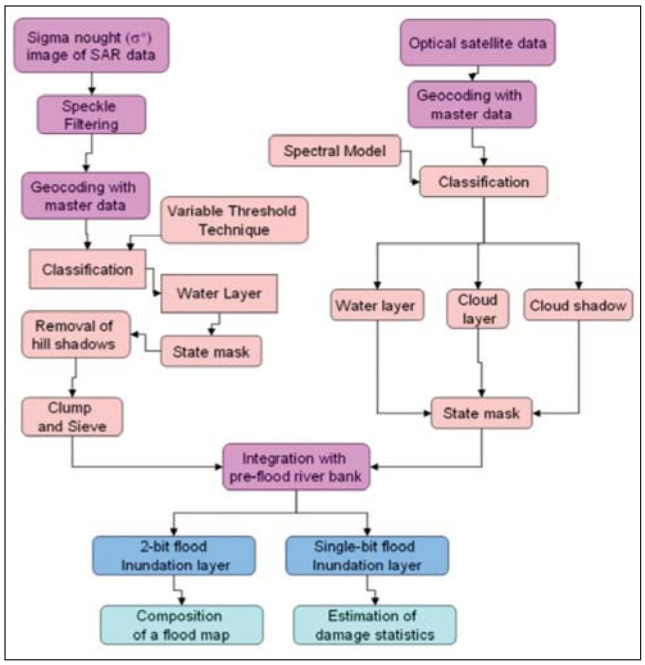

Figure 12.15: Methodology for analysis of satellite data during floods

different pockets. A cloud mask and a cloud shadow mask are also prepared. Since signature of cloud edges mixes with the water signature, a model was developed to classify water and cloud using different spectral bands for AWiFS data. Figure 12.15 shows the steps involved in the analysis of satellite data.

In case of SAR data, sigma nought is generated and using variable threshold model, water is classified (Srinivasulu *et al.*, 2005). Post editing tools are applied and final flood layer is prepared. The flood inundation layer is prepared by integrating the water layer with the pre-flood active river channel, permanent water bodies and

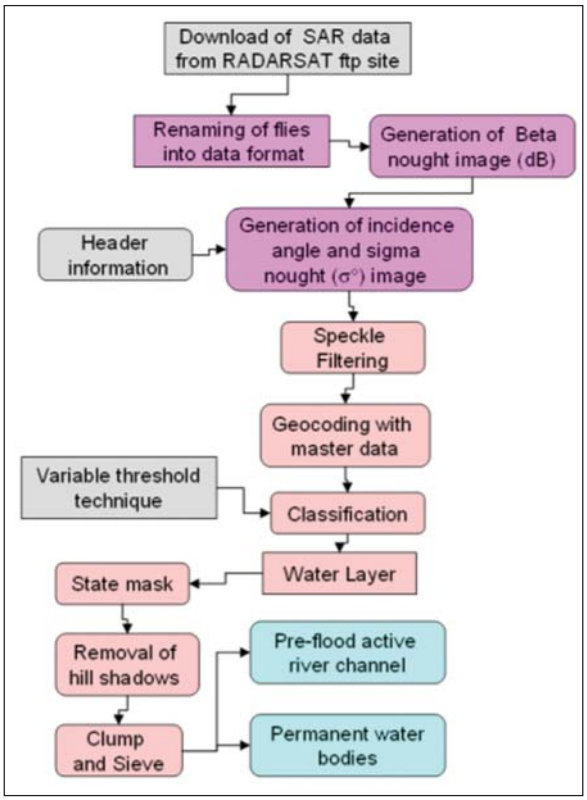

Figure 12.14: Flow chart for pre-flood analysis of microwave SAR data

villages, landuse/landcover are prepared for each state. Flood map templates are created at 1: 1 Million, 1:500,000 1:250,000 and 1:50,000 scale using the above layers. From the satellite data, pre-flood river bank and permanent water bodies layers are prepared before the onset of the flood season, as discussed earlier. During flood season, the flood inundation layer which is generated after the analysis of satellite data, is also stored and updated in the database. Table 12.5 shows the database layers used for generation of flood inundation information. Using flood templates and the inundation layer, flood maps are composed at state / district level and for selected areas at detailed level.

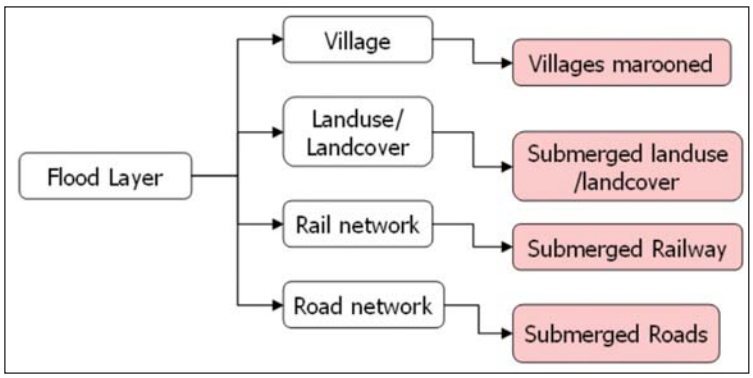

Figure 12.16: Generation of damage statistics

villages marooned, length of road and rail network submerged are estimated. Figure 12.16 illustrates the steps diagrammatically.

A detailed flood report is prepared describing the flood situation, the actions taken, the observations made from the analysis and the flood damage statistics.

The flood products are disseminated to the concerned user departments by digital means through e-mail system as well as by surface mail.

For effective and fast dissemination of the flood products and to reduce the turn-around-time, the control room at Decision Support Centre (DSC) is equipped with an extended C-band network through EDUSAT satellite linkage. It is connected to 9 primary user nodes (NRSC, PMO, CWC, IMD, SAC, NEOC, knowledge institutes, etc.) with the central hub at New Delhi. Through this VPN network, all the flood products in pdf format are transferred to the data computer system at the user end.

12.3. Case Study – 2006 Floods in Bihar, India

Bihar, the land-locked central Indian state that lies in the Gangetic basin, accounts for 16.5% of the flood-prone area and 22.1% of the flood-affected population in India. Out of 94.16 Lakh ha of geographical area, 68.80 Lakh ha is flood prone and 30 out of 37 districts of Bihar are flood-prone. According to statistics, the flood-prone area of Bihar has nearly tripled from 2.5 million hectares in 1954 to 6.8 million hectares in 1994.

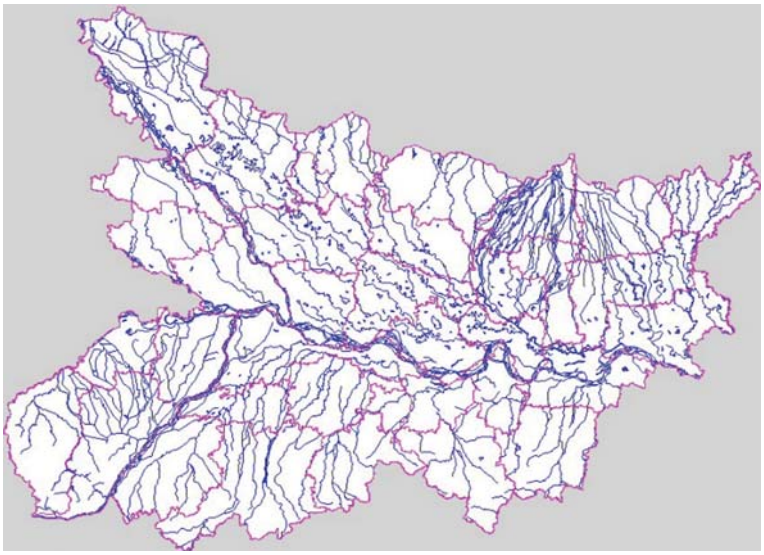

Figure 12.17: River stream network in Bihar

The rivers that regularly inundate the plains are the Ganga, Kosi, Gandak and Son. North Bihar plains are drained by an extensive networks of rivers most of which flow into the Ganga and has their part of catchment in the Nepal, Himalaya. These rivers carry high discharges and large quantities of sediments from the slopes of Himalayas and to the depth of the sediments in the lower flatter areas before their confluence with the Ganga causing reduction in channel

12.2.4.2. Flood Damage Assessment

The flood inundation layer is intersected with the district layer and district-wise flood inundation area statistics are generated. Similarly, for detailed damage assessment, the flood layer is intersected with village boundaries; transport network; landuse/ landcover; and damage statistics such as

Table 12.5: Database layers

S.No	Layers
1	**Administrative boundaries** – International – State – District – Taluk/Mandal/Block – Village Road – National Highway – Major Roads – State Highway – District Road – Village Road – Other Roads Railway Settlements Landuse/Landcover – Kharif crop – Double crop
2	**Pre-flood/water bodies**
3	Flood Inundation layer
4	Cloud cover

capacities. South Bihar also experiences floods due to excess discharges in the tributaries of the Ganga like the Sone, the Punpun, the Kiul and the Harohar which accumulate in the lower natural depressions whose drainage depend on the stages prevailing in the Ganga. Figure 12.17 shows drainage networks in Bihar state with Districts boundaries.

During 2006, Bihar reeled under floods during the months of June, July, and September. The water levels of River Ganga, its tributaries, Kosi, Bagmati and few others were above the danger level. Most of the districts in the state were affected due to floods. DSC has monitored the flood extent by analysing 12 satellite data sets and prepared 16 flood maps at different levels. Flood damage statistics were estimated and the information was disseminated to the concerned user departments.

Figure 12.18a shows the IRS-P6 AWiFS pre-flood image of Bihar, Figure 12.18b shows the extracted river bank and water bodies from this image, Figure 12.18c shows the Radarsat image of 28-29 Sep 2006 acquired during floods and Figure 12.18d shows the extracted flood inundation layer from Radarsat image.

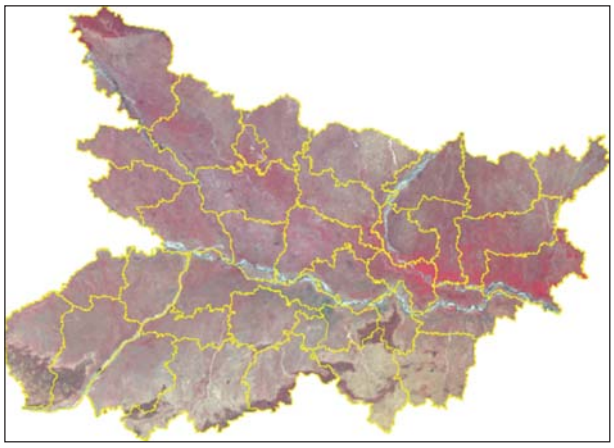

Figure 12.18a: Pre-flood AWiFS image of Bihar state

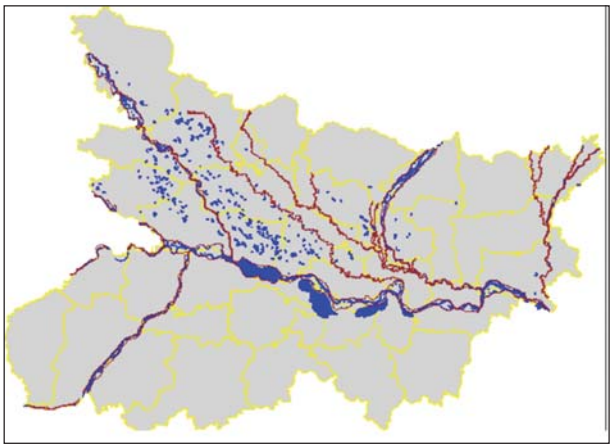

Figure 12.18b: River bank and permanent water bodies

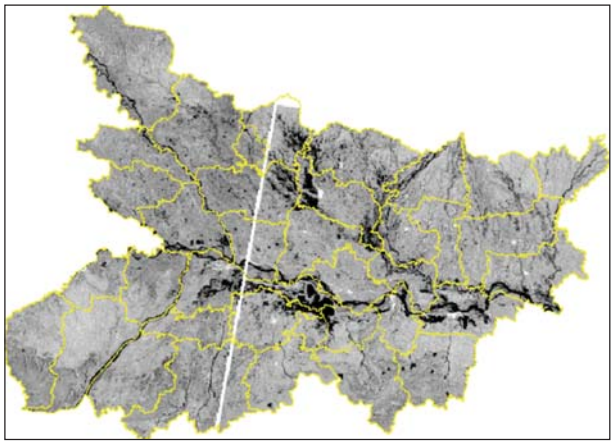

Figure 12.18c: Combined Radarsat image of 28 & 29 Sep., 2006 acquired during flooding

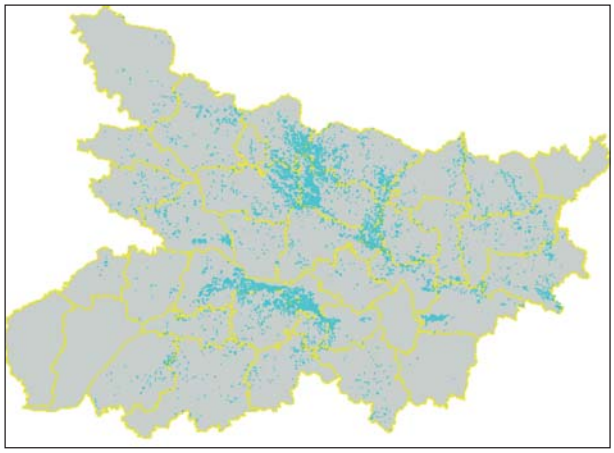

Figure 12.18d: Extracted single-bit flood inundation layer from 28 & 29 Sep., 2006 image

The flood layer of 28th and 29th September 2006 were combined and the map was prepared for the entire state.

Figure 12.19 shows the flood map at state level showing the spatial flood extent in each district overlaid with transport network and pre-flood water bodies layer.

Figure 12.20 shows a district flood map for Nalanda district in Bihar based on the analysis of Radarsat data of 18-July-2006. This map shows the submerged railway and roads with settlements and taluk boundaries.

Figure 12.21 shows the detailed flood map at 1:50,000 scale for part of Darbhanga district showing the inundated villages in the district, based on the analysis of IRS-LISS-IV MX data of 28-Sep-2006. LISS-IV MX sensor aboard IRS-P6 satellite has a spatial resolution of 5.8 m with a swath of 23 Km is suitable for detailed level flood mapping.

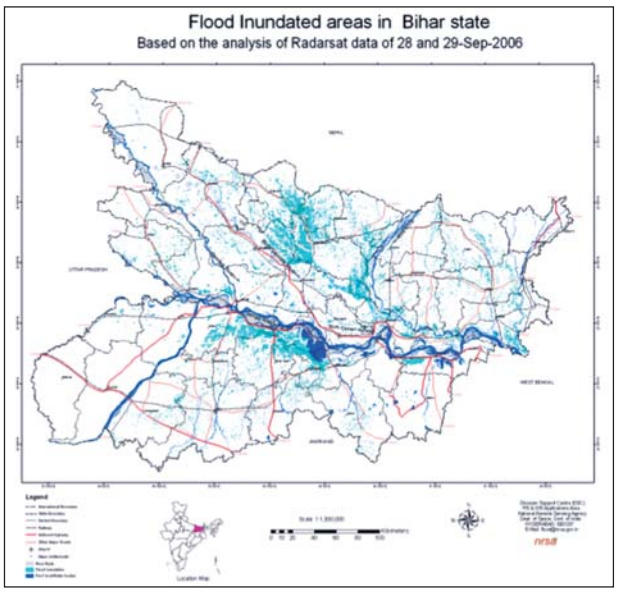

Figure 12.19: Bihar state flood map based on the analysis of Radarsat data of 28 & 29 Sep., 2006

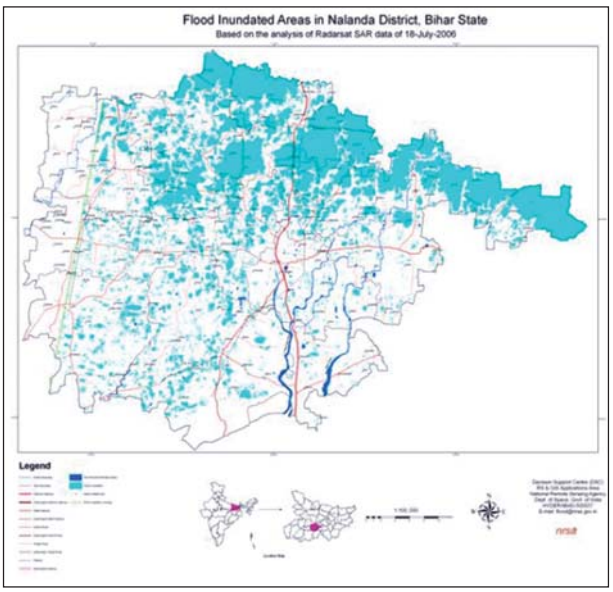

Figure 12.20: A district-wise flood map for Nalanda district based on the analysis of Radarsat data of 18 July., 2006

Figure 12.22 shows the increase in the flooded area in part of Bagmati river basin during June to Oct 2006. This monitoring of floods at regular interval of time was possible through meticulous planning and acquisition of satellite data.

Further, all the flood inundation layers acquired during 2006 were integrated and the maximum extent of flooding observed from these datasets was extracted. During 2006 flood season, about 11, 28,902 hectares of area was inundated in Bihar. Figure 12.23 shows the maximum flood inundation in Bihar during 2006.

12.4. River Configuration and Bank Erosion Aspects in Flood Control Planning

Most of the flood prone rivers in India change their course frequently after every flood wave attacking strategic locations at different times. During floods, bank erosion takes place due to high inflows, excessive sediment charge and channel shift of the river on either side of the river banks takes place. As the discharge of the stream increases, the depth and the mean velocity increases, due to which river banks are subjected to greater erosive action. An increase in the discharge increases high stream power of the flow and would cause more bank erosion. As the severity and effect of hydraulic forces increase manifold during the flood, the rate of erosion increases rapidly. Further physical modelling studies for river flood control planning to study river behaviour needs latest accurate information on river configuration. Hence, it is necessary to understand the behaviour of the river and its latest configuration so as to plan the flood control measures effectively. At the same

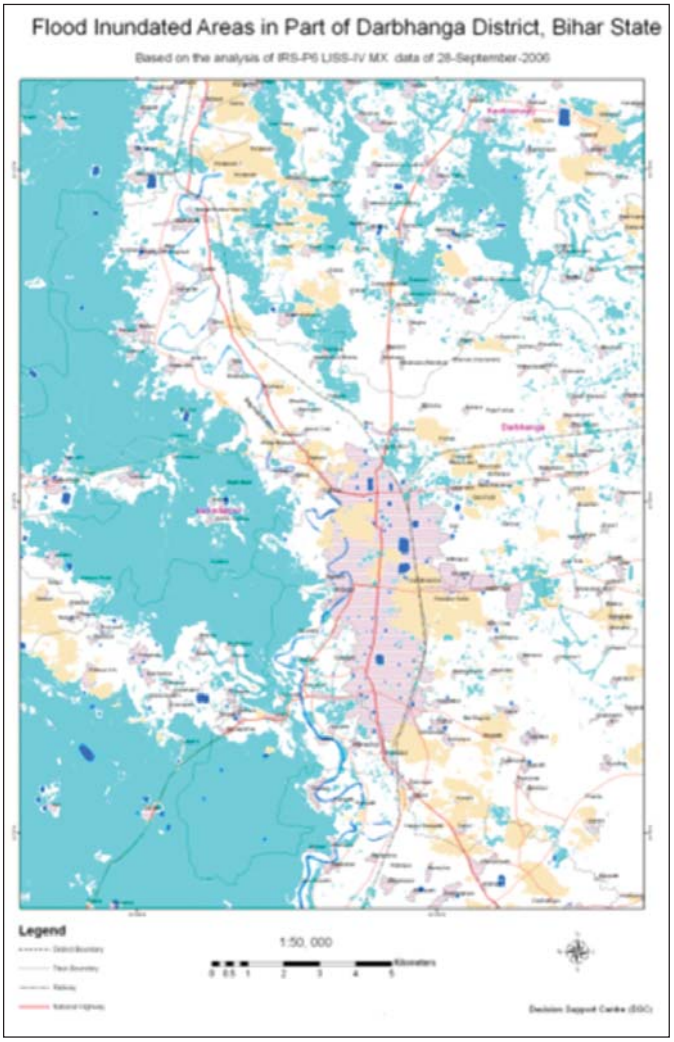

Figure 12.21: Detailed flood map showing the inundation in and around Darbhanga town in Bihar based on the analysis of IRS-P6 LISS-IV MX data

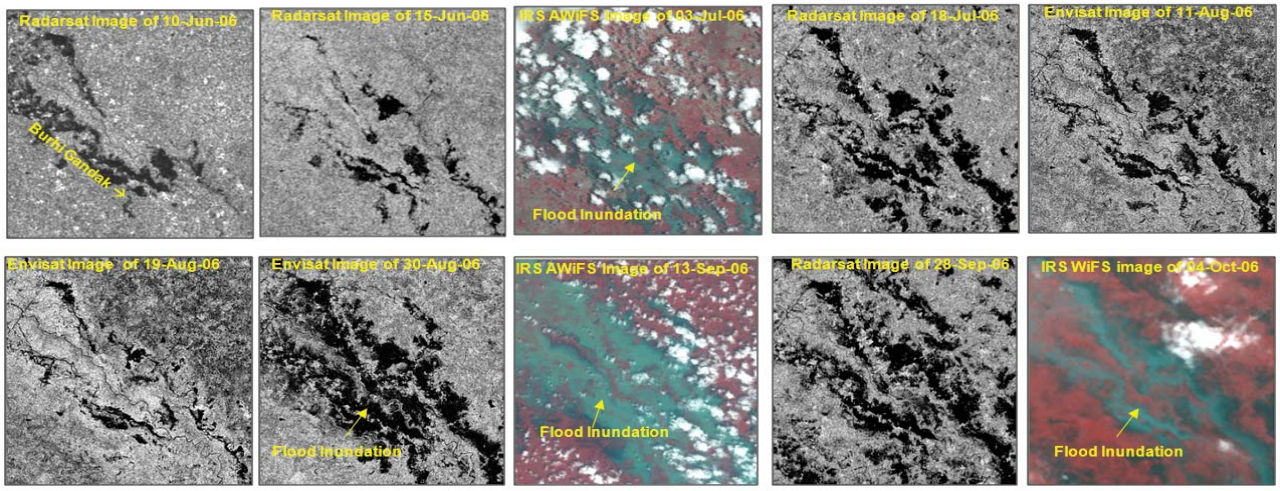

Figure 12.22: Continuous monitoring from June to Oct., 2006

time it is equally important to monitor the existing flood control structures from time to time to avoid breaches in view of the frequent changes in river configuration.

For flood mitigation, major thrust was given for structural measures such as construction of embankments mostly in Assam, Bihar, UP & West Bengal in India. Other measures like channel improvements, raising villages, selective dredging etc., have been tried at some locations. Though embankments have controlled the flood to some extent, but they have inadvertently added severe problems like drainage congestion in the countryside. Greater threat to the people was created in cases of failures of embankments. The building up of the riverbeds because of the high silt content which deposits down is another problem that has been faced. Anti erosion measures that are needed to protect the embankments in vulnerable reaches are found to be very costly and often required more than the original outlay on the embankments they seek to protect. Therefore flood risk zone mapping was found to be one of the non-structured measures.

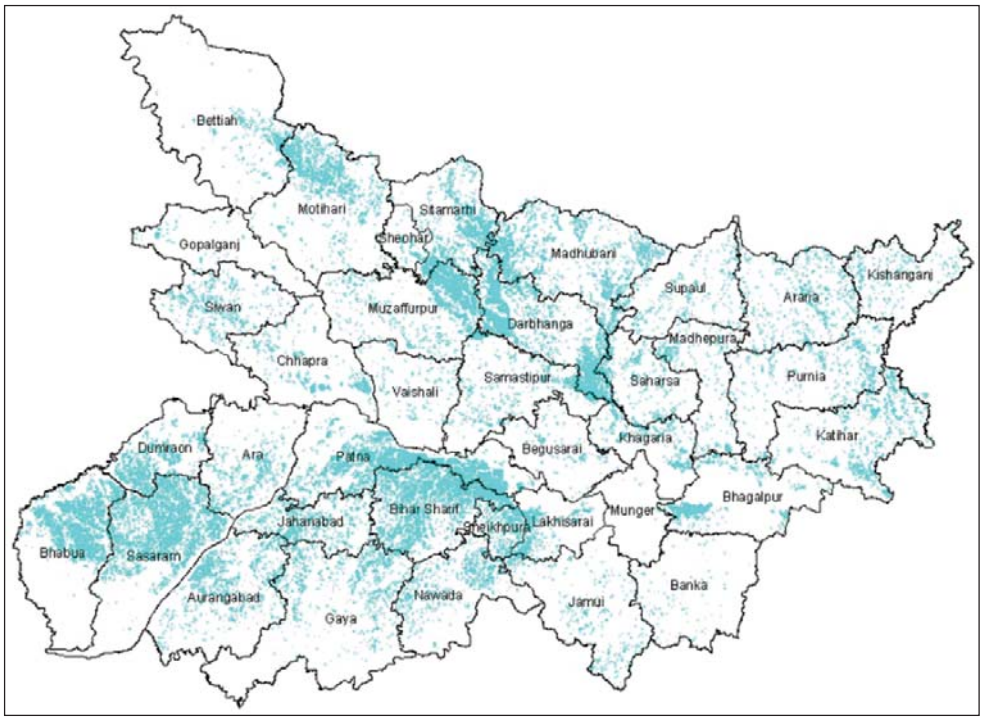

Figure 12.23: Maximum flood inundation map for Bihar during 2006

12.4.1. Potential use of Satellite Data

Conventional method for river configuration mapping is time consuming and expensive. In the recent years, Satellite Remote Sensing Technology has successfully proven itself as a valuable information generator for various river engineering studies. The potential of remote sensing data is that it is highly reliable, accurate and cost effective. Using LISS-III/IVMX and CARTOSAT -1 & 2 PAN data of Indian Remote Sensing (IRS) satellites, the latest river configuration, shift in the river courses, formation of new channels/oxbow lakes, bank erosion/deposition, drainage-congested areas, etc. can be mapped at different scales. Since accurate river configuration is obtained, it can be

nrsc

Remote Sensing Applications

P. S. Roy
R. S. Dwivedi
D. Vijayan

National Remote Sensing Centre

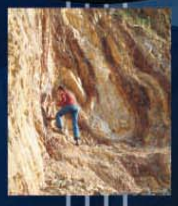

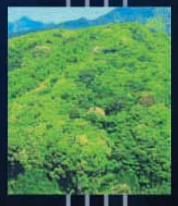

Remote Sensing Applications

Agricultural Drought Monitoring and Assessment

13.1. Introduction

Drought is a climatic anomaly, characterized by deficient supply of moisture resulting either from sub-normal rainfall, erratic rainfall distribution, higher water need or a combination of all the three factors. Several definitions of drought are available in literature. In India, National Commission on Agriculture (1976) has categorized drought into three types, viz., meteorological drought, hydrological drought and agricultural drought based on the concept of its utilization.

In meteorological terms, a drought is "a sustained, regionally extensive, deficiency in precipitation". All other definitions are related to the effect or impact of below normal precipitation on water resources, agriculture and social and economic activities; hence the terms hydrological drought and agricultural drought. In quantitative terms, the definitions could vary among countries and regions. In India, the definition for "meteorological drought" adopted by the Indian Meteorological Department (IMD) is a situation when the deficiency of rainfall at a meteorological sub-division level is 25 per cent or more of the long-term average (LTA) of that sub-division for a given period. The drought is considered "moderate", if the deficiency is between 26 and 50 per cent, and "severe" if it is more than 50 per cent. Based on this definition, the National Commission on Agriculture has given the following broad classifications:

Hydrological drought is a prolonged meteorological drought situation resulting in depletion of surface water from reservoirs, lakes, streams, rivers, cessation of spring flow and fall in groundwater levels causing severe shortage of water for livestock and human needs.

Agricultural drought is a situation when rainfall and soil moisture are inadequate during the crop growing season to support healthy crop growth to maturity, causing crop stress and wilting. It is defined as a period of four consecutive weeks (of severe meteorological drought) with a rainfall deficiency of more than 50 per cent of the LTA or with a weekly rainfall of 5 cm or less during the period from mid-May to mid- October (the Kharif season) when 80 per cent of the country's total crop is planted, or six such consecutive weeks during the rest of the year. The National Oceanic and Atmospheric Administration (NOAA) defines agricultural drought as a combination of temperature and precipitation over a period of several months leading to substantial reduction (less than 90%) in yield.

Drought differs from other natural hazards in many respects -most complex and least understood of all disasters. While it is difficult to demarcate the onset and end of drought but the effects of drought accumulate for a considerable period of time. Prolonged droughts or abnormal weather conditions such as extended winters, cold summers, floods, biological factors like plague of locusts or rodents result in famines.

13.1.1. Drought impacts – the vicious circle

Practically all the developing countries, being primarily agrarian, are very much dependent on the vagaries of seasonal rainfall and climatic conditions. On an average, severe drought occurs once every five years in most of the tropical countries, though often they occur on successive years causing misery to human life and live stock. The crisis brought out by this hazard directly hit poorest and most deprived sections of our society thus destroy the life, economy, infrastructure, environment and society because all are inter linked.

Drought results from adverse (figure 13.1) climatic conditions leading to deleterious impacts on various sectors of the economy. The immediate impact is on crop area, crop production and farm employment. Reduction in income and purchasing power of farmers forces the small and marginal farmers to join the band of agricultural labourers leading to increase in unemployment. Speculation of poor farm harvest drives the food prices upwards. Market failure and advantage-seeking group work in perfect nexus to intensify the impact of drought. The effect of this nexus are catastrophic particularly to small and marginal farmers who constitute the large chunk of farming community, who tend to migrate obviously to urban areas in search of employment opportunities. Shortage of drinking water and starvation for food are the other consequences that emerge. Fodder problem drives away the animals to distress sales. Thus climate is the initial causative factor for drought, the implications and intensity of drought are manifested by human interactions with the situation leading to famines.

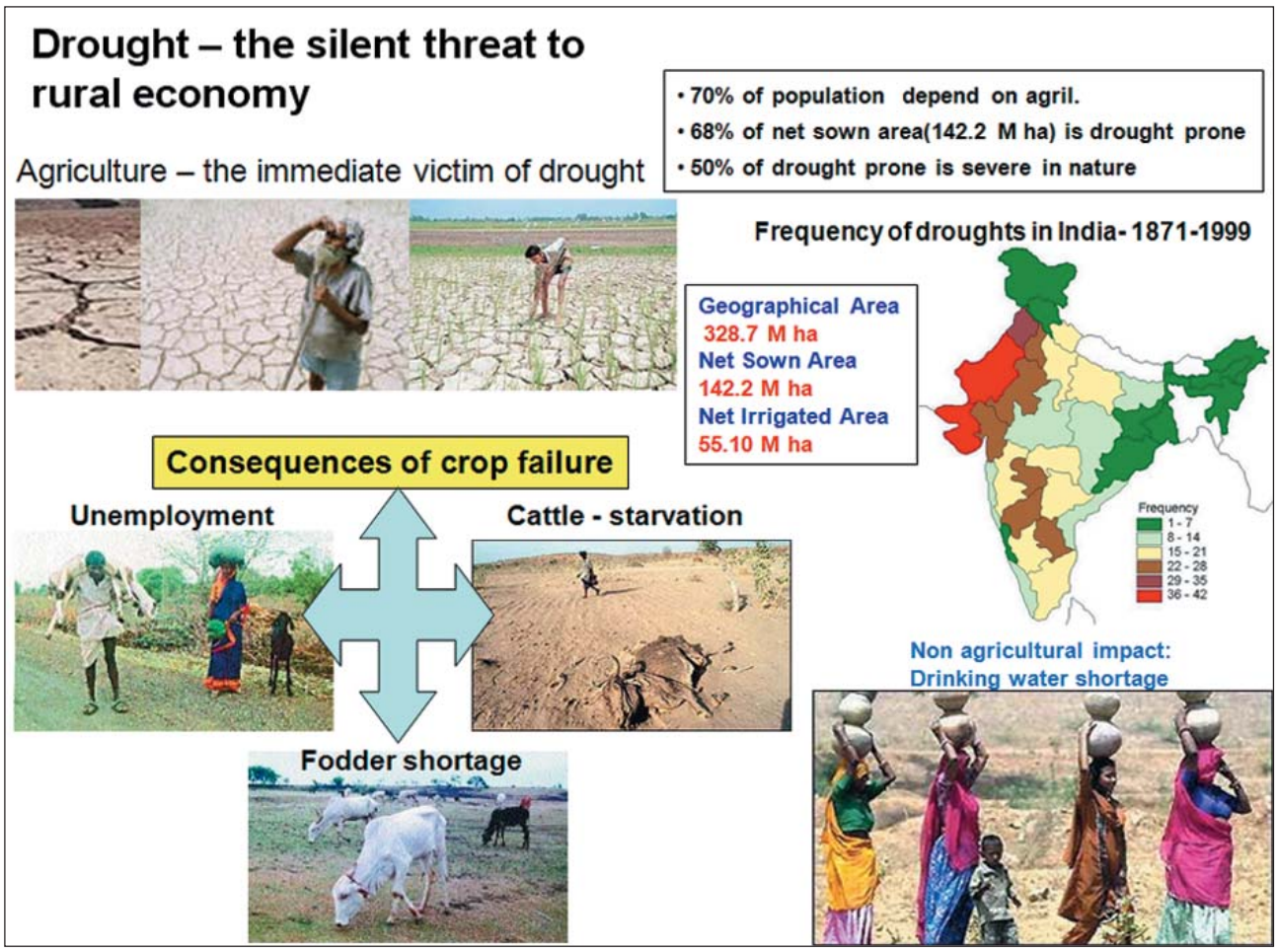

Figure 13.1: Multidimensional impacts of drought

13.1.2. Drought scenario in India

Indian economy is largely dependent on agriculture with more than 70% of the population depending either directly or indirectly on agriculture for their livelihood. Owing to abnormalities in the monsoon precipitation, in terms of spatial and temporal variation, especially, late onset of monsoon, prolonged break and early withdrawal of monsoon; drought is a frequent phenomenon over many parts of India. About two thirds of the geographic area of India receives low rainfall (<1000 mm), which is also characterized by uneven and erratic distributions. Out of net sown area of 140 million hectares about 68% is reported to be vulnerable to drought conditions and about 50% of such vulnerable area is classified as 'severe', where frequency of drought is almost regular. India experiences localized drought almost every year in some region or other. In the post independence era, major droughts that affected more than 1/3rd of the country were reported during 1951, 1966-67, 1972, 1979, 1987-88 and 2002-03 (Subbaih, 2004). Thus, despite significant technological advances since independence, Indian agriculture continues to be periodically affected by droughts (Table 13.1).

Abnormally low rainfall in 1979, reduced the overall food grain by as much as 20%. The 1987 drought damaged 58.6 million hectares of cropped area affecting over 285 million people. The 2002 drought had reduced the sown area to 112 million hectares from 124 million hectares and the food grain production to 174 million tons from 212 million tons, thus leading to 3.2% decline

Table 13.1: Drought history of India

Period	Drought years	No. of years
1801-25	1801,04,06,12,19,25	6
1826-50	1832,33,37	3
1851-75	1853,60,62,66,68,73	6
1876-1900	1877,91,99	3
1901-25	1901,04,05,07,11,13,15,18,20,25	10
1926-50	1939,41	2
1951-75	1951,65,66,68,72,74	6
1976-02	1979,82,85,87,2002	5

(Source: Kulshreshta and Sikka, 1989)

in agricultural GDP. The total food grain production in India has to be stepped up from 212 million metric tons to 300 million metric tons by 2020 to meet the food demands of growing population.

13.1.3. Droughts – the global scenario

All the developing countries, being primarily agrarian, are very much dependent on the vagaries of seasonal rainfall and climatic conditions and hence more vulnerable to droughts. On an average, severe drought occurs once in every five years in most of the tropical countries, though often they occur on successive years causing severe losses to agriculture and allied sectors. More than 500 million people live in the drought prone areas of the world and 30% of the entire continental surface is affected by droughts or desertification process. In 2004, wide spread drought in much of Asia resulted in loss of agricultural production of hundreds of million dollars. In Thailand, drought hit 70 of 76 provinces and affected more than 8 million people. Southern Chines island of Hainan suffered its worst drought in 50 years during 2004. Vietnam's eight central highland provinces suffered severe drought in 2004. The direct impacts of droughts are wide ranging; physical, social, economical and environmental (Rathore, 2004). Drought prone areas of the world are depicted as (1) frequent and intensive (2) less intensive drought prone areas in Figure 13.2. Nearly 50 per cent of the world's most populated areas are highly vulnerable to drought. More importantly, almost all of the major agricultural lands area located there (USDA 1994). In the world's two largest agricultural producers, the United States and the former Soviet Union (FSU), drought occur almost every year.

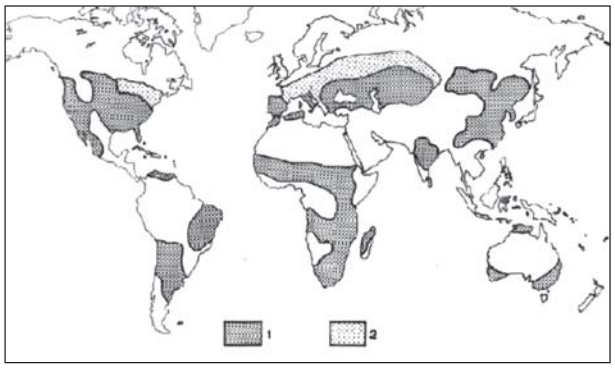

Figure 13.2: Drought prone areas of the World (source: Goldsberg,1972)

USA is the world's second largest grain producer accounting for 70% of corns and 60% of coarse grains and 30% of wheat (FAO 2000). Drought is typical for north American climate and occurs almost every year. USA had experienced many droughts and dry spells in the last century which had significant impact on economic, social and environmental sectors. Recent drought with devastating effect is that of 1988 drought which cost around $40 billions. The 1988 drought ranks as one of the nation's greatest disasters of 20th century. Yields of agricultural crops dropped so sharply that grain production fell below domestic consumption probably for the first time in the last half century (Kogan 1995). Other major droughts of the last 15 years included 1989 and 1996 which were quite similar.

In Europe, drought is a problem in the southern countries along the rim of the Mediterranean (Croatia, France, Greece, Italy, Slovenia and Spain). Over the past 1000 years of Russian history, catastrophic droughts occurred eight to twelve times in every century (Kogan 2000).

In Latin America and the Caribbean, the drought associated with the El Nino has severe impact. For example, after the El Nino of 1983, Peru's GDP fell by 12 percent, mostly because of a reduction in agricultural output and fishery. The national economy took a decade to recover. Damage in the Andean community countries (Bolivia, Colombia, Ecuador, Peru and Venezuela) due to the 1997-98 El Nino was estimated at more than US$7500 million (www.octi.gov.ve). The Caribbean countries that are highly vulnerable for drought are Antigua, Cuba, Guyana, Haiti and Jamaica.

West Asia is arid and vulnerable to drought with rainfall scanty and variable (ACSAD 1997). Nearly 80% of the region is classified as semi-desert or desert (AOAD 1995). Drought is the most important natural disaster in the region. The rainfall appears to be declining in some countries bordering the Mediterranean Sea. Over the past 100 years, precipitation has decreased by more than 5 per cent over much of the land bordering. Mediterranean with few exceptions such as Libya and Tunisia (IPPC 1996). The region suffered from drought during 1930s, 1960s and the 1990s. Cycles of drought have become intense and more frequent. The 1998-99 drought affected many countries and Syria was the worst hit, suffering its worst drought in 25 years (FAO 1999).

13.2. Monsoon pattern in India

About 70% of the annual rainfall over India is contributed by south west monsoon which commences in the month of May from the southern tip. Normally, the monsoon arrives in Sri Lanka and over the islands of the Bay

of Bengal in the last week of May and reaches the extreme south of the Indian peninsula a week later. Then the monsoon advances in two directions as the Arabian sea branch (covering towards Mumbai) and Bay of Bengal branch (covering towards Assam). On reaching the southern periphery of the Himalayans, the Bay of Bengal branch deflects towards west covering gangetic plains. The Arabian seas branch covers central India and merge with Bay of Bengal branch to form a single current. Western UP, Haryana and Rajashtan states experience the first showers by first of July. By mid July, the monsoon extends to Kashmir area. The normal duration is roughly 100 days and its withdrawal starts from Punjab and Rajasthan by mid of September.

The normal rainfall during south west monsoon rainfall is 890 mm for the country as a whole, and it is 611 mm in north-west India, 994 mm in central India, 723 mm in southern India and 1427 mm in north east India. Out of 890 mm of normal rainfall in the country, June month accounts for 162 mm followed by 293 mm in July, 262 mm in August and 175 mm in September (www.imd.gov.in).

The onset of north east monsoon is not well defined and on many occasions there is no clear indication on the withdrawal of south west monsoon and onset of north east monsoon. Therefore, it is a general understanding that the rainfall in the winter months from October to December represents the northeast monsoon. Tamil Nadu state receives significant rainfall from north east monsoon, and it is about 463 mm representing 48 % of annual rainfall of the state (Das, 1968).

13.3. Agricultural Drought Monitoring & Assessment

The immediate and more devastating impact of drought is on agricultural crops leading to loss of production, unemployment, fodder shortage etc. The water needs in agricultural sector are going to be very high, as several thousand tons of water is required to produce each metric ton of food grains. Therefore, there is a need for effective monitoring of agricultural drought, its onset, progression and impact on crops to minimize the damages.

Monitoring and assessment of drought conditions at different scales and timely dissemination of information constitute the most vital part of drought management system. Inadequate system for monitoring the drought, unreliable data points, lack of standard procedures to calculate indices of drought prevalence and intensity could lead to inefficient management strategies. Therefore, the need is to have a sound, operationally feasible, objective and economically viable system for drought monitoring and analysis. Conventionally agricultural drought conditions are characterized by ground observations on meteorological parameters such as rainfall, aridity and agricultural parameters such as sown crop area, crop condition and crop yield.

13.3.1. Meteorological indicators

Rainfall is the most important single factor influencing the incidence of drought and practically all definitions use this variable either singly or in combination with other meteorological elements. Many studies have studied the nature and frequency of droughts based on simple relation between actual and average rainfall.

Based on rainfall, temperature, soil moisture and evaporation, various indicators of meteorological drought have been developed by researchers as shown in Table 13.2. Some of these indices like Palmer's index, Standardized Precipitation Index, Crop Moisture Index are being used operationally in some of the countries. Gibbs and Meher (1967) made a study of drought in Australia by using annual rainfall deciles as drought indicator. Using a network of 100 stations, maps have been prepared showing the decile ranges in which rainfall for each year has occurred. Van Rooy (1965) developed a drought anomaly index based on the ratios of rainfall departure from normal to the departure of threshold value from normal. The threshold value was taken as the average of the lowest ten values in series. Bhalme and Mooley (1980) developed a numerical index which is comparable in space and time, based on monthly rainfall and duration. They devised a scale, which ranged from -4 to +4 on the basis of which droughts were classified.

Table 13.2: Meteorological indicators of drought

Year	Index
1916	Munger's Index
1919	Kincer Index
1930	Morkowitch Index
1942	Blumenstock Index
1954	Antecedent precipitation index
1957	Moisture adequacy index
1965	Palmer's index (PDSI, PHDI)
1968	Crop Moisture Index
1968	Keetch Byram Drought Index
1981	Surface water supply index
1993	Standardized precipitaion index

Standardised precipitation index was developed by Colarado state university (Mc Kee *et al.*, 1993, 1995) to improve drought detection and monitoring capabilities. It is based on precipitation alone. Its fundamental strength is that it can be calculated for a variety of time scales. This versatility allows the SPI to monitor short term water supplies, such as soil moisture, important for agricultural production and long term water resources such as ground water supplies, stream flow and lake and reservoir levels. The ability to examine different time scales also allows droughts to be readily identified and monitored for the duration of the drought. Calculation of SPI for a specific time period at any location requires a longterm precipitation database with 30 years or more of data. The probability distribution functions are determined from the long term record by fitting a function to the data. The cumulative distribution is then transformed using equal probability to a normal distribution with a mean zero and standard deviation one, so the values of SPI are really in standard deviations. SPI values generally ranges from +2 to -2, from extremely wet to extremely dry conditions respectively (Mc Kee *et al.*, 1993, Wu *et al.*, 2006).

In 1965, WC Palmer developed an index to measure the departure of the moisture supply (Palmer, 1965). Palmer based his index on the supply-and-demand concept of the water balance equation, taking into account more than just the precipitation deficit at specific locations. The objective of the Palmer Drought Severity Index (PDSI), as this index is now called, was to provide measurements of moisture conditions that were standardized so that comparisons using the index could be made between locations and between months (Palmer 1965). The PDSI is a two layer moisture model. Palmer introduced the concept of CAFEC (Climatically approximate for the existing conditions) rainfall, which was normal for a given place. The anomaly between the CAFEC and actual precipitation is used as a drought indicator. To make this anomaly comparable in space and time, it is multiplied by a weighting factor K which depends on average moisture demand and supply and mean of the absolute values of anomaly of the place. The classification of drought intensity based on Palmer drought index is +4 representing extremely wet and -4 representing extremely dry conditions.

There are considerable limitations when using the Palmer Index, and these are described in detail by Alley (1984) and Karl and Knight (1985). Apart from the climatological parameters, physical parameters like canopy-air temperature differences have also been used for assessing the stress degree days (SDD) to indicate the impact of drought. The SDD have been found to correlate well with the yield fluctuations as a result of moisture stress. Also spectral ratios of infrared to red reflectance obtained from radiometers (Satellite or ground based) can be used to monitor the agricultural effects of drought based on the observed rate of change of absorbed radiation expressed as a fraction of the maximum rate.

The India Meteorological Department (IMD) prepares rainfall maps on sub-divisional basis every week throughout the year. These maps show the rainfall received during a week and corresponding departures from normal. During monsoon season, these maps are indicative of development of drought. In addition, IMD also provides the information on weekly rainfall and its deviation from normal at district level for the entire country. This information is useful to identify the districts with deficit/scanty rainfall and the prevailing meteorological drought.

IMD also monitors drought using water balance technique which addresses agricultural drought. The aridity index is calculated using the formula;

Aridity Index = (Actual Evapotranspiration – Potential Evapotranspiration) / Potential Evapotranspiration

The departure of aridity index from normal percentage terms is used to define the various categories of drought severity. Anomaly upto 25 % is attributed to mild drought, 26-50% to moderate drought and >50% to severe drought. IMD has been bringing out weekly aridity anomaly charts from 1979 onwards, based on data from different observatories, covering south west monsoon period. These charts show the departures of actual aridity from normal aridity giving indication of the severity of water deficit to water demand relationship on weekly basis. IMD is also preparing detailed maps of rainfall, temperature (maximum and minimum), cloud cover, relative humidity and analyze this information with prevailing crop conditions and an Agromet Advisory Bulletin is prepared and disseminated to users.

13.3.1.1. Limitations of using rainfall as agricultural drought indicator

Many studies have proved that spatial and temporal distribution of rainfall is more important than the total rainfall in a month or season. A review of past agricultural droughts in the country reveal the lack of unique

relationship between incident ground measured rainfall (only a part of which replenishes soil moisture and thus available to vegetation) and the resulting vegetation development within and between seasons as well as across space. The “rainfall use – efficiency” varying over both time and space and the vegetation species dependence limits the use of rainfall as a sole or major agricultural drought indicator. Rainfall as an agricultural drought indicator is limited by the sparse ground observations (especially in view of high spatial variability of tropical rainfall) as well as the lack of spatially and temporally unique relationship between incident rainfall and vegetation development. Though the daily reporting network of IMD is supplemented by the State Government rain-gauge network in each state, real-time information from the latter is normally limited to rain-gauges located at Tahsil Headquarters. The possibility of observational errors also makes it necessary to process this data prior to its use leading to time delays. Aridity anomaly data currently available is only representative of large areas such as meteorological sub-divisions. The aridity anomaly also suffers from the same limitations as that of rainfall.

13.3.2. Water Balance Approach

Using the soil characteristics and initial soil moisture values, weekly/monthly water balance computations can be carried out. If monthly water balances are to be calculated input data required by the model consists of monthly values of precipitation, $\boldsymbol{P_m}$, and potential evapo-transpiration, $\boldsymbol{PET_m}$ (calculated by any method appropriate to the region and available data). These values can be climatic-average values of a time period or actual monthly averages of a series of annual registers.

Also the model requires the soil-water storage maximum capacity, S_{max}

and the initial soil moisture content, $\boldsymbol{S_0}$. The water balance model will then calculate soil moisture content, actual evapotranspiration and runoff (here water surplus).

Soil moisture content

If for a given month $P_m > PET_m$, the soil moisture at the end of that month is then obtained as:

$S_m = \min \{(P_m - PET_m) + S_{m-1}, S_{max} \}$.

Otherwise, if $P_m < PET_m$, the soil moisture is given as:

$S_m = S_{m-1} * \exp (P_m - PET_m / S_{max})$

ii. Actual evapotranspiration (ET_m)

For the first of the cases, $P_m > PET_{m,}$

$ET_m = PET_m$, otherwise

$ET_m = P_m + S_{m-1} - S_m$

Water surplus

It is assumed that soils will only produce water surplus whenever the soil moisture content at the end of a month will equal its maximum water storage capacity. In that case water surplus, $\mathbf{T_m}$, will be calculated as

$T_m = P_m - PET_m + S_{m-1} - S_m$

Rainfall departures and Soil Moisture Index (SMI) values are useful for contingency crop planning based on the climatic conditions. Spatial distribution of weekly SMI (actual / available moisture) maps reveals moisture status spatially and temporally in a given area. Time to time contingencies can be suggested to the farmers, by closely monitoring the weather conditions during the season. The crop production strategies situation-wise alternate crops / cropping systems could be suggested.

13.3.3. Agricultural observations

Agriculture departments of different states collects information on crop sown areas, crop development, pests and diseases, etc., to assess the drought situation. A special task force known as Crop Weather Watch Group is constituted in India by Ministry of Agriculture. This group reviews the progress of monsoons, crop situations, water levels in reservoirs/dams, availability of fertilizers etc. Though the ground observations of agricultural conditions by the State Departments of Agriculture and Revenue are exhaustive such a system involves a significant amount of subjective judgment at various stages. The periodicity and extent of ground observations also

vary significantly between different states. The nature of sparse ground observations also make it difficult to assess, in near real-time, average drought conditions over the district. Thus ground monitoring of both causative factors as well as impact of drought assessment suffer from various limitations such as sparse observations, subjective data etc.

13.4. Drought information needs

Objective information on the prevalence of drought and its intensity along with its spatial and temporal dimensions is very critical for evolving drought combating strategies either of short term or long term. The information requirements of scientific/research organizations for effective drought assessment and the requirements of government functionaries and farming community for drought management at community level or farm level differ in various issues are shown in Table 13.3. For example, the needs of federal government are mostly at district level while district administration requires detailed drought information at sub district level such mandals/ taluks for generating and implementing technically feasible and economically viable drought management strategies.

Table 13.3: Requirements of drought information (Source: Roy et al., 2006)

	A. Information requirements for drought assessment
	Spatial rainfall on weekly basis
	Spatial aridity
	Spatial soil moisture (real time)
	Spatial crop condition
	B. Information requirements for drought management
1	**Beginning of the season** (a) Extent of delay in sowings (no. of days/weeks) (b) Extent of reduction in sown area (c) Expected sown area
2	**Middle/end of the season** (a) Impact of drought on standing crops. (b) Expected reduction in crop yield
3	**Scale of information** At different spatial units (mandals/taluks) within district Weekly/fortnightly information
4	**Quantitative assessment of drought impact** (a) Area affected by drought - list of drought affected mandals/taluks along with severity level.
5	Early warning on drought occurrence/severity
6	**Drought relief management** Prioritization of the areas in terms of drought severity level.

13.4.1. Gap Areas

The gap areas for technology development to meet the information needs for drought assessment and drought management are mentioned below:

- Geospatial data bases
- Use of new indices for drought assessment
- Data bases of drought related information
- Advanced tools for geospatial data analysis
- Spatial Decision Support System
- Climatic models for simulation of drought events
- Drought assessment at local scales
- Drought early warning
- Quantitative assessment of drought impact
- Institutional framework
- Drought information delivery mechanism

High quality data on drought related parameters and powerful geospatial tools for analyzing such data are required to address these gap areas.

13.5. Application of Geospatial Information Technology

Dynamic nature of droughts with complex phenomenon having multiple effects form a major challenge in planning, monitoring, predicting, assessing impact and offering solutions to drought hit areas. Because of these complexities, high quality data and improved tools to capture the spatial and temporal dimensions of drought is required.

Geoinformatics constitute the geospatial data i.e., mostly available from various satellite platforms and the technology available for analysis of such data such as Geographic Information System (GIS), and other integrative tools like Global Positioning System (GPS). The ever increasing pressure on natural resources to meet the requirements of growing population calls for the development of plans that maintains equilibrium environment, ecology and human needs. The use of contemporary technology tools like Geoinformatics to find solutions for sustainable use of land and water resources has been found to be an indispensable management and decision making tool. Geoinformatics facilitate the cost effective, timely, customized and simplified solutions for resource use. Geoinformatics has become a new tool in the hands of modern cartographers and the technology has been proved beyond doubt for its efficiency to generate maps with accuracy and time effectively particularly to depict the physically devastated areas by disasters, impact assessment and quick dissemination of disaster information to people (Dutta, 2002). The application of Geoinformatics for resource management at micro level was successfully demonstrated by integrating both satellite imagery and ground data to generate action plans for land development (www.gisdevelopment.net/application/ nrm/overview/ma03226pf.htm).

The Risk Management Agency (RMA) of US Department of Agriculture in collaboration with the University of Nebraska, the National Drought Mitigation Center, and the High Plains Regional Climate Center started the development of geospatial decision support tools to address agricultural drought hazards and identify regions of vulnerability in the management of drought risk. The objective of this joint research project National Agricultural Decision Support System (NADSS) is to develop a support system of geospatial analyses that will enhance drought risk assessment and exposure analysis. The NADSS is a collection of decision support tools designed to help agricultural producers assess a variety of risks. The architecture is separated into four layers: knowledge, information, data, and presentation ({kozaldg, culvermg, harmssk}@unk.edu).

University of Nebraska developed hydrological drought index map for the great plains region of the USA using an approach called Intelligent Joint Evaluation of Data and Information (IJEDI) using geospatial data. The data base from a variety of parameters related to hydrological drought such as surface water, ground water, above ground climate and geomorphology was integrated and analysed using GIS based tools. The data analysis module of IJEDI consists of four modules namely knowledge acquisition, knowledge discovery and data mining, data and information fusion and Multi agent Intelligence. The output products for IJEDI include hydro climatic products such as state of water resources report, seasonal water supply outlooks, stressed streams and lakes and stressed community and public lands (Zhang *et al.*, 2004).

Today's powerful geospatial tools, especially remote sensing, positioning, navigation and timing (PNT), and geographic information systems (GIS), can assist the characterization of a disaster situation. Remote sensing technologies, together with other geospatial technologies such as GIS and PNT systems, have a significant role to play in the improvement of disaster management and critical infrastructure condition assessment. Remote sensing from space combines a broad synoptic view with the ability to detect changes in surface features quickly and routinely.

Geospatial data from satellites provide a complete inventory of natural and biological resources at different spatial and temporal scales which is the fundamental requirement for the assessment and management of droughts. It is important to determine the vulnerability of these resources to periods of water shortage that result from drought. The most obvious natural resource of importance is water – its location, quality, quantity, accessibility and optimal use. Biological resources refer to the quantity and quality of grasslands/rangelands, forests, wildlife, and so forth.

The capabilities of remote sensing technology to provide the information on land and water management issues that is critical to drought/famine management process have been proved through various studies. Today, remote sensing has been operationalised to cover diverse themes such as agricultural crop acreage and yield estimates, forestry, drought monitoring, flood monitoring, land use/land cover studies, waste land delineation and reclamation, water resources development and management, ground water prospecting, marine resources survey, urban planning, mineral targeting, environmental impact assessment and so on, thus encompassing every facet of sustainable development and management. The synoptic and repetitive information provided by satellite data is useful to map surface water bodies, monitor their spread and estimate volume of water. This information is useful to measure the loss of storage capacity of reservoirs. Water bodies of the order of 0.5 ha size and above can be mapped using IRS-LISS III data. Satellite data analysis enables estimation of pre-harvest acreage and production besides assessment of crop condition. High-resolution data are useful for estimating minor crops. IRS LISS-III data merged with PAN data provides information on the extent of horticultural crops such as mango, coconut etc.

The spatial and temporal information on cropping pattern, crop intensity and crop condition form basic inputs for assessing the performance of irrigated command areas. Satellite data derived geological, geomorphological and hydrogeomorphological maps on 1:50,000 scales are useful to generate ground water prospecting maps. Generation of forest cover maps and monitoring changes in forest areas can be achieved through the analysis of satellite data. Information on all natural resources of the watershed namely soils, geology, geo-morphology, ground water, land use/cover, slope generated from satellite data are very useful inputs for watershed development plans.

13.6. Space Technology for Agricultural Drought Monitoring

Unlike point observations of ground data, satellite sensors provide direct spatial information on vegetation stress caused by drought conditions and the information is useful to assess the spatial extent of drought situation. Satellite remote sensing technology is widely used for monitoring crops and agricultural drought assessment. Over the last 20 years, coarse resolution satellite sensors are being used routinely to monitor vegetation and detect the impact of moisture stress on vegetation. AVHRR on NOAA's polar orbiting satellites has been collecting coarse resolution imagery world wide with twice daily coverage and synoptic view. The NOAA AVHRR NDVI has been extensively used for drought/vegetation monitoring, detection of drought and crop yield estimation (Batista *et al.,* 1997, Beneditte and Rossini, 1993, Moulin *et al.*, 1998, Goward *et al.*, 1985, Justice at al., 1985 and Tucker *et al.*, 1985). The 10 bit resolution digital data from the AVHRR is processed in the Spacecraft's Manipulated Information Rate Processor (MIRP) to produce four products namely (1) direct readout to ground stations of High Resolution Picture Transmission, HRPT world wide, (2) direct readout to ground stations of Automatic Picture Transmission (APT) worldwide, (3) Global Area Coverage, GAC at relatively low resolution (4 km) for central processing and (4) Local Area Coverage, LAC, from selected portions of each orbit at high resolution 1 km (Cracknell, 1997). Space technology has become a global potential tool for detection and mitigation of natural disasters like drought and the availability of long term satellite data enhance the accuracy of hazard detection, monitoring and impact assessment (Kogan, 2001). Integration of remote sensing derived inputs on land cover and bio physical parameters with crop simulation models under GIS environment would enhance the accuracy of crop monitoring and crop yield estimation methods in agriculture. The Drought Monitor of USA using NOAA-AVHRR data **(**www.cpc.ncep.noaa.gov**)**, Golbal Information and Early Warning System (GIEWS) and Advanced Real Time Environmental Monitoring Information System (ARTEMIS) of FAO using Meteosat and SPOT – VGT data (Minamiguchi, 2005), International Water Management Institute (IWMI)'s drought assessment in South west Asia using Modis data (Thenkabail, 2004) and NADAMS drought monitoring in India with IRS–WiFS/AWiFS and NOAAAVHRR (Murthy *et al.*, 2007) data are the proven examples for successful application of satellite remote sensing for operational drought assessment.

Spatial information technology like remote sensing from a wide range of satellite sensor systems currently available, offer a different dimension to agricultural drought assessment compared to conventional subjective, non spatial and non consistent mechanisms being practiced.

13.6.1. Drought Indices from satellite data

The crop/vegetation reflects high in the near infrared due to its canopy geometry, the health of the standing crops / vegetation and absorbs high in the red reflected radiance due to its biomass and accumulated photosynthesis (Figure 13.3). Using these contrast characteristics of near infrared, red and middle infra red bands which indicate both the health and condition of the crops/ vegetation, different types of vegetation indices have been developed. Parry and Lautenschlager (1984) provide an extensive review of vegetation indices based on LANDSAT and NOAA satellite data as shown below:

- Difference Vegetation Index
- Ratio Vegetation Index
- Infrared Percent Vegetation Index
- Perpendicular Vegetation Index
- Soil Adjusted Vegetation Index
- Weighted Difference Vegetation Index
- Greenness Vegetation Index
- Atmospherically Resistant Vegetation Index
- Normalized Difference Vegetation Index

- Normalized Difference Wetness Index
- Enhanced Vegetation Index

13.6.1.1. Normalised Difference Vegetation Index (NDVI)

Among the various vegetation indices that are now available, Normalized Difference Vegetation Index (NDVI) is widely used for operational drought assessment because of its simplicity in calculation, easy to interpret and its ability to partially compensate for the effects of atmosphere, illumination geometry etc., (Malingreau 1986, Tucker and Chowdhary 1987, Jhonson, *et al.*, 1993, Kogan 1995). NDVI is a transformation of reflected radiation in the visible and near infrared bands of NOAA AVHRR and is a function of green leaf area and biomass.

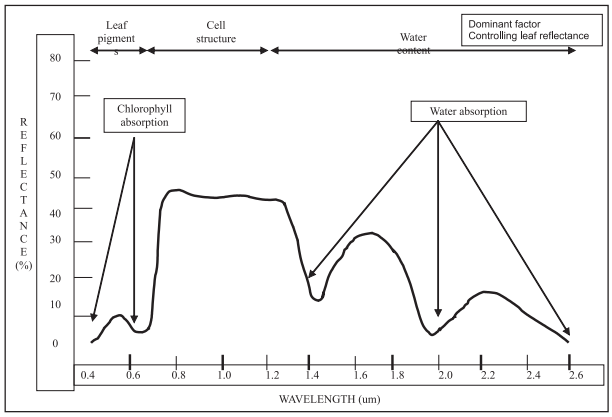

Figure 13.3: Spectral response of vegetation (source: Swain and Davis, 1978)

NDVI is derived as under:

NDVI = (NIR-Red) / (NIR+Red)

where, Near Infra Red and Red are the reflected radiations in these two spectral bands.

Water, clouds and snow have higher value in the visible region and consequently NDVI assumes negative values for these features. Bare soil and rocks exhibit similar value in both visible and near IR regions and the index values are near zero. The NDVI values for vegetation generally range from 0.1 to 0.6, the higher index values being associated with greater green leaf area and biomass (Tucker, 1979). Currently, NDVI products can be generated from the data of most of the satellite sensor systems. The MODIS NDVI of 250 m and 1000 m, SPOT VGT NDVI of 1000 m, NOAA AVHRR NDVI of 1000 m, IRS WiFS NDVI of 188 m and IRS AWiFS NDVI of 56 m are widely used for drought monitoring purpose because of the advantages of spatial and temporal coverage of these products.

In general, growth and decay of crop canopy represents similarities in the temporal vegetation index profile during the crop growth. The peak of this profile corresponds to peak vegetation cover of the crop. Interpretation of vegetation index (VI) profile can be used to derive information on the crop stage. Further, VI at peak vegetative stage or the time integration of VI profile is related with accumulated biomass in the crop or crop condition or crop yields. Lowering of VI values reflects moisture stress in vegetation, resulting from prolonged rainfall deficiency. Such a decrease in VI could also be caused by other stresses such as pest/disease attack, nutrient deficiency or geochemical effects. The seasonal VI profile is thus reflective of vegetation dynamics and condition. Comparison of VI profile of the reporting year and a previous normal agricultural year provides assessment of drought impact in the scale of previous agricultural scenario.

NDVI shows a lag correlation of up to 4 weeks with rainfall and aridity anomaly. However, the correlation is not unique either through the season or between the areas. The rainfall use efficiency varies in time and space making direct satellite monitoring of vegetation development essential for reliable and objective monitoring of agricultural drought conditions. However, conjunctive use of rainfall/aridity anomaly and VI provides greater reliability.

NDVI values contaminated by high residual (after time compositing) cloud cover or by thin clouds unidentified by visible band cloud masking or due to off-nadir viewing or as a result of insufficient cloud free passes in compositing period require validation before use in drought assessment. Heavy rainfall at the time of heading/flowering can disturb grain development and lead to yield reduction which however may remain undetected by the satellite which will show healthy canopy conditions. Excessive wide spread rainfall or flooding can also decrease VI value.

The general growing period in regard to start, peak growth and senescence can be identified through the seasonal NDVI profile. However, NDVI can be an indicator of crop development/condition only after significant spectral emergence of crops, which has a lag of 2-3 weeks after the completion of significant sowings in the district.

13.6.1.2. Normalised Difference Water Index (NDWI)

Shortwave Infrared (SWIR) band is sensitive to moisture available in soil as well as in crop canopy. In the beginning of the season, soil back ground is dominant hence SWIR is sensitive to soil moisture of top 1-2 cm. As the crop progresses, SWIR becomes sensitive to leaf moisture content. SWIR band has got no penetrating capability. It provides only surface information. When the crop is grown-up, SWIR response is only from canopy and not from the underlying soil. NDWI using SWIR can complement NDVI for drought assessment particularly in the beginning of the season.

NDWI is derived as under;

NDWI = (NIR-SWIR) / (NIR+SWIR)

where Near Infra Red and SWIR are the reflected radiations in these two spectral bands. Higher values of NDWI signify more surface wetness.

13.6.1.3. Drought indices derived from NDVI and Temperature

Kogan (1990, 1995) developed Vegetation Condition Index (VCI) using the range of NDVI and Temperature Condition Index (TCI) with brightness temperature data as under;

$VCI = (NDVI-NDVI_{min}) / (NDVI_{max}-NDVI_{min})*100$

$TCI = (BT_{max}-BT) / (BT_{max}-BT_{min})*100$

$VTI = a*VCI + b*TCI$

Where,

$NDVI$, $NDVI_{max}$ and $NDVI_{min}$ are smoothed weekly NDVI absolute maximum and its minimum

BT, BT_{max} and BT_{min} are smoothed weekly brightness temperature absolute maximum and its minimum

VCI is Vegetation Condition Index

TCI is Temperature Condition Index

VTI is Vegetation Health Index

The severity of drought situation is assessed by the extent of NDVI deviation from its long term mean. The concept of relative greenness i.e., the ratio of current NDVI to the historic mean NDVI for the same period was introduced by Burgan and Hartford (1993) and is given by

$NDVI_{dev} = NDVI_i - NDVI_m$

$NDVI_i$ is the NDVI in the i th month

$MDVI_m$ = long term average for the same month

Maps produced using relative greenness are quite useful to assess drought situation and hence this indicator is being used widely (Johnson *et al.*, 1993).

Peters *et al.*, (2002) developed Standardised Vegetation Index based on NDVI which indicates the probability of vegetation condition's deviation from normal using z scores of NDVI distribution derived from long term historic NDVI data sets.

13.6.1.4. Process based indicators

By modeling the energy and matter transfer between atmosphere and surface, a process based indicator known as Evaporative Fraction (EF) is derived. EF is defined as the fraction of available energy used for evapotranspiration. EF is derived as under;

$R_n = G + H + lE$

Where,

R_n = Net Radiation

G = Soil heat flux *lE*

H = Sensible heat flux

lE **=** Latent heat flux

$lE = (R_n\text{-}G) - c_p * \gamma_{air} * 1 / r_a * (T_s\text{-}T_x)$

c_p= Sp. Heat of air

γ_{air}= Air density

r_a= Surface roughness

T_s= Surface temperature

T_x= Maximum temperature

$EF = lE / (R_n - G)$

EF is Evaporative fraction

As long as adequate soil moisture is available, energy will be used for its evapotranspiration and EF will be close to one (no water stress). In the absence of soil moisture, all available energy will be directed into warming up surface and the ambient air and EF will approach zero indicating serious water stress (Bastiaanssen, 1998). Although there are many vegetation indices and derived indices, VCI and NDVI deviation from historic NDVI are being widely used on operational basis to assess drought situation (Kogan 1995, Burgan *et al.*, 1996, Hayes and Decker, 1998).

13.7. Rainfall and Soil Moisture Estimation from Satellites

Observations from Meteorological Geostationary satellites may be more useful in indicating or forecasting an eminent drought rather than its monitoring. However, the prediction of such situations is still a major challenge for atmospheric scientists. In a recent significant study, Goswami and Xavier (2003) have shown that by analysis of past observations of rainfall and circulation, it is possible to predict the monsoon breaks with a lead time of ~ 20 days. Fortunately with the advent of high resolution microwave sensors onboard new generation satellites, it is now possible to make quantitative estimates of precipitation on global scales. Adler *et al.*, (1998) suggested a method to merge the information from microwave sensors onboard polar orbiting satellites and that from the geostationary satellite to produce more frequent and regionally continuous maps of quantitative precipitation.

The availability of real-time rainfall observations may be useful for defining the indicators of drought. Other important meteorological observations are the global patterns of sea surface temperature (SST) and Outgoing long-wave radiation (OLR). Recent studies have indicated that there is a relationship between equatorial convection patterns and the variations of Indian summer monsoon rainfall. The authors of this study found that the link of the Indian monsoon to events over the equatorial Indian Ocean is as important as the well-known link to the dramatic events over the Pacific (El Niño Southern Oscillation; ENSO). Over the equatorial Indian Ocean, enhancement of deep convection in the atmosphere over the western part is found to be associated with suppression over the eastern part and vice versa. The reliable drought prediction technique based on the analysis of global patterns of convection and other satellite observations is not available today, but the availability of high quality satellite observations can definitely boost the efforts in this direction.

Drought is a consequence of the prolonged period of dry soil due to lack of rainfall and could be inferred from soil moisture conditions over a long period of time. This, in turn, could be monitored regularly using microwave remote sensing techniques. In recent years satellite-based microwave radiometers have been used widely to monitor soil moisture conditions (Schmugge *et al.,* 1986, Chaudhury and Golus 1988, Owe *et al.,* 1988, Jackson 1993, Njoku and Entekhabi 1996). Recently, Rao *et al*., (2001), Thapliyal (2003) and Thapliyal *et al.,* (2003, 2005) have demonstrated the potential of microwave radiometers for surface soil moisture estimation over India.

Lower microwave frequencies are preferred for soil moisture observation as they are least affected by vegetation, surface roughness and atmospheric cloud liquid water. Theoretically 1.4 GHz is considered best for soil moisture observations. However, due to power constraints, the lowest frequency used so far by satellite microwave radiometers

is 6.6 GHz, e.g., Scanning Multi-frequency Microwave Radiometer (SMMR) onboard Nimbus (1978 to 1987) and Multi-frequency Scanning Microwave Radiometer (MSM R) onboard IRS-P4 (1999 to 2001). Currently, the TRMM Microwave Imager (TMI) launched in 1998 with lowest frequency at 10.7 GHz is providing observations at higher spatial resolution (~40 km as compared to ~100 km for a similar channel in SMMR and MSMR). Jackson and Hsu (2001) compared TMI 10.7 GHz brightness temperatures with observed soil moisture over the Southern Great Plains of USA and concluded that it has great potential for soil moisture estimation. Thapliyal (2003) showed that 10.7 GHz show high sensitivity to the surface soil moisture over India, which is comparable to that of 6.6 GHz of MSMR and SMMR.

The SSMI on board DMSP satellites is 7 channel, four frequency, linearly polarized passive microwave system, that measures micro wave brightness temperatures from atmosphere, ocean and terrain with different foot prints ranging from 13 X 15 km to 43 X 69 km. Soil moisture is one of the important derivatives from SSMI foot prints that has potential applications for regional level drought studies.

Advanced Microwave Scanning Radiometer AMSR-E onboard Aqua satellite provide the data that is useful to derive the soil moisture in the top few millimeters by averaging over the retrieval footprint. The soil moisture data can be generated at a spatial resolution of 25 Km.

European Space Agency's (ESA) Soil Moisture and Ocean Salinity (SMOS) is the second Earth Explorer Opportunity mission scheduled for launch in 2009. SMOS is capable of providing observations on soil moisture and ocean salinity by capturing emitted microwave radiation around 1.4 GHz frequency. This information will be useful for forecasting extreme weather events and seasonal climate changes (www.esa.int).

13.8. National Agricultural Drought Assessment and Monitoring System (NADAMS)

In India, National Agricultural Drought Assessment and Monitoring System (NADAMS) was initiated towards the end of 1986, with the participation of National Remote Sensing Agency, Dept. of Space, Government of India, as nodal agency for execution, with the support of India Meteorological Department (IMD) and various state departments of agriculture. NADAMS was made operational in 1990 and has been providing agricultural drought information in terms of prevalence, severity and persistence at state, district and sub-district level. Over a period of time, NADAMS project has undergone many methodological improvements such as use of high resolution data for disaggregated level assessment, use of multiple indices for drought assessment, augmentation of ground data bases, achieving synergy between ground observations and satellite based interpretation, providing user friendly information, enhanced frequency of information etc.

The complete chain of activities of NADAMS project starting from procurement of satellite data till dissemination of information to user community are currently being undertaken by Decision Support Centre located at National Remote Sensing Centre, Hyderabad, India under the preview of Disaster Management Support Program (DMSP) of Department of Space, Government of India.

The coverage of the project includes 13 agriculturally important and drought vulnerable states of the country. Monitoring of agricultural drought is restricted to Kharif season (June-Oct/November), since this season is agriculturally more important and rainfall dependent. Since drought declaration by the State Government involves the use of a large number of drought indicators, many of which are not amenable to satellite sensing, the emphasis of NADAMS is on agricultural drought conditions. Agricultural conditions are monitored at state/district/sub-district level using daily observed coarse resolution (1.1 km) NOAA AVHRR data for 9 states. Moderate resolution data from Advanced Wide Field Sensor (AWiFS) onboard Resourcesat 1 (IRS P6) of 56 m and Wide Field Sensor (WiFS) of IRS 1C and 1D of 188 m are being used for detailed assessment of agricultural drought at district and sub district level in four states namely, Andhra Pradesh, Karnataka and Maharashtra. Details of satellites/sensors being used for drought assessment are shown in Table13.4.

Indian Remote sensing Satellite (IRS) series (IRS 1A, IRS 1B, IRS 1C, IRS 1D and IRS P3) have unique payloads to monitor and assess various natural resources available in the country and around globe at different spatial resolutions. Among the payloads available IRS 1C, IRS 1D and IRS P3 have WiFS (Wide Field Sensor) payload (Table 13.4). WiFS sensor collects data in two spectral bands 0.62-0.68 μm (red) and 0.77-0.86 μm (near infrared) with spatial resolution of 188 m and ground swath of 810 km with a revisit period of 5 days. The combined use of three satellites cover any part of the country once in 3-4 days. The Advanced WiFS (AWiFS) sensor onboard IRS P6 provides data in 56 metres resolution with a swath of about 700 km. Due to higher spatial resolution use of WiFS/AWiFS data enables detailed monitoring at district and sub-district level.

Table 13.4: Satellites/sensors being used for drought monitoring in NADAMS project

S.No	Satellite/sensor	Spectral resolution (microns)	Spatial resolution (metres)	Radiometric resolution (bits)	Temporal resolution
1	NOAA-AVHRR (Swath= 2700 km)	0.58-0.68 0.725-1.10 3.55-3.93 10.3-11.3 11.5-12.5	1100	10	Twice a day
2	IRS 1C/1D-WiFS (Swath= 810 km)	0.62-0.68 0.77-0.86	188	7	5 days
3	IRS P3 WiFS (Swath = 810 km)	0.62-0.68 0.77-0.86 1.55-1.75	188	7	5 days
4	Resourcesat-1-AWiFS (Swath= 740 km)	0.53-0.59 0.62-.068 0.77-0.86 1.55-1.70	56	10	5 days

13.8.1. Integration of satellite derived indicators and ground data

In NADAMS, compositing of NDVI with maximum value approach for the period of 15 days and one month is being adopted. Drought assessment is carried out on fortnightly basis and reporting of information to the User departments is done on monthly basis. The assessment of agricultural drought situation in each district/block/taluk takes in to consideration the following factors; (1) seasonal NDVI/NDWI progression – i.e transformation of NDVI/NDWI from the beginning of the season, (2) comparison of NDVI/NDWI profile with previous normal years – relative deviation and vegetation condition index, (3) weekly rainfall status compared to normal and (4) weekly progression of sown. The relative deviation of NDVI/NDWI from that of normal and the rate of progression of NDVI/NDWI from month to month gives the indication about the agricultural situation in the district which is then complemented by ground situation as evident from rainfall and sown area. The ground data from different states has been organized in to a data base along with satellite derived NDVI/NDWI data. Concept and basic details of drought assessment in NADAMS is depicted in Figure 13.4. The seasonal AWiFS NDVI progression and drought assessment over Haryana state was shown in Figure 13.5. The Modis NDWI 250 metres images comparing a drought year (2008) and a normal year (2007) shown in Figure 13.6 indicate surface dryness caused by deficit rainfall in selected districts of Maharashtra state.

The methodology being adopted in NADAMS essentially reflects the integration of satellite derived crop condition with ground collected rainfall and crop area progression to evolve decision rules on the prevalence, intensity and persistence of agricultural drought situation. Some of the coarse resolution products being used for drought assessment are shown in Figure 13.7. The agricultural drought warning and declaration procedures being followed are shown in Table 13.5. During June to August, drought warning information is issued in terms of “watch, alert and normal” categories. In case of ‘watch’, external intervention is required if similar drought like conditions persist during the successive month while ‘alert’ calls for immediate external intervention, in terms of crop contingency plans. During September and October, based on NDVI anomalies corroborated by ground situation, drought declaration is done in terms of mild, moderate and severe drought.

13.8.2. Drought reports and user feedback

Since inception in 1989, NADAMS has transformed from biweekly bulletins to detailed monthly drought reports. The reports are sent to the Central relief department (nodal agency for relief for the country), Planning Commission, State Relief department (nodal agency for relief for the state) and agricultural department and host of other organizations, which are dealing with drought. Currently, monthly drought reports from June to November are being disseminated. Whenever need arises, drought information is also disseminated on fortnightly basis, subject to availability of cloud free satellite data. The NDVI images describing the spatial pattern of vegetation development

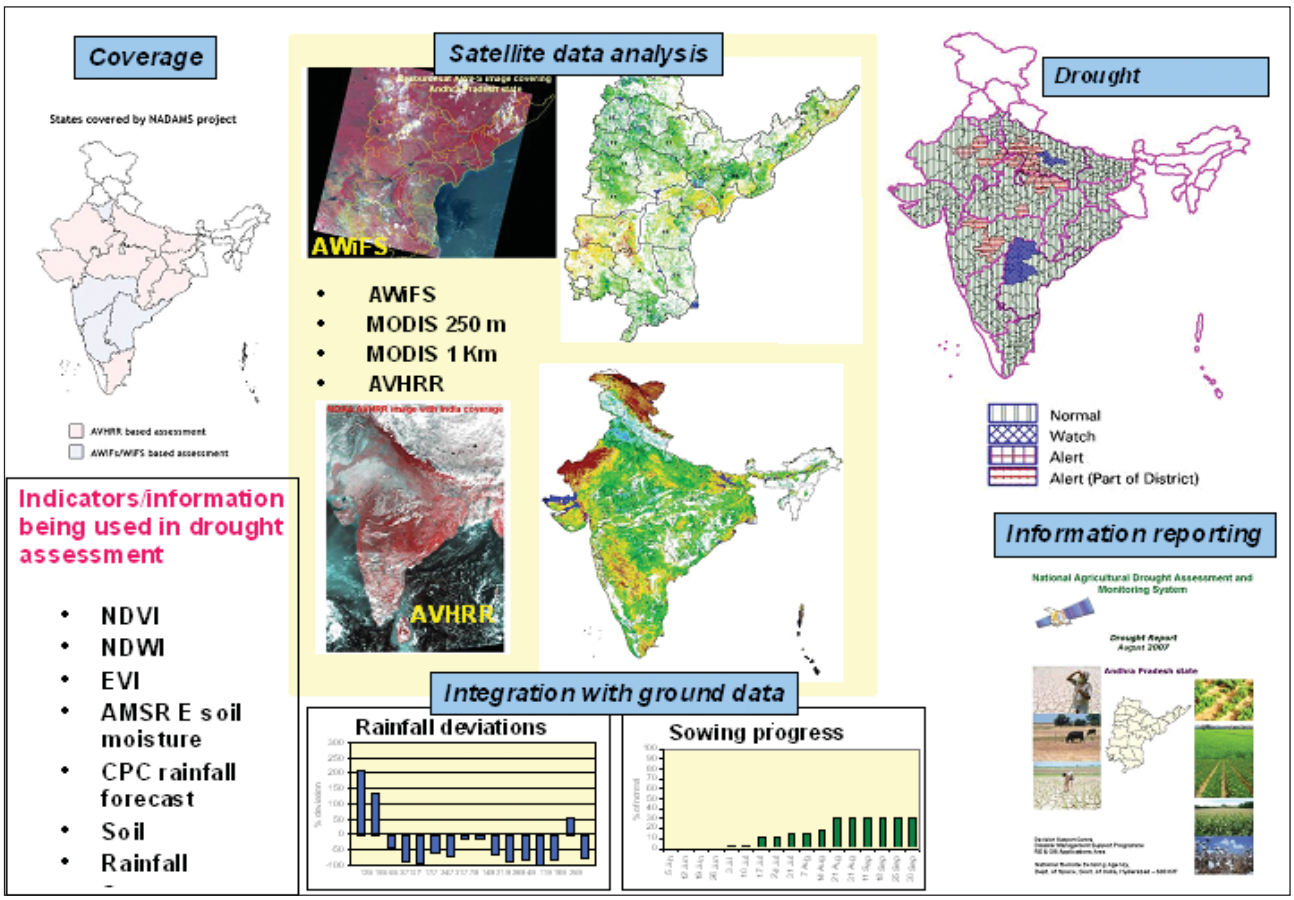

Figure 13.4: Details of NADAMS project

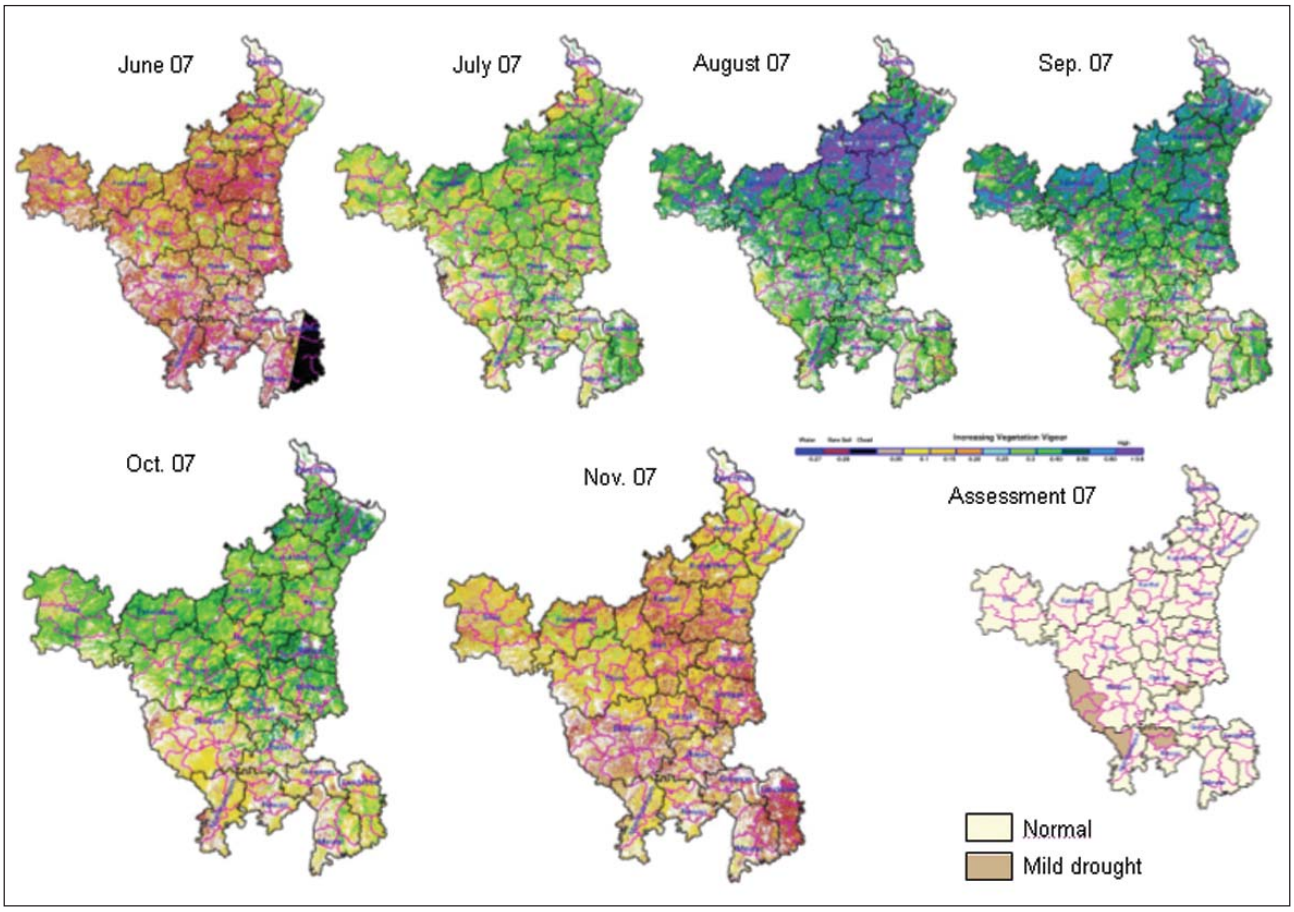

Figure 13.5: Seasonal NDVI progression and drought assessment over Haryana state – Kharif 2007

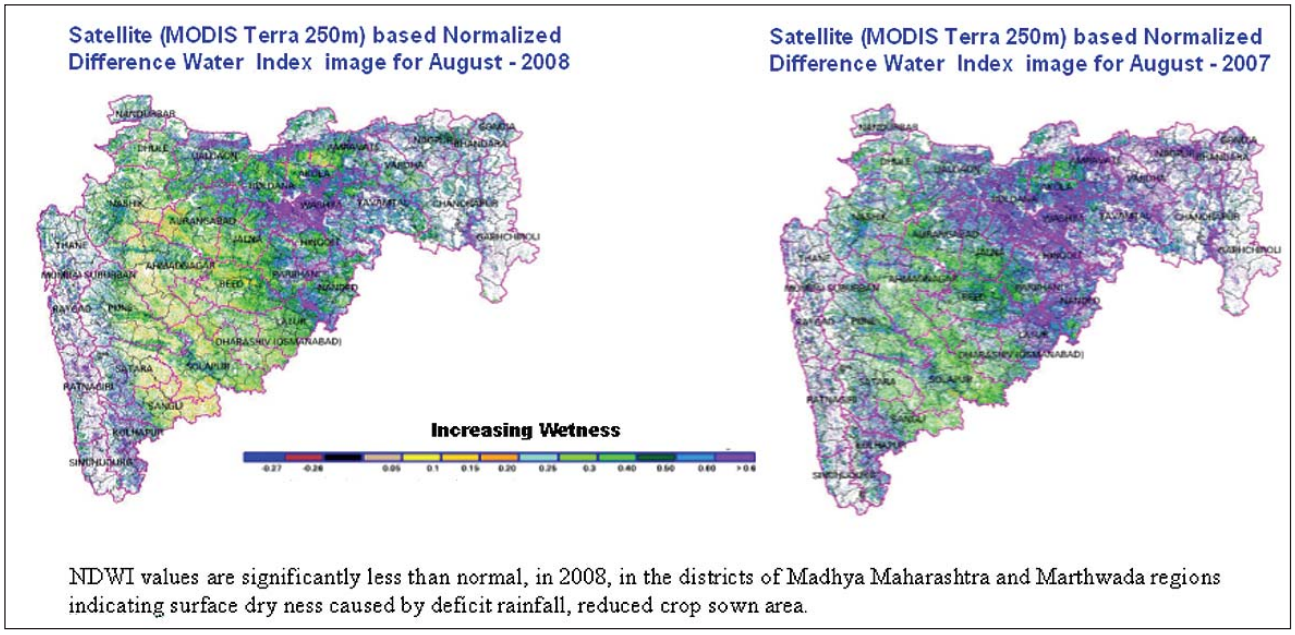

Figure 13.6: MODIS – 250 m – NDWI images of drought year (2008) and normal year (2007), Maharashtra state

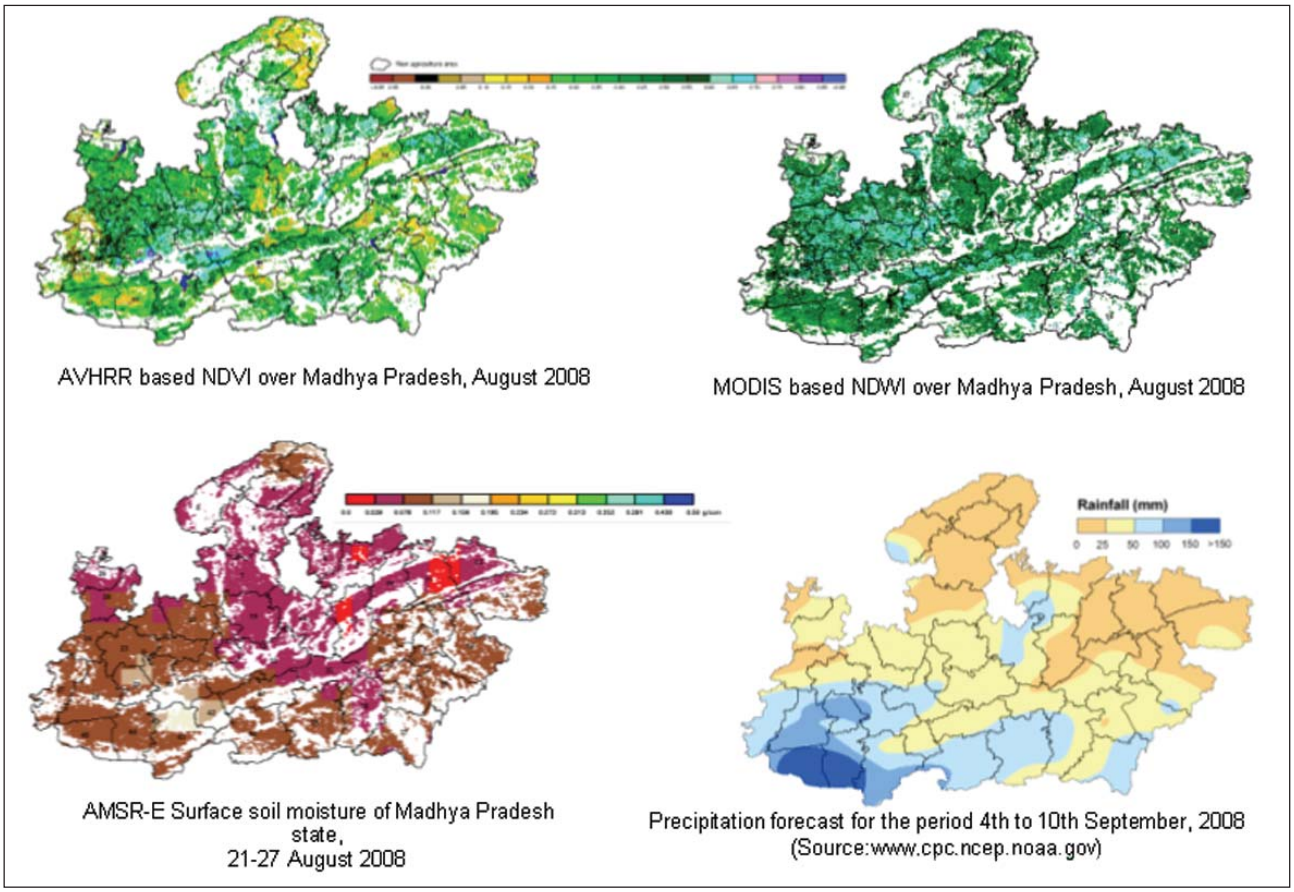

Figure 13.7: Coarse resolution products being used in NADAMS project for drought assessment

are being given to state agriculture departments on request for their crop and seasonal conditions review meetings.

The NADAMS report is useful for the decision makers for the management of agricultural drought at state/district/ sub-district level. This report provides a comprehensive picture of the drought situation which acts as a complimentary information along with their ground based information.

Feedback received from some of the states indicates that the drought reports are being used as inputs in their review meetings on agricultural situation. The agricultural drought information of NADAMS reports are being used

as inputs in the development of contingency plans and in relief management. It was also found that there is good correlation between NDVI images of NADAMS and aridity maps being provided by India Meteorology Department.

Today, the real strength of NADAMS project lies in the operational use of moderate resolution AWiFS/WiFS images for detailed assessment of agricultural situation within a district at regular intervals of one month to enable the User departments taking strategic decisions in drought management.

Table 13.5: Agricultural drought warning and declaration in NADAMS project

Month	Assessment	Implications
June	Normal	Agricultural situation is normal
July August	Watch	• Progress of Agricultural situation is slow • Ample scope for recovery • No external intervention needed
	Alert	• Very slow progress of agricultural situation • Need for intervention. • Develop and implement contingency plans to minimise loss
Sept. Oct.	Mild drought	Crops have suffered stress slightly
	Moderate drought	• Considerable loss in production. • Take measures to alleviate suffering
	Severe	• High risk Significant reduction in crop yield • Management measures to provide relief

13.9. Drought declaration by different states

Declaration of drought is the subject matter of State Governments. During the season, after examining the various aspects on rainfall, crops, irrigation, ground water etc., the state government identifies the number of administrative units - Taluks or blocks, affected by drought. The drought declaration helps assessment of relief requirements and guides relief management. Some states declare drought in middle of season and some states declare at the end of season.

Existence of considerable disagreement about the definition of drought itself makes it impossible to devise a universal drought index. Furthermore, drought characteristics and the wide range of economic sectors on which it has an impact make its effects difficult to quantify. Because of the complexities of drought, no single index has been able to adequately capture the intensity and severity of drought and its potential impacts on such a diverse group of users. Different states are adopting different methodologies for drought assessment, preparation of drought memorandums, drought declaration and relief assessment etc.

The criteria adopted in different states also vary depending on the rainfall and crops grown in the region. Tamil Nadu considers regions receiving less than 900 mm rainfall as drought affected, while Karnataka considers regions which received rainfall less than 400 mm during *kharif* and less than 30 per cent during the cropping season and 20 per cent deficiency of rainfall during critical stage of crop growth as drought affected areas. Rajasthan on the other hand considers an year as scarcity year when the productivity decreases by 50 per cent compared to a good crop year. Many of the states also follow the 'Annawary' system wherein the crop conditions are assessed through visual estimates. The criteria followed is production above 75% of normal – no drought, 50 to 75% normal – moderate drought, 25-50 % - severe drought, <25 per cent – disastrous drought. Karnataka state has recently revised its norms for drought declaration in the light of four consecutive years of chronic drought. It was felt that the current norms to define drought affected areas were inadequate and inappropriate. The taluks of the state are divided in to four categories based on annual rainfall. The threshold values for rainfall deviations and number of dry weeks for drought declaration vary across the four groups of taluks. The criteria also differ for year to year, for the taluks experiencing consecutive years of drought. Details are available in the annual report (2005-06) of Revenue Department of Government of Karnataka.

13.10. Drought Management

There is lot of confusion still existing between science and policy communities about the characteristics of drought as a result of which drought management practices all over the world is progressing slow. Governments respond to drought through adhoc or crisis management approach rather than through coordinated or strategies. The specific goals, the task of drought management is expected to deliver are:

Food production & security: for procurement, storage and distribution of food grains from food surplus to deficit areas, distribution of essential through public distribution system.

Employment generation: Employment generation schemes need to be prepared, technically evaluated and kept ready for implementation to provide jobs to the drought affected population.

Contingency crop plan: Alternate crop plan with sufficient infrastructure availability to stabilise farm level production.

Livestock management: Fodder supply, prevent distress sales, cattle camps

Drinking water: Augment the fleet of rigs available for drilling tube wells to provide drinking water.

Economic aspects: Waiving loan and providing monitory relief.

Social security schemes: Infrastructure facility can be expanded to cover the vulnerable section of the population.

There are two types of management measures namely (short term measures and long term measures). Short term measures include adoption of contingent crop plans, cultivation of drought tolerant crops, mulching, cultivation practices like optimal spacing, rationing, nutrient management and rainwater management. Long term management include land and water management practices to enhance the productivity in a sustainable manner.

Drought management in India was evolved as a national approach and has undergone changes in the light of status of resources and technological developments. The famine codes based on recommendations of Indian Famine commission (1880) constituted a mile stone in the history of drought management in India. This was the first time systematic approach was used. In the 1950s famine codes were replaced by scarcity relief with the objective of preventing starvation deaths. In mid 60's drought response mechanisms were built up to ensure physical and economic access to food. Since 1970 drought management is being carried out by providing relief and by adopting drought impact minimization thought short and long term drought mitigation measures.

While India struggled to manage the 1965-66 drought by importing more than 10 millions of tons of food grains, in 1987-88 drought which is of greater severity in terms of rainfall deficiency and twice as that of population affected, was efficiently managed. The difference in impact can be explained by resilience in terms of distress indicators such as rise in food grain prices, increase in crimes, sale and mortgage of land etc., starvation level which were very low in 1987 and also due to improved level of drought preparedness and management which was considered as an integral part of country's development programs.

The primary responsibility for management of drought in India vests with the State Governments. The Central Government supplements the efforts of the State Governments in dealing with disaster situations and also provides the major part of the financial resources for disaster response. There is an institutional arrangement at the national, state, district and sub-district levels to deal with emergency situations. A National Contingency Action Plan exists for ensuring emergency assistance in the wake of natural disasters at the national, state and district levels. The State Governments have their Relief Manuals/Codes which lay down the procedures and powers for emergency management and provision of relief.

A Calamity Relief Fund (CRF) is allocated to each state on an annual basis, 75% of which is contributed by the Central Government. The quantum of the CRF is determined by independent Finance Commissions once in five years. In the process, the drought relief management has become high sensitive to political and financial implications and hence a reliable drought assessment and monitoring mechanism has evolved using remote sensing in the country.

13.10.1. Drought Preparedness

Drought preparedness activities include identifying drought prone area which generally refers to the area frequently affected by drought and to carry out the long term drought mitigation activities that minimize the impact. Irrigation commission in 1972 suggested following criteria for determining drought proneness (i) low rainfall regions, (ii) areas that receive irrigation support less than 30 % of net sown area (iii) frequency of famine and scarcity. Later in 1976 National Commission on Agriculture suggested areas based on four rainfall categories (i) rainfall below 375 mm create conditions of extreme aridity, (ii) semi arid zones have rainfall between 375 mm and 750 mm (iii) the dry sub humid areas receive rainfall between 750 mm and 1125 mm and (iv) certain areas which receive above

1125 mm experience failure of crops. The task force on Drought prone area program and Desert Development Program evolved broad indicator comprising of rainfall and irrigation with relaxed irrigation yardstick to 40 per cent for areas having less than 750 mm rainfall and 30 per cent for areas having rainfall higher than 750 mm. However, the drought prone area identified based on limited data on rainfall and irrigation details of 1970's was not revised so far in spite of increase in the irrigated area and changes in the land use during recent years. The frequent change in the land use, irrigation development, cropping pattern and agricultural practices, it is necessary for frequent updating of drought prone area with enhanced understanding of drought impact using satellite data is essential.

13.10.2. Prediction of Drought

The prediction of drought is carried out mainly based on rainfall predictions. The rainfall predictions are of three kinds:

- Long range rainfall prediction: Since 1875 seasonal rainfall forecast for the entire country as a whole is being provided by India Meteorological Department. Over recent years, since 1989, forecasts are fairly accurate due to the use of parametric, dynamic, stochastic transfer and power regression models. These forecasts are issued in two stages, the first tentative forecast is issued in mid April and final forecast in last week of May. The seasonal total rainfall for the entire country is predicted in the forecast
- Medium range rainfall prediction: National Center for Medium Range Weather Forecasting (NCMRWF) provides in advance the weather forecast at every 2.5° x 2.5° grid. Operationally for 24 stations, 3 day forecasts are provided and Agriculture advisory committee members from various departments and universities meet and decide about necessary advice to farmers of these regions. This prediction is still in experimental mode and needs improvement in the accuracy
- Short range rainfall predictions: Based on INSAT data supported with weather observation, qualitative predictions of weather valid for 24 to 72 hours are being issued daily

NCMRWF is currently providing extended range forecasts through monthly predictions based on simulations from global T80/L18 atmospheric model. The extended range forecasts are useful for planning and management of water resources. Efforts are in progress at NCMRWF, to develop a more accurate 'Atmosphere- Ocean-Land' coupled system, to predict the monsoon environment a season in advance.

13.11. Drought proneness/drought vulnerability

Vulnerability mapping and hazard zonation are indispensable requirements to evolve more effective long term drought disaster management strategies. In India, the identification of drought prone districts and blocks was done by Hanumanth Rao Technical committee in 1994 using the criteria of percent irrigated area in different climatic zones and found that 1173 blocks representing 185 districts and 13 states, occupying 120 M ha of geographic area was drought prone area. However, the rapidly changing agricultural scenario with increasing irrigated area on one hand and significant climatic changes on the other hand, indicate the need for the development of new set of criteria for delineation of drought prone areas. Recently to be in tune with changing environmental concerns and agricultural scenario globally, the Parthasarathy Committee (2005) was asked to re-look into the criteria related to drought prone areas delineation in the country.

Drought proneness of a given area is largely determined by the response of agricultural situation and crop condition to the combined effects of causative factors - rainfall variability, irrigation support and soil type etc. Therefore, drought proneness- its characterization and delineation can be done using two approaches – one on the basis of causative factors and the other on the basis of response factor.

13.11.1. Drought vulnerability based on causative factors

Central Research Institute for Dryland Agriculture (CRIDA) carried out a pilot study to delineate drought prone blocks in Mahaboobnagar and Anantpur districts of Andhra Pradesh. Long term block wise rainfall data (for 30 years) and percent irrigated area was the data used in the analysis. A composite drought index with weighted drought index derived from rainfall data and weighted irrigation index derived from percent of source wise irrigated area was developed. Blocks of the two districts were delineated using this index in to more prone and less prone classes. The procedure is being fine tuned with different weighing factors to arrive at more objective criteria for application to rest of the districts in the country.

13.11.2. Drought vulnerability based on response factors

Vulnerability analysis and hazard zonation from the point of view of response of agricultural situation and crop condition to rainfall variability and irrigation support at sub district level would be possible using the indicators derived from agricultural area NDVI of the season. NDVI based assessment of drought proneness takes in to account the actual condition of standing crops during the season and its comparison among different years of normal and abnormal years. The fluctuations of crop condition as triggered by weather and water supply conditions determine the drought proneness of a given area. Long term NDVI data base consisting of extreme drought events and normal season facilitates quantification of NDVI variability which directly indicates drought vulnerability.

Pilot studies on drought proneness using agricultural area NDVI data sets from 1999-2005 for kharif seasons for two districts namely, Anantpur and Mahaboobnagar were undertaken by NRSC. Drought proneness at block level in Anantpur and Mahaboobnagar districts was identified using a set of NDVI based indicators namely, relative NDVI differences, inter annual NDVI variability, probability of occurrence of low NDVI etc. (Murthy *et al.*, 2008). Based on this study, blocks with more drought proneness and less drought proneness could be delineated (Figure 13.8). The NDVI based criteria are now being integrated with ground parameters such as rainfall, irrigation support to better represent the drought proneness at sub district level.

13.12. Challenges in drought assessment

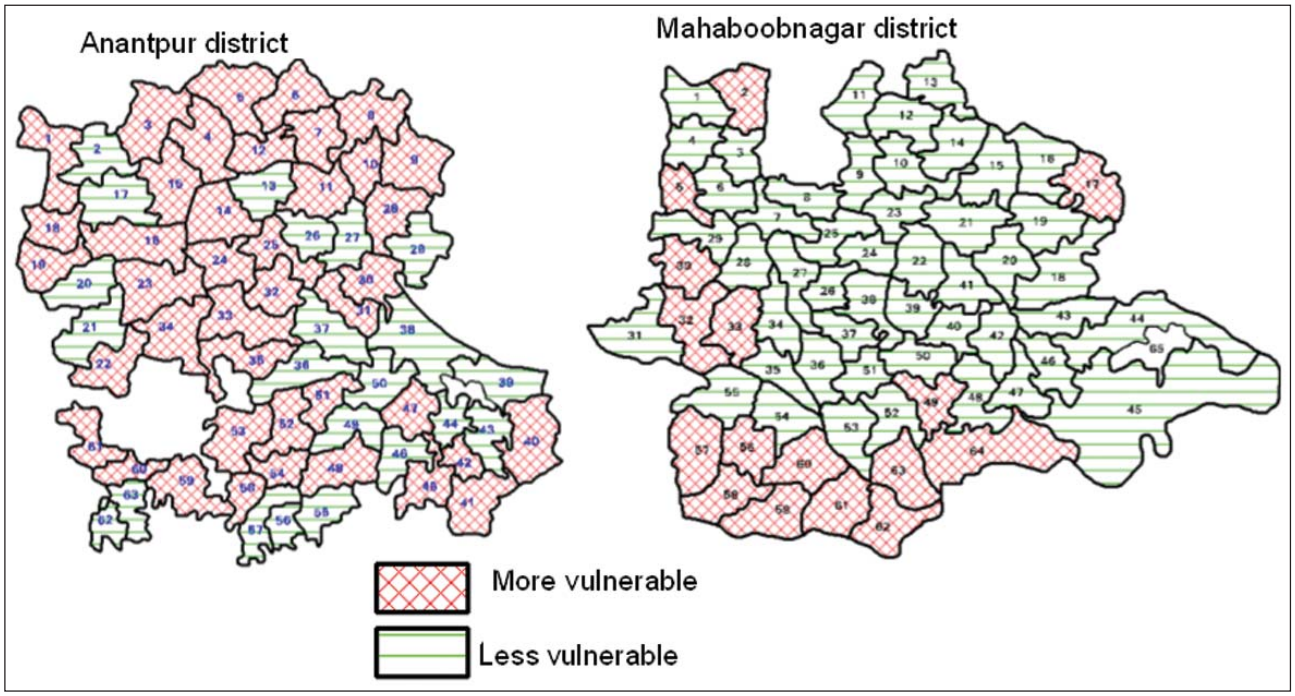

Figure 13.8: Drought proneness assessments on the basis of historic NDVI

13.12.1. Future Satellite Systems for Drought Analysis

Future missions are planned to meet the requirements of the meteorology community. The INSAT-3D to be launched in the year 2010 will carry improved VHRR and vertical sounders for temperature/humidity profiles. The imager will have six channels and the sounder will have nineteen channels. The Oceansat – 2, next in oceansat series of satellites, proposes to carry a scatterometer for surface wind retrieval. These surface winds are essential inputs for the weather prediction models.

The Megha-Tropiques mission will be a joint effort of ISRO and CNES, France towards study of the water cycle in the tropical region, which is very critical for forecast of monsoon. The unique payloads of the Megha-Tropiques are MADRAS (multi-frequency microwave radiometer – including 89 and 157 GHz), ScaRab (radiation budget – for both short and long wavelengths) and SAPHIR (atmospheric sounder – six channels). The mission will operate with an inclined equatorial orbit for repetitive coverage of tropical areas. The mission is expected to give insights into the convective processes in tropics and their characterization (Table 13.6).

Radar Imaging Satellite (RISAT), scheduled to be launched in 2009, is expected to boost the utilization of microwave images in the fields of agriculture and disaster management. One of the major constraints of using optical data is persistent cloudy conditions during monsoon season resulting in non-availability of sufficient cloud free data. In this context, microwave remote sensing offers great potential for monitoring crop and soils especially during the monsoon season due to capability of radar systems to acquire data under all weather conditions. The multi mode, multi polarization SAR images of RISAT will be useful to study the crop sown area progression, crop condition and soil moisture during the monsoon season to strengthen the existing drought assessment methodology.

Resourcesat-2 is planned to be launched in 2010 as a continuation to existing Resourcesat-1. With the availability

Table 13.6: Payload characteristics of and applications of future Indian satellites

Satellite	Payload	Bands/Resolution	Resolution(in Km.)	Applications
INSAT-3D	6 Channel IMAGER	Spectral bands (µm) Visible : 0.55-0.75 Short wave IR:1.55-1.70 Mid wave IR: 3.70-3.95 6.50-7.10 Thermal IR: 10.30-11.30 11.30-12.50	 1km 1km 4km 4km 4km 8km	 Cloud characterization Mesoscale processes
	19 Channel Vertical SOUNDER	Spectral bands (µm) Short wave infra red : six bands Mid wave infra red: five bands Long wave infra red: seven bands Visible :one band	10×10 for all bands	Atmospheric water vapour/temperature
Megha Tropiques	SAPHIR	Six bands around 183 GHz	10 km Horizontal Resolution	Water vapour profile Six atmospheric layers upto 12 km height
	SCARAB	4 Channels: Sc-1 (Visible), Sc-2 (Solar), Sc-3 (Total) Sc-4 (IR window)	25 km at nadir	Radiation budget
	MADRAS	Radiation instrument in short& long wave 89&157GHz radiometer 10,18&37GHz radiometer	40km Horizontal Resolution 10 km Horizontal Resolution	Ice particles in cloud tops cloud liquid water and precipitation; sea surface wind speed 23 GHz : integrated water vapour
	GPSROS			Vertical profile of temperature and humidity

of AWiFS sensor on both Resourcesat 1 and 2 from 2010, the frequency of moderate resolution AWiFS images would significantly increase permitting improved drought assessment at subdistrict level by way of minimizing cloud cover in the images.

13.12.2. Unified index

Development of a unified index for drought severity assessment by integrating the data from different sources is an important activity recently undertaken to enhance the scope of drought assessment. There is a need to arrive at a scientifically true measure cutting across various rainfall zones and socio economically acceptable indicator of drought for the country. The index should be completely and comprehensively explain the phenomenon of drought. The index should give appropriate weightages to the rainfall, soil moisture and crop condition. To make the criteria uniform irrespective of region or state, Standardized Precipitation Index will be used to assess the deficiency of

rainfall, since it has been standardized with mean zero and variance one. The impact of rainfall can be measured in terms of soil moisture availability through Soil Moisture Index (SMI), retrievable through water balance procedures. This index allows incorporating variability of soil parameters, crops and weather, which lead to better assessment of drought over the growing season. However, the spatial variability in the soil moisture index within a district depends largely on the spatial rainfall data and spatial Available Water Content (AWC) of soils that are representative of blocks/mandals. NDVI which indicates the agricultural vegetation condition is a response factor. Thus, a drought index which encompasses rainfall, soil moisture and crop condition would become complete and comprehensive. Combination of three parameters-rainfall, SMI and NDVI, if available at sub district level on weekly/fortnightly basis provide scope to evolve a unified index. A pilot study has been proposed for block level drought assessment by integrating rainfall, soil moisture and crop condition.

Procedures have to be developed for early drought detection and assessing the quantitative impact of drought on agricultural production through the use of satellite data and assimilation of data from ground segments, routinely collected by various agricultural related departments of the country. Empirical models, process based models and ground surveys with sampling techniques need to be explored in this context.

13.12.3. Enhanced exploitation of space technology

Activities planned towards retrieval of additional information from currently available satellite sensor systems, for improving the drought assessment, include;

- exploitation of SWIR region to detect crop water stress
- analysis of crop area progression using microwave data
- improved vegetation indices using BRDFs
- improved temperature retrievals for quantification of ET to develop process based indicators
- exploration of soil moisture retrievals operationally at different canopy closures
- extended data support from geo-stationary satellites
- estimation of spatial rainfall
- process based indicators

13.12.4. Data base

Collection of high quality information related to a variety of physical, meteorological, agricultural, environmental and socio-economic at different spatial and temporal scales in standard formats. Rainfall, temperature, evaporation, soil moisture, stream flow, vegetation health are some of the crucial parameters that are required to be measured continuously at different spatial and time scales during the season for drought assessment. These data bases enable adoption of an integrated approach for timely assessment and early warning.

13.12.5. Early warning systems

Green revolution has increased the yields of various crops but at the same time the amplitude of fluctuations in yields have also raised parallelly. In good years hybrids yield better, but generally in poor years the yield are worse, thus has led to increased sensitivity to rainfall variations. Since drought is a slow phenomenon, information on early warning is more relevant. However, the difficulty is to detect the start of the drought process even when variety of data is available. The monitoring/early warning system should provide decision makers at all levels with information about the onset, progress and termination of drought conditions and should become an integral part of drought management process.

Early warning systems help in formulating drought intervention strategies that respond to the needs of the people and enables individuals/community to face the risk with reduced damage. Objective and scientific information on the possibilities of the occurrence of drought situation in a given area enhance the credibility of early warning signals. An ideal early warning system should provide periodical information on meteorological, agriculture, hydrological conditions and their impact on the environment along with advisory services. Traditional early warning systems consist of physical indicators of the recent meteorological conditions. A good early warning system should have a composite database on meteorological conditions, agricultural situation, production estimates, availability of drinking water, fodder, price trends of food and feed etc. Early warning system should not end in the collection and processing of data but should be designed to mitigate/respond to the crisis (Buchanan-Smith, 1994). Vulnerability profile of the area should also form an important component of early warning methodology. Vulnerability information include trends in recent rainfall, production, prices, nutritional status,

environmental status, soil fertility and house holed status. The physical aspects of an early warning system should be able to provide information on spatial extent of drought, duration of drought, time of occurrence of drought in relation to the crop calendar and severity of drought.

United States Agency for International Development has evolved a Famine Early Warning System NetWork (FEWSNET) by integrating the composite information on temperature, winds, humidity, soil and topography, observations on conflict, civil interest, health, market prices, field observations on agriculture, satellite derived rainfall and NDVI. FEWSNET is operationally issuing monthly food security reports for decision makers in Africa and USA (http://ltpwww.gsfc. nasa.gov/bsb/hqvisit/16MAR2004/tucker.GIMMS_FEWS.pdf).

Remote sensing data provides major input to all the three types rainfall prediction systems currently in operation in India. In the long term rainfall prediction by 16 parameters which include global and regional atmosphere, land and ocean parameters (Temperature, pressure, wind, snow, El-Nino, etc.) remote sensing data from geo-stationary and polar orbiting weather satellites such as INSAT, NOAA and other global data is used. In the medium range weather prediction, the NCMRWF uses satellite based SST, NDVI, snow cover area and depth, surface temperature, altitude, roughness, soil moisture at surface level and TOVS and Radio sonde data on water vapour, pressure and temperature at vertical profile data in the T86/NMC Model. However at present only global data with poor spatial resolution is being used. In the short range rainfall prediction also INSAT based visible and thermal data is being used.

13.12.6. Improved deliverables

The deliverables from drought monitoring projects should lead to enhance the capabilities of administration and farming community to evolve action plans to minimize the impact of drought. Therefore value addition to the drought assessment has to be done on the following aspects;

- Vulnerability mapping - drought prone area identification need to be updated at least once in five years due to change in the land use, irrigation development, cropping pattern and rainfall, etc.
- Rainfall predictions- quantitative predictions over smaller regions
- Crop monitoring – early season drought detection, stress detection at local level
- Crop specific crop condition assessment and early warning on expected yield at district and sub district level
- Quantitative assessment – drought impact on sown area, crop production
- Regular monitoring of water availability at minor, medium and major irrigation tanks and reservoirs with the help of remote sensing is required for better accuracy and timeliness
- Action plan for sustainable development in all drought prone area need to be taken up
- Decision support system drought assessment in all the drought prone districts for planning and operation of various drought relief management activities

13.12.7. Delivery mechanism

The information on drought assessment, predictions produced by different agencies is very often technical, complex and do not follow any standardized format. Many potential users do not even know the existence of such information. Therefore there is a need for evolving an effective mechanism to disseminate the information to the user agencies. The delivery mechanism should allow active interaction in the identification of problems and providing solutions with the use of scientific information. This can be achieved through internet portals in an interactive environment. Internet will also provide access to related research that is not always disseminated in a timely way or through easily accessible modes. User feedback on the functional aspects of the system and utility of the information will form essential part of management approach. Communication satellites have significant potential for real-time dissemination of information.

13.12.8. Integration between Science and Policy

An essential aspect of the planning process is integrating the science and policy of drought management. The policy maker's understanding of the scientific issues and technical constraints involved in addressing problems associated with drought is often limited. Likewise, scientists generally have a poor understanding of existing policy constraints for responding to the impacts of drought. In many cases, communication and understanding between the science and policy communities must be enhanced if the planning process is to be successful.

Integration of science and policy during the planning process will also be useful in setting research priorities and synthesizing current level of understanding and capabilities.

13.12.9. Institutional frame work

Drought management requires a joint efforts of individuals/institutions originating from multidisciplinary aspects and together should evolve a mechanism to understand the inter relations of various aspects and generate the action plan. For example meteorologists foresee the availability of water through rainfall; natural resource managers or environmental specialists focus on the analysis of the impact of different water availability situations on various interests like agriculture, live stock and people. The major challenge lies in bringing these groups together with inter connectivity and synergy to evolve group actions. The different institutions in the drought management plan should include water institution, meteorology, agriculture, ground water, environment and socio-economic. These groups collectively should address various issues such as identification of human, biological, financial and legal constraints, identification of research needs, integration of science and policy, formulation of drought plan, creation of public awareness, implementation of planned activities either short term or long term etc. A model for institutional participation is shown in Figure 13.9.

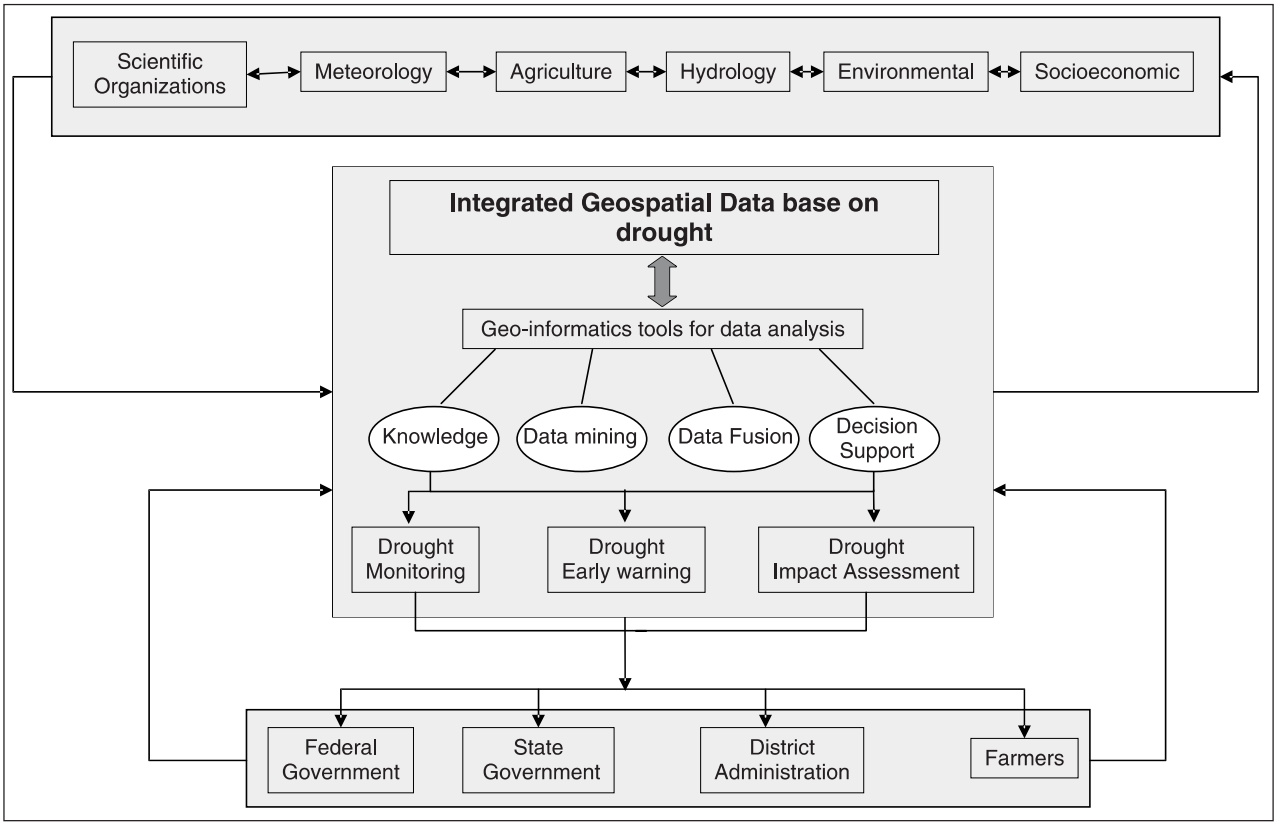

Figure 13.9: Frame work of Institutional linkages, data flow, application of Geoinformatics for drought assessment and use of information for drought management

13.13. Conclusions

Drought is a weather related disaster affecting a large portion of the most productive agricultural areas of the world. With spatial and temporal abnormalities in monsoon precipitation and 68% of agricultural area depending on rainfall, agriculture in India is increasingly affected by droughts of different intensities. A number of indicators related to weather, soils and crops are currently available for assessing the agricultural drought situation.

Dynamic nature of drought in terms of its onset, progression, intensity and impacts requires improved tools and high quality data to capture the spatial and temporal dimensions of drought by complementing and supplementing different indicators.

Geoinformatics with geo-spatial data from various satellites, Geographic Information System (GIS) and integrative tools provide immense opportunities to evolve a variety of drought indicators and integrate the same with ground based indicators for objective assessment of drought at different spatial scales.

The unique capabilities of remote sensing satellites to provide comprehensive synoptic and multi- temporal coverage of large areas at regular intervals help in the development of sound, operationally feasible, objective driven and economically viable system for near real time agricultural drought monitoring and assessment.

Geospatial technologies are also useful for hazard and vulnerability mapping to help development of long term strategies of drought management.

The proposed launch of state of the art indigenous microwave satellite RISAT, in the year 2009 gives scope for studying cropped area progression and soil moisture in the monsoon season, thereby enhancing the drought monitoring capabilities.

Institutionalization of contemporary technologies, development of spatial decision support systems, impact assessment and early warning are some of the issues that needs to be addressed to strengthen the agricultural drought management system of the country.

References

Bastiaanssen, 1998, *Remote Sensing in Water Resources Management: The state of the art*, IWMI publication, p118.

Batista TT, Shimabukuro YE and Lawrence WT, 1997, The long term monitoring of vegetation cover in the Amazonian region of northern Brazil using NOAA-AVHRR data, *International Journal of Remote Sensing*, **18**: 3195-3210.

Benedetti R and Rossini P, 1993, On the use of NDVI profiles as a tool for agricultural statistics – the case study of wheat yield estimate and forecast in Emilia Romanga, *Remote Sensing of Environment,* **45**: 311-326.

Bhalme HN and Mooley DA, 1980, Large scale droughts/floods and monsoon circulation. *Monsoon Weather Review,* **108(8)**: 1197-1211.

Burgan R E, Hartford RA and Eidenshink JC, 1996, Using NDVI toassess departure from average greenness and its relation to fire business, Gen. Tech. Report INT-GTR-333, US Department of Agriculture, Forest Service, Intermountain Research Station, Ogden, Utah,p 8.

Chaudhury BJ and Golus RE, 1988, Estimating soil wetness using satellite data, *International Journal of Remote Sensing*, **9**: 1251-1257.

Doraiswamy, Paul C, Thomas R Sinclair, Steven Hollinger, Bakhyt Akhmedov, Alan Stern and John Prueger, 2005, Application of MODIS derived parameters for regional crop yield assessment, *Remote Sensing of Environment,* **97**: 192-202.

Gibbs WJ and Meher JV, 1967, Rainfall deciles as drought indicators. Bureau of Meteorology, Melbourne, *Australia Bulletin*, **48**,pp 33.

Goldberg I, Ed., 1972, *Agro climatic atlas of the World*, Hydrometizdat, p 133.

Goswami and Prince K Xavier, 2003, Potential predictability and extended range prediction of Indian summer monsoon breaks, *Geophysical Research Letters,* **30(18)***:* Doi:10.1029/2003gl017810.

Goward SA, Tucker CJ and Dye, 1985, North Americal vegetation patterns observed with the NOAA-7 advanced very high resolution radiometer, *Vegetation*, **64**: 3-14.

Hayes MJ and Decker WL, 1998, Using satellite and real-time weather data to predict maize production, *International Journal of Biometeorology,* **42**: 10-15.

Jackson TJ, 1993, Measuring surface soil moisture using passive microwave remote sensing, *Hydrological Processes*, **7**: 139-152.

Jhonson E, Gary, Rao Achutuni V, Thiruvengadachari S and Kogan Felix, 1993, The role of NOAA satellite data in Drought early warning and monitoring: Selected studies, in Drought Assessment, Management and Planning: Theory and case studies, edited by Donald A. Wilhite, Kulwer Academic Publishers.

Justice CO, Townshend JRG, Holbenand BN and Tucker CJ, 1985, Analysis of phenology of global vegetation using meteorological satellite data, *International Journal of Remote Sensing*, **6**: 1271-1318.

Kogan FN, 1995, Droughts of late 1980s in the USA as derived from NOAA polar orbiting satellite data, Bulletin of *American Meteorological Society,* **76**: 655-668.

Kogan FN, 2001, Operational Space Technology for Global Vegetation Assessment, *Bulletin of the American Meteorological Society*, **82**: 1949-1964.

Kulshreshta SM and Sikka DR, 1989, Monsoons and Droughts in India: Long term trends and policy choices, National workshop on drought management, New Delhi.

Malingreau JP, 1986, Global vegetation dynamics: Satellite observations over Asia, *International Journal of Remote Sensing,* **7**: 1121-1146.

Mc Kee TB, Doesken JL and Kliest, 1993, Drought monitoring with multiple time scales, Eighth Conference on Applied Climatology, Anaheim, California.

Minamiguchi Naoki, 2005, The application of Geospatial and Disaster information for food insecurity and agricultural drought monitoring and assessment by the FAO GIEWS and Asia FIVIMS, Workshop on Reducing Food Insecurity Associated with natural Disasters in Asia and the Pacific, Bangkok, Thailand.

Moulin SA, Bondeau A and Delecolle R, 1998, Combining agricultural crop models and satellite observations: from field to regional scales, *International Journal of Remote Sensing*, **19**: 1021-1036.

Murthy CS, Sesha Sai MVR, Bhanuja Kumari V, Prakash VS and Roy PS, 2007, Study of crop condition and assessment of agricultural drought in rabi season using IRS – AWiFS images, *Journal of Agrometeorology*, **9**:19-26.

Murthy CS, Sesha Sai MVR, Dwivedi RS, Roy PS, Rao GGSN and Rama Krishna YS, 2008, An integrated approach for characterization and delineation of drought prone areas, Procedingson International Symposium on Agromet and Food Security, Hyderabad, India.

Murthy CS, Sesha Sai MVR, Bhanuja Kumari V and Roy PS, 2007, Agricultural drought assessment at disaggregated level using AWiFS/WiFS data of Indian Remote Sensing satellites, *Geocarto International*, **22**: 127-140

Murthy CS, Sesha Sai MVR, Chandrasekar K and Roy PS, 2008, Spatial and Temporal Responses of Different Crop Growing Environments to Agricultural Drought – A Study in Haryana State, India using NOAA AVHRR data, *International Journal of Remote Sensing.*

Njoku EG and Entekhabi D, 1996, Passive microwave remote sensing of soil moisture, *Journal of Hydrology*, **184**: 101-129.

Owe M, Chang A and Golus RE, 1988, Estimating surface soil moisture from satellite microwave measurements and satellite derived vegetation index, *Remote Sensing of Environment*, **24**: 331-345.

Palmer WC, 1965, Meteorological Drought, Research Paper, *Weather Bureau US*, **45**, p 58.

Palmer WC, 1965, Meteorological drought, Research Paper No. 45, *US Weather Bureau* (NOAA Library and Information Services Division, Washington DC, 20852).

Palmer WC, 1968, Keeping track of crop moisture conditions, nationwide: The new crop moisture index, *Weatherwise,* **21**: 156-161.

Perry CR and Lautenschlager LF, 1984, Functional equivalence of spectral vegetation indices, *Remote Sensing of Environment,* **14**: 169-82

Peters J Albert, Elizabeth A. Walter-Shea, Lei Ji, Andres Vina, Michael Hayes and Mark D Svoboda, 2002, Drought monitoring with NDVI-based Standardised Vegetation Index, *Photogrammetric Engineering and Remote Sensing*, **68**: 71-75.

Rao BM, Thapliyal PK, Pal PK, Manikiam B and Dwivedi A, 2001, Large scale soil moisture estimation using microwave radiometer data, *Journal of Agrometeorology*, **3**: 179-187.

Rathore MS, 2004, State level analysis of drought policies and impacts in Rajasthan, India, Working paper 93, International Water Management Institute (IWMI), Colombo, Srilanka, p 40.

Roy PS, Joshi PC, Murthy CS and Kishtawal CM, 2006, Geoinformatics for Drought Assessment, in Drought Management Strategies in India (Eds. Samra JS, Gurbachan Singh & Dagar JC), 23-60. ICAR, NEW Delhi, India.

Schmugge TJ, O'Neil PE and Wang JR, 1986, Passive Microwave soil moisture research, *IEEE Transaction on Geoscience and Remote Sensing,* **24**: 12-22.

Subbaiah AR, 2004, *State of the Indian Farmer – A Millenium study, Natural Disaster Management,* **21**, Published by Department of Agriculture and Cooperation, Ministry of Agriculture, Government of India, New Delhi. p 226.

Swain PH and Davis SM, 1978, *Remote Sensing; The Quantitative Approach*, McGraw Hill, New York

Thapliyal PK, 2003, Estimation of soil moisture from satellite microwave radiometers and its impact on the simulation of Indian summer monsoon, Ph.D.Thesis, Department of Mechanical Engineering, Indian Institute of Science, Bangalore, INDIA.

Thapliyal PK, Pal PK, Narayanan MS and Srinivasan J, 2005, Development of a time series based methodology for estimation of large area soil wetness over India using IRS-P4 microwave radiometer data, *Journal of Applied Meteorology*, **44**: 127-143.

Thapliyal PK, Rao BM, Pal PK and Das HP, 2003, Potential of IRS-P4 Microwave Radiometer Data for Soil Moisture Estimation over India, *Mausam*, **54**: 277-286.

Thenkabail PS, Gamage MSDN and Smakhtin VU, 2004, The use of remote sensing data for drought assessment and monitoring in Southwest Asia, International Water Management Institute (IWMI) *Research Report* no.85, Srilanka.

Thornthwaite CW, 1948, An approach toward a rational classification of climate, *Geographical Review*, **21**: 633–655.

Tucker CJ, Townshend JRG and Goff TE, 1985, African land covers classification using satellite data, *Science*, **227**: 369-375.

Tucker CJ, 1979, Red photographic infrared linear combinations for monitoring vegetation, *Remote Sensing of Environment,* **8**: 127-50.

Tucker CJ and Chowdhary BJ, 1987, Satellite remote sensing of drought conditions, *Remote Sensing of Environment*, **23** : 243-251.

Van Bavel CHM, 1953, A drought criterion and its applications in evaluating drought incidence of hazard, *Agronomy Journal*, **45**: 167-172.

Van Dijk A, Callis SL, Sakamoto CM and Decker WL, 1987, Smoothing vegetation index profiles; An alternative method for reducing radiometric disturbance in NOAA/AVHRR data, *Photogrammetry Engineering and Remote Sensing,* **53**: 1059-67.

Van-Rooy MP, 1965, A Rainfall anomaly index (RAI) independent of time and space, *Notos*, **14**: 43.

Wu Hong, Svoboda D Mark, Hayes J Michael, Wilhite A Donald and Fujiang Wen, 2006, Appropriate application of the standardizes precipitation index in arid locations and dry seasons, *International Journal of Climatology*, **27(1)**: 65-79.

Suggested readings

Drought – A Global Assessment, Vols. I and II, - Ed. Donald A Wilhite, 2000, Routledge, p396 and 304 respectively.

Drought – Assessment, monitoring, management and resources conservation,Nagarajan R, Capital Publishing Company, pp 312.

Drought and Water Crises – Ed. Donald A Wilhite, 2005, Taylor & Francis, p406.

Methods and tools for drought analysis and management- Ed. Giuseppe Rossi, Teodoro Vega and Brunella Bonaccorso, 2007, Springer, pp 422.

The Advanced Very High Resolution Radiometer- Cracknell AP,1997, Taylor & Francis, p534.

The Monsoons – Das PK, National Book Trust India, New Delhi, p254.

nrsc

Remote Sensing Applications

P. S. Roy
R. S. Dwivedi
D. Vijayan

National Remote Sensing Centre

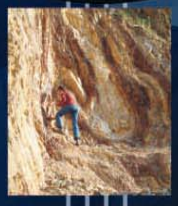

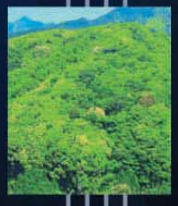

Remote Sensing Applications

Landslides

14.1. Introduction

A frequently used definition of landslide is “a movement of mass of rock, earth or debris down a slope” (Cruden, 1991). They can occur on many types of terrain given the right conditions of soil, rock, moisture condition and slope. Integral to the natural process of the earth’s surface geology, landslides serve to redistribute soil and sediments in a process that can be in abrupt collapses or in slow gradual slides. Classification of landslides was first formally proposed by Varnes (1978) based on types of movement and types of material. A landslide can be classified and described by two nouns; the first describes the material and the second describes the movement. The material can be rock, debris and earth or a mix. The movement can be fall, topple, slide, spread and flow. Hence, a landslide can be named as rock fall (‘rock’ is the material type + ‘fall’ is the movement type), debris flow and so on. It is recommended to use a combination of one/ two of these nouns to describe a landslide, though in nature, we notice a mix of materials and movements and then we are tempted to use the term ‘complex landslide’, which normally should be avoided. The features and geometry of a landslide is explained in figure 14.1. Details of various landslide types and processes can be found in Cruden and Varnes (1996).

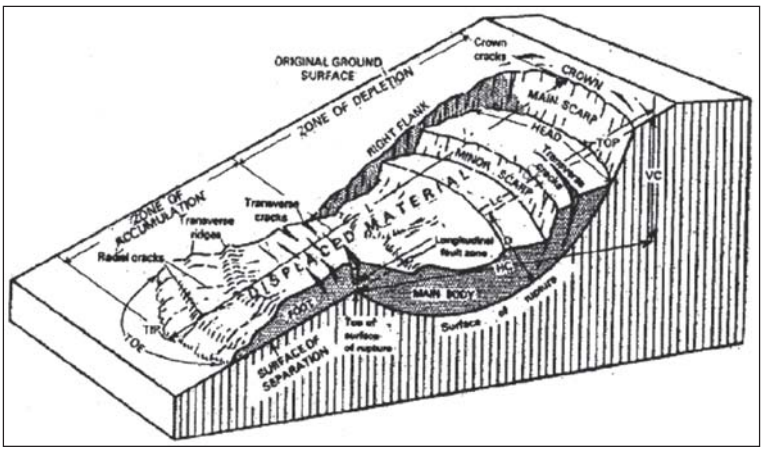

Figure 14.1: Block diagram of a landslide (source: Varnes, 1976)

Zonation refers to “the division of the land into homogenous areas or domains and their ranking according to degree of actual/potential hazard caused by mass movement” (Varnes, 1984). Landslide Hazard Zonation (LHZ) is defined as the “mapping of areas with an equal probability of occurrence of landslides of a given type and magnitude within a specified period of time” (Guzzetti *et al.*, 1999; Varnes, 1984). Landslide hazard is commonly shown on maps as areas or zones, which display the spatial distribution of landslide hazard classes. To do this, the fundamental steps are the spatial prediction of susceptible zones, estimation on the probability of magnitude of future landslide and then temporal prediction of landslide recurrence in different susceptible zones. Landslide hazard estimates in turn, are the most crucial input to risk analysis, the latter being defined as “the expected number of lives lost, persons injured and damage to property and disruption of economic activity due to a particular landslide hazard phenomenon for a given area and reference period” (Varnes, 1984).

14.1.1. Cause of Landslide

The terrain factors such as slope, lithology, geological structure, land use, lineament density, geomorphology etc., are important for a landslide to occur in an area. If terrain factors are favourable e.g., high lineament density, unconsolidated rock, steep slope etc., then the area is susceptible to landslide. Landslides can be triggered by rainfall, undercutting of slopes due to flooding or excavation, earthquakes, snowmelt and other natural causes as well as human-made causes, such as over grazing by cattle, terrain cutting and filling and excessive development. Rainfall increases the pore water pressure. So the shear strength of the rock decreases. This leads to landslide in an area. In India, most of the landslides occur during rainy season due to heavy downpour in a short time.

14.1.2. Role of remote sensing in Landslide Inventory

Comprehensive landslide inventory is a prerequisite for landslide hazard and risk analysis. A landslide inventory map not only shows the time and date of occurrence but also the types of landslide. Landslide inventories can make use of a variety of approaches, ranging from digital stereo image interpretation to automatic classification based either on spectral or altitude differences, or a combination of both. The multi temporal images can be used to prepare a landslide activity map. The stereo-images are not only useful for the derivation of height information but also for landslide inventory mapping as it provides a 3-dimensional visualisation opportunity (Vinod Kumar *et*

al., 2006, 2008). Updation of landslide inventory map after earthquake / rainfall can be done with satellite data (Vinod Kumar *et al.*, 2006).

Very high resolution imagery (QuickBird, IKONOS, CARTOSAT-1 and 2) has become the best option now for landslide mapping, and the number of operational sensors with similar characteristics is growing year by year (van Westen *et al.*, 2007). Other remote sensing approaches of landslide inventory mapping include shaded relief images produced from Light Detection and Ranging (LiDAR) DEM and Synthetic Aperture Radar (SAR) interferometry. Lidar is an active sensor and the signal from the sensor from onboard aircraft has the capability of penetrating through the tree crown (most of the times) and thus provides data about subtle elevation variation of the bare ground. Lidar data have been used even to prepare landslide inventory under forest areas in hilly regions and to refine the boundaries of landslides prepared during field investigations. This data is not only useful for mapping old landslides but also can improve field survey based investigation in regions with subdued morphology (Van Den Eeckhaut *et al.*, 2007). SAR images are useful in identifying critical terrain elements such as faults and slope characteristics. Also subtle movement due to landslides can be picked up from interferograms generated from SAR images. Another advantage of SAR data over optical sensor data is its all weather monitoring ability. So, combination of SAR imagery with high resolution optical multispectral is useful for monitoring debris hazard in mountainous areas (Tsutsui *et al.*, 2004). However the problems such as foreshortening and layover effects associated with SAR data in mountainous areas have to be addressed carefully.

14.2. Global and National Scenario

Landslides are among the main natural catastrophes, which have caused major problems in mountainous terrain by killing hundreds of people every year besides damaging property and blocking transportation links. In some areas, such as the western coastal parts of North and South America, Central America, Alpine regions of Italy, France, Switzerland and Austria in Europe, Himalayan regions of India, Nepal in Asia and parts Central Asia, the effects of landslides are more pronounced mainly due to the spurred developmental activities to meet the ever growing demand of people. As per the official figures of United Nations International Strategy for Disaster Reduction (UN/ISDR) and the Centre for Research on the Epidemiology of Disasters (CRED) for the year 2006, landslide ranked 3rd in terms of number of deaths among the top ten natural disasters. Approximately 4 millions people were affected by landslides in 2006 (OFDA/CRED, 2006). Regions with the highest landslide risk are found in Colombia, Tajikistan, India, and Nepal where the estimated number of people killed per year per 100 km^2 was found to be greater than one (Nadim *et al.*, 2006).

Incidences of landslides are not uncommon in India. Approximately 0.49 million km^2 or 15% of land area of the country is vulnerable to landslide hazard. Out of this, 0.098 million km^2 is located in north eastern region and rest 80% is spread over Himalayas, Nilgiris, Ranchi Plateau and Eastern and Western Ghats (GSI, 2006). The states of Uttarakhand, Himachal pradesh have been facing landslide problems for a long time. Some of the big landslides of Uttarakhand in recent years are Vishnuprayag, Baldora, Lambaghar Chatti, Jharkula, Phata Byung landslides and Amiya landslide. One of the major landslides in the recent history of India is the 1998 Malpa landslide in which 221 persons were killed. Hence, there is an urgent need to formulate strategies for minimising the societal impact of landslides. One of the first steps in this direction is the preparation of Landslide Hazard Zonation (LHZ)/susceptibility and landslide risk maps and making them available to the concerned governmental as well as non-governmental/local bodies for taking up necessary actions.

14.3. Methods of Landslide Hazard Zonation (LHZ)

14.3.1. Conventional method

Conventional methods of landslide investigation are the most accurate as it focus on a small area and relies on extensive field investigations. In this method, an expert visits the area and based on his/her knowledge about the geology, geomorphology of the area, assigns a susceptibility class of landslide to it. But it has a serious limitation as it is labour intensive and it is also impossible to carry out this method of hazard zonation for large country like India.

14.3.2. Statistical method

Landslide susceptibility can be determined through deterministic method, which is followed in smaller areas on larger scales (larger than 1:10000). These methods are process-based and give more detailed results, expressing the hazard in terms of factor of safety to each mapping unit. The deterministic method can quantitatively represent

the landsliding processes by considering the detailed physical and dynamic in-situ parameters of slope forming material and can easily be used to retrieve temporal probability information by modeling different groundwater scenarios caused by different rainfall event (triggering factor). The deterministic methods highly depend on a large number of detailed site-specific geotechnical and groundwater parameters, otherwise its results are oversimplified (Moon and Blackstock, 2004) and that is why for medium scale (1:25,000 to 1:50,000) analysis in a large area, the use of such deterministic method may not be feasible. Deterministic models are also difficult to represent as 2D GIS spatial data product because it considers depth wise data variability for calculation of factor of safety. That is why for hazard assessment of bigger areas on medium scale, empirical methods based on various statistical and mathematical techniques are followed.

In medium scale landslide susceptibility analysis, knowledge-driven/ heuristic and data-driven empirical methods are prevalent. The knowledge-driven methods are mostly qualitative (direct) but semi-quantitative methods (indirect) based on heuristics are also followed. The data-driven methods are mostly statistical (bivariate and multivariate) and few are mathematical (artificial neural network).

The knowledge-driven/heuristic direct approaches to spatial prediction of landslide susceptibility involve detailed geomorphological mapping using uniquely coded polygons, which are evaluated one-by-one by an expert to assess the type and degree of hazard (Barredo *et al.*, 2000; Hansen, 1984; Varnes, 1984). Indirect heuristic approach utilizes data integration techniques, including qualitative parameter combination, in which the analyst assigns weighting values to a series of terrain parameters and to each class within each parameter**.** The relative importance of each terrain parameter as a predisposing determining factor of slope instability is quantitatively determined by pair-wise comparison using the so-called analytical hierarchy process (AHP) (Saaty, 1996) or is incorporated through spatial multi-criteria evaluation (SMCE). In direct heuristic methods, use of detailed geomorphological factor maps in general raised the overall accuracy of the susceptibility maps**,** though the accuracy of such direct qualitative model largely depends on the experience of the expert using the method. Whereas, in indirect heuristic methods, similar weight values are considered for all locations within the same factor. The addition of such unique weight values tends to "flatten out" the results of indirect methods. Thus, the main limitations of the knowledge-driven methods are the subjectivity involved both in the direct mapping as well as in the assignment of weights in indirect methods and general non-availability of any quantitative technique of model validation.

Since the late eighties, the increasing popularity of geographic information system (GIS) has facilitated development of various *quantitative or data-dependent* landslide spatial prediction methods (Aleotti and Chowdhury, 1999). GIS is very suitable for such methods, in which all possible landslide contributing terrain geofactors (evidence) are combined with landslide inventory map (target) using data-integration techniques (Bonham-Carter, 1996; Chung *et al.*, 1995; van Westen, 1993). Thus, in such quantitative methods of hazard estimation, spatial associations of past and present landslides and associated geofactors act as the key parameters to predict future landslides (Carrara *et al.*, 1991; Zezere *et al.*, 2004). These data-dependent methods aim to introduce objectivity in analysis by reducing subjectivity or generalisation of the true knowledge-driven methods.

Amongst the quantitative methods, the application of the *bivariate statistics* (e.g., weight of evidence method) in landslide spatial prediction is common and it needs to be weighed in light of following limitations because of mis-applications by many researchers, which include i) generalisation by assuming that landslides happen under the same combination of factors throughout the study area, ii) ignorance of the fact that each landslide type has its own set of causal factors, and should be analysed individually and iii) lack of suitable expert opinion on different landslide types and processes and of slides of different periods, which may be inevitable if these methods are solely applied by GIS-experts, and not by earth scientists (Westen *et al.*, 2003). Another debate regarding bivariate methods is that, instead of partitioning the study area into unique domains or mapping/ terrain/ slope unit, the conditional probabilities are determined for separate geofactors and then added sequentially under the assumption that such factors are weakly correlated to each other (assumption of conditional independence amongst independent variables). It has been argued by some researchers (Carrara *et al.*, 1995) that this method perhaps holds true where very few environmental factors are only responsible for landslides, and a sound expert knowledge exists about the landslide processes.

Bivariate or multivariate methods may be found statistically suitable to predict future landslides at medium scales (1:25,000 to 1:50,000), but logical explanations of the results or outputs and exact knowledge about the dependencies of causal parameters with the target are sometimes absent in these type of methods. Since these methods are

mostly based on various statistical data treatments focused mainly for objective elimination or reduction of errors and uncertainty in prediction, the aspects of data quality, reasoned selection of input parameters and inherent fuzziness of some geofactor data etc., are frequently overlooked. Multivariate methods, in spite of limitations and pitfalls in applications, are used nowadays as among the most feasible quantitative tools for assessing different levels of landslide susceptibility. For example, when a set of independent variables include both good and bad predictors (the latter having no clear physical relationship with mass movement processes), a step wise regression technique in multivariate statistics is followed with an aim to eliminate statistically non-significant factors, but sometimes the output of these analyses may generate unreliable and meaningless results. In similar way, artificial neural network (ANN) – a mathematical technique is also used for spatial prediction of landslide hazard. The ANN method is not sensitive to any statistical distribution of data, and can integrate both continuous as well as categorical data set. The ANN methods are adaptive and generic in nature. They are construed to handle imperfect or incomplete datasets and can capture non-linear and complex interactions among variables of a system (Lee *et al.*, 2003). Since ANN is almost independent of the quality of input variable; chances of getting unreasonable goodness in results are sometimes highly abstract and misleading. Like multivariate techniques, in ANN method also, the internal processes which train the input dataset and minimise the statistical errors and uncertainties are difficult to follow.

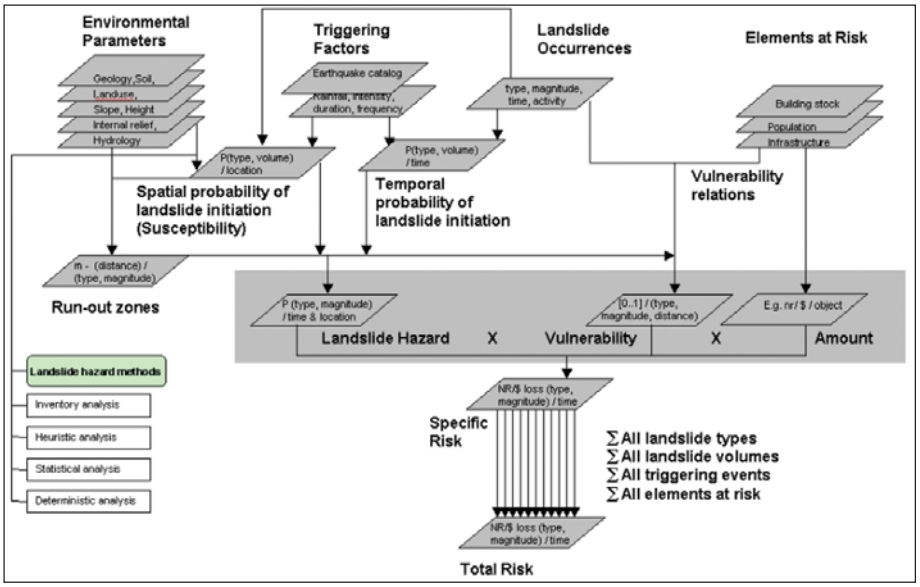

Figure 14.2: A generalised flowchart for LHZ and landslide risk mapping (source: van Westen et al., 2008)

Landslide risk mapping is a step forward to hazard zonation. The elements at risk and the vulnerability of these elements to a landslide are the key factors to calculate the landslide risk. Figure 14.2 shows the general methodology for landslide hazard and risk mapping.

14.4. Gap Areas

Understanding of the processes that lead to landslide is very crucial to any successful landslide hazard zonation. Landslide is an active field of research. The methodology of landslide hazard zonation mapping is changing with availability of new datasets and tools.

In order to prepare an accurate landslide susceptibility map, it is important to know the terrain factors favourable for landslide. Instead of considering all the factors, research is required to find out the critical factors of the landslide susceptibility mapping.

Determination of temporal probability of landslides in given set of terrain condition is required to prepare the landslide hazard map from the landslide susceptibility map. Normally it is done by calculating the return period of landslide using rainfall data, which is a common triggering factor for landslides. It is a difficult task as we require historical rainfall, which in most cases is not available. Research is required to calculate of return period of the landslide not only due to rainfall but also due to earthquake and snowmelt, which can be integrated with the landslide susceptibility map.

As we know, the areas under high landslide hazard category may not be always at high risk. Elements at risk and calculation of vulnerability are important factors for preparation of landslide risk map, which are often difficult to determine. Finally we need to have proper policies and laws where these maps prepared can be implemented on the ground so that life and property can be saved.

14.5. Major Application Projects

The following major landslide projects are carried out by NRSC.

14.5.1. LHZ mapping in Uttarakhand and Himachal Pradesh

Landslide hazard zonation (LHZ) map for important pilgrimage/tourist routes covering 2000 km road length for the states of Uttarakhand and Himachal Pradesh are prepared using satellite data and GIS. This project was carried out in association with other scientific organisations such as CBRI, WIHG. Total 14 thematic layers such as lithology, geomorphology, geological structure, and slope are prepared and integrated in GIS to prepare the landslide hazard maps. Figure 14.3 shows the landslide susceptibility map prepared for Uttarkashi. These maps are prepared in the year 2001 on 1:25 000 scale and two Atlases are published separately for both the states. Subsequently theses maps are validated using the landslides that have occurred after 2001.

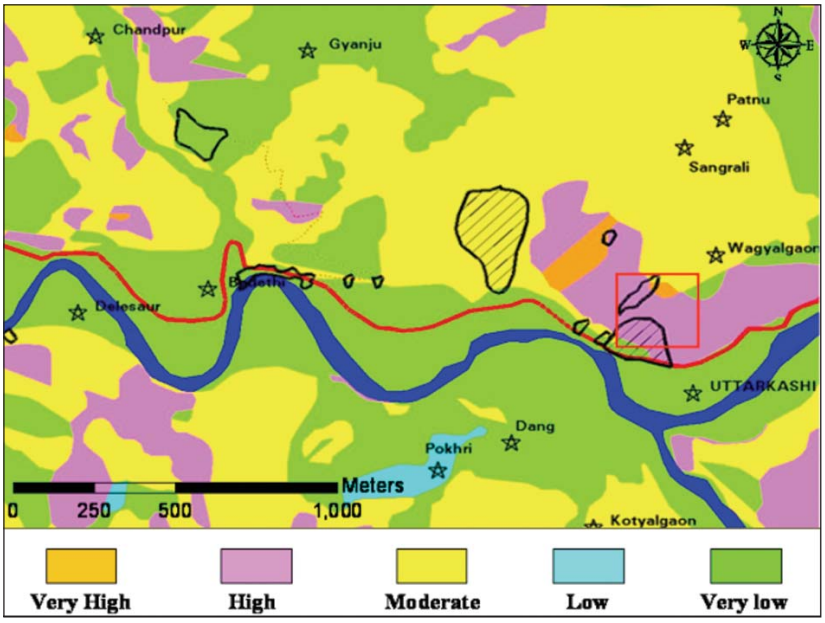

Figure 14.3: Landslide susceptibility map of Uttarkashi and its surrounding, Uttarakhand prepared using remote sensing data and GIS analysis

14.5.2. Mumbai – Goa (NH-17) Route

This project is being carried out in association with Geological Survey of India (GSI). The objective of this project is to prepare landslide hazard zonation map on 1:50,000 scale. This project is of similar nature to the previous project. The types of landslides are different in this area from the Himalayas. Mostly they are shallow translational landslides. They are controlled by the depth of the soil cover.

14.5.3. Varunawat Landslide

The town of Uttarkashi is situated on the foothill of Varunawat Parbat. It is on the right bank of Bhagirathi river in the Uttarakhand. Himalaya witnessed a serious landslide crisis, which started on 23 September 2003 and continued for two weeks, but the situation became grave by 1 October 2003. Severe damage was caused to the residential areas and infrastructure facilities such as power sub-station and the Rishikesh–Gangotri national highway around the small township of Uttarkashi. Fortunately, there was no loss of human and animal lives due to the timely and combined efforts of the local administration in warning and evacuating the people.

A detail study was carried out using aerial photographs acquired by NRSC after the landslide. The objective was to find out the cause of the landslide. The landslide map is prepared on 1:10,000 scale, which can be used for post landslide management measures (Vinod Kumar *et al.*, 2008).

14.5.4. DSC Activity

Landslide is identified as one of the disasters in the DMSP programme of ISRO. As a part of this activity, every year landslides are monitored using the high resolution Indian satellite data in Decision Support Centre (DSC) at NRSC.

14.6. Methods to solve problem

Similar to other geo-hazards, landslide can not be avoided in mountainous terrain. Better understanding of this hazard will help people to live in harmony with the pristine nature.

Since India has 15% of its land area prone to landslides, preparation of LHZ maps for these areas is of paramount importance for prioritising the areas critical to landslides. These LHZ maps will also be an important input for

preparing the landslide management maps. Ministry of Home Affairs, Government of India has identified GSI as the nodal office to prepare landslide hazard map on 1:50,000 scale for the vulnerable areas of India in association with Survey of India and NRSC. These maps will act as guideline for the developmental activities such as road, dam, building construction in the mountainous areas.

Big landslides are a perennial problem by blocking transportation routes should be treated geotechnically on the ground. The methods that are normally practiced for such purpose are explained below.

- Minimising the infiltration of rain /surface water into the slide zones
- Channelisation of water in the crown portion by constructing line horizontal gravity drains drilled either from the slope surface or from drainage wells or galleries
- Modifying / resloping unstable weathered material in the crown portion
- The scarp portions where the fragmented and fractured rocks are exposed can be reinforced through anchoring of rocks
- Removal of the roots of trees growing in cracks and grouting the natural fracture zones in the primary zones of accumulation
- In order to stabilise the loose soil debris, soil nailing can be used to stabilise the potentially stable slopes where the creeping process is in progress
- In order to minimise the hazard of rock-fall the best process is to let the fall occur and to control their distance and direction of travel. This includes catchments ditches and barriers, wire mesh fences and rock sheds at the toe of slope
- Proper measurements to prevent forest fire in the slide-affected areas
- Retention wall, terracing is useful as it modifies the slope

14.7. Monitoring of Landslides

Monitoring of landslides can be carried out on two scales; one for the regional scale using remote sensing data and the other for specific sites using ground instruments.

14.7.1. Remote sensing

Satellites have a limitation on the frequency of observation. So they are used to find out the changes in terms of number of landslides over a period of time. High resolution satellite data are very helpful for this purpose. Though there are limitations of satellite remote sensing for site specific monitoring due to poor revisit period, terrestrial remote sensing techniques using SAR interferometry, terrestrial laser scanner are emerging as alternate tools. These methods are very precise and can predict movement with centimeter level of accuracy. Terrestrial laser scanner can observe continuously the change in the density of joint density pattern and indicate the areas of new stress built up.

14.7.2. Ground instruments

Ground instruments in the landslide prone areas are used to measure parameters such as surface and sub surface movements, surface and sub-surface water movement. From site specific monitoring, we can get a real time data and then fit a slope stability model and then predict the time of occurrence of a landslide. Though the correct predication of occurrence of landslides is uncommon, it happened once in China, when a landslide in the year 1995 was predicted one day ahead

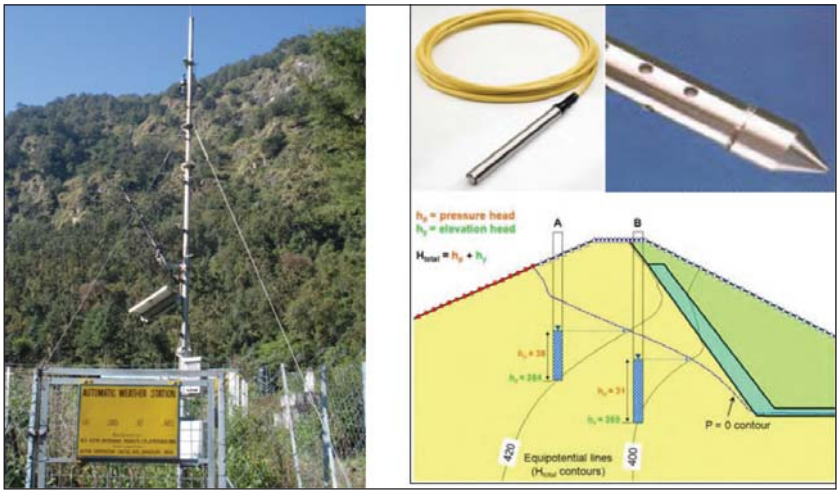

Figure 14.4: (a) AWS of ISRO near Kandi landslide, Uttarakhand and 4(b) Piezometer

along the Yellow river. Success of site specific monitoring may lead to a landslide early warning, which will save people and property. Instruments useful for site specific monitoring of landslides are GPS, piezometer (figure 14.4(b)), raingauge, extensometer, inclinometer, tiltmeter, automatic weather station (AWS) in figure 14.4(a). AWS is useful in measuring rainfall, humidity, windspeed, etc.

14.8. Cost benefit analysis

Previously aerial photo interpretation (API) was used extensively to prepare landslide inventories. But now with the availability of high resolution imageries, the focus has shifted away from the aerial photographs. A cost comparison between aerial photos and IKONOS image, carried out by Nichol *et al.*, (2006) shows that, if air photos have already been taken and are available, the overall cost of the air-photo-based approach is similar to that of the IKONOS-based approach. If flying costs to take new air photos are added, the cost of the air-photo-based approach becomes 46% higher or 41% higher if tasking of IKONOS is required.

Use of remote sensing data in conjunction with field investigation is a cost effective method for landslide studies. Again, landslide mostly occurs in inaccessible areas, where it is difficult to carry out field investigations. Now with the lowering of the prices of some satellite data and free availability of some satellite data such as Landsat TM/ETM+ and SRTM DEM, the cost of such studies has further reduced.

14.9. Summary

The physical processes that lead to a landslide are very important for successful landslide hazard zonation of an area. Satellite remote sensing data is now exetensively used for preparation of thematic layers. DEM derived from satellite data will now provide important parameters such as slope but also help in better geovisualisation. Moreover, GIS has contributed substantially to the processes of making spatial analyses of landslides.

However, we know very much less about how non-scientists, including public administrators, view the landslide hazard. As mentioned by Alexander (2008), there is a disjuncture between the ability to understand, on the one hand which slopes will fail, as well as when and how that will happen, and, on the other hand, why the public seems to find it so hard to recognise and avoid situations of slope failure hazard.

Earth scientists are vigorously responding to the technical challenge of coupling GIS, remote sensing and slope monitoring systems to yield accurate, timely information on landslide hazard (Soeters and Westen, 1996). But at the same time we must listen to the concerns of public safety officials and providing information of a kind that is useful to them.

References

Aleotti P and Chowdhury R, 1999, Landslide hazard assessment: summary review and new perspectives, *Bulletin of Engineering Geology and Environment*, **58**: 21-44.

Alexander DE, 2008, A brief survey of GIS in mass-movement studies, with reflections on theory and methods, *Geomorphology*, **94(3-4)**: 261-267.

Barredo J, Benavides A, Hervas J and Van Westen CJ, 2000, Comparing heuristic landslide hazard assessment techniques using GIS in the Tirajana basin, Gran Canaria Island, Spain, *International Journal of Applied Earth Observation and Geoinformation,* **2(1)**: 9-23.

Bonham-Carter GF, 1996, *Geographic Information Systems for Geoscientists: Modeling with GIS*, Pergamon, Elsevier Science Ltd.,p 398.

Carrara A, Cardinali M, Detti R, Guzzetti F, Pasqui V, Reichenbach P,, 1991, GIS techniques and statistical models in evaluating landslide hazard, *Earth surface processes and landforms,* **16(5)**: 427-445.

Carrara A, Cardinali M, Guzzetti F and Reichenbach P, 1995, GIS technology in mapping landslide hazard, ACF Guzzetti (Editor), *Geographical information systems in assessing natural hazards*, Kluwer Academic Publishers, 135-175.

Chung CJF, Fabbri AG and Westen CV, 1995, Multivariate regression analysis for landslide hazard zonation. In: Carrara A and Guzzetti F (Editors), *Geographical Information Systems in Assessing Natural Hazards,* Kluwer Academic Publishers, Netherlands, 107-133.

Cruden D and Varnes DJ, 1996, Landslide types and processes, In: AK Turner and R.L. Schuster (Editors), *Landslides Investigation and Mitigation*, Special Report 247, Transportation Research Board, National Academy of Sciences, Washington, D.C., 36-75.

Cruden DM, 1991, A simple definition of a landslide, *Bulletin of the International Association of Engineering Geology*, **43**: 27-29.

Guzzetti F, Carrara A, Cardinali M and Reichenbach P, 1999, Landslide hazard evaluation: a review of current techniques and their application in a multi-scale study, Central Italy, *Geomorphology*, **31(1-4)**: 181-216.

Hansen A, 1984, Landslide hazard analysis. In: Brunsden&Prior (Editor), Slope Instability. John Wiley & Sons, New York, 523-602.

Lee S, Ryu JH, Lee MJ and Won JS, 2003, Use of an artificial neural network for analysis of the susceptibility to landslides at Boun, Korea, *Environmental Geology*, **44**: 820-833.

Moon V and Blackstock H, 2004, A Methodology for Assessing Landslide Hazard Using Deterministic Stability Models, *Natural Hazards*, **32(1)**: 111-134.

Nadim F, Kjekstad O, Peduzzi P, Herold C and Jaedicke C, 2006, Global landslide and avalanche hotspots, *Landslides*, **3(2)**: 159-173.

Nichol JE, Shaker A and Wong MS, 2006, Application of high-resolution stereo satellite images to detailed landslide hazard assessment, *Geomorphology*, **76(1-2)**: 68-75.

OFDA/CRED, 2006, EM-DAT International Disaster Database - www.em-dat.net., Université Catholique de Louvain, Brussels, Belgium.

Saaty TL, 1996, *The Analytic Hierarchy Process*, McGraw Hill, 1980, New York.

Soeters R and Van Westen CJ, 1996, Slope Instability. Recognition, analysis and zonation, Turner AK and Schuster RL (Editors), *Landslide: Investigations and Mitigation* ,Special Report 247, Transportation Research Board, National Research Council, National Academy Press, Washington, DC, 129-177.

Tsutsui K, Miyazaki S, Nakagawa H, Shiraishi T and Rokugawa S, 2004, Data fusion techniques of heterogeneous sensor images for debris hazard assessments, IGARSS, Anchorage, Alaska.

Van Den Eeckhaut M, Poesen J, Verstraeten G, Vanacker V, Nyssen J, Moeyersons J, Van Beek LPH, Vandekerckhove L, 2007, Use of LIDAR-derived images for mapping old landslides under forest, *Earth Surface Processes and Landforms*, **32(5)**: 754-769.

Van Westen C, 1993, Remote Sensing and Geographic Information Systems for Geological Hazard Mitigation, *ITC-Journal*, **4**: 393-399.

Van Westen CJ, Castellanos E and Kuriakose SL, 2008, Spatial data for landslide susceptibility, hazard, and vulnerability assessment: An overview. Engineering Geology.

Van Westen CJ, Rengers N and Soeters R, 2003, Use of geomorphological information in indirect landslide susceptibility assessment, *Natural Hazards,* **30(3)**: 399-419.

Varnes DJ, 1978, Slope movements types and processes, In: Schuster RL and Krizek RL (Editors), *Landslides: Analysis and Control*, Special Report 176, Transportation Research Board, National Academy of Sciences, Washington, DC, 11-33.

Varnes DJ, 1984, Landslide Hazard Zonation: a review of principles and practice, UNESCO, Darantiere, Paris, p 61.

Vinod Kumar K, Lakhera RC, Martha TR, Chatterjee RS and Bhattacharya A, 2008, Analysis of the 2003 Varunawat Landslide, Uttarkashi, India using Earth Observation data, *Environmental Geology,* **55(4)**: 789-799.

Vinod Kumar K, Martha TR and Roy PS, 2006, Mapping damage in the Jammu and Kashmir caused by 8 October 2005 Mw 7.3 earthquake from the Cartosat–1 and Resourcesat–1 imagery, *International Journal of Remote Sensing*, **27(20)**: 4449-4459.

Zêzere JL, Reis E, GarciaR,. Oliveira S, RodriguesML , Vieira G,and Ferreira AB, 2004, Integration of spatial and temporal data for the definition of different landslide hazard scenarios in the area north of Lisbon (Portugal), *Natural Hazards and Earth System Sciences*, **4**: 133-146.

http://www.gsi.gov.in/lndslde/lhs.htm., Geological Survey of India,GSI, 2006, Landslide Hazard Studies.

nrsc

Remote Sensing Applications

P. S. Roy
R. S. Dwivedi
D. Vijayan

National Remote Sensing Centre

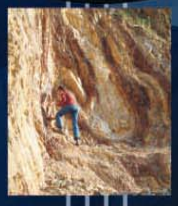

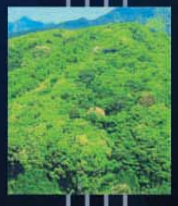

Remote Sensing Applications

Earthquake and Active Faults

15.1. Introduction

Natural hazards and catastrophes are recurring phenomena which affect one or the other part of the world every now and then. Among all such hazards, the most devastating are the earthquakes with intensity over 5 on Richter scale. This is because occurrences of earthquakes are quite uncertain. An earthquake is the result of a sudden release of energy in the Earth's crust that creates seismic waves. The earthquakes are, generally, recorded with a seismometer, also known as a seismograph. The moment magnitude of an earthquake is conventionally reported and this data speaks about the intensity of earthquake. It is seen that magnitude 3 or lower earthquakes are, generally, imperceptible and the earthquakes with magnitude 7 cause serious damage over large areas. Intensity of tremor is measured on the modified Mercalli scale. Tectonic earthquakes occur anywhere within the earth where there is sufficient stored elastic strain energy to drive fracture propagation along a fault plane. In the case of transform or convergent type plate boundaries, which form the largest fault surfaces on earth, plates will move past each other smoothly and seismically only if there are no irregularities or asperities along the boundary that increase the frictional resistance.

Most boundaries do have such asperities and this leads to a form of stick-slip behaviour. Once the boundary has locked, continued relative motion between the plates leads to increasing stress and therefore, stored strain energy in the volume of the rock around the fault surface. This continues until the stress has risen sufficiently to break through the asperity, suddenly allowing sliding over the locked portion of the fault, releasing the stored energy. This energy is released as a combination of radiated elastic strain seismic waves, frictional heating of the fault surface, and cracking of the rock, thus causing an earthquake. This process of gradual build-up of strain and stress punctuated by occasional sudden earthquake failure is referred to as the Elastic-rebound theory. It is estimated that only 10 percent or less of an earthquake's total energy is radiated as seismic energy. Most of the earthquake's energy is used to power the earthquake fracture growth or is converted into heat generated by friction. Therefore, earthquakes lower the Earth's available elastic potential energy and raise its temperature.

Although researchers relentlessly work on earthquake prediction; operationally earthquake is difficult to predict or forecast. Remote sensing based studies are being attempted to detect thermal anomaly associated with earthquake to demonstrate its potentials in earthquake-related studies. Moreover, remote sensing-based study also attempts to relate ionosphere disturbances associated with earthquake to use it as a tool for prediction. A specialized technique called DinSAR (Differential Interferometric Synthetic Aperture Radar) technique is used to record the dynamic movement in parts of earth with the help of spaceborne SAR (Synthetic Aperture Radar). Moreover, the delineation of active faults with help of active fault-related morphometric and geomorphic signature using satellite images helps in long term prediction of earthquake.

Generally, intensity and magnitude of earthquake is known only after the earthquake has actually occurred in a region and causes immense destruction and loss of life and property. This requires all time preparedness for the authorities and the people. The use of satellite imagery and remote sensing techniques also play a vital role in the post earthquake management in the short run as well as in the long run. Availability of high resolution satellite data with short revisit offers immense potential in post earthquake disaster management related studies. Moreover, satellite data helps in creating information for seismic hazard zonation. The integrated analysis of geologic and seismologic data, field observations, lineament data, derived from satellite radar images if integrated with historical data on earthquake, demographic data, soil type, soil deformation analysis etc., data would help to generate seismic hazard zonation map of an area. These maps would evaluate the potential of occurrences of earthquake in an area so that proper pre-earthquake management/engineering practices can be chalked out.

15.2. Global, National Issues and Scneario Development

Although no proper methods are proved as suitable for earthquake prediction with approximate idea of the magnitude of the earthquake. Remote sensing-based study used to detect the thermal anomaly associated with earthquake. But no earthquake has been predicted based on remote sensing based study. Remote sensing-based study also proved useful in detecting active faults; which believed to have activated in recent geological past (<10,000 years) and therefore these zones are very useful for establishing the seismic stations to monitor the deformations or any

future earthquake. In India, in the recent past several active faults have been identified using remote sensing based study in the lower Himalayas.

Seismic hazard zonation is another approach that helps minimizing the devastative impact of earthquake. Seismic hazard assessment requires knowledge not only of the earthquake sources and propagation of seismic waves, but also of the effect of local geology on earthquake ground shaking. However, the lack of empirical data and efficient earthquake microzonation tools have precluded a general integration of local site effects into earthquake hazard assessment schemes. Therefore, simple and fast methods for first-order site classification and methods based on rapid surveys of seismic noise in conjunction with shallow geophysical investigations are being developed. Besides advanced methods of seismic noise analysis suitable for near-surface investigations are being developed and tested. Furthermore, we examine the applicability of remote sensing techniques with the aim of mapping the topography gradient as a proxy. Investigating the role of "soil-city" interaction for local ground shaking and assessing the effect of ground motion duration on earthquake damage are additional challenging issues that have found no or only inadequate consideration in previous microzonation studies. Studies related to adequate magnitude determination, wave propagation, and ground motion prediction equations are to be incorporated, in the earthquake microzonatioin studies.

15.3. Conventional and Scientific Methods in practice

Remote sensing has been used for earthquake research from 70s, with the availability of satellite images. Initially it began with the structural geological and geomorphological studies. Active faults and structures were mapped on the basis of satellite images (Trifonov, 1984). The active faults and structures thus delineated do not form the sound base for time series analysis. Hence, there is no possibility to measure short-term processes before and after the earthquake. The current scenario of remote sensing applications for earthquake studies indicates a few phenomena related to earthquakes: These are earth's deformation, surface temperature and humidity, air humidity, gas and aerosol content. Both horizontal and vertical deformations scaled about tens of centimeters and meters after the shock. Such deformations; specially vertical deformations are recorded by interferometric SAR (DInSAR) technique with confidence. Pre-earthquake deformations are rather small – in term of centimeters. A few cases of deformation mapping after the shock using satellite data are known. Future development lays in precision SAR systems with medium spatial resolution and in combination with GPS technique. There are numerous observations of surface and near-surface temperature growth of the order of 3–5 degree centigrade prior to earthquakes. Methods of earthquake predictions have been developed using thermal IR survey. Well-known cases of gas and aerosol content change also have been observed before the earthquake. Satellite methods allow us to restore the concentrations of gases in the atmosphere: O_3, CH_4, CO_2, CO, H_2S, SO_2, HCl and aerosol. However the spatial resolution and sensitivity of currently available spaceborn sensors is not adequate for the estimation of the concentration of atmospheric gases. First promising results were obtained only for ozone, aerosol and air humidity.

Another important element of the study related to earthquake is active fault/ active tectonic related studies. In the geological sciences, tectonic refers to the processes, structures and landforms associated with the process of deformation of earth crust. In a broader sense it refers to the evolution of these structures and landforms over time. The time scale of tectonics depends on the spatial scale at which the process acts. For example, it takes billion of years for continents to develop; hundreds of million years for large ocean basin, whereas a fault scarp may be produced almost instantaneously during the earthquake (Kellar, 1997). The term active tectonic refers to those tectonic processes that produce deformation in the earth crust on a time scale of significance of human society. But the time frame required for studying these process needs to be longer- at least few hundred years to few thousand years –because earthquake on particular faults may have longer return period. One indirect way to study the tectonic process is to analyze the geological record of quaternary period to find out information indicative of deformation (e.g., presence of sand dykes within the column of particular quaternary unit such as cross bedded sandstone). Landform also bears the information on tectonic processes operated in recent geological past. Geomorphic tools used for such study are the set of landforms and quaternary deposits present at an area generally encompasses the last few thousand to two million thousand years (Kellar, 1997). Active fault or a neotectonic fault causes formation of variety of landform features including fault scarps, warped and tilted ground, subsidence features such as sag ponds and offset features such as stream channels. Each major category of faulting- strike-slip, normal, reverse – may be discussed in terms of a characteristic assemblage of landforms. There is fair amount of over lap between these different assemblages because many faults have oblique displacement, partially strike slip and partially vertical. The study of these features can provide valuable information regarding

tectonic processes operated in recent geological past. Remote sensing data plays an important role in delineating such active fault signatures specially high resolution data plays significant role in delineating delicate signatures such as sag ponds; pressure ridge, benches, etc. DEM generated from stereo pair of spaceborne SAR sensors/ aerial photographs facilitates deriving geomorphic indices indicative of neotectonic signatures. Some of the critical geomorphic signatures (figure 15.1) associated with active fault/ neotectonic terrain is discussed below:

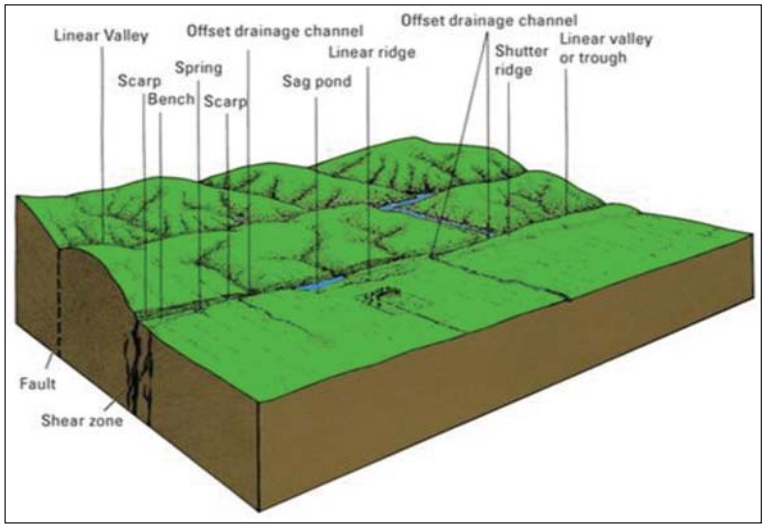

Figure 15.1: Geomorphic Signatures

- Landform analysis around active fault area is a significant exercise; which would help in delineating the trend of active fault. Some of the Landforms are very characteristic and associated with active fault
- Some faults, called creeping faults, move very slowly all the time. Structures such as bridges, sidewalks, and buildings on top of these faults will be offset by a small amount each year as the faults move. One can try to find a creeping fault by looking for bent or offset curbs and sidewalks
- Most faults don't creep, however, so geologists look for other ways that faults affect the landscape. Usually these evidences are easiest to spot from the air. For example, natural features such as streams, valleys, and ridges may have offset where they cross faults as movement from many earthquakes is accumulated. Active faults also create their own landscape features. For example, if one side of a fault moves up or down, a straight, low ridge called a scarp is created. As faults accumulate offset, the rock along the fault is broken and ground down, and the resulting shattered zone is more easily eroded than the surrounding rock. This type of erosion produces many common fault-related landforms, such as benches, saddles, and linear valleys along the fault. Faults also can disrupt the movement of underground water, forcing it to the surface to form springs and ponds. Finally, faults can be recognized by the offset they produce in the rocks that underlie the landscape, which can be recognized by careful study
- Important landforms associated with active faults (figure 15.1) are:
  - Shutter Ridge: A shutter ridge is a ridge which has moved along a fault line, blocking or diverting drainage. Typically, a shutter ridge creates a valley corresponding to the alignment of the fault that produces it
  - Fault Scarp: Fault scarp is the topographic expression of faulting due to the displacement of the land surface by movement along the fault. It can be caused by differential erosion along an old inactive fault (a sort of old rupture) with hard & weak rock, or by an active geologic fault. In many cases, bluffs form from the up thrown block and can be very steep. The height of the scarp formation is equal to the vertical displacement along the fault. Active scarps are usually formed by tectonics, e.g. when an earthquake changes the elevation of the ground, and can be caused by any type of fault, including strike-slip faults, whose motion is primarily horizontal. This movement is usually episodic, with the height of the bluffs being the result of multiple movements over time. Displacement of around 5 to 10 meters per tectonic event is common. Due to the dramatic uplift along the fault, the fault scarp is very prone to erosion, especially if the material being uplifted consists of unconsolidated sediment. Weathering, mass wasting and water runoff can soon wear down these bluffs. Fault scarps may be only a few centimeters or many meters high. Fault-line scarps are coincident with faults, but are most typically formed by the erosion of weaker rocks that have been brought alongside more resistant ones by the fault's movements. In the case of old eroded fault scarps, active erosion may have moved the physical cliff back away from the actual fault location which may be buried beneath a talus (fan) or the valley fill
  - Sag ponds: A sag pond is a body of water, which forms as water collects in the lowest parts of the depression that forms between two strands of an active strike-slip fault. The relative motion of the two faults strands results in a stretching of the land between them, causing the land between them to sink

- Beheaded Streams: Portion of a channel downstream from a fault, which is separated from its headwaters by strike-slip movement along the fault. In the process of abandoning the older downstream portion of the channel (and thereby "beheading" the downstream portion of the channel), the headwaters carve a new path straight across the fault. In subsequent earthquakes, the new channel will be offset, and it will eventually become beheaded as well. Thus the cycle will continue
- Offset drainages are streams displaced by faulting; they indicate the direction of relative displacement. The offset may reflect cumulative offset of several earthquake. Eventually the stream may erode a more direct route across the fault zone, producing a beheaded stream at the fault trace
- Linear valleys are troughs along main fault trace. These often develop because continued movement along recent fault traces crushes the rock, making it vulnerable to erosion. Streams commonly follow these zones of weakness
- Deflected streams are streams that enter a fault zone at an oblique angle and flow parallel to fault zones for some distance before returning to original orientation of flow
- River terraces are generally found in graded river. When a uplift occurs or base levels falls due to tectonic activity; river try to incise to reach to new graded profile and begin cutting new flood plain. In this manner; old flood plain become river terrace an inactive bench stranded over the new level of river. When down cutting of terraces are accompanied by regional tiling then tilted terraces are formed
- Geomorphic indices are the quantitative tools to understand the processes associated with any geomorphic element. Hypsometric integral, topographic asymmetry factor, stream length gradient indices, mountain sinuosity indices are a few geomorphic indices used for delineating landforms evolved primarily due to tectonic processes

15.4. Literature Review

The technique of interferometric synthetic aperture radar (InSAR) is used to examine small-scale features in the deformation field associated with the earthquakes. Satellite interferometry is based on multitemporal radar observations. InSAR is a method by which the phase differences of two or more SAR images are used to calculate the differences in range from two SAR antennae having slightly different viewing geometries to targets on the ground. As a result, displacements on the Earth's surface can be measured in a range of centimeters and millimeters. The InSAR results show significant deformation signatures associated with faults, fractures and subsidence. The interferogram also clearly indicates surface deformation related to earthquakes. First application of satellite interferometry for earth-quake research was demonstrated in '90 s by Massonnet *et al.*, (1993). The well-known ''butterfly'' image of the Landers earthquake (M = 7.3, 28 June 1992) was compiled on the basis of pre-seismic image of April 24, 1992 and post-seismic scenes: August 7, 1992; 3 July, 1992 and June 18, 1993. Similar images were obtained for the Kobe earth quake, Japan, date 16.01.1995, M = 6.8, Hector Mine earth quake, USA, M = 7.1, 16.10.99, Izmit earthquake, Turkey, 17.08.1999, M = 7.8 and others. All these cases demonstrate co-seismic and post-seismic deformations. There were no applications

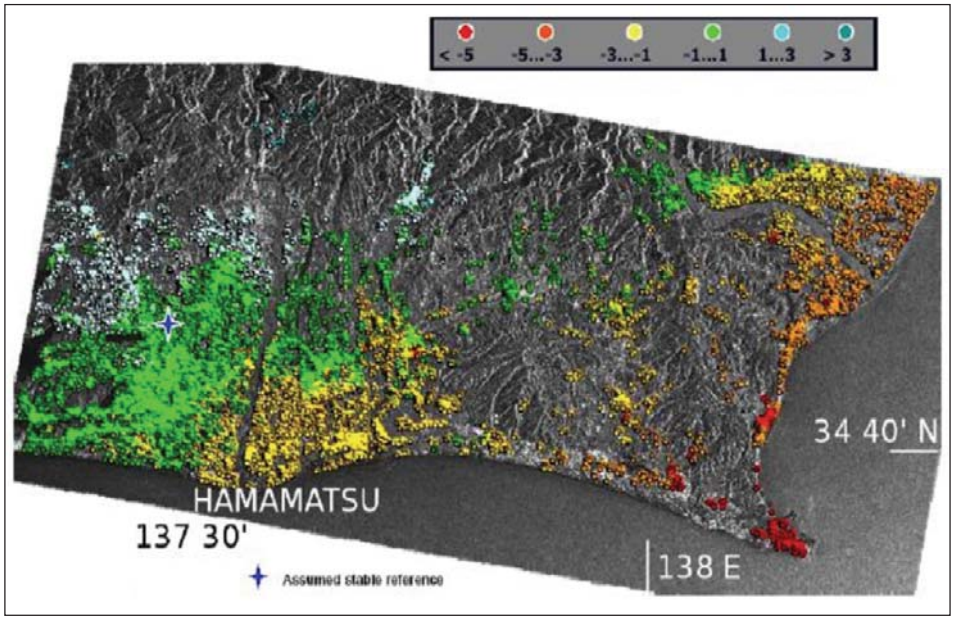

Figure 15.2: Average displacement rate 1992-2000 Years, mm/year (source: Kuzuoka and Mizuno, 2004)

showing the pre-seismic deformation. Only recent results from Japan (Figure 15.2) indicate probable pre-seismic deformation in the Tokai region (Kuzuoka and Mizuno, 2004). The vertical deformation recorded on the basis of InSAR data coincides with ground GPS observation.

Extensive researches have resulted to the identification of many precursors to the invincible earthquake phenomena. The latest one in the list of earthquake precursor that has been gaining a lot of attention and support from the scientific community across the world is thermal anomaly, i.e., a sudden rise in land surface temperature (LST) a few days or weeks before the earthquake occurrence. Prior to the earthquake event the region undergoes long preparation during which development of tectonic stress within the earth takes place. During this process various physical and electrical changes occur in the earth media. A change in the thermal regime of the epicentre region is one of the most prominent changes and can be detected by spaceborne sensors like Advanced Very High Resolution Radiometer (AVHRR) and MODIS. Pre-earthquake thermal anomaly and its spatial and temporal variations are controlled by various factors. Stresses acting before an earthquake in tectonically active regions generally increase ground temperature of the region. Such changes detected through thermal remote sensing can provide important clues about future earthquakes. Chowdhury *et al.*, (2007) demonstrated the capability of MODIS data in detecting the thermal anomaly related to earthquake in Iran. Panda *et al.*, (2005) detected the thermal anomaly just before the Kashmir earthquake.

The modern operational space-borne sensors in the infra-red (IR) spectrum allows monitoring of the Earth's thermal field with a spatial resolution of 0.5–5 km and with a temperature resolution of 0.12–0.5^{o}C. Surveys are repeated every 12 hours for the polar orbit satellites, and 30 minutes for geostationary satellites. The operational system of polar orbit satellites (2–4 satellites on orbit) provides whole globe survey at least every 6 hours or more frequently. Such sensors may closely monitor seismic prone regions and provide information about the changes in surface temperature associated with an impending earthquake. Natural phenomena and data availability stimulated the analysis of the long time series of thermal images in relation to earthquake hazard. Historically, the first application of thermal images in earthquake study was carried out in '80s for Middle Asia (Tronin, 1996). Later, similar researches were carried out in China (Qiang and Du, 2001), Japan (Tronin *et al.*, 2002), India (Singh and Ouzounov, 2003), Italy (Tramutoli *et al.*, 2001), Spain and Turkey, USA (Ouzounov and Freund, 2003) and other countries.

Thermal observations from satellites indicate the significant change in the Earth's surface temperature and near-surface atmosphere layers. Significant thermal anomalies prior to earthquakes related to high seismic areas have been reported in Middle Asia, Iran, China, Turkey, Japan, Kamchatka, India, Italy, Greece and Spain. Large volumes of thermal data were collected. Middle Asia database include seven years of observations for more than 100 earthquakes. Statistically significant correlation between thermal anomalies and seismic activity was observed (Tronin, 1996, 1999, 2000, 2002). Chinese scientists started operational earthquake forecast with spaceborne thermal measurements (Qiang and Du, 2001). The Destructive Bam earthquake in Iran took place on 26 Dec 2003. The magnitude of the earthquake was 6.6 and the city of Bam was destroyed. Before the earthquake the background distribution of the surface temperature was observed (Figure 15.3a) five days before the earthquake on 21 Dec 2003, and thermal anomaly was detected to the south of Bam city (Figure 15.3b). The observed thermal anomalies are related to the strong lithosphere-atmospheric coupling (Tronin *et al.*, 2004).

The causes of the thermal anomalies lie in the lithosphere and are related to the change of stress. The geological structures (faults, cracks, fractures etc.,) act as preferred conduits because the convective flow of fluids and gas in the upper levels of the lithosphere, and thereby the transport of heat, is one order of magnitude higher than the diffusive flow. The thermal anomalies are typically observed above large faults and their intersections. Depending on the geological and tectonic setting, near the surface, at depths of a few kilometers, the fluid is divided into water and gas. The water causes change of chemical composition in the wells and springs. Gas (H_2, He, CH_4, CO_2, O_3, H_2S moves to the atmosphere.The heat, water vapour and gas reach the Earth's surface, as a result of the lithosphere-atmospheric coupling. Few mechanisms of interaction are considered. First, convective heat flux (hot water and gas) changes the temperature of the Earth's surface. Second, change of the water level with usual temperature leads to a change in soil moisture, and consequently the physical properties of the soil. The difference in physical properties determines the different temperatures on the surface. Third is the greenhouse effect, when the optically active gases are escaped from the surface. Result of space borne thermal measurements for different areas looks similar: 1) thermal anomalies appeared about 6–24 days before and continued for about a week after an earthquake; 2) the anomalies are sensitive to crustal earthquakes with magnitude greater than 4.5;

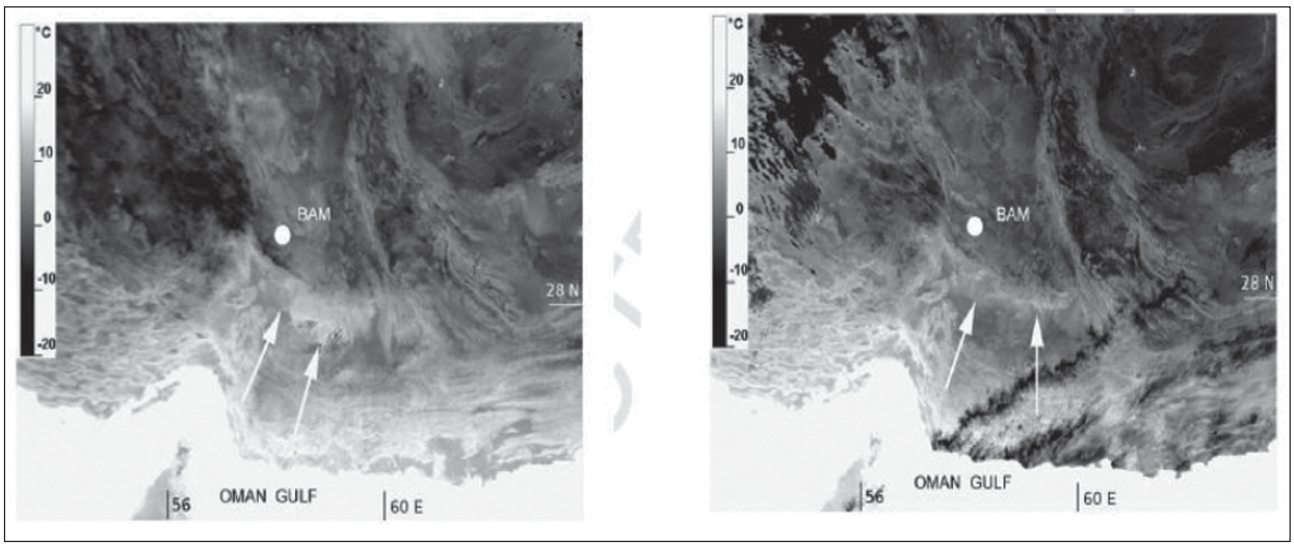

Figure 15.3: (a) NOAA thermal image , South Iran, background situation, 23 December, 2003. Arrows shows thermal anomaly and white circles Earthquake epicenter on 26th December, 2003. (b) NOAA thermal image 25 December, 2003. (Source: Tronin,2006)

3) thermal anomalies are attached to large faults; 4) the response of water in wells and surface temperature in thermal anomaly on earthquake look similar; 5) increase of air and surface temperature as a consequence of the hot water eruption a few days before strong earthquakes could lead to atmospheric perturbations (atmospheric gravity waves) and could be helpful to explain an origin of some preseismic electromagnetic effects (in the ULF, VLF, LF frequency range) (Gokhberg *et al.*, 1982; Hayakawa and Molchanov, 2002).

Case studies on various remote sensing applications for earthquakes have been reported recently. Pinty *et al..* (2003) have found the significant emergence of surface moisture growth after the Gujarat earthquake, 26 Jan 2001, using MISR data. Dey and Singh (2003) found significant surface latent heat flux change prior to the Gujarat earthquake. Dey *et al.*, (2004) found a change in the total water vapor column after the Gujarat earthquake. Water content was retrieved by SSM/I microwave radiometer on Tropical Rainfall Measuring Mission (TRMM) satellite. Okada *et al.*, (2004) found changes in atmospheric aerosol parameters after the Gujarat earthquake. Aerosol above sea surface was recorded by SeaWiFS satellite. Singh *et al.*, (2002) found changes in water colour and Earth's surface related to the Gujarat earthquake using IRS satellite data. A few examples of ozone concentrations changes measured by TOMS related with earthquakes are reported by Tronin (2002).

The use of satellite-based remote sensing technology for seismic risk mitigation purposes goes back to early 70s. One of the first related techniques that can be mentioned is "Side-Looking Radar Imagery" (Kedar and Hsu, 1972). In recent decade more attention has been paid to the use of remote sensing for natural hazards mitigation, and it has been claimed that remote sensing has a unique role in natural hazard assessment and mitigation (Wadge, 1994). Airborne and satellite are among the newly developed ones for gathering information on damage due to earthquake (Yamazaki *et al.*, 1998; Matsuoka and Yamazaki, 2000).

A similar damage detection study was carried out on the 1999 Kocaeli, Turkey earthquake (Estrada *et al.*, 2000) by using Landsat/TM images. Another similar study has been done with regard to 2001 Gujarat, India earthquake (Yusuf *et al.*, 2002). The damage of 2001 Bhuj, India earthquake has been also studied through a multidisciplinary approach based on high resolution satellite imagery (Chiroiu *et al.*, 2002). It has been claimed that the results could be very useful for the rescue teams deployed immediately after the catastrophe. Very recently in an MCEER publication a study has been reported entitled "Resilient Disaster Response: Using Remote Sensing Technologies for Post-Earthquake Damage Detection" (Eguchi *et al.*, 2003). Eguchi and his colleagues have studied the damages caused by the 1999 Marmara (Kocaeli), Turkey earthquake. The proposed techniques have been claimed to an effectively employed to determine the extent of damages in urban buildings. However, their results show that their techniques are basically useful for heavily damaged buildings rather than moderately or slightly damaged ones. This can be considered as a limitation in the use of their proposed techniques. Teeuw (2007) demonstrates as to how various types of remote sensing technique can be applied to mapping and monitoring riverine and coastal geohazards. The study focuses on flooding, ground instability, erosion and sedimentation, mainly drawing on examples from the UK. The study has shown as to how remote sensing offers a wide range of useful techniques

for mapping coastal and riverine features, especially in inaccessible terrain. Seismic hazard assessment requires knowledge not only of the earthquake sources and propagation of seismic waves, but also of the effect of local geology on earthquake ground shaking. However, the lack of empirical data for efficient earthquake microzonation tools have precluded integration of local site effects into earthquake hazard assessment schemes. Therefore, simple and fast methods for first-order site classification are being developed, as well as methods based on rapid surveys of seismic noise and combined with shallow geophysical investigations. Advanced methods of seismic noise analysis suitable for near-surface investigations are also being developed and tested.

15.5. Gap Areas

The low revisit frequency of thermal and DinSAR satellites limits the use of advance remote sensing technology in earthquake prediction and deformation monitoring-related studies. The observations made by satellites needs to be validated with more ground-based observations detecting anomalous soil moisture concentration, thermal anomaly, radon gas concentration for improving the accuracy of the methods can be enhanced. Moreover, low visit frequency of high resolution data limits the use of satellite data in post-earthquake damage assessment. Moreover, the lack of empirical data on various geophysical parameters influenced by earthquake deformation is main obstacle information for efficient earthquake microzonation. Suitable models needs to be developed which can incorporate satellite-based and ground information to provide accurate seismic micro zonation.

15.6. Case Study

A case study on the use of remote sensing for assessment of Post earthquake damages that occurred in 8th october, 2005 in J & K.

An earthquake of magnitude Mw=7.3 (USGS) ML=7.4 (IMD), Ms=7.6 (USGS) shook entire Northern India at 9.30am on Oct 8, 2005. The preliminary location of the earthquake epicenter was close to Muzuffarabad of Pak administered Kashmir and west of Uri Sector of Baramullah district. The severe shaking has been felt in most of the Northern India which includes Jammu and Kashmir, Uttarkhand, Himachal Pradesh, Rajastan state in the range of several hundred kilometers from the epicenter. People in Srinagar, New Delhi, Chandigar, Ajmer cities came out of their houses and the duration was about 40 to 70 seconds. Several people have experienced significant shaking in southeastern part of New Delhi and some of them witnessed sway in tall buildings. Massive destruction has been reported in Uri sector where one of the villages has been completely destroyed and a report of fire causing damage to some houses has been reported. The 200 year old Moti Mahal fort at Poonch district has been reported to be completely destroyed. At least 39 people which includes 15 soldiers have been killed in the Kashmir region of India (Source: Press Trust of India). Over 300 injured as more than 400 houses were flattened in J&K after a massive earthquake that also jolted Pakistan claiming at least 35 lives and injuring hundreds there, after a 19-storey building collapsed in Islamabad (Source: DD News). The Pakistani media has reported that the destruction has been severe in Islamabad.

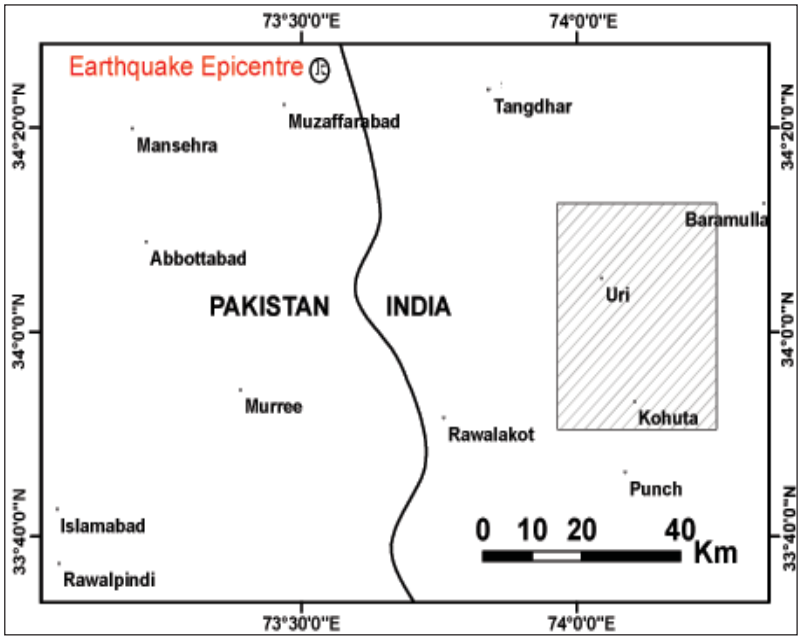

Figure 15.4: Study area map

Objective

- Geological assessment of the earthquake
- Damage assessment of the earthquake

15.6.1. Study Area

Geological assessment was carried out for a larger area covering the epicentre (Muzzaffarabad) using AWIFS, LISS-3 and LISS-IV data – (Figure 15.4). Damage assessment was carried using stero-cartosat data.

15.6.2. Data Used

The following data has been used for the study :-

- LISS-IV Mx data for the most damaged Uri sector was acquired by tilting the camera on 9th October,2005
- AWiFS data acquired on 9th October 2005
- No IRS-P5 data coverage for this area on 8th October and hence it was tilted for 9th October,2005 for Uri sector

15.6.3. Analysis

15.6.3.1. Geological Assessment

Geological assessment was carried out using the satellite data and published seismo-tectonic atlas by GSI (2000) and the USGS report on the earthquake (2005). AWiFS data having a wider spatial coverage was co-registered with the published seismo-tectonic map and the boundaries were transferred to satellite image. The boundaries were updated using the image expression. The past and the present epicentre were plotted on the satellite data. There are basically two major tectonic elements which has played a major role for this earthquake. These are main central thrust and the Jhelum strike slip fault. Earthquakes and active faults in northern Pakistan and adjacent parts of India and Afghanistan are the direct result of the Indian subcontinent moving northward at a rate of about 40 mm/yr (1.6 inches/yr) and colliding with the Eurasian continent. This collision is causing uplift that produces the highest mountain peaks in the world including the Himalayan, the Karakoram, the Pamir and the Hindu Kush ranges. As the Indian plate moves northward, it is being subducted or pushed beneath Eurasian plate. Much of the compressional motion between these two colliding plate has been and continues to be accommodated by slip on a suite of major thrust faults that are at the Earth's surface in the foothills of the mountains and dip north beneath the ranges. These include the Main Frontal thrust, the Main Central thrust, the Main boundary thrust, and the Main Mantle thrust. These thrust faults have a sinuous trace as they arc across the foothills in northern India and into northern Pakistan

15.6.3.2. Tectonics Framework of the Kashmir Region

The epicenter was located very close to Shinkiari fault and north of Jhelum fault which is regionally most extensive and it separates Kashmir basin of India from the Peshawar basin of Pakistan. From north to south, three main thrust system exists. The northernmost is the Main Karakoram Thrust (MKT). Towards south, it is separated from Peshawar and Kashmir basin by the Main Mantle Thrust (MMT). The southernmost is the Main Boundary Thrust (MBT), which separates the main Himalayan system from the sedimentary sequence of the frontal belt. The local geology strongly points the possibility of large amplifications of ground motion due to the influence of Peshawar basin and basin edges near Jhelum fault. The region is moderately active and has experienced several earthquakes of magnitude greater than 5.0 during last 300 years. The largest earthquake occurred on 30th May 1885 (Kashmir EQ) 19.5 km west of Srinagar and took 3000 lives. The earthquake of Badgam (M5.1) on 2nd Sept 1963 and Pattan earthquake (M5.9) on 28th Dec 1974 was deadliest and has affected several towns in the region which includes Indus Kohistan and Swat region. The Karakoram highway was reported to be badly damaged during this earthquake (Source: GSI 2000).

The AWiFS data analysis has highlighted the following important changes. A set of landslides has developed along the main central thrust and jhelum Fault.

15.6.4. Damage Assessment

A detail damage assessment was carried out using PAN stero + Cartosat-1 data. The area coverage was limited by the tilting of the camera. Monoscopic and stereoscopic analysis was carried out to assess the damages. Uri and Baramaulla sector of J& K was considered for damage assessment since it is nearer to epicentre.

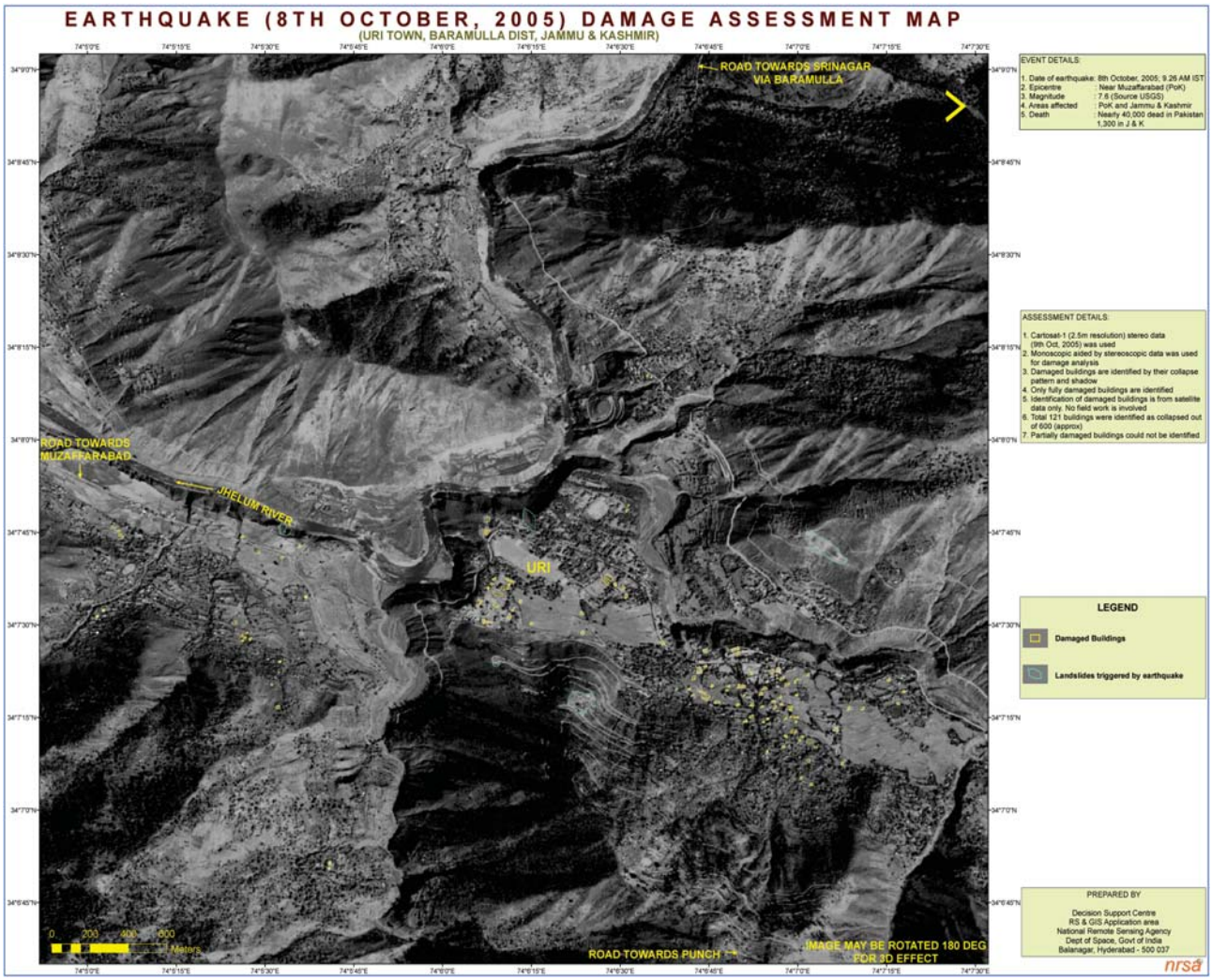

Figure 15.5: The Damaged Building/infrastructures in Uri town, Baramulla District, Jammu & Kashmir due to Earthquake- identified from high resolution Satellite image

The damages were classified into (Figure 15.5)

- Collapsed building
- Infrastructure damage especially roads , bridges and any other vital installations

15.7. Future

Advancement in DinSAR technology will allow us to record very fine differences in surface displacement. The COSMO/SkyMed mission aims at providing daily observations from 2007, overcoming limited observational frequency by using a constellation of four satellites. Existing satellite INSAR instruments have C- band (a wavelength of 5.66 cm) offering high resolution, but they only provide reliable interferograms for coherent, non-vegetated surfaces. Data from the JERS-1 satellite demonstrated during its lifetime that L-band satellites offer reduced resolution but provide interferograms over a far greater range of surface cover types.

Furthermore, the role and the applicability of remote sensing techniques with the aim of mapping the topography gradient as a proxy would be an important aspect of study. Investigating the role of “soil-city” interaction for local ground shaking and assessing the effect of ground motion duration on earthquake damage are additional challenging issues that have found no or only inadequate consideration in previous microzonation studies. Studies related to adequate magnitude determination, wave propagation, and ground motion prediction equations are also being integrated. On the other hand, recent earthquakes in Turkey and India showed that the main cause of human casualty in developing countries due to earthquake is the collapsed buildings. Therefore, it is quite reasonable for developing countries to plan for conjunctive use of optical and SAR systems for detection of collapsed buildings. This will provide the emergency management authorities with the more reliable information on the casualties distribution, which is a key point in the success of disaster mitigation actions.

15.8. Summary

Remote sensing can play an important role in earthquake prediction, seismic microzonation and post earthquake disaster management-related studies. The major limitations of remote sensing based earthquake studies is ascribed to rare validation of satellite based measurement with ground data and the lack of consistency in trend in the relations of observed anomaly with the earthquake. The high repetitivity, varied satellite-based observations are required for earthquake related studies of all relevant domain such as prediction, seismic zonation and post-earthquake disaster management.

References

Chiroiu L, Andre G, Guillande R, 2 and Bahoken F, 2002, Earthquake Damage Assessment Using High Resolution Satellite Imagery, 7th US National Conference on Earthquake Engineering, *Earthquake Engineering Research Institute, Oakland*, California.

Choudhury S, Dasgupta S, Saraf AK and Panda S, 2006, Remote sensing observations of pre-earthquake thermal anomalies in Iran, *International Journal of Remote Sensing,* **27(20)** :4381–4396.

Dey S, Sarkar S and Singh RP, 2004, Anomalous changes in column water vapor after Gujarat earthquake, *Advnces in Space Research,* **33(3)**: 274–278.

Dey S and Singh RP, 2003, Surface Latent Heat Flux as an Earthquake Precursor, Natural earthquake, *International Journal of Remote Sensing,* **28(20)** : 4587–4596

Eguchi RT, Huyck CK, Adams BJ, Mansouri B, Houshmand B and Shinozuka M, 2003, Resilient Disaster Response: Using Remote Sensing Technologies for Post-Earthquake Damage Detection, in MCEER Research Progress and Accomplishments, 2001-2003, State University of New York at Buffalo, 125-137.

Estrada Miguel, Matsuoka Masashi and Yamazaki Fumio, 2000, Spectral Analysis of Optical Remote Sensing Images for the Detection of Damage due to the 1999 Kocaeli, Turkey earthquake, *Seisan-Kenkyu*, **52(12):** 586-589.

Ferretti A, Prati C and Rocca F, 2000, Non-linear subsidence rate estimation using permanent scatterers in differential SAR interferometry, *IEEE Transactions Geoscience Remote Sensing*, **38** : 2202-2212.

Ferretti A, Prati C and Rocca F, 1999, Permanent Scatterers in SAR Interferometry, Proceedings International Geoscience Remote Sensing Symposium, Hamburg, Germany, 1528-1530.

Ferretti A., Prati C., Rocca F. (2001). *Permanent Scatterers in SAR Interferometry. IEEE Transactions On Geoscience and Remote Sensing.* **39**(8): 8 - 20.

Gokhberg MB, Morgunov VA, Yoshino T and Tomizawa I, 1982, Experimental measurement of electromagnetic emissions possibly related to earthquakes in Japan, *Journal of Geophysical Research*, **87**: **7824-7828.**

Hayakawa M (Ed.), Atmospheric and Ionospheric Electromagnetic Phenomena Associated with Earthquakes,TERRA-PUB, Tokyo, 717–746.

Hayakawa M and Molchanov OA, (Eds.), 2002, Seismo Electromagnetics: Lithosphere-Hazards and Earth System Sciences 3 (6), 749–755, *IEEE Transactions on Geoscience and Remote Sensing*, **39(1)**: 8-20.

Kedar EY and Hsu SY, 1972, Side-Looking Radar Imagery Applied in Seismic-Risk Mapping, Eighth International Symposium on Remote Sensing of the Environment, Willow Run Laboratories, University of Michigan, Ann Arbor, Oct. 2-6.

Kuzuoka S and Mizuno T, 2004, Land Deformation Monitoring Using PSInSAR Technique, International Symposium on Monitoring, Prediction and Mitigation of Disasters by Satellite Remote Sensing, MPMD, 176-181.

Massonnet D, Rossi M, Carmona C, Adaragna F, Peltzer G, Feigl K and Rabaute T, 1993, The displacement field of the Landers earthquake mapped by radar interferometry, *Nature*, **364** : 138-142.

Matsuoka Masashi, Yamazaki and Fumio, Mar.- 2000, Satellite Remote Sensing of Damaged Areas due to the 1995 Kobe Earthquake, Confronting Urban Earthquakes: Report of Fundamental Research on the Mitigation of Urban Disasters Caused by Near-Field Earthquakes, Kyoto University, Kyoto, Japan, 259-262.

Okada Y, Mukai S and Singh RP, 2004, Changes in atmospheric aerosol parameters after Gujarat earthquake of January 26, 2001, *Advances in Space Research*, **3(3)**: 254–258.

Ouzounov D and Freund F, 2003, Mid-infrared emission prior to strong earthquakes analyzed by remote sensing data, *Advances in Space Research*, **(33/3)**: 268–273.

Panda, S. K., S. Choudhury, A. K. Saraf and J. D. Das, (2007), MODIS land surface temperature data detects thermal anomaly preceding 08 October 2005 Kashmir earthquake, *International Journal of Remote Sensing*, 28(20): 4587-4596.

Pinty B, Gobron N, Verstraete MM, Me´lin F, Widlowski JL, Govaerts Y, Diner DJ, Fielding E, Nelson DL, Madariaga R and Tuttle MP, 2003, Observing earthquake-related dewatering using MISR/Terra satellite data, *EOS Transactions of the American Geophysical Union*, **84**: 37–48.

Qiang ZJ and Du LT, 2001, Earth degassing, forest fire and seismic activities, Earth Science Frontiers, 8, 235–245. regions, *International Journal of Remote Sensing*, **17(8)** :1439–1455.

Rodriguez, E., and Martin, J. M., 1992, Theory and design of interferometric synthetic aperture radars: IEE Proceedings-F, v. 139, no. 2, p. 147–159.

Singh RP, Bhoi S and Sahoo AK, 2002, Changes observed on land and ocean after Gujarat earthquake of January 26, 2001 using IRS data, *International Journal of Remote Sensing*, **23(16)** : 3123–128.

Singh RP and Ouzounov D, 2003, Earth processes in wake of Gujarat earthquake reviewed from space, *EOS Transactions of the American Geophysical Union*, **84**: 244.

Teeuw R, 2007, Applications of remote sensing for geohazard mapping in coastal and riverine environments; *Geological Society, London*, Special Publications, **283** : 93-106, temperature data detects thermal anomaly preceding 8 October 2005 Kashmir.

Tramutoli V, Bello GD, Pergola N and Piscitelli S, 2001, Robust satellite techniques for remote sensing of seismically active areas, *Annali di Geofisica*, **44**: 295–312.

Trifonov VG, 1984, Application of space images for neotectonic studies Remote sensing for geological mapping, vol. 18, IUGS Publication, Paris, 41–56.

TRONIN, A.A. (1996): Satellite thermal survey – A new tool for the study of seismoactive regions, Inter. J. Remote Sensing, 41 (8), 1439-1455.

Tronin, A. A. (Ed.): Satellite thermal survey application for earthquake prediction, 717–746 pp., Terra Sci. Publ., Tokyo, Japan, 1999.

Tronin AA, 2000, Thermal IR satellite sensor data application for earthquake research in China, *International Journal of Remote Sensing*, **21(16)**: 3169–3177.

Tronin AA, 2002, Atmosphere-litosphere coupling. Thermal anomalies on the Earth surface in seismic processes, In: Hayakawa, M., Molchanov, O.A. (Eds.), Seismo Electromagnetics: Lithosphere-Atmosphere- Ionosphere Coupling, TERRAPUB, Tokyo, 173–176.

Tronin AA, 2006, Remote sensing and earthquakes: a review, Physics and Chemistry of the Earth, parts A/B/C, **31(4-9)** : 138-142

Tronin AA, Hayakawa M and Molchanov OA, 2002, Thermal IR satellite data application for earthquake research in Japan and China, *Journal of Geodynamics*, **33** : 519–534.

Wadge G, ed., 1994, Natural Hazards and Remote Sensing, Natural Environment Research Council, London, p 101.

Yamazaki Fumio**,**Airborne and Satellite Remote Sensing Technologies for Gathering Damage Information: F. Yamazaki, M. Matsuoka, N. Ogawa, H. Hasegawa and H. Aoki, Multi-lateral Workshop on Development of Earthquake and Tsunami Disaster Mitigation Technologies and Their Integration for the Asia-Pacific Region,p 187-200, 1998.11

Yusuf Y, Matsuoka M and Yamazaki F, 2002, Detection of Building Damages due to the 2001 Gujarat, India Earthquake Using Satellite Remote Sensing, 7th US National Confence on Earthquake Engineering, Earthquake Engineering Research Institute, Oakland, California.

Zebker HA and Goldstein RM, 1986, Topographic mapping from interferometric SAR observations, *Journal of Geophysical Research*, **91**: 4493-4999.

Zebker HA and Villasenor J, 1992, Decorrelation in Interferometric Radar Echoes, *IEEE Transactions on Geosciences and Remote Sensing*, **30(5)** : 950-959.

nrsc

Remote Sensing Applications

P. S. Roy
R. S. Dwivedi
D. Vijayan

National Remote Sensing Centre

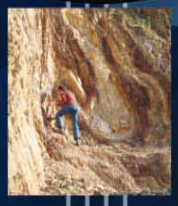

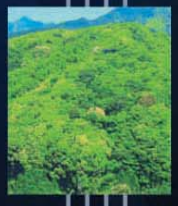

Remote Sensing Applications

Forest Fire Monitoring

16.1. Introduction

Vegetation fires have been acknowledged as an environmental process of global scale, which affects the chemical composition of the troposphere, and has profound ecological and climatic impacts. However, considerable uncertainty remains, especially concerning intra and inter-annual variability of fire incidence.

Within the total global vegetation, forests constitute a large part of earth's renewable natural resources, which plays a pivotal role in maintaining a near ideal environmental condition for life sustenance, besides serving as an important source of food, fuel wood, fodder, timber etc. Global Forest Resources Assessment 2000 (FRA 2000) concluded that the world's forest cover as of 2000 was about 3.9 billion hectares, or about 0.6 ha per capita. The regional distribution of global forests showed that Europe (including the Russian Federation) has 27 percent of the forests; South America, 23 percent; Africa, 17 percent; North and Central America, 14 percent; Asia, 14 percent; and Oceania, 5 percent.

FRA 2000 also conducted a remote sensing survey of tropical forests to assess forest change. This survey used sampling techniques with satellite imagery. The results indicated that the world's tropical forests were lost at a rate of about 8.6 million ha annually in the 1990s, compared to a rate of around 9.2 million ha per year during the previous decade. During the same period, the annual rate of loss of closed forests decreased from 8.0 million ha in the 1980's to 7.1 million ha in the 1990s. While the reduction in deforestation rates between the two decades was likely not significant in itself, the change estimate for the 1990s coincided well with the country specific findings.

Forest ecosystems are subjected to a variety of environmental threats of which fire is a potentially serious hazard. Fire depending on where, when and why it occurs, can be either an essential factor or otherwise, in the ecological cycle of the forested landscape and the survival of associated plants and animals it is merely a destructive unnatural threat. In tropical deciduous forests, fire is a natural phenomenon due to higher levels of water stress during summer. Traditional land use practices and changes in the weather pattern have affected the incidence of fires. Fire being a good servant and a poor master, has been responsible for causing immense damage to both forest fauna and flora, including the soil inhabitants. Forest fires can have large impacts on both, ecosystems and economy.

The ecological role of fire is to influence several factors such as plant community development, soil nutrient availability and biological diversity. Forest and wild land fire are considered vital natural processes initiating natural exercises of vegetation succession. However, uncontrolled and misuse of fire can cause tremendous adverse impacts on the environment and the human society.

Continued high annual rate of loss of tropical forest cover and outbreak of major wildfires over the past decade, in contrast to increased plantation development, successes in sustainable forest management and increases in protected areas show a complex picture of the past and possible future of the world's forests and mankind's interaction with them.

During the last decade, increased availability of time series of satellite data has contributed to improve our understanding of fire as a global environmental process. Dwyer *et al.* (2000a, b), used one year of the Advanced Very High Resolution Radiometer (AVHRR) fire data to characterise global patterns of fire seasonality and their relationships with climate. More recently, a new generation of satellites sensors brought further advances through enhanced fire monitoring capabilities, resulting in the production of various burned area and fire hotspots datasets at regional or global scales (Arino *et al.*, 2005; Giglio *et al.*, 2003; Giglio *et al.*, 2006; Carmona-Moreno *et al.*, 2005; Ria˜no *et al.*, 2007).

In spite of these studies, considerable uncertainties remain, especially regarding the spatial and temporal variability of global vegetation burning and its relationship with climate dynamics. The Global Climate Observing System (GCOS, 2006) considered fire disturbance an "Essential Climate Variable" and highlighted the need for long data time series to quantify the links between climate and fire (Le Page, 2007).

16.1.1. Causes of fire

Intentional : Forest fires are mostly anthropogenic in nature and caused intentionally. These may occur due to the following reasons (Negi, 1986).

- Forest floor is often burnt by villagers to get a good growth of grass in the following season or for a good growth of mushrooms
- Wild grass or undergrowth is burnt to search for animals
- Firing by miscreants
- Attempt to destroy stumps of illicit fallings

Unintentional :These fires are caused due to man's carelessness i.e., without intention to set fire. Such fires may be due to the following reasons:

- Un-extinguished campfires of trekkers, laborers, camp of roadside charcoal panniers etc.
- Spark of fire from railway engines
- Careless throwing of fire after honey collection
- Un-extinguished bidis, cigarette butts, matchsticks etc., by grazers, travelers, picnickers or even forest laborers
- Burning of agricultural fields adjacent to forested areas. Such fires is left unattended may spread to forest areas
- Careless handling of acid by resin tapers
- During controlled burning by the department, fire may spread to the forest due to negligence of the staff

Figure 16.1: Ground fire

Natural: Natural causes of fires include:

- Fires caused by lighting
- Fires caused by rolling stones
- Fires may be caused by volcanic eruptions

In our country there was no report forest fire due to natural cause.

16.1.2. Classification of forest fire

According to a classification of forest fires by type and causes, three major types of forest fires are prevalent (P S Roy, 2003);

Ground fires: Ground fires occur in the humus and peaty layers beneath the litter of undecomposed portion of forest floor with intense heat but practically no flame. Such fires are relatively rare and have been recorded occasionally at high altitudes in Himalayan fir and spruce forests (Figure 16.1)

Figure 16.2: Surface Fire

Surface fires: Surface fires occurring on or near the ground in the litter, ground cover, scrub and regeneration, are the most common type in all fire-prone forests of the country (Figure 16. 2)

Figure 16.3: Crown Fire

Crown fires: Crown fires, occurring in the crowns of trees, consuming foliage and usually killing the trees, are met most frequently in low level coniferous forests in the Siwaliks and Himalayas (NCA Report, 1976) as shown in figure 16.3.

16.1.3. Global and National Issues, Scenario and Developments

Forest fire is a major cause of degradation of India's forests. While statistical data on fire loss are weak, it is estimated that the proportion of forest areas prone to forest fires annually ranges from 33% in some states to over 90% in others. About 90% of the forest fires in India are started by humans (Roy, 2003). Forest fires cause wide ranging adverse ecological, economic and social impacts. In a nutshell, fires cause: indirect effect on agricultural production; and loss of livelihood for the tribals as approximately 65 million people are classified as tribals who directly depend upon collection of non-timber forest products from the forest areas for their livelihood.

A combination of edaphic, climatic and human activities account for the majority of wild land fires. High terrain steepness along with high summer temperature supplemented with high wind velocity and the availability of high flammable material in the forest floor accounts for the major damage and wide wild spread of the forest fire. The vast majority of wild fires are intentional for timber harvesting, land conversion, slash – and- burn agriculture, and socio-economic conflicts over question of property and landuse rights. In recent years extended droughts (prolonged dry weather), together with rapidly expanding exploitation of tropical forest and the demand for conversion of forest to other land uses, have resulted in significant increase in wild fire size, frequency and related environmental impacts.

Past wild fires have an immense impact in Indonesia, Brazil, Mexico, Canada, USA, France, Turkey, Greece, India and Italy. Large-scale fires and fire hazards were also reported in eastern parts of the Russian Federation and in China northeastern Mongolia autonomous region. There has been a continuous increase of application of fire in landuse system in forest of South East Asian region. This has resulted in severe environmental problems and impacts on society. Wild fires often escape from landuse fire and take unprecedented shape causing problems of transboundary pollution. Author (Roy, 2003) analyzes the forest and wild land fires issues with particular reference to South East Asia and emphasizes on development of national and regional fire management plans considering the complexity and diversity of fire.

Impact of the Forest Fire on the Global Environment: Forest fires controlled or uncontrolled have profound impacts on the physical environment including land cover, land use, biodiversity, climate change and forest ecosystem. They also have enormous implication on human health and on the socio-economic system of affected countries. Economic cost is hard to quantify but an estimate by the economy and environment can be provided. The fire incidence problem for South East Asia put the cost of damages stemming from the Southeast Asian fires (all causes) at more than $4 billion. Health impacts are often serious. As per one estimate 20 million people are in danger of respiratory problems from fire in Southeast Asia. Most pronounced consequence of forest fires causes their potential effects on climate change. Only in the past decade researchers have realized the important contribution of biomass burning to the global budgets of many radiatively and chemically active gases such as carbon dioxide, carbon monoxide, methane, nitric oxide, tropospheric ozone, methyl chloride and elemental carbon particulate. Biomass burning is recognized as a significant global source of emission contributing as much as 40% of gross Carbon dioxide and 30% of tropospheric ozone.

There is a strong need for a comprehensive international set of comparable data on forest fires and other wildland fires, as a tool for policy makers, and for operational planning (for both prevention and suppression), as an essential part of improving understanding of climate change and the factors influencing it, and as a part of an effort to monitor the state of the world's forests.

In recent years the scientific community has shown renewed interest in forest (vegetation) fires, notably because of their significant role in climate change, and new methods of collecting information using remote sensing techniques are being developed. Furthermore, the research community needs global geo-referenced data (although not necessarily at a very fine degree of resolution).

To collect the Fire Statistics in the Countries of the United Nations Economic Commission for Europe (UNECE) has the following commitment.

The Resolution S3 of the Ministerial Conference at Strasbourg committed the signatories (including the EU) to creating a decentralised data base on forest fires. Since then a data base, with fire-by-fire information, has been built up, in those countries/regions of the European Union with a particularly severe forest fire problem. In

this system, for each fire, information is collected on first alert and extinction times, location, area, cause, etc., according to a “common core” of parameters. 19 countries of the 27 signatories of Resolution S3 expressed their willingness to adhere to a data base network based on the common core system adopted by EU members, considering it a good, feasible starting point of collecting data on a common base at the pan-European level.

FAO Silva Mediterranea, like the Working Party a subsidiary body of the European Forestry Commission (EFC), covers a region where forest fires are one the most serious dangers to sustainable forest management, and has also stated its interest in moving towards a fire-by-fire information system, based on the EU system.

At the global level, FAO has collected data on forest fires, using the FAO/ECE conceptual framework and definitions, as part of its monitoring of the state of the world’s forests within the context of the Global Forest Resource Assessment.

International Forest Fire News (IFFN), prepared by JG Goldammer, leader of the ECE/FAO. Team of Specialists on Forest Fires, contains both technical and statistical information on forest fires world wide. Goldammer is also developing a Global Vegetation Fire Inventory (GVFI), collecting information by a network of correspondents. GVFI is an activity of the International Global Atmospheric Chemistry (IGAC) project, a core project of the International Geosphere-Biosphere Programme (IGBP).

16.2. Review of Literatures

During last two decade especially in last decade, much work has been carried in the field of forest fire detection, assessment, risk management and other related study considering the global acknowledgment of environmental degradation and direct consequences in climatic change.

16.2.1. Fire Detection

Traditionally, forest fires have been detected using fire lookout towers located at high points in a forested area. A fire lookout tower houses a person whose duty is to look for fires using binocular or other sophisticated equipment such as Osborne fire finder (Fleming and Robertson, 2003). Osborne fire finder is comprised of a topographic map printed on a disk with graduated rim. A pointer aimed at the fire determines the location and the direction of the fire. Once the fire location is determined, the fire lookout alerts fire-fighting crew. Fire lookout towers are still in use around the world with simple binocular or other related sophisticated equipment

Unreliability of human observations in addition to the difficult life conditions for fire lookout personnel have led to the development of automatic video surveillance systems (Fire Watch Web Page ; Breejen *et al.*, 1998; Khrt *et al.*, 2001). Most systems use Charge-Coupled Device (CCD) cameras and Infrared (IR) detectors installed on top of towers. CCD cameras use image sensors, which contain an array of light sensitive capacitors or photodiodes. In case of fire or smoke activity, the system alerts local fire departments, residents, and industries. Current automatic video surveillance systems used in Germany, Canada, and Russia are capable of scanning a circular range of 10 km in less than 8 minutes. (Fire Watch Web Page). The accuracy of these systems is largely affected by weather conditions such as clouds, light reflection, and smoke from industrial activities. Automatic video surveillance systems cannot be applied to large forest fields easily and cost effectively, thus for large forest areas either aeroplanes or Unmanned Aerial Vehicles (UAV) are used to monitor forests. Aeroplanes fly over forests and the pilot alerts the base station in case of fire or smoke activity. UAVs, on the other hand, carry both video and infrared cameras and transmit the collected data to a base station on the ground that could be up to 50 km away. UAVs can stay atop for several hours and are commanded by programming or joystick controls (Aerovision Web Page) .

More advanced forest fire detection systems are based on satellite imagery. Advanced Very High Resolution Radiometer (AVHRR), Moderate Resolution Imaging Spectroradiometer (MODIS), Indian Remote Sensing Satellite-Advanced Wide Field Sensor (IRS AWiFS) are being used for active forest fire detection. Current satellite-based forest fire detection systems use data from these instruments for forest fire surveillance. The accuracy and reliability of satellite-based systems are also (unlike ground surveillance) largely impacted by weather conditions. Clouds and rain absorb parts of the frequency spectrum and reduce spectral resolution of satellite imagery, which consequently affects the detection accuracy. Although satellite-based systems can monitor a large area, relatively low resolution of satellite imagery means a fire can be detected only after it has grown large. More importantly, the long scan period—which can be as long as 2 days—indicates that such systems cannot provide timely detection.

There are many existing techniques used for detection of forest fires. One of the most important is described by Boyd M, Harden *et al.*, (1973). Their paper outlines a model, which can be readily adapted for analysis of any forest, and has actually been used to examine various fire detection strategies for the Footner Forest in Northern Alberta. Some research is based on image processing techniques, capturing camera segments and processing and classifying these images for fire detection. Using image processing methods, Roy and UNEP have used a satellite for capturing images from forests and, have detected whether there is a fire possibility or not. Another satellite application in forest fires detection is by Lafarge *et al.*, (2007). They present a fully automated method of forest fire detection from TIR satellite images based on the random field theory where preprocessing is used to model the image as a realization of a Gaussian field. This study shows some interesting properties because the fire areas considered to be in the minority are considered as anomalies of that field. Nakau *et al.*, (2006) developed a fire detection information system from receiving AVHRR satellite to output fire detection map and validated the early detection algorithm using AVHRR satellite imagery.

Another study is computer vision based forest fire detection and monitoring system where fixed cameras are used (Toreyin *et al.*, 2007). Furthermore, there is a great many forest fire detection studies and systems available (Fujiwara *et al.*, 2002, Casanova *et al.*, 2004, Ertena *et al.*, 2002 and Filizzola *et al.*, 2007). Ollero *et al.*, 1998. have studied a scheme using multi-sensorial integrated systems for early detection of forest fires. Several information and data sources in Olleros's study were used, including infrared images, visual images, data from sensors, maps and models, Casanova *et al.*, 2004. present the MSGSEVIRI sensor's ability to detect forest fires and subsequent fire monitoring. There are a number of similar studies on fire detection using sensors.

Justice *et al.*, 2002 and Giglio *et al.*, 2003 developed a multi-year daily active fire product from the Moderate Resolution Imaging Spectroradiometer (MODIS). This product has a good detection rate, due to its 4 daily overpasses. This method is the most popular all over the world but is only available since 15 November 2000. Hence, for global fire mapping is being done since year 2000 only.

The authors (Doolin and Sitar 2005), in their study shown the feasibility of wireless sensor networks for forest fire monitoring. Experimental results are reported from two controlled fires in San Francisco, California. The system is composed of 10 GPS-enabled MICA motes (Crossbow Inc. Web Page) collecting temperature, humidity, and barometric pressure data. The data is communicated to a base station which records it in a database and provides services for different applications. The experiments show that most of the motes in the burned area were capable of reporting the passage of the flame before being burned. In contrast to this system which reports raw weather data, Mohamed H *et al.*, 2007 design processes weather conditions based on the Fire Weather Index System (Canadian Forest Fire Danger Rating System (CFFDRS) Web Page) and reports more useful, summarized, fire indexes. His study addresses the Fire Weather Index (FWI) System, which notes that different components can be used in designing efficient fire detection systems FWI. He has presented the design of a wireless sensor network for early detection of forest fires. Their design is based on the Fire Weather Index (FWI) System, which is backed by decades of forestry research. The FWI System is comprised of six components: three fuel codes and three fire indexes. The three fuel codes represent the moisture content of the organic soil layers of forest floor, whereas the three fire indexes describe the behavior of fire. By analyzing data collected from forestry research, they showed how the FWI System can be used to meet the two goals of a wireless sensor network designed for forest fires: (i) provide early warning of a potential forest fire, and (ii) estimate the scale and intensity of the fire if it materializes. To achieve these goals, they have designed their sensor network based on two main components of the FWI System: the Fine Fuel Moisture Code (FFMC), and the Fire Weather Index (FWI). The FFMC code is used to achieve the first goal and the FWI index is used to achieve the second.

Using animals for disaster detection is not a new idea but it has been limited to a few of disaster types such as earthquake. Yeung, 2007 describes an example of observing animals' behavior for early earthquake alert, but the author gives no guaranty that his study works correctly for every earthquake. Kahn, 2007 suggested an idea that the best and the cheapest biosensors are already distributed globally but generally ignored: They're called animals. Kahn's idea leads the scientists to start new investigations to be made on animals. Lee *et al.*, 2007, in their study, they offered a Bio-adhoc sensors network for early forest fire warning system for mountain areas, and they used animals as wireless adhoc nodes.

However, the proposal presented by Yasar, 2007, is based on the usage of many access points explicitly constructed in the forests instead of an adhoc network structure. Although it may not seem to be feasible to install sufficient number of access points to cover whole forests, some critical points which are highly under the

risk of fire, can be selected for the access point locations. Moreover, the usage of the access points would remove the risk of interruption of communication (network failure) that usually occurs in adhoc networks, if animals are used as wireless nodes. Furthermore, Lee *et al.*, in their study focused on the usage of animals' behavior only for detection of fire possibilities. This paper, however, focuses on using both animal behavior classification and thermal detection methods. In this paper (Yasar, 2007), a proposal for a fire detection system combining methods from both animal tracking and current fire detection systems is presented. The system proposed does not claim to detect every possible fire, and can readily be used to augment others.

The main idea presented in this paper is to utilize animals with sensors as Mobile Biological Sensors (MBS). The devices used in this system are animals which are native animals living in forests, sensors (thermo and radiation sensors with GPS features) that measure the temperature and transmit the location of the MBS, access points for wireless communication and a central computer system which classifies of animal actions. The system offers two different methods, firstly: access points continuously receive data about animals' location using GPS at certain time intervals and the gathered data is then classified and checked to see if there is a sudden movement (panic) of the animal groups: this method is called animal behavior classification (ABC). The second method can be defined as thermal detection (TD): the access points get the temperature values from the MBS devices and send the data to a central computer to check for instant changes in the temperatures. The proposed system, additionally, has a classifier which built-in measures to use animal action (panic) to signal a fire alarm in situations where thermal sensors usage is inappropriate. Furthermore, this system may assist in preventing poaching, monitoring animals' death, and understanding animals' group behavior.

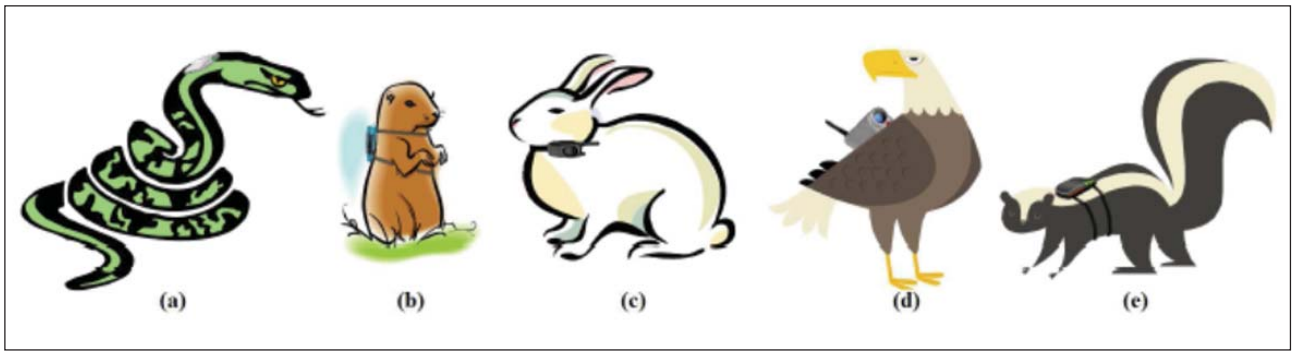

Figure 16. 4: Some animals that can be used as MBS in the system

In this paper he has suggested to choose animals and sensors in accordance with characteristic the forest such as climate zone, natural specifications, and density. Selection of animals which are native to the forest areas, and the choice of sensors depend on which method (TD or ABC) will be applied. The usual pattern of fire spread for a particular forest is another criterion in the selection of animals and sensors. Figure 16. 4 shows examples of animals that can be used as MBS (these animal species can vary in accordance with the territory's specifications), and Figure 16.5 shows sample sensors, which can be attached to animals (Cochran *et al.*, 2007). The most important issue in the selection of sensors is that they must all have GPS features with both methods (TD and ABC).

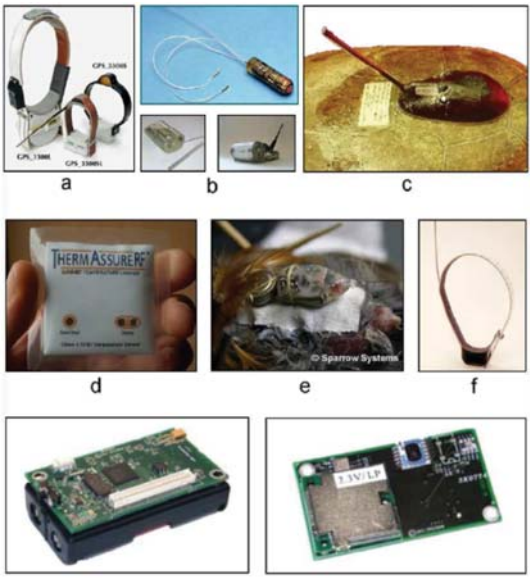

Figure 16.5: Sample sensors which can be attached to animals

More advanced approach of surveillance is automatic surveillance and automatic early forest fire detection. Today there are several different approaches but the most feasible is the system based on video cameras sensible in visible spectra. In almost every country, which encounters high risk of forest fires, at least one such system was developed and proposed. Some of them are on the market under various commercial names. Croatia also has its own system called Integral Forest Fire Monitoring System (in Croatian IPNAS) developed at the Faculty of Electrical Engineering, Mechanical Engineering and Naval Architecture

University of Split. The system was experimentally tested during 2005 and 2006 fire seasons on three locations but it is also in everyday use in National Park Paklenica from June 2006.

IPNAS structure is shown in Figure 16.6. The system is based on field units and a central processing unit. The field unit is conceived of pan/tilt/zoom controlled video cameras and a mini meteorological station connected by Wireless LAN to a central processing unit where all analysis, calculation, presentation, image and data archiving is done. The system is Web based because the user interface is displayed in a standard Web browser, and the user can reach any system module through tunnelled SSL (Secure Socket Layer) VPN (Virtual Private Network). Multiple level of authentication stop the potential intruders.

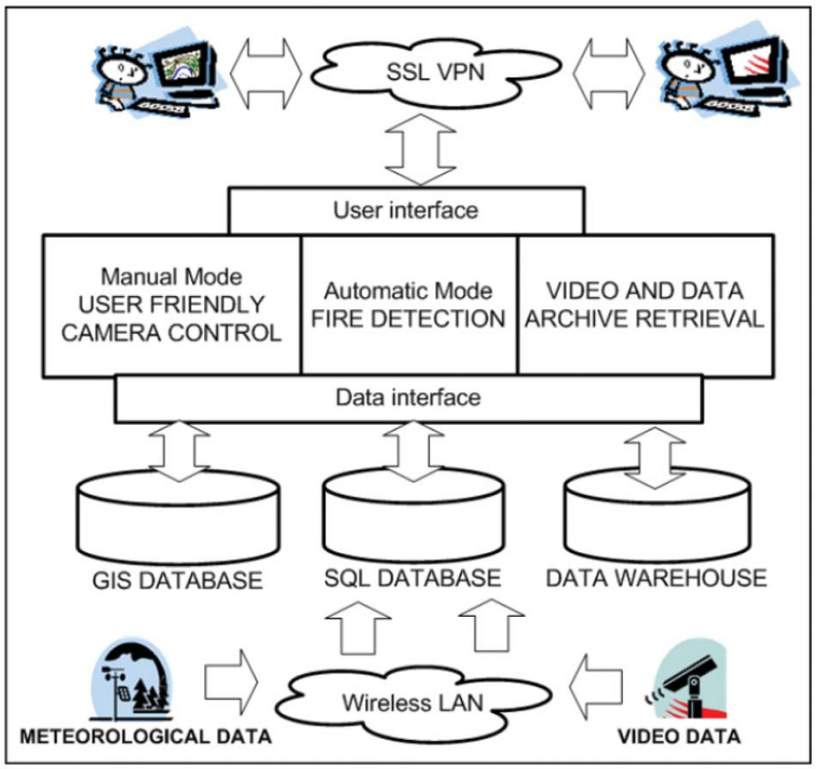

Figure 16.6: Structure of Croatian Integral Forest Fire Monitoring System (IPNAS) (Source :http://www.fesb.hr/~ljiljana/radovi/279548)

IPNAS is based on three types of data

- Real-time video data – Digital video signal is used both in automatic and manual mode. In automatic mode it is a source of images for automatic forest fire detection and in manual mode it is used for distant video presence and distant monitoring using pan/tilt control and powerful zoom
- Real time metrological data –The meteorological data is today used in a postprocessing unit for false alarm reduction, and tomorrow will be useful for local fire risk index calculation in prevention phase and fire spread estimation in fire fighting phase
- GIS (Geographical Information System) database – stores information on pure geographical data (elevations, road locations, water resources, etc.), and all other relevant information related to a geographic position, like fire history, rain-water resource locations, land cover – land use, soil characteristics, local forest corridor map, tourist routes and similar. This data tomorrow will be quite useful for fire management activities and today it is used for user-friendly camera pan/tilt control.

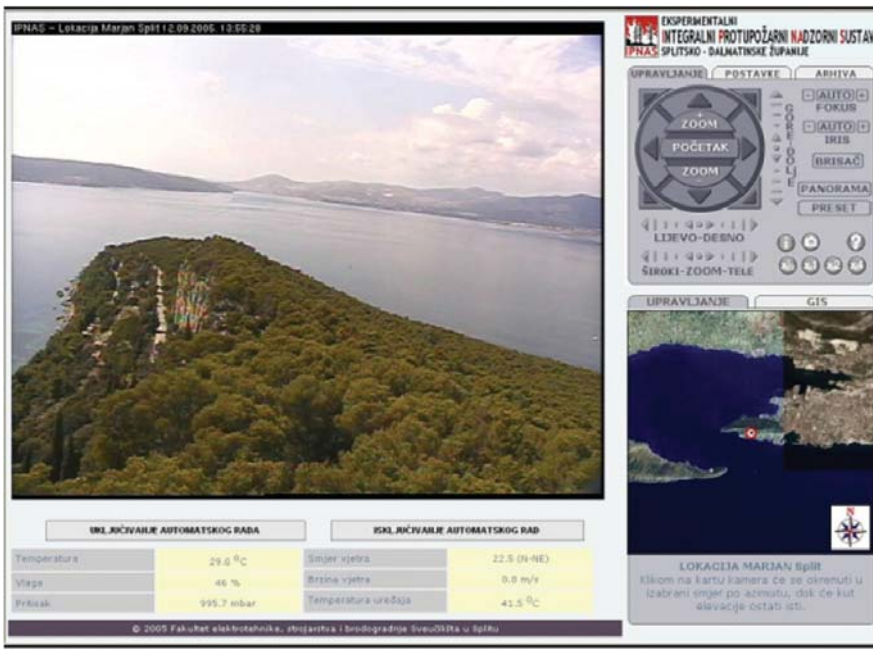

Figure 16.7 (a): IPNAS user interface is a dynamic and interactive Web page with the all real-time data and a user friendly interface for camera control in manual mode(Source :http://www.fesb.hr/~ljiljana/radovi/279548)

Figure 16.7 (b): IPNAS user screen in automatic mode. Detection algorithms has few parameters which could be adjusted in real time to decrease the false alarm rate(Source :http://www.fesb.hr/~ljiljana/radovi/279548)

The user interface is a dynamic and interactive Web page where real time video and meteorological data is shown together with GIS data and user friendly interface for camera pan/tilt/zoom control in manual mode. Figure 16.7 shows the main user interface page for experimental monitoring unit.

During this experimental period they have acquired a big collection of false alarms that help them to improve the fire detection algorithm and functionality of the whole system. New improved version of Integral Forest Fire Monitoring System was released during 2006.

B. Zhukov *et al.*, have investigated the effect of the resolution on the recognition of fire fronts and on the estimation of their characteristics, as well as on the estimation of the total fire radiative power (FRP) emitted from a fire scene. Data of the spectroradiometers MODIS on the Terra and Aqua satellites, which are obtained on a global scale 4 times a day, are widely used for global and regional monitoring of active fires. A disadvantage of MODIS is a relatively low resolution of 1 km. For this purpose, they compared images of fire scenes in Siberia, Portugal and Australia that were obtained nearly simultaneously by MODIS and by the dedicated small satellite BIRD, which provides a resolution of 370 m in its infrared channels and allows the detection of fires with an area a factor of 7 smaller than MODIS. The results show that BIRD allows the recognition of fire fronts and the estimation of their characteristics, while in the MODIS data fire fronts are usually not clearly distinguished. On the other hand, MODIS proves to be a marginally adequate sensor for the estimation of the total FRP in fire scenes, which is related to the rates of biomass burning and of gas and aerosol emissions. Only in cases of fires with a relatively small front depth, which is typical for bush fires in Australia, MODIS may significantly underestimate the FRP by a factor of 1.8 compared to the BIRD-based FRP estimates.

The results of this study show that the MODIS sensor, with a spatial resolution of 1 km, is marginally adequate for the estimation of the radiative power of forest fires. FRP can be related to the rates of biomass burning and of gas and aerosol emissions. Though MODIS may miss a significant portion of small fires in comparison to BIRD, it underestimated the total FRP of the fire scenes in Siberia only by ~4%. The reason is that in these scenes the major part of FRP (and consequently of the fire pollutant emissions) are produced by large fires that are reliably detectable by MODIS. In cases of fires with a relatively small front depth, which is typical for the bush fires in Australia, MODIS may significantly underestimated the FRP by nearly 50% compared to the BIRD-based FRP estimates. As a conclusion, it is recommended to combine the data of wide swath sensors, such as MODIS and of high-resolution instruments of the BIRD type for effective fire monitoring from space.

Young Gi Byun *et al.*, 2005 proposed a graph-based forest fire detection algorithm which is based on spatial outlier detection methods. Spatial outliers in remotely sensed imageries represent observed quantities showing unusual values compared to their neighbor pixel values. There have been various methods to detect the spatial outliers based on spatial autocorrelations in statistics and data mining. These methods may be applied in detecting forest fire pixels in the MODIS imageries from NASA's AQUA satellite. This is because the forest fire detection can be referred to as finding spatial outliers using spatial variation of brightness temperature. Authors have tested the proposed algorithm to evaluate its applicability. For this the ordinary scatter plot and Moran's scatter plot were used. In order to evaluate the proposed algorithm, the results were compared with the MODIS fire product provided by the NASA MODIS Science Team, which showed the possibility of the proposed algorithm in detecting the fire pixels.

16.2.2. Fire burnt Area Assessment

Devastating fires affected Greece in the summer 2007, with the loss of more than 60 human lives, the destruction of more than 100 villages and hundreds of square kilometers of forest burned. Luigi boschetti *et al.*, have mapped the extent burned and the approximate day of burning in Greece using MODIS burned area product for 22 June to 30 August 2007. Their mapping is independent that of European Forest Fires Information Service (EFFIS). The characteristics of the two datasets, and an evaluation of the areas burned comparing the MODIS and EFFIS data for the same temporal interval are analysed.

The MODIS burned area product (MCD45) mapped 292657 ha as burned from 22 June to 30 August 2007 across the whole of Greece (including the islands), and the EFFIS reported 272163 ha burned for the same period. Of these 242 900 ha were identified as burned by both products, corresponding to approximately 2% of Greece. Differences between the two products occur primarily along the borders of EFFIS mapped polygons, in agricultural regions which are not considered by EFFIS, and for small burned areas that were mapped by EFFIS but not by MCD45.

GeoSpatial Experts' GPS-Photo Link software has been deployed by U.S. Forest Service in the Cleveland National Forest to speed the creation of soil burn severity maps following the devastating California wildfires in October 2007. The software enabled Forest Service personnel to complete the damage assessment more rapidly than would have otherwise been possible, so that plans could quickly be made to protect surviving infrastructure from flooding, landslides and debris flows. The GPS-Photo Link software maps digital photographs to their correct georeferenced locations in geospatial map layers. Requiring only a standard digital camera and handheld GPS device, the software links the photographic images with GPS location data and then accurately integrates them into a geospatial data set along with important attribute data, such as the time, date, and location coordinates of each photo. The software enables users to display their photo locations as icons in digital mapping environment, including GIS and Google Earth map layers.

Roy *et al.*, 2008, have analyzed NASA MODIS Collection 5 burned area product. Total annual and monthly area burned statistics and missing data statistics are reported at global and continental scale and with respect to different land cover classes. Globally the total area burned labeled by the MODIS burned area product is 3.66×106 sq.km for July 2001 to June 2002 while the MODIS active fire product detected for the same period a total of 2.78×106 sq.km, i.e., 24% less than the area labeled by the burned area product. A spatio-temporal correlation analysis of the two MODIS fire products stratified globally for pre-fire leaf area index (LAI) and percent tree cover ranges indicate that for low percent tree cover and LAI, the MODIS burned area product defines a greater proportion of the landscape as burned than the active fire product; and with increasing tree cover (>60%) and LAI (>5) the MODIS active fire product defines a relatively greater proportion. This pattern is generally observed in product comparisons stratified with respect to land cover.

The reasons for the observed product differences are complex, and require further research and independent validation data. The demonstrated complementary nature of the MODIS burned area and active fire products imply that with further research their synergistic use may provide improved burned area estimates. The MODIS burned area product has been recently implemented in the MODIS land production system to systematically map burned areas globally for the 6 year MODIS observation record. Collection 5 is underway, reprocessing the Terra data record starting in 2000 to present.

16.2.3. Fire Risk Assessment

Forest fires can cause substantial damage to natural resources and human lives regardless of whether it is caused by natural forces or human activities. To minimize threat from wildfires, fire managers must be able to plan protection strategies that are appropriate for individual local areas. A prerequisite for the planning is the ability to assess and map forest fire risk zones across both broad areas and local sites. Forest fire risk zones are locations where a fire is likely to start, and from where it can easily spread to other areas.

People studied forest fire risk zones (FFRZ) with a variety of mapping methods. Most of them mapped forest fire risk zones by directly using remote sensing and geographic information systems (GIS) that contain topography, vegetation, land use, population, and settlement information (Chuvieco and Congalton 1989; Chuvieco and Salas 1996). A common practice was that forest fire risk zones were delineated by assigning subjective weights to the classes of all the layers according to their sensitivity to fire or their fire-inducing capability.

XU Dong *et al.*, 2005, have developed a RS & GIS based methodology to map forest fire risk zones (Baihe forestry bureau, Jilin, China) to minimize the frequency of fires, avert damage, etc. Satellite images were interpreted and classified to generate vegetation type layer and land use layers (roads, settlements and farmlands). Topographic layers (slope, aspect and altitude) were derived from DEM. The thematic and topographic information was analyzed by using ARC/INFO GIS software. Forest fire risk zones were delineated by assigning subjective weights to the classes of all the layers (vegetation type, slope, aspect, altitude and distance from roads, farmlands and settlements) according to their sensitivity to fire or their fire-inducing capability. Five categories of forest fire risk ranging from very high to very low were derived automatically. The mapping result of the study area was found to be in strong agreement with actual fire-affected sites.

Patah *et al.*, have developed a model using the integration of remote sensing and GIS to produce Fire Risk Index (FRI) maps which could be modified interactively with changing weather conditions. The model resided on three sub-indices - (i) Topographic danger index (TDI), (ii) Weather Danger Index (WDI) and (iii) Fuel Danger Index (FDI). The TDI was computed based on two parameters – slope, aspect and elevation which were generated from a DEM. The WDI was calculated from the ratio of mean maximum air temperature to mean maximum air relative humidity. In the development of the FDI the research has adopted the integration of digital classification product of the Tasselled Cap Transformed (TCT) datasets and the Forest Canopy Density (FCD) Map which gave a significantly more accurate fuel type map of the study area.

16.2.4. Fire Ecology

Fire ecology is a branch of ecology that concentrates on the origins, cycles, and future stages of fire. It probes the relationship of fire with living organisms and their environment. Following concepts provide the basis for fire ecology.

Fire Dependence: This concept applies to species of plants that rely on the effects of fire to make the environment more hospitable for their regeneration and growth. (2) Fire History: This concept describes how often fires occur in a geographical area. Fire scars, or a layer of charcoal remaining on a living tree as it adds a layer of cells annually, provide a record that can be used to determine when in history a fire occurred. (3) Fire Regime: Fire regime is a generalized way of integrating various fire characteristics, such as the fire intensity, severity, frequency, and vegetative community. (4) Fire Adaptation: This concept applies to species of plants that have evolved with special traits contributing to successful abilities to survive fires at various stages in their life cycles.

One major effect of fire is a change in soil nutrients and soil temperature. Fire may be a chief factor maintaining productivity in colder soils where the lack of nutrients is a major factor limiting plant growth. Fires release nitrogen and other nutrients from woody vegetation back into the soil in the form of mineral-rich ash, which makes them readily available for new plant growth. Plant regeneration begins almost immediately following a fire. At any given location, vegetation develops over time in orderly stages called succession. Each successive stage is determined by climate, soil conditions, available sunlight, and natural disturbances such as wildland fire. Although fire may destroy individual trees and understory plants, the species themselves are well adapted to survive. In many cases, this is accomplished through a high regeneration capacity.

The effects of fire on habitat- an animal's surroundings or home- are generally more significant than the effects on animals themselves. Forests of different ages support different kinds of wildlife. Different types of birds and mammals seeking food and shelter are attracted to different types of forest types. All of these animals need a variety of resources to provide shelter, food, water, and space. These resources are often found on the borders of two or more plant communities, such as meadow/black spruce or birch/shrubland. These "edges" are created by fires and other disturbances and are beneficial to maintaining a healthy wildlife habitat. Small fires that occur in an area create more "edges" than one large burn. In fact a majority of species generally do best in forests that provide a combination of habitats.

Many wildlife species thrive on the occurrence of fire. The grasses, seedling shrub, and trees that reestablish burned areas provide an ideal environment for many small seed-eating mammals and birds, such as sparrows. Burned trees provide sites for cavity nesting birds like flickers, kestrels, and chickadees, while woodpeckers thrive on the insects that inhabit fire-killed trees.

Although the common conception is that fire is a destroyer of the natural environment, the opposite is actually true, where a carefully planned prescribed burning program can be beneficial and even enhance the health of an ecosystem. Prescribed fires can reduce the amount of combustible fuel buildup that can cause larger more destructive fires. Other benefits of prescribed fire include: insect pest control, removal of undesirable plants competing for nutrients, addition of nutrients from ash, and removal of sunlight inhibiting brushy undergrowth.

However, incorrectly managed prescribed fires can have very adverse effects causing excessive soil heating, loss of nutrients, and removal of woody debris needed to protect seedlings. Wildfires are suppressed in developed and high-fuel areas where intense fire could destroy a plant community or human built structures. Modern fire policy permits the burning of some natural fires and recognizes the use of prescribed fire as a management tool.

16.2.5. Agricultural burning

Agriculture and climate are inextricable related. Dependence of agriculture to climate change has only been established over the last few decades. Agricultural activities including clearing of forests, burning plant matter, cultivating rice, raising livestock and using fertilizers, leads to increased concentration of greenhouse gases in the atmosphere. Present agricultural practices contribute towards 17% of the global warning.

Badrinath *et al.*, have studied the agriculture crop residue burning in Punjab during wheat and rice crop growing periods. Indian Remote Sensing Satellite (IRS-P6) Advanced Wide Field Sensor (AWiFS) data during May and October 2005 have been analysed for estimating the extent of burnt areas and thereby greenhouse gas (GHG) emissions from crop residue burning. Emission factors available in the literature (Jun Wang *et al.*, 2003, Dennisa, *et al.*, 2002 and Reddy *et al.*, 2003) were integrated with satellite remote sensing data for estimating the emissions. Results suggested that emissions from wheat crop residues in Punjab are relatively low compared to those from paddy fields. It is inferred that incorporation of agricultural residues into the soil in rice–wheat systems is highly sustainable and eco-friendly, rather than burning the crop residues.

16.2.6. Biomass burning

Land clearing, an agriculture related activity, has made significant contribution to the greenhouse gas build-ups. When land is cleared, carbon dioxide is released through the burning or decomposition of plant matter and the oxidation of organic matter in the soil. Clearing forestlands for agricultural purpose results in increased carbon emission, because forest ecosystem store 20-100 times more carbon per unit area than cropland. Moreover burning of biomass for agriculture and pasture farming result in significant carbon dioxide emissions.

Biomass burning, in a broad sense, encompasses different burning practices, including open and confined burnings, and different types of vegetation. Emission factors of gaseous or particulate trace compounds are directly dependent both on the fuel type and the combustion process. Emission factors are generally calculated using the carbon mass balance method, applied either to combustion chamber experiments or to field experiments based on ground-level measurements or aircraft sampling in smoke plumes. There have been a number of experimental studies to investigate wildfires in tropical, temperate, or boreal regions. Delmas *et al.*, 1995, presented in their article, an overview of measurement methods and experimental data on emission factors of reactive or radiatively active trace compounds, including trace gases and particles. It focuses on fires in tropical regions, that is, forest and savanna fires, agricultural burns, charcoal production, use of fuelwood, and charcoal combustion.

The MOPITT (Measurement Of Pollution In The Troposphere) aboard the NASA Earth Observing System (EOS) Terra satellite is a thermal and near IR gas correlation radiometer designed specifically to measure CO profiles and total column CH_4. The resolution is 22 km horizontal resolution, though the refresh is 3 days. Pinpointing the sources of airborne chemical species is an important role for MOPITT. Although it cannot distinguish between individual industrial sources in the same city, it can map different points of origin that cover a few hundred square miles. This is accurate enough to differentiate air pollution from a major metropolitan area, for example, from a major fire in a national forest. In addition to being a pollutant, CO gas is a useful tracer for other pollutants, such as ozone at or near ground level. CO can also be used to calculate the level of pollutant-cleansing chemicals in the atmosphere, such as the hydroxyl radical. When CO levels are high, the level of the hydroxyl radical is usually lower and fewer pollutants are removed from the atmosphere. Generally radiative transfer model is being used to determine the amount of CO required to agree with MOPITT observations of elevated CO in conjunction with biomass burning.

MODIS data are also used to predict and monitor emissions from forest fires. This data are used to monitor area recently burned using two methods: a preliminary near-IR spectral test being developed at NASA and the convex hull of the cumulative active fire pixel centers (hot spots) when thick smoke obscures the burn scar. Emission factors from previous studies are used to estimate fire emissions from the MODIS observations. The emission estimates are used by a NOAA model to predict the dispersion of the emissions at three-hour intervals over several days (Wei Min Hao *et al.*).

A new instrument in orbit aboard NASA's ICESat satellite—the Geoscience Laser Altimeter System (GLAS)—reveals another dimension of the California wildfires. By transmitting a green beam of laser light downward at the Earth and then precisely measuring how much of that light is backscattered back up into space, GLAS can determine the vertical structure of clouds, pollution, or smoke plumes in the atmosphere.

Streets *et al.*, 2006 have studied biomass burning and associated atmospheric emission for Asian country. They estimated that 730 Tg of biomass are burned in Asia in a typical year from both anthropogenic and natural causes. Forest burning comprises 45% (330 Tg) of the total; the burning of crop residues in the field comprises 34% (250 Tg), and 20% (150Tg) comes from the burning of grassland and savanna. China contributes 25% of the total, India 18%, Indonesia 13%, and Myanmar 8%. Regionally, forest burning in Southeast Asia dominates. In their study National annual totals are converted to daily and monthly estimates at $1^0 \times 1^0$ grid resolution using distributions based on AVHRR fire counts for 1999-2000. Several adjustment schemes are applied to correct for the deficiencies of AVHRR data, including the use of moving averages, normalization, TOMS Aerosol Index, and masks for dust, clouds, landcover, and other fire sources.

To calculate emissions from biomass burning, the mass of dry matter burned of each type (forest, savanna grassland, or crop residues) is multiplied by an appropriate emission factor from Andreae and Merlet [2001], using the equation

$$E = M * F$$

where, E = total emissions of the source type;
M = mass of dry matter burned; and
F = source-specific emission factor

Biomass burning amounts are converted (using the above equation) to atmospheric emissions, yielding the following estimates: 0.37 T_g of SO_2, 2.8 T_g of NO_x, 1100 T_g of CO_2, 67 T_g of CO, 3.1 T_g of CH_4, 12 T_g of NMVOC, 0.45 T_g of BC, 3.3 T_g of OC, and 0.92 T_g of NH_3. Uncertainties in the emission estimates, measured as 95% confidence intervals, range from a low of ±65% for CO_2 emissions in Japan to a high of ±700% for BC emissions in India.

Annual emissions inventories, although necessary, are notoriously inaccurate, especially when emission factors from developed countries are applied (Guttikunda *et al.*, 2008) to developing countries.

16.2.7. Forest Fire Management System

Reliable up-to date information is critical for effective and efficient prevention and suppression of fires. Hence forest fire information system is a driving force for improved communication with the user department. Presently there are many number of forest fire information systems available globally/country level viz., Canadian wild land fire information system (http://cwfis.cfs.nrcan.gc.ca/en/index_e.php), European forest fire information system (http://ies.jrc.cec.eu.int/94.html), Web fire mapper (http://maps.geog.umd.edu/). Indian Forest Fire Response and Assessment System (INFFRAS).

Fire Information for Resource Management System (FIRMS) is a transitioning from a Research to an Operational System with an Emphasis on Protected Areas. This project integrates Remote Sensing and GIS technologies to provide Global fire information in easy to use formats for decision making, with an emphasis on supplying Protected Area managers. This work builds on Web Fire Mapper, a decision support tool built by researchers in the Department of Geography using NASA research and observations. The project will refine Web Fire Mapper - expanding the prototype into an operational system called the Fire Information for Resource Management System (FIRMS). This operational system will ultimately be housed at the United Nations (FAO and UNEP) to ensure data continuity and aid the UN in meeting its mandate to assist developing countries in protecting biodiversity. FIRMS will consist of a WebGIS with interactive maps, near-real time NASA imagery and email and text message alerts warning of fires in or around Protected Areas. FIRMS is likely to be integrated with INFFRAS soon.

Although fire is an established ecosystem process, and has an important role in conservation areas, frequent and uncontrolled fires can be detrimental. Uncontrolled fires can damage natural resources, diminish the range and diversity of species and erode fragmented forest edges. To be able to manage fires, natural resource managers need timely information both on fires occurring within their area of jurisdiction and within its immediate surroundings. Obtaining fire information in a user-friendly format and in time to use it for operational fire management has not been easy for park managers in remote locations and with limited access to the internet. FIRMS will provide resource managers with a system that delivers fire products with the minimum possible file size and using a delivery system that anyone with Internet connectivity can access.

16.3. Forest Fire Study under Decision Support Centre (DSC), Disaster Management Support Programme (DMSP) at National Remote Sensing Centre (NRSC), India

16.3.1. Indian Forest Fire Response and Management System (INFFRAS)

The Decision Support Center (DSC) at the National Remote Sensing Centre is an integral part of the National Disaster Management Support Program (DMSP) activities of Department of Space. The Indian Forest Fire Response and Assessment System (INFFRAS) have been established under the DSC to facilitate forest fire management. INFFRAS integrates multi sensor satellite data with GIS databases to address forest fire management at following levels

- Pre fire: Preparatory planning for fire control;
- During fire: Near real time active fire detection and monitoring;
- Post fire: Damage and recovery assessment and mitigation planning

Website of INFFRAS is available at NRSC home page as shown in Figure 16.8.

With the advent of series of satellite onboard, it is possible to detect active fires to a minimum of 4 times in a day (viz. MODIS-Terra/Aqua, NOAA-17/ 18, IRS P6) and at least 2 times during nighttime by DMSP-OLS (F15 & F16). In an integrated approach, daytime fire signals using MODIS Terra/Aqua and nighttime fire signals using DMSP-OLS are disseminated to the user (State Forest Department), through INFFRAS. Different spatial & temporal satellite data viz. IRS 1D/P6, MODIS are analysed for fire monitoring and burnt area assessment on the basis of daily fire alert or based on special request from any user and are made available at INFFRAS for the users. In addition to the above, Remote Sensing & GIS based inputs for recovery/ mitigation planning also been provided to the user through INFFRAS. All the activities done under INFFRAS are described in the following sections.

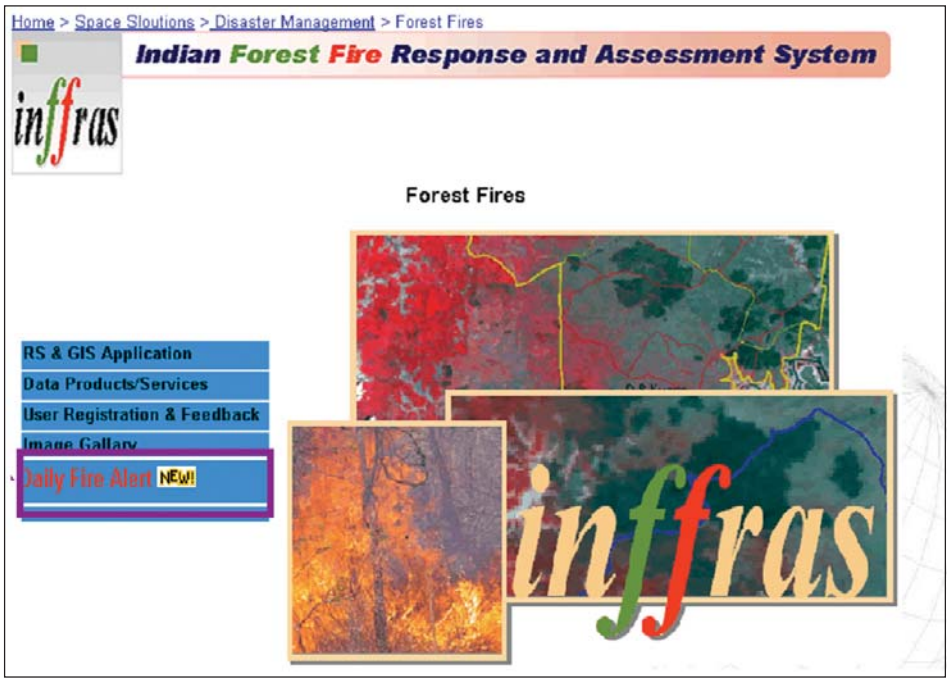

Figure 16.8: INFFRAS web site

16.3.1.1. Active fire detection using Moderate Resolution Imaging Spectroradiometer (MODIS) Terra/ Aqua data

16.3.1.1.1. Introduction

Coarse resolution (1 Km.) satellite data of sensors like MODIS, AATSR and NOAA detect active fires based on the brightness temperature levels recorded in short wave and thermal IR wavelength bands. Detection of active fires as a function of the pixel brightness temperature above that of background depends on fire temperature and size (area under burning) relative to the ground resolution of the sensor, fire and smoldering intensity levels, vegetation type and background land cover and atmospheric interferences.

Active fire locations detected using MODIS satellite data are placed on WEB on daily basis for the entire globe. Based on our initial studies conducted using these databases, it was found that a lot of improvement is required in terms of positional accuracy, detection of small fires and reduction of false alarms. The methods available globally need to be fine tuned while applying them over tropical regions like India by taking into account small

extent of fires, different vegetation types and forest boundaries to exclude false alarms. This calls for development of region specific algorithms for detection of fires with improved accuracy.

Experience with the previous few years of high quality data from the (MODIS) through quality control and validation has suggested several improvements to the original MODIS active fire detection algorithm described by Kaufman *et al.*,1998. An improved active fire detection algorithm was developed which offers increased sensitivity to smaller, cooler fires as well as a significant lower false alarm rate. (Kaufman *et al.*, 2003). The improved algorithm can detect fires roughly half the minimum size that could be detected with the original algorithm while having an overall false alarm rate 10-100 times smaller.

The original fire detection algorithm suffered from persistent false detections in deserts and other sparsely vegetated land surfaces. As an example over Pakistan version -3 algorithm yielded nearly 4800 false fire pixels. These pixels were deemed false based on an examination of MODIS 250 m, 500 m, and 1 km imagery and the fact that the large cluster persisted over long periods of time (e.g., weeks). All fire pixels were located in areas of sparsely vegetated soil, and none of the fire pixels have sufficiently high 4 μm brightness temperatures to definitively suggest that true fires might be present. In addition, the top-of-atmosphere visible channel reflectances reveal a complete absence of smoke. This suggests that the majority (if not the entirety) of the fire pixels within a mosaic land cover of vegetative and non-vegetative surface are indeed false alarms. These studies stress a need for fine-tuning the fire detection algorithm on a continuous mode with region specific thresholds especially for sparsely vegetated forest areas in India.

In view of this, present study is proposed with the following objectives:

- To fine tune region specific forest fire detection algorithms using MODIS –Terra/Aqua satellite data
- To provide active fire locations along with forest infrastructure boundaries (if available) on daily basis for entire the country

16.3.1.1.2. Methodology for detection of active fire locations using MODIS Terra/Aqua data

A complete MODIS technical specification is given in Table 16.1 and operational procedure adapted for identification of active fire using MODIS Terra/Aqua satellite data is shown in figure 16.9. Raw MODIS Terra/Aqua satellite data acquired at NRSA ground station has undergone a series of process for the generation of active fire products. The raw satellite data in PDS format has been pass through MS2GT algorithm (down lowed from MODIS fire site) for

Table 16. 1: MODIS Technical Specifications

Orbit	:	705 km, 10:30 a.m. descending node (Terra) or 1:30 p.m. ascending node (Aqua), sun-synchronous, near-polar, circular
Scan Rate	:	20.3 rpm, cross track
Swath Dimensions	:	2330 km (cross track) by 10 km (along track at nadir)
Telescope	:	17.78 cm diam. off-axis, afocal (collimated), with intermediate field stop
Size	:	1.0 x 1.6 x 1.0 m
Weight	:	228.7 kg
Power	:	162.5 W (single orbit average)
Data Rate	:	10.6 Mbps (peak daytime); 6.1 Mbps (orbital average)
Quantization	:	12 bits
Spatial Resolution	:	250 m (bands 1-2)
		500 m (bands 3-7)
		1000 m (bands 8-36)
Design Life	:	6 years

Primary Use	Channel	Bandwidth 1	Spectral Radiance 2	Required SNR3
Land/Cloud/Aerosols Boundaries	1	620 - 670	21.8	128
	2	841 - 876	24.7	201
Land/Cloud/Aerosols Properties	3	459 - 479	35.3	243
	4	545 - 565	29	228
	5	1230 - 1250	5.4	74
	6	1628 - 1652	7.3	275
	7	2105 - 2155	1	110
Ocean Color/ Phytoplankton Biogeochemistry	8	405 - 420	44.9	880
	9	438 - 448	41.9	838
	10	483 - 493	32.1	802
	11	526 - 536	27.9	754
	12	546 - 556	21	750
	13	662 - 672	9.5	910
	14	673 - 683	8.7	1087
	15	743 - 753	10.2	586
	16	862 - 877	6.2	516
Atmospheric Water Vapor	17	890 - 920	10	167
	18	931 - 941	3.6	57
	19	915 - 965	15	250
Surface/Cloud Temperature	20	3.660 - 3.840	0.45(300K)	0.05
	21	3.929 - 3.989	2.38(335K)	2
	22	3.929 - 3.989	0.67(300K)	0.07
	23	4.020 - 4.080	0.79(300K)	0.07
Atmospheric Temperature	24	4.433 - 4.498	0.17(250K)	0.25
	25	4.482 - 4.549	0.59(275K)	0.25
Cirrus Clouds Water Vapor	26	1.360 - 1.390	6	150(SNR)
	27	6.535 - 6.895	1.16(240K)	0.25
	28	7.175 - 7.475	2.18(250K)	0.25
Cloud Properties	29	8.400 - 8.700	9.58(300K)	0.05
Ozone	30	9.580 - 9.880	3.69(250K)	0.25
Surface/Cloud Temperature	31	10.780 - 11.280	9.55(300K)	0.05
	32	11.770 - 12.270	8.94(300K)	0.05
Cloud Top Altitude	33	13.185 - 13.485	4.52(260K)	0.25
	34	13.485 - 13.785	3.76(250K)	0.25
	35	13.785 - 14.085	3.11(240K)	0.25
	36	14.085 - 14.385	2.08(220K)	0.35

[1] Bands 1 to 19 are in nm; Bands 20 to 36 are in µm
[2] Spectral Radiance values are (W/m^2 - µm-sr)
[3] SNR = Signal-to-noise ratio
[4] NE(delta)T = Noise-equivalent temperature difference
Note: Performance goal is 30-40% better than required

the production of bow tie and geo-corrected satellite data. Geo-corrected satellite data is used as the input to the revised fire algorithm to produce value added fire products.

NRSC followed Version 4 contextual algorithm (Louis Giglio *et al.*, 2003), which is based upon the original MODIS fire detection algorithm (Kaufman, Justice *et al.*, for the generation of fire maps. The above algorithm is modified with region specific needs. The algorithm uses brightness temperatures derived from MODIS 4µm and 11µm channels, denoted by T_4 and T_{11} respectively. Thermal channels 21 and 22 ranging from 3.929 µm to 3.989µm

of MODIS were considered for the present study. Channel 21 saturates at nearly 500 K and channel 22 saturates at 331 K. Since the low–saturation channel (22) is less noisy and has less quantization error; T4 is derived from channel 22. Brightness temperature T_{11} was derived from channel 31, which saturates approximately at 400K. Brightness temperatures derived from channel 32 is denoted by T_{12} and is used in cloud masking.

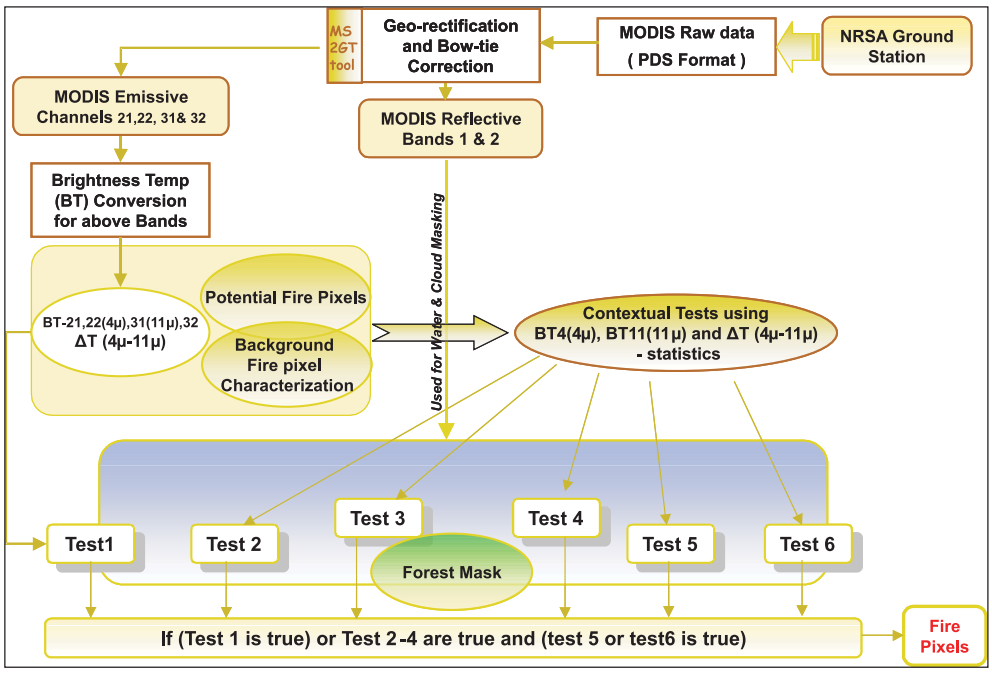

Figure 16.9: Operational procedure of Active fire detection

The 250 m resolution Red and Infrared channels (1 and 2) were aggregated to 1km and were used to reject false alarms and in masking clouds and water bodies. Reflectance of these channels (R,NIR) are denoted by $r_{0.65}$ and $r_{0.86}$ respectively. The details of the adopted algorithm are as follows

16.3.1.1.3. Cloud and water masking

Day time pixels are considered as clouds and obscured if following conditions are satisfied

(ρ 0.65 + ρ0.86 > 0.5) or (T_{12} < 295 K) for small clouds and

(ρ0.65 + ρ0.86 <. 15) or (T_{12} < 298 K) for larger clouds.

16.3.1.1.4. Identification of potential fire pixels

A preliminary classification is used to eliminate obvious non-fire pixels. Remaining pixels are considered in subsequent tests. A daytime pixels are identified as potential fire pixels

if T_4 > 290 K, ΔT > 3K and $\boldsymbol{\rho}$0.86 < 0.185, where $\Delta T = T_4 - T_{11}$

16.3.1.1.5. Absolute threshold test

The 4 and 11 µm channels in MODIS are designed to be sensitive to temperatures reaching 500 K and 400 K respectively. Therefore except for large wild fires (less possible events in India) these MODIS channels with resolution 1 km at nadir are not expected to saturate. According to Weins displacement law, shorter the wavelength (4 µm), the stronger the sensitivity to the higher temperature region. Moreover 4 µm channel is not affected by water vapor absorption and weakly affected by other gaseous absorption.

Fire pixels are detected based on certain criterion. These are (1) The 4 µm channel brightness temperature to be elevated above a set threshold indicating a fire. (2) The difference between the 4 and 11 µm temperatures must be at least some specific value to avoid hot exposed soils, and the (3) used the 11 µm temperature to eliminate false detections from cool clouds, with small drop size, that are highly reflective in the 4 µm band. Based on the above considerations brightness temperatures for 4 and 11 µm channels were examined. Scatter plot of brightness temperatures of fire pixels represented by 4 and 11 µm channels is shown in Figure 16.10. It has been observed from brightness temperature received by 4 µm channel is always showing greater than 310 K. Hence, for absolute temperature threshold, a brightness temperature of 310 K is identified for picking up fire pixel. Similarly the difference of temperature received by 4 and 11 µm channels are plotted in Figure 16.11 wherein it is clear that delta BT is always higher than 17 K for fire pixels.

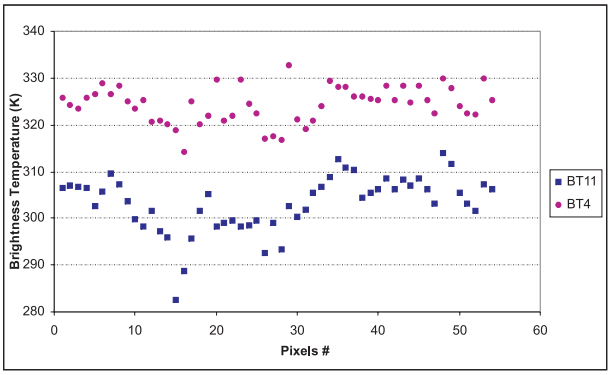

Figure 16.10: Scatter plot of Brightness Temperatures (BT4 &BT11)

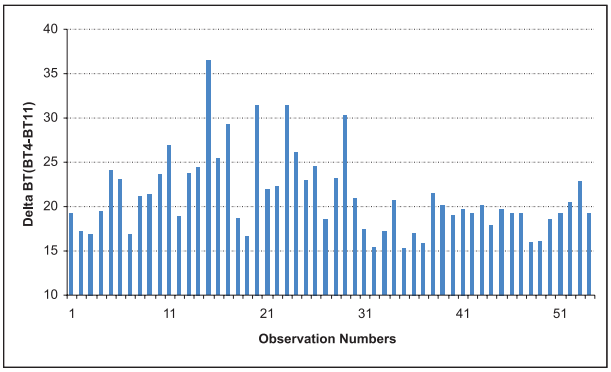

Figure 16.11: Delta BT (BT4-BT11) plotted for different fire pixels

Hence, the absolute threshold criterion considered as

$T_4 > 310$ K and $\Delta T >= 17$ K Test (1)

16.3.1.1.6. Background characterization

Background characterization was performed using the neighboring pixels to estimate the radiometric signal of the potential fire pixel in the absence of fire. Valid neighboring pixels in a window centered on the potential fire pixel are identified and used to estimate background value. Valid pixels are defined as those that (1) contain useful observations, (2) are located on land, (3) are not cloud-contaminated and (4) are not background fire pixels.

Background pixels are in turn defined as those having $T_4 > 323$K and $\Delta T > 20$.

Excluding the background fire pixels, mean and mean absolute deviations of T_4, T_{11} and ΔT for valid neighboring pixels are computed where

$\check{T}_4$ and δ_4 are the respective mean and absolute deviation of T_4;

$\check{T}_{11}$ and δ_{11} are the respective mean and absolute deviation of T_{11} and

$\Delta\check{T}$ & $\delta_{\Delta T}$ are respective mean and absolute deviation of ΔT.

The 4 µm brightness temperature mean and mean absolute deviations for rejected background fire pixels were also computed as $\check{T}_4^I$ and δ_4^I, respectively.

16.3.1.1.7. Contextual tests

Successful background characterization is followed by a series of contextual tests, which use T_4, T_{11} and ΔT to perform relative fire detection. Relative thresholds are adjusted based on natural variability of the background. They are

$\Delta T > \Delta\check{T} + 3.5\ \delta_{\Delta T}$	Test (2)
$\Delta T > \Delta\check{T} + 6$ K	Test (3)
$T_4 > \check{T}_4 + 3\delta_4$	Test (4)
$T_{11} > \check{T}_{11} + \delta_{11} - 4$ K	Test (5)
$\delta_4^I > 5$ K	Test (6)

16.3.1.1.8. Creation of forest mask

A forest mask is created to retain fire pixels under forested area and remove fire pixels outside forest (appear as false alarm).

16.3.1.1.9. Tentative fire detection

A daytime pixel is tentatively classified as a fire pixel if {Test(1) is true} or {Tests (2) – (4) are true and {Test (5) or Test (6) is true} and under forest mask. Otherwise it is classified as non-fire.

16.3.1.1.10. Validation / Accuracy Assessment

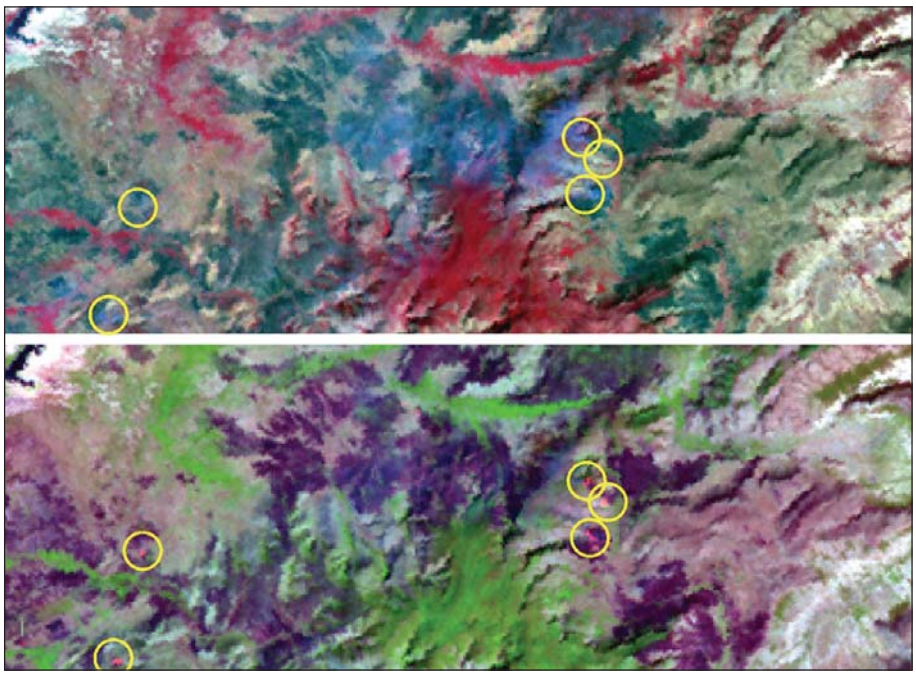

Figure 16.12: Reference active fire location identified using IRS P6 AWiFS data of 24 Feb, .2004 (Top-NIR,R,G and Bottom- SWIR,NIR,R channels were assigned to Red, Green and Blue Channels to enhance fire source location)

Since 1.65 µm (IRS P6 – AWiFS/LISS-III) in the electromagnetic spectrum is very sensitive to flame and flaming energy and not very sensitive to smoldering and its energy, FCC with the SWIR, NIR, R combination highlights the active fire pixels (figure 16.12). IRS-P6 satellite pass is at 1030 IST local time and MODIS Terra satellite 1st pass is also around similar time but with slight variation of pass time based on MODIS orbital calendar. Hence, it is expected that fire location as observed by IRS-P6 AWiFS data are also identified by MODIS Terra data based on duration of fire incident and the time lag between two satellite pass. Therefore in synchronization IRS-P6 AWiFS data and MODIS derived fire products are comparable for active fire identification. Thus, MODIS web based algorithm, revised algorithm based and IRS-P6 AWiFS data based fire locations in conjunction with ground data were used in synchronization for the validation of active fire locations.

16.3.1.2. Active fire detection using Defense Meteorological Satellite Program (DMSP) Operational Line scan System (OLS) data

16.3.1.2.1. Introduction

DMSP OLS is a two band (visible and thermal imaging) system designed for global observation of cloud cover. At night the visible band is intensified with a photo-multiplier tube to permit detection of clouds illuminated by moonlight. The light intensification enables the observation of faint sources of visible-near infrared (VNIR) emissions present at night on the Earth's surface including cities, towns, villages, gas flares, heavily lit fishing boats and fires (Croft 1973, 1978, 1979). By analyzing a time series of DMSP-OLS images, it is possible to define a reference set of "stable" lights, which are present in the same location on a consistent basis. Fires are identified as lights detected on the land surface outside the reference set of stable lights. The Operational Line scan System (OLS) is an oscillating scan radiometer with two spectral bands (visible and TIR) and a swath of ~3000 km. The "visible" bandpass straddles the visible and near-infrared portion of the spectrum (0.5 to 0.9 µm). The thermal band pass covers the 10.5 to 12.5 µm region. Satellite attitude is stabilized using four gyroscopes (three axis stabilization), a star mapper, Earth limb sensor and a solar detector. The OLS visible band signal is intensified at night using a photomultiplier tube (PMT), for the detection of moonlit clouds. The low light sensing capabilities of the OLS at night permit the measurement of radiances down to 10^{-9} watts/cm^2/sr/µm. This is four times lower in magnitude than the OLS daytime visible band or the visible-near infrared bands of other sensors, such as the NOAA AVHRR or the Landsat Thematic Mapper. Fires present at the Earth's surface at the time of the nighttime overpass of the DMSP are readily detected in the visible band data. In contrast, fires rarely show up as hot spots in the OLS thermal band data. The OLS thermal band position (10.5 to 12.5 µm) is not well placed for fire detection.

16.3.1.2.2. Methodology and description of Algorithms

Procedure adapted has been shown in Figure 16.13. The procedures rely on the existence of a stable lights data set derived from a time series of night time OLS observations. The basic procedures used to generate the stable lights have been described by Elvidge *et al.*, (1997). The fire product processing can be grouped into two divisions:

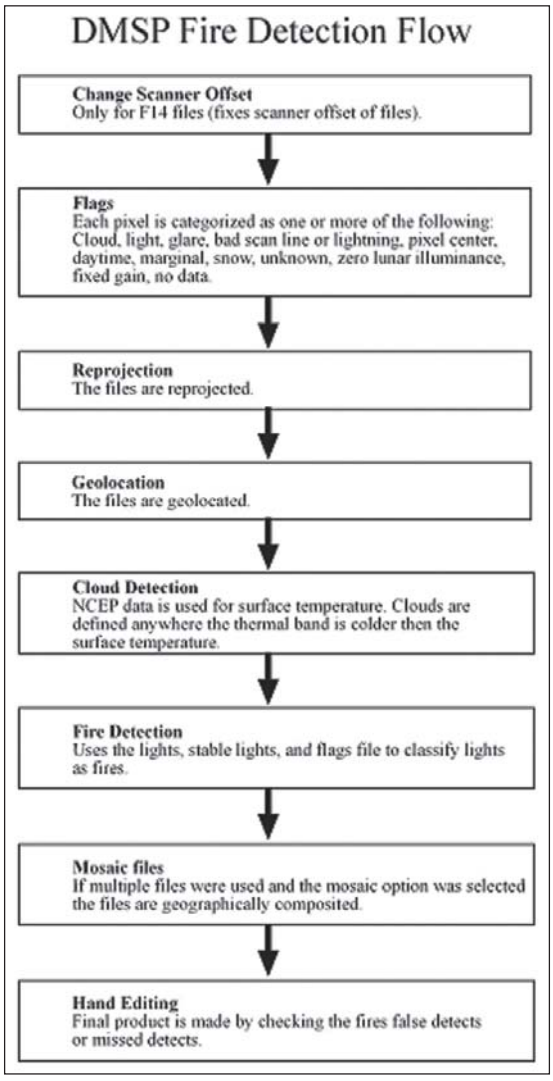

Figure 16.13: DMSP fire detection procedure

processing done on raw OLS data and processing done on geo-referenced OLS data. Certain steps are logically applied while the data are in their raw scan line format. In addition, the raw data has less data volume, which allows the processing to run faster. Processing steps applied to the raw data include: orbit assembly and sub orbiting, cloud identification, light detection, geo-location and girding. Following the light detection there are options for the removal of single pixel light detections and light detections that coincide with clouds on heavily moonlit nights. Pixels identities (e.g., lights, clouds, clouds with lights, missing scan lines) are marked in a flag file which overlays the OLS image data. Steps performed on the geo-referenced data include the removal of lights associated with stable lights, lights over water surfaces, and final editing by an image analyst.

16.3.1.2.3. Factors influencing DMSP fire detection

There are a number of factors or conditions, which will impede the detection of fires with DMSP-OLS data, including: high levels of lunar illumination, cloud cover, and solar glare, moonlit clouds, incomplete stable light set used etc. Thus it is important that the stable lights database be kept up to date and that it is constructed with sufficient numbers of cloud-free observations to ensure that all stable lights are included. Because of the manner in which the stable lights are removed, fires that are adjacent to stable lights can not be readily detected (errors of omission). As final steps in generating a DMSP fire product are performed on 30 arc second grids instead of OLS pixels. Since a single OLS pixel usually occupies nine 30 arc second grid cells, a simple estimate of the number of OLS fire pixels can be made by dividing the total number of 30 arc second cells tagged as fire by nine. Day and Night time operational forest fire products are shown in figure 16.14.

16.3.1.3. Burnt Area Assessment

16.3.1.3.1. Introduction

Currently burnt area reporting in the country is done by individual State Forest Department by integrating the ground reports. The ground-based assessment is very laborious and time taking. As the fires occur simultaneously at several places between January to June many of the cases might also go undetected. The burnt area assessment assumes importance in terms of local and National relevance. The near real time damage assessment can only be achieved through satellite based burnt area

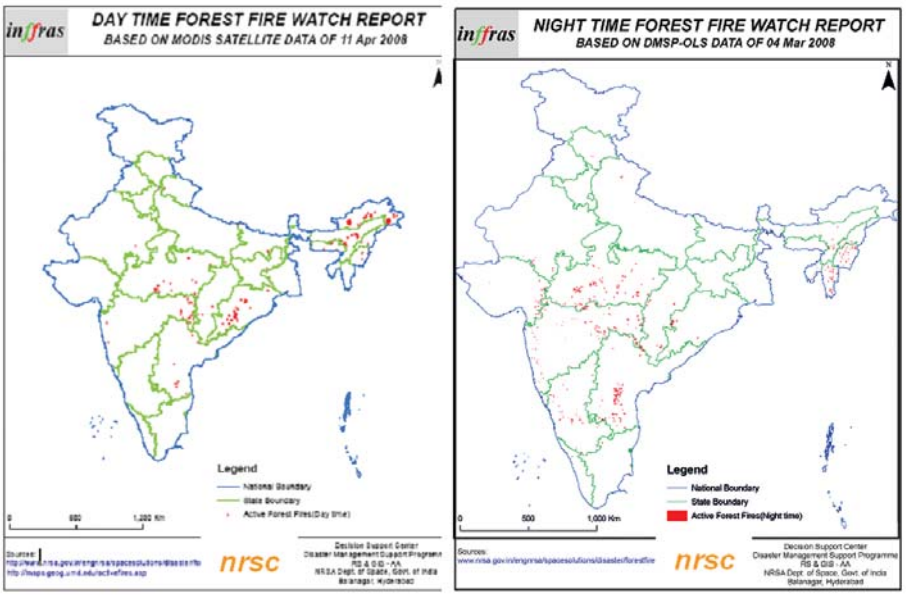

Figure 16.14: MODIS and DMSP-OLS active fire product

assessment and would be critical inputs essentially for protected areas and other ecologically important forested areas. On the other hand National level burnt area assessment has relevance in terms of following issues. This calls for moderate resolution satellite data application to make more precise assessment. In this regard remote sensing & GIS would helps for

- Reliable assessment in terms of area, no of patches and spatial spread
- Base line for temporal monitoring and fire recurrence assessment
- Identification and prioritization of vulnerable areas
- Understanding the impacts on regeneration, succession, biodiversity and wild life
- Assessment in terms of GHGS towards
- Scope for developing web enabled national forest burnt area reporting system
- Fire mitigation planning

The local level burnt area studies were made limited extent to provide inputs for vulnerable assessment and mitigation planning. An operational mechanism, which can provide information on burnt area assessment on real time basis, does not exist in the country. The National Commission on Agriculture (NCA) for the period 1968 to 1973 carried out a study on the incidence of fire. According to NCA, the average number of annual fires was 3,406, affecting an area of 2,576 Sq.Km (0.76 km per fire). In 1986, Ministry of Environment and Forests (MOEF) compiled data on fires for the five-year period 1980 to 1985, and found that 17,852 fires occurred in the country burning an area of 5,724 Sq.Km. This amounts to an average of 3,570 fires affecting 1,145 Sq.Km annually (i.e., 0.32 Sq.Km per fire). Based on the data for 1985 to 1988 compiled by MOEF, Forest Survey of India (FSI) estimated that the stand replacing fires affect about 10,000 Km^2 of forest area annually (FSI, 1988). In the present study, the same percentage of area (estimates by FSI, 1988) has been taken as annual area affected by stand-replacing fires for the reference year 1993.

Table 16.2: Forest range wise area statistics of Rajiv Gandhi National Park using IRS-P6 LISS-III of 14 February 2004

SL #	Forest Range Name	Area (Sq.Km.)	Burnt Area (Sq.Km.)	% Area Burnt
1	Anechowkur	101.21	0.41	0.41
2	Veeranahosahalli	74.44	0.11	0.15
3	Kalhalla	111.96	0.14	0.13
4	Mettikuppe	75.27	9.05	12.02
5	Nagarhole	103.55	0.02	0.02
6	Antarasante	78.83	2.05	2.60
7	D. B. Kuppe	144.78	3.67	2.53
	TOTAL	**690.04**	**15.45**	**2.24**

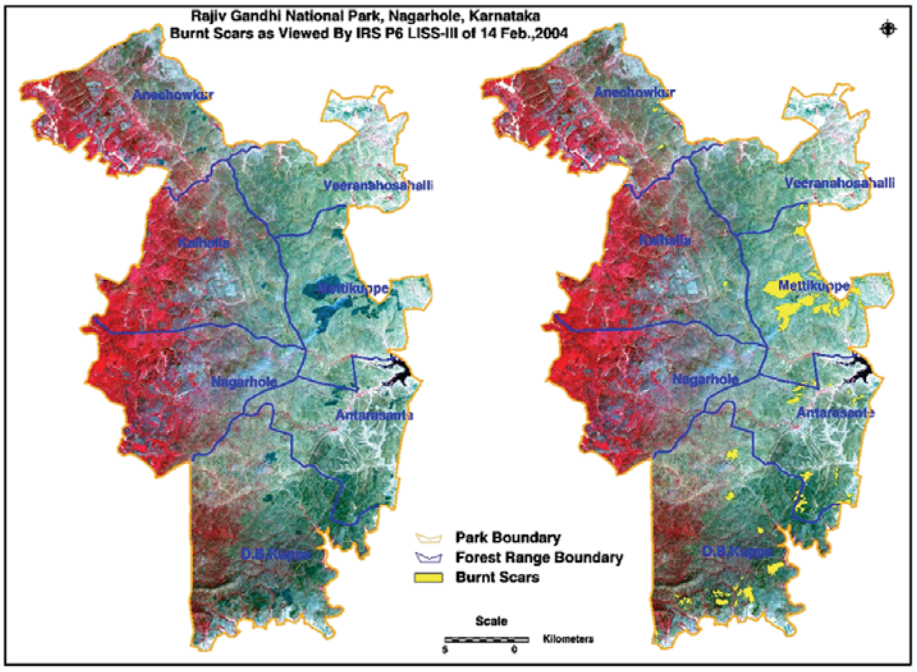

Figure 16.15: Forest Range boundary overlaid on FCC of 14th February 2004

On the other hand the global forest burnt area assessment made by ESA (European Space Agency) using coarse resolution (1.1 km^2) SPOT4-VEGETATION (SPOT-VGT) reported forest burnt area as 9% (47,134 km^2) of the total forest area for the year 2000. The reports are found to be over estimates because of the coarse resolution satellite data used. The global assessments do not reflect the realistic small-scale burning and also associated trace gas emissions due to forest fires. So far reliable spatial accounting of forest burnt area for the entire country is not done.

In view of this, an effort is initiated to undertake burnt area assessment on a regular basis on the following lines.

- Based on trigger from fire watch report
- Response from user departments against the announcement of DSC
- Direct request from user departments
- Internal DSC studies to develop data base

16.3.1.3.2. Burnt area assessment for Rajiv Gandhi National Park

Burnt area assessment for Rajiv Gandhi National Park has been done using IRS P6 LISS-III data of 14 February 2004 as shown in Figure 16.15 and corresponding Forest Range wise burnt area statistics are given in Table 16.2.

16.3.1.3.3. Burnt area assessment in Bhandavgarh National Park, Madhya Pradesh

There was a TV news report on 16th April, 2005 at 2030 hrs that forest caught fire in Bhandavgarh National Park, Madhya Pradesh. Report says that fire incidence started in the morning of 16th April, 2005. According to this report, we have browsed all possible satellite data and procured IRS-P6 AWiFS data of 16th April 2005. Study revealed that, no fire burnt scars observed within the Park extent, which indicates that fire started after 1030 hrs morning satellite pass. Hence, next possible satellite pass of 17th April 2005 (IRS 1D WiFS) data was procured and analysed and found burnt scars within the park extent as shown in Figure 16.16. The information was communicated to concerned official on 17th April 2005.Study demonstrated the efficacy of Indian Remote Sensing Satellite in meeting the near real time requirement.

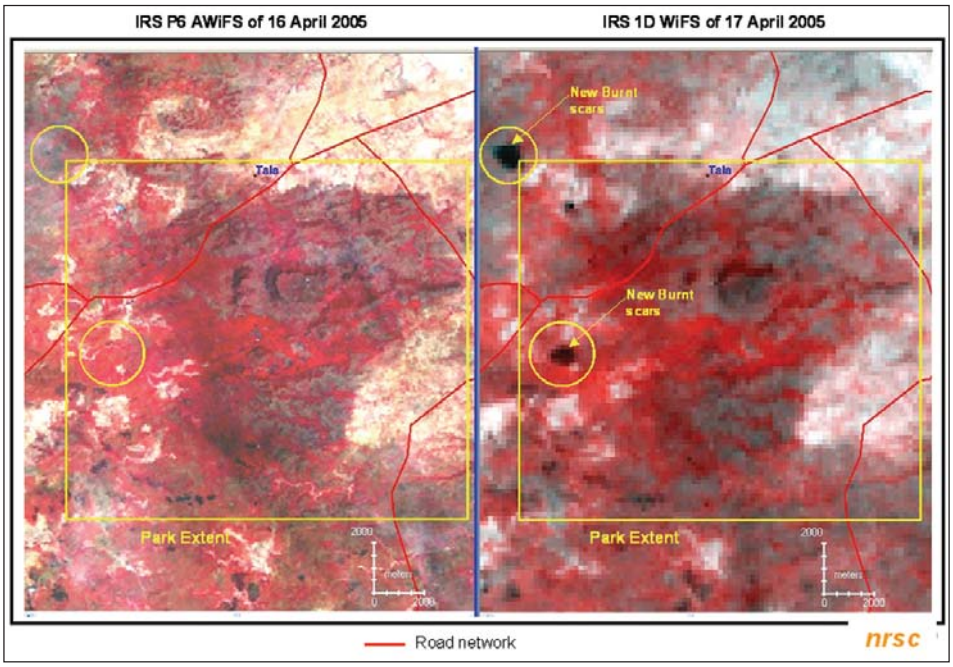

Figure 16.16: Near real time damage assessment in and around Bhandavgarh National Park, Madhya Pradesh

16.3.1.4. Fire progression Monitoring

Fires, whether of human or natural origin, have profound effects on land cover, land use, production, local economies, global trace gas emissions, and health. A fire analysis cycle can be defined that moves from mapping the potential for a fire start if there is ignition, to detecting the start of a fire, through monitoring the progression of a fire, to mapping the extent of the fire scars and the progression of vegetation regeneration. Such information would be useful to managers, policy makers and scientists interested in mitigating and evaluating the effects of fires.

Fire monitoring differs from fire detection in emphasis rather than in fundamental methods. Fire monitoring measures and describes the growth of known fires; three characteristics of interest are the growth of the fire, extent of the smoke plume, and Monitoring the movement and dispersion of fires is a variant of fire detection, where the focus is the analysis of changing fire patterns. As in fire detection, thermal and nighttime visible images are effective for mapping changing fire patterns. Monitoring the extent of the fire burnt scars requires analysis of visible, near infrared and short wave infrared wavelengths.

In India, effective fire control and assessment is tedious due to their randomness of occurrence and their size. Here, numbers of fire occurrence are high but most of them are small in nature. With the advent of series of IRS satellites on board, it is quite possible to monitor the fire progression on a high temporal basis. IRS AWIFS/WIFS temporal images clearly show the spatial and temporal changes in burnt and unburnt areas. This spatial information

on progression could be useful in effective planning for ground control operation during the summer month by identifying the areas still prone to fire during the remaining period of current summer season.

Continuous fire burnt area monitoring using high temporal satellite data like IRS P6/1D AWiFS/ WiFS data helps in assessment of progression of fires at frequent intervals to facilitate control operations. As an example during the fire season 2004, Different protected area in India is being monitored and progression of fire was studied using Indian satellite data. Fire burnt areas overlaid with forest infrastructure boundaries were sent to respective State Forest Department to facilitate control planning during current fire season. The information provided has been found to be quite useful to different State Forest Departments for strategic planning. Forest Fires over Indian region mostly occur during the months of February May and the progression of fires depends on the forest types in different parts. The southern dry deciduous forests had more fire episodes during mid February to the end of March. The tropical and temperate forests of North Eastern Region also show fire episodes during the same period and the fires in these regions are associated with shifting cultivation practices. The fires progress from southern to central regions of India during March and April and the central Himalayan region experiences fires during end of May to early June each year. Fire progression in and around Rajiv Gandhi National Park, Nagarhole & Bandipur Tiger Reserve, Karnataka is shown in Figure 16.17.

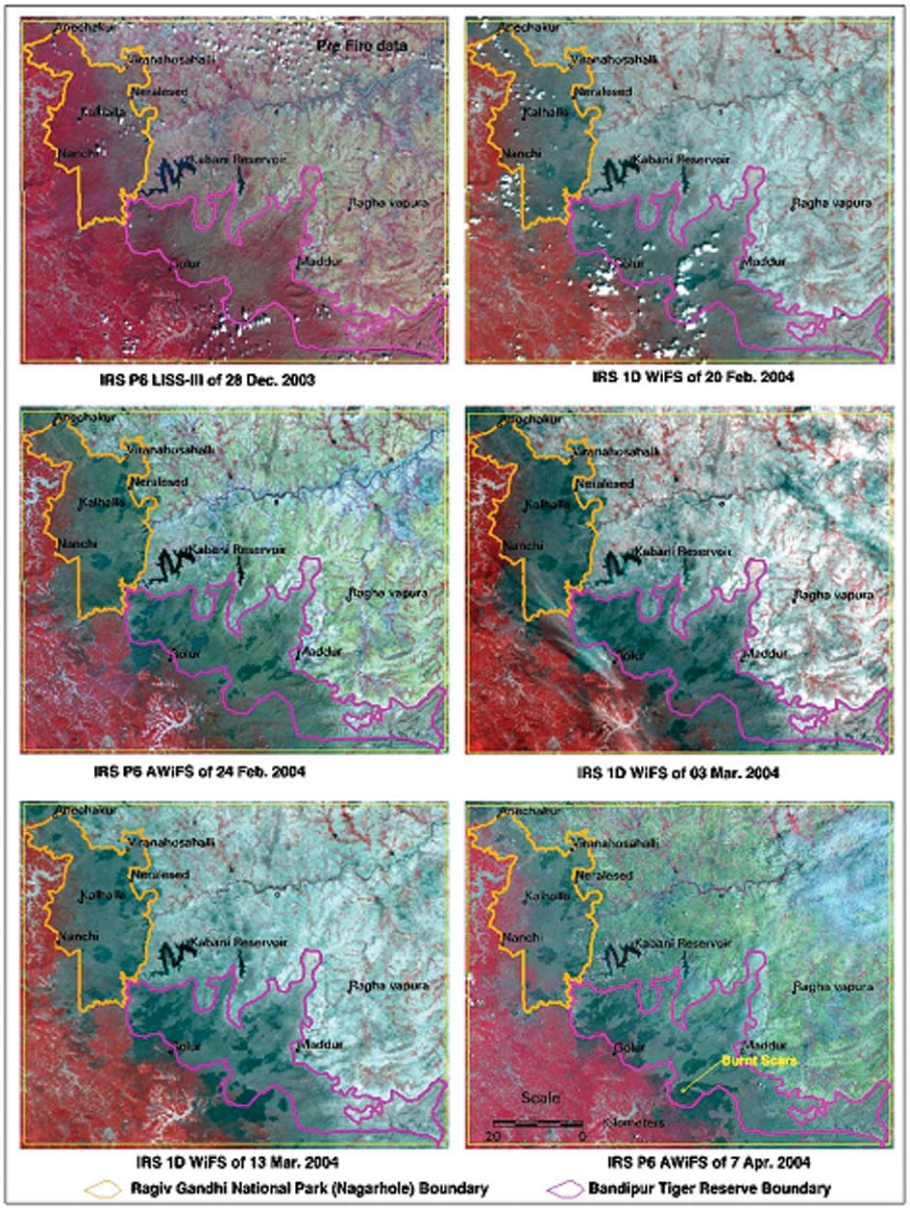

Figure 16.17: Forest Fire monitoring in Rajiv Gandhi National Park and Bandipur Tiger Reserve, Karnataka

16.3.1.5. Fire Risk Assessment- Case Study in India

Badrinath *et al.*, have studied and prepared a Fire danger index map for the Nagarjunasagar Srisailam Tiger Reserve (NSTR) of Andhra Pradesh, India. Two major steps are involved in arriving at the danger indices. The first step is to generate danger variable maps such as fire frequency, topography, surface temperature and relative humidity. The second step involves derivation of intermediate indices using multiple regressions taking fire frequency as dependent variable. The methodology used in the study has been adapted from Roberto Castro *et al.*, 1998. Two major steps are involved in arriving at the danger indices. The first step is to generate danger variable maps such as fire frequency, topography, surface temperature and relative humidity. The second step involves derivation of intermediate indices using multiple regressions taking fire frequency as dependent variable.

Results of the study (figure 16.18) suggests high Fire Danger Index (FDI) values in the proximity of village locations, water bodies and road points. The study area is inhabited by local tribal populations who depend more upon the

forest for fuel wood. They cut the grasses and burn the base so as to facilitate the re-growth of the grasses by the on setting of monsoon. Traditional practices such as these account for most of the fire episodes. More over, the study area also being a pilgrim place is more subjected to visitors all round the year. Lighting of cigarettes and cooking practices of these pilgrims have their contribution in forest fires along highways and road points. This suggests that fires in the study area are more of anthropogenic activities than due to natural episodes. Although the proportional weights between variables might be applied to other areas or periods, the specific coefficients are restricted to the area and interval in which fire statistics were collected. The approximations on danger variable calculations such as fuel types, relative humidity are some of the limitations of the study which can be overcome by more ground knowledge and detailed measurements.

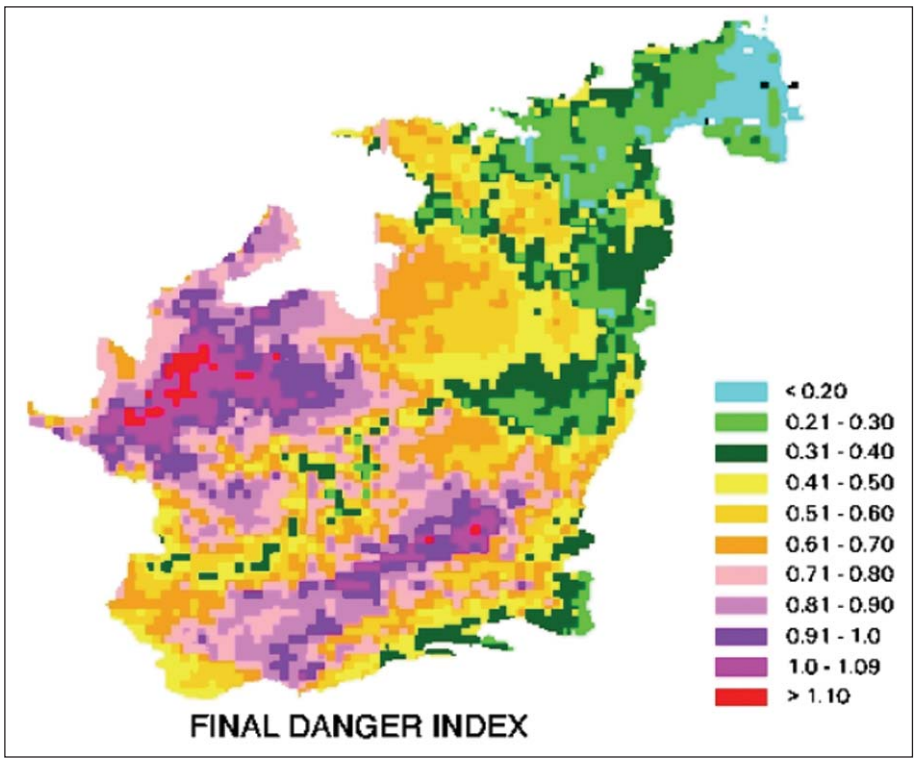

Figure 16.18: Final Fire Danger Index map of Nagarjunasagar Srisailam Tiger Reserve

16.3.1.6. Recovery / Mitigation Planning

As part of recovery / mitigation plan during fire season, a study was conducted to identify the recurrence fire zone map of Rajiv Gandhi National park using satellite data. The study also investigates about, whether the existing watchtowers are adequate for their mitigation planning or not? Towards this, forest fire recurrence and visibility analysis were done and are shown in Figure 16.19 & 20, respectively.

The study has identified the necessity of an additional fire watch tower and its location for monitoring the recurrent fire areas. New locations were suggested based on visibility range identified using canopy heights, terrain heights and forest canopy density.

16.4. Conclusion and Future Aspect

The only effective way to minimize damage caused by forest fires is their early detection and fast reaction, apart from preventive measures. Great efforts are therefore made to achieve early forest fire detection, which is traditionally based on human surveillance. Technically more advanced forest fire surveillance systems is based on video camera monitoring units mounted on monitoring spots and distant monitoring from operation center in conjunction with satellite monitoring. Infrared and laser-based systems are more sensitive and they generate less false alarms, but their price is quite high in comparison to video (CCD) cameras sensitive in visible spectra. For example the price of one typical high quality outdoor pan/tilt CCD camera is 3.000 EUR, and the price of one typical IR thermal imaging camera is 25,000 EUR. Additional feature of CCD video cameras which are today on the market is their dual sensitivity. They are color cameras sensitive in visible spectra during the day, and black and white cameras sensitive in near IR spectra during the night.

The terrestrial systems based on CCD video cameras sensitive in visible and near IR spectra are today the best and the most effective solution for realizing automatic surveillance and automatic forest fire detection systems. In almost every country, which encounters high risk of forest fires, at least one such system are developed or proposed. Some of them are on the market under various commercial names like FireWatch (Germany), FireHawk (South Africa), ForestWatch (Canada), FireVu (England), UraFire (France) etc. In all those systems automatic forest fire detection is based on smoke recognition during the day and flame recognition during the night.

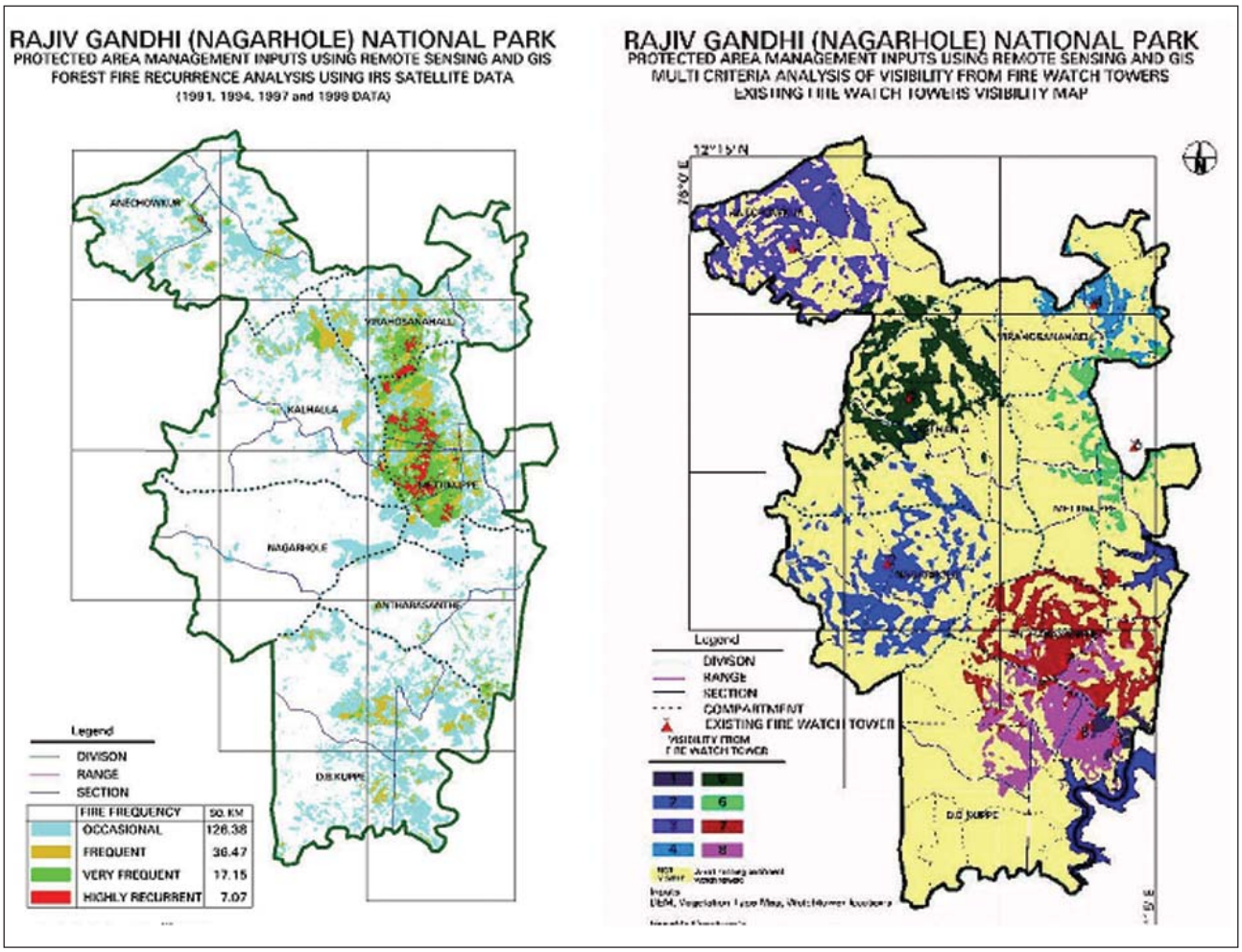

Figure 16.19: Forest fire recurrent analysis

Figure 16.20: Existing watch towers visibility map

With the advent of series of satellites onboard, it is possible to monitor the fires to a minimum of 5 times in a day, facilitating to monitor large episodic fires. In India, with the current capabilities of data processing and data dissemination, it is possible to generate fire signals within one hour of satellite pass. Presently INFFRAS provide one day time (MODIS-Terra/Aqua) and one night time (DMSP-OLS) fire alarm to all the State Forest Department through electronic mail (available in NRSC web site also). In our country, fire watching from ground has also to be strengthened and equipped with sophisticated instrument/system so that mitigation will be done in more effective way.

A new Geostationary Meteorological Satellite INSAT-3D is being designed by ISRO with the capability for fire detection/characterization. Preliminary plans include fire product generation and distribution (GOFC-GOLD Report No 32, October 2007). It will have a six channel advanced imager and a nineteen channel sounder. In addition to satellite imageries in six channels, several new derived products useful in NWP and in day-to-day weather forecasting will be available in the new system. Vertical profiles of atmospheric temperature, moisture and ozone will be available for the first time from an Indian Satellite.

Since, on orbit no of satellites with different sensors are available, it is very important that data pre-processing steps need to be fully characterized. Data fusion of different products types (e.g., burned area and active fire) and between different sensors (polar orbiting and geostationary) needs to be explored.

The quality and consistency of the different geostationary imagers with regard to fire detection and fire characterization needs to be examined. We need to improve communication between data providers and product developers, especially in light of the new instruments becoming operational. Image generation processes should be clearly documented and accessible to product developers, and ideally the applications of active fire detection and characterization should be taken into account when developing new generation sensors (e.g., in terms of dynamic range) and pre-processing procedures (e.g., geolocation and re-gridding).

References

Andreae MO, Fishman J, Garstang M, Goldammer JG, Justice CO, Levine JS, Scholes RJ, Stocks BJ and Thompson AM, 1994, Biomass burning in the global environment: first results from the IGAC/BIBEX Field Campaign STARE/ TRACE-A/SAFARI-92, *Global Atmospheric-Biospheric Chemistry,* Ed. Prinn R, Plenum Press, New York, 83-101.

Andreae MO and P Merlet, 2001 ,Emissions of trace gases and aerosols from biomass burning, Global Biogeochem. Cycles, 15, 955-966, 2001 aperture radars, Proceedings of Institution of Electrical Engineers F, **139**: 147-159.

Arino O, Plummer S and Defrenne D, 2005, Fire disturbance: the ten years time series of the ATSR world fire atlas, H. Lacoste, Proceedings of the MERIS (A)ATSR Workshop 2005 (ESA SP-597).

Badrinath KVS, Kiran Chand TR and Krishna Prasad V, 2006, Agriculture crop residue burning in the Indo-gangetic plains – A study using IRS P6 AWiFS satellite data, *Current Science*, **91(8)**: 1085-1089.

Bjorn Larsen, Guy Hutton and Neha Khanna, 2008, Copenhagen Consensus 2008 Challenge Paper on Air Pollution, Copenhagen.

Boyd M, Harnden P, Michael Maher and Gregory AM, 1973, Forest Fire Detection Systems Design Management Science. Application Series, Part 2, *Management Science in Canada*, **20(4)**: 617-628.

Breejen E, breuers M, Cremer F, Kemp R, Roos M, Schutte K and Vries J, 1998, Autonomous forest fire detection. In Proc. of Third International Conference on Forest Fire Research and Fourteenth Conference on Fire and Forest Meteorology, Luso, Portugal, 2003–2012.

Carmona-Moreno C, Belward A, Malingreau JP, Hartley A, Garcia-Alegre M, Antonovskiy M, Buchshtaber V and Pivovarov V,2005, Characterizing interannual variations in global fire calendar using data from Earth observing satellites, *Global Change Biology*, **11**: 1537–1555.

Casanova JL, Calle A, Romo A, Sanz J, 2004, Forest Fire Detection and Monitoring By Menas of an Integrated MODIS-MSG SYSTEM, Satellite-based fire monitoring network in Northern Eurasia: Methods, Data Products, Applications. Moscow, Space Research Institute, 409-415.

Castro R and Chuveico E, 1998, Modeling Forest Fire Danger from Geographic Information Systems, *Geocarto International*, **13(1)**: 15-23.

Chuvieco E and Congalton RG, 1989, Application of remote sensing and geographic information systems to forest fire hazard mapping, *Remote Sensing of Environment*, **29**: 147-159.

Cochran J, 2007, Sparrow Systems, Automated radio telemetry system initiative, Retrieved from: http://www.princeton.edu/ ~wikelski/research/physiology.htm, Accessed on Oct, 20th 2007.

Croft TA, 1973, Burning waste gas in oil fields. *Nature*, **245**: 375-376.

Croft TA, 1978, Night time images of the earth from space, *Scientific American*, **239**: 68-79.

Croft TA 1979, The brightness of lights on Earth at night, digitally recorded by DMSP satellite. Stanford Research Institute Final report prepared for the US Geological Suevey , p 57.

Crossbow INC. Web page. http://www.xbow.com/.

Delmas R, Lacaux JP and Brocard D, 1995, Determination of biomass burning emission factors: Methods and results, Environmental Monitoring and Assessment, **38**: 181-204.

Dennisa A, Fraserb M, Andersonc S and Allena D, 2002, Air pollutant emissions associated with forest, grassland, and agricultural burning in Texas, *Atmospheric Environment*, **36**: 3779–3792.

Doolin DM and Sitar N, 2005, Wireless sensors for wildfire monitoring, In Proc. of SPIE Symposium on Smart Structures and Materials. San Diego, CA, 477–484.

Dwyer E, Pereira JMC, Gregoire JM and DaCamara CC, 200a, Characterization of the spatio-temporal patterns of global fire activity using satellite imagery for the period April 1992 to March 1993, *Journal of Biogeography,* **27**: 57–69.

Dwyer E, Pinnock S, Gregoire JM and Pereira JMC, 200b, Global spatial and temporal distribution of vegetation fire as determined from satellite observations, International Journal of Remote Sensing, **21**: 1289–1302.

Ertena E, Kurgunb V and Musaoglu N, 2002, Forest Fire Risk Zone Mapping From Satellite Imagery And GIS: A Case Study, *International Journal of Applied Earth Observation and Geoinformation*, **4**: 1-10.

Evidencia, ThermAssure RF,2007, Retrieved from: http://www.evidencia.biz/products/ prototemp_pr.htm/ ThermAssureRF.htm, accessed on 20th 2007.

Filizzola C, Marchese F, Mazzeo G, Pergola N and Tramutoli V, 2007, Robust satellite techniques (RST) for forest fire Detection Geophysical Research Abstracts, **9**, 06506.

Fleming J and robertson RG, 2003, FireManagement Tech Tips: The Osborne Fire Finder, Tech. Rep. 0351 1311-SDTDC, USDA Forest Service, October.

Forest Survey of India (FSI), 1988, State Forest Report –Ministry of Environment and Forests, Dehradun.

Fornaro R, Coblentz D, Hawkins D, Lewis J and Noffsinger B, 2005, NEAT-Networks for Endangered Animal Tracking, Computer Society International Design Competition, Final Report.

Fujiwara K, Kushida K, Fukuda M and Kudoh J, 2002, Forest fire detection in far east Russian region with NOAA AVHRR images, Geosciences and Remote Sensing Symposium, 2002, IGARSS '02. 2002, *IEEE International*, **4**: 2054-2056.

GCOS-107, 2006, Systematic Observation Requirements for Satellite-based Products for Climate – Supplemental details to the satellite-based component of the Implementation Plan for the Global Observing System for Climate in Support of the UNFCCC, prog/gcos/Publications/gcos-107.pdf, Accessed on 14 September 2007.

Giglio L, Descloitres J, Justice CO and Kaufman YJ, 2003, An enhanced contextual fire detection algorithm for MODIS, *Remote Sensing Environment*, **87**: 273–282.

Giglio L, van der Werf GR, Randerson JT, Collatz GJ and Kasibhatla P, 2006, Global estimation of burned area using MODIS active fire observations, *Atmospheric Chemestry & Physics*, **6**: 957–974.

Guttikunda S, Wells GJ, Johnson TM, Artaxo P, Bond TC, Russell AG, Watson JG and West J, 2008, Source apportionment of urban particulate matter for air quality management: Review of techniques and applications in developing countries. Prepared by World Bank, Washington DC.

Hefeeda M, 2007, Forest Fire Modeling and Early Detection using Wireless Sensor Networks, Technical Report TR 2007-08, School of Computing Science, Simon Fraser University.

International Forest Fire News (IFFN), 2004, **31**:140 - 141.

Jun Wang and Christopher SA, 2003, Intercomparison between satellite- derived aerosol optical thickness and PM2.5 mass: Implications for air quality studies, *Geophysical Research Letter,* **30 (21)**: doi:10.1029/2003GL018174.

Justice CO, Giglio L, Korontzi S, Owens J, Morisette JT, Roy D, Descloitres J, Alleaume S, Petitcolin F and Kaufman Y, 2002, The MODIS fire products, *Remote Sensing of Environment,* **83**: 244–262.

Kahn LH, 2007, Animals: The world's best (and cheapest) biosensors, The Bulletin Online 14 March 2007, Retrieved from : http://www.thebulletin.org/columns/laura-kahn/20070314.html, Accessed on Nov, 13, 2007.

Kaufman YJ, Ichoku C, Giglio L, Korntzi S, Chu DA, Hao WM, LiR R and Justice CO, 2003, Fire and smoke observed from Earth Observing System MODIS instrument products, validation and operational use, *International Journal Of Remote Sensing,* **24 (8)**: 1765-81.

Khrt E, knollenberg J and Mertens V, 2001, An automatic early warning system for forest fires, *Annals of Burns and Fire Disasters*, **14**, 3.

Lafarge F, Descombes X, Zerubia J, 2007, Forest Fire Detection based on Gaussian field analysis, Proc. European Signal Processing Conference (EUSIPCO), Poznan, Poland.

Le Page Y, Pereira JMC, Trigo R, da Camara C, Oom D, and Mota B, Global fire activity patterns (1996–2006) and climatic influence: an analysis using the World Fire Atlas, *Atmospheric Chemistry & Physics Discussion,* **7**: 17299–17338, 2007.

Lee GY, Lee DE, Jeong CK, 2007, Bio-adhoc sensor networks for early disaster warning, *IEICE Transaction On Communications,* **5**: 1241-1244.

Lotek Corp, 2002, Retrieved from http://www.lotek.com, Accessed on Nov, 13th 2007.

Luigi Boschetti, David Roy, Paulo Barbosa, Roberto Boca and Chris Justice, 2008, A MODIS assessment of the summer 2007 extent burned in Greece, *International Journal of Remote Sensing*, **29(8)**: 2433–2436.

Nakau K, Fukuda M, Kushida K, Hayasaka H, Kimura K, Tani H, 2006, Forest fire detection based on MODIS satellite imagery, and Comparison of NOAA satellite imagery with fire fighters' Information, IARC/JAXA Terrestrial Team Workshop, 18-23.

Negi SS, 1986, *A handbook of Forestry,* International Book Distributors, Dehradun, India.

Ollero A, 1998, Martinez-De Dios, J-R.; ARRÚE, B.C. Integrated Systems For Early Forest-Fire Detection. III International

Conference on Forest Fire Research 14th Conference on Fire and Forest Meteorology, Luso, 16/20 November 1998, VOL II, 1977-1988.

Patah NA, Mansor S and Mispan MR, An application of remote sensing and geographic information system for forest fire risk mapping, Malaysian Centre for Remote Sensing (MACRES).

Reddy BVS, Reddy SP, Bidinger F and Blummel M, 2003, Crop management factors influencing yield and quality of crop residues, *Fields Crop Research*, **84** : 57–77.

Ria˜no D, Ruiz JAM, Isidoro D and Ustin SL, 2007, Global spatial patterns and temporal trends of burned area between 1981 and 2000 using NOAA-NASA Pathfinder, Glob. Change Biol., 13, 40–50, 2007.

Roberto Castro and Chuvieco E, 1998, Modeling forest fire danger from geographic information systems, *Geocarto Internationa*l, **13(1)** :15-23.

Rodriguez E and Martin JM, 1992, Theory and design of interferometric synthetic. *Proceedings of IKE,* **139(2)**: 147-159.

Roy DP, Boschetti L, Justice CO, Ju J, 2008, The collection 5 MODIS burned area product — Global evaluation by comparison with the MODIS active fire product. Remote Sensing of Environment, *112* :3690–3707.

Roy PS, 2003, Forest fire and degradation assessment using satellite remote sensing and Geographic Information System, Satellite Remote Sensing and GIS Applications in Agricultural Meteorology, Proceedings of a Training Workshop, Dehra Dun, India, 361-400.

Stipanièev D, Vuko T, Krstiniæ D, Štula M and Bodro•iæ L, 2006, Forest Fire Protection by Advanced Video Detection System - Croatian Experiences, Third TIEMS Workshop - Improvement of Disaster Management System, Trogir.

Streets DG, Yarber KF, Woo JH and Carmichael GR, 2003, Biomass burning in Asia: annual and seasonal estimates and atmospheric emissions.*Global Biogeochemical Cycles*, 17(4), doi:10.1029/2003GB002040.

Toreyin BU, Dedeoglu Y, Cetin AN, 2007,Computer vision based forest fire detection and monitoring system, 4th International Wildland Fire Conference, Seville.

UNEP, 2007, UNEP Assists ASEAN Countries to Combat Forest Fires, Retrieved from : http://www.rrcap.unep.org/projects/forestfires.cfm, Accessed on 20th October, 2007.

Wei Min Hao J, Meghan Salmon and Bryce Nordgren, 2003. Development of A Forest Fire Smoke Emission and Dispersion Model Using Real-time MODIS Data USFS Rocky Mountain Research Station, Missoula Fire Sciences Laboratory. Paper presented at the workshop on " innovatrive methods for emission inventory development & evaluation" held at Pickle Research Centre, University of Texas, Austin, TX, USA.

XU Dong , DAI Li-min, SHAO Guo-fan, TANG Lei, WANG Hui:, ~2005, Forest fire risk zone mapping from satellite images and GIS for Baihe Forestry Bureau, Jilin, China, *Journal of Forestry Research,* **16(3)**: 169-174.

Yasar Guneri Sahin, 2007, Animals as Mobile Biological Sensors for Forest Fire Detection, *Sensors,* **7**: 3084-3099.

Yeung J, 2007, Animals to be used as quake sensors (China Daily), Retrieved from : http://english.peopledaily.com.cn/200705/22/eng20070522_376760.html, Accessed on Oct, 20th, 2007.

Young Gi Byun, Yong Huh, Kiyun Yu and Yong Il Kim, 2005, Evaluation of Graph-based Analysis for Forest Fire Detections Proceedings of world academy of science, engineering and technology,**10** .

Zhukov B, Oertel D, Lorenz E, Ziman Ya and I Csiszar - Comparison of fire detection and quantitative Characterisation by MODIS and BIRD.

http://www.nofc.forestry.ca/fire,Canadian Forest Fire Danger Rating System (Cffdrs) Web Page

http://www.aerovision-uav.com., Aerovision Web page.

http://www.cccturtle.org/satellitetracking.php? page=satintro, Accessed on Nov, 13th 2007,Caribbean Conservation Corporation & Sea Turtle Survival League, How Tracking Sea Turtles by Satellite Works, Retrieved from

http://www.fire-watch.de/.Fire watch web page.

http://www.fesb.hr/~ljiljana/radovi/279548, TIEMS-Stipanicev_i_ostali.pdf, Forest Fire Protection by Advanced Video Detection System, Croatian Experiences, Darko Stipaniev, Tomislav Vuko, Damir Krstini, Maja Štula, Ljiljana Bodro